AN INVESTIGATION INTO THE PHYSICO-CHEMICAL AND NEUROPROTECTIVE PROPERTIES OF MELATONIN AND 6-HYDROXYMELATONIN

THESIS

Submitted in Fulfilment of the
Requirements for the Degree of

DOCTOR OF PHILOSOPHY
(PHARMACY)

of

Rhodes University

By

Deepa Sukhdev Maharaj

DECEMBER 2003

Dedicated to the memory of my grandmother.

"The wonderful thing about melatonin is that it can extend your life and support your health and vitality. However, the really wonderful thing about melatonin is the great effect it will have on our generation as well as on future generations. We are embarking on a common adventure and are the first generation which has the power to avoid diseases and ailments which are considered typical for a 'normal' senescence. For the first time we have the power to maintain our youthfulness and to stay strong and fit for all our life. For the first time we cannot only avoid physical decline caused by the ageing process but we are also in a position to delay and even to reverse it. This is the real melatonin miracle."

Citation from the book of Dr. Walter Pierpaoli and Dr.William Regelson

(The Melatonin Miracle, August 1995)

ABSTRACT

Until the beginning of this decade the antioxidant, melatonin, had been considered as little more than a tranquilizing hormone, responsible for regulating certain circadian and circannual rhythms. However, it is the discovery of melatonin as a free radical scavenger that has generated the most interest in recent years. The reduction of melatonin with age has been associated with neurodegenerative diseases such as Alzheimer's disease (AD) and therefore, melatonin has been implicated to have an important clinical role in neuroprotection. Thus, for several years melatonin has attracted increasing attention from the general press with many advertisements touting this indoleamine to act as an aphrodisiac, rejuvenator, protector against diseases and a general wonder drug. However, melatonin formulations appear with no labelling for the correct storage conditions, dosage and side effects, as well as no control for purity and self-medicating with an unregulated product. In addition, there is much controversy surrounding the antioxidative properties of the indolemaine, 6-hydroxymelatonin (6-OHM). Therefore, the first part of this study aims to elucidate the physico-chemical and various stability characteristics of the pineal antioxidant, melatonin, while the second part is devoted to investigating the neuroprotective properties of the primary hepatic metabolite of melatonin, 6-OHM.

The physical properties of melatonin were determined using various chemical techniques. This information served to both characterize and confirm the identity of melatonin raw material used in this study. In addition, this information serves to be essential as the physical properties of melatonin have not been reported in detail in literature, to date. Thereafter, using a validated high performance liquid chromatography (HPLC) method, the various physico-chemical and stability characteristics of melatonin were determined. Melatonin was shown to be extremely lipophilic, while the hygroscopic study indicates that melatonin raw material is extremely hygroscopic at temperatures above 40^{o}C, whereas melatonin tablets are hygroscopic when left out of the original container. This study highlights the need for consumers to be aware of the proper storage of melatonin tablets to improve the stability and ensure long term integrity of the compound.

Since, melatonin is most often administered orally, thus exposing it to a large variations in pH, within the gastrointestinal tract, it was decided to investigate the stability of melatonin over a range of pH's and temperatures. The findings imply that melatonin is

relatively stable at body temperature when ingested orally and that orally administered slow release preparations of melatonin should be relatively stable and therefore exhibit favourable bioavailability. However melatonin was shown to be unstable in solution. This provides important information and a challenge to the formulators of this drug substance in a liquid dosage form. An assessment of the photostability of melatonin dosage forms using International Committee on Harmonization (ICH) conditions revealed melatonin to be light sensitive and thus indicates a need for careful consideration of the packaging of these drug products. In addition a detailed assessment of the photochemistry and photoproducts formed during the UV photodegradation of melatonin is reported. Melatonin is shown to rapidly degrade in the presence of UV light, with the presence of oxygen accelerating the photodegradation. N^1-acetyl-N^2-formyl-5-methoxykynurenamine (AFMK) and 6-OHM were identified as the major photoproducts formed and these agents have been shown previously to retain antioxidant activity. One of the concerns of using melatonin in sunscreens is its photostability. However, it is reported in this study that the degraded solution of melatonin still possesses equipotent free radical scavenging ability as melatonin, despite the absence of melatonin in solution. In addition, melatonin is shown to reduce UV-induced oxidative stress in rat skin homogenate. Thus, these results make melatonin a likely candidate for inclusion in sunscreen preparations.

Neuronal damage due to oxidative stress has been implicated in several neurodegenerative disorders. 6-OHM is not only formed as the major hepatic metabolite of melatonin, but also when melatonin reacts with toxic radicals as well as UV light. Thus the second part of the study aims to elucidate and further characterize the mechanism behind 6-OHM's neuroprotection. The results show 6-OHM to be a more potent singlet oxygen and superoxide anion scavenger than melatonin. In addition, the results show 6-OHM to offer protection against, oxidative stress and lipid peroxidation induced by several neurotoxins in the rat brain and hippocampus.

The hippocampus is an important region of the brain responsible for the formation of memory and any agent that induces stress in this area has detrimental effects and could lead to various types of dementia. Such agents include quinolinic acid (QA) and iron (II). Histological studies undertaken reveal that 6-OHM is able to protect hippocampal neurons against QA and iron (II) induced necrotic cell death. Immunohistochemical investigations showed that QA moderately induces apoptotic cell death in the

hippocampus which is inhibited by both melatonin and 6-OHM. The study sought to elucidate possible mechanisms by which 6-OHM exerts its neuroprotective capabilities and the results show 6-OHM to inhibit the action of cyanide on the mitochondrial electron transport chain (ETC), one of the most common sources of free radicals. In addition, 6-OHM treatment alone, increased ETC activity above basal control levels and the results show 6-OHM to increase complex I activity in the mitochondrial ETC.

Electrochemical, ultraviolet/visible spectroscopy (UV/Vis) and HPLC assessment show that an interaction exists between 6-OHM and iron (III) and 6-OHM is able to reduce iron (III) to a more biologically usable form viz. iron (II) which can be incorporated into important biomolecules such as heme. One dire consequence of this interaction is the ready provision of iron (II) to drive the Fenton reaction. However the biological and histological assessments show 6-OHM to prevent iron (II)-induced lipid peroxidation and necrotic cell death and thus, provide evidence of its antioxidant properties. The results also show 6-OHM to promote Hsp70 induction in the hippocampus. Heat shock proteins, especially Hsp 70 plays a role in cytoprotection by capturing denatured proteins and facilitating the refolding of these proteins once the stress has been relieved. 6-OHM treatment alone and together with QA was shown to increase the level of expression of Hsp70, both inducible and cognate forms of the protein. This suggests that 6-OHM helps to protect against cellular protein damage induced by any form of stress the cell may encounter. Melatonin treatment alone and in combination with QA was shown to prevent increases in the level of Hsp70 in the hippocampus, indicating that melatonin was able to reduce oxidative stress induced by QA such that Hsp70 expression was not required.

The discovery of neuroprotective agents, such as melatonin and 6-OHM, is becoming important considering the rapid rise in the elderly population and the proportionate increase in neurological disorders. The findings of this study indicate the need for important information regarding the correct storage conditions and stability characteristics of melatonin dosage forms. In addition, the results indicate that 6-OHM has a definite role to play as an antioxidant. Thus further research may favour the use of these agents in the treatment of several neurodegenerative disorders.

TABLE OF CONTENTS

CHAPTER TWO HPLC CHROMATOGRAPHY METHOD DEVELOPMENT AND VALIDATION

CHAPTER THREE MELATONIN: PHYSICO-CHEMICAL PROPERTIES

CHAPTER NINE MITOCHONDRIAL FUNCTION

CHAPTER TEN LIPID PEROXIDATION

LIST OF FIGURES

LIST OF TABLES

LIST OF PUBLICATIONS

The articles in press and published thus far as a result of this work is listed below.

1. B.D. Glass, ME. Brown, S. Daya, MS. Worthington, P. Drummond, E. Antunes, M. Lebete, S. Anoopkumar-Dukie, and **D. Maharaj**. Influence of cyclodextrins on the photostability of selected drug molecules in solution and the solid-state. *International Journal of Photoenergy*, 3: 1-7. (2001).

2. **D.S. Maharaj**, B.D. Glass, and S. Daya. Exposure of rat skin homogenate to UV light in the presence of melatonin reduces lipid peroxidation and superoxide anion generation, *Int. J. Biogenic Amines*, 16(6), 531-540 (2001).

3. **D.S. Maharaj**, S. Anoopkumar-Dukie, B. D. Glass, E.M. Antunes, B. Lack, R.B. Walker and S. Daya. Identification of the UV degradants of melatonin and their ability to scavenge free radicals, *JPR,* 32 (4), 257-261 (2002).

4. **D.S. Maharaj,** B.D. Glass, S. Daya. The photostability of Ibuprofen under ICH conditions in solution and in the gel formulation is dependent on the packaging. *South African Pharmacy Journal* 69(2): 29-31, (2002).

5. **D. S. Maharaj**, Janice L. Limson, and Santy Daya. 6-Hydroxymelatonin converts Iron (III) to Iron (II). *Life Sciences*, 72 (12), 1367-1375 (2003).

6. **D. S. Maharaj**, RB Walker, BD Glass and S. Daya. 6-Hydroxymelatonin protects against cyanide-induced free radical attack in rat brain homogenates. Journal of Chemical Neuroanatomy. (In Press.).

LIST OF SYMBOLS AND ABBREVIATIONS

AdSV	Adsorptive cathodic stripping voltammogram
AD	Alzheimer's Disease
AFMK	N^1-acetyl-N^2-formyl-5-methoxykynurenamine
AIF	Apoptosis inducing factor
Ag/AgCl	Silver/Silver chloride
Al	Aluminium
ANOVA	One way analysis of variance
ATP	Adenosine Triphosphate
BBB	Blood brain barrier
BHT	Butylated hydroxytoluene
BSA	Bovine Serum Albumin
CA1	Cornu Ammonis *1*
CA3	Cornu Ammonis *3*
Ca^{2+}	Calcium (II)
CaCaM	Ca^{2+}-calmodulin
CNS	Central nervous system
C_o	DPBF concentration at time 0
C_t	DPBF concentration at time t
$C_{octanol}$	Molar Concentration of solute in octanol
C_{water}	Molar Concentration of solute in water
CTL	Cytotoxic T lymphocytes
CV	Cyclic voltammogram
DHBA	Dihydroxybenzoic acid
DMSO	Dimethylsulfoxide
DNA	Deoxyribonucleic Acid
DPBF	1, 3-diphenylisobenzofuran
DPI	2, 6-dichlorophenolindophenol
DSC	Differential scanning calorimetry
EAA	Excitatory amino acid
EDTA	Ethylenediaminetetraacetic acid
Em	Emission
ESR	Electron spin resonance
ETC	Electron transport chain
Ex	Excitation
Fe^{2+}	Iron (II)
Fe^{3+}	Iron (III)
GCE	Glassy carbon electrode
GC-MS	Gas chromatography – mass spectrometry
GPx	Glutathione peroxidase
GRd	Glutatione reductase
GSH	Reduced glutathione
GSSG	Oxidized glutathione
HAD	Hydroxyalkenals
HAO	Hydroxyanthranilic acid oxygenase
HCl	Hydrochloric acid
H_2O	Water
H_2O_2	Hydrogen peroxide

$HO^{\bullet}_2$	Hydroperoxyl radical
HPLC	High performance liquid chromatography
Hsp	Heat shock protein
ICH	International Committee of Harmonisation
i.p.	Intraperitoneal
i_{pa}	Anodic peak current
i_{pc}	Cathodic peak current
IR	Infrared
ISEL	*In situ* end labelling
ISNT	*In situ* nick translation
K^+	Potassium
KA	Kainic acid
KCN	Potassium cyanide
KF	Karl Fischer
K_{ow}	Octanol-water Partition Coefficient
LC-MS	Liquid chromatography – mass spectrometry
LDH	Lactate dehydrogenase
LOD	Limit of detection
LOQ	Limit of quantitation
$LOO^{\bullet}$	Peroxyl radical
LTP	Long term potentiation
MDA	Malondialdehyde
MEL	Melatonin
$MEL^{\bullet}$	Melatonin radicals
mg/Kg	milligram per Killogram
min	Minute
mL	Millilitre
mM	Millimolar
MOPS	3-[*N*-morpholino]propanesulfonic acid
MPc	Metallated phthalocyanines
MPTP	1-methyl-4-phenyl-1, 2, 3, 6-tetrahydropyridine
mRNA	Messenger ribonucleic acid
n	Number of replicates
Na^+	Sodium
NAD	Nicotinic acid dinucleotide
NADH	Reduced nicotinamide adenine dinucleotide
NADP	Nicotinamide Adenine dinucleotide phosphate
$NaHCO_3$	Sodium Hydrogen Carbonate
NAT	Serotonin-N-acetyltransferase
NBD	Nitroblue Diformazan
NBT	Nitroblue Tetrazolium
NK	Natural killer
NMDA	N-methyl-D-aspartate
NMR	Nuclear magnetic resonance
$NO^{\bullet}$	Nitric oxide
NOCD	Naturally occurring cell death
NOS	Nitric oxide synthase
ns	Not significant
$O_2^{\bullet-}$	Superoxide anion radical
$^{\bullet}OH$	Hydroxyl radical

$^1O_2$	Singlet oxygen
O_2	Oxygen
6-OHM	6-Hydroxymelatonin
p	Probability
PARS	Poly-ADP ribose polymerase
Pb	Lead
PBS	Phosphate buffered saline
PCD	Programmed cell death
PDT	Photodynamic therapy
Ppm	Parts Per Million
PTP	Permeability transition pore
PUFA	Polyunsaturated fatty acid
QA	Quinolinic acid
QPRT	Quinolinate phosphoribosyl transferase
RNS	Reactive nitrogen species
Rpm	Revolutions per minute
R_T	Retention Time
ROS	Reactive oxygen species
s	seconds
SAR	Structure activity relationships
s.c.	Subcutaneous
SCN	Suprachiasmatic nucleus
SEM	Standard error of the mean
SOD	Superoxide dismutase
SPE	Solid-phase extraction
TBA	2-Thiobarbituric acid
TCA	Trichloroacetic acid
TdT	Terminal deoxynucleotidyl transferase
THA	Terephthalic acid
Tris	Tris (hydroxymethyl)-aminomethane
TUNEL	TdT-mediated dUTP nick end labeling
UK	United Kingdom
USA	United States of America
USP	United States Pharmacopoeia
UV/Vis	Ultraviolet/Visible Spectroscopy
V	Volts
v/v	Volume by volume
ZnPc	Zinc Phthalocyanines
$\propto$	Alpha
µA	Microamperes
µg	Micrograms
µL	Microlitre
µM	Micromolar
^oC	Degrees celcius
λmax	Lambda Maximum
Φ_Δ	Singlet oxygen quantum yield
Φ_F	Fluorescence quantum yield
Φ_P	Phototransformation quantum yield

ACKNOWLEDGEMENTS

I would like to express my sincerest gratitude to the following people for their contributions toward this thesis:

My supervisor, Professor Santy Daya, for his expert supervision, constant encouragement, unfailing support and guidance throughout this study. It was truly a privileged to work as part of his research group.

My co-supervisor, Professor Beverly Glass, for all her supervision, enthusiasm, support and guidance. I would also like to thank her for her patience and expertise in helping me understand the inorganic chemistry part of this study.

Dr. Janice Limson, for her help with understanding the electrochemical part of this study and the interest she took in my work.

Dr. Edith Antunes, for her assistance and guidance with the use of the LC-MS and Nd-Yag laser.

Emily, for her help in explaining the apoptosis technique to me.

Professor Blatch and Tondi for their help with the heat shock protein studies.

Professor, Ted Botha, for lending his invaluable time and expertise to assist me with the use of the fluorescence miscroscope.

The National Research Foundation, Medical Research Council and Andrew Mellon Scholarship, for financial assistance during my studies.

The staff of the department of pharmacy and my lab mates for the warmth and encouragement extended towards me and my work. Mr and Mrs Morley, for always being there to help me, for their support and providing a well-organised work environment.

My family for their unconditional love, support and encouragement without which this work would not be possible. I would especially like to thank my mom and dad for their unwavering belief in my capabilities and for the sacrifices that they made to help me realise my dreams.

My close friends, Abi, Terry, Melanie, Angel, and Nestor for their companionship. Himant for his encouragement, support, enthusiastic help and above all for being “so sweet” and caring. Josephine, for being her cheerful self and always encouraging me.

Ashley for always being there to talk to and for his undying support and faith in me, without whom this thesis would not have been possible. Thank you for your patience during the last few months and in believing in me.

Above all, I give thanks to God for opening doors for me and making my dreams come true.

CHAPTER EIGHT

SUPEROXIDE ANIONS

8.1. INTRODUCTION

Reactive oxygen species (ROS) are continually generated under normal conditions as a consequence of aerobic metabolism. ROS are particularly transient species due to their high chemical reactivity and can react with DNA, proteins, carbohydrates and lipids in a destructive manner (DiFiglia, 1990).

Cells are endowed with extensive and highly effective antioxidant defence mechanisms to protect neurons against ROS (Braughler & Hall, 1989), either directly by interception or indirectly through reversal of oxidative damage (Curtin *et al.*, 2002). Under normal conditions these defence mechanisms are quite capable of protecting neurons. However, under conditions when ROS overcome the defence systems of the cell and redox homeostasis is altered, the result is oxidative stress and neurotoxicity (Curtin *et al.*, 2002; DiFiglia, 1990).

The reduction of oxygen by its acceptance of a single electron produces the superoxide free radical also referred to as superoxide anion ($O_2^{\bullet-}$) (Reiter *et al.*, 2002). The major source of $O_2^{\bullet-}$, under physiological conditions is the mitochondrion and these radicals are usually generated as a result of electron "leakage" from the electron transport chain located in the mitochondria (McCord, 1985), and by activation of certain enzymes. Other sources of $O_2^{\bullet-}$ include enzymes such as cytochrome *P*450 in the endoplasmic reticulum, lipoxygenases, cyclooxygenases, xanthine oxidase and NADPH oxidase (Curtin *et al.*, 2002). Figure 8.1 diagrammatically illustrates the different sources of $O_2^{\bullet-}$.

In normal resting cells, the respiratory chain loses two to three percent of the electrons during their transfer to molecular oxygen, most of them participating in the production of $O_2^{\bullet-}$ (Boveris, 1977).

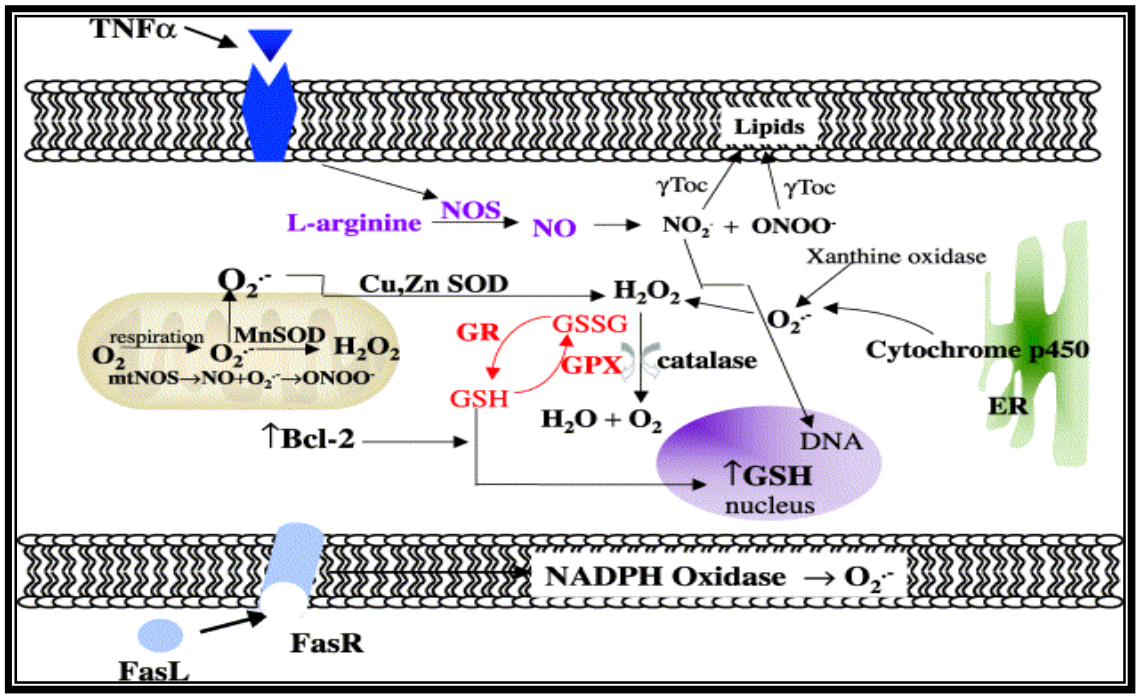

Figure 8.1: Diagrammatic representation of the Intracellular sources of ROS and principle defence mechanisms. Major sources of ROS production include the mitochondria, endoplasmic reticulum, plasma membrane and cytosol. The mitochondria generate $O_2^{\bullet-}$ during respiration, which is converted to H_2O_2 by Mn-SOD. In the cytosol, $O_2^{\bullet-}$ is converted to H_2O_2 by Cu,Zn-SOD. The two major defence systems against H_2O_2 are the GSH redox cycle present in both the cytosol and mitochondria and catalase present only in the peroxisome fraction. Other sources of $O_2^{\bullet-}$ include the enzymes xanthine oxidase in the cytosol, NADPH oxidase in the membrane and cytochrome *P*450 in the ER (Cooney *et al*., 1993).

Briefly, Complex I, NADH-ubiquinone oxidoreductase, and Complex III, ubiquinol-cytochrome *c* oxidoreductase are the two sites in the ETC where O_2 is initially converted to $O_2^{\bullet-}$ (Raha & Robinson, 2000) and this is diagrammatically represented in figure 8.2. Electrons enter the ETC at either Complex I or Complex II (succinate dehydrogenase) following the oxidation of NADH and succinate, respectively. Ubiquinone is a lipid-soluble electron carrier and carries the electrons from Complex I and Complex II to Complex III. It is believed that semiquinone formation at both Complex I and Complex III results in the production of $O_2^{\bullet-}$ (Curtin *et al*., 2002). $O_2^{\bullet-}$ is generated by the cycling of ubiquinol in the inner mitochondrial membrane and is produced primarily in the mitochondrial matrix (Raha *et al*., 2000). Complex III is however shown to be the primary site of ROS and $O_2^{\bullet-}$ production (Waypa & Schumacker, 2002). In the Q cycle, a free radical (ubisemiquinone) is normally generated during the electron transport process and this radical can potentially donate its unpaired electron to O_2, thereby generating $O_2^{\bullet-}$ (Waypa & Schumacker, 2002).

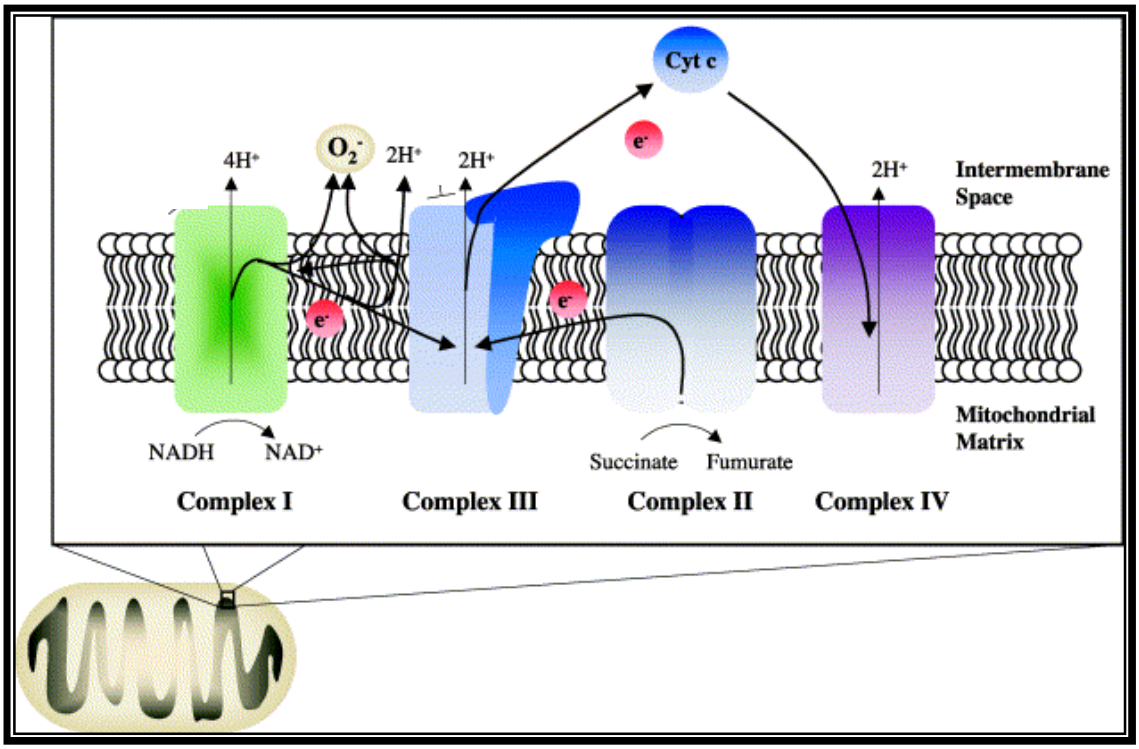

Figure 8.2: Schematic diagram illustrating the major subunits of the electron transport chain (ETC) and sites of $O_2^{\bullet-}$ production (Curtin *et al*., 2002).

Superoxide toxicity appears to be through an indirect action on living cells as $O_2^{\bullet-}$ is capable of producing the more powerful and damaging hydroxyl radical ($^{\bullet}OH$) in the presence of hydrogen peroxide (Haber – Weiss reaction). Since these reactions are reversible, there is a constant generation of superoxide and the promotion of free radical reactions is allowed for (Curtin *et al*., 2002).

$O_2^{\bullet-}$ can be very reactive and leads to neurodegeneration (Patel *et al*., 1996). It has been proposed (Fahn & Cohen, 1992) that the excitatory amino acids (EAA's) are neurotoxic because they lead to increased production of $O_2^{\bullet-}$. Overstimulation of EAA receptors results in the influx of Ca^{2+}, Na^{+}, and K^{+} into the neuron (Poeggeler *et al*. 1993). As these ions cause a change in the osmotic pressure, the neuron attempts to pump the ions out of the cell. The transport of ions is an active process that requires energy. Thus the mitochondria are forced to produce more ATP, and so there is a chance of greater electron leakage. Enzymes such as xanthine dehydrogenase (Dykens *et al*., 1987) and nitric oxide synthetase (Iadecola, 1997) are also activated by Ca^{2+} so the influx of Ca^{2+} into the neurons results in greater activity of these enzymes and one of the by-products of the activities of these enzymes is the production of $O_2^{\bullet-}$.

The aim of the present chapter is to investigate the ability of the neurotoxin, cyanide, on the production of $O_2^{\bullet-}$ in rat brain homogenate *in vitro* and to determine the ability firstly of degraded melatonin solution to reduce cyanide-induced $O_2^{\bullet-}$ generation. Secondly, a comparative study was done to determine if melatonin and 6-OHM administration *in vitro* and *in vivo* could prevent or reduce cyanide-induced $O_2^{\bullet-}$ production *in vitro* and quinolinic acid-induced $O_2^{\bullet-}$ formation in the rat hippocampus *in vivo*. Furthermore, the ability of melatonin to reduce UV-induced $O_2^{\bullet-}$ generation in rat skin homogenate was assessed *in vitro*.

The nitro-blue tetrazolium (NBT) assay was used to determine $O_2^{\bullet-}$ levels. This method is generally accepted as a simple and reliable method for assaying the superoxide and possibly other free radicals (Halliwell & Gutteridge, 1989). The spectrophotometric assay involves the reduction of the yellow dye nitro-blue tetrazolium (NBT) ion to the blue insoluble diformazan form i.e. nitroblue diformazan (NBD) in the presence of $O_2^{\bullet-}$, which is extracted with glacial acetic acid and measured at 560nm using a UV spectrophotometer.

8.2. EFFECT OF CYANIDE ON SUPEROXIDE ANION FORMATION IN RAT BRAIN HOMOGENATE *IN VITRO.*

8.2.1. INTRODUCTION

Cyanide is a well-established respiratory poison, which exerts its primary toxic effect by inhibiting Complex IV (cytochrome *c* oxidase) which is the terminal electron acceptor enzyme of the mitochondrial electron transport chain (Isom & Way, 1984) and it must give up its reducing equivalents to allow continued electron transport and ATP production (Cadenas & Davies, 2000) as demonstrated in figure 8.3.

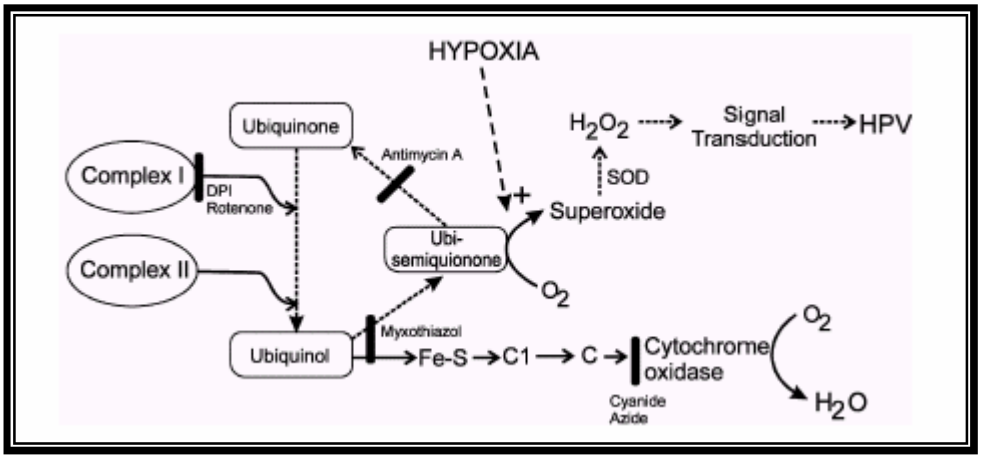

Figure 8.3: Schematic diagram showing mitochondrial ROS and $O_2^{\bullet-}$ production at Complex III. Solid arrows show electron transfer steps; solid bars show sites of electron transport inhibition. The Q cycle converts the dual electron transfer in Complex I and II into single electron transfer steps in Complex IV. Ubisemiquinone (a free radical) created in this process can generate $O_2^{\bullet-}$ (Waypa & Schumacker, 2002).

Cyanide causes inhibition of sites distal to Complex III and thus tends to augment ROS and especially $O_2^{\bullet-}$ generation (figure 8.3). Therefore, the consequence of this inhibition is impaired tissue utilisation of oxygen, and with time, oxidative metabolism is brought to a halt. Due to its high dependence on oxidative metabolism and limited anaerobic capacity, the CNS is particularly vulnerable to cyanide intoxication (Way, 1985) and the brain is seen as a primary target organ in cyanide toxicity (Gunasekar *et al*., 1996).

Furthermore, cyanide has been shown to play an important role in neurotoxicity by elevating intracellular calcium (Johnson *et al*., 1987) levels and inhibiting a number of antioxidant enzymes (Ardelt *et al*., 1989). Therefore, the aim of the present study was to investigate the effect of incubating homogenized rat whole brain with increasing concentrations cyanide on $O_2^{\bullet-}$ production.

8.2.2. MATERIALS AND METHODS

8.2.2.1. Chemicals and Reagents

Potassium cyanide (KCN), nitro-blue tetrazolium and nitro-blue diformazan (NBD) were purchased from the Sigma Chemical Company, St. Louis, MO (USA). Glacial acetic acid was purchased from Saarchem (PTY) Ltd, Krugersdorp (South Africa). All other chemicals used were of the highest quality available from commercial sources.

8.2.2.2. Animals

Adult male rats of the Wistar strain, weighing between 200-250g were used in this experiment. The rats were randomly assembled into groups of five, and housed in separate cages, in a controlled environment as described in appendix one. Protocols for the experiments were approved by the Rhodes University Animal Ethics Committee.

8.2.2.3. Sample Preparation

A 0.1% NBT solution was made by dissolving the NBT in ethanol before making up to the required volume with Milli-Q water. The final ethanol concentration in the incubation flasks was less than 0.5%.

Stock solutions were prepared so that on addition of 250µL of the toxin, the stock solution would be diluted to the correct incubation concentration. KCN was tested at the following concentrations; 0, 0.25, 0.5, 1, 1.5mM. The KCN was dissolved in Milli-Q water.

8.2.2.4. Preparation of Standards

NBD was used as a standard. A series of reaction tubes, each containing appropriate aliquots of NBD dissolved in glacial acetic acid was prepared to a final volume of 1ml. A calibration curve (appendix four) was generated by measuring the absorbance at 20µmoles/ml intervals. The absorbance was read at 560nm using a Shimadzu UV-160A UV-visible recording spectrophotometer.

8.2.2.5. Brain Removal

Rats were sacrificed swiftly by cervical dislocation and rapidly decapitated. The brains were removed for use in experiments as described in appendix two. The brains were either used immediately or stored at -70^{o}C until needed.

8.2.2.6. Tissue Preparation

Rat brain homogenate is a useful model for determining the efficacy of agents to reduce or potentiate $O_2^{\bullet-}$. Each brain was homogenised in a glass teflon homogenizer with 0.1M phosphate-buffered saline buffer (PBS), pH 7.4 so as to give a final concentration of 10% w/v. This is necessary to prevent lysosomal damage of the tissue. PBS buffer was used as it has been shown not to scavenge free radicals (Anoopkumar-Dukie *et al*., 2001) unlike Tris-HCl buffer which by itself is a hydroxyl radical scavenger (Yamamoto & Tang, 1996a). The homogenate was either used immediately or frozen in liquid nitrogen and stored at -70°C until use. All samples were used within 7 days of homogenate preparation. Test samples revealed that storage of the homogenate did not alter the $O_2^{\bullet-}$ levels compared to fresh brains.

8.2.2.7. Nitroblue Tetrazolium Assay (NBT)

A modified method of Sagar *et al*., (1992) and Das *et al*., (1990) was used for this assay. The lipid source viz. rat brain homogenate (1mL) containing varying concentrations of KCN (0, 0.25, 0.5, 1, 1.5mM) was incubated with 0.4ml of a 0.1% NBT solution in an

oscillating water bath for 60 min at 37°C. Termination of the assay and extraction of reduced NBT was carried out by centrifugation of the suspensions at 2000 x g for 10 mins. The supernatant was decanted and the pellet was resuspended with 2ml glacial acetic acid. The relative absorbance of the glacial acetic acid fraction was measured at 560nm and converted to µmoles Diformazan using a standard curve generated from nitroblue diformazan (NBD) in appendix three. Final results are expressed as µmoles Diformazan/mg protein.

The mg of protein in each homogenized rat brain tissue was determined by carrying out protein assays as described in section 8.2.2.8. All results were analyzed to show statistical significance as described in section 8.2.2.9.

8.2.2.8. Protein Determination

All protein determinations were performed using the method described by Lowry *et al*., (1952). A standard curve was generated using bovine serum albumin (BSA) as a standard at concentration intervals of 60µg/ml, described in appendix three.

8.2.2.9 Statistical Analysis

The results were analyzed using a one-way analysis of variance (ANOVA). If the F values were significant, the Student Newman-Keuls test was used to compare the treated and control groups. The level of significance was accepted at $p<0.05$ (Zar, 1974).

8.2.3. RESULTS

The final results were corrected for any dilutions and are expressed as µmoles of diformazan produced/mg protein. The data represents the mean ±SEM of five determinations. The *in vitro* exposure of whole rat brain homogenate to increasing concentrations of KCN caused a significant increase in $O_2^{\bullet-}$ generation, in a concentration-dependent manner when compared to the control value. The 1mM concentration of KCN caused a ±60% increase in $O_2^{\bullet-}$ in comparison to the control value (figure 8.4). It is evident from figure 8.4, that no further increase in $O_2^{\bullet-}$ formation is

evident for KCN concentrations higher than 1mM. Therefore, this concentration of KCN (1mM) was chosen for subsequent studies as it yielded the highest amount of $O_2^{\bullet-}$.

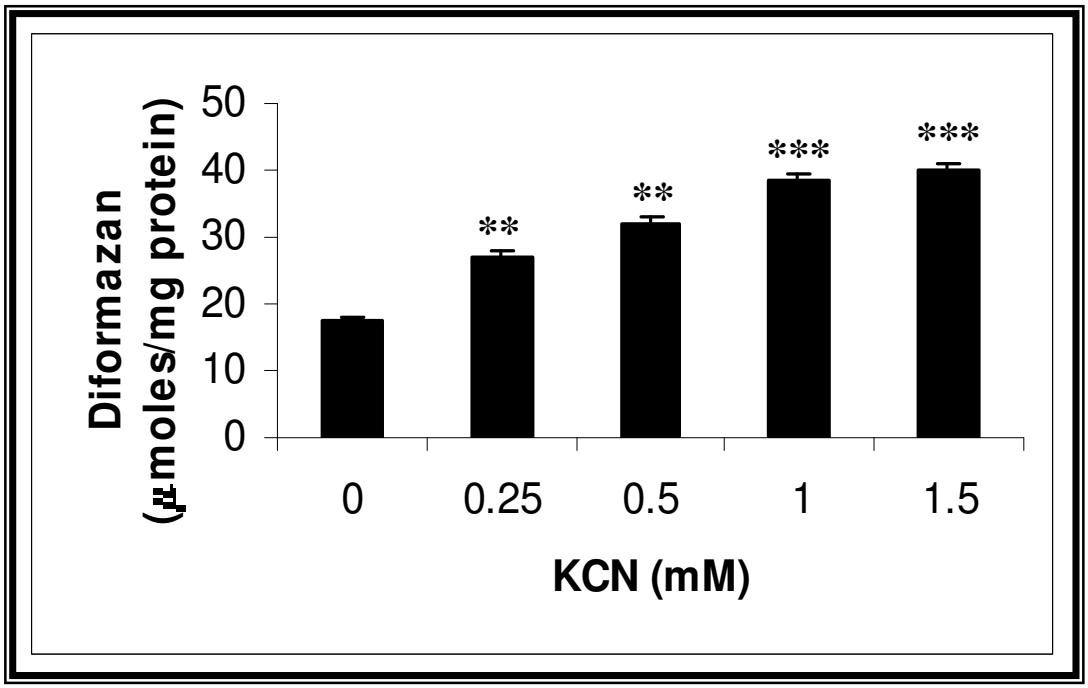

Figure 8.4: Concentration-dependent effect of KCN on $O_2^{\bullet-}$ generation in whole rat brain homogenates. Each bar represents the mean ± SEM; n=5; *p<0.05 ; **p<0.01 ; ***p<0.001 in comparison to control. (Student-Newman-Keuls Multiple Range Test).

8.2.4. DISCUSSION

The mitochondria possess a mechanism known as mild uncoupling and this prevents a marked increase in $O_2^{\bullet-}$ formation. Mild uncoupling is the first line of mitochondrial antioxidant defence since it reduces $O_2^{\bullet-}$ generation (Skulachev, 1999). If, nevertheless, some $O_2^{\bullet-}$ is still formed, the next line of defence is activated. This role is carried out by the cytochrome *c* oxidase (cyt c) which oxidizes $O_2^{\bullet-}$ back to O_2 (cyt c^3 + $O_2^{\bullet-}$ = cyt c^2 + O_2), whereas reduced cyt c can then be oxidized by O_2 (4cyt c^2 + O_2 + $4H^+$ = 4 cyt c^3 + $2H_2O$). This mechanism represents the most effective way to scavenge $O_2^{\bullet-}$, since it is merely converted back to O_2 (Skulachev, 1999). It is well known that $O_2^{\bullet-}$ production occurs primarily within Complex I and Complex III. Cyanide is a Complex IV inhibitor of the mitochondria ETC and thus inhibits this defence mechanism of mitochondria. Distal inhibition of the ETC by cyanide augments ROS production in contrast to proximal site inhibitors such as rotenone (Complex I inhibitor) or myxothiazol (Complex III

inhibitor), as seen in figure 8.3, which allows for the ubiquinone pool to become fully oxidised and ROS generation at Complex III is thus abrogated (Waypa & Schumacker, 2002).

Due to a number of antioxidant enzymes being inhibited by cyanide, it is also believed that oxidative stress plays an important role in cyanide induced neurotoxicity (Ardelt *et al*., 1989). In the present study, it is evident that cyanide causes a rapid and concentration dependent rise in $O_2^{\bullet-}$ generation, thus providing further evidence that cyanide is able to produce oxidative stress and induce neurotoxicity.

Cyanide interacts with the hem-a-3 portion of cytochrome oxidase in the electron transport chain, in the mitochondria (Slater, 1967) to prevent oxygen utilization and causes a loss of oxidative phosphorylation resulting in the disruption of the homeostatic ATP-dependent Na^{2+}/K^{+} and Ca^{2+} pumps. The latter pump will cause an increase in intracellular calcium and this will initiate a cascade of events, culminating free radical generation that will affect the lipids, proteins, and DNA (Southgate & Daya, 1999). Johnson *et al*., (1987) further confirmed this by showing cyanide to elevate brain calcium levels and produce an increase in free cytosolic calcium in an isolated neuronal cell model. Elevated calcium levels can lead to activation of numerous neuronal calcium-dependent events and ultimately results in oxidative stress and free radical generation. Isolated cerebral and cerebellar mitochondria have been shown to produce free radicals when exposed to elevated levels of Ca^{2+} (Dykens, 1994). Hence, the elevation of calcium levels by cyanide in the mitochondria could be another mechanism by which it induces oxidative stress.

8.3. EFFECT OF UV-IRRADIATED SOLUTION OF MELATONIN ON CYANIDE-INDUCED SUPEROXIDE ANION FORMATION IN RAT BRAIN HOMOGENATE *IN VITRO*.

8.3.1. INTRODUCTION

The brain is especially susceptible to free radical formation and damage as a result of its high consumption of total body oxygen and the relatively low concentration of antioxidant enzymes (Colye & Puttfarcken, 1993). Free radicals induce lipid destroying chain reactions in polyunsaturated lipid rich areas like the brain (Southgate & Daya, 1999). Toxic oxygen radicals are formed normally during respiration, but unless these can be scavenged effectively, these agents will cause cellular damage.

The pineal indoleamine, melatonin has been shown to reduce neurodegeneration under a number of different conditions that involve the production of $O_2^{\bullet-}$ (Reiter, 1997). However, in chapter six, the photo-instability of melatonin was shown, with less than 20% of melatonin remaining after 20 minutes of UV irradiation. In addition two of the major photoproducts of melatonin were identified to be AFMK and 6-OHM, in chapter six. Melatonin is also localized in the skin (Roberts *et al*., 2000) and the skin transmits both UVA and UVB radiation (Sterenborg & Van der Leun, 1990), allowing light of both wavelength ranges to reach melatonin. This raises concerns about the antioxidant properties of melatonin and the use of melatonin in sunscreen preparations (Maharaj *et al*., 2002).

Thus, in the present study, the protective effect of incubating homogenized rat whole brain tissue with melatonin solution, which has been irradiated with UV light at different time intervals, against cyanide-induced $O_2^{\bullet-}$ production was investigated. This would then provide an idea of the antioxidant ability of these photoproducts as at time 60 minutes of UV irradiation. The percentage of melatonin in solution after such UV irradiation is almost zero.

8.3.2. MATERIALS AND METHODS

8.3.2.1. Chemicals and Reagents

Melatonin was purchased from the Sigma Chemical Company, St. Louis, MO (USA). All other chemicals used were of the highest quality available from commercial sources.

8.3.2.2. Sample Preparation

Samples for the NBT assay were prepared according to the method described in section 8.2.3.5. A 0.1 mg/ml solution of melatonin was prepared by dissolving it in absolute ethanol, and subsequently diluting it with Milli-Q water so that the final ethanol concentration in the brain homogenate was less than 0.5%. Fresh solutions of melatonin were prepared each day and the beakers containing the melatonin solutions were covered with aluminium foil to protect melatonin from light.

8.3.2.3. Irradiation Studies

Melatonin (0.1 mg/ml) was placed in the immersion-well photoreactor (figure 6.1, chapter 6) and irradiated according to the method described in chapter six, section 6.2.2.5. The selected times for UV irradiation were predetermined and 5mL aliquots were removed at each time interval and assayed for $O_2^{\bullet-}$ scavenging ability.

8.3.2.4. Nitroblue Tetrazolium Assay (NBT)

Adult male rats of the Wistar strain housed in separate cages, in a controlled environment as described in appendix one were used for the experiments. Rats were sacrificed and their brains were removed according to the protocol described in appendix two. The rat brain homogenate was prepared as described in section 8.2.2.6 and the nitro-blue tetrazolium (NBT) assay was carried out as described in section 8.2.2.8. The only modification was the incubation of the lipid source (1mL) containing 1mM KCN alone or in combination with melatonin (0.1 mg/ml) that was subjected to UV irradiation at different time intervals (0, 5, 10, 20, 30, 60 min) together with 0.4ml of NBT reagent. The

relative absorbance of the glacial acetic acid fraction was measured at 560nm and converted to µmoles diformazan using a standard curve generated from nitroblue diformazan (NBD) in appendix four. Final results are expressed as µmoles Diformazan/mg protein.

8.3.3. RESULTS

The *in vitro* exposure of whole rat brain homogenate to 1mM KCN caused a significant increase in $O_2^{\bullet-}$ in comparison to the control value as is evident from figure 8.5. The unirradiated melatonin at zero time significantly reduced the 1mM cyanide-induced rise in $O_2^{\bullet-}$ with a ± 24% reduction in $O_2^{\bullet-}$ is noted by the unirradiated melatonin solution. However, melatonin irradiated for 5-60 min provided an equivalent level of reduction in $O_2^{\bullet-}$ levels in comparison to the unirradiated melatonin at time zero (figure 8.5).

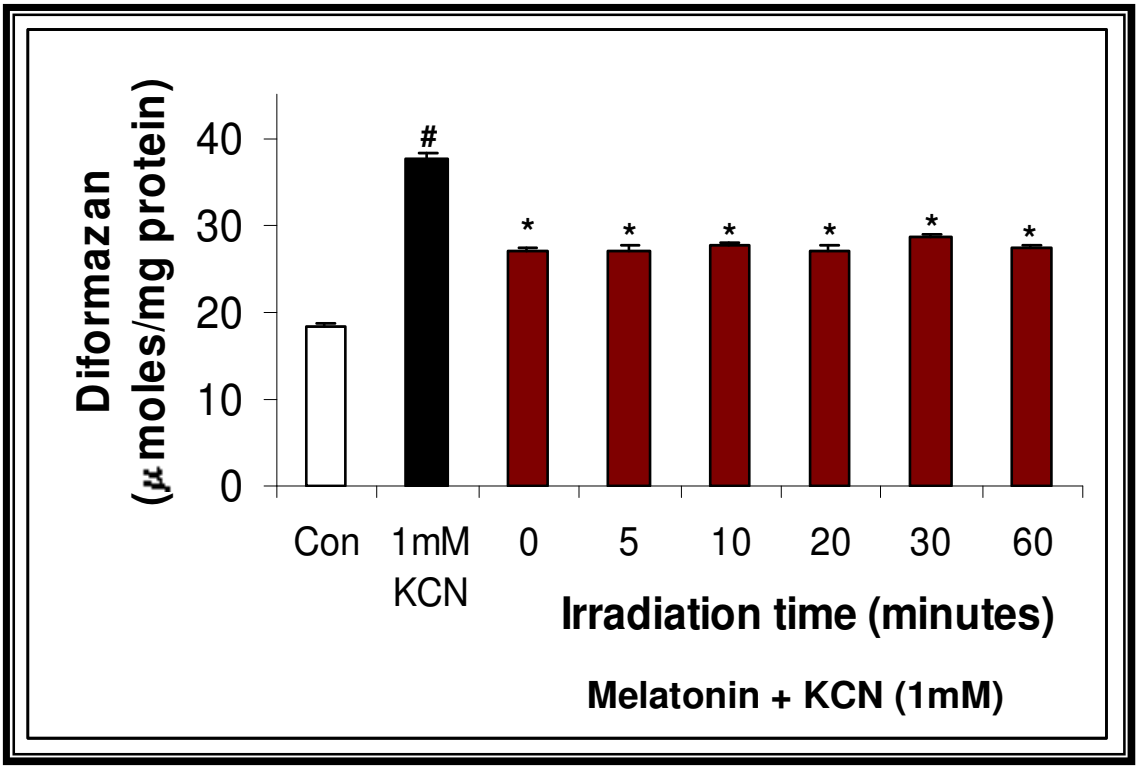

Figure 8.5: The effect of irradiated melatonin (MEL) on KCN-induced $O_2^{\bullet-}$ formation. Each bar represents the mean ± SEM of three determinations. $^{\#}p<0.05$ 1mM KCN versus control; *p<0.05 MEL versus 1mM KCN. (Student-Newman-Keuls Multiple Range Test).

8.3.4. DISCUSSION

Free radical scavengers are becoming increasingly popular as a means of reducing or preventing the hazardous effects of free radicals and their inducers. Melatonin has been reported to be more potent that α-tocopherol as a free radical scavenger at physiological concentrations (Gilchrest, 1996). The possibility of using melatonin as an additive to sunscreens to prevent the hazards of UV light has been raised (Maharaj *et al*., 2002). Furthermore, in chapter six, the rapid inactivation of melatonin in the presence of UV light was demonstrated. These results demonstrate that although melatonin is degraded in the presence of UV light, the degraded solution still provides equipotent protection against reducing the generation of $O_2^{\bullet-}$, despite the absence of melatonin. This implies that the photoproducts that are produced i.e. 6-OHM and AFMK, due to the UV-irradiation of melatonin in solution, retain the $O_2^{\bullet-}$ scavenging properties of the parent compound, melatonin. Furthermore, these melatonin photoproducts, i.e. AFMK and 6-OHM have been shown by a number of authors to possess antioxidant activity (Tan *et al*., 1998, 2000b, 2001; Pierrefiche *et al*., 1993; Maharaj *et al*., 2002; Maharaj *et al*, 2003a, b). Therefore, it can be speculated that the use of melatonin to protect the skin against UV-induced free radicals is a realistic possibility.

8.4. COMPARISON OF THE EFFECT OF MELATONIN AND 6-OHM ON CYANIDE-INDUCED SUPEROXIDE ANION FORMATION IN RAT BRAIN HOMOGENATE *IN VITRO AND IN VIVO.*

8.4.1. INTRODUCTION

Cyanide induces inhibitory effects on superoxide dismutase (SOD) and catalase. SOD and catalase, as well as reduced glutathione and the antioxidant vitamins A, C and E are involved in the protection of biological membranes from the harmful effects of free radicals (figure 8.6.) (Halliwell and Gutteridge, 1989; Bunce & Hess, 1988; Tessier *et al*., 1999; Paolisso *et al*., 1998).

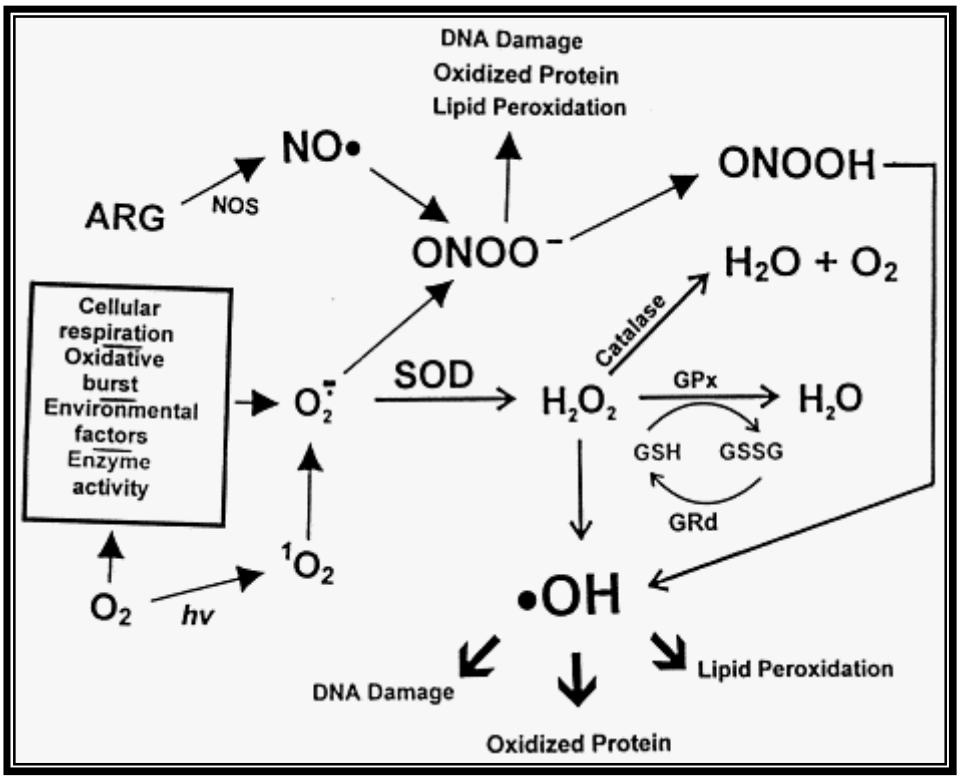

Figure 8.6: Oxygen reactants which are generated in abundance. Melatonin acts to stimulate activities of SOD, catalase and GPx thus promoting the detoxification of oxygen radicals (Reiter & Tan, 2003).

These free radicals, which are generated in all biological systems can cause tissue damage. Thus, if indeed the tissue damage caused by cyanide is due to inhibition of the free radical scavenging enzymes, then administration of antioxidants to cyanide toxified animals should exert an ameliorating influence on the severity of resultant tissue injury.

Melatonin has been shown to have little ability to directly scavenge $O_2^{\bullet-}$ (Chan & Tang, 1996). However, there are a number of ways in which melatonin may influence the intracellular concentration of $O_2^{\bullet-}$. The indolyl cation radical (Hardeland *et al*., 1993), when melatonin donates an electron to a highly reactive free radical such as $^{\cdot}OH$, is believed to secondarily scavenge $O_2^{\bullet-}$ thereby reducing its levels within the cells. Furthermore, melatonin has been reported to increase mRNA levels for SODs (Antolin *et al*., 1996; Kotler *et a*l., 1998). Southgate (1999) demonstrated that melatonin is effective as an $O_2^{\bullet-}$ scavenger only at high concentrations i.e. concentrations of 500μM and higher.

In the previous study, the ability of the degraded solution of melatonin to scavenge $O_2^{\bullet-}$ was demonstrated implying that the photoproducts possess free radical scavenging ability (Maharaj *et al*., 2002). Furthermore, in chapter six, 6-OHM was identified as the one of the major photoproducts of melatonin. Pierrefiche *et al*., (1993) identified 6-OHM to possess greater anti-oxidative capacity than melatonin. Thus the present study investigates the protective effects of incubating homogenized rat whole brain with increasing concentrations of 6-OHM on cyanide-induced $O_2^{\bullet-}$ production *in vitro*. A comparative study was conducted using melatonin. A further study was conducted to investigate the potential protective effects of the chronic treatment of rats with a pharmacological dose of melatonin or 6-OHM, on cyanide-induced $O_2^{\bullet-}$ generation.

8.4.2. MATERIALS AND METHODS

8.4.2.1. Chemicals and Reagents

6-hydroxymelatonin was purchased from the Sigma Chemical Company, St. Louis, MO (USA). All other chemicals used were of the highest quality available from commercial sources.

8.4.2.2. Sample Preparation

Melatonin and 6-OHM were prepared by dissolving it in absolute ethanol, and subsequently diluting it with Milli-Q water so that the final ethanol concentration in the brain homogenate was 0.5%. Fresh solutions were prepared daily and the solutions were covered with aluminium foil to protect against light. Melatonin and 6-OHM were dissolved in sweet oil for the purpose of *in vivo* administration of this agent to the rats.

8.4.2.3. *In vitro* Exposure of Rat Brain to Melatonin or 6-OHM

The experiments were conducted as described in section 8.2.2.8. The brain homogenate (1ml) was incubated at 37^0C for one hour, with the highest concentration of cyanide (1mM) used previously, alone and in combination with increasing concentrations of melatonin or 6-OHM. Following this, the NBT assay was performed.

8.4.2.4. *In vivo* Administration of Melatonin or 6-OHM

For the *in vivo* study rats were divided into three groups, each group consisting of six animals each. Each group of animals received the respective drug or vehicle via a subcutaneous injection (s.c.). Menéndez-Peláez *et al*., (1993) found that 30 min after subcutaneous injection of 0.5mg/kg melatonin, the concentration of melatonin in cell nuclei in rat cerebral cortex and cerebellum were five times higher than those of control rats. Given this information, melatonin and 6-OHM in the present study was administered subcutaneously at a dose of 10mg/kg. The control group received sweet oil, s.c.; while group 2 received a dose of 10mg/kg/day, s.c. of melatonin and group 3 received 6-OHM, 10mg/kg/d, s.c. The injections of melatonin, 6-OHM and sweet oil were administered at the same time (14H00) each day, so as to increase circulating melatonin concentration, when levels should have been physiologically at their lowest (Southgate, 1999). These animals were treated for seven days and thereafter were sacrificed and the brains removed and stored at -70^{o}C as described in appendix two.

The experiments were conducted as described in section 8.2.2.2 and in this case, the homogenate (1mL) was allowed to incubate with 1mM concentration of cyanide at 37^0C for one hour, after which the NBT assay was performed.

8.4.3. RESULTS

As shown in figure 8.7, co-treatment of the rat brain homogenate with 1mM KCN caused a significant increase in $O_2^{\bullet-}$ generation in comparison to the control. However, the treatment of the homogenate with increasing concentrations MEL (0.5, 1 and 1.5mM) resulted in an overall decline in cyanide-induced $O_2^{\bullet-}$ generation in comparison to the 1mM KCN alone. All the concentrations of 6-OHM used significantly reduced the cyanide induction of $O_2^{\bullet-}$ generation. In addition, all the concentrations of 6-OHM significantly reduced the diformazan levels in comparison to the respective melatonin concentrations. Furthermore, the 1.5mM 6-OHM concentration was able to lower the $O_2^{\bullet-}$ levels below that measured in control homogenate (no drug or toxin present).

From figure 8.8, it is evident that 1mM KCN induced a marked rise in $O_2^{\bullet-}$ generation in the control treated rats which was blunted by the chronic treatment of animals with either melatonin or 6-OHM. It is also clearly evident from figure 8.7, that 6-OHM was able to significantly reduce $O_2^{\bullet-}$ generation in comparison to melatonin. Furthermore, no significant difference was noted between the protection offered by 6-OHM and that of the control value.

8.4.4. DISCUSSION

The inhibition of antioxidant enzymes by cyanide is believed to produce oxidative stress and induce neurotoxicity (Ardelt *et al*., 1989). Free radical scavengers have become increasingly popular as a means of reducing or preventing the hazardous effects of free radicals and their inducers.

In the present study, it is clearly evident that the indoleamines, melatonin and 6-OHM are able to reduce the cyanide-induced rise in $O_2^{\bullet-}$. A dose dependent response is noted for 6-OHM while melatonin only in high concentrations i.e. 1 and 1.5mM decreased $O_2^{\bullet-}$

generation. The hepatic metabolite of melatonin, 6-OHM (Matuszak *et al.*, 1997) is shown to significantly reduce the production of $O_2^{\bullet-}$ below that of the melatonin value both *in vitro* and in the rats that were treated *in vivo*. Furthermore, the 1.5mM 6-OHM was also able to reduce the $O_2^{\bullet-}$ levels below that of the control values. Thus, the results indicate that 6-OHM serves as a more efficient scavenger of $O_2^{\bullet-}$ induced by cyanide than melatonin. The fact that 6-OHM was able to lower $O_2^{\bullet-}$ below that of the control value indicates that this agent in high concentrations offers complete protection against the effects of this neurotoxin. Since 6-OHM is able to reduce $O_2^{\bullet-}$ levels below that of the control value, it is suggested that this agent possibly acts also to prevent the distal inhibition of the ETC by cyanide and increases mRNA levels for SODs, the family of enzymes that play a role in the dismutation of $O_2^{\bullet-}$ (figure 8.6). However, this has to be further investigated.

Melatonin is minimally reactive with $O_2^{\bullet-}$ as evidenced in this study and other reports (Chan & Tang, 1996; Marshall *et al.*, 1996). In one study, in which electron spin resonance (ESR) was used to identify DMPO-$O_2^{\bullet-}$ adducts, melatonin was reported to be modestly interactive with $O_2^{\bullet-}$ (Zang *et al.*, 1998). Melatonin's actions against cyanide-induced toxicity is probably attributed to it's ability to counteract the cyanide induced distal inhibition of the ETC (Yamamoto and Tang, 1996a) and its ability to increase mRNA SOD.

However, the results of this study is in accordance with the findings of Yoshida *et al.*, (2003), where the authors demonstrated that melatonin does not prevent $O_2^{\bullet-}$ formation, although in contrast 6-OHM significantly decreased the intensity of the ESR signal of the $O_2^{\bullet-}$, indicating that 6-OHM is a more potent scavenger of $O_2^{\bullet-}$ generation than melatonin. Therefore 6-OHM has a definite role to play as a free radical scavenger.

Petrone *et al.*, (1980) suggests a chemotactic role for superoxide anions in inflammation. Neutrophil generated superoxide reacts with an extracellular precursor to generate a substance chemotactic for neutrophils and this appears to play a major role in communication in neutrophil-mediated inflammatory events. Superoxide dismutase inhibits the appearance of this chemotactic activity but catalase does not. Prevention of production of this factor appears to be the major anti-inflammatory action of superoxide

dismutase (Petrone *et al.*, 1980). Melatonin has been shown to be an effective anti-inflammatory agent; its ability to secondarily scavenge and inactivate $O_2^{\bullet-}$ contributes to melatonin reducing inflammation (Cuzzocrea & Reiter, 2001). Hence it could be postulated that the anti-inflammatory activity of melatonin may be attributable to its superoxide scavenging properties. In addition, since 6-OHM is shown to be a potent scavenger of $O_2^{\bullet-}$, it could act to reduce inflammation, like melatonin. In order to confirm these hypotheses more studies need to be conducted in this respect.

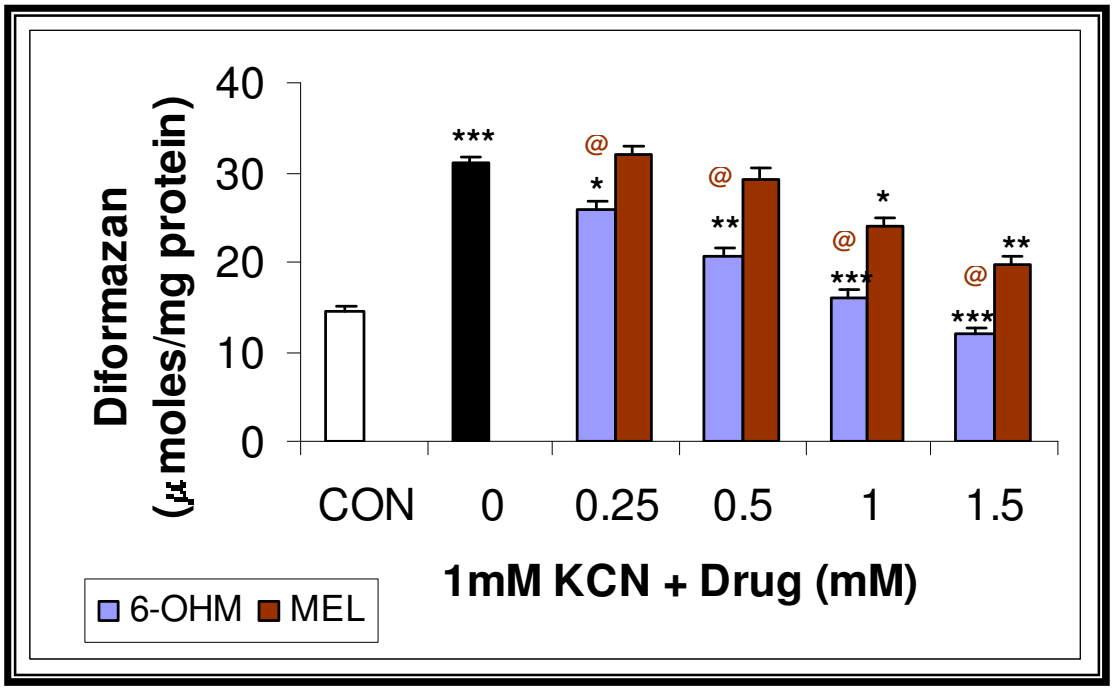

Figure 8.7: Dose-dependent effect of 6-OHM and MEL on cyanide-induced $O_2^{\bullet-}$ generation in whole rat brain homogenates *in vitro*. Each bar represents the mean ± SEM; n=5; *p<0.05 ; **p<0.01 ; ***p<0.001 in comparison to 1mM KCN and $^{@}$p<0.05 in comparison to the respective melatonin doses. The 1.5mM 6-OHM concentration also significantly reduces (p<0.05) the levels of superoxide anion generation below those measured in control homogenates (no drug or toxin present) (Student-Newman-Keuls Multiple Range Test).

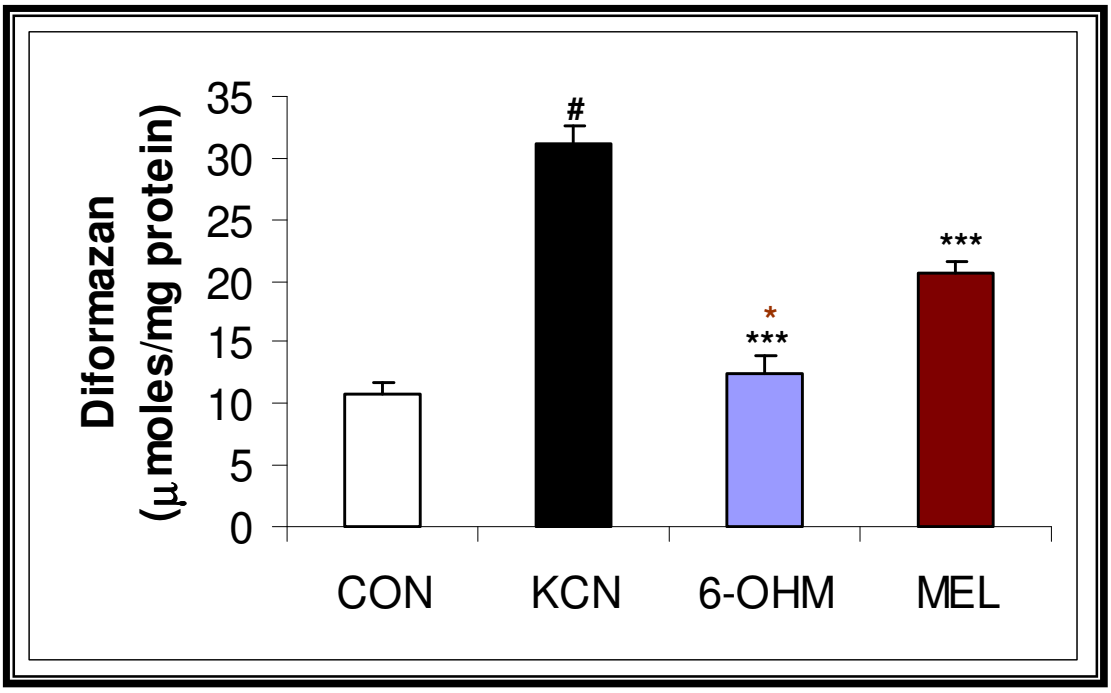

Figure 8.8: The effect of the *in vivo* administration of 6-OHM and MEL on 1mM cyanide-induced $O_2^{\bullet-}$ generation in whole rat brain homogenates. Each bar represents the mean ± SEM; n=6; $^{\#}p<0.001$ in comparison to control, ***$p<0.001$ in comparison to 1mM KCN and *$p<0.05$ in comparison to the melatonin value). The 6-OHM dose is able to significantly reduce ($p<0.05$) the levels of superoxide anions generated below those measured in melatonin homogenates. There is no significant difference between the protection offered by 6-OHM and the control (no drug or toxin present) rats against KCN-induced $O_2^{\bullet-}$ generation. (Student-Newman-Keuls Multiple Range Test).

8.5. COMPARISON OF THE EFFECT OF MELATONIN AND 6-OHM ON QA-INDUCED SUPEROXIDE ANION GENERATION IN THE RAT HIPPOCAMPUS *IN VIVO*.

8.5.1. INTRODUCTION

Quinolinic acid (QA) is a naturally produced metabolite of the tryptophan metabolism (Foster *et al*., 1983; Heyes & Morrison, 1997; Heyes *et al*., 1996). QA has been shown to be present in normal post-mortem human brains at levels similar to those of other species (Wolfensberger *et al*., 1983), and with concentrations not varying greatly among the different regions of the brain. Heyes & Morrison (1997) demonstrated that the brain naturally synthesises QA, and that the rate of QA formation increases in conditions of brain and systemic immune activation. QA concentrations have also been shown to increase during the natural aging process in rats (Moroni *et al*., 1984a). The neurotoxic effects of QA are well known. Injection of QA into various brain regions in adult rats produces neurodegenerative effects similar to those caused by kainic and ibotenic acids (Schwarcz & Köler, 1983). The administration of quinolate is known to induce seizures in various species of mammals (Lapin, 1981; Lapin *et al*., 1998). The most vunerable brain structures appear to be the striatum, globus pallidus and hippocampus (Schwarcz & Köler, 1983).

Quinolinic acid is an endogenous ligand of the NMDA receptor in the brain (Stone & Perkins, 1981). Since it is not readily metabolized in the synaptic cleft, it stimulates the NMDA receptor for prolonged periods and this sustained activation results in the opening of the Ca^{2+} channels and causes an increase in Ca^{2+} influx through these membrane channels. Intracellular Ca^{2+} levels rise and Ca^{2+}-calmodulin-dependent enzymes become activated (Choi, 1988; Lipton & Rosenberg, 1994). This is followed by a Ca^{2+} dependent enhancement of free radical production which leads to molecular damage and often cell death (Stone & Perkins, 1981). In cultured neurons, QA stimulation of the NMDA receptors is known to generate ROS, such as the $O_2^{\bullet-}$, H_2O_2 and NO (Gunasekar *et al*.,

1995; Reynolds and Hastings, 1995; Kucukkaya *et al*., 1996; Lafon-Cazal *et al*., 1993; Lysko *et al*., 1992).

Southgate (1999) demonstrated that the incubation of rat brain homogenate with varying concentration of QA *in vitro* failed to cause an increase in $O_2^{\bullet-}$. However, for QA to cause an increase in $O_2^{\bullet-}$ production, the process would only be initiated by an increase in intracellular Ca^{2+} levels. In homogenates, any Ca^{2+} control is effectively destroyed, and thus the binding of QA to the receptors would have had no regulatory effects. However, Southgate (1999) showed that QA increase $O_2^{\bullet-}$ production significantly in cultured neuronal cells.

Therefore, in the present study it was decided to investigate whether an intrahippocampal injection of QA could cause an increase in $O_2^{\bullet-}$ generation and whether co-treatment with melatonin or 6-OHM, *in vivo*, could reduce this $O_2^{\bullet-}$ production in rat hippocampii.

8.5.2. MATERIALS AND METHODS

8.5.2.1. Chemicals and Reagents

Quinolinic acid (2, 3-pyridinedicarboxylic acid) and diethylether were purchased from the Sigma Chemical Company, St. Louis, MO (USA). All other chemicals used were of the highest quality available from commercial sources.

8.5.2.2. Dosing of the Animals

Adult male rats of the Wistar strain were housed in separate cages, in a controlled environment as described in appendix one. The animals were separated into four groups of six animals each. Animals were dosed according to the procedure described in section 8.3.2.4 (Table 8.1). The dose and treatment period was chosen according to Southgate (1999) who showed this to be an effective dose to protect brain homogenate against oxidative damage. The control group received sweet oil, s.c.; while the animals in group 3 received a dose of 10 mg/kg/d of melatonin in 100µl sweet oil, injected subcutaneously, 20 min prior to intrahippocampal QA injection. Similarly the animals in group 4 received

a dose of 10mg/kg/d of 6-OHM in 100µl of sweet oil, administered in the same way. The injections of melatonin, 6-OHM and sweet oil were administered at the same time (14H00) each day, so as to increase circulating melatonin concentration, when levels should have been physiologically at their lowest (Southgate, 1999). The animals in groups 1 and 2 received the vehicle for these drugs, viz. sweet oil. On day one, 20 mins after dosing the animals with the respective drug or vehicle, the animals were injected with QA directly into the hippocampal region. QA was dissolved in PBS made up to pH 7.4. A dose of QA (120nmol) was used to induce neurotoxicity as this concentration of QA is known to cause severe behavioural disturbances and total loss of hippocampal neurons in rats (Lekieffre *et al*., 1990; Schwarcz *et al*., 1984).

Following the intrahippocampal injections of QA, the animals in groups 3 and 4 received subsequent daily doses of melatonin and 6-OHM respectively, each day for seven days, while as before, the animals in groups 1 and 2 received daily doses of sweet oil for seven days. All animals were treated for 7 days following surgery, and injections of sweet oil, melatonin or 6-OHM were administered at the same time (14H00) each day, so as to increase the circulating melatonin concentration, when levels should have been physiologically at their lowest (Southgate, 1999).

Table 8.1: Treatment regime for each group of animals

Treatment Group	**Received 20 mins prior to surgery (s.c.)**	**Intrahippocampal injection**	**Daily treatment for 7 days after surgery (s.c.)**
1 Control	100µl Sweet oil	PBS	100µl Sweet oil
2 QA	100µl Sweet oil	120 nmol QA in PBS	100µl Sweet oil
3 MEL(+)	100µl MEL in sweet oil	120 nmol QA in PBS	100µl MEL in sweet oil
4 6-OHM(+)	100µl 6-OHM in sweet oil	120 nmol QA in PBS	100µl 6-OHM in sweet oil

8.5.2.3. Surgical Procedures

8.5.2.3.1. Anaesthesia

Ether anaesthesia was employed for all surgical procedures carried out. Animals were placed, one at a time, in a dessicator containing cotton wool soaked in ether. Once the animals were sedated, they were removed and placed on the operating surface as shown in figure 8.9. A small conical flask containing cotton wool soaked in ether was placed approximately 3cm from the rats' nose. This flask remained in this position throughout surgery, except in cases where respiration became too weak. A good indication of the depth of anaesthesia was monitored by the colour of the limbs and tail, which displayed a faint, almost pale pinkness. This was indicative of the optimum level of anaesthesia, meaning a satisfactory rate and depth of respiration with good narcosis. A purple colour of the limbs was an indication of cyanosis.

Diethylether is a desirable anaesthetic to use because the mortality rate of the animals is lower than with halothane or phenobarbitone. Ether is also easy to administer and it is easy to monitor the depth of anaesthesia.

8.5.2.3.2. Bilateral Intrahippocampal QA Injection

QA was injected intrahippocampally using stereotaxic surgical techniques. Each animal was anaesthetized as described above in section 8.5.2.3.1. QA was dissolved in phosphate buffered saline (PBS), pH= 7.4, and (120 nmol in 2µl) was infused bilaterally into the hippocampii employing rat brain stereotaxic apparatus (Stoelting, IL, USA) (figure 8.9). The skull was orientated according to the König and Klippel stereotaxic atlas (1963). After a saggital cut in the skin of the skull, the bregma and lambda suture were located (figure 8.10) and holes were drilled with a Bosch electrical drill fitted with a drill bit of 0.5mm in diameter at the following coordinates; 4.0mm caudal to the bregma, 2.5 mm lateral to the saggital suture, and 3.2mm ventral of the dura. Care was taken not to lesion the meninges. A Hamilton syringe, with a cannula of diameter 0.3mm held rigidly in the stereotaxic micromanipulator, was used to inject 120 nmol of quinolinic acid in 2 µl of PBS, 3.2mm ventral of the dura.

The injection was administered at a rate of 1 µl per minute and the cannula was left *in situ* for a further 3 minutes following the drug injection, to allow for passive diffusion away from the canulla tip and to minimise spread into the injection tract. The cannula was then slowly removed and the scalp was closed with sutures. Animals recovered from the anaesthesia after approximately 3-4 hours. Since QA is known to stimulate seizure activity behavioural disturbances in rats, the rats from all the treatment groups were monitored for any behavioural changes.

8.5.2.3.3. Sham Lesioned Rats

The rats used as controls were subjected to the same surgical procedures described in section 8.5.2.3 (i). However, stereotaxic injections into the hippocampus were free of QA and comprised solely of PBS.

8.5.2.4. Dissection of the Hippocampus

On the eighth day following the intrahippocampal injection of QA, the brains were removed as described in appendix two and the hippocampi rapidly dissected according to a modified method of Glowinski and Iversen, (1966). Briefly, the rhombencephalon is separated by a transverse section from the rest of the brain (figure 8.11., section 1). A transverse section is then made at the level of the optic chiasma, which delimits the anterior part of the hypothalamus and passes through the anterior commissure (section 2). This section separates the cerebrum into two parts, B and C. Part B is divided into five fractions. The easiest way to reach the hippocampus is to first dissect the hypothalamus and the striatum from section B.

The midbrain is then gently separated from the remaining part of the brain. The hippocampus is then dissected.

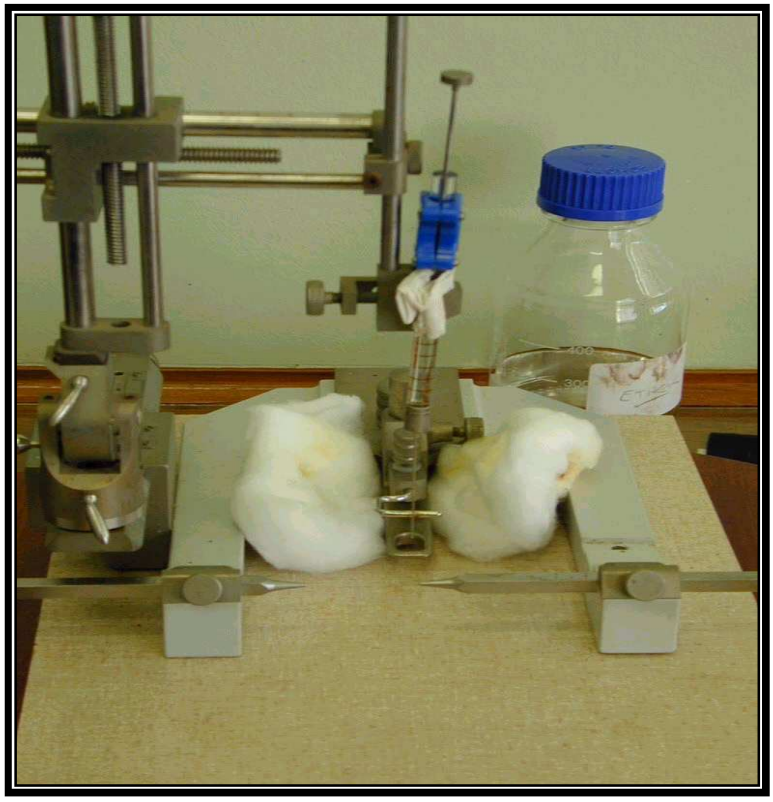

Figure 8.9: A view of the stereotaxic apparatus and Hamilton syringe used for the bilateral intrahippocampal injection of QA (Stoelting, IL, USA).

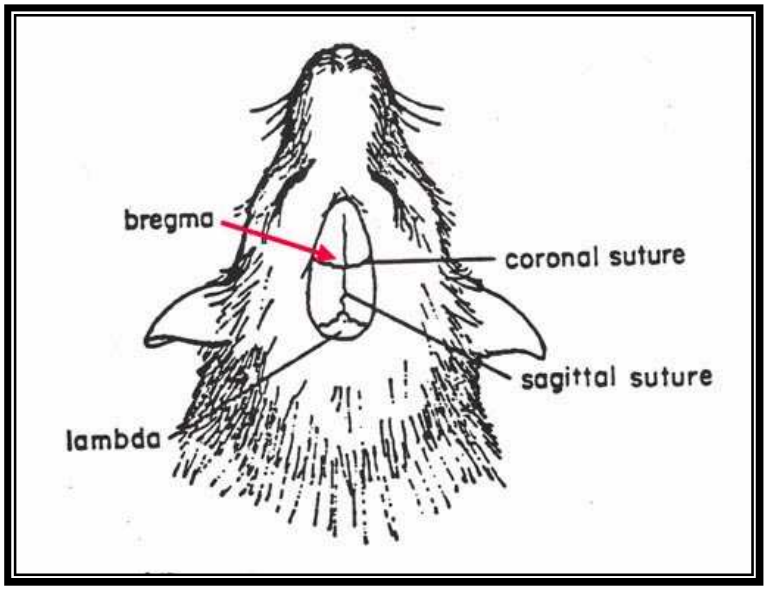

Figure 8.10: A view of the rat skull after the skin has been cut. The sutures shown are used as a reference point for the measurement of the coordinates for the intrahippocampal injection.

8.5.2.5. Nitroblue Tetrazolium Assay (NBT)

The rat hippocampii were homogenized in PBS, pH 7.4, to yield a 10% w/v homogenate as described in section 8.2.2.6. The nitro-blue tetrazolium (NBT) assay was performed as described in section 8.2.2.8. The only difference was that the lipid source viz. rat hippocampii homogenate (1mL) was incubated with 0.4ml of a 0.1% NBT solution in an oscillating water bath for 1 hr at 37^{o}C.

8.5.3. RESULTS

Since, QA is known to stimulate seizure activity; the animals injected with QA displayed several behavioural changes. In particular, seizure episodes varied from chewing and scratching movements often associated with a frozen appearance of the animal and intermittent "wet dog shakes". Ataxia and the classical sign of arching of the tail were also apparent in the QA treated animals. This provides evidence that neurological damage has occurred. However, the rats treated with melatonin or 6-OHM together with QA failed to produce any detectable behavioural changes.

The bilateral intrahippocampal injection of QA (120nmols) induced a significant increase in hippocampal $O_2^{\bullet-}$ production in comparison to the control value (figure 8.12). However, the co-treatment of rats with melatonin or 6-OHM in combination with QA was able to significantly reduce this QA-induced increase in $O_2^{\bullet-}$ levels. Furthermore, the 6-OHM was able to decrease the $O_2^{\bullet-}$ levels below that observed for the melatonin and control treated rats.

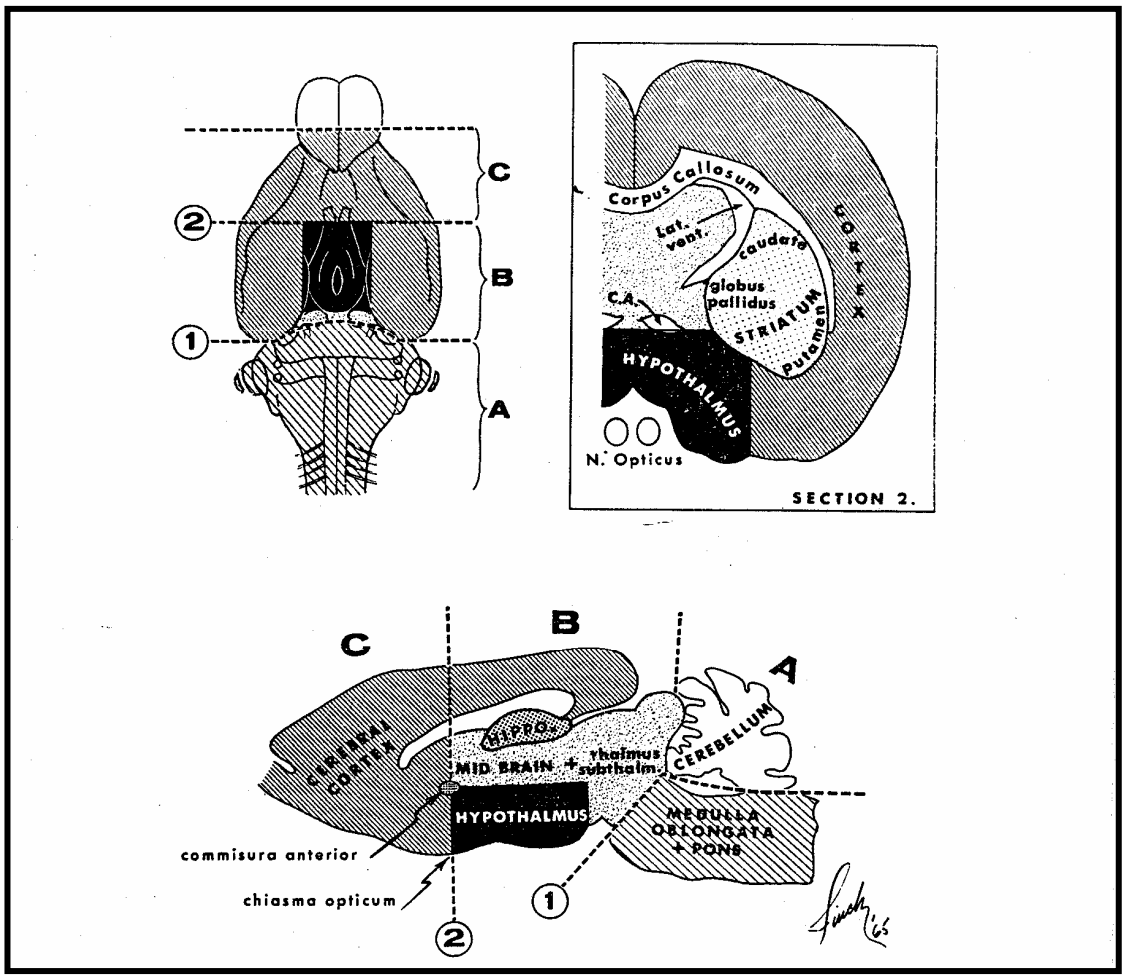

Figure 8.11: Diagrammatic representation of the dissection procedure for rat brain (Glowinski & Iversen, 1966).

8.5.4 DISCUSSION

The rats treated with QA only showed severe behavioural disturbances as indicated in the results and this in itself provides evidence that neurological damage has occurred. However, the rats treated with melatonin or 6-OHM together with QA failed to produce any detectable behavioural changes. This is evidence that melatonin and 6-OHM are able to prevent the seizure-induced activity of QA in rats and thus possibly reduce the QA-induced neurodegeneration.

The results show that intra-hippocampal injections of QA cause a significant induction of $O_2^{\bullet-}$ generation in the rat hippocampus. This is a result of the activation of the NMDA receptors in the hippocampus by QA which results in Ca^{2+} dependent increase in oxidative stress (Stone & Perkins, 1981). However, the chronic treatment of rats with

melatonin or 6-OHM (10mg/kg/d) together with QA significantly reduces this QA-induced generation of $O_2^{\bullet-}$. The results of this study show that both melatonin and 6-OHM are effective scavengers of $O_2^{\bullet-}$ radicals generated by QA in the hippocampus. However, 6-OHM is a more potent scavenger of this free radical than melatonin. Furthermore, 6-OHM decreases the hippocampal $O_2^{\bullet-}$ levels below that of the basal control value. These results are supported by Yoshida *et al.*, (2003) where 6-OHM significantly decreased the intensity of $O_2^{\bullet-}$. In addition, Kawanishi and Sakurai (2002) demonstrated that 6-OHM effectively scavenges $O_2^{\bullet-}$ more effectively than Trolox. Furthermore, Chang & Tang (1996) and Marshall *et al.*, (1996) demonstrated in different studies, that melatonin possesses little ability to directly scavenge the $O_2^{\bullet-}$.

The 6-OHM like melatonin is extremely lipophilic (Shida *et al.*, 1994). Thus it will readily penetrate the BBB and gain access to the brain where it can serve as an effective scavenger of $O_2^{\bullet-}$.

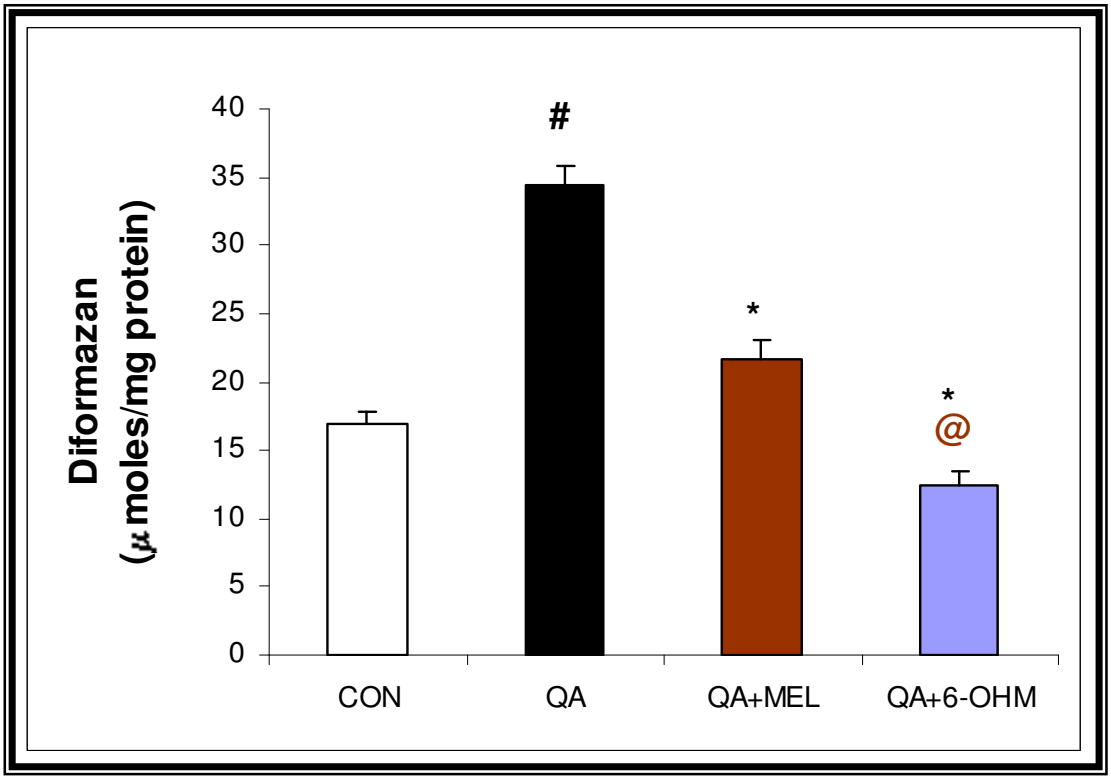

Figure 8.12: The effect of the *in vivo* administration of 6-OHM and melatonin on intrahippocampally injected QA-induced $O_2^{\bullet-}$ generation in rat hippocampal homogenate. Each bar represents the mean ± SEM; n=6; #p<0.001 in comparison to control, *p<0.001 in comparison to QA and $^{@}$p<0.05 in comparison to the melatonin (10mg/kg/d) value. The 10mg/kg/day 6-OHM dose is able to significantly reduce $^{@}$(p<0.05) the levels of $O_2^{\bullet-}$-generated to below those measured in the control value. (Student-Newman-Keuls Multiple Range Test).

8.6. EFFECT OF UV-IRRADIATION ON SUPEROXIDE ANION FORMATION IN RAT SKIN HOMOGENATE *IN VITRO* AND THE PROTECTION OFFERED BY MELATONIN.

8.6.1. INTRODUCTION

By far the most obvious agent the skin has contact with is the sun. The ultraviolet (UV) component from between ≈ 290nm and 400nm (wavelengths below 290nm being absorbed by atmospheric ozone, for now) is accepted as being the most damaging portion of the solar spectrum (Darr & Fridovich, 1994). UV radiation has been shown to produce DNA damage directly and indirectly through oxidative stress (Ichihashi *et al*., 2003). Free radical generation is believed to be the major source of damage by UV light (Nishi *et al*., 1991).

Photochemical reactions with UV light result in the formation of reactive oxygen species (ROS). In particular $O_2^{\bullet-}$ and $^1O_2$ are probably involved in chronic photodamage, since topical antioxidants that scavenge these species are photoprotective in the hairless mouse (Bissett *et al*., 1990a). $^1O_2$ produced by UVA and UVB radiation targets the skin causing DNA damage (Cadet *et al*., 2000). However, $^1O_2$ which has a lifetime shorter than 1s (Merkel *et al*., 1972) can be readily converted to the highly reactive $O_2^{\bullet-}$ (Reiter *et al*., 2002) that can induce further and prolonged cellular damage. Also, these oxygen radicals are probably a primary factor in chronic photodamage, since chelators, which prevent iron-catalyzed production of oxygen radicals, are dramatically photoprotective in the mouse (Bissett *et al*., 1991). Furthermore, inflammatory cells appear to play a role in photodamage. With chronic UV radiation exposure of mouse skin, there is an increase in dermal cellularity, including inflammatory cells (Kligman *et al*., 1985; Bissett *et al*., 1987). It is also known that topical anti-inflammatory agents are protective against chronic photodamage (Bissett *et al*., 1990b), suggesting that the inflammatory cell infiltrate contributes to the damage; although it is not clear what specific role these cells play in the damage process.

The skin possesses antioxidant defence mechanisms contained in the keratinocytes, which are located in the outermost surface of the skin (Sasaki *et al*., 2000). The keratinocytes contain specific enzymes such as superoxide dismutase. However, the generation of free radicals following UV irradiation depletes the skin of endogenous enzymic and/or nonenzymic antioxidants (Shindo *et al*., 1993), leaving it vulnerable to oxidative stress. Supplementation of the skin with antioxidants may therefore increase the skins' resistance to UV-induced oxidative stress. Therefore, supplementation of the skin with antioxidants such as melatonin is a further approach in limiting or preventing UV-induced skin damage. It has been shown that neutrophilic granulocytes irradiated with UV light in the presence of melatonin, dose-dependently exhibit less free radical generation (Fischer *et al*., 2001). One of the concerns of using melatonin in sunscreens is its photoinstability (Maharaj *et al*., 2002) which was demonstrated in chapter six.

Thus, the basis of the present study was to provide evidence that the irradiation of rat skin homogenate with UV light results in the production of $O_2^{\bullet-}$, and to determine whether the protection of rat skin homogenate with melatonin prior to exposure with UV light, results in a decline in $O_2^{\bullet-}$ formation.

8.6.2. MATERIALS AND METHODS

8.6.2.1. Sample Preparation

A Stock solution of 0.1 mg/ml of melatonin was prepared by dissolving 40mg of melatonin in 400ml of a mixture of absolute ethanol and water. The final concentration of ethanol in the incubation samples was less than 0.5%.

8.6.2.2. Skin Tissue Preparation

Adult male rats of the Wistar strain were housed in separate cages, in a controlled environment as described in appendix one. Rats were sacrificed and the skin was removed as described in appendix two. The rat skins were weighed before being homogenised in

0.1M Phosphate buffer saline (PBS), pH 7.4 in a Warring Blender and a glass homogeniser to give a final concentration of 2% (w/v) homogenate.

8.6.2.3. Irradiation Studies and NBT assay

Rat skin homogenate in the absence and presence of melatonin (0.1 mg/ml) was placed in the immersion-well photoreactor and irradiated continuously with a 400-W high pressure mercury lamp for 90 minutes, whilst bubbling air through the solution, at ambient temperature as described in chapter six, section 6.2. Aliquots of 5mL were removed periodically and analysed for $O_2^{\bullet-}$ generation using the NBT assay.

The nitro-blue tetrazolium (NBT) assay was used as described in section 8.2.2.8. Briefly, the lipid source viz. rat skin homogenate (1mL) alone or in combination with melatonin at the different time intervals of UV irradiation was incubated with 0.4ml of a 0.1% NBT solution in an oscillating water bath for 1 hr at 37^{o}C.

The protein content in each homogenized rat brain tissue was determined by carrying out protein assays as described in section 8.2.2.7. All results were analyzed for statistical significance as described in section 8.2.2.8. Final results were expressed as μmoles Diformazan/mg protein.

8.6.3 RESULTS

As shown in figure 8.13. UV-irradiation of rat skin homogenate results in a significant time-dependent increase in $O_2^{\bullet-}$ generation with an ± 80% increase in $O_2^{\bullet-}$ generation at 90 min of UV irradiation in comparison to the time zero sample.

As is evident in figure 8.14, the presence of melatonin is able to significantly retard the $O_2^{\bullet-}$generated by the presence of UV light at each irradiation time interval. It is also evident that there is no significant difference in the $O_2^{\bullet-}$ scavenging ability shown by melatonin at each irradiation time interval.

8.6.4 DISCUSSION

The skin is such a specialized organ that it has its own immune system. It has been proposed that faulty skin immunity affects the entire immune system. Sunlight can penetrate deep into the skin and alter immunity directly, or it can cause changes in dermis and epidermis that provoke immune changes. Ultraviolet (UV) radiation-induced skin damage includes acute reactions such as erythema, oedema, as well as premature skin aging (Dreher *et al*., 1999). Photochemical reactions with UV light result in the formation of reactive oxygen species (ROS) including the $O_2^{\bullet-}$ and the highly toxic hydroxyl radical (Sasaki *et al*., 2000). The results of the present study further support this and show that the exposure of rat skin to UV light results in a time dependent increase in $O_2^{\bullet-}$.

Chronic exposure of skin to ultraviolet radiation produces multiple deleterious responses including photoaging (Gilchrest, 1996). There is ample evidence that UV radiation produces toxic free radical intermediates, which are implicated in the pathogenesis of UV-induced skin damage. Under normal conditions the skin antioxidant defence mechanisms, which include superoxide dismutase (SOD), are able to protect the skin (figure 8.6). However, the generation of free radicals depletes the skin of these antioxidant defence mechanisms, rendering it vulnerable to UV-induced oxidative stress (Gilchrest, 1996). Additionally, and importantly, a very reproducible finding is that UV radiation of skin and/or skin cells leads to a compromised anti-oxidant defence system, superoxide dismutase, catalase and glutathione peroxidase activities decline, and lipid soluble antioxidants (vitamin E and ubiquinones) and vitamin C levels can drop precipitously after UV irradiation (Shindo *et al*., 1993). These changes almost certainly impose additional oxidative stress to the skin, as basal levels of the anti-oxidants are lost for some time after the initial insult. Not specifically during UV-irradiation, melatonin has been shown in a number of cases to promote the metabolism of O_2-based reactants to innocuous or less toxic substances (Reiter & Tan, 2003). For example, melatonin stimulates gene expression and augments activity of the SOD enzyme, an important antioxidative enzyme involved in the dismutase of $O_2^{\bullet-}$ to H_2O_2 (figure 8.6) (Antolin *et al*., 1996). Thereafter, the two enzymes assigned the function of metabolizing H_2O_2, i.e. catalase and glutathione peroxidase (GPx), and thereby reducing the formation of the

devastatingly toxic $^{\bullet}OH$, have been shown to be stimulated by melatonin as well (Montilla *et al*., 2000; Okatani *et al*., 2001; Reiter *et al*., 2000b). These indirect antioxidant actions of melatonin could certainly magnify its protective actions in the skin and other cells under conditions of high oxidative stress e.g. UV radiation, aging, diseases etc. Also of significance is a report by Urata *et al*., (1999), who have shown that melatonin increases the levels of glutathione, an important intracellular antioxidant, by stimulating its rate limiting enzyme, glutamylcysteine synthase.

Melatonin, the principal antioxidant of the pineal gland, now known to be a potent free-radical scavenger at physiological concentrations (Tan *et al*., 1993a; Southgate & Daya, 1999), is an ideal candidate for scavenging such radicals. The results of the present study show that exposure of rat skin homogenate to UV irradiation induces $O_2^{\bullet-}$. This phenomenon is significantly reduced when the homogenate is exposed to UV light in the presence of melatonin. Melatonin is a potent free radical scavenger and is known to curtail the damaging properties of these agents. However, whilst it was originally thought that only melatonin has these attributes, we recently showed that degradants which arise on exposure of melatonin to UV light are equally potent as free radical scavengers (Maharaj *et al*., 2002). Thus, it is a possibility that the protection offered against UV-induced $O_2^{\bullet-}$ generation in the rat skin is actually due to the melatonin photoproducts and not melatonin itself.

A combination of antioxidant and anti-inflammatory agent applied topically to mice provides UV photoprotection that overall is approximately additive to the effects provided by the individual components (Bissett *et al*., 1992). Since, melatonin serves as both an antioxidant and anti-inflammatory, this further supports its use in sunscreens to prevent or reduce the deleterious effects of UV radiation.

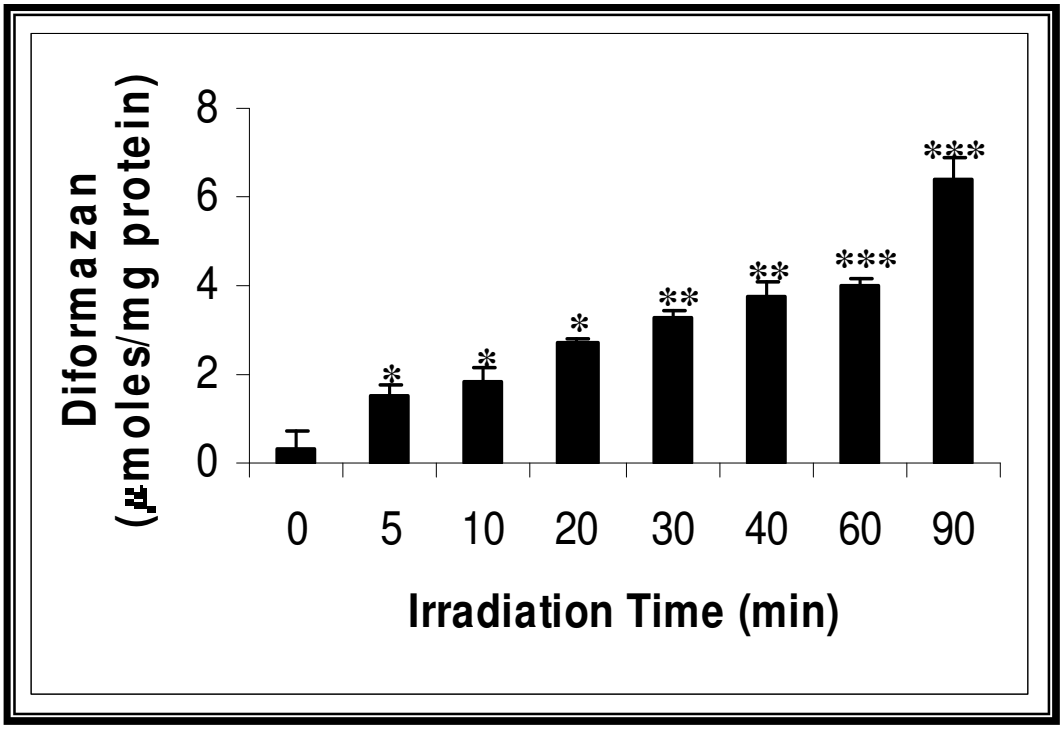

Figure 8.13: The effect of increase in UV-irradiation time on $O_2^{\bullet-}$ generation in rat skin homogenate. Each bar represents the mean ± SEM of five determinations. *($p<0.05$) 5-20 min irradiation time versus zero time; **($p<0.01$) irradiation time 30 and 40 mins versus zero time; and ***($p<0.001$) irradiation time 60 and 90 mins versus zero time (Student-Newman-Keuls Multiple Range Test).

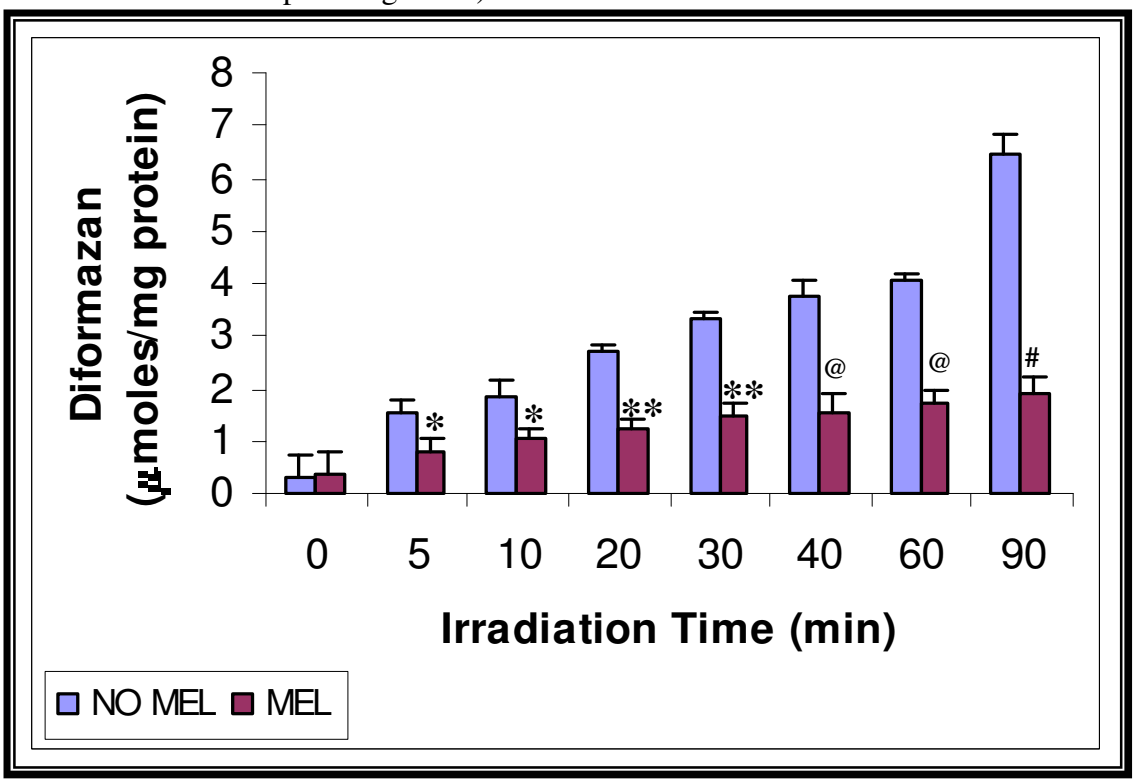

Figure 8.14: The effect of increase in UV-irradiation time on $O_2^{\bullet-}$ generation in rat skin homogenate in the presence of melatonin. Each bar represents the mean ± SEM of five determinations. *($p<0.05$); **($p<0.01$); $^{@}$($p<0.001$); $^{\#}$($p<0.0001$) MEL versus NO MEL for each respective irradiation time interval. (Student-Newmans-Keuls Multiple Range Test).

8.7. CONCLUSION

The brain is especially susceptible to free radical formation and damage as a result of its high consumption of total body oxygen and the relatively low concentration of antioxidant enzymes (Colye & Puttfarcken, 1993). Toxic oxygen radicals form normally during respiration, but unless these can be scavenged effectively, these agents will cause cellular damage. Moreover, the $O_2^{\bullet-}$ is capable of producing the hydroxyl radical in presence of hydrogen peroxide (Haber – Weiss reaction). Since these reactions are reversible, there is a constant generation of superoxide and the promotion of free radical reactions is allowed for. In pH environments of approximately 7.4, superoxide partially protonates to form the hydroperoxyl radical ($HO_2^{\bullet}$) a more reactive oxidising species (Rao & Hayon., 1973). In a study by Antunes *et al*. (1996) the perhydroxyl radical is estimated to inflict more than 5 times the damage that the hydroxyl radical is capable of. The protective measures that the cells employ in response to such damage are usually sufficient except when there is excessive ROS production, causing the biological defences to be overwhelmed, thus leading to oxidative stress (DiFiglia, 1990).

In this study, both cyanide and QA were shown to cause an increase in $O_2^{\bullet-}$. Cyanide is known to inhibit a number of antioxidant enzymes and also inhibit Complex IV activity of the ETC but it is also believed that oxidative stress plays an important role in cyanide induced neurotoxicity (Ardelt *et al*, 1989). Johnson *et al* (1987) proposed that increased intracellular calcium after cyanide treatment generates reactive oxygen species leading to peroxidation of lipids and subsequent neuronal damage. It has also been proposed that nitric oxide, a promoter of hydroxyl radical formation, is a mediator of convulsions associated with cyanide toxicity (Yamamoto & Tang, 1996a). The QA production of $O_2^{\bullet-}$ and neurotoxicity has been ascribed to the activation of the NMDA receptor Complex (Schwarcz *et al*., 1983; Beal *et al*., 1986).

Melatonin was able to also offer some protection against cyanide and QA-induced $O_2^{\bullet-}$ production by scavenging $O_2^{\bullet-}$ in rat hippocampus. However, 6-OHM offered complete protection against QA-induction of $O_2^{\bullet-}$ by reducing the levels of $O_2^{\bullet-}$ below that of the control value. In addition, the chief hepatic metabolite of melatonin, namely 6-OHM proved to be superior to melatonin as a $O_2^{\bullet-}$ scavenger, 6-OHM is also reportedly an

effective free radical scavenger (Maharaj *et al*., 2002). Thus, even when melatonin itself is metabolically converted to 6-OHM before it can function in the direct detoxification of a radical(s), its major hepatic metabolic product may be capable of doing so (Reiter & Tan, 2003). The results demonstrate that melatonin and 6-OHM are able to reduce $O_2^{\bullet-}$ levels in rat brain homogenate. High concentrations of melatonin (1mM) significantly reduce $O_2^{\bullet-}$ levels, although the effect appears to be rather limited. 6-OHM, on the other hand, is effective at low concentrations (0.25mM) in significantly reducing cyanide-induced $O_2^{\bullet-}$ generation. Similar results were obtained with rats treated with melatonin or 6-OHM chronically. The 6-OHM is not only the major hepatic metabolite of melatonin but has been shown to be formed when melatonin reacts with peroxynitrite (Zhang *et al*., 1998). Peroxynitrite is formed via the rapid reaction of $O_2^{\bullet-}$ with nitric acid (Beckman *et al*., 1990; Huie *et al*., 1993). Thus, even when melatonin itself is metabolically converted to 6-OHM before it can function in the direct detoxification of a radical(s), its major metabolic product may be capable of doing so (Reiter & Tan, 2003).

In chapter six, the rapid photodegradation of melatonin was demonstrated in the presence of UV light. This raised concerns about its antioxidant properties. However the results demonstrate that although melatonin is degraded in the presence of UV light, the degraded solution still provides equipotent protection against reducing the generation of $O_2^{\bullet-}$, despite the absence of melatonin. In addition, it is evident that melatonin, when present in the skin, can be an effective in reducing UV-induced $O_2^{\bullet-}$ generation. These results provide supportive evidence for the use of melatonin in sunscreen preparations. Furthermore, melatonin is known to increase the activities of SOD which is involved in converting $O_2^{\bullet-}$ to H_2O_2, and this indirect action of melatonin further supports its function as an antioxidant.

In conclusion the results of the present studies imply that 6-OHM is a more potent scavenger of $O_2^{\bullet-}$ than melatonin and that it has a definite role to play as an antioxidant and in the protection of the brain against oxidative stress.

CHAPTER ONE

LITERATURE REVIEW

1.1. NEUROSCIENCE

1.1.1. Introduction

The word "neuroscience" is young, however the study of the brain is as old as science itself. Two hundred years ago the brain was thought by our forefathers to consist of a concoction of spirits, which might be pure and tranquil, or riotous and evil. Recovered writings from the early physicians of ancient Egypt, dating back almost 5000 years, indicate that they were well aware of many symptoms of brain damage. However, the heart and not the brain was considered to be the seat of conciousness until the time of Hippocrates (Bear *et al.*, 2001). Historically, the scientists that devoted themselves to an understanding of the nervous system came from different scientific disciplines and the neuroscience revolution came when these scientists realised that the best hope for understanding the workings of the brain came from an interdisciplinary approach, combining the traditional approaches to yield a new synthesis, a new perspective (Bear *et al.*, 2001). The discovery that the CNS consists of an immense universe of highly complex units has been a slow and gradual one. In recent decades the brain and its mechanisms have become the focal point of much interest and research, and indeed many important and life changing discoveries and contributions have been made in the field of neuroscience.

If history has taught us nothing else, it has clearly shown that understanding how the brain works is a big challenge. Modern neuroscience research is expensive but more greatly the cost of ignorance about the brain is far greater. The continued and increased growth of older population age groups in many countries, irrespective of whether they fall under the "developed" or "developing" status, is possibly one of the main driving forces fuelling neuroscience and the study of neurodegenerative diseases particularly Alzheimer's disease, as well as age-related dementias in general. The economic costs of

brain dysfunction are enormous but they are pale in comparison with the staggering emotional toll on victims and their families. However, the prevention and treatment of brain disorders require an understanding of normal brain function, and this basic understanding is the goal of neuroscience.

Neuroscience research has already contributed to the development of increasingly effective treatments for many neurodegenerative diseases. Over the years, neuroscientists have continued to unveil more and more, and have gained tremendous insight into the pathophysiology and etiology of several neurodegenerative disorders. As a result, the field of neuroprotection has become a rapidly advancing area of neuroscience, which has led to the ongoing search of suitable agents for therapeutic intervention. The pineal antioxidant, melatonin and its main enzymatic metabolite, 6-hydroxymelatonin (6-OHM) are such agents that have been shown to elicit a wide range of actions in the brain. In order to understand the specific mechanism of acion that these indoleamines have on the brain, it is imperative to understand the role played by oxidative stress in the brain, particularly the hippocampus.

1.2. NEUROANATOMY

1.2.1. The Hippocampus: Structure and Function

The limbic system comprises of the olfactory areas, hippocampus, amygdala, the septum, cingulate cortex, and regulates the hypothalamic area. The significance of the limbic system lies in the role it plays in emotion, motivation and memory (Butler, 1993). Figure 1.1 shows the components of the limbic system involved in memory. The hippocampus is a region of the brain that is the most medial portion of the cerebral cortex and is developed from the stalk of the orginal cerebral vesicle (Smythies, 1970). This region forms part of the cerebral cortex and is a single cell layer, which is folded onto itself in a peculiar shape (Bear *et al*., 2001).

The hippocampus is derived from the Greek word meaning “seahorse” because of its shape. The hippocampus is the main relay station that determines whether a new memory should go into long-term storage or be deleted after its short-term usefulness is over.

Figure 1.2 shows the area of the rat brain in which the hippocampus is located, which can easily be dissected from the whole brain. The main pathway involved in hippocampal function is the glutamatergic system, requiring glutamate as the major neurotransmitter, which causes the activation of postsynaptic receptors such as N-methyl –D-aspartate (NMDA) receptors involved in memory. The hippocampus is also the primary target for neuronal degeneration in the brains of patients with Alzheimer's disease (Behl *et al.*, 1997). The rat hippocampus is located approximately 1mm anterior to where the cerebrum starts (from where the cerebellum ends, if one looks at the dorsal view of the brain) and extends about 4mm posterior and approximately 2.5mm lateral of the midline separating the two hemispheres.

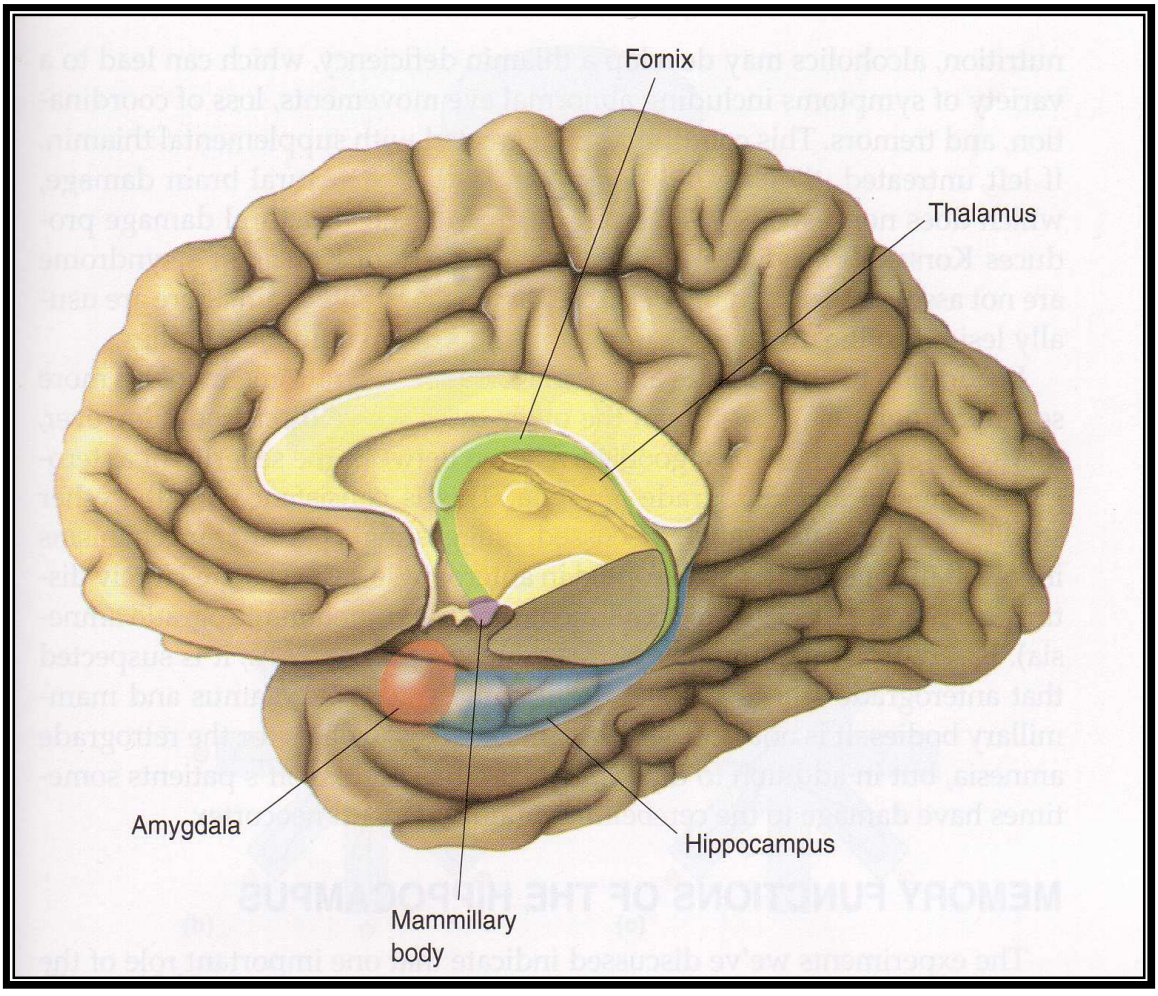

Figure 1.1: Components of the limbic system involved in memory. The thalamus and mammillary bodies receive afferents from structures in the medial temperal lobe (Bear *et al.*, 2001).

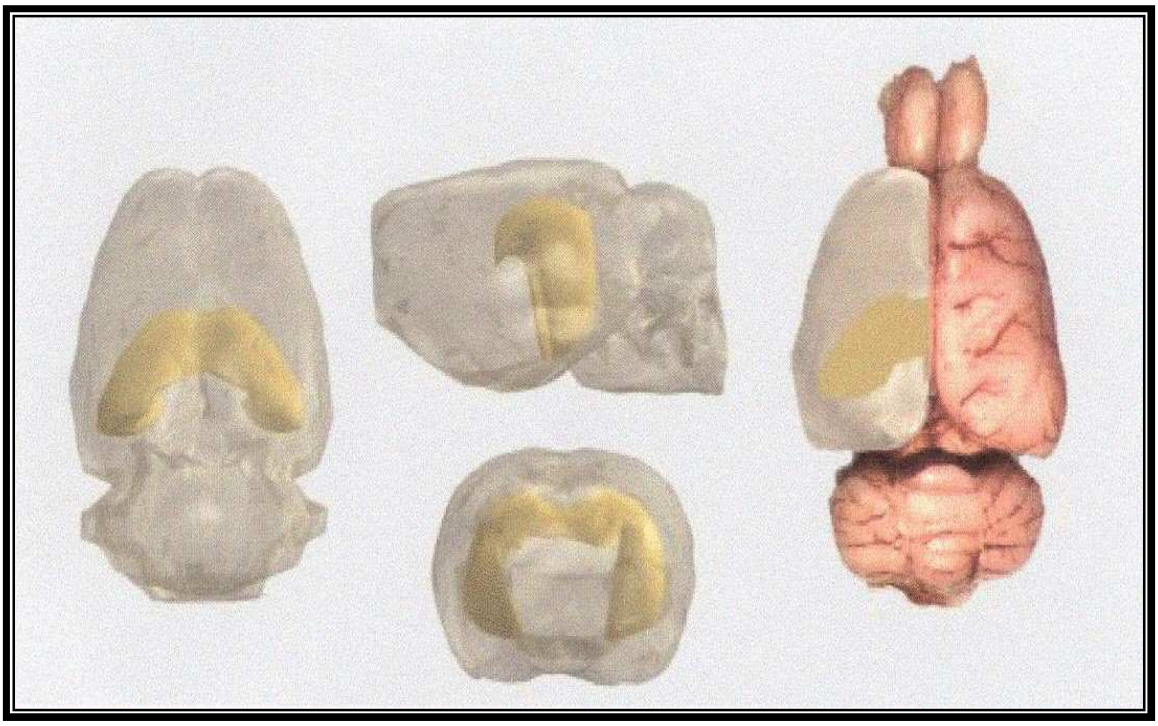

Figure 1.2: Various sections of the rat brain displaying the hippocampus shown in yellow. (Left and Far Right) A dorsal view of the rat brain; (Middle, Top) A midsaggital section through the brain; (Middle, bottom) A coronal section through the brain.

The hippocampus formation is a bi-lateral limbic structure, which resembles two "C's" that lean together at the top and spread apart at the base. The top portion is known as the "dorsal hippocampus", and because of its proximity to the septum, the dorsal tip of the hippocampus is called the "septal pole" and the bottom tip is called the "temporal pole" (Amaral & Witter, 1989). The hippocampus consists of two thin sheets of neurons folded onto each other; one sheet is the dentate gyrus and the other is the Ammon's horn. The Ammon's horn has four divisions, of which the most important are the CA1 and CA3 (figure 1.3). CA stands for *Cornu Ammonis* (CA1-CA3), also known as the "Hippocampus proper" meaning Ammon's Horn in Latin. The major input to the hippocampus is the entorhinal cortex, which sends information to the hippocampus via a bundle of axons called the perforant path. These axons synapse on neurons of the dentate gyrus. Dentate gyrus neurons give rise to axons, called mossy fibres, which synapse on cells in the CA3 region. The CA3 cells give rise to axons that branch; one branch leaves the hippocampus via the fornix and the other branch called Schaffer collateral, forms synapses on the neurons of CA1 (figure 1.3).

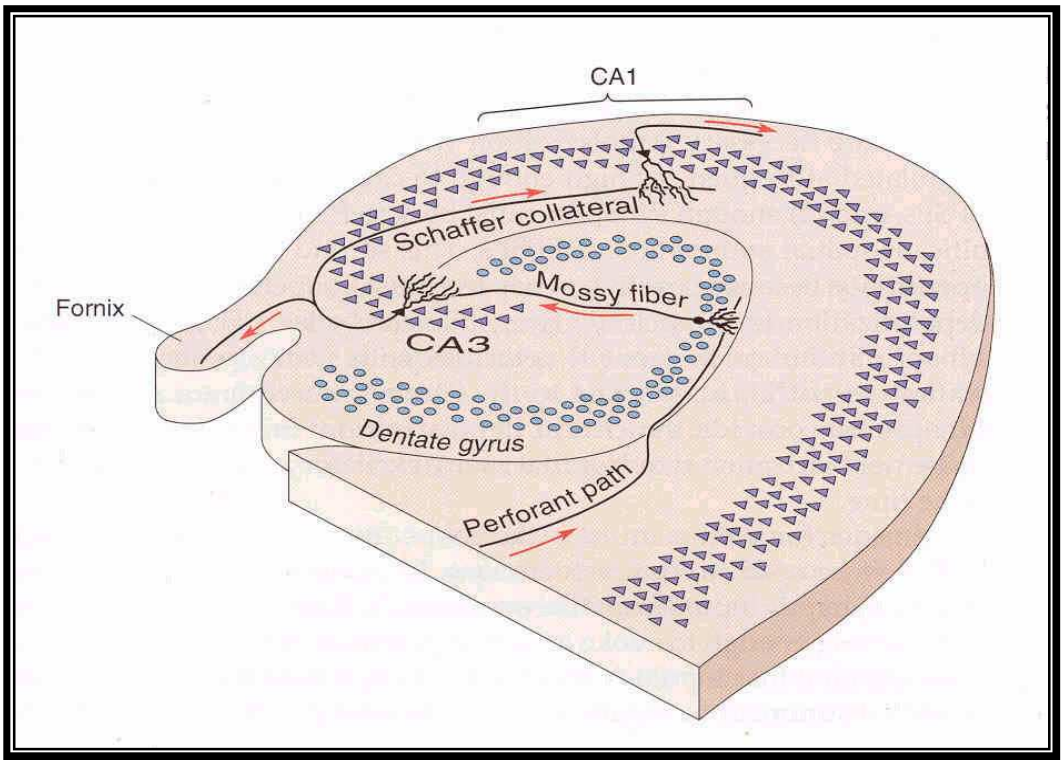

Figure 1.3: An illustration of some microcircuits of the hippocampus (Bear *et al.*, 2001).

The intrinsic connections between the principle cell layers of the dentate gyrus and CA regions of the hippocampus are very clear. The hippocampus, when cut transverse to its longitudinal (septal-temporal) axis, exhibits a strong afferent set of three connected pathways known as the "trisynaptic" circuit or loop (Amaral & Witter, 1989). The second and third layers, which are referred to as the “surface layers” of the entorhinal cortex, project to the granule cells of the dentate gyrus through the perforant-path. The granule cells of the dentate gyrus then project to the large pyramidal cells of CA3 region via the mossy fibers system. Finally, the CA3 pyramidal cells project to the pyramidal cells of the CA1 subfield, via the Schaffer collateral system (Amaral, 1978).

1.3. OXIDATIVE STRESS

1.3.1. Introduction

Oxygen is essential to life and it plays a vital role in diverse biological phenomena, however, it can also provoke damaging oxidative events within cells. Although there are a variety of free radicals produced by molecules, those that are produced from molecular

oxygen have received the most investigative interest (Reiter *et al.*, 1995). An estimated 1-4% of the O_2 taken up into cells forms, partially reduced O_2 species, the ROS. Some of these contain unpaired electrons and are therefore referred to as free radicals. In the strictest sense of the word, 'free' preceding 'radical' is not necessary since all radicals are free (Leigh, 1990). The diatomic oxygen molecule, that is, O_2 itself qualifies as a radical in as much as it possesses two unpaired electrons, each located in a different orbital but both having the same spin quantum number.

The oxygen species that are typically linked to oxidative stress are superoxide ($O_2^{\bullet -}$) anion radical, hydroxyl radical ($^{\bullet}OH$), hydrogen peroxide, nitric oxide (NO) and peroxynitrite. The collective term for these chemicals is "reactive oxygen species" (ROS), but not all of these species are particularly active in aqueous biological solutions (Dawson & Dawson, 1996). These reactive oxygen species cause an oxidative stress that could lead to cell damage or death (Hoyt *et al.*, 1997). Oxygen, via the transformation to these more reactive forms, can cause damage to DNA, proteins, essential enzymes, provoke uncontrolled chain reactions such as lipid peroxidation and dissolution of plasma and mitochondrial membranes. Normally there exists a balance in living cells between oxidative events and antioxidative forces. When the normal balance is upset, either by loss of reducing agents or protective enzymes or by the increased production of reactive oxygen species, or by both events simultaneously, the cell is said to be under oxidative stress (Fahn & Cohen, 1992). Thus, oxidative stress refers to cell damage induced by free radicals or reactive oxygen species.

Oxidative stress induces cell injury in a number of neuronal cell culture models and by a variety of proposed mechanisms. Hydrogen peroxide causes apoptosis of immature cultured cortical neurons (Whittemore *et al.*, 1995). ROS increases intracellular free calcium, which leads to the activation of endonucleases that degrade DNA (Floyd & Carney, 1992). Proteins that control calcium homeostasis, such as ATPase is sensitive to oxidative attack, the inhibition of which, leads to dysregulation of calcium levels. Mitochondria are important in buffering excessive calcium in neurons (Werth & Thayer, 1994) and ROS exposure disrupts mitochondrial function preventing accumulation of mitochondrial calcium as well as decreasing ATP production, both of which have toxic consequences.

1.3.2. Free Radicals

Free radicals are unstable, highly reactive molecules characterized by the presence of unpaired electrons in their outermost shells (Schipper, 1998). This definition encompasses a wide range of species (table 1.1.). Free radicals are known to play critical roles in many biochemical reactions that maintain normal cell functions. Usually, electrons associated with atoms or molecules are paired because this makes atoms relatively stable and unreactive. The loss of an electron leaves a molecule much more reactive than its paired counterpart. If two radicals react, both radicals are eliminated, while if a radical reacts with a non-radical, another free radical is produced. This characteristic allows free radicals to participate in chain reactions, which may be thousands of events long (McCord, 1985). Figure 1.4, illustrates the formation of free radicals and toxic reactants from molecular oxygen. The oxygen centred radicals or "oxyradicals" such as $O_2^{\bullet-}$, $^{\bullet}OH$ and hydrogen peroxide, mediate oxygen toxicity. The radicals are connected via the transfer of a single electron for example; the acceptance of a single electron by an oxygen molecule forms the $O_2^{\bullet-}$, while the acceptance of an electron by $O_2^{\bullet-}$ along with two protons forms hydrogen peroxide. Similarly, the acceptance of an electron by hydrogen peroxide forms the highly reactive $^{\bullet}OH$.

Table 1.1: Types of free radicals (Halliwell, 1992).

Type of radical	**Example**
Hydrogen centred	Hydrogen atom, $H^{\bullet}$
Carbon centred	Trichloromethyl, $CCl_3^{\bullet}$
Sulphur centred	Glutathione thiyl, $GS^{\bullet}$
Oxygen centred	Superoxide, $O_2^{\bullet-}$
	Hydroxyl, $^{\bullet}OH$
	Lipid peroxyl, Lipid-$O_2^{\bullet}$
Electron delocalized	Phenoxyl, $C_6H_5O^{\bullet}$ (electron delocalized into benzene ring)
	Nitric oxide, $NO^{\bullet}$

1.3.2.1. Superoxide Radical

When molecular oxygen accepts an electron from a reducing agent, the primary product generated is the superoxide anion ($O_2^{\bullet-}$). The $O_2^{\bullet-}$ is produced *in vivo* in a variety of ways (figure 1.4). A major source is via the cellular electron transport chains, such as those of mitochondria, chloroplasts and the endoplasmic reticulum (Halliwell & Gutteridge, 1990) where some electrons passing through the chain leak directly from the intermediate electron carriers onto O_2. Since oxygen accepts one electron at a time, $O_2^{\bullet-}$ is formed (Halliwell, 1992). Some leakage of $O_2^{\bullet-}$ can occur, however, mitochondria normally contain high levels of the protective enzymes, superoxide dismutase (SOD) and glutathione peroxidase (GPx) to remove toxic species (Jesberger & Richardson, 1991). It is generally held that $O_2^{\bullet-}$ is not highly reactive in an aqueous environment. Moreover, once formed, $O_2^{\bullet-}$ quickly undergoes dismutation to generate H_2O_2; this reaction is markedly accelerated by a family of enzymes, the SOD (Fridovich, 1989). Since SOD removes an oxidant, that is $O_2^{\bullet-}$, form the cell it is generally considered an important antioxidative enzyme (Touati, 1989). In solution $O_2^{\bullet-}$ actually exists in equilibrium with the hydroperoxyl radical ($HO^{\bullet}_2$). The $O_2^{\bullet-}$ and its conjugate acid, the $HO^{\bullet}_2$ has been shown to be reactive to a number of compounds *in vitro*. Superoxide oxidises alpha-tocopherol to 8-alpha-tocopherone, which spontaneously forms α-tocopherol quinone (Nishikimi *et al*., 1980). The reduction of cytochrome c by xanthine and xanthine oxidase is mediated by $O_2^{\bullet-}$ (McCord & Freidovich, 1968) and this reduction is used as the basis of assays for both $O_2^{\bullet-}$ and SOD. The SOD enzymes are catalysts that have evolved a surface charge arrangement to facilitate the specific use of $O_2^{\bullet-}$ as a substrate (Benovic *et al.*, 1983).

The $O_2^{\bullet-}$ has come to occupy an amazingly central role in a wide variety of diseases. The toxicity of superoxide is seen in its ability to inhibit certain enzymes and thereby attenuate vital metabolic pathways, as well as in its effects on other major classes of biological molecules (McCord, 2000). *E. coli* deficient in SOD activity show increased rates of mutagenesis (Touati & Farr, 1990), illustrating the role of the radical, directly or indirectly, in DNA damage. In conditions of ischaemia and reperfusion, the most acute problem resulting from the overproduction of superoxide appears to be greatly increased

rates of lipid peroxidation. Here the $O_2^{\bullet-}$ plays paradoxical roles, in that it can both initiate and terminate lipid peroxidation chains.

The reduction of molecular oxygen to form $O_2^{\bullet-}$ also occurs in normal biochemical oxidation-reduction reactions, both enzymatic (xanthine oxidase) and non-enzymatic (autoxidation of catecholamines). In addition, activated phagocytic cells (such as monocytes, neutrophils, eosinophils and macrophages including microglia) produce superoxide, which plays an important part in the mechanism by which bacteria are engulfed and destroyed (Colton & Gilbert, 1987). Thus excessive activation of phagocytic cells (as in chronic inflammation) can lead to free radical damage. The $O_2^{\bullet-}$ can also be generated chemically by auto-oxidative reactions with catecholamines, tetrahydrofolates and reduced flavins. The Ca^{2+}-dependent activation of phospholipase A_2 also yields $O_2^{\bullet-}$ through the metabolism of arachidonic acid by the lipoxygenases and cyclooxygenases to form eiconasoids (Chan & Fishman, 1980). However, most of the $O_2^{\bullet-}$ generated in a cell is converted to H_2O_2 by SOD as mentioned earlier.

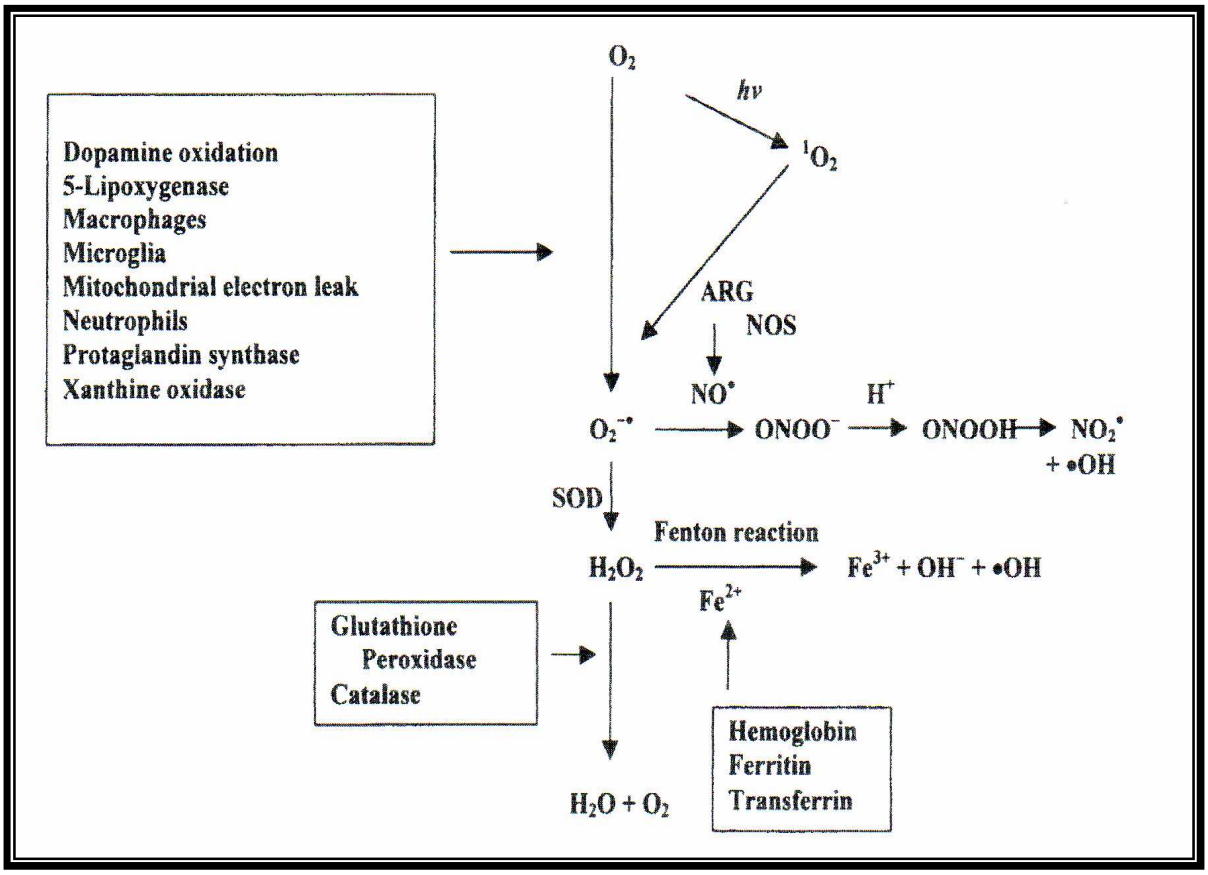

Figure 1.4: A summary of the multiple by-products generated by the partial reduction of O_2 (Reiter, 1998).

1.3.2.2. Hydrogen Peroxide

A system generating $O_2^{\bullet-}$ would produce H_2O_2 by non-enzymatic or SOD-catalyzed dismutation. SOD enzymes in human cells usually work in conjunction with H_2O_2-removing enzymes such as catalases and GPx's (Halliwell & Gutteridge, 1990). Besides SOD several other enzymes that generate H_2O_2 also exist in human tissues; these include L-amino acid oxidase, glycolate oxidase and monamine oxidase.

H_2O_2 itself is not especially toxic unless it is in high concentrations within the cells. There are features of the molecule, however, which make it hazardous. H_2O_2 readily diffuses through cellular membranes and can thereby distribute to sites distant from where it was generated. Also, in the presence of transition metals, most often Fe^{2+} (figure 1.4.) but also Cu^{1+}, H_2O_2 is reduced to the hydroxyl radical ($^{\bullet}OH$) via either Haber-Weiss or Fenton reactions (Halliwell & Gutteridge, 1990). The ultimate fate of H_2O_2 is not always the $^{\bullet}OH$. In most cells H_2O_2 is converted to innocuous products by the actions of two important antioxidative enzymes, that is catalase and selenium dependent GPx (figure 1.4). In the brain GPx are considerably more important than catalase because of the low activity of the latter enzyme in most parts of the central nervous system (CNS) (Jain *et al*., 1991). GPx utilizes H_2O_2 and hydroperoxides as substrates during the conversion of reduced glutathione (GSH) to its disulfide oxidized glutathione (GSSG) (Griffith, 1985).

1.3.2.3. Hydroxyl radical

The $^{\bullet}OH$ is perhaps not the only destructive species that is formed during the Fenton reaction (Bielski, 1991) but its formation is well documented as is its ability to oxidize adjacent moleucles (Halliwell & Gutteridge, 1989). The $^{\bullet}OH$ is thus, probably the most reactive of the ROS species (Poeggler *et al*., 1993; Dawson & Dawson, 1996) as it will react with almost all molecules in living cells (Fridovich, 1996). The $^{\bullet}OH$ are formed from $O_2^{\bullet-}$ and H_2O_2 through the Haber-Weiss reaction or through the interaction of metals such as Fe^{2+} or Cu^{1+} and H_2O_2 through the Fenton reaction (figure 1.4) as shown in equation 1 and 2 below. An intermediate in the reaction of H_2O_2 with Fe^{2+} may be the iron-oxygen complex refered to as ferryl which itself is highly oxidixing and which degrades to form the $^{\bullet}OH$.

$O_2^{\bullet-} + H_2O_2 \rightarrow H_2O + OH^- + {}^{\bullet}OH$ Haber-Weiss Reaction (equation 1)

$Fe^{3+} + O_2^{\bullet-} \rightarrow Fe^{2+} + O_2$

$Fe^{2+} + H_2O_2 \rightarrow Fe^{3+} + {}^{\bullet}OH + OH^-$

} Fenton Reaction (equation 2)

There is universal agreement that once formed, the $^{\bullet}OH$ reacts rapidly with any molecule within a few Angstroms of where it is produced. Because of its high reactivity its estimated half-life at 37°C is on the order of 1 x 10^{-9} sec. The $^{\bullet}OH$ readily damages nuclear and mitochondria DNA, proteins, membrane lipids and carbohydrates (Bird & Iversen, 1974). When the $^{\bullet}OH$ is produced within mammalian cells, it virtually always leaves in its wake damaged DNA products (Cochrane, 1991). There are at least two ways in which DNA damage is achieved. In many cases the mutilated DNA may occur because H_2O_2 reacts with either Fe^{2+} or Cu^{1+}, that is bound to molecules in the immediate vicinity of DNA so when the toxic $^{\bullet}OH$ is formed its first target is the adjacent nucleic acids (Halliwell & Arouma, 1989). Alternatively, during excitatory neurotransmitter stimulation of neurons, the large increases in intracellular Ca^{2+} activates nuclease enzymes in the nucleus with results in the formation of $^{\bullet}OH$ which subsequently leads to DNA damage (Orrenius *et al*., 1989).

Besides its destructive actions at the level of the genetic material in the nucleus, the $^{\bullet}OH$ does not reserve itself specifically for this action. Thus, the semi-reduced oxygen species also interacts with membrane lipids to initiate lipid peroxidation. This is accomplished when the $^{\bullet}OH$ removes an allelic H^+ from a polyunsaturated fatty acids (PUFA); this results in a radical chain reaction wherein lipid peroxidation is self-propogating. The brain is a favourate site for lipid peroxidation because of its regionally high iron and due to the fact that neural membranes phopholipids are composed of a high content of easily oxidized PUFA such as linoleic and arachidonic acid (Reiter, 1998).

1.3.2.4. Singlet Oxygen

Singlet oxygen ($^1O_2$) is formed under photoxidative conditions when energy is transferred to O_2 from photoexcited sensitizers, for example, rose bengal or methylene blue (figure 1.4). $^1O_2$ is not a diradical like molecular O_2 and it is highly reactive towards most olefins; thus, it can abstract a H^+ from a PUFA to initiate lipid peroxidation. In biological systems, $^1O_2$ may play a prominent role in the peroxidation of membrane lipids (Halliwell & Gutteridge, 1989).

1.3.2.5. Peroxyl Radical

Perhaps the most thoroughly studied of all oxidative processes is that of the break down of lipids in cellular membranes during which the peroxyl radical is formed (Asano *et al.*, 1991). Lipid peroxidation, once underway generated a number of toxic products. These include lipid hydroperoxides and the peroxyl radical ($LOO^\bullet$). The $LOO^\bullet$ can then attack a nearby PUFA and re-initiate (propagate) the process. Vitamin E (α-tocopherol) is known to be the premier $LOO^\bullet$ scavenger and chain breaking antioxidant.

1.3.2.6. Nitric Oxide and Peroxynitrite Anion

Nitric oxide ($NO^\bullet$) is often characterized as a double-edged sword. Under normal physiological conditions this nitrogen-centered radical has important functions as a neuronal messenger molecule and is responsible for relaxation of the pyloric sphincter in the gastrointestinal tract (Yun *et al.*, 1996), mediation of penial erections (Melis *et al.*, 1994) and vasodilation (Holscher, 1997); however, when $NO^\bullet$ increases intracellularly to unusually high concentrations it initiates a toxic cascade of events which can lead to the death of neurons (Zhang *et al.*, 1994). A common example of $NO^\bullet$ toxicity is seen in glutamate neurotransmission in the CNS where N-methyl-D-aspartate (NMDA)-receptor activation leads to large rises in intracellular calcium concentration followed by the stimulation of neuronal nitric oxide synthase (NOS) (Dawson *et al.*, 1991) leading to the generation of $NO^\bullet$. As seen in figure 1.4, this induces a series of events that can lead to neuronal destruction.

During focal ischemic events in the CNS, the release of excitatory amino acid neurotransmitters including glutamate causes large increases in $NO^{\bullet}$ (Malinski *et al.*, 1993). $NO^{\bullet}$ then interacts with $O_2^{\bullet-}$ to generate the peroxynitrite ($ONOO^-$) (Radi *et al.*, 1991a). It is this latter molecule which accounts for much of the toxicity of $NO^{\bullet}$. Hastening $O_2^{\bullet-}$ removal with exaggerated SOD activity reduces infarct volume following focal cerebral ischemia in mice (Kinouchi *et al.*, 1991) as does inhibition of NOS (Dawson & Snyder, 1994). These findings are consistent with $ONOO^-$ being the culprite in $NO^{\bullet}$ toxicity. Therefore, the formation of $ONOO^-$ depends on the concentration of $O_2^{\bullet-}$ and $NO^{\bullet}$ in the cell (figure 1.4).

Whereas $ONOO^-$ is a simple molecule, it is chemically highly complex. Its reactivity is roughly the same as that of $^{\bullet}OH$ and $HO^{\bullet}_2$. The toxicity of $ONOO^-$ derives from its ability to directly nitrate and hydroxylate the aromatic rings of amino acid residues (Beckman *et al.*, 1992), with zinc-thiolate moieties (Crow *et al.*, 1995) as well as with lipids (Radi *et al.*, 1991b), proteins (Moreno & Pryor, 1992) and DNA (King *et al.*, 1992). This ubiquitous acitivity makes the $ONOO^-$ a molecule that can have devastating effects on neuronal physiology as well as viability.

1.3.3. Antioxidant Defence Mechanisms

The body has many defence mechanisms to deal with oxidative stress (Machlin & Bendich, 1987) see table1.2. These enzyme systems are normally distributed evenly inside cells (McCord, 1985), and under normal circumstances these defence mechanisms can deal with the production of ROS in the neuron. Antioxidants usually refer to molecules that inhibit the chain reaction of lipid peroxidation by scavenging intermediate peroxy radicals (Halliwell, 1992). The toxicity of free radicals can be mitigated by direct free radical scavengers and by indirect antioxidants (Sies, 1993). These protective mechanisms can be classified into two main categories (Dawson & Dawson, 1996), namely the enzymatic defence mechanisms, which include SOD and the non-enzymatic cellular antioxidants, which include vitamins A and E.

Table 1.2. Cellular defence / anti-oxidant mechanisms accessible to neurons to protect against ROS species (Dawson & Dawson, 1996).

Enzymatic	**Non-Enzymatic**
Cu / Zn – $O_2^{\cdot}$ Dismutase	Ascorbic Acid (Vitamin C)
Mn – $O_2^{\cdot}$ Dismutase	α-tocopherol (Vitamin E)
Glutathione Peroxidase	Glutathione
Glutathione-S-Transferase	Melatonin
Glutathione Reductase	
Catalase	

The principal defence system against oxygen free radicals are SOD, GSH, GPx, glutathione reductase (GRd), catalase (a haem enzyme), and antioxidant nutrients (figure 1.5). These enzymes scavenge reactive chemical species and help to maintain cells in a reduced state. Cellular reducing agents such as glutathione and α-tocopherol, appear predominantly in the reduced state rather than their oxidized form to enable them to gain electrons (Fahn & Cohen, 1992).

The breakdown of $O_2^{\bullet -}$ by SOD yields hydrogen peroxide and oxygen (reaction 1). There are two distinct SOD's in eukaryotes ; the manganese-containing SOD localized in the mitochondrial matrix and the copper- zinc-containing SOD found in the cytoplasm.

$$2O_2^{\bullet -} + 2H^+ \rightarrow H_2O_2 + O_2 \qquad (1)$$

$$2GSH + H_2O_2 \rightarrow GSSG + 2H_2O \qquad (2)$$

$$GSSG + NADPH + H^+ \rightarrow 2GSH + NADP^+ \qquad (3)$$

$$2H_2O_2 \rightarrow O_2 + 2H_2O \qquad (4)$$

Hydrogen peroxide is decomposed by two reactions. At low concentrations, H_2O_2 is removed by reacting with GSH to form GSSG and water, catalyzed by GPx (reaction 2). GSH is regenerated by the action of GRd (reaction 3). At high concentrations, however, H_2O_2 is removed by the enzyme catalase (reaction 4), (Fahn & Cohen, 1992).

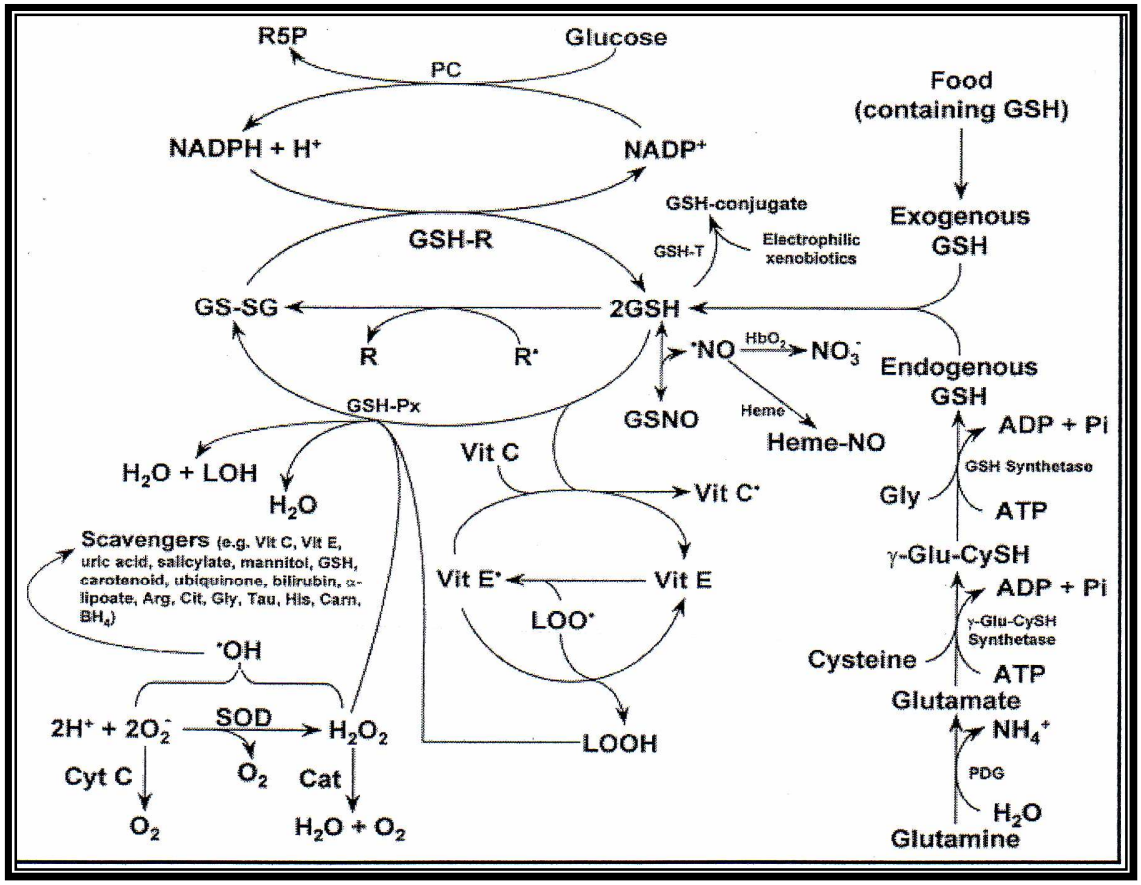

Figure 1.5: Removal of oxygen and nitrogen free radicals and other reactive species in mammalian cells (Fang *et al*., 2002).

An important antioxidant in the brain is α-tocopherol. This is the most potent antioxidant that can break the propagation of the free radical chain reaction in the lipid part of the biological membrane. In rats, it was shown that in the long term, low levels of antioxidants, such as vitamin E, ascorbic acid (vitamin C), and GSH in all tissues could lead to tissue peroxidizability. Vitamin E deficiency also influences the activities of SOD, catalase and GPx (DeKumar & Rukmini, 1988). In addition, severe and prolonged deprivation of this antioxidant produces severe neurological derangements (Muller & Goss-Sampson, 1990).

Among the antioxidants vitamin E has shown some promise in the treatment of AD (Vatassery, 1992). The hypothesis that oxidative stress is implicated in the pathogenesis of AD prompted a large, two year, double blind placebo-controlled, randomized multi-center clinical trial of vitamin E in 341 AD patients. The treatment was found to delay functional deterioration in moderately impaired AD patients (Sano *et al*., 1997). However, one antioxidant agent that has generated a vast amount of interest in recent

years, is melatonin. Melatonin has been shown to be more potent than α-tocopherol, mannitol, and glutathione as a free radical scavenger (Reiter, 1997). Unlike classical antioxidants such as vitamin C, vitamin E and glutatione that undergo redox cycling, melatonin being and electron rich molecule, may interact with free radicals via an additive reaction to form several stable end products which are eliminated in the urine (Maharaj *et al*., 2002). The ability of melatonin to act as a free radical scavenger is further described below in section 1.4.

1.3.4. Neurotoxins

1.3.4.1. Introduction

Brain damage also results from chemical neurotoxicity, either from administered drugs or environmental toxins. Many neurotoxic agents are available which mimic human pathologies or are useful for the study of neurodegeneration because of their specificity in effect e.g. quinolinic acid (QA), cyanide and iron.

1.3.4.2. Quinolinic Acid

Quinolinic acid (QA) was first identified in human brain in 1983. However, the role played by this neurotoxin in neuropathology was uncertain. QA is a naturally occurring amino acid and a structural analogue of the neurotransmitter candidates L-glutamate and L-aspartate. This neurotoxin is a metabolite of the tryptophan-kynurenine pathway in the brain, and is normally present in nanomolar concentrations in human brain and cerebrospinal fluid. The concentration of QA varies among different brain regions, with the cerebral cortex containing approximately 1.8 nmol/g wet weight; almost 2 fold that in the hippocampus with 1nmol/g wet weight (Moroni *et al*., 1984b). When introduced into the CNS, QA is a potent excitotoxin acting through excitatory amino acid receptors to cause neuronal excitation (Stone & Perkins, 1981), seizure activity and lesions (Schwarcz *et al*., 1984), and neuronal degeneration (Southgate & Daya, 1999). More recent reports describe QA as an endogenous agonist at the NMDA glutamate receptor subtype that is able to cause neuronal damage and cell loss (Santamaria *et al*., 1996).

Substantial increases in QA have however been found in the brain and CSF in response to a broad spectrum of infectious and other inflammatory neurological diseases (Heyes *et al*., 1996). Furthermore, Moroni *et al*., (1984a), showed that the concentration of QA in the CNS changes after treatments capable of modifying brain tryptophan content; the QA concentration can increase by 150% in response to tryptophan loading. Paradoxically, administration of a tryptophan-free diet to rats for 15 days resulted in a doubling of QA concentrations in the cortex. One explanation for this may be that QA can also be synthesized by a pathway distinct from the kynurenine pathway, particularly as some bacteria and plants are able to synthesize QA from the condensation of aspartic acid and dihydroxyacetate (Stone, 1993). It has also been reported that the concentrations of QA present in the human brain is similar to those in the rat brain (Wolfensberger *et al*., 1983), and that these concentrations increase in the cortex during the aging process (Moroni *et al*., 1984b).

Some studies demonstrate that QA exerts its toxicity in the CNS via glutamatergic receptors (Stone, 2001). Glutamate neurotoxicity is implicated in acute neurological disorders as well as in neurodegenerative diseases (Lipton & Rosenberg, 1994). Evidence suggests that QA is associated with neuronal damage through the overactivation of the postsynaptic NMDA subtype of glutamate receptors (Stone, 2001). Many factors come into play to render this compound a potent neurotoxin. One such factor is the performance of the two enzymes involved in QA synthesis and metabolism respectively. A detailed analysis of the properties of both 3-hydroxyanthranilic acid oxygenase (3-HAO) and quinolinate phosphoribosyl transferase (QPRT) indicate that both have similar Km values but that the reaction velocity of 3-HAO was 80-fold higher than that for QPRT (Foster *et al*., 1986). Consequently, the production of QA occurs at a much faster rate within the brain than the conversion to nicotinic acid dinucleotide (NAD). This has implications for the accumulation of QA in the brain under certain pathological conditions.

Other factors that promote QA's ability to cause neuronal damage are the lack of uptake systems and extracellular metabolism that exist within neurons. An experiment in which radiolabeled QA was injected into the hippocampus, the radiolabeled compound was cleared from brain with a half life of 22 minutes, all residual radioactivity recovered after 2 hours still being present as QA, assayed by HPLC. Thus this region (as well as the

striatum) does not appear to possess mechanisms either for the rapid removal of QA or for its metabolic degradation in the extracellular space by QPRT (Foster *et al*., 1984).

Striatal administration of QA is associated with neurotoxicity and development of neurological damage, which resembles that, observed in Huntington's disease, and probably results from excessive NMDA receptor activation (Beal *et al*., 1991; Malcon *et al*., 1997). Moreover, intracerebroventricular injection of QA has been shown to induce seizures (Schmidt *et al*., 2000; Lara *et al*., 2001).

The neurotoxicity produced by QA may also depend at least partly on the formation of ROS, since its neurotoxic activity can be prevented by spin-trap reagents such as α-phenyl-*t*-butylnitrone (Nakao & Brundin, 1997) and free radical scavengers (Nakai *et al*., 1999). QA has also been shown to induce lipid peroxidation (Rios & Santamaria, 1991) which can be prevented by nitroarginine and potentiated by L-arginine, suggesting that NO, a free radical itself and a precursor of potent toxic radicals such as peroxynitrite, may contribute to the activity of QA (Santamaria *et al*., 1997).

1.3.4.3. Cyanide

Cyanide is one of the most potent poisons known to man. The toxicity of cyanide is a consequence of its high potency as a respiratory poison in all aerobic forms of life (Yen *et al*., 1995). Numerous biochemical, morphological and physiological studies have shown that cyanide is a potent and selective neurotoxin whose toxicity is mediated through histotoxic hypoxia, consequent to mitochondrial dysfunction (Bhattacharya & Lakshmana Rao, 2001). Acute doses of cyanide are usually fatal, due to the marked susceptibility of the nerve cells of the respiratory centre to hypoxia (Greer & Jo, 1995). The cascading effects of cyanide-induced impairment of mitochondrial energy production include failure of ionic homeostasis, acidosis, elevated Ca^{2+} levels and lipid peroxidation, leading to activation of proteases, lipases, xanthine oxidase, etc. (Madhu, 1989). The elevation of brain calcium (Johnson *et al*., 1987) and increase in free cytosolic calcium leads to increased oxidative stress and excitotoxicity.

The implication of oxidative stress and activation of endonucleases in oligonucleosomal cleavage of DNA following cyanide exposure is well documented (Trump & Berezesky, 1995). Subsequent to oxidative stress, widespread DNA fragmentation leading to an apoptotic type of cell death has been documented in cyanide poisoning (Mills *et al*., 1996; Mills *et al*., 1999), with Mills *et al*., (1996) reporting an apoptotica effect of cyanide in terminally differentiated PC12 cells. Cyanide also causes surface blebbing and cytoarchitectural defects of neuronal cells as a consequence of Ca^{2+}-activated phospholipases and proteases (Nicotera *et al*., 1989).

1.3.4.4. The Involvement of Metal Ions

Ions of transition metals such as copper and iron are involved in many free radical reactions, and often these lead to the generation of very reactive species (Halliwell & Gutteridge, 1989). In the case of iron, only free iron is able to stimulate free radical reactions, whereas iron bound to protein such as transferrin found in human plasma, is not normally available to stimulate such reactions. Iron (II) (Fe^{2+}) reacts with hydrogen peroxide in the Fenton reaction to produce the harmful $^{\bullet}OH$ and the oxidized form of the metal ie. iron (III) (Fe^{3+}) as shown in equation 2 above.

The Fenton reaction can be augmented by the reduction of ferric ion by superoxide thus regenerating ferrous ion. The net result is the production of $^{\bullet}OH$ as in the iron-catalyzed Haber-Weiss type of reaction (equation 1 above).

The iron dependent formation of the hydroxyl radical is detrimental to the cell, since, the hydroxyl radical is the most reactive of all oxygen radicals, so much so that no enzyme systems involve it as a substrate. Cells try to prevent its formation, and remove hydrogen peroxide and transition metals to inactive sites (Fahn & Cohen, 1992). The hydroxyl radical does not travel far and has a short half life. However, hydrogen peroxide is able to cross the blood-brain barrier and thus its conversion to the $^{\bullet}OH$ in the brain causes severe damage to neurons as described above.

There is considerable evidence, which demonstrates that endogenous iron stores are partially available for participating in peroxidative events in tissue (Halliwell &

Gutteridge, 1986). Iron accumulates in human and rat brain during aging, and there has been speculation that several degenerative changes in brain functions which occur during aging and in certain pathological states of the CNS may be mediated through or accelerated by iron-induced peroxidative processes (Viani *et al*., 1991). More recently, Keyer & Imlay (1996) reported that superoxide accelerates DNA damage by elevating free-iron levels. However, iron also plays essential roles in the brain, especially in learning and memory and these ions are required for the correct binding of certain neurotransmitters to their receptors (Youdim, 1988).

1.3.5. Iron Source For Fenton Chemistry

The iron contained in the body is absorbed from the gut, and originates from food and beverages we consume that are fortified with iron. Most body iron is found in haemoglobin, with smaller amounts in myoglobin, various enzymes and the transport protein transferrin. Iron not required for these is stored as ferritin, which can hold up to 45 000 ions of iron (Halliwell & Gutteridge, 1989). Transferrin enters the cytoplasm in a vacuole, which is acidified to release the iron. The transferrin is then ejected leaving a pool of non-protein-bound iron, which will be used in the synthesis of iron proteins. In this way the cells minimize the size of the intracellular iron pool (Halliwell & Gutteridge, 1989).

Oxidant stress can provide the iron necessary for Fenton chemistry by mobilizing iron from ferritin or by degrading haeme proteins to release iron. Reports have stated that the formation of OH^- *in vivo* may be limited by the supply of iron ions, and tissue injury can exacerbate radical reactions if it liberates metal ions from broken cells into the surrounding environment. This is especially true in brain, since CSF has no significant iron-binding capacity, and mechanical disruption of the brain releases iron that can stimulate radical reactions such as lipid peroxidation.

1.3.6. Lipid Peroxidation

The detection and measurement of lipid peroxidation is the evidence most frequently cited to support the involvement of free radical reactions in toxicology and in human

disease. Lipid peroxidation has been defined as the oxidative deterioration of polyunsaturated lipids, ie. those lipids containing more than two carbon-carbon double covalent bonds (Halliwell, 1992). Cell membranes are rich in polyunsaturated lipids, which together with saturated fatty acids give rise to membrane fluidity. Damage to these polyunsaturated fatty acid side chains reduces membrane fluidity and as a result the biological membrane is not able to function properly.

Schematic diagram of the sequence of events in lipid peroxidation:

- Cell damage $\rightarrow OH^{\cdot} + CH_2 \rightarrow C^{\cdot}H \rightarrow$ conjugated diene + $O_2 \rightarrow CHO_2^{\cdot} + CH_2 \rightarrow C^{\cdot}H$ + lipid peroxide
- Fe^{2+}-complex + lipid peroxide $\rightarrow CHO^{\cdot}$
- Fe^{3+}-complex + lipid peroxide $\rightarrow CHO_2^{\cdot} + H^{+} + Fe^{2+}$-complex

Lipid peroxidation is initiated by the attack of any species that has sufficient reactivity to abstract a hydrogen atom from a methylene group ($-CH_2-$). A hydroxyl radical can do this, as well as various iron-oxygen complexes. Abstraction from a methylene group leaves a carbon radical, which then stabilizes by molecular rearrangement to form a conjugated diene. This then combines with oxygen (which is hydrophobic and thus concentrates into the interior of membranes) to give a peroxyl or "peroxy" radical ($CHO_2^{\bullet}$). This radical can then abstract a hydrogen from another lipid molecule or it may attack membrane proteins. Once the peroxyl radical is formed it can abstract another hydrogen atom from say a methylene group and combines with this hydrogen to form a carbon radical and lipid peroxide. This carbon radical may then react with oxygen to form a peroxyl radical and so the chain of lipid peroxidation can continue as shown in figure 1.6.

Iron plays an important role in lipid peroxidation. Not only can it generate hydroxyl radicals via the Fenton reaction, which initiates the chain of events leading to the formation of the alkoxyl radical, but it also plays a second important role in lipid peroxidation. Lipid peroxides are fairly stable at physiological temperatures, but in the presence of iron, their decomposition is greatly accelerated. Thus a reduced iron complex can react with lipid peroxides in a way similar to its reaction with H_2O_2; it causes fission of O-O bonds to form alkoxyl radicals. A Fe^{2+} complex can form peroxy radicals and by

further reaction with the Fe^{2+}–complex can form alkoxyl radicals (Halliwell & Gutteridge, 1990).

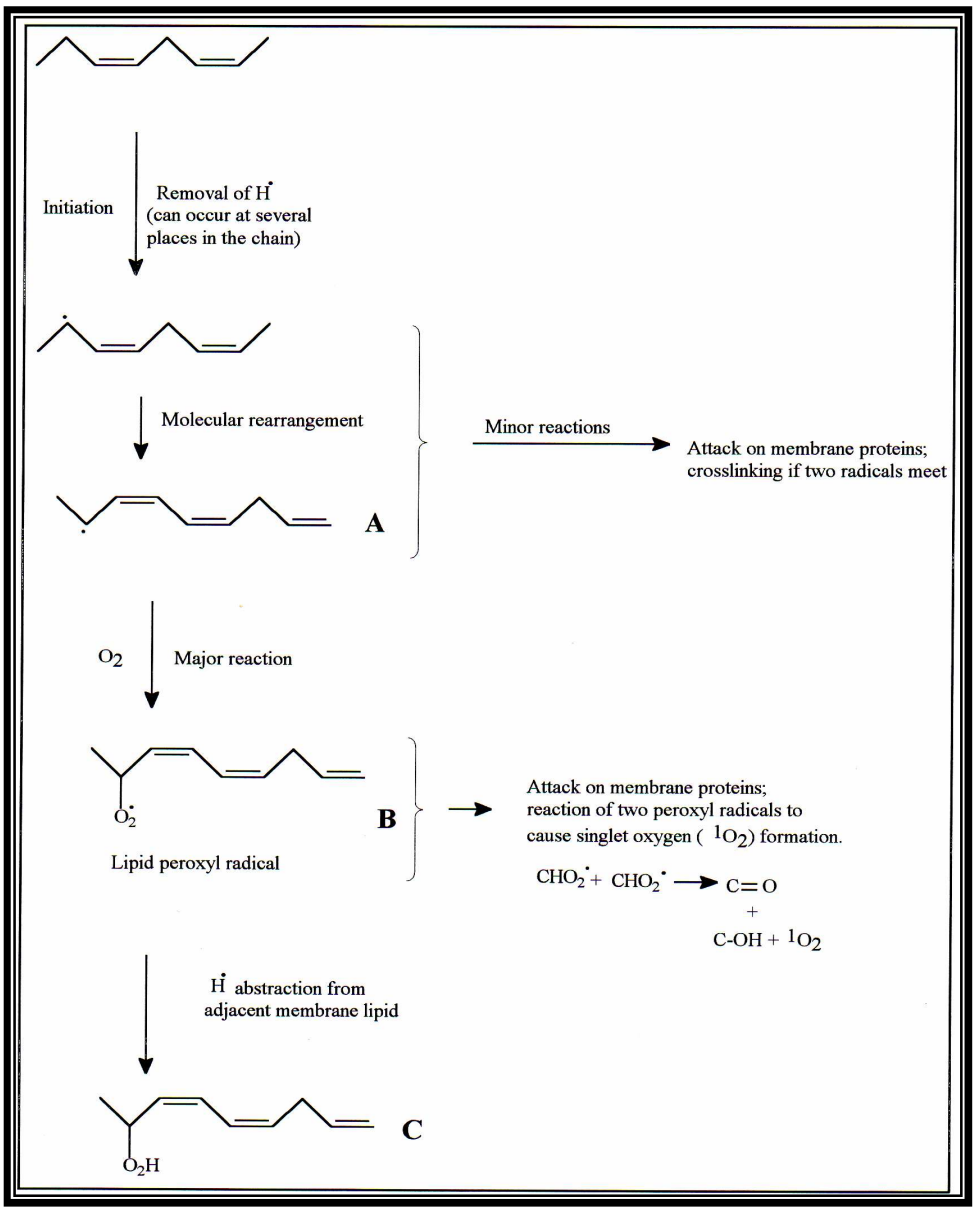

Figure 1.6: An outline mechanism of lipid peroxidation (Gutteridge & Halliwell, 1990).

1.3.7. Free Radicals and Disease

1.3.7.1. Introduction

In a structure as complex as the human brain, a multitude of things can go wrong. The amount of abuse the brain takes from free radicals is generally considered to be extensive

(Poeggeler *et al*., 1993; Reiter, 1995a; Reiter *et al*., 1997). Perhaps the major reasons for this are its high utilization of O_2, its relatively poorly developed antioxidant network, and the fact that it contains large amounts of easily oxidizable fatty acids and iron (Reiter, 1998). Although estimates vary, it is believed that up to 5% of the oxygen (Reiter *et al*., 1995; Chan *et al*., 1993) taken up by an organism may eventually end up as damaging oxygen-based radicals. In the human, this means that there could be the equivalent of 2 kg of O_2 radicals produced each year (Reiter *et al*., 1995). As a consequence, the molecular carnage and cytotoxicity that is measured in the brain after toxin exposure and during aging is often substantial. This oxidative damage has been considered a common link in the pathogenesis and neuropathology of a variety of neurodegenerative disorders.

Free radicals have been reported to be involved in aging as well as many disease states including, iron-overload disease, arthritis, neurological damage, Down's syndrome and diabetic cataract. Undoubtedly, one of the major challenges for contemporary neurology is the deferral and prevention of age-associated neurodegenerative conditions that are commonplace in a population whose life span has shown substantial increases in recent decades. The debilitating consequence of brain deterioration and malfunction obviously compromise the quality of life and longevity and are financially taxing to society. The scientific quest to identify the causes and effective treatments for these devastating conditions is diverse and intensive. While oxidative stress may be one feature that links many neurological deficits, it is also obvious that these diseases have extremely complex etiopathologies and it is unlikely that a single agent will totally combat their development. There are a number of neurodegeneration disease models. However, for the purpose of this study, ageing and Alzheimer's disease (AD) will be explored.

1.3.7.2. Aging

Aging in mammalian species appears to be the result of normal developmental and metabolic processes responsible for the graying of the hair, decreases in the rate of wound healing and increases in susceptibility to disease and death. The most reliable risk factor for neurodegenerative diseases is normal aging. Studies have found evidence of oxidative damage to macromolecules (DNA, lipids and proteins) especially in brains from elderly subjects, supporting the hypothesis that oxidative injury might directly cause the aging

process (Gilgun-Sherki *et al.*, 2001). The lifespan of individuals in a population varies with stress and free radicals play an important role in stress (Pryor, 1986). Free radicals increase ageing both by influencing the rate of development of specific chronic diseases and by causing general "wear and tear" on biopolymer molecules. The argument that free radicals cause general, non-specific damage to biopolymer molecules is called the "free radical theory of ageing" (Harman, 1982). This theory is a popular hypothesis that has been used to explain the ageing process (Fantone & Ward, 1985). The intracellular generation of free radicals results in a progressive accumulation of defective molecules in the cells. This causes an alteration in the physiological function including the accumulation of the lipofuscins ("age-pigments"). Biochemical characterisation of these pigments indicates that they consist largely of oxidised lipids (Taubald *et al.*, 1975). Several other studies support a relationship between that of free-radical production within tissues and life span (Fantone & Ward, 1985).

Additional links between oxidative stress and aging focus on mitochondria. Direct biochemical measurements of mitochondrial function demonstrate age-dependent increases in mitochondrial deletions, point mutations, and oxidative damage to the DNA. The mitochondrial DNA is particularly susceptible to oxidative stress probably due to its close proximity to the respiratory chain, limited repair mechanisms, few non-coding sequences and absence of histones (Beal, 1995). It has been postulated that a reduced caloric intake could result in the decreased production of free radicals as by-products of normal biochemical reactions in cells, especially oxygen metabolic products of mitochondrial respiration (Harman, 1982). The correlation that exists between age and the onset of specific diseases in which free radical reactions are important, further supports the hypothesis that free radicals are intimately involved in the aging process (Fantone & Ward, 1985).

1.3.7.3. Alzheimer's Disease

A case report was published by Alois Alzheimer in 1907, describing the cerebral cortex of a 55-year old woman with progressive dementia (Alzhemier, 1977). The famous "note" pointed out the presence of abnormal nerve cells that contained tangles of fibres (neurofibrillary tangles) and clusters of degenerative nerve endings (neuritic plaques).

This presenile dementia later became known as Alzheimers disease (AD). AD is a progressive neuropsychiatric disorder of unknown etiology. It is characterized by neuronal degeneration and cognitive deterioration especially in the elderly (Flynn & Runho, 1999). It affects an estimated 15 million people worldwide with this number expected to increase with the continuing rise in mean longevity. A triad of neuromorphophysiological features characterize AD and include β-amyloid plaques (senile plaques), neurofibrillary tangles and extensive neural loss particularly in the hippocampus and cerebral cortex (O'Banion *et al*., 1994; Mattson *et al*., 1997); these changes are associated with dementia and characteristic neurobehavioural consequences. The signs of the disease changes in the majority of cases appear to arise sporadically and usually have a late life onset (after 65-years of age) (Harman, 1995). In a less common form of familial AD, the onset of the condition is typically much earlier (40-50 years of age).

Oxidative stress has been implicated in the pathogenesis of AD (Markesbery, 1997) by the finding of several characteristics, such as enhanced lipid peroxidaiton in specific areas of the brain in postmortem studies (Lovell *et al*., 1995). Several investigators detected an increase in the activity of catalase, SOD, GPx, GRd in the hippocampus and amygdala (Pappolla *et al*., 1992). The suggestion that oxidative stress causes oxygen radical formation with resultant neurodegeneration and possibly plaque formation in the CNS, was supported by the study of Frautschy *et al*., (1991). Moreover, Pappolla *et al*., (1998) provided evidence for the hypothesis that β-amyloid plaque, the major constituent of the senile plaque, is neurotoxic and that such toxicity is mediated by free radicals *in vitro* and in a transgenic mouse model of AD.

1.3.8. Free Radicals and Mitochondria

Free radicals are sometimes formed as intermediates in mitochondrial and microsomal electron transport systems (Fantone & Ward, 1985). A deleterious consequence of energy production by the mitochondria is the production of free radicals such as the superoxide anion and hydroperoxides. This is because oxygen acts as the terminal electron acceptor within the ETC (Fantone & Ward, 1985).

Impaired mitochondrial function leads to impaired cellular Ca^{2+} buffering and secondary activation of voltage-dependent NMDA receptors. This can, in turn, lead to further influxes of Ca^{2+}, which are buffered in mitochondria, leading to increased production of the $O_2^{\bullet-}$. Moreover, the increase in Ca^{2+} results in an activation of neuronal NOS. Nitric oxide reacts with $O_2^{\bullet-}$ to generate $ONOO^-$ (as discussed in section 1.3.1.3), which results in oxidative damage to DNA, proteins and lipids (Beal, 1997). This is shown in figure 1.7 below.

As figure 1.7 depicts, the production of superoxide radicals can also lead to increased H_2O_2 production, which can react with transition metals like Fe^{2+}. This results in damage to cellular macromolecules like DNA, which leads to the activation of poly-ADP ribose polymerase (PARS). Activation of PARS leads to ATP and NAD depletion, which leads to death. Both mitochondrial accumulation of Ca^{2+} and oxidative damage lead to activation of the permeability transition pore (PTP) that is linked to excitotoxic cell death. The release of cytochrome c, caspase 9 and apoptosis inducing factor (AIF) by the mitochondria is also linked to increased mitochondrial Ca^{2+} and free radical production. These mediators lead to the activation of a caspase cascade, and finally apoptotic death (Beal, 1997).

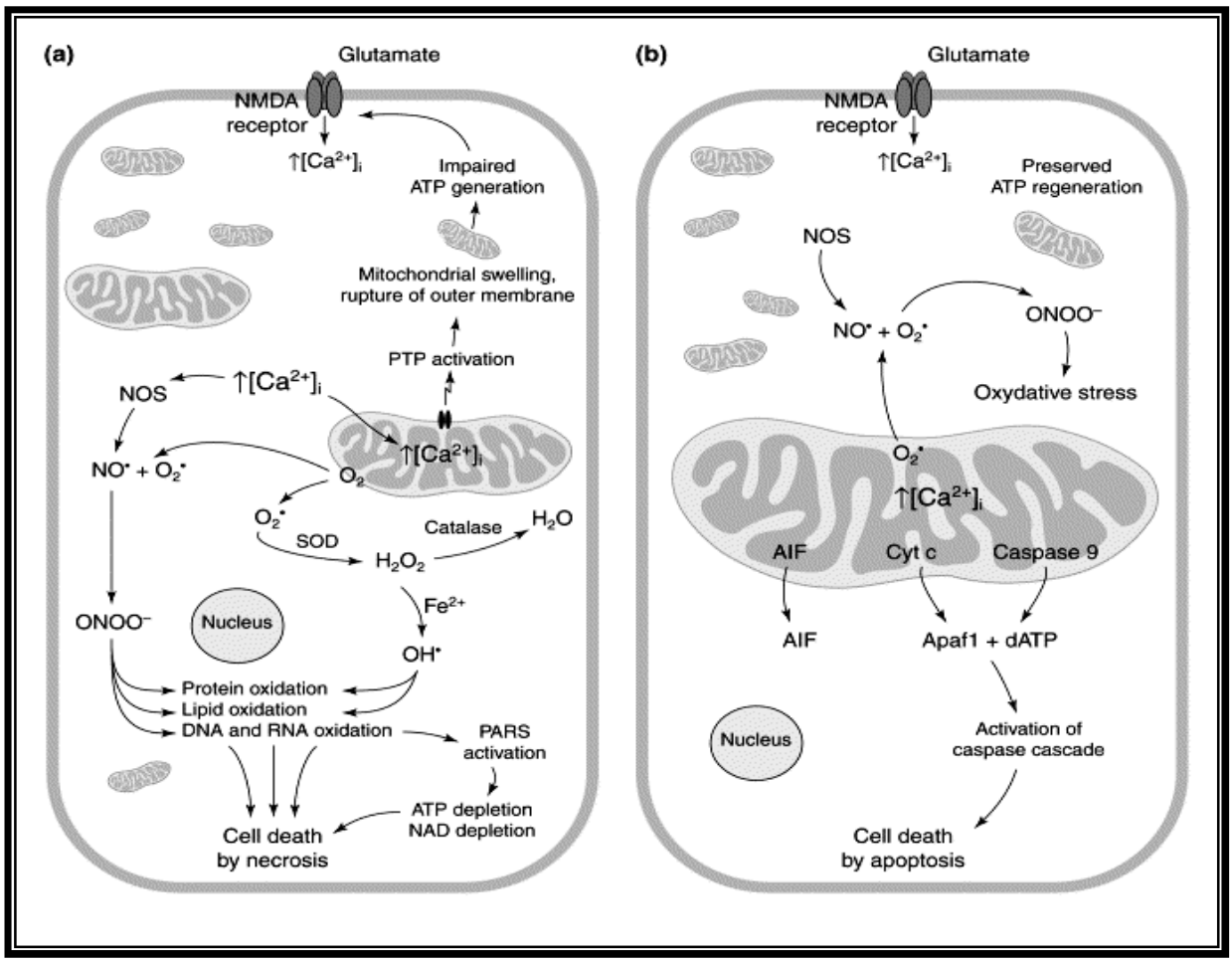

Figure 1.7: The Mitochondrion: A major source of cellular free radicals. (a) depicts the effects of a severe excitotoxic insult that results in cell death by necrosis, whereas (b) depicts the results of a mild excitotoxic insult that results in apoptosis (Beal, 1997).

1.3.9. Molecular Targets of Oxidative Stress

Oxidative damage does not always lead to the formation of lipid peroxides in injured nervous tissue. Damage to DNA and proteins are of equal or greater importance *in vivo* (Halliwell, 1987). Early events in human cells subjected to oxidative stress, include DNA damage and consequent activation of poly (ADP-ribose) synthetase, decreases in ATP content and increases in calcium, with consequent activation of calcium-stimulated proteases that can cause such phenomena as ‘ bleb’ formation on the plasma membrane of the cells (Orrenius *et al*., 1989).

Protein damage is frequently an important consequence of oxidative stress, and Oliver *et al*., (1990) showed that radicals can damage brain proteins, including the enzyme glutamine synthetase (GS), which is responsible for the removal of glutamate. Oxidative

inactivation renders GS and other enzymes highly susceptible to proteolysis by proteases such as trypsin and subtilisin as well as by a class of cytosolic proteases that selectively degrade the oxidized protens *in vivo* and *in vitro*. Oliver *et al*., (1990) proposed that oxidative modification of proteins is a marking step for selective proteolysis. Additional evidence suggests that this process is important in a variety of normal and pathological processes, such as aging, neutrophil function, rheumatoid arthritis and oxygen toxicity (Oliver *et al*., 1990).

1.3.10. Heat Shock Response to Oxidative Stress

Heat shock proteins are synthesized in response to any form of stress in the cell that results in a denaturing of proteins. Oxidative stress is one condition in which the inappropriate folding of proteins is favoured. This results in a heat shock response in the cell, which is characterized by a shutdown of protein synthesis and a dramatic increase in the synthesis of heat shock proteins (Hsp's), (Smith *et al*., 1998). There are several types of Hsp families, each differing with respect to sequence and expression patterns, as well as function and subcellular localization of the respective gene products. Major Hsp families, named to reflect the approximate molecular size (in kilodaltons) of family members, are Hsp100, Hsp90, Hsp70, Hsp60, Hsp40 and the small Hsp family (typically 20 to 25 kDa), (Smith *et al*., 1998).

Hsp70 is the molecular chaperone mainly involved in the refolding of proteins. Chaperones achieve this by controlled binding and release of the substrate protein, facilitating its correct folding, oligometric assembly and transport to a particular subcellular compartment (Hendrick & Hartl, 1993). In addition, this chaperone exhibits a protective effect following tissue injury. Currie *et al*., 1988, first demonstrated that heat stress promotes recovery of heart tissues from ischemic injury. This protection correlated with the time course of Hsp70 levels (Yellon & Latchman, 1992), and transgenic mice overexpressing Hsp70 exhibit reduced postischemic injury (Marber *et al*., 1995). A recent article reported that Hsp70 protects a stressed cell via an anti-apoptotic function (Beere *et al*., 2000). Apoptosis is programmed cell death. The mechanism underlying this Hsp70-mediated suppression of apoptosis is only just beginning to unfold. However, evidence suggests that Hsp70 targets the APAF-1 (apoptotic protease-activating factor)

apoptosome, thereby inhibiting the activation of procaspase-9, which occurs during apoptosis (Beere *et al*., 2000).

It is believed that one of the major causal factors of senescence is the accumulation of damaged protein induced by oxidative stress (Jazwinski, 1996). Thus molecular chaperones may cope with and suppress the accumulation of these damaged proteins, thereby contributing to the delay of senescence and an increased life span. Naturally extreme overexpression of molecular chaperones has some deleterious effects on the growth of an organism (Krebs & Feder, 1997).

1.4. CELL DEATH

1.4.1. Introduction

Cell death can occur by either of two distinct (Vermes & Haanan, 1994) mechanisms, necrosis or apoptosis. In addition, certain chemical compounds and cells are said to be cytotoxic to the cell, that is, to cause its death. Necrosis is briefly described as "accidental" cell death (Wylie *et al*., 1998). It is the pathological process which occurs when cells are exposed to a serious physical or chemical insult. Apoptosis is described as "normal" or programmed cell death and is the physiological process by which unwanted or useless cells are eliminated during development and other normal biological processes (Wylie *et al*., 1998). Cytotoxicity is the cell-killing property of a chemical compound (such as a food, cosmetic, or pharmaceutical) or a mediator cell (cytotoxic T cell). In contrast to necrosis and apoptosis, this term cytotoxicity does not indicate a specific cellular death mechanism. For example, cell-mediated cytotoxicity (that is, cell death mediated by either cytotoxic T lymphocytes (CTL) or natural killer (NK) cells combines some aspects of both necrosis and apoptosis (Berke, 1991). There are many observable morphological and biochemical differences between necrosis and apoptosis and these are highlighted in figure 1.8 and table 1.3.

Table 1.3: Differential features and significance of necrosis and apoptosis as adapted from Wylie *et al*., (1998).

NECROSIS	APOPTOSIS
Morphological Features	
• Loss of membrane integrity. • Begins with swelling of cytoplasm and mitochondria. • Ends with total cell lysis. • No vesicle formation, complete lysis. • Disintegration (swelling) of organelles.	• Membrane blebbing, but no loss of integrity. • Aggregation of chromatin at the nuclear membrane. • Begins with shrinkage of cytoplasm and condensation of nucleus. • Ends with fragmentation of cell into smaller bodies. • Formation of membrane bound vesicles (apoptotic bodies). • Mitochondria become leaky due to pore formation involving proteins of the bcl-2 family.
Biochemical Features	
• Loss of regulation of ion homeostasis. • No energy requirement (passive process, also occurs at 4^{o}C). • Random digestion of DNA (smear of DNA after agrose gel electrophoresis). • Postlytic DNA fragmentation (late event of death).	• Tightly regulated process involving activation and enzymatic steps. • Energy (ATP)-dependent (active process, does not occur at 4^{o}C). • Non-random mono-and oligonucleosomal length fragmentation of DNA (Ladder pattern after agrose gel electrophoresis). • Prelytic DNA fragmentation • Release of various factors (cytochrome c, AIF) into cytoplasm by mitochondria. • Activation of caspase cascade • Alterations in membrane asymmetry (i.e. translocation of phosphatidyl-serine from the cytoplasmic to the extracellular side of the membrane).
Physiological Significance	
• Affects groups of contiguous cells. • Evoked by non-physiological disturbances (complement attack, lytic viruses, hypothermia, hypoxia, ischemia, metabolic processes). • Phagocytosis by macrophages. • Significant inflammatory response.	• Affects individual cells • Induced by physiological stimuli (lack of growth factors, changes in hormone environment). • Phagocytosis by adjacent cells or macrophages. • No inflammatory response.
Chemotactic factors stimulate neurtophil infiltration to degrade dead cells.	Apoptotic bodies are phagocytosed and intact; generally no neutrophil infiltration occurs.

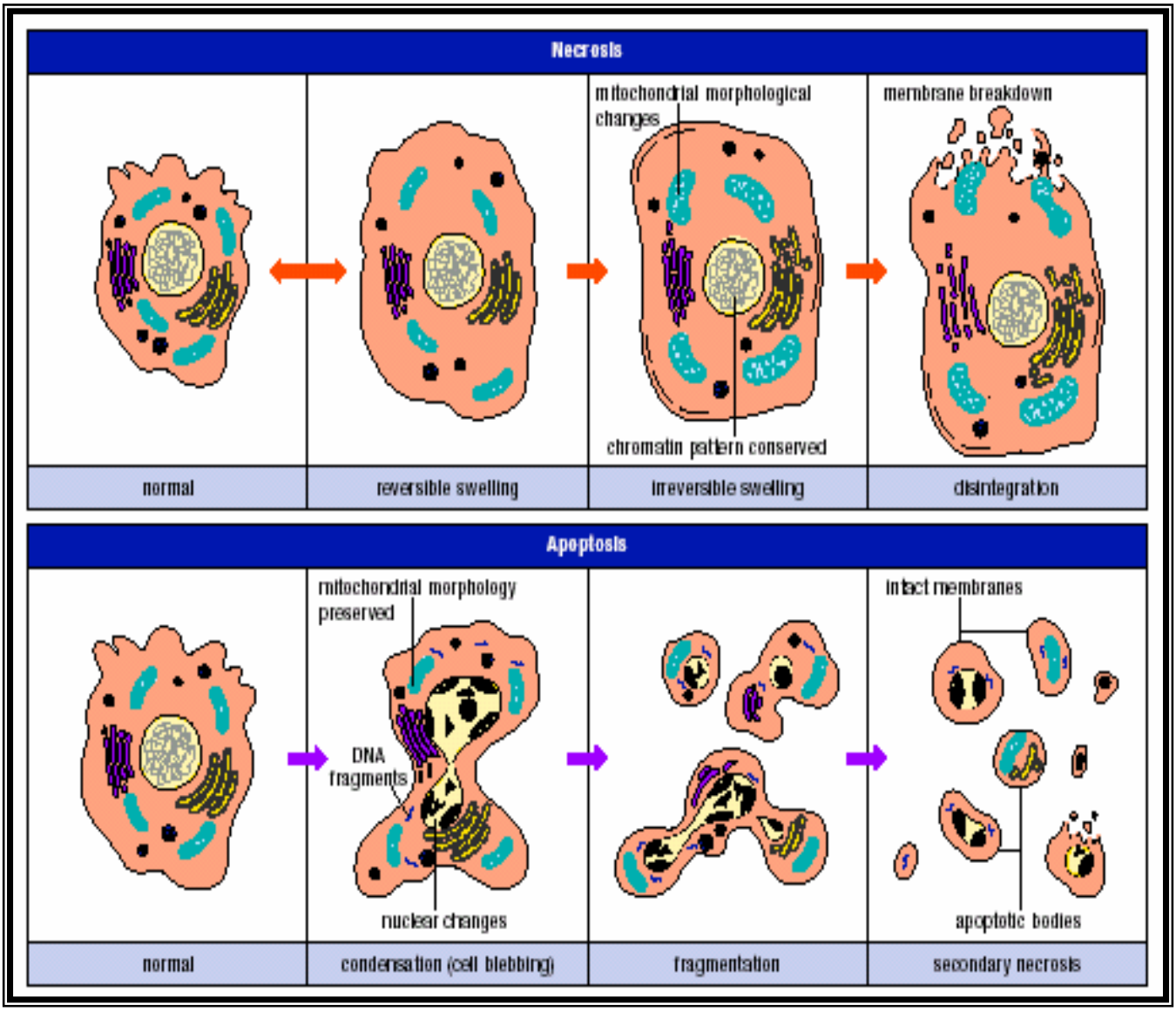

Figure 1.8: Illustration of the morphological features of necrosis and apoptosis. (Wylie *et al*., 1998).

1.4.2. Necrosis

Necrosis is normally the result of a severe insult resulting in cell damage characterized by rapid breakdown of all membrane systems and disruption of organelles as the whole cell swells and increases in size. Necrosis occurs when cells are exposed to extreme variance from physiological conditions (e.g. hypothermia, hypoxia) which may result in damage to the plasma membrane. Under physiological conditions direct damage to the plasma membrane is evoked by agents like complement and lytic viruses (Wylie *et al*, 1998). Necrosis begins with an impairment of the cell's ability to maintain homeostasis, leading to an influx of water and extracellular ions. Intracellular organelles, most notably the

mitochondria, and the entire cell swell and rupture (cell lysis). Due to the ultimate breakdown of the plasma membrane, the cytoplasmic contents including lysosomal enzymes are released into the extracellular fluid. Therefore, *in vivo*, necrotic cell death is often associated with extensive tissue damage resulting in an intense inflammatory response (Van Furth & Van Zwet, 1988) and randomly degraded DNA (Gschwind & Huber, 1997).

1.4.3. Apoptosis

Naturally occurring cell death (NOCD) has been recognized for many years as a critical phase in the development of the nervous system (Hamburger & Levi-Montalcini, 1949). During this process, immature neurons undergo an active process of cell death, probably because they receive in sufficient quantities of trophic factors from their target cells. Active cell death implies a molecular program of cellular-self-destruction and is therefore often called programmed cell death (PCD) (Schwartz & Osborne, 1993). Diverse morphological types of PCD have been described with apoptosis being the most commonly encountered (Kerr *et al*., 1972). After NOCD period, neuronal apoptosis is considered to be pathological and is found to be implicated in clinical outcomes, such as Alzheimer's disease, Parkinson's disease, or Huntington's disease (Martinou *et al*., 1997).

Over the past five or six years there has been a near-exponential increase in publications on apoptosis. The term apoptosis first appeared in biomedical literature in 1972, to delineate a structurally-distinctive mode of cell death responsible for cell loss within living tissues (Kerr *et al*., 1972). Cells undergoing apoptosis show characteristic morphological and biochemical features (Cohen, 1993). These include chromatin condensation, nuclear and cytoplasmic condensation, partition of cytoplasm and nucleus into membrane bound-vesicles (apoptotic bodies) which contain ribosomes, morphologically intact mitochondria and nuclear material (Savill *et al*., 1989). The transient morphological features are cell shrinkage, accompanied by transient but violent bubbling and blebbing from the surface, and culminating in separation of the cell into a cluster of membrane-bounded bodies. Organellar structure is usually preserved intact, but the nucleus undergoes a characteristic condensation of chromatin, initiated at sublamellar foci and often extending to generate torodial or cap-like, densely heterochromatic regions

(Savill *et al*., 1989). Changes in several cell surface molecules also ensure that, in tissues, apoptotic cells are immediately recognized and phagocytosed by their macrophages or adjacent epithelial cells (Savill *et al*., 1989, Wylie *et al*., 1998). Due to the efficient mechanism for removal of apoptotic cells *in vivo* no inflammatory response is elicited. *In vitro*, the apoptotic bodies as well as the remaining cell fragments ultimately swell and finally lyse. This terminal phase of *in vitro* cell death has been termed "secondary necrosis" (figure 1.8).

Apoptosis is a remarkable process responsible for cell death in development, normal tissue turnover, atrophy induced by endocrine and other stimuli, negative selection in the immune system, and a substantial proportion of T-cell killing. It also accounts for many cell deaths following exposure to cytotoxic compounds, hypoxia, or viral infection. It is a major factor in the cell kinetics of tumors, both growing and regressing. Many cancer therapeutic agents exert effects through initiations of apoptosis, and even the process of carcinogenesis itself seems sometimes to depend upon a selective, critical failure of apoptosis that permits the survival of cells after mutagenic DNA damage. Apoptosis probably contributes to many chronic processes, including Alzheimer's disease, Parkinson's disease, and heart failure (Wylie *et al*., 1998). In oncology, extensive interest in apoptosis comes from observation, that this mode of cell death is triggered by a variety of antitumor drugs, radiation, and hypothermia, and that the intrinsic propensity of tumor cells to respond by apoptosis is modulated by expression of several oncogenes and may be a prognostic marker for cancer treatment (Hickman, 1992).

Apoptosis, or programmed cell death, is a normal component of the development and health of multicellular organisms. Apoptosis is the most common form of eukaryotic cell death. It is a physiological suicide mechanism that preserves homeostasis, in which cell death naturally occurs during normal tissue (Wylie *et al*., 1998; Kerr *et al*., 1972). In general, cells undergoing apoptosis display a characteristic pattern of structural changes in nucleus and cytoplasm, including rapid blebbing of the plasma membrane and nuclear disintegration.

These biological events occurring with apoptosis are induced by such stimuli as hormones, growth factor withdrawal, oxidative stress, DNA damaging reagent, and antitumour drugs which kill tumors through the induction of apoptosis (Ogata *et al*.,

2000). The mechanism for apoptosis is not well known, but numerous studies have implicated the cascade of caspases (cysteine aspartate-specific proteases) in the process of apoptosis (Martin & Green, 1995). Particularly caspase-3 protease cleaves one of its substrates, poly (ADP-ribose) polymerase, to generate the 85-kDa fragment during apoptosis in many eukaryotic cells (Lazebnik *et al*., 1994). NAD is an impotant coenzyme in oxidation-reduction reactions and is also a subtrate for PARP (Ogata *et al*., 2000).

1.4.3.1. Induction of Apoptosis

Scientists now recognise that most, if not all, physiological cell death occurs by apoptosis, and that alteration of apoptosis may result in a variety of malignant disorders (Wylie *et al*., 1998). Cells die in response to a variety of stimuli and during apoptosis they do so in a controlled, regulated fashion. This makes apoptosis distinct from another form of cell death called necrosis in which uncontrolled cell death leads to lysis of cells, inflammatory responses and, potentially, to serious health problems. Apoptosis, by contrast, is a process in which cells play an active role in their own death, which is why apoptosis is often referred to as cell suicide. (www.sghms.ac.uk/depts/immunology/.html).

There are a number of mechanisms through which apoptosis can be induced in cells. The sensitivity of cells to any of these stimuli can vary depending on a number of factors such as the expression of pro- and anti-apoptotic proteins (eg. the Bcl-2 proteins), the severity of the stimulus and the stage of the cell cycle. Some of the major stimuli that can induce apoptosis are outlined in the illustration below (figure 1.9). Apoptosis is essential in many physiological processes, including maturation and effector mechanisms of the immune system (Allen *et al*., 1993; Cohen & Duke, 1992), embryonic development of tissue, organs and limbs (Clarke, 1990), development of the nervous system (Johnson & Deckwerth, 1993; Batistatou & Greene, 1993) and hormone-dependent tissue remodeling (Strange *et al*., 1992). Inappropriate regulation of apoptosis may play an important role in many pathological conditions like ischemia, stroke, heart disease, cancer, AIDS, autoimmunity, hepatotoxicity and degenerative diseases of the CNS (Edgington, 1993; Gougeon & Montagnier, 1993).

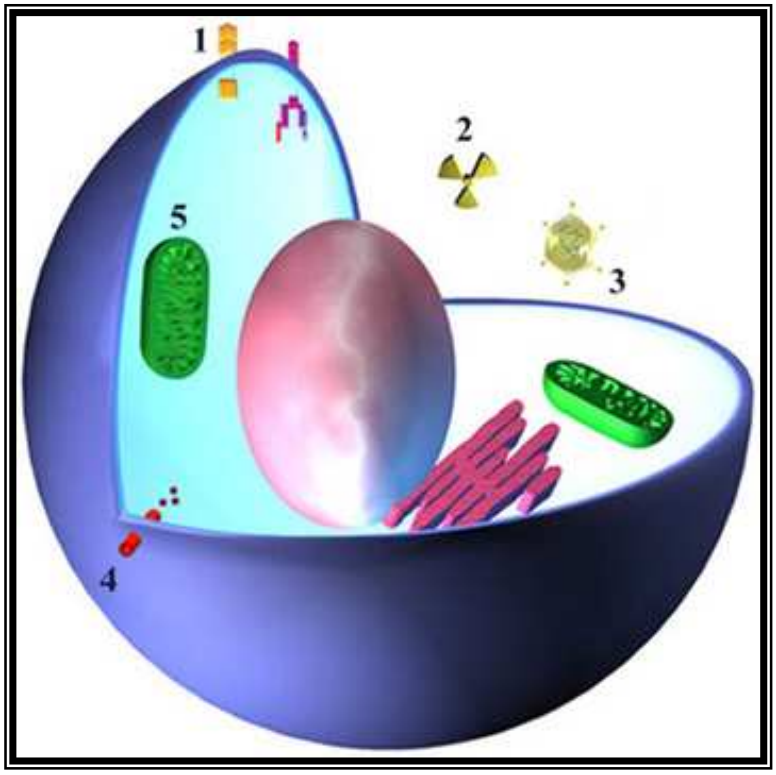

Figure 1.9: Some of the major stimuli that can induce apoptosis. In some cases the apoptotic stimuli comprise extrinsic signals such as the binding of death inducing ligands to cell surface receptors **(1)** or the induction of apoptosis by cytotoxic T-lymphocytes by granzyme **(4)**. The latter occurs when T-cells recognise damaged or virus infected cells and initiate apoptosis in order to prevent damaged cells from becoming neoplastic (cancerous) or virus-infected cells from spreading the infection. (www.sghms.ac.uk/depts/immun.html).

In other cases apoptosis is initiated following intrinsic signals that are produced following cellular stress. Cellular stress may occur from exposure to radiation **(2)** or chemicals or to viral infection **(3)**. It might also be a consequence of growth factor deprivation or oxidative stress. In general intrinsic signals initiate apoptosis via the involvement of the mitochondria **(5)**. The relative ratios of the various bcl-2 proteins can often determine how much cellular stress is necessary to induce apoptosis.

1.4.3.2. Nuclear Effects of Apoptosis

Upon receiving specific signals instructing the cells to undergo apoptosis a number of distinctive biochemical and morphological changes occur in the cell. A family of proteins known as caspases are typically activated in the early stages of apoptosis. These proteins breakdown or cleave key cellular substrates that are required for normal cellular function including structural proteins in the cytoskeleton and nuclear proteins such as DNA repair

enzymes. The caspases can also activate other degradative enzymes such as DNases, which begin to cleave the DNA in the nucleus. The result of these biochemical changes is appearance of morphological changes in the cell.

The nuclear collapse is associated with extensive damage to chromatin and DNA-cleavage into oligonucleosomal length DNA fragments after activation of a calcium-dependent endogenous endonuclease (Compton, 1992). However, very rare exceptions have been described where morphological features of apoptosis are not accompanied with oligonucleosomal DNA cleavage (Cohen & Duke, 1992). One of the hallmarks of apoptosis is the cleavage of chromosomal DNA into nucleosomal units. The degradation of DNA in the nuclei of apoptotic cells is accomplished in a number of ways following activation of caspases. The processes leading to DNA cleavage and nuclear changes are illustrated in figure 1.10.

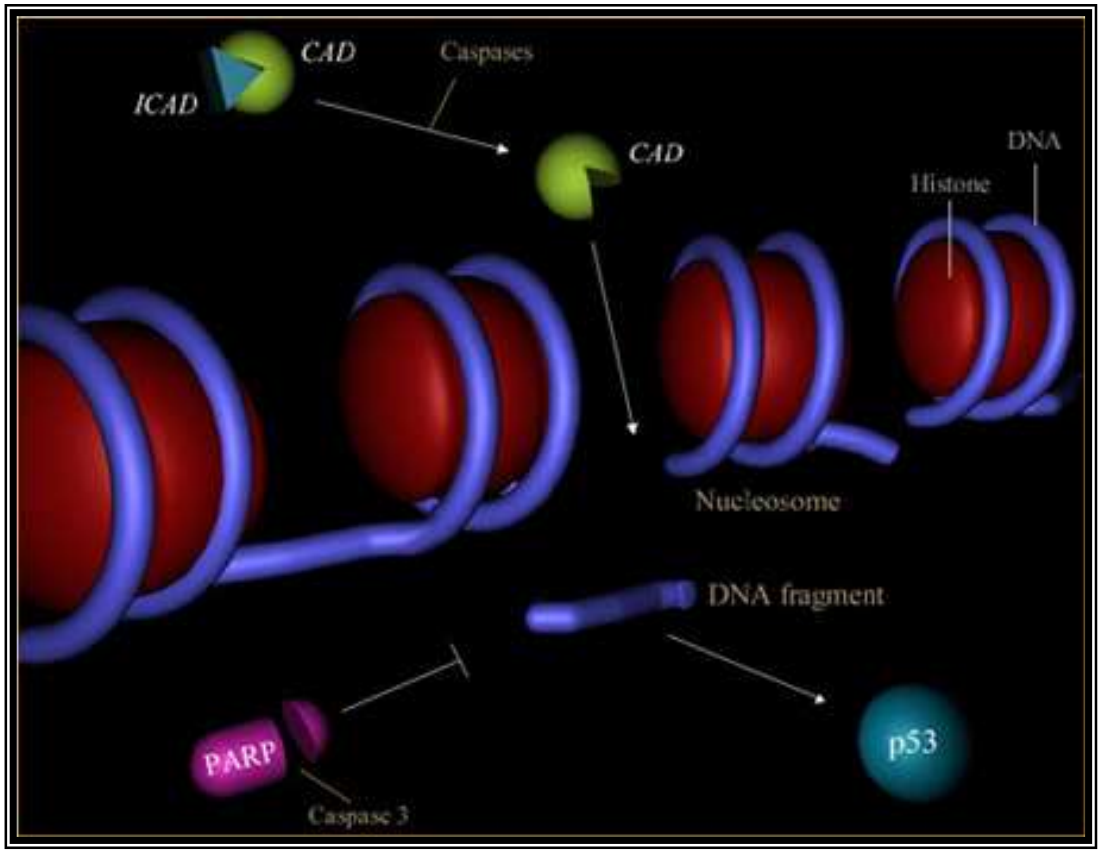

Figure 1.10: Processes leading to DNA cleavage and nuclear changes in the cell. (www.sghms.ac.uk/depts/immunology/%7Edash/apoptosis/intro.html).

1.5. MELATONIN

1.5.1. Introduction

Most scientists believed that the pineal gland or pineal body did not serve any particular purpose and that it was a relic of early days of human development, which eventually became obsolete due to the evolution of the organism. After centuries of disregard and unfounded philosophical ideologies, the pineal gland has, over the past decade, finally been acknowledged as an important functional neuroendocrine gland. Herophilos (325-280BC) is credited with discovering the human pineal gland. At the time of discovery he and other investigators were examining the brain in an attempt to find the soul in the body. For the next 2000 years, very little knowledge was accumulated on the pineal gland, although both doctors and philosophers from Europe and Asia considered the pineal to be a prime candidate for the seat of the soul. The pineal gland was implicated as the regulator of the flow of the spirit, and this lead the philosopher, René Descartes, to proclaim that the pineal gland was the seat of the soul (Pevét, 1984). The full extent of the function of the pineal gland is not yet known. This has stimulated vast research worldwide in an attempt to elucidate the role of the pineal gland in the mammalian body. Presently, the pineal gland is recognised as an endocrine gland and its major metabolite, melatonin, as a antioxidant. Melatonin which is the principal pineal neurohormone, has been the focus of the larger part of pineal research.

1.5.2. History

Melatonin is phylogenetically very old. Melatonin is known to be produced in virtually all organisms in the animal kingdom. In 1917, McCord and Allen reported that extracts of bovine pineals produced a dramatic blanching of skins in amphibians (Pevét, 1984). Forty-two years later, in 1958, the compound responsible for this blanching was isolated from the mammalian pineal gland by Lerner and Case, and chemically analysed for the first time (Reiter, 1997). This compound was identified as N-acetyl-5-methoxytryptamine. Since it caused aggregation of melanin granules with melanophores, Lerner and collegues named the compound melatonin (Pevét, 1984). Melatonin comes from the Greek word *melas* which is black and *tosos* which is laboratory. They found that

in certain laboratory frogs this substance could cause a change in the pigment cells of the skin, and thus a change in skin colour. By 1963, it had been proven that melatonin had an effect on the sexual function of rats, and subsequently it was categorised as a hormone (Kuchowsky, 2001). For a small number of selected scientist, this development marked the beginning of an interesting and exciting journey into an area, which had until then, remained relatively untouched.

1.5.3. Biosynthesis

Melatonin, 5-methoxy-N-acetyltryptamine is a derivative of the amino acid tryptophan with a phylogenetic ubiquitous distribution. Melatonin is found in plants (Reiter *et al.*, 2001; Van Tassel *et al.*, 2001), bacteria (Manchester *et al.*, 1995), unicells (Hardeland *et al.*, 1995) and invertebrates (Hardeland & Fuhrberg, 1996) as well as in vertebrates (Reiter, 1991) including man (Brzezinski, 1997). In mammals, it is likely produced in a variety of organs and cells (Bubenik, 2001) but it is best known as the major secretory product of the pineal gland (Reiter, 1991). Melatonin is primarily synthesized in the pineal gland by the pinealocytes. The different stages are outlined in figure 1.11. It commences with the uptake of tryptophan from the blood stream. Some of the tryptophan is utilised in the synthesis of pineal proteins, but the majority is converted to 5-hydroxytryptophan by the enzyme tryptophan hydroxylase (Lovenberg *et al.*, 1967). This step occurs in the presence of O_2, Fe^{2+} and a reduced pteridine cofactor (Snyder & Axelrod, 1964). The enzyme has a low affinity for tryptophan, which is its substrate. Tryptophan availablity is therefore the rate-determining factor for this enzyme.

5-Hydroxytryptophan is then decarboxylated by L-aromatic amino acid decarboxylase. This leads to the formation of 5-hydroxytryptamine or serotonin (Lovenberg *et al.*, 1967). Serotonin is allowed to accumulate in the pineal gland, before it is converted to melatonin. Thus, the major fraction of serotonin is then converted to melatonin via a two step process. First, N-acetyltransferase transfers an acetyl group from acetyl coenzyme A to the amino group of serotonin to form N-acetylserotonin. This process occurs during the hours of darkness. This is because N-acetyltransferase is the rate-limiting enzyme in melatonin synthesis (Saarela & and Reiter, 1993), with its function in the pineal gland being regulated by the release of noradrenaline (Freur, 1990) by the postganglionic

synaptic fibres. N-acetylserotonin is the precursor of melatonin (Klein *et al*., 1971). N-acetylserotonin is then O-methylated by hydroxyindole-O-methyltransferase to form melatonin (see figure 1.11).

Melatonin synthesis is not confined to the pineal gland. Presently, melatonin is known to be synthesized in the retina, the Harderian gland, the intra-orbital lacrimal glands, and the enterochromaffin cells of the gastro-intestinal tract (Raikhlin & Kvetnoy, 1976).

1.5.4. Circadian Variation in Melatonin Synthesis

In vertebrates, melatonin production in the pineal gland exhibits a circadian rhythm, with the highest levels of melatonin being produced during the night. Fiske *et al*., (1960), reported that the pineal gland decreases in size and mass following continuous exposure to light. This was the first report of the influence of light on the pineal gland.

The rhythm of melatonin synthesis depends primarily on the activity of the enzyme serotonin-N-acetyltransferase (NAT) (see figure 1.12). This enzyme is the rate-limiting enzyme in the synthesis of melatonin (Reiter *et al*., 1994). The circadian rhythm in NAT-activity is responsible for the circadian rhythm in melatonin production. Activation of NAT is controlled by signals from photoreceptor cells. Melatonin synthesis in the mammalian pineal gland is regulated by endogenous oscillators and photoreceptors in the retina of the eye. Thus, the production of melatonin is controlled by a visual signal that originates in the retina. The eye is functionally and anatomically connected to the pineal gland by a neural network. During the hours of darkness, the retina initiates the production of melatonin, by passing a signal along unmyelinated fibres (Saarela & Reiter, 1993; Hendrickson *et al*., 1972) suprachiasmatic nucleus (SCN) of the hypothalamus (Illnerová *et al*., 1993). In mammals the endogeous oscillator is believed to be located in the SCN. The suprachiasmatic nucleus is the body's internal clock which controls circadian rhythmicity of biological events and behaviour (Saarela & Reiter, 1993; Delagrange and Guardiola-Lemaître, 1993; Tenn & Niles, 1993). Light synchronises this clock to the external environment by daily adjustments in the circadian oscillation (Ding *et al*., 1994). The SCN has been shown to contain melatonin receptors named the ML1

receptor (Hagan & Oakley, 1995). The effect of light on pineal function is attributed to the inhibitory effects of light on the sympathetic nerves to the pineal gland (Klein, 1973).

A pathway then stretches from the SCN, through the lateral hypothalamus to the upper thoracic intermedio-lateral cell column. Impulses are conveyed via the medial forebrain to the spinal cord by preganglionic cell bodies synapsing in the superior cervical ganglion (Saper *et al.*, 1976). Finally, post ganglionic fibres approach the pineal together with the pineal blood vessels. When stimulated during darkness, the postganglionic sympathetic fibres release noradrenaline which binds to specific β-adrenergic receptors on the pinealocyte cell membrane (Saarela & Reiter, 1993), so activating melatonin production in the pineal gland.

NAT activity has been shown to be lower during the day (Reiter, 1997), resulting in lower melatonin production during the day. At night, NAT is activated as described earlier, and melatonin production increases. The activity of NAT is 30-70 fold greater at night than during the day (Arendt, 1988; Daya, 1999). As a result of this circadian rhythm, the physiological levels of melatonin in body fluids and tissues vary according to the light/dark cycle. At night, blood melatonin levels reach values of 150pg/ml, which is ten times higher than daytime values (Arendt, 1988).

1.5.5. Secretion and Distribution

Melatonin is not stored in large pools in the pineal gland. Due to its high lipophilicity, melatonin is secreted from the pinealocytes by diffusion. Melatonin is released directly into the blood vascular system, and secondarily into other body fluids which include blood and saliva (Lewis *et al.*, 1990). The normal route of melatonin secretion comprises of the pineal capillaries draining into the surrounding venous sinuses. This view is based on animal experiments as well as human data (Freuer, 1990). Melatonin is transported in the blood non-covalently bound to high-capacity (60-70%), low affinity binding sites on plasma albumin (Van Wyk, 1993), while in cerebrospinal fluid, melatonin is present in its free form (Freuer, 1990). Due to its unique lipophilic and hydrophilic nature (Cagnacci, 1996), melatonin is able to easily diffuse into most tissue and cells in the body. Melatonin has a relatively short life in blood, and during a single passage through the body,

approximately 90% is taken up into the tissues (Lewis *et al*., 1990). In addition melatonin is not in equilibrium in the body (Reiter and Tan, 2003) and since melatonin is derived from multiple sites in the body, concentrations of melatonin in the CSF may be greatly elevated over the concentrations in the blood (Skinner and Malpaux, 1999; Tricoires *et al*., 2002).

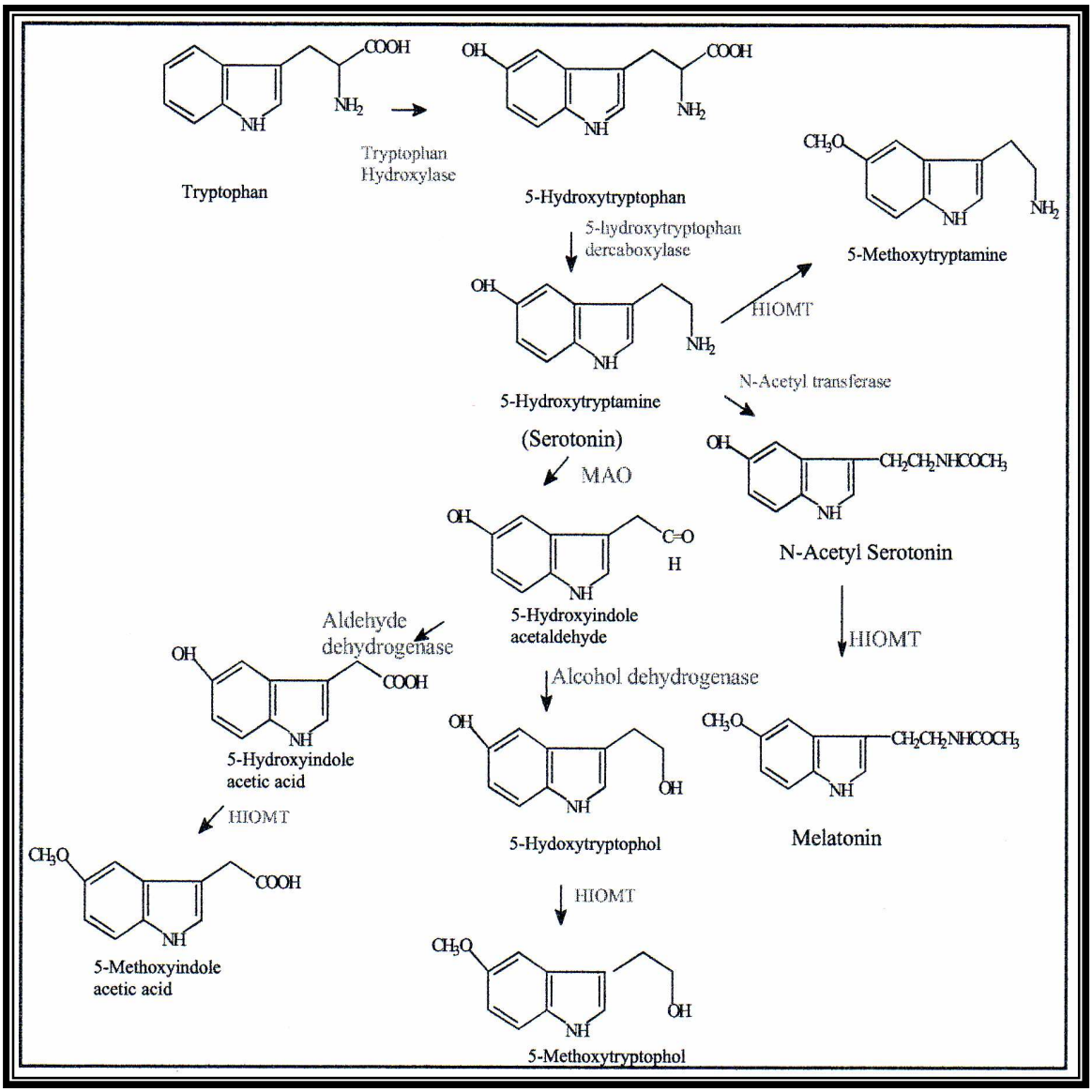

Figure 1.11: The pathway of melatonin and other indole metabolism (modified from Young and Silman, 1982).

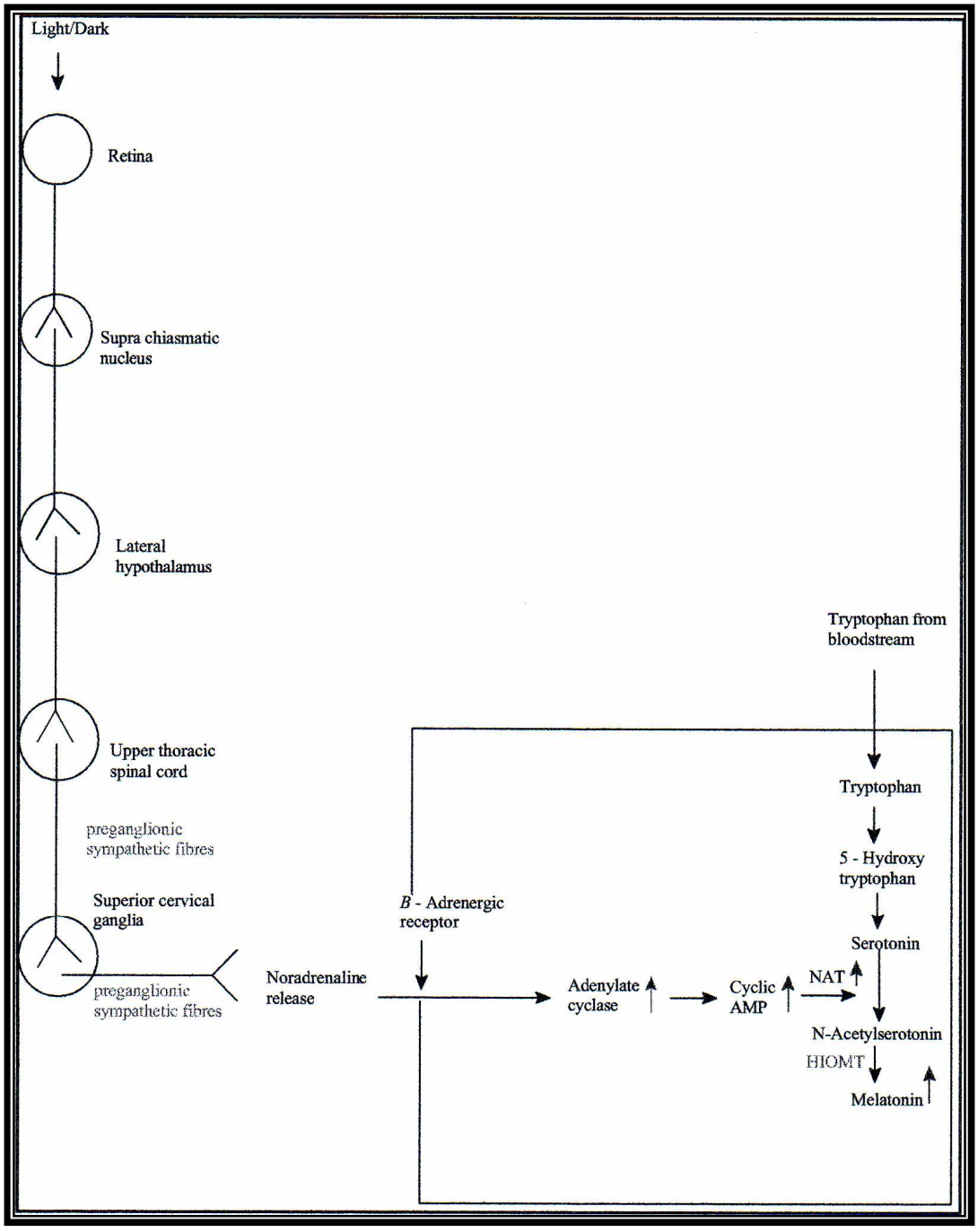

Figure 1.12: Schematic representation of the actions of light and innervation on melatonin synthesis in the pineal gland (Freuer, 1990).

1.5.6. Metabolism

The turnover of melatonin is fairly quick. The half-life of melatonin in rats (Gibbs & Vriend, 1981) and sheep is only about 20 minutes. Approximately 75% of the melatonin taken up by the liver is inactivated by hepatic cytochrome P-450-dependent microsomal enzymes, via hydroxylation, to form 6-hydroxymelatonin (6-OHM) (Kopin *et al.*, 1961).

Most of the 6-hydroxymelatonin is further conjugated to sulphate, rendering 6-sulphatoxymelatonin as the major urinary metabolite (Saarela & Reiter, 1993; Kopin *et al.*, 1961; Valtonen *et al.*, 1993; Wurtman *et al.*, 1964), although 6-hydroxymelatonin can also be conjugated to glucuronic acid (Cagnacci, 1996; Kopin *et al.*, 1961). These products are excreted in the urine. The catabolism pathway of melatonin in the CNS is different from that in the liver. In the brain, excess melatonin is converted to N-acetyl-5-N-methoxykynurenamine by the enzyme indoleamine-2, 3-dioxygenase which cleaves the pyrrole ring of melaotnin (Reiter, 1991). This is then converted to N-acetyl-5-methoxykynurenine by hydrolysis (figure 1.13).

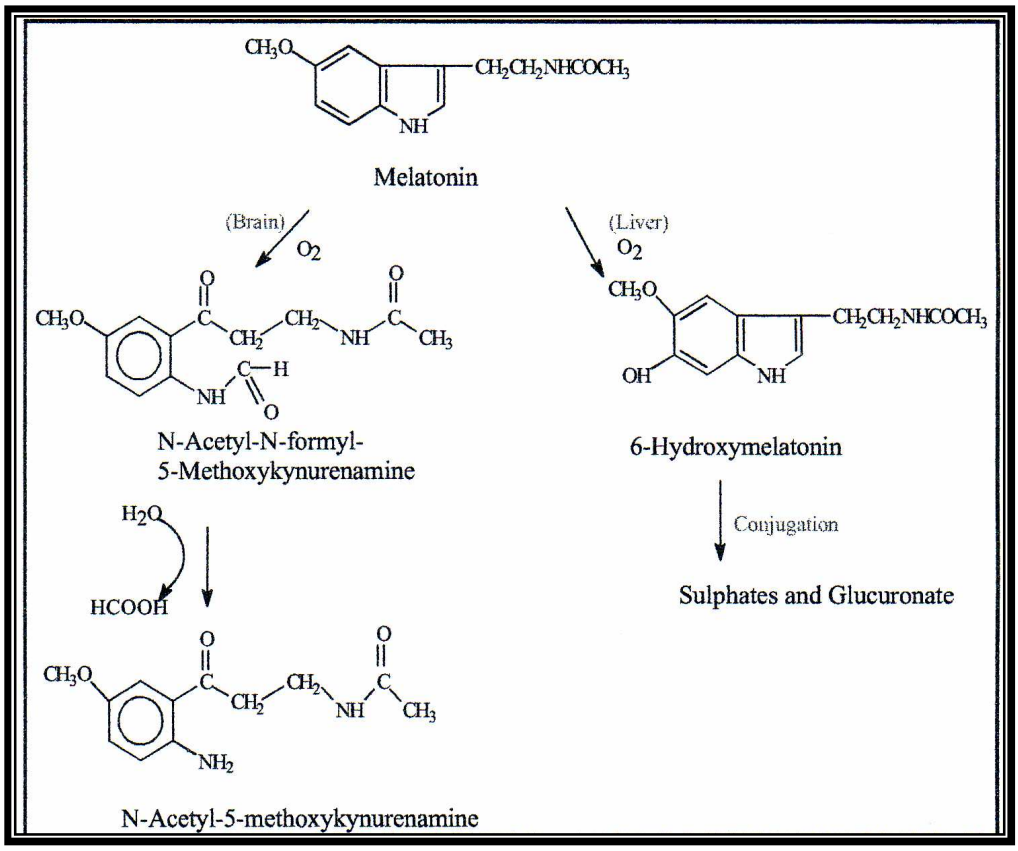

Figure 1.13: The catabolism of melatonin in the brain and liver (Freuer, 1990)

1.5.7. Effects of Disturbances to the Diurnal Melatonin Cycle

Because the production of melatoin is regulated by the intensity of the light falling on the retina, the time of the day and even the season of the year (Van Someren *et al.*, 1993) affect melatonin production. Any disturbances that throw the melatonin cycle out of phase with the natural circadian rhythms of the body can harm human well-being (Savides *et al.*, 1986).

Seasonal Affective Disorder is characterized by periodically recurring depressive episodes (Lingjaerde *et al*., 1993; Koehler *et al*., 1993; Harris & Dawson-Hughes, 1993), which normally occur during winter. This disorder is especially prevalent in Scandinavian countries, where it is proposed that a patient's circadian clock does not adjust correctly in accordance with the changes in day length, that occur during the different seasons. Normally the acrophase of the melatonin cycle is either, phase advanced or phase delayed with respect to healthy subjects, in patients with this disorder. This results in a melatonin cycle out of phase with the patient's general environment, and leads to the periods of depression or mania. Treatment involves synchronizing the melatonin rhythm with the day / night cycle over a period of 4-14 days (Lewy, 1987). This is done by exposing phase advanced patients to 2 500 lux light for 2 hours in the morning, and phase delayed patients to the same amount of light in the evening. Morning appears to be the most beneficial time to give light treatment in most cases, indicating that circadian rhythms are more likely to be delayed in seasonal affective disorder patients when compared to controls (Lingjaerde *et al*., 1993; Lewy, 1987).

Jet-lag results from a similar shift in the melatonin acrophase. Flying over many time zones results in a melatonin circadian rhythm that is out of phase with the general environment (Oakley, 1993). Symptoms such as sleep disturbance, loss of appetite, reduced psychomotor efficiency and general malaise may occur. Fortunately most people are able to adjust their circadian rhythms to suit the new environment within a few days (Reinberg & Smolensky, 1983). Taking 5mg of melatonin (Lino *et al*., 1993) at the local bed time, for the first two days in the new time zone, can be beneficial for helping to speed up changes in the circadian rhythm. However, melatonin given for 3 days prior to arrival and 5 days after return showed a worse recovery than placebo (Petrie *et al*., 1993). Therefore, the correct usage of melatonin is advisable. The use of melatonin as a therapeutic agent against jet-lag does not appear to have any undesirable endocrine effects (Wright *et al*., 1986), with the only side effect being the promotion of drowsiness (Sugden, 1983).

It has also been reported (Waterhouse, 1993) that the depressive effects and feelings of disorientation that many night workers experience could be caused by a circadian rhythm that is out of phase with the environment. In this case however, melatonin treatment

would not be therapeutic as the work environment is completely out of phase with the signals from the natural environment that help to regulate the circadian rhythms.

1.5.8. Mechanism of action of Melatonin

From a phylogenetic point of view, melatonin is a molecule present in organisms from unicells to mammals. Since tryptophan and serotonin (melatonin precursors) are present at early stages of cell phylogeny, the presence of melatonin is also suggested. Tryptophan metabolites including melatonin are antioxidants, and from a hypothetical point of view, the first function of melatonin may have been as an antioxidant (Acuña-Castroviejo *et al*., 2001). The discovery of different targets in the cell suggests a variety of mechanisms of action for this compound. At the present, melatonin's mechanism of action seems to fall into three catogories (Acuña-Castroviejo *et al*., 2001):

a) receptor-mediated,
b) protein-mediated,
c) and non protein-mediated effects.

Receptor-mediated melatonin events involve both membrane and nuclear receptors. Although membrane melatonin receptors have been identified and are well characterized in humans (Conway *et al*., 2000), some of the receptor-related antioxidant effects of melatonin seen also to be related to its nuclear receptors (Acuña-Castroviejo *et al*., 1994; Becker-André *et al*., 1994; Garcia-Mauriño *et al*., 2000). The expression of some enzymes, mainly related to the endogenous antioxidant system of the cell, such as GPx, GRd, SOD and NOS (Antolin *et al*., 1996; Crespo *et al*., 1999), are under genomic regulation by melatonin. The interaction between membrane and nuclear melatonin signaling has been proposed (Carlberg & Wiesenberg, 1995).

Experimental evidence has clearly demonstrated the interaction of melatonin with Ca^{2+}-calmodulin (CaCaM), a ubiquitous protein in the cell. High affinity binding of melatonin to CaM has been characterised (Romero *et al*., 1998). The significance of melatonin-CaCaM interaction was emphasized in a series of experiments showing changes in the cytoskeletal rearrangements due to this interaction (Benitez-King, 2000). Also the binding of melatonin to CaCaM inhibits intracellular CaCaM-dependent enzymes such as NOS

(León *et al*., 2000). Hence, melatonin inhibits $NO^{\bullet}$ production. The non-protein-mediated effects of melatonin deals directly withs its direct free radical scavenging actions. Which is described in detail in section 1.5.9.2.

1.5.9. Melatonin and Oxidative Stress

1.5.9.1. Introduction

Of significance is that melatonin levels wane with increasing age such that, in the elderly, melatonin concentrations in the blood are only a fraction of those in the young (Reiter, 1992). Functionally, melatonin has been linked to the regulation of seasonal reproduction (Reiter, 1980), strengthening of circadian rhythms (Ardent, 1988), stimulation of the immune system (Guerrero & Reiter, 1992; 2002; Maestroni, 2001), inhibition of cancer initiation (Reiter, 1999; Karbownik & Reiter, 2000) and tumour growth (Blask *et al*., 1991; Sauer *et al*., 2001) and sleep processes (Garfinkel *et al*., 1995; Dijk & Cajochen, 1997). That melatonin functions as a powerful free radical scavenger and antioxidant was only uncovered in the last decade (Poeggeler *et al*., 1993; Tan *et al*., 1993a ; Hardeland *et al*., 1995; Reiter *et al*., 1995; 2002a). Considering the diminished melatonin production in aged organisms (Reiter, 1992), the functions of melatonin are likewise attenuated in the elderly.

1.5.9.2. Melatonin and Free Radicals

Hundreds of reports have appeared in the last 8 years that have documented melatonin's ability to directly neutralize free radicals and related toxicants. The bulk of the reactants are listed in table 1.2 have been shown to be detoxified by melatonin. When injected into animals or given orally, melatonin levels quickly rise in the blood and, followed shortly thereafter, by its uptake into tissue (Menéndez-Peláez *et al*., 1993; Menéndez-Peláez & Reiter, 1993). Its levels in tissues can exeed blood concentrations manifold. There are no morphophysiological barriers to melatonin; this is apparent in reference to the brain were melatonin concentrations increase soon after peripheral administration of the indoleamine (Menéndez-Peláez *et al*., 1993). The first indication that melatonin may be a direct free radical scavenger actually appeared in 1991, but the details relating to what was done and

the specific findings are difficult to unravel because of incomplete methodological details and poor English composition of the report (Ianas *et al*., 1991). However the authors did conclude, that melatonin possesses both antioxidant and pro-oxidant activity, a feature common to a number of so-called antioxidants. Two years later, Tan *et al* (1993a,b) provided strong evidence that melatonin was highly effective in detoxifying the highly reactive $^{\bullet}OH$.

1.5.9.3 Melatonin: Direct Scavenging Actions

1.5.9.3.1. Melatonin and Superoxide Anions

Melatonin is minimally reactive with $O_2^{\bullet-}$ (Chan and Tang, 1996; Marshall *et al*., 1996) although one study in which electron spin resonance (ESR) was used to identify DMPO-$O_2^{\bullet-}$ adducts, melatonin was reported to be modestly interact with $O_2^{\bullet-}$ (Zang *et al*., 1998).

1.5.9.3.2. Melatonin and Hydrogen Peroxide

Recent evidence, however has uncovered a pathway whereby melatonin directly interacts with H_2O_2 to diminish its levels in a pure chemical system (Tan *et al*., 2000a). The product that results from the melaotnin-H_2O_2 interaction is N^1-acetyl-N^2-formyl-5-methoxykynuramine (AFMK) (Tan *et al*., 2001) (see figure 1.14). Additionally, AFMK was shown to be capable of donating two electrons and, therefore, being a direct free radical scavenger in its own right (Reiter *et al*., 2002). In specific experiments, AFMK reduced DNA damage induced by a combination of H_2O_2 and the transition metal Cr^{3+}, and also limited the destruction of lipids resulting from their exposure to H_2O_2 and other transition metals, Fe^{2+} (Tan *et al*., 2001).

1.5.9.3.3. Melatonin and Hydroxyl Radical

Definitive evidence that melatonin functioned as a direct scavenger of $^{\bullet}OH$ was provided by Tan *et al*., (1993a) and Poeggeler *et al*., (1994). For these studies H_2O_2 was exposed to 254nm ultraviolet light to generated $^{\bullet}OH$ that was captured with the spin-trapping agent 5,5-dimethylpyrrolien *N*-oxide (DMPO) using a well defined cell free system. The

resulting adducts ($^{\bullet}$OH-DMPO) were identified and quantified using electron spin resonance (ESR) spectroscopy, widely accepted as the most definitive method for identifying such adducts. When melatonin was added to the mixture in increasing concentrations, it progressively reduced $^{\bullet}$OH-DMPO, proving it had scavenged $^{\bullet}$OH so it was no longer available for adduct formation. Tan *et al*., (1993a) compared melatonin to two well-known $^{\bullet}$OH scavengers, glutathione and mannitol, and found that melatonin was significantly better than those agents. Structure activity studies revealed that the acetyl group on the side chain and the methoxy group at position 5 of the indole nucleus were both important for melatonin's $^{\bullet}$OH scavenging activity. Thus, melatonin scavenges $^{\bullet}$OH by contributing an electron, thereby rendering the radical non-reactive, but becoming itself a radical, the indolyl cation radical (Reiter *et al*., 1996) (see figure 1.14.) This product is not very reactive and is therefore non-toxic in the cell (Lewis *et al*., 1990). It is then believed that the indolyl cation radical then scavengers the $O_2^{\bullet-}$, thereby becoming AFMK which is excreted through the urinary system.

In 1998 it was shown that each melatonin molecule actually scavenges two $^{\bullet}$OH and generates the product cyclic-3-hydroxymelatonin (Tan *et al*., 1998). Many other studies have confirmed melatonin's ability to detoxify $^{\bullet}$OH (Matuszak *et al*., 1997; Susa *et al*., 1997; Bandyopadhyay *et al*., 2000; Brömme *et al*., 2000; Poeggeler *et al*., 2002). The calculated biomolecular rate constant for the melatonin/$^{\bullet}$OH reaction is $0.6x10^{11}{}_{M}{}^{-1}$ (Poeggeler *et al*., 1996).

The $^{\bullet}$OH scavenging ability of melatonin *in vitro* has also been confirmed by Pähkla *et al*., (1998) who used terephthalic acid (THA) as a chemical dosimeter of $^{\bullet}$OH since it forms an adduct that is, THA-$^{\bullet}$OH (Barreto *et al*., 1994). In this system melatonin in a concentration dependent manner reduced the formation of this adduct.

Poeggeler *et al*., (1994; 1995; 1996) further showed that melatonin is also an efficient radical scavenger in other *in vitro* systems. By measuring changes in indole fluorescence they showed that melatonin was quickly oxidized by $^{\bullet}$OH generated with Fenton reagents but not by iron itself. Likewise, they found that melatonin was oxidised in the presence of H_2O_2 only and found that melatonin synergised with other antioxidants for example, vitamin C and E, in the scavenging of radicals. This is an important observation because

it suggests that *in vivo*, particularly in the presence of other free radical scavengers, melatonin could have a role as a physiologically relevant antioxidant.

Evidence that exogenously administered melatonin acts *in vivo* to scavenge $^{\bullet}$OH was recently provided by Li *et al*., (1997). This group used the salicylate trapping method to show that melatonin administration to rats undergoing ischemia-reperfusion of the brain reduced dihydroxybenzoic acid (DHBA) in the microdialysate retrieved from the ischemic brain. DHBA is a specific product formed by the interaction of the $^{\bullet}$OH and salicylate and its reduction indicated that melatonin scavenged $^{\bullet}$OH thereby leading a reduced DHBA formation. This is the first evidence which showed that melatonin functions as a $^{\bullet}$OH quencher *in vivo*.

The significance of melatonin as an $^{\bullet}$OH scavenger relates to the fact that this reactant is generally considered the most damaging of all endogenously generated reactive agents. Once produced it plunders any molecule it encounters in its immediate vicinity (Reiter *et al*., 2002). Indeed, its high reactivity prevents it from moving more than a few molecular diameters from where it was produced before it biochemically alters a neighbouring molecule. Thus, for any scavenger to combat $^{\bullet}$OH-mediated damage it must be essentially at the site where the radical is produced to prevent its destructive actions. Unlike some other well known antioxidants that are exclusively lipid (e.g. vitamin E) or water (e.g. vitamin C) soluble and, therefore, exhibit a limited intracellular distribution, melatonin is amphiphilic allowing it to reduce $^{\bullet}$OH-mediated damage in both lipid and aqueous subcellular compartments (Reiter *et al*., 2002). Evidence has shown that melatonin is clearly highly soluble in lipid-based medium (Costa *et al*., 1997) and it has shown to dissolve to some extent in aqueous medium (Shida *et al*., 1994).

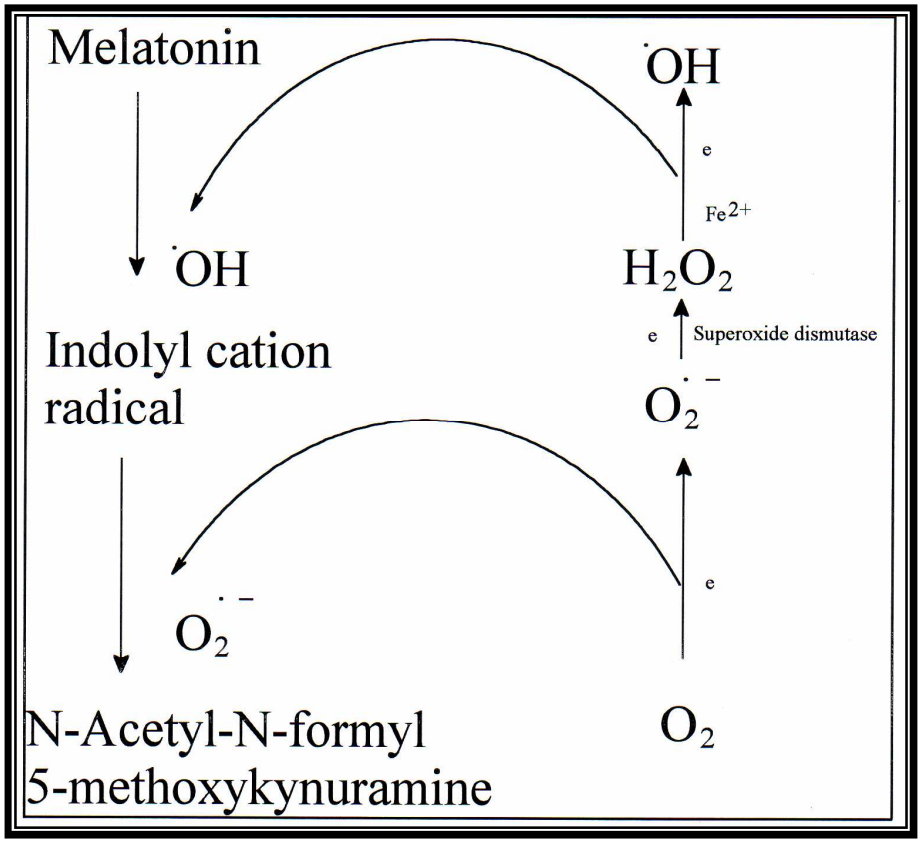

Figure 1.14: The presumed mechanism whereby melatonin detoxifies and reduces the formation of the highly toxic •OH (Reiter *et al.*, 1996).

Previous studies have established that •OH reacts very rapidly with melatonin in aqueous solution (Matuszak *et al.*, 1997) to form a number of metabolites. The secondary and tertiary metabolites formed *in vitro* and *in vivo*, for example, 6-OHM, N-acetyl-5-methoxykynuramine and AFMK (Horstman *et al.*, 2002) are believed to be generated when melatonin interacts with free radicals, are also regarded as effective free radical scavengers (Tan *et al.*, 2000b). Figure 1.15. shows the proposed pathway for the formation of the products following incubation of melatonin with a •OH. Melatonin metabolites are able to neutralize O_2 by-products like melatonin (Reiter *et al.*, 2002). This effect of melatonin and its metabolites has been referred to as the antioxidant cascade and allows melatonin and its metabolites to scavenge additional radicals beyond what the parent compound, in this case melatonin, is capable of doing (Tan *et al.*, 2000b). This metabolic cascade permits melatonin to directly or indirectly scavenge a number of radicals unlike the classic antioxidants where the ratio of scavenger to radicals neutralized is 1:1.

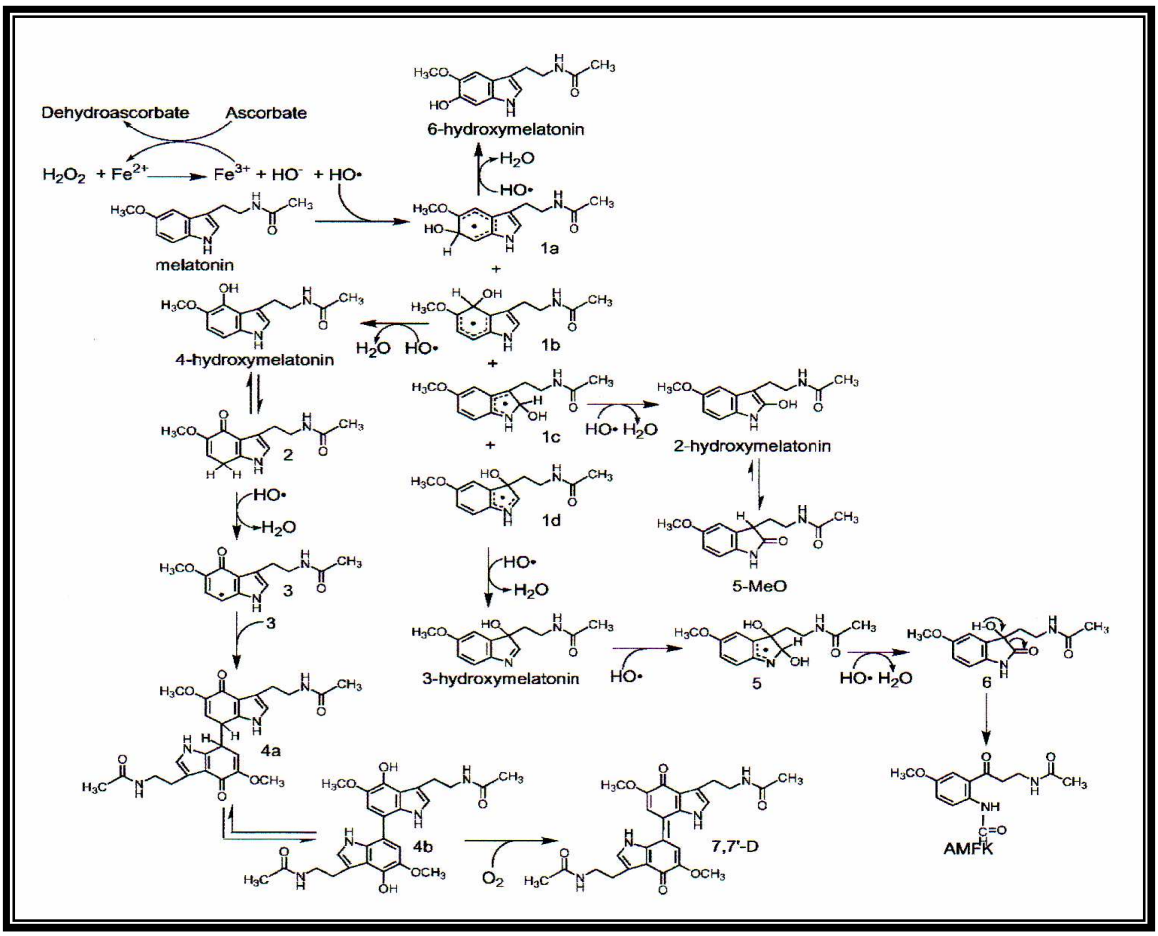

Figure 1.15: Proposed pathway for the formation of the products following incubation of melatonin with a recycling Fenton-type $^{\bullet}OH$ generating system (Horstman *et al*., 2002)

1.5.9.3.4. Melatonin and Singlet Oxygen

Indirect evidence suggesting that melatonin neutralizes $^1O_2$ was first provided by Cagnoli *et al*., (1995) when they showed that the brain of photosensitized rose bengal treated rats was protected by melatonin administration. In addition, Poeggeler *et al*., (1994) and Zang *et al*., (1998) found melatonin to reduce $^1O_2$ generation. Melatonin was also shown to prevent both neuronal apoptosis and inhibition of creatine kinase activity. Since melatonin in pharmacological concentrations overcome the photodynamic injury to neurons, the authors surmised that melatonin directly neutralised $^1O_2$. Furthermore, the ability of melatonin to scavenge $^1O_2$ was further investigated in chapter seven.

1.5.9.3.5. Melatonin and Peroxyl Radical

One of the most extensively studied processes in free radical biology is lipid peroxidation wherein the $LOO^{\bullet}$ radical is generated; this radical then oxidizes another adjacent lipid

molecule to maintain the chain reaction of lipid peroxidation. Earlier studies by Pieri *et al*., (1994; 1995) claimed that melatonin was a more efficient $LOO^{\bullet}$ scavenger than is vitamin E, which is considered the premier chain-breaking antioxidant. This claim however, has not been verified in subsequent studies (Livrea *et al*., 1997; Antunes *et al*., 1999). Thus, it appears that melatonin's ability to reduce lipid peroxidation *in vivo* is probably not related to its function as a chain-breaking antioxidant but could be associated with melatonin's ability to scavenge the initiating radicals (Reiter *et al*., 2000a) and to other actions within the molecular lipid bilayer (Garcia *et al*., 1997; 1998; Tesoriere *et al*., 1999). While melatonin seems not to have any particular ability to scavenge the $LOO^{\bullet}$, it does neutralize the trichloromethylperoxyl radical, an interaction that has a rate constant of $2.7 \times 10^{8}{}_{M}{}^{-1}s^{-1}$ (Marshall *et al*., 1996).

1.5.9.3.6. Melatonin and Nitric Oxide/Peroxynitrite Anions

In test of melatonin's proficiency to scavenge $ONOO^{-}$, it met the challenge and neutralized this reactant (or its metabolites) (Gilad *et al*., 1997; Zhang *et al*., 1998; 1999; Blanchard *et al*., 2000). Likewise, in many situations where $ONOO^{-}$ was induced *in vivo*, exogenously administered melatonin curtailed the molecular and physiological damage that normally accompanies $ONOO^{-}$ exposure (Cuzzocrea & Reiter, 2001; Dugo *et al*., 2001). Cuzzocrea *et al*. (1997) showed that melatonin *in vivo* reduced the inflammatory response induced by carageenan where both $NO^{\bullet}$ and $ONOO^{-}$ are believed to be mediate the inflammation (Beckman & Koppenol, 1996; Szabo, 1996). In the comprehensive study of Cuzzocrea *et al*., (1997) thes authors demonstrated, using several different endpoints, melatonin's anti-inflammatory ability and theorized that this is related to the ability of the indole to inhibit NOS activity and to scavenge $ONOO^{-}$ and the $^{\bullet}OH$. These findings were extended by the same group (Cuzzocrea *et al*., 1998) where melatonin was found to potently inhibit the severe inflammatory response in rats following the injection of a non-bacterial proinflammatory moleucle, zymosan; this moleucle, in addition to initiating a marked inflammatory response, causes multiple organ failure (Mainous *et al*., 1995). Again, Cuzzocrea *et al*., (1998) speculated that melatonin's protective effects are a consequence of its ability to reduce $NO^{\bullet}$ formation and scavenge $ONOO^{-}$ and associated oxidants.

In addition, melatonin has been shown to incapacitate $NO^{\bullet}$ (Mahal *et al*., 1999; Noda *et al*., 1999; Blanchard *et al*., 2000). Although, inherently relatively unreactive, $NO^{\bullet}$ quickly couples with $O_2^{\bullet-}$ to form $ONOO^-$ (Beckman *et al*., 1990) that is capable of meting out significant molecular destruction (Villa *et al*., 1994; Phelps *et al*., 1995). Thus, by scavenging $NO^{\bullet}$, melatonin indirectly limits oxidative stress (Reiter *et al*., 2002). Besides directly scavenging $NO^{\bullet}$, melatonin curtails its generation under some circumstances by inhibiting the activity of its rate-limiting enzyme, NOS (Pozo *et al*., 1997; Crespo *et al*., 1999).

1.5.9.4. Melatonin: Indirect Antioxidant Actions

Whereas the repertoire of melatonin as a direct free radical (and associated reactants) scavenger is obviously extensive, precisely how these reactions relate to the indole's ability to protect against such a wide variety of toxicants *in vivo* remains to be resolved (Reiter *et al*., 2002). This relates to the fact that melatonin, in addition to its ability to directly neutralize reactive species, also limits their generation or metabolizes intermediates to innocuous products. As noted earlier melatonin inhibits NOS (Pozo *et al*., 1997; Crespo *et al*., 1999) under some circumstances which lowers tissue damage that is a consequence of either $NO^{\bullet}$ itself or of the product formed (i.e. $ONOO^-$), when it couples with $O_2^{\bullet-}$. At physiological concentrations, melatonin has been shown to inhibit NOS activity in rat cerebellar (Pozo *et al*., 1994) and hypothalamus (Bettahi *et al*., 1996). The melatonin-induced suppression of NOS acitivity is believed to be a consequence of the binding of calmodulin by melatonin (Pozo *et al*., 1997; Anton-Tay *et al*., 1998). NOS is a calmodulin-activated enzyme (Bredth & Snyder, 1990) and by binding calmodulin, melatonin may limit its availability for this function. With a drop in $NO^{\bullet}$ synthesis, the formation of $ONOO^-$ is curtailed, and the potential oxidative damage is averted (Pryor & Squadrito, 1995). Whether melatonin reduces NOS activity in all tissues that contain this enzyme is unknown. Furthermore, melatonin stimulates several other important antioxidative enzymes including SOD (Antolin *et al*., 1996; Kotler *et al*., 1998; Albarran *et al*., 2001), GPx (Barlow-Walden *et al*., 1995; Pablos *et al*., 1995; 1997; Okatani *et al*., 2001; Wakatsuki *et al*., 2001) and GRd (Pablos *et al*., 1997). SOD is the family of enzymes that play a role in the dismutation of $O_2^{\bullet-}$ from cells thereby lowering the formation of the highly reactive and damaging $ONOO^-$ (Beckman *et al*., 1990).

Usually when one considers the removal of H_2O_2 from cells, it is via its enzymatic conversion to innocuous agents. The two major enzymes involved in these conversions are GPx and catalase. The GPx and catalase enzymes are involved in converting H_2O_2 to non-toxic products in the body (Chance *et al*., 1979). Recent evidence, however has shown melatonin to stimulate the activity of GPx in several organs including the brain (Barlow-Walden *et al*., 1995; Pablos *et al*., 1995; 1997). In addition, melatonin has been reported to increase the activity of GRd, another important antioxidant enzyme. Recent studies by Montilla *et al*., (2000) and Reiter *et al*., (2000b) have further confirmed melatonin's ability to stimulate catalase, GPx and GRd activity. The enzyme GPx utilizes GSH, an intracellular thiol that is typically in mM concentrations, as a substrate. Maintaining high intracellular concentrations of GSH seems to be a function of melatonin since this indole stimulates the activity of its rate-limiting enzyme, gama-glutamylcysteine synthase (Urata *et al*., 1999). When GSH is metabolised by GPx, a reaction that also requires H_2O_2 or other hydroperoxides, it is converted to GSSG. Within cells the GSH:GSSG ratio is normally greatly in favour of the former, and to maintain this ratio GSSG is rapidly metabolized back to GSH by GRd. As noted above experimental evidence has shown that melatonin also promotes the activity of GRd thereby helping to maintain high levels of reduced glutathione (Hara *et al*., 2001).

Although membrane receptors for melatonin have been identified in many cells (Reppert, 1997; Dubocovich *et al*., 1999), nuclear binding sites for the indole have also been documented (Garcia-Mauriño *et al*., 1998; Guerrero *et al*., 2000). Either or both of these may be involved in the mechanisms by which melatonin promotes the activity of SOD, GPx and GRd. Indeed, in one case, Pablos *et al*. (1997) showed that a nuclear melatonin receptor agonist, like melatonin itself, stimulated both GPx and GRd in mouse brain. Whether this is a common mechanism by which melatonin increases the activity of these enzymes (or prevents their decrease in high oxidative stress conditions) remains to be investigated. In reference to the stimulation of GSH synthesis as reported by Urata *et al*., (1999), it is assumed that this action of melatonin likewise involves a receptor-mediated process although the location of the receptor remains unresolved.

Beyond these actions, melatonin has additional means whereby it curtails the oxidative mutilation of essential macromolecules. Melatonin maintains the optimal fluidity of cellular membranes (Garcia *et al*., 1997; 1998). This is accomplished by reducing the

peroxidation of inherent polyunsaturated fatty acids (PUFA) and indirectly reducing increased membrane rigidity (Garcia *et al.*, 1998) by positioning itself within cellular membranes to restrict damage to PUFA by toxic reactants (Tesoriere *et al.*, 1999). Even more important in reducing oxidative damage may be melatonin's action at the level of the electron transport chain (ETC) in mitochondria (Acuña-Castroviejo *et al.*, 2001). In addition to the indirect evidence suggesting an action of melatonin on mitochondrial electron transfer (Yamamoto & Tang 1996a, b; Gilad *et al.*, 1997), several studies have shown that the indole directly stimulates mitochondrial enzyme activity associated with oxidative phosphorylation (OXPHOS); these include NADH-conenzyme Q reductase (complex I) and cytochrome c oxidase (complex IV) (Absi *et al.*, 2000; Martin *et al.*, 2000a; 2000b). Additionally, besides stimulating OXPHOS that could reduce electron leakage and free radical generation (Acuña-Castroviejo *et al.*, 2001), melatonin treatment of rat brain and liver mitochondria *in vitro* increases ATP production (Martin *et al.*, 2002). This action of melatonin may be highly significant in reducing accumulated oxidative damage by providing energy for molecular repair processs. How melatonin influences the mitochondrial enzymes and processes remains enigmatic (Reiter *et al.*, 2002).

Clearly, the number of mechanism at melatonin's disposal to reduce molecular destruction and cellular dysfunction due to oxygen and nitrogen based reactants is extensive. These actions have been shown, for the most part, to be operative *in vitro* and *in vivo* situations and are summarized in figure 1.16.

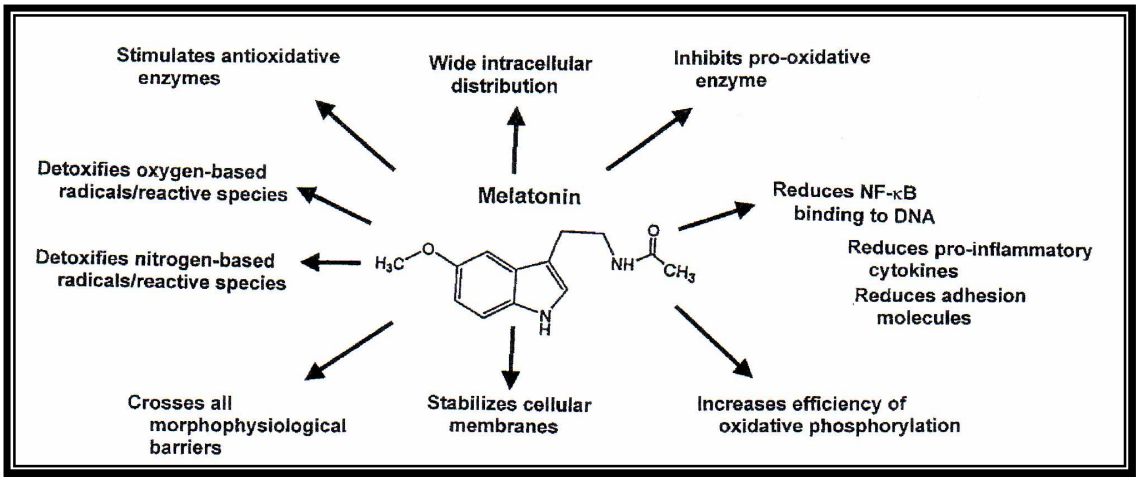

Figure 1.16: Multiple Actions melatonin has in protecting against toxicity. Besides its ability to directly detoxify free radicals and related reactants, melatonin has other actions that enhance its capacity to reduce molecular damage caused by oxidative stress (Reiter *et al.*, 2002).

1.5.10. Melatonin and Neurodegeneration

Undoubtedly, one of the major challenges for contempory neurology is the defferal and prevention of age-associated neurodegenerative conditions that are commonplace in a population whose lifespan has shown substantial increases in recent decades. The debilitating consequences of brain deterioration and malfunction obviously compromise the quality of life and longevity and, additionally, they are financially taxing to society. The scientific quest to identify the causes and effective treatments for these devastating conditions is diverse and intensive. While oxidative stress may be one feature that links many neurological deficits, it is also obvious that these diseases have extremely complex etiopathologies and it is unlikely that a single agent will totally combat their development (Reiter, 1998).

Melatonin, is of interest in the context of neurodegenerative diseases for several reasons:

1. the endogenous production of this molecule falls dramatically with age (Reiter *et al*., 1980; 1981; Touitou *et al*., 1981; Iguchi *et al*., 1982; Reiter, 1992) coincident with the onset of many of the age-associated neurodegenerative conditions (Beal, 1995; Hurn *et al*., 1996; Hensley *et al*., 1997);
2. melatonin readily crosses the BBB and after its exogenous administration it is found in high concentrations in the brain, sometimes exceeding those in the blood manifold (Menéndez-Peláez & Reiter, 1993; Menéndez-Peláez *et al*., 1993; Finnochiaro & Glikin, 1998);
3. melatonin is a ubiquitously acting free radical scavenger and antioxidant (Hardeland *et al*., 1993; Poeggeler *et al*., 1993; Reiter *et al*., 1994; Reiter, 1995b,c) which in models of neurological diseases has proven effective in reducing oxidative damage and preserving neurological function (Reiter, 1995a; Reiter *et al*., 1998a);
4. the only procedure, that is, food restriction, in animal models of aging that significantly delays senescence also retards the age-associated loss of melatonin (Stokkan *et al*., 1991) suggesting a potential association between the loss of melatonin and the signs of aging.

1.5.11. 6-Hydroxymelatonin as a Free Radical Scavenger

The chief, hepatic metabolite, 6-OHM is also reportedly an effective free radical scavenger (Maharaj *et al*., 2002). Thus, even when melatonin, itself is metabolically converted to 6-OHM before it can function in the direct detoxification of radical(s), 6-OHM may be capable of doing so (Reiter & Tan, 2003). In addition, 6-OHM is formed when melatonin is reacted with peroxynitrite in the absence of bicarbonate (Zhang *et al*., 1998). The 6-OHM, has been shown to have some physiological activities similar to those of melatonin (Reiter & Vaughan, 1975; Vaughan *et al*., 1976). It has been claimed this degradation product may be more potent than melatonin in inhibiting lipid peroxidation (Pierrefiche *et al*., 1993; Hara *et al*., 1997). Pierrefiche *et al*., (1993), reported 6-OHM to be 30-fold more potent than melatonin in reducing lipid peroxidation. Furthermore, Hara *et al*., (1997) and Lui *et al*., (2002) supported this finding and showed that 6-OHM was as potent as melatonin in regard to its antioxidant activity. In addition, Hara *et al*., (2001) demonstrated that 6-OHM treatment prevents the cisplatin-induced increase in GSSG in renal tissue. However, Matuszak *et al*., (1997), reported that this hydroxylated indole, in contrast to non-hydroxylated melatonin, functions as both an $^{\bullet}OH$ promoter and $^{\bullet}OH$ scavenger. As evident from these numerous studies there is much controvesy surrounding whether 6-OHM serves as a more potent or equipotent antioxidant agent to melatonin.

1.6. RESEARCH OBJECTIVES

The first objective of this study was to develop a validated selective and sensitive isocratic HPLC method for the quantitative analysis of melatonin which would then be applied to stability studies and the determination of melatonin in dosage forms. With the use of melatonin increasing rapidly, there is to date limited information regarding its physicochemical properties of melatonin including hygroscopicity and partition coefficient. Thus, a number of chemical techniques were employed including, x-ray powder diffraction pattern, differential scanning calorimetry, spectroscopy, nuclear magnetic resonance spectrometry, and mass spectrometry, and the information gained provided a detailed characterization of melatonin and confirmed the identity of the melatonin raw material used in this study. In addition, the analytical HPLC method also served as the basis for the assessment of the partition coefficient, hygroscopic, pH, temperature and photostability characteristics of melatonin raw. This part of the study was essential as with the use of melatonin increasing rapidly, there is to date no or very little information in literature regarding these properties of melatonin. It is also imperative that consumers be informed of the proper storage conditions for melatonin formulations to improve its stability and ensure the long term integrity of the product and these studies provide important information on the proper manufacturing and storage of melatonin. The photostability studies on melatonin were based on the recent report that melatonin is extremely photoliable. For this reason, if melatonin is to be incorporated into pharmaceuticals, its stability in the presence of light needs to be thoroughly investigated. Thus, the photostability of melatonin was assessed according to ICH guidelines. In addition, detailed investigations on the photochemistry and the photoproducts resulting from the exposure of melatonin to UV light have not been reported, thus a detailed study was conducted to determine the melatonin photoproducts.

The second objective was to determine whether 6-OHM could act as a neuroprotective agent under a number of neuropathological conditions and to attempt to elucidate the mechanism of neuroprotection, should it be occuring. Thus, this part of the study was undertaken to observe the neuroprotective properties of 6-OHM in comparison to melatonin against damage induced by various neurotoxins in the hippocampus. The role of oxidative stress, endogenous toxins such as quinolinic acid, mitochondrial inhibitors

like cyanide, and metal such as iron, in various neurodegenerative disorders are well established. Thus, it was decided to observe the effects of 6-OHM on damage induced by these factors through the employment of various biological assays as well as inorganic studies. Furthermore, this study also entails the elucidation of possible mechanisms by which 6-OHM may exert any protective effects against oxidative stress and damage caused by these above mentioned neurotoxins in the rat brain and hippocampus. This part of the study was imperative due to the controversy surrounding whether 6-OHM serves as a pro-oxidant or antioxidant. In addition, the ability of 6-OHM to serve as an antioxidant was compared to that of melatonin, to determine which indoleamine was superior, as different researchers have named each agent as superior. In addition, the hippocampus was chosen as the area of brain to study, since this is the primary region involved in memory formation and it is one of the areas of the brain that is most vunerable to free radical attack.

It was hoped that following this investigation, this would provide scientists with a better understanding of the physico-chemical properties of melatonin., its pH and temperature stability and photostability. In addition, the potential neuroprotective properties of 6-OHM would be better understood, and that knowledge gained could ultimately be used by future researchers in the treatment of a number of neurodegenerative diseases.

CHAPTER TWO

HIGH PERFORMANCE LIQUID (HPLC) CHROMATOGRAPHY METHOD DEVELOPMENT AND VALIDATION

2.1. INTRODUCTION

The analysis of drug substances and products within a pharmaceutical industry is carried out to satisfy both the manufacturer companies and the regulatory authority, equally, about the integrity, quality, and stability of the medicine to be administered to the patient. Several reports are available containing guidelines for the validation of analytical methods, (Hokanson, 1994; Boehlert, 1984; ICH, 1996) with some reports describing practical minimum requirements (Carr & Wahlich, 1990).

Chromatography, in general, uses a range of techniques to separate a mixture of solutes by using a mobile phase and an immobile, immiscible stationary phase, allowing solutes to be separated based on their different affinities within the system (USP, 1999; Lindsay, 1987). Prior to the 1970's there were few reliable chromatographic methods available for use in the laboratory. However, during this period, pressure liquid chromatography was increasingly used (Guell & Holcombe, 1990), although consistent flow rates were not achieved.

In the last decade high performance liquid chromatography (HPLC) has become the method of choice for the separation of pharmaceutical and chemical compounds and the quantitation of the active ingredient and related substances. The advantages of HPLC include the separation and measurement of the desired components making HPLC without a doubt, the most popular and versatile techniques in laboratories today.

After the method has been developed, validation for effectiveness and suitability of the analysis is required to be undertaken. Parameters include: linearity, range, specificity,

accuracy and precision, detection limit and ruggedness. If HPLC is used to quantitate the amount of drug present, peak purity i.e. photodiode array and or liquid chromatography mass spectrometry (LC-MS) is required to ensure the integrity of the analyte peak. Method development then is only complete when acceptable analytical performance has been demonstrated (Edwardson *et al*., 1990).

The discovery of melatonin (N-acetyl-5-methoxytryptamine), as a free radical scavenger has generated a vast amount of interest (Reiter, 1995a). Previously published methods used to analyze melatonin have involved the use of HPLC with UV/Vis (Cavallo & Hassan 1995), fluorescence (Torano *et al*., 2000) and electrochemical detection (Bechgaard, 1998; Kumar *et al*., 1999). Hartter *et al*., (2001) used LC-MS to determine exogenous melatonin levels in human plasma while gas chromatography – mass spectrometry (GC-MS) was used to assay for the urinary metabolites of melatonin (Leone *et al*., 1987). However, a major disadvantage of these methods is that they are time consuming, complex and costly.

Thus, the possible use of melatonin as a therapeutic agent prompted the development of a simple, reliable, cost-effective HPLC method to analyze melatonin raw material. In addition, this method may be applied to the determination of melatonin in dosage forms and to quantitate the amount of melatonin in combination with selected drugs remaining during and after photostability studies. A key to the success of drug formulation research is the availability of a rapid and sensitive analytical method to analyze the large number of samples collected in development studies. It is therefore important to develop a rapid, reliable analytical method to expedite the analytical process (Mandal & Womack 1999).

The method described in this chapter involves the use of HPLC with UV/Vis detection and is a selective, sensitive, simple, reliable, and cost-effective isocratic HPLC method developed for the quantitation of melatonin.

2.2. MATERIALS AND METHODS

2.2.1. Chemicals and Reagents

All chemicals used were at least of analytical reagent quality. Melatonin was purchased from the Sigma Chemical Corporation, St Louis, MO, USA and ammonium acetate from Saarchem, Krugersdorp, South Africa. HPLC grade acetonitrile was obtained from BDH Laboratory Supplies, Poole, England, while HPLC grade water was obtained by purification using a Milli-Ro®-15 water purification system (Millipore, Bedford, MA, USA), consisting of a Super-C® carbon cartridge, two Ion-X® ion-exchange cartridges and an Organex-Q® cartridge. The water was then filtered through a 0.22µm Millipak® stack filter prior to use.

2.2.2. Stock Sample Preparation

A stock solution of melatonin (0.1 mg/ml) was prepared, by accurately weighing out 1mg of melatonin and dissolving it in 10ml of mobile phase. Dilutions of this stock solution were made to prepare the required standard solutions for the concentration range of 2.5µg/ml - 50µg/ml.

2.2.3. HPLC Instrumentation System

The modular, isocratic HPLC system consisted of a Spectraphysics IsoChrom pump (Spectraphysics, San Jose, California, USA), a Linear UV/Vis 200 Detector and a Perkin Elmer Model 561 flat-bed chart recorder (Hitachi, Japan). Samples were injected onto the system using a Rheodyne Model 7125 (Rheodyne, Cotati, California, USA) fixed 20µl loop injector using a 100µl syringe (Hamilton Company, Reno, USA).

2.2.4. Chromatographic Conditions

2.2.4.1 Column Selection

C18 columns have been most frequently used for the HPLC analysis of melatonin. Thus, separation was achieved on a 5µm C18 Waters Spherisorb (Waters Corporation, Milford, Massachusetts, USA) (250H4.6mm i.d.) analytical column. This column offered adequate separation of compounds and resulted in well-resolved peaks.

2.2.4.2 Mobile Phase Selection

The mobile phase or eluent interacts with the solute molecules and the stationary phase itself, with the strength of these interactions determining the resolution obtained and hence the efficacy and efficiency of the separation, resulting in the selection of an appropriate mobile phase being imperative (Lindsay, 1987; Hadden, *et al*., 1971). The mobile phase selected must not alter the characteristics of, or be miscible with the stationary phase, as this is potentially detrimental to the life span of the column.

Solutions for use in HPLC systems must be filtered to remove particulate matter that could interfere with the pumping action of the solvent delivery device, cause damage to the seals and valves, or collect on the top of the column causing irregular behaviour and subsequent column blockages (Lindsay, 1987). Solutions must also be degassed to remove dissolved or suspended air bubbles so that they do not collect in the pump or the detector cell and cause erratic behaviour of the detector or an irregular pumping action.

The viscosity of the mobile phase is also an important consideration and should not exceed 0.5cps (Lindsay, 1987) as high viscosity solvents reduce solvent diffusion coefficients, hence decreasing column efficiency (Hadden, *et al*., 1971). The solvents selected must also exhibit very low absorbance at the operating wavelength; for example, if a wavelength of 245nm is selected, aromatic solvents cannot be used as all such solvents absorb UV light to some extent at this wavelength (Hadden *et al*., 1971).
An assessment of 10mM- 50mM buffers showed that increasing the buffer molarity led to an increased retention time (R_T). As shown in figure 2.1, the 25mM buffer resulted in the

shortest R_T for melatonin of 7.2 min. The 25mM buffer resulted in sharp, well resolved peaks for melatonin exhibiting no tailing.

A change in buffer pH influenced both the R_T and resolution of melatonin. As evident in figure 2.2, a pH of 7.0 was selected as it produced peaks with good shape and resolution in a short R_T and would minimize damage to the column.

The initial organic modifier used was acetonitrile. The ration of aqueous phase: organic phase is of importance particularly with respect to R_T and optimal proportions of acetonitrile were determined by assessing the impact of varying the organic content of the mobile phase. An increase of the organic modifier composition resulted in sharper, well-resolved peaks and decreased R_T for melatonin; however, the inclusion of methanol resulted in broader peaks. Acetonitrile was selected as the organic modifier for use, as a good resolution and sharp peaks were obtained when it was included in the mobile phase. The proportion of acetonitrile: buffer selected as optimal was 40:60%v/v. Furthermore, the possibility of an incompatibility, which may result between the organic modifier in the mobile phase and acetonitrile used in the preparations of melatonin solutions, would be minimized. Therefore, the mobile phase chosen for the analysis of melatonin was 25mM ammonium acetate buffer, pH 7.0 with acetonitrile (40%v/v). Prior to use the mobile phase was filtered through a 0.45µm filter and degassed.

2.2.4.3 Flow Rate Selection

A commonly used mobile phase flow rate is 1-5cm^2/min (Lindsay, 1987). However, slower flow rates are more advantageous in terms of maximizing the life span of the pump and the column and would thus be more economical. Consequently, a flow rate of 1.0ml/min was selected for use in this method.

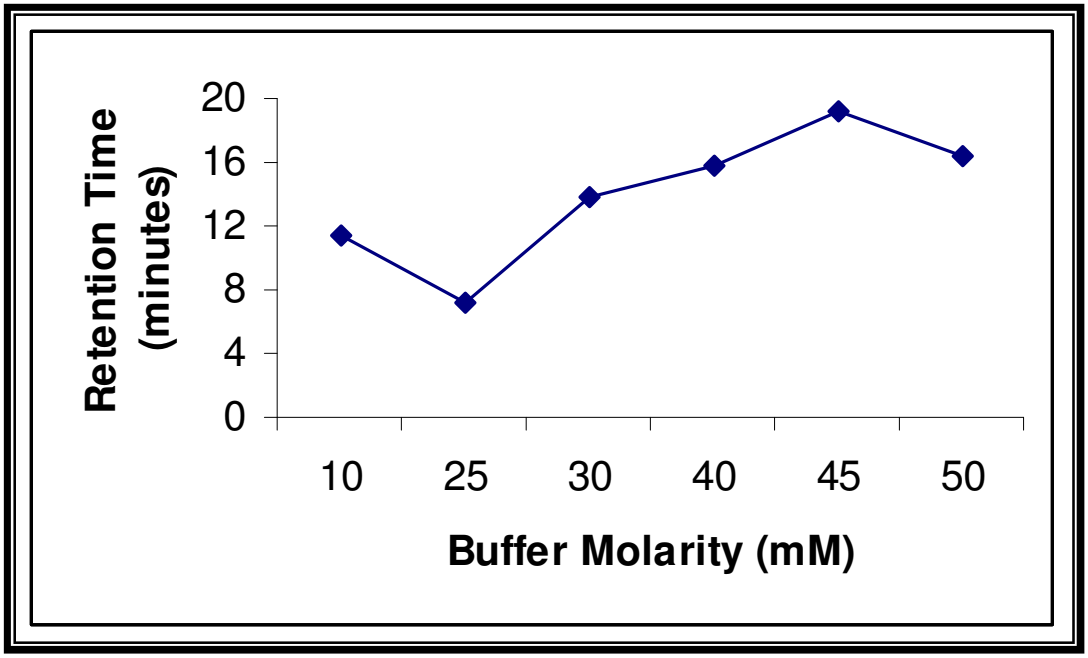

Figure 2.1: The effect of buffer molarity on the retention time of melatonin.

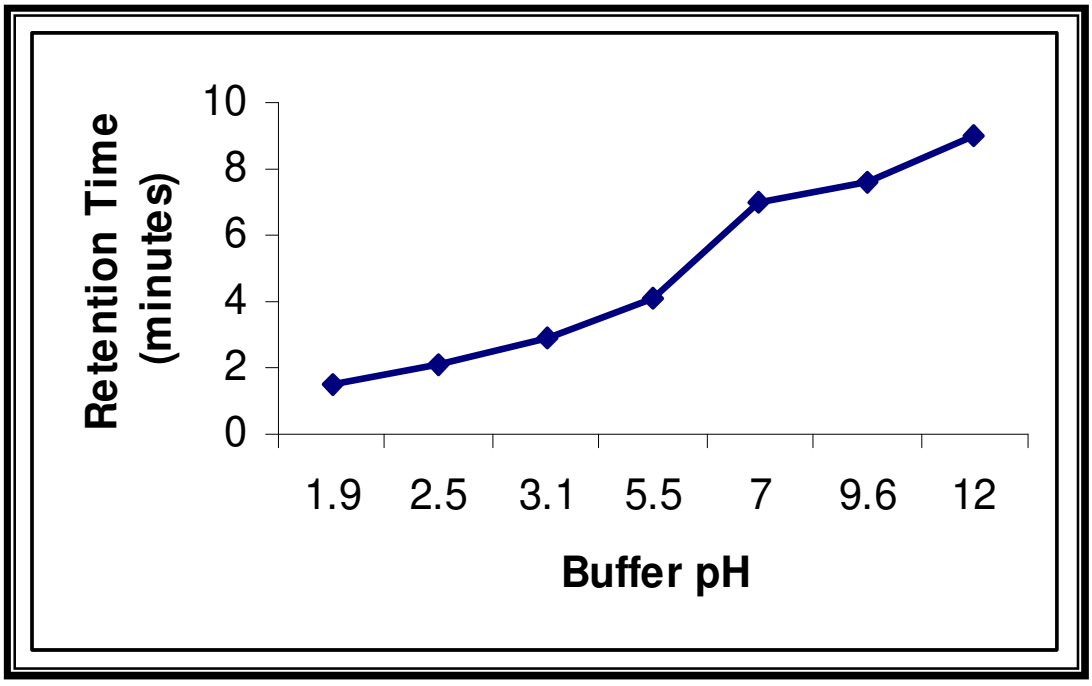

Figure 2.2: The effect of buffer pH on the retention time of melatonin.

2.2.4.4. UV/Vis Detection

A wavelength of 304nm was chosen for the detection of melatonin. This wavelength was found to produce reproducible, well resolved peaks and allowed for the detection of sufficiently low concentrations of melatonin, such that samples did not require dilution prior to analysis.

The response time on the detector was set at 0.1s. An attenuation of 0.2 absorbance units full scale (AUFS) was selected as it offered adequate sensitivity for the detection of melatonin in solution and early detection of degradation products. Data was recorded at a chart speed of 5mm.min^{-1}.

2.2.4.5. Final Chromatographic Conditions.

The optimal chromatographic conditions that were established are described below in table 2.1.

Table 2.1: Optimal Chromatographic Conditions Used for the HPLC Analysis of Melatonin.

Mobile Phase	25mM ammonium acetate (pH 7.0): acetonitrile, 60:40 v/v
Flow Rate	1.0mL/min.
Detection Wavelength	304nm
AUFS	0.2
Injection volume	20µL
Temperature	Ambient
Retention Time	7.2 min

A typical chromatogram obtained for melatonin in solution is shown in figure 2.3.

2.2.4.6. Conclusions

The variables investigated indicate that buffer pH and molarity have a significant effect on peak shape and retention time of melatonin in solution. The choice of a suitable wavelength is also important, in terms of method precision, selectivity and sensitivity. The chromatographic conditions were optimized to yield a well-resolved peak with a reasonable retention time.

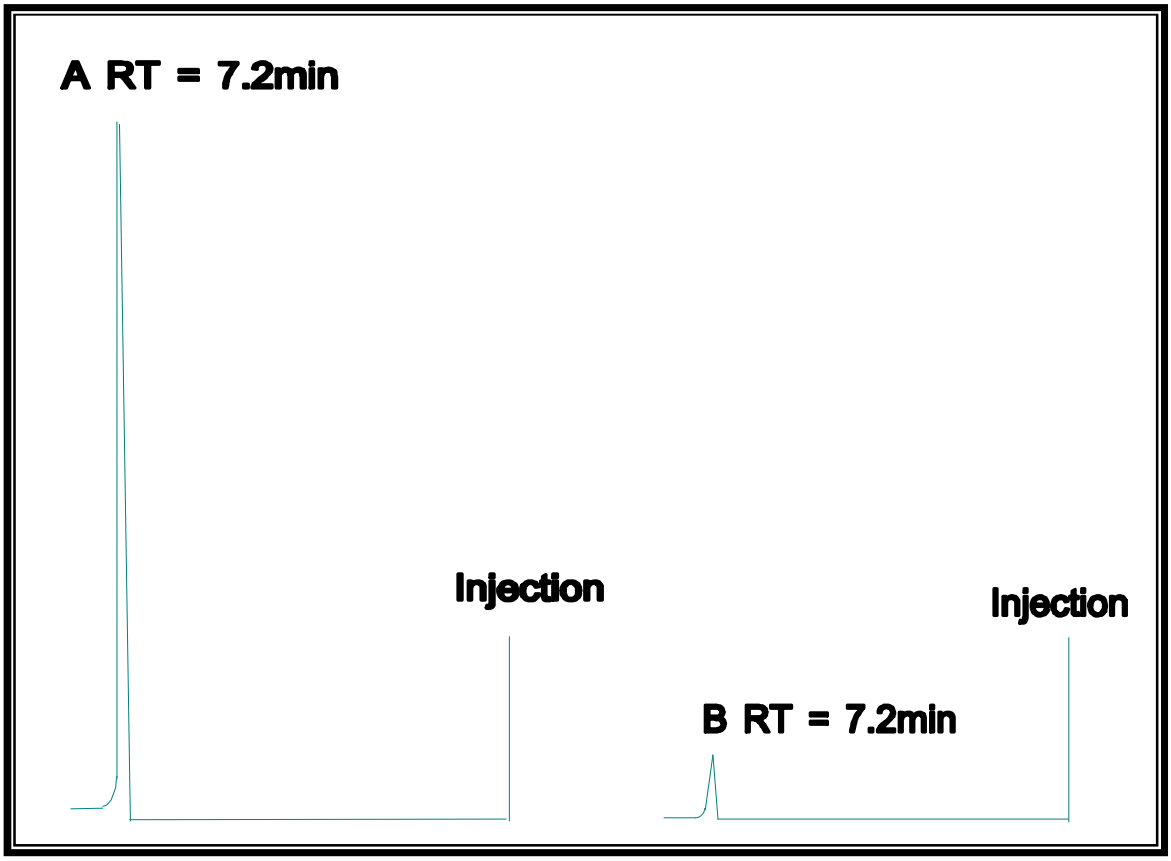

Figure 2.3: A typical chromatogram of the separation of melatonin at concentration of A= 50µg/ml; B= 2.5µg/ml.

2.3 METHOD VALIDATION

2.3.1. Introduction

Validation is a process whereby the performance characteristics of an analytical method are established and the analytical method meets the requirements for its intended purpose (USP, 1999; Edwardson *et al*., 1990). A validation process is essential as it serves to ensure that the quality of analytical data generated is both reliable and accurate, and it is also capable of identifying potential problems of a particular method. Such problems include column degeneration, changes in column behaviour due to changes in the manufacturing process, and the co-elution of impurities, derived from the synthesis of active compound (Edwardson *et al*., 1990). Thus, a method development is complete only when the method has been tested and shown to demonstrate acceptable analytical performance (Edwardson *et al*., 1990).

The validation parameters outlined by the United States Pharmacopoeia (USP), the FDA, regulatory bodies in Europe and Canada and International Conference on Harmonization (ICH) may vary slightly. The USP and ICH include eight parameters for evaluation, namely accuracy, precision (intermediate precision and repeatability /reproducibility), specificity, limit of detection (LOD) and limit of quantitation (LOQ), linearity and range. However, the ICH guidelines also include robustness and system suitability, and suggest that precision be assessed at three levels, namely repeatability, intermediate precision and reproducibility (USP, 1999; Swartz & Krull, 1997). Most validation methods for HPLC analyses include some or all of these parameters described (Hokanson, 1994; Wielinski & Olszanowski, 2001).

In order to facilitate the evaluation of the validation parameters, acceptance criteria should be universally applicable, mathematically explicit, complete and achievable. The acceptance limits for a number of validation parameters such as specificity, linearity, precision, accuracy and sensitivity (LOD and LOQ) were reported by Jenke (1996) and are shown in table 2.2.

Table 2.2: Summary of acceptable limits of validation parameters (Jenke, 1996).

Validation Parameters	Acceptable Limits
Specificity	Should have baseline separation between peak of interest and all other analytical responses
Linearity	Correlation coefficient should be between 0.98 - 1.00
Precision	4% RSD
Accuracy	98 to 102% of the theoretical value
LOD and LOQ	No specific criteria exist in the literature

2.3.2. Specificity

Specificity is defined as the method's ability to measure, unequivocally, the analyte in the presence of other components that may be expected in the sample matrix, accurately and specifically. This may include degradation products, impurities, matrix, placebo ingredients, etc (ICH, 1996; USP, 1999; Swartz & Krull, 1997). Specificity was assessed by comparing chromatograms obtained from analysis of a standard solution containing the analyte only with a sample mixture obtained by dissolving commercial tablets of melatonin in the dissolution medium as well as chromatograms obtained when melatonin was irradiated with UV light to show its photoproducts.

Melatonin tablets were crushed weighed out and dissolved in sufficient mobile phase and the resultant samples were chromatographed on HPLC. For the melatonin photolysis study, melatonin solution was irradiated with UV light continuously with a 400-W high pressure mercury lamp, emitting over the UV/Vis range (300-575nm) with maximum irradiance in the UVA at 365nm and 565nm in the visible region, for three hours, whilst bubbling air through the solution, at ambient temperature. Melatonin solutions were removed at different time intervals of irradiance and were subjected to chromatography.

2.3.3. Linearity

A linearity study is used to verify that the sample solutions are in a concentration range where the analyte response is linearly proportional to the concentration (USP, 1999). The linearity of the range of detectability is dependent on Beer's Law, such that the absorbance of a solute is directly proportional to its concentration in the solution (Jeffry *et al*., 1989). Linearity in this range is dependent on both the compound analyzed and the detector used (http://pubs.acs/hotaartcl/ac/96/may/may.html).

The ICH guidelines recommend that five concentrations spanning the concentration range to be studied must be used (Swartz & Krull, 1997), and it is necessary that a minimum of twenty assays be performed for statistical validity (Weed, 1999).

Samples were prepared by serial dilution of a stock solution to yield concentrations over the range 2.5 – 50 μg/ml and linearity assessed by repeated measurements (n=20) of six concentrations over the concentration range. Acceptability of linearity data was judged by examining the correlation coefficient (r^2) on the regression line for the response versus concentration plot. An r^2 value of >0.990 was considered to be sufficient to demonstrate linearity of the method and it falls in the range specified in table 2.2.

2.3.4. Precision

Precision is a measure of the closeness of data values to one another when a number of measurements are taken under the same analytical conditions. The ICH defines precision as having three components, namely: repeatability, intermediate precision and reproducibility (Swartz & Krull, 1997). Precision is usually expressed as the percentage relative standard deviation (%RSD) (USP, 1999; Swartz & Krull, 1997) and the tolerance for %RSD was set at ±4% in our laboratory.

2.3.4.1 Repeatability

Repeatability refers to inter-assay precision and is expressed as the degree of variation arising from consecutive and non-consecutive injections run on the same day. It should be determined using a minimum of nine determinations covering the specified analytical range, for example three determinations at three concentration levels (Swartz & Krull, 1997). Consecutive measurements were obtained by repeated injection of the same concentration taken from different vials in succession. Interspersing vials of the same concentration with those of different concentrations was the method used to obtain non-consecutive measurements. Repeatability of this system was assessed by repeat measurements (n=6) of high, middle and low concentration calibration solutions. Samples were run in both consecutive and non-consecutive sequence.

2.3.4.2 Intermediate Precision

Intermediate precision is used to evaluate the reliability of the method in different environments other than that used for the development of the method, and depending on the time, the method may be tested on different days, using different analysts and instruments (Segall *et al*., 2000). Inter-day precision was determined using calibrators of the same concentration as described in 2.3.4.1. Samples were run over a one week period.

2.3.4.3 Reproducibility

Reproducibility is used to express the precision of an analytical method when used in different laboratories; however this is not always possible, therefore tests for reproducibility are not normally expected if intermediate precision is accomplished (Segall *et al*., 2000) and thus no tests were performed.

2.3.5. Accuracy and Bias

Accuracy is a measure of the closeness between the true and measured values of a sample (USP, 1999; Swartz & Krull, 1997). A tolerance of 3% was set for %RSD for this parameter. Accuracy and bias were evaluated by making repeat measurements of three

samples of varying concentration. Accuracy studies for drug products are recommended to be performed at 80, 100, and 120% of the target concentration (http://pubs.acs/hotaartcl/ac/96/may/may.html). Accuracy studies were performed in triplicate on melatonin samples representative of high, medium and low concentrations prepared in mobile phase.

2.3.6. Limit of Quantitation (LOQ) and Limit of Detection (LOD)

The LOQ is a measure of the level of analyte that can be measured with the required accuracy and precision, and LOD is the lowest analyte that is detectable above the baseline noise of the system (USP, 1999; http://pubs.acs/hotaartcl/ac/96/may/may.html.; Swartz & Krull, 1997). The USP method was selected for the determinations of the requisite validation parameters. This method describes the LOQ as having a signal to noise ratio of 10:1 and the LOD as having a signal to noise ration of 2:1 or 3:1. Although, this concept is widely used, it must be noted that these values are likely to vary with changes in detector, which may include deterioration of the detector lamp on prolonged use (USP, 1999). Repeat measurements (n=6) of blank injections were used to establish the baseline noise.

2.3.7. Ruggedness

This is expressed as the lack of influence of environmental and instrumental conditions on the analytical method. It is usually determined by analyzing samples under a variety of test conditions such as the analysis on different days, with different analysts, and using different temperatures and reagents. Results from different day analysis have been described for intermediate precision and thus no further tests were conducted.

2.4. RESULTS

2.4.1. Specificity

In order to develop a suitable chromatographic system, knowledge of the susceptibility of the drug to degradation and its degradation pathway is necessary. Any interference on the assay by possible degradants, or synthesis precursors, or by chemicals employed in sample preparation, and excipients present in the formulation needs to be investigated. This is a standard procedure in the development of a method (Edwardson *et al*., 1990).

The chromatograms obtained for melatonin in tablet formulation and melatonin after UV irradiation are shown in figures 2.4 and 2.5. The chromatogram of an injection of mobile phase (on a 20µl loop), used to overfill the loop, showed no observable peaks indicating that the mobile phase would not interfere with the melatonin peak. The resultant peak obtained for melatonin made up in mobile phase was well resolved from the solvent front with no interference observed. For the chromatogram obtained for melatonin tablets (figure 2.4) the melatonin peak eluted at 7.2 min with an excipient peak obtained at an earlier R_T of 3.1 min. The irradiated melatonin solution at 60 min eluted at 7.2 min with the photoproducts eluting at earlier R_T as is evident in figure 2.5. As evident from the chromatograms, the melatonin peaks were well resolved, sharp and symmetrical with no interference from the excipients or degradation products, indicating that the method was specific for melatonin. Two of the four photoproduct peaks were also well resolved from each other, symmetrical and sharp as is evident in figure 2.5, indicating that the HPLC method can be used to quantitate the amount of the photoproducts formed with an increase in irradiation time.

Furthermore, LC-MS scans were run for the melatonin irradiated with UV light at different times of irradiation to prove that the melatonin peak was due to melatonin only. The LC-MS traces shown in appendix six show that the molecular mass (MM) of melatonin does not change over the peak i.e. on the up-slope, peak and down slope, the same MM of melatonin was obtained. The MM of melatonin i.e. $(M+H)^+$ of 233; did not change with an increase in irradiation time. Furthermore, the photodegradants showed up on the LC-MS scans with different MM from that of melatonin (appendix six) i.e. the two

major photoproducts had a MM of 265 and 249, respectively. Thus, these results provide evidence that this HPLC method is specific under these experimental conditions for quantitating and measuring melatonin in the presence of other components e.g. photodegradants, excipients etc.

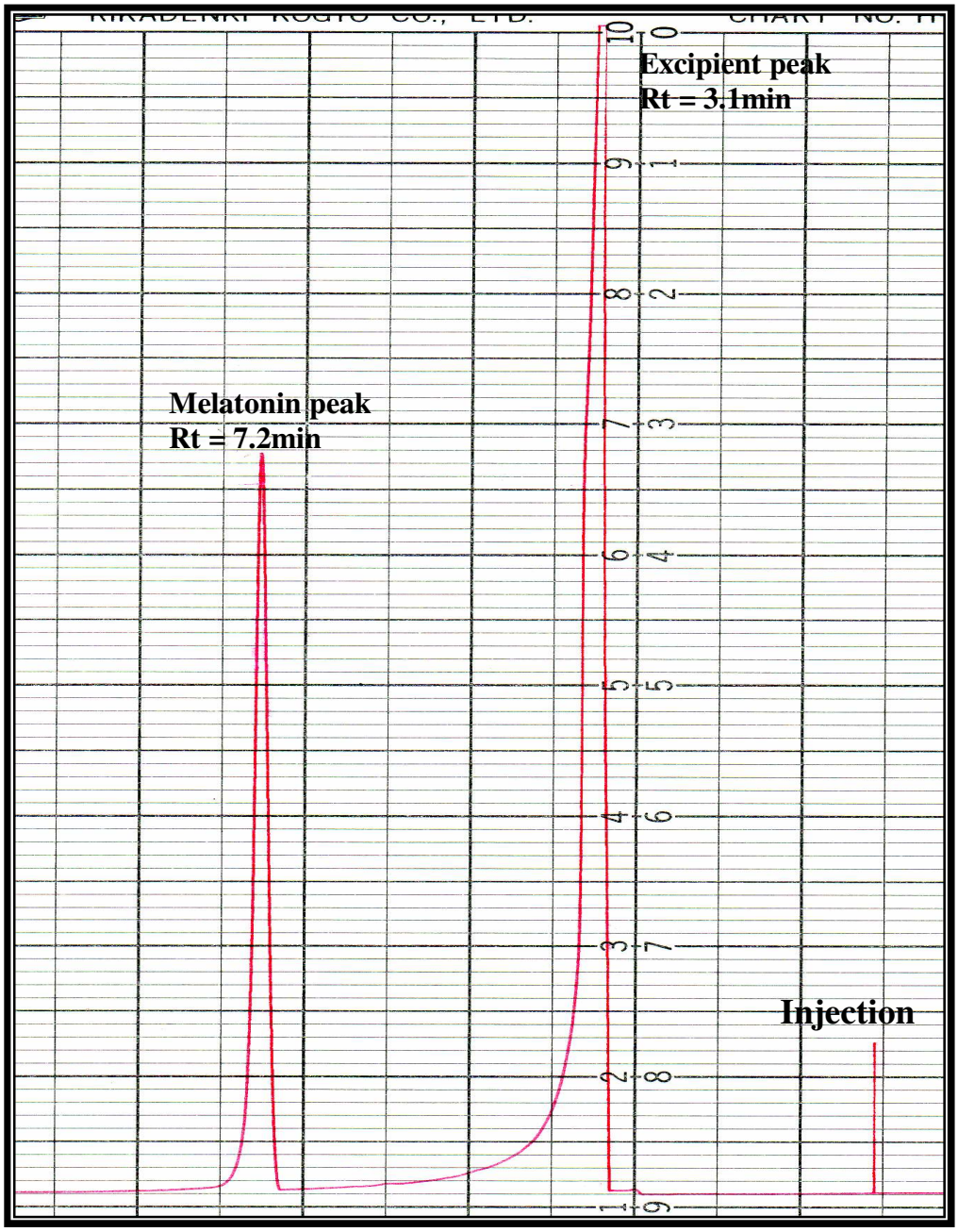

Figure 2.4: A typical chromatogram of the separation of melatonin from a melatonin tablet formulation.

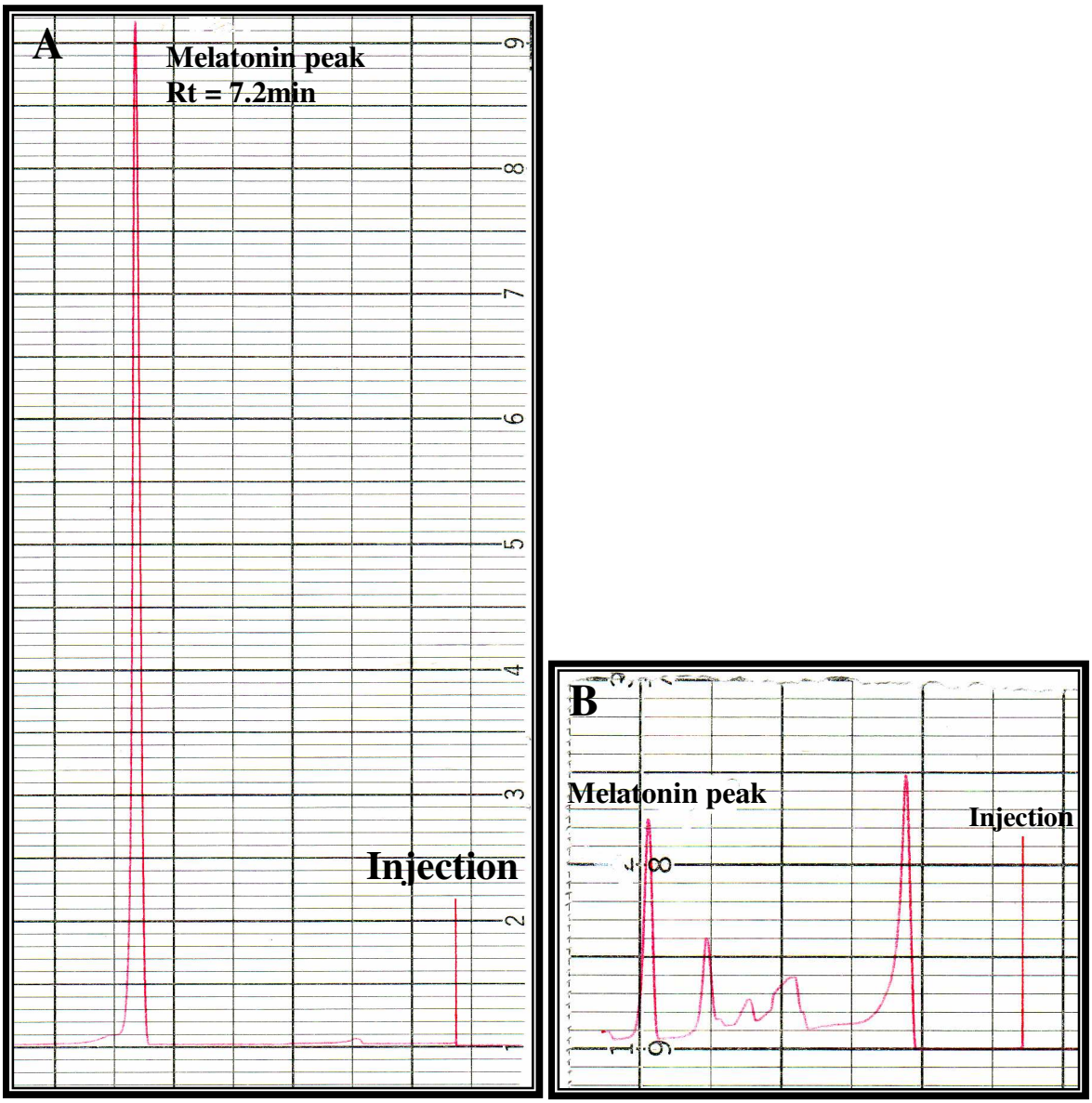

Figure 2.5: A typical chromatogram of the separation of melatonin after UV-irradiation of melatonin. A= irradiation time 0 min; B= irradiation time 60 min.

2.4.2. Linearity

Figure 2.6 shows a typical calibration curve for melatonin over the concentration range of 2.5-50 µg/ml, with an excellent correlation coefficient of $r^2 = 0.9993$. The r^2 is within the acceptable limits set (see table 2.2).

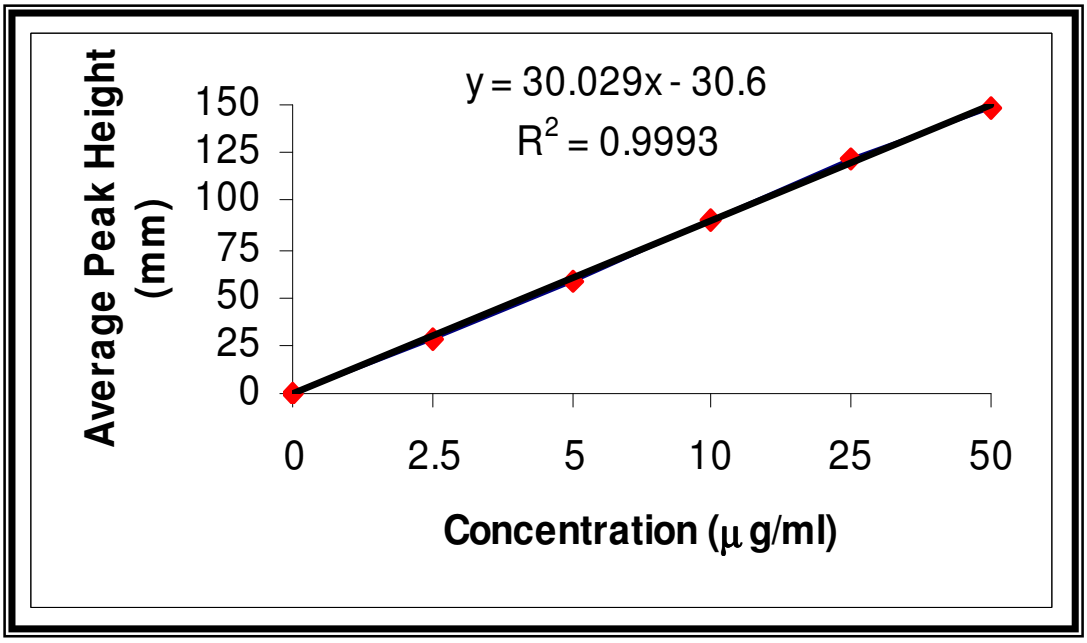

Figure 2.6: Typical calibration curve constructed by plotting mean peak height against the concentration of melatonin.

2.4.3 Precision

2.4.3.1 Repeatability

The standard deviations and % relative standard deviation (RSD) values obtained were less than 4% (figure 2.7), which was the limit set in our laboratory, indicating that the method displayed adequate repeatability.

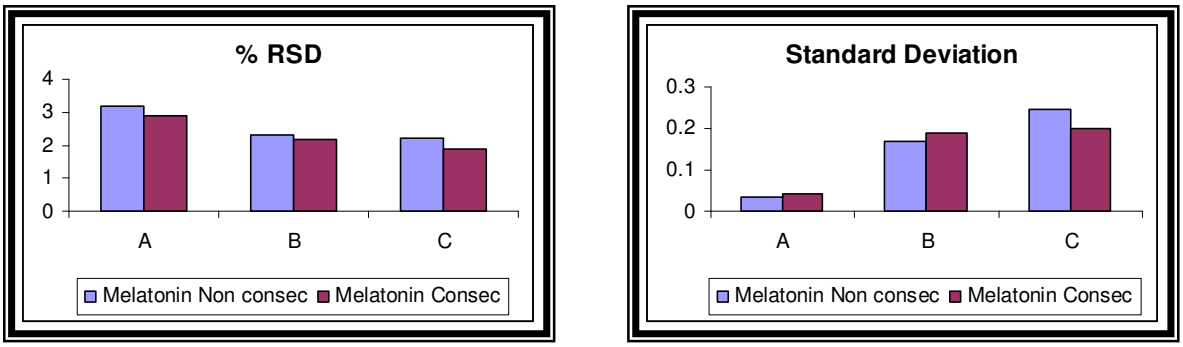

***A, B, C represents High, Middle and Low concentrations, respectively.**

Figure 2.7: Precision data (repeatability) for the analytical method developed.

2.4.3.2 Intermediate Precision

The intra-assay precision revealed RSD % values of 0.17-3.5% and the inter-assay precision revealed values of 0.19-3.93% (table 2.3). Results shown in table 2.3 shows that all standard deviations were within the acceptable range, resulting in a %RSD values less than 4 %. Thus, the data shows acceptable precision as the results are within the specified range set out in table 2.2.

Table 2.3: Melatonin assay validation data.

	% RSD	
Concentration(µg/ml)	**Intra-assay (n=6)**	**Inter-assay (n=6)**
2.5	3.45	3.93
5	3.5	3.76
10	1.9	1.9
25	0.17	0.19
50	0.39	0.34

2.4.4 Accuracy and Bias

The results are shown in table 2.4. The test concentrations were close to the theoretical value and fell within the acceptable range of 98 to 102% theoretical value shown in table 2.2. The % bias is between 0.4 to -8% and this falls within the bias acceptance criteria of ±3%. The largest value obtained for % bias was -8.420%, indicating the no concentration value deviated by greater than approximately 8% of the stated concentration value.

Table 2.4: Percent error obtained during determination of blinded samples in accuracy testing.

Theoretical concentration (µg/ml)	**Actual concentration (µg/ml)**	**% Bias**
5	5.42	-8.420
25	25.05	-0.208
50	49.7	0.610

2.4.5 LOQ and LOD

Repeat injections of decreasing sample concentrations (n=6) yielded a LOD value of 1µg/ml and a LOQ value of 2.5µg/ml. The %RSD values were higher than for samples of higher concentration, all %RSD values were less than 6%.

2.5. DISCUSSION

Validation forms an integral part of the quality assurance in the pharmaceutical industry in order to provide quality medicine. A survey conducted by the Pharmaceutical Analytical Sciences Group (PASG) in 1992 determined the current practice employed in the validation of analytical methods for drug substances and drug products in pharmaceutical laboratories in the United Kingdom (UK). The survey was divided into method validation parameters employed for drug substances and those for drug products. The investigation indicates that the highest degree of consistency is seen in the application of validation parameters to chromatographic techniques, specifically in the case of HPLC, where there was good agreement over which parameters should be applied to method validation, reflecting the widespread application and dependence on this technique within the pharmaceutical industry (Clarke, 1994).

This HPLC protocol that has been developed is rapid, simple and cost effective for the determination of melatonin in solution. Thus, this method may be applied to the analysis of melatonin in dosage forms and to the assessment of melatonin stability studies without using expensive and highly sensitive electrochemical detection techniques. The principal aspects of method validation have been examined and the validation studies indicate that the method is specific, accurate, precise and linear over the concentration range of 2.5 to 50µg/ml and this method provides a cheap tool for the successful analysis of the material in studies that are necessary for the successful development of a useful dosage form.

This analytical method also serves as the basis for the assessment of the partition coefficient, hygroscopic, pH, temperature and photostability characteristics of melatonin, which is discussed in the subsequent chapters i.e. chapter 3-6. Furthermore, this method

has been used successfully in a number of studies (Daya *et al*., 2001; Maharaj *et al*., 2002) to analyze melatonin.

2.6. CONCLUSION

Melatonin is available commercially from several unregulated health food suppliers. Soon after the publication of the Wurtman report (Wurtman and Axelrod, 1965), health stores began selling melatonin and consumers flooded Wurtman's lab with requests for melatonin for insomnia and jet-lag. The responses to these requests have been to point out that melatonin is not FDA approved. However the melatonin formulations appear with no labelling for dosage and side effects, as well as no control for purity and self-medicating with an unregulated product. However, melatonin use has not yet declined. In 1994, one manufacturer of melatonin in USA increased the amount of melatonin sold the previous year by three fold (www.ch.ic.ac.uk/local/project). In brief, melatonin has been administered in both physiological and pharmacological amounts to humans and animals, and there is widespread agreement that it is a non-toxic molecule (Reiter, 2003). However, the main disadvantage of the current methods available to analyze melatonin is that these are very expensive to conduct. However, this is a selective and sensitive isocratic high-performance liquid chromatography method developed for the quantitative analysis of melatonin and may be applied to stability studies and the determination of melatonin in dosage forms.

CHAPTER THREE

MELATONIN - PHYSICOCHEMICAL PROPERTIES

3.1 INTRODUCTION

Melatonin, a hormone that is formed in the pineal gland and secreted at night plays an important role in the regulation of the circadian sleep-wake cycle. Normal average physiological plasma levels of melatonin during daytime hours are 10pg/mL, increasing to an average of 60pg/mL at night (Epstein, 1997). Numerous publications report the therapeutic applications of melatonin in circadian rhythm, sleep disorders, insomnia in blind people, intercontinental flight dysrhythmia (jet-lag syndrome) and insomnia in elderly patients (Nowak & Zawilska, 1998). Bergstrom and Hakanson (1998) reported that the small doses required for sleep disorders have few side effects when reputable firms supply the compound. However, because neither the synthetic process nor tablet strength is inspected or regulated, there is obvious potential for harm, such as resulted not so long ago from the indiscriminate use of tryptophan, a closely related molecule to melatonin.

With the use of melatonin increasing rapidly, there is to date limited information regarding its physicochemical properties including hygroscopicity and partition coefficient. Knowledge of the hygroscopicity of the drug substance will allow us to adequately store the raw material and to comment of the packaging of commercially available dosage forms, and the partition coefficient while providing information on the solubility of the drug substance is a molecular property which influences the release, transport and the extent of absorption (ability to cross the BBB) of drugs in the body. There is good correlation between the BBB penetration *in vivo* and the lipid solubility of a drug i.e. the more lipid soluble a drug, the easier it is for it to penetrate the BBB and gain access to neurons (Gilgun-Sherki *et al*., 2001).

The resulting octanol-water partition coefficient (K_{ow}) is also one of the most effective parameters to evaluate the toxicity of a single organic chemical (Hansch, 1978). A

description and physical properties (including X-ray powder diffractometry, differential scanning calorimetry, UV/Vis spectroscopy and vibrational spectroscopy, nuclear magnetic resonance (NMR) and mass spectrometry) of melatonin is presented and where possible comparison of known literature values is made in order to both characterize melatonin and confirm the identity of the raw material (drug substance) used in this study.

3.2 DESCRIPTION OF MELATONIN

Melatonin is a practically odourless, off-white powder having a melting point of 118.1ºC determined in our laboratory. The molecular formula of melatonin [N-acetyl-5-methoxytryptamine; N- {2-(5-methoxyindol-3-yl) ethyl} acetamide] is $C_{13}H_{16}N_2O_2$ and the molecular weight 232.3 $g.mol^{-1}$ {elemental analysis: C (Calculated) 67.22%; C (Found) 67.27%: H (Calculated) 6.94%; H (Found) 6.79%: N (Calculated) 12.06%; N (Found) 11.89%} The molecular structure of melatonin is depicted in figure 3.1.

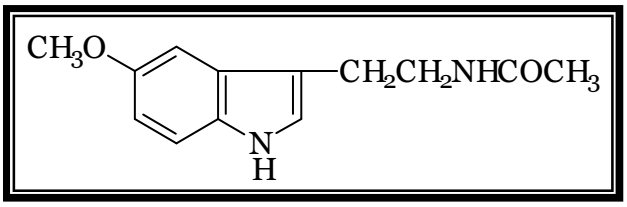

Figure 3.1: Molecular Structure of Melatonin.

Melatonin may be synthesized by the conversion of 5-methoxyindole to a gramine derivative, displacement with cyanide, lithium aluminium hydride reduction and acetylation according to the following scheme as shown in figure 3.2:

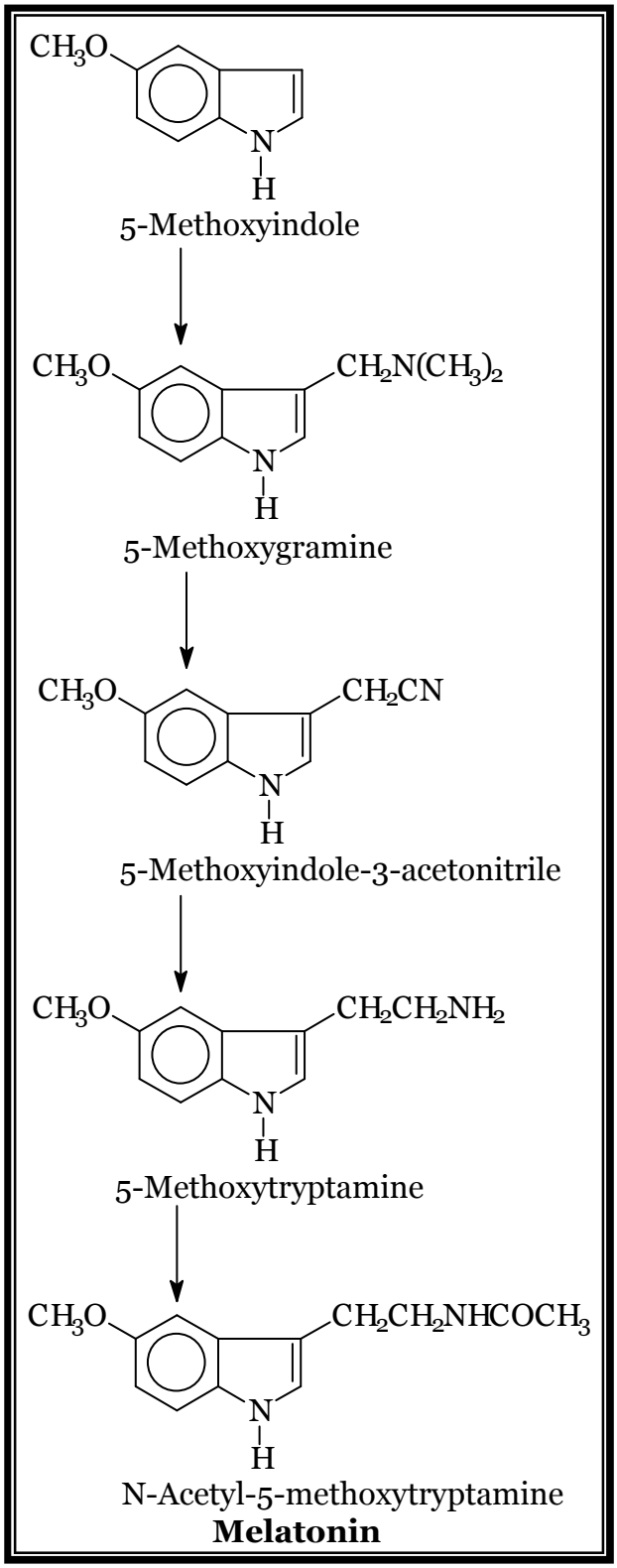

Figure 3.2: Synthesis of Melatonin from 5-Methoxyindole

3.3. PHYSICAL PROPERTIES OF MELATONIN

3.3.1 MATERIALS AND METHODS

3.3.1.1. Chemicals and Reagents

Melatonin, DMSO and methanol (deuterated) were purchased from Sigma Chemical Corporation, St Louis, MO, USA. All other chemicals were HPLC grade purchased from commercial distributors and contained no impurities, which could interfere with the determination of the test compound.

3.3.1.2. X-Ray Powder Diffraction Pattern

X-rays are electromagnetic radiation of wavelength about 1Å (10-10m), which is about the same size as an atom. They occur in that portion of the electromagnetic spectrum between gamma rays and the ultraviolet. The discovery of x-rays in 1895 enabled scientists to probe crystalline structure at the atomic level. X-ray diffraction (XRD) has been in use in two main areas, for the fingerprint characterization of crystalline materials and the determination of their structure. Each crystalline solid has its unique characteristic X-ray powder diffraction pattern, which may be used as a 'fingerprint' for its identification (Whittingham, 1997).

The X-Ray diffraction (XRD) pattern of melatonin was obtained in our laboratory and the data was collected on a Philips PW 1050/25 XRD-spectrogoniometer using CuKα (1.541 Å) with a Ni filter as a radiation source. The data was acquired at a rate of 2^{o} min^{-1}.

3.3.1.3. Differential Scanning Calorimetry

DSC thermograms are used to determine the physical state of a drug and determine what happens to the drug upon heating (El-Gibaly, 2002). In addition DSC is used to determine complex formation between drugs and other polymers. El-Gibaly (2002) used DSC to

determine the complex formation between chitosan and sodium dioctyl sulfosuccinate in melatonin-loaded chitosan microcapsules.

The differential scanning calorimetry (DSC) of melatonin was obtained using a Perkin-Elmer Series 7 DSC system, using a sample size of 2-5 mg and a heating rate of 10°C / minute, under a constant flow of nitrogen gas.

3.3.1.4. UV/Vis Spectroscopy

Ultraviolet-visible spectroscopy (UV = 200-400nm, visible = 400-800nm) corresponds to electronic excitations between energy levels that correspond to the molecular orbitals of the systems. A solution of 0.1mg/ml of melatonin was made up by accurately weighing out 1mg of melatonin and dissolving it in 10ml of 95% ethanol and in a mixture of 10% ethanol and water. The UV absorbance spectra of these solutions were recording on a GBC UV/Vis Model 916.

3.3.1.5. Vibrational Spectroscopy

Infra-red (IR) analysis simplistically determines the functional group chemistry of a compound. The IR spectrum of melatonin as a dispersion in a KBr pellet was obtained in this laboratory using a Perkin-Elmer FTIR 2000 spectrometer. Szmuszkovicz (1960) has reported that the principle infrared absorption peaks of melatonin are found at energies of 800, 810, 828, 1180, 1217, 1492, 1555,1587, 1620, 1627 and 3240 cm^{-1}. Therefore the melatonin samples were scanned between 400cm^{-1} to 4000cm^{-1}.

3.3.1.6. Nuclear Magnetic Resonance (NMR) Spectroscopy

Nuclear magnetic resonance spectroscopy is the use of the NMR phenomenon to study physical, chemical and biological properties of matter. As a consequence NMR spectroscopy finds applications in several areas of science. NMR spectroscopy is routinely used by chemists to study chemical structure using simple one-dimensional techniques. Two-dimensional techniques are used to determine the structure of more complicated molecules. These techniques are replacing x-ray crystallography for the

determination of protein structure (Hornak, 1999). The ^{1}H and ^{13}C nuclear magnetic resonance spectra of melatonin were recorded in deuterated-DMSO and deuterated methanol, respectively, on a 400.14 MHz Bruker Avance NMR spectrometer with the probe temperature regulated at 303∀0.1K.

3.3.1.7. Mass Spectrometry

Mass spectrometry is based on slightly different principles to the other above mentioned spectroscopic methods. The physics behind mass spectrometry is that a charged particle passing through a magnetic field is deflected along a circular path on a radius that is proportional to the mass to charge ratio, m/e. In an electron mass spectrometer, a high energy beam of electrons is used to displace an electron from the organic molecule to form a radical cation known as molecular ion. If the molecular ion is too unstable then it can fragment to give other smaller ions. The most useful information obtained from a mass spectrometry spectrum is the molecular weight of the sample and this is normally the heaviest ion from the sample provided that this ion is stable enough to be observed (www.chem.ucalgary.ca/courses/351/Carey/Ch1.html). The mass spectrum of melatonin was obtained using a Finnigan GCQ mass spectrometer.

3.3.2. RESULTS

3.3.2.1 X-Ray Powder Diffraction Pattern

The x-ray powder diffraction pattern of melatonin is presented in figure 3.3 and the scattering angles, interplanar distances, and peak relative intensities are collected in table 3.1.

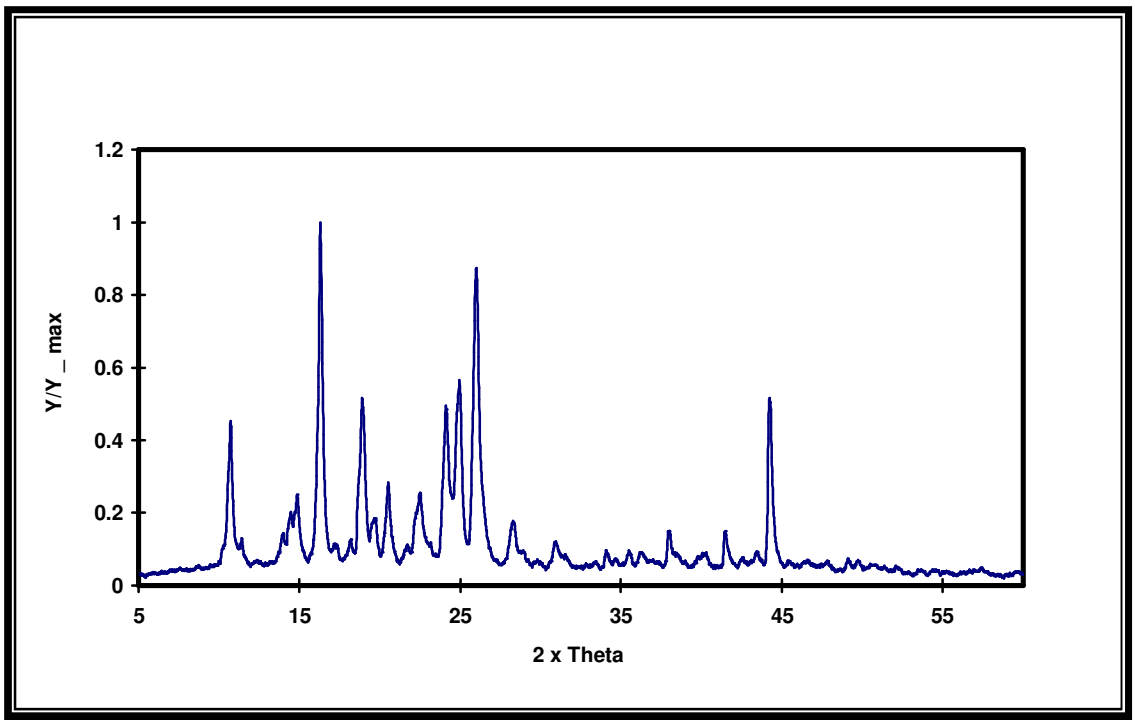

Figure 3.3: X-Ray Powder Diffraction Pattern of Melatonin.

Table 3.1: Crystallographic Data from the X-Ray Powder Diffraction Pattern of Melatonin.

Scattering angle (2θ)	Scattering angle (θ)	d spacing (Å)*	Relative Intensity (I)
10.734	5.367	8.237567381	0.449256
10.969	5.485	8.060875143	0.451000
14.815	7.408	5.975922956	0.228687
16.309	8.155	5.431735906	0.975643
18.946	9.473	4.681533845	0.489851
19.618	9.809	4.522661556	0.177267

20.540	10.270	4.321682863	0.273342
22.437	11.219	3.960225306	0.242219
24.083	12.042	3.693164785	0.483085
24.940	12.470	3.568312517	0.565629
26.015	13.008	3.423119325	0.863329
28.365	14.183	3.144644661	0.180000
37.954	18.977	2.369394453	0.148850
38.071	19.036	2.362321735	0.136671
38.122	19.061	2.359338298	0.121786
44.301	22.151	2.043501880	0.504736

*where $d_{h,k,l} = \lambda / (2 \text{ Sin } \theta)$

3.3.2.2 Differential Scanning Calorimetry

The DSC thermogram of melatonin is shown in figure 3.4. The strong endothermic peak which has its maximum at 117.33°C corresponding to the melting transition, an onset at 116.11°C and an end at 118.37°C is characterized by a heat of fusion equal to 130.34J/g. The equivalence of the baseline prior to and subsequent to the melting endotherm suggesting that the compound melts without decomposition has been confirmed by the melting point determination conducted in our laboratory.

3.3.2.3 UV/Vis

UV spectroscopic studies of melatonin were been conducted in 95% ethanol and resulted in a maximum at 272.5 and inflections at 295 and 308 nm. These ultraviolet absorptions are characteristic of hydroxyindoles. In a 10% ethanol in water solution, the spectrum of melatonin recorded between 200 and 400 nm exhibits a maximum at 278 nm as shown in Figure 3.5.

3.3.2.4 Vibrational Spectroscopy

The Fourier transform infrared spectrum of melatonin as a dispersion is shown in figure 3.6 and structural assignments have been correlated with group frequencies in table 3.2.

3.3.2.5 NMR Spectrometry

The ^{1}H and ^{13}C nuclear magnetic resonance spectra of melatonin are shown in figure 3.7 and 3.8. Assignments for the observed resonance bands are presented in table 3.3 together with the atomic numbering system

3.3.2.6 Mass Spectrometry

The mass spectrum of melatonin is presented in figure 3.9. The molecular ion peak was observed at m/z=232, and the base peak was at m/z=173. Assignments for the fragmentation pattern, the peak relative intensities, and the proposed structures are found in table 3.4.

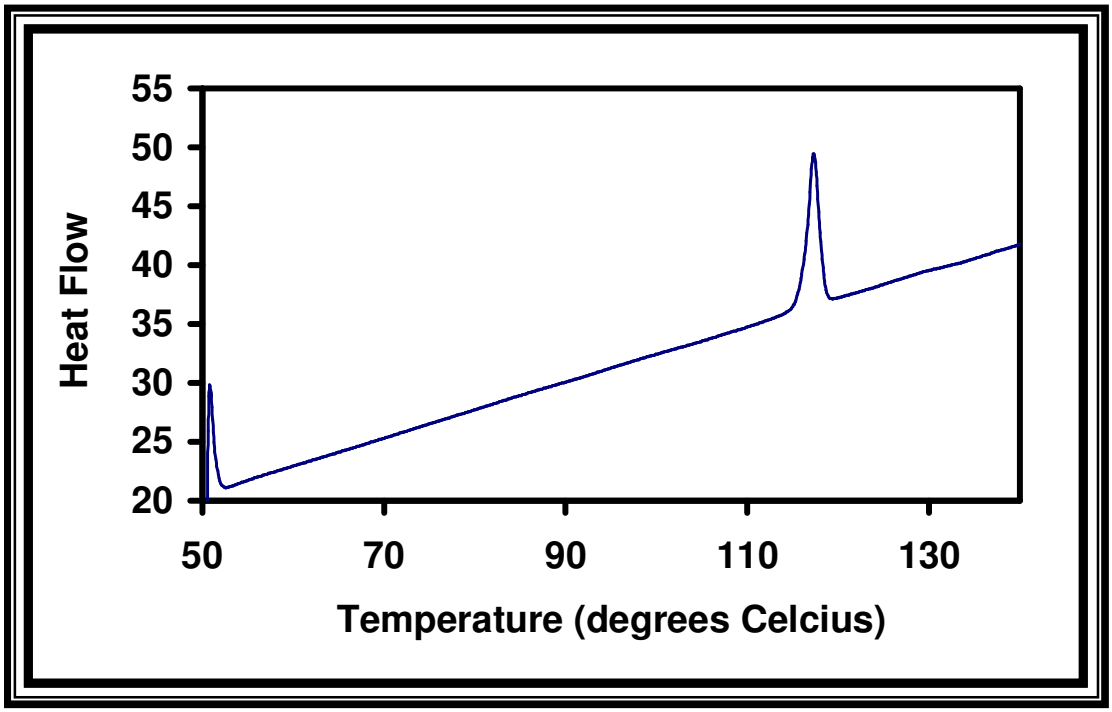

Figure 3.4: Differential scanning calorimetry thermogram of melatonin

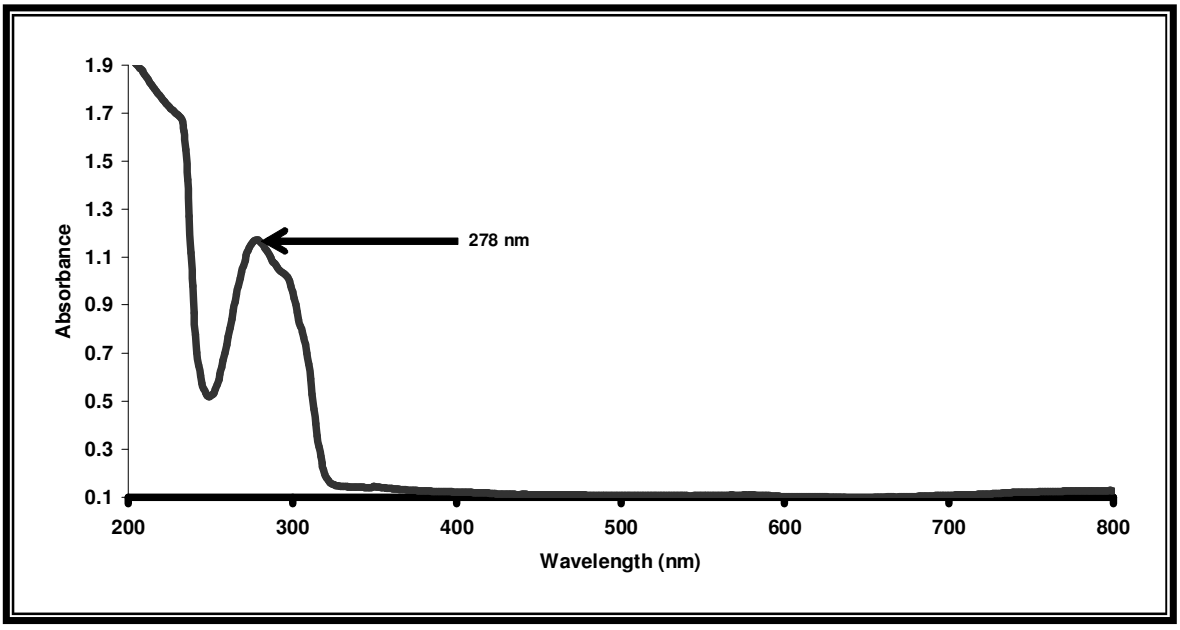

Figure 3.5: Ultraviolet absorption spectrum of melatonin in 10% ethanol in water

Table 3.2: Assignments for the Infrared Absorption Bands of Melatonin

Assignment	Frequency (cm^{-1})
-NH (indole), amide	3306, 3260
-C=O	1627
Aromatic –C=C	1587, 1492
-C-O	1212, 1175
Aromatic substitution	797, 825

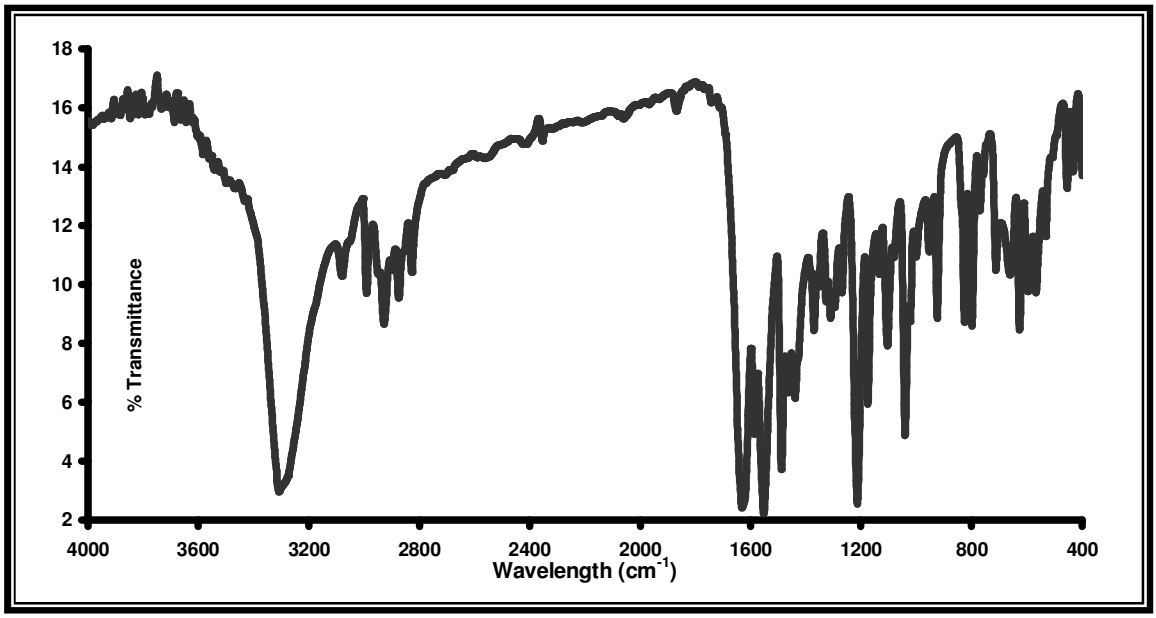

Figure 3.6: Infrared absorption spectrum of melatonin

Table 3.3: Assignments for the ^{1}H-NMR and ^{13}C-NMR Spectra of Melatonin

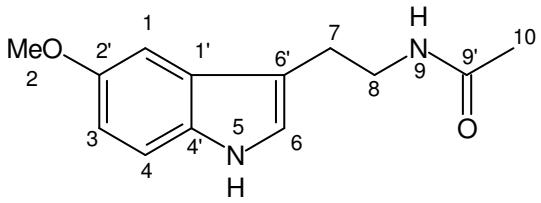

Atom No.	δ_C	δ_H (mult) DMSO-d_6	δ_H (mult, *J*, Hz) CD_3OD
1	100.1, d	7.1, s	7.1; d; 2.4
1’	110.9, s	-	-
2	55.2, q	3.8, s	3.8; s
2’	152.9, s	-	-
3	111.6, d	6.7, dd	6.7; dd; 2.4, 8.8
4	111.8, d	7.2, d	7.2; d; 8.8
4’	131.3, s	-	-
5	-	10.6, s	-
6	122.9, d	7.0, s	7.0; s
6’	127.4, s	-	-
7	25.1, t	2.8, t	2.9, t; 14.4
8	40.5, t	3.3, m	3.4, t; 14.8
9	-	7.9 s	-
9’	168.9, s	-	-
10	22.6, q	1.8, s	1.9; s

Figure 3.7: ^{1}H-NMR Spectra of Melatonin

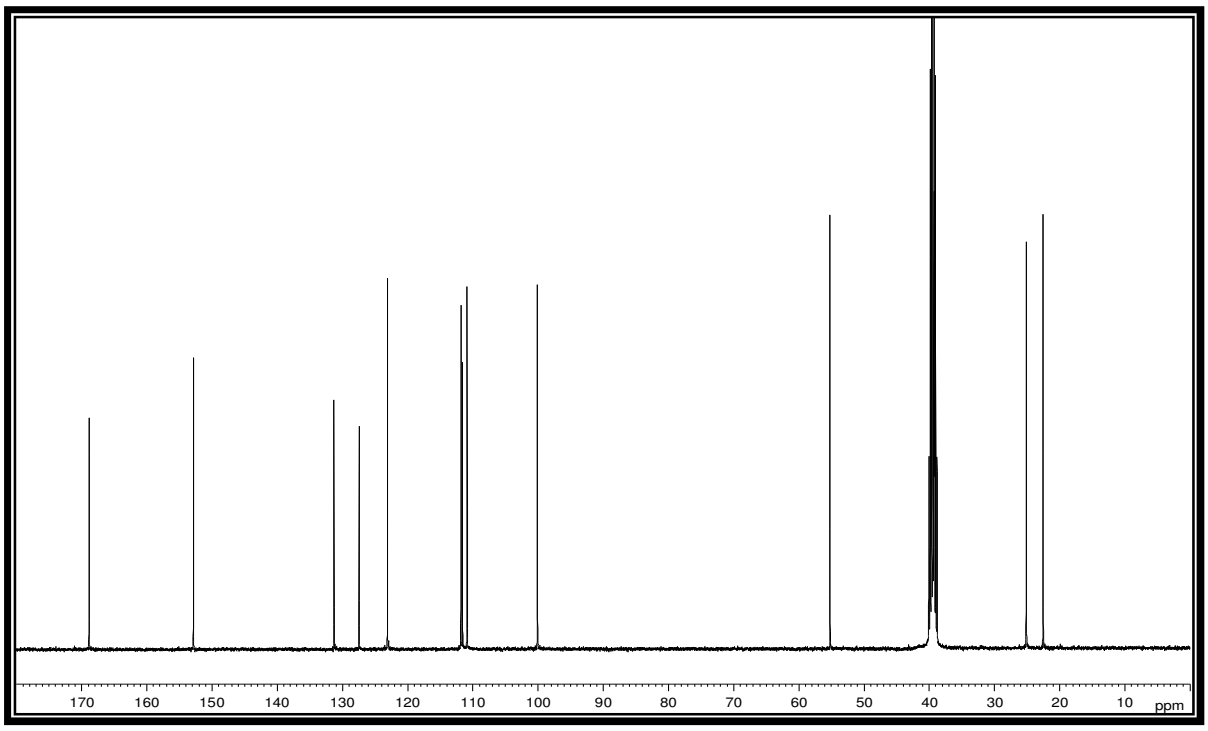

Figure 3.8: ^{13}C-NMR Spectra of Melatonin

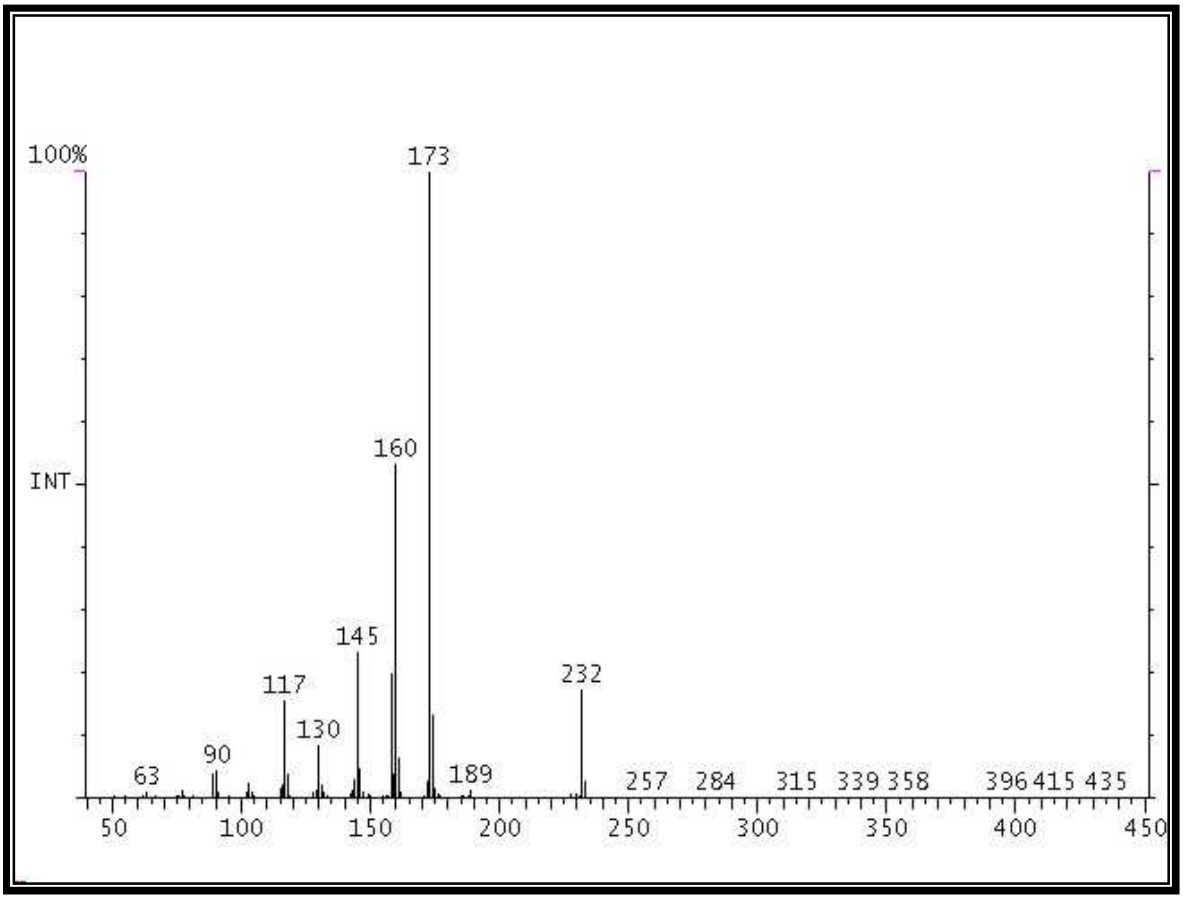

Figure 3.9: Mass spectrum of melatonin

Table 3.4: Assignments for the Prominent Fragments in the Mass Spectrum of Melatonin

m/z	Relative intensity %	Fragment
232	17.31	$M^{+\cdot}$
173	100.00	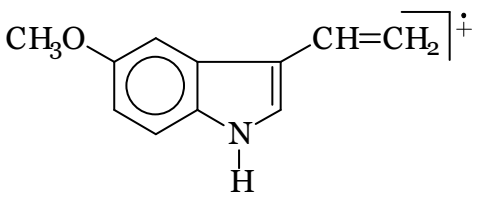
160	53.38	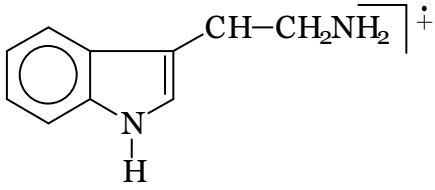

145	23.25	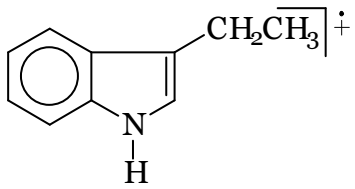
130	8.36	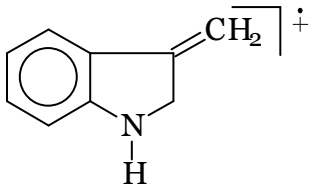
117	15.65	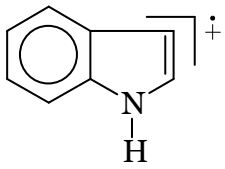

3.3.3 DISCUSSION

The conformational flexibility of the N-acetyl-ethylamine side chain in melatonin plays an important role in its binding to receptor sites. Also because of its pharmacological importance, melatonin has been studied by x-ray crystallographic and molecular orbital methods, investigating the relationships between their pharmacological activities and molecular configurations (Thewalt & Bugg., 1978; Quarles *et al*., 1974a; Quarles *et al*., 1974b). However, it should be noted that x-ray powder diffraction, DSC, UV/Vis, IR, NMR, and MS data on melatonin has not been reported in the literature

The results of this study describe the x-ray powder diffraction pattern, DSC, UV/Vis, IR, NMR and MS spectra of melatonin. El-Gibaly (2002) reported that melatonin possesses an endothermic peak at about 120^{o}C and this has been further confirmed in this study. In addition the X-ray powder diffraction pattern of melatonin and IR spectrum recorded for melatonin corresponds to the results recorded by Bayari and Ide (2003) for melatonin, while the MS data obtained above corresponds with the data that Harumi and Matsushima (2000) reported melatonin to possess.

This information provides a detailed characterization and confirms the identity of the melatonin raw material used in this study.

3.4 PARTITION COEFFICIENT OF MELATONIN

3.4.1 INTRODUCTION

Since the pioneering work of Fujita (1981) in the measurement and estimation of the octanol-water partition coefficient (K_{ow}), this property has become the cornerstone of a myriad of structure-activity relationships (SAR). The solubility of liquids and solids in water (S_w) as well as partition coefficient of solutes in different solvents viz. partition coefficient in octanol-water (K_{ow}), partition coefficient in water-hexadecane (P_{16}), partition coefficient in water-alkane (P_{alk}), and partition coefficient in water-cyclohexane (P_{cyc}) are very important molecular properties that influence the release, transport and the extent of absorption of drugs in the body (Abraham *et al*., 2000; Khadikar *et al*., 2002). Hansch and Leo (1979) have used the coefficient extensively for correlating structural changes in drugs with changes observed in biological, biochemical or toxic effects. These correlations are then used to predict the effect of a new drug for which a K_{ow} could be measured.

Water solubility is the most important property that can be estimated from K_{ow}, because it affects the fate and transport of chemicals. For example, compounds that are more soluble in octanol (more hydrophobic/ lipophilic) such as melatonin would be expected to partition out of the water and into the lipophilic tissue. Thus K_{ow} can be used to predict the potential for drug substances to accumulate in living tissue.

The K_{ow} is defined as the ratio of the molar concentrations of a chemical in n-octanol and water, in dilute solution and the coefficient K_{ow} is a constant for a given chemical at a given temperature. Since K_{ow} is the ratio of two molar concentrations, it is dimensionless. Sometimes, K_{ow} is reported as the decadic logarithm ($\log_{10}K_{ow}$). The mathematical statement of K_{ow} is:

$$\mathbf{K_{ow} = C_{octanol} / C_{water}} \qquad \textbf{.....Equation 1}$$

Where: $C_{octanol}$ and C_{water} are the molar concentration of the solute in *n*-octanol and water, respectively, at a given temperature.

UV spectrophotometry or HPLC are both suitable for determining the K_{ow} of single chemicals. However, the use of HPLC would be required in the determination of the K_{ow} of a mixture (Lin *et al*., 2001). To date there is no reference in the literature to the determination of the K_{ow} of melatonin. in dilute solution at a given temperature. In this study, the K_{ow} of melatonin was determined using the validated HPLC method (chapter two) to quantitate the amount of melatonin in the water and octan-1-ol layers.

3.4.2. MATERIALS AND METHODS

3.4.2.1 Chemicals and Reagents

Melatonin was purchased from Sigma Chemical Corporation, St Louis, MO, USA, while certified Octan-1-ol was purchased from Fisher Scientific Co. All other chemicals were HPLC grade purchased from commercial distributors and contained no impurities that could interfere with the determination of the test compound.

3.4.2.2 Instrumentation

The modular, isocratic HPLC system used for this determination was the same as that described in chapter two, section 2.2.3.

3.4.2.3 Chromatographic Conditions

The chromatographic conditions for this assessment were the same as that described in chapter two, section 2.2.4.

3.3.2.4 Sample Preparation

Melatonin powder was accurately weighed out and dissolved in a 1:1 mixture of octan-1-ol and water to give a final concentration of 0.1mg/ml of melatonin. The melatonin mixture was gently shaken for about 10 mins to avoid the formation of an emulsion. The two layers were then allowed to separate with the water layer remaining at the bottom. A

calibration curve in the range of 0.01-0.1 mg/ml was constructed for the accurate quantitation of melatonin. After separation of the octan-1-ol and water, 20µl of each layer (n=4) was injected onto the column. This was repeated on five different days. The temperature was maintained at 25 (± 0.05°C) throughout the experiment.

3.4.3 RESULTS

The chromatograms obtained from the partition coefficient determinations showed sharp and symmetrical peaks that were well resolved from the solvent peak (figure 3.10). The peak for melatonin in the water layer was about five times smaller than the melatonin peak in octan-1-ol (figure 3.10).

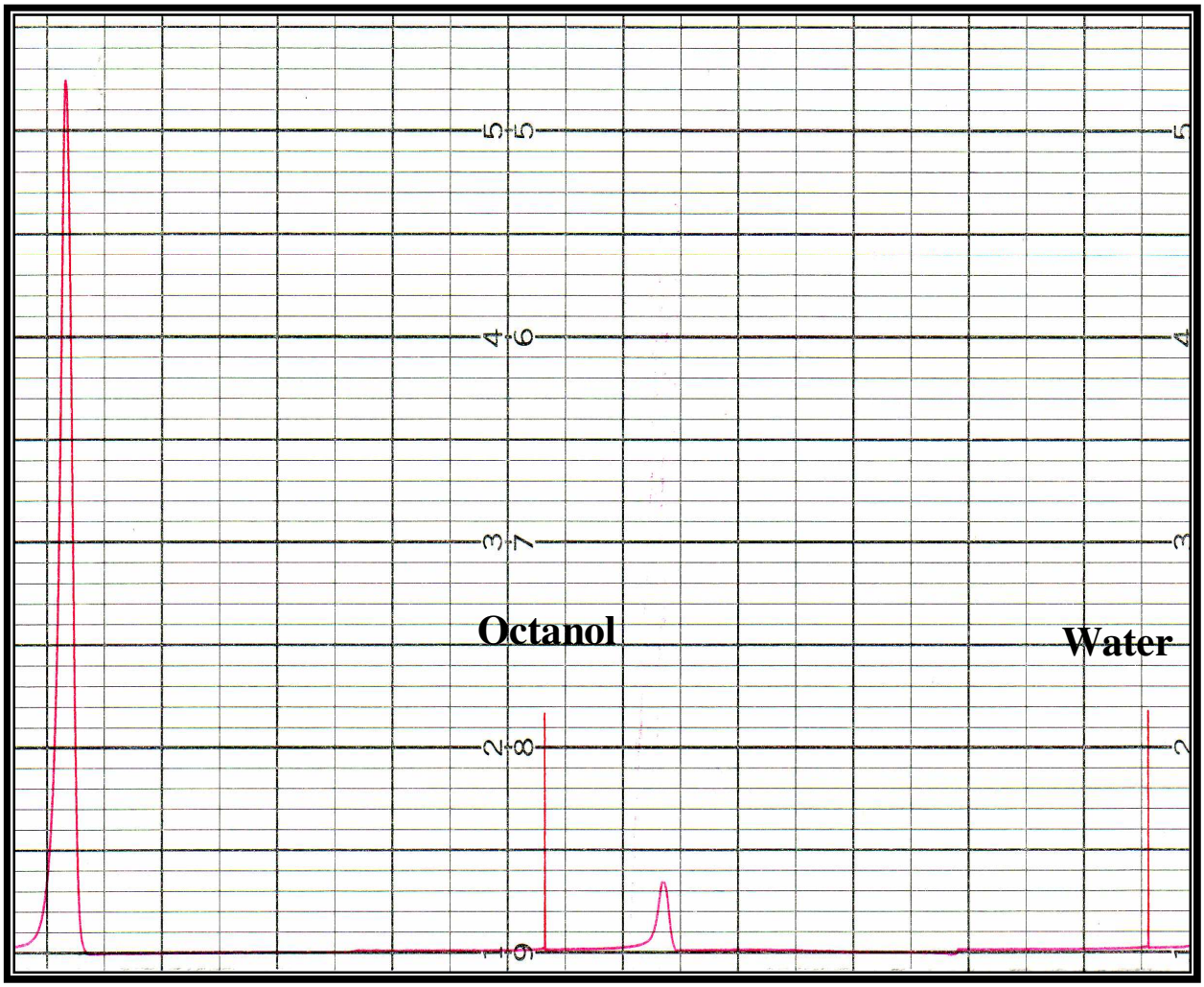

Figure 3.10: A chromatogram showing the separation of melatonin in the aqueous and octan-1-ol phases.

The calibration curve was linear for melatonin concentrations (0.01 – 0.1mg/ml) and the r^2 value of 0.9992 was obtained. The melatonin concentration in each phase was determined using a calibration curve constructed on the day of analysis (figure 3.11).

Table 3.5 represents the ratio of the melatonin in octan-1-ol and water as well of the concentration of melatonin in each phase. The K_{ow} of melatonin was calculated using equation 1. From the table it is evident that melatonin partitions to a greater extent in octan-1-ol than in water, with the partitioning ratio on all five days being ± 14. The concentration of melatonin in octanol on all five days was between 0.09-0.092 mg/ml indicating that 91% of the melatonin was present in the octanol phase, while the concentration of melatonin in water was between 0.006-0.0068 mg/ml indicating that only 6.4% of melatonin was present in the water phase. However this only accounts for 97.4% of the original melatonin mixture (0.1 mg/ml), with acceptable recovery loss of 3.6%. This loss could be due to some of the melatonin not being dissolved and thus remaining in the separating funnel.

3.4.4 DISCUSSION

From the above results it is evident that melatonin partitions to a greater extent in octan-1-ol than in water at a temperature of 25°C, with 90% of the original melatonin concentration (0.1mg/ml) being present in the octan-1-ol phase and only 6.4% in the water phase. Since K_{ow} does influence the release, transport and extent of absorption in the body, these findings have important implications. Thus, it can be concluded that melatonin is hydrophobic and as a result of this lipophilicity will be able to cross membranes easily and thus be able to cross all types of lipophilic biological barriers such as the blood brain barrier (BBB) and placenta and thus would be able to easily enter into all cytoplasmic and nuclear compartments (Dobsak *et al.*, 2003).

Normally the tight junctions of the BBB permit the diffusion of only very small amounts of water-soluble compounds (paracellular aqueous pathway), while the large surface area of lipid membranes of the endothelium offers an effective diffusive route for lipid-soluble agents such as melatonin via the transcellular lipophilic pathway. Therefore, a potential route through which a therapeutic substance may cross the endothelium is by the lipid

pathway. There is good correlation between BBB penetration *in vivo* and the lipid solubility of the drug. Furthermore, the presence of hydrophobic groups on a molecule may help it to penetrate the brain (Gilgun-Sherki *et al*., 2001). Melatonin as shown in this study is highly lipophilic and furthermore, the presence of the hydrophobic groups on the melatonin molecule will assist it in crossing the BBB to access neurons and glial cells. Melatonin has been shown because of its high lipophilic nature to easily penetrate the BBB (Reiter *et al*., 1997; Reiter *et al*., 1995); thereby its concentration in the brain rises rapidly (Menéndez-Peláez *et al*., 1993; Reiter *et al*., 1997) when administered exogenously. Immunocytochemistry and radioimmunoassay has been used to show that melatonin concentrates in the cell nucleus (Menéndez-Peláez *et al*., 1993) after administration. The indoleamine, melatonin concentrates into cellular organelles such as the nucleus (Menéndez-Peláez *et al*., 1993) and mitochondria, where it may help to preserve them from oxidative damage and subsequent ATP depletion (Martin *et al.,* 2000b; Acuña-Castroviejo *et al*., 2001). Thus, melatonin's lipophilic nature and potent antioxidative actions make it a useful agent that can be used in reducing damage to the brain from oxidative stress and ageing.

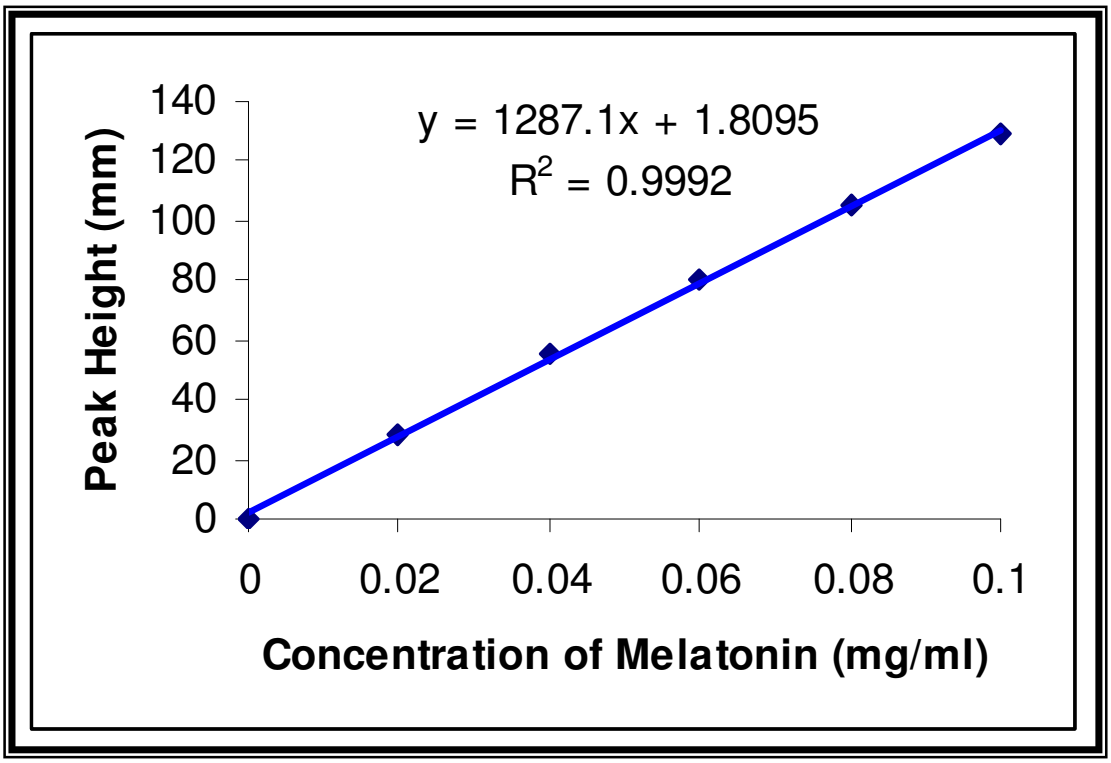

Figure 3.11: Linear Calibration curve for the quantitation of melatonin in the K_{ow} determination.

Table 3.5: Partitioning ratio of melatonin between octan-1-ol and water

	Peak Height (mm) and Melatonin Concentration (mg/ml) (n=4)		**K_{ow} Ratio**	**Log K_{ow}**
Day	**Octan-1-ol phase**	**Water phase**		
1	120.0 (**0.092**)	10.0 (**0.006**)	14.11	1.15
2	120.0 (**0.092**)	9.5 (**0.006**)	13.24	1.12
3	119.5 (**0.091**)	10.5 (**0.007**)	13.38	1.13
4	118.0 (**0.090**)	9.0 (**0.006**)	14.76	1.16
5	115.0 (**0.090**)	10.0 (**0.006**)	14.06	1.15
Average	118.5 (**0.091**)	10.0 (**0.006**)	14.09	1.15

3.5 HYGROSCOPICITY OF MELATONIN

3.5.1 INTRODUCTION

Hygroscopicity is the capacity of a product to react to the moisture content of the air by absorbing or releasing water vapour. The water content of the product is significant for the absorption or release of water vapour. A measure of the hygroscopicity of a product is consequently the magnitude of the increase or decrease in its water content as a function of relative humidity at a certain temperature. Weakly hygroscopic products exhibit no or only a slight change in their water content as a consequence of variations in relative humidity. In strongly hygroscopic products, water content may vary widely (http://www.tis-gdv.de/tis_e/misc/hygro,htm). In an unventilated container, filled with a hygroscopic product, the product determines the relative humidity in the hold, i.e. the product creates its own atmospheric environment. During these balancing processes, the product itself undergoes only slight changes to its water content, since this quantity of water is a multiple of the total (absolute) humidity of the container air. However, in a ventilated container filled with a hygroscopic product, the relative humidity of the container depends on the external air values, the product being able to absorb or release water vapour accordingly.

Determination of the hygroscopicity is essential for the determining the correct conditions for the handling, distribution, packaging, and storage conditions of a particular chemical compound. Containers carrying hygroscopic compounds should protect their contents from moisture, light and oxygen and must be tested for moisture permeability.

It is essential that an accurate assessment of the moisture content of the compound be made. These total values may often be obtained by drying under defined conditions that are appropriate to the proposed substance. Sometimes this may not be possible or may yield misleading results. In such cases, thermogravimetric analysis may be used to determine the water content.

Moisture is sometimes determined in the laboratory by the technique of weighing the sample following loss on drying (LOD). However, in this technique volatile substances

other than water will evaporate, giving an inaccurate reading (weight) for the moisture content. In order to determine water by distillation, large quantities of both sample and solvent are necessary. In addition to being time-consuming, distillation does not give accurate measurement when testing for low water concentrations (Wieser, 1993).

Gas chromatography can determine water concentration, but only in samples that have been transformed into a volatile derivative. A very accurate and practical method for water analysis in a wide range of sample matrices is the Karl Fischer (KF) titration. Overcoming the drawbacks of water analysis by LOD, KF titration is a test *specific* for water content. Analytical results from KF titrations combined with evaporation are more reliable than measurements by LOD because in evaporation-titration, only water content is measured.

Compared to gas chromatography, KF titration is a universal method, one that can be used for all types of samples regardless of their state of matter. And unlike the distillation method, KF titrations take just a few minutes, need only small quantities of samples and reagents, and deliver very precise measurements even for very low water concentrations (Wieser, 1993).

The most frequently used method of moisture analysis today is the coulometric KF titration technique. Redox chemistry forms the basis of this method. Moisture reacts stoichiometrically with iodine and sulfur dioxide to form iodide and SO_3. KF reagent consists of iodine, sulfur dioxide, a base and a solvent, such as alcohol:

$$I_2+SO_2+3Base+ROH+H_2O \rightarrow 2\ Base\ .\ HI+Base\ .\ HSO_4R \quad (1)$$

The current required to electrolytically generate iodine at the anode

$$2I^- - 2e^- = I_2 \quad (2)$$

is measured and stoichiometrically related to the amount of moisture introduced. The technique is highly accurate and precise, and extremely sensitive.

The KF technique is widely used by practicing analysts and continues to be actively investigated (Nordmark & Cedergren, 2000; Margolis, 1998). Moisture has been quantitatively correlated with a wide range of useful properties in an even wider array of

diverse material including foodstuffs, petrochemicals, pharmaceuticals, and cosmetics (Masa, 1998). Owing to its widespread utility, the technique represents an important application of redox chemistry and electrochemistry (Mendham *et al*., 2000; Skoog *et al*., 2000). The KF reagents consist of iodine, sulphur dioxide, a base, and a solvent. Originally, pyridine was the base of choice for the reaction. However, health concerns sent chemists in search of less hazardous bases to perform volumetric KF titrations. Coulometric reagents have also contained hazardous chemicals, particularly halogenated hydrocarbons. Recent research has provided substitute reagents that are safer for the environment (Wieser, 1993).

Coulometric reagents that are free of halogenated hydrocarbons are currently available for routine analyses. However, some samples (particularly those containing aldehydes and ketones) engage in side reactions with standard KF reagents. Therefore, the reagents used for any particular titration must be carefully selected (Wieser, 1993)

The KF instrument is relatively inexpensive, simple to operate, robust toward student use and microprocessor driven (there is no software to master), and its scientific principles are easily understood. Furthermore, accurate and precise determinations can be accomplished in a short period of time.

At present, there are no publications or reports on the moisture content of the melatonin and its oral dosage forms, raising concerns about the packaging and storage of melatonin raw material and oral dosage forms. The present study looks at the moisture content of melatonin under different moisture and temperature conditions in order to determine its hygroscopicity.

3.5.2. MATERIALS AND METHODS

3.5.2.1 Chemicals and Reagents

Commercially available capsules/tablets packaged in white securitainers/ amber plastic containers were utilised in this study. KF reagents (anode and cathode solutions) containing iodine, sulphur dioxide, a base, and a solvent were of the highest quality available and were purchased from commercial distributors.

3.5.2.2 Instrumentation

The KF apparatus (Mettler DL 18 Karl Fischer Titrator) shown in figure 3.12 was used to determine the water content of melatonin raw material only. A modular, isocratic HPLC system as described in chapter 2.2.3 was used.

Figure 3.12: Photograph of the Karl Fischer Titration Apparatus (Mettler DL 18).

3.5.2.3 Chromatographic Conditions

Quantitation of melatonin was achieved according to the chromatographic conditions described in chapter 2.2.4. This analytical procedure for melatonin determination has been validated for linearity, repeatability, precision, and LOQ and LOD (refer to chapter two, section 2.3).

3.5.2.4. Sample Preparation

Melatonin powder (10mg) was accurately weighed, introduced into the KF apparatus and its moisture content was measured and reported as a percentage (n=3).

10 melatonin tablets were crushed, weighed and dissolved in sufficient mobile phase to yield a concentration of 0.1mg/ml melatonin. Similarly, the powder from the melatonin capsules was weighed and dissolved in sufficient mobile phase to yield a 0.1mg/ml melatonin concentration and these samples were analysed using HPLC (n=3). HPLC analysis was used for the determination of hygroscopicity of the melatonin tablets and capsules in order to ensure that the value obtained was only of that of melatonin and not the excipients used in the melatonin formulations.

Thereafter, melatonin powder samples (10mg); tablets (10); and capsules (10) were placed onto clear petri-dishes. Ten melatonin tablets and capsules were also kept in their original packaging. These were then exposed to different conditions for 1 month i.e.

- at 40^{o}C/75% relative humidity (RH)
- at 25^{o}C/ dry heat
- at 30^{o}C/ dry heat
- and at 60^{o}C/ dry heat

Samples were withdrawn each day at the same time for the first 7 days, after which they were sampled on the 14th and 21st days and analysed according to the abovementioned procedures.

3.5.2.4. Statistical Analysis

The results were analysed using a one-way analysis of variance (ANOVA). If the F values were significant, the Student Newman-Keuls test was used to compare the treated and control groups. The level of significance was accepted at $p<0.05$ (Zar, 1974).

3.5.3. RESULTS

The control hygroscopicity value obtained for melatonin raw material using the KF apparatus was 4.067%. Table 3.6 shows the % hygroscopicity obtained and the % increase in moisture content of the melatonin raw material under various conditions over the time period. It is evident from the table that the water content (%) did not vary to a great extent for the melatonin raw material maintained at 25°C and 30°C, with % increases in water content of ± 2% occurring on the 21st day of analysis. No statistically significant difference was noted between the day 21 value and the day 0 obtained. It is evident from the results in table 3.6 that significant increases in the water content (%) are noted for the melatonin raw material maintained at 40°C / 75% RH and at 60°C, with increases of 4.5 and 15% respectively.

Table 3.6: Water content (%) in melatonin raw material.

	Average % Water Content and % Increase (n=3)			
Day	**40°C / 75% RH**	**25°C**	**30°C**	**60°C**
0	4.067	4.067	4.067	4.067
0.25	4.067 **(0%)**	4.069 **(0%)**	4.066 **(0%)**	4.067 **0%)**
1	4.082 **(1.5%)**	4.067 **(0%)**	4.067 **(0%)**	4.155 **(9%)**
2	4.097 **(3%)**	4.067 **(0%)**	4.067 **(0%)**	4.163**(9.6%)**
3	4.095 **(2.8%)**	4.066 **(0%)**	4.069 **(0%)**	4.167**(10%)**
4	4.106 **(3.9%)**	4.067 **(0%)**	4.066 **(0%)**	4.167**(10%)**
5	4.105 **(3.8%)**	4.080 **(1.5%)**	4.080 **(1.5%)**	4.180 **(11%)**
6	4.105 **(3.8%)**	4.080 **(1.5%)**	4.080 **(1.5%)**	4.185**(12%)**
7	4.1060 **(3.9%)**	4.084 **(2%)**	4.081 **(1.5%)**	4.207**(14%)**
14	4.1085 **(4.2%)**	4.084 **(2%)**	4.084 **(2%)**	4.217**(15%)**
21	4.112 **(4.5%)** *	4.080 **(1.5%)ns**	4.081 **(1.5%)ns**	4.217**(15%)** **

***p<0.05 in comparison to day 0 and **p<0.01 in comparison to the day 0 value.**

The chromatograms obtained for the hygroscopicity study of melatonin powder and tablet formulations using HPLC analysis showed sharp and symmetrical peaks that were well resolved from the solvent peak. The peaks for melatonin capsules was 141mm and for melatonin tablets was 136.5 mm on day zero and were taken as 0% increase in moisture content, thereafter any decreases that occurred in the peak height were calculated as % increase in moisture content. However, there is a possibility that the excipients present in the melatonin tablets may be contributing to the increased moisture uptake in the tablets since this increase in moisture content is not the case with the raw material. Therefore, the possibility that the excipients are hygroscopic cannot be ruled out.

Table 3.7: Water content (%) of melatonin capsules and tablets using HPLC analysis.

Average Peak Height (mm) and Average % Increase in Moisture Content (n=3)					
Melatonin	**Day**	**40°C/75%RH**	**25°C**	**30°C**	**60°C**
Capsule (unpackaged)	21	138 (2%)	139 (1.4%)	139 (1.4%)	136.5 (3%)
Capsule (packaged)	21	140 (0.7%)	141 (0%)	140 (0.7%)	140 (0.7%)
Tablet (unpackaged)	21	122 **(11%)****	130 **(11%)****	132 **(8%)****	119 **(13%)****
Tablet (packaged)	21	132 (3%)	136.5 (0%)	134(2%)	132(3%)

****p<0.01 in comparison to day 0 value**

Over the days chosen for analysis the % increase in water content for melatonin capsules (unpackaged and packaged) and melatonin tablets (packaged), over the various conditions, did not increase significantly, however for the melatonin tablets (unpackaged) there was an increase in % moisture content.

Table 3.7 shows the results obtained on day 21 of analysis. It is clearly evident from table 3.7 the melatonin capsules (packaged and unpackaged) were stable in terms of absorption of water, with the highest % increase in moisture content occurring at 60°C of 3% and 0.7%, respectively. The melatonin tablets in their original packaging did not show a significant increase in % moisture content in comparison to the day 0 values. The highest value obtained for % increase in moisture content was 3% at 40°C/75%RH and 60°C**.**

The melatonin tablets (unpackaged) showed significant increases in % increase in moisture content at all the storage temperatures, with increases of 11%, 11%, 8% and 13% observed at 40°C/75% RH, 25°C, 30°C, and 60°C respectively**.**

3.5.4 DISCUSSION

Although there are many reports on the use of melatonin, not much information is available to researchers concerning the moisture content of this drug substance, which will aid in the determining the correct conditions for the handling, distribution, packaging, and storage conditions for melatonin.

Precise control of moisture can be very important in the processing, testing and stability of manufactured goods. Moisture can affect the storage life of pharmaceuticals and foods. From the above results it can be noted that melatonin raw material is not hygroscopic when stored for a prolonged period of time at 25°C and 30°C with a % increase in moisture content of only 2%. However, significant increases in % increase in moisture content is noted for melatonin raw material stored at 40°C / 75% RH and at 60°C, with increase of 15% and 4.5%, respectively. The melatonin tablets (packaged) and capsules (unpackaged and packaged) are stable in terms of absorption of moisture under various conditions of storage used in the above experiment. However, from the above results it is evident that there was a significant increase in moisture content for the melatonin tablets (unpackaged).

3.6 CONCLUSION

This chapter has described melatonin and examined the different physical properties of melatonin, allowing both the characterization and confirmation of the identity of melatonin raw material used in this study.

There are a number of routes of administration of melatonin. However despite the common use of melatonin, to our knowledge the octanol-water partition coefficient and hygroscopic properties of melatonin is not known. The present study shows that melatonin partitions to a greater extent in octan-1-ol than in water, with the partitioning ratio on all five days being ± 14. Thus, it is evident that melatonin is highly lipophilic and thus be able to enter the blood brain barrier (BBB). Thus, since melatonin is highly lipophilic and can easily cross the BBB after peripheral administration (Reiter *et al*., 1995; Reiter *et al*., 1997) and thus exogenous melatonin may be highly useful in preventing oxidative damage to neural tissue as it can easily gain access to the brain. This also provides essential experimental evidence regarding the preparation of melatonin in solution, since melatonin has low water solubility. Thus we can conclude that melatonin raw material is extremely hygroscopic at 40°C / 75% RH and at 60°C conditions and thus handling, distribution, packaging, and storage of melatonin raw material should rather be done at 25°C or 30°C. While melatonin tablets (packaged) and melatonin capsules (unpackaged and packaged) are not hygroscopic at the above conditions.

These results are important because melatonin tablets should not be left out of the original packaging at any of the above tested conditions, as it tends to absorb water vapour and increase the water content of melatonin. It is important as people buying the product should be informed on the proper storage of melatonin tablets to improve its stability and ensure long-term integrity of the compound. In addition, this chapter examines the different physical properties of melatonin, which would assist researchers in the identification of melatonin in different dosage forms and experimental specimens.

CHAPTER FOUR

pH AND TEMPERATURE STUDY OF MELATONIN

4.1 INTRODUCTION

The pineal hormone melatonin is present in all mammalian species studied to date (Reiter, 1991). Since Wurtman *et al*., (1965) reported the inhibitory action of melatonin injections on the reproductive axis in rats, numerous experiments have been conducted in various animal species and in humans, utilizing administration of exogenous melatonin (Reiter *et al*., 1983; Cavallo, 1993). Numerous dosage forms and brands of melatonin have appeared on the market. Various authors have used different routes of administration of melatonin, for example, oral (Aldhous *et al*., 1994), subcutaneous (Colmenero *et al*., 1991), intranasal (Vollrath *et al*., 1981), intramuscular (Lissoni *et al*., 1986), intravenous (Mallo *et al*., 1990) and transdermal (Lee *et al*., 1994).

The most common route of administration melatonin is the oral route, thus exposing the indole group to large variations in pH, within the gastrointestinal tract. It has been shown that melatonin is stable for at least 6 months in aqueous solution when stored in vials under vacuum at 4^{o}C. (Cavallo & Hassan, 1995). Also, despite the common use of aqueous solutions of melatonin, its stability in solution has not been reported. In fact, it is a lack of this information that has led researchers to utilize freshly prepared solutions, increasing experimentation and therefore cost. In addition, at present, there is very little information on the stability of melatonin in over a range of pH's and temperatures. Such information would be important to researchers when considering the bioavailability of melatonin from the gastrointestinal tract and when preparing melatonin solutions at different pH's and temperatures.

The aim of this study was thus to investigate the stability of melatonin in aqueous solution over a pH range, at both room and body temperature using the validated HPLC method developed in chapter 2.

4.2. MATERIALS AND METHODS

4.2.1 Chemicals and Reagents

All other chemicals were of the highest quality available and were purchased from commercial distributors.

4.2.2. Instrumentation

The HPLC instrumentation used for this experiment was the same as that as described in chapter 2, section 2.2.3.

4.2.3 Chromatographic Conditions

Separation was achieved according to the chromatographic conditions described in chapter 2, section 2.2.4.

4.2.4. Sample Preparation and pH Measurement

A stock solution of melatonin (0.1 mg/ml) was freshly prepared by accurately weighing out 1mg of melatonin and dissolving it in mobile phase. Dilutions of this stock solution were made to prepare the required standard solutions in the desired concentration range. Solutions of melatonin at a concentration of 50µg/ml were prepared in phosphate buffer at the following pH's using a Crison Basic 20 pH meter: 1.2, 2, 4, 7.4, 10, 12 and stored in 20mL glass volumetric flasks. These pH's and temperatures were chosen in order to assess melatonin's stability both under physiological conditions as well as in chemical conditions i.e. when melatonin is prepared to be used in the laboratory.

4.2.5 Stability Assessment

These solutions were stored at room temperature (25± 2°C). A duplicate set of solutions was kept at 37±2°C in an incubator with both sets of solutions stored for 21 days. A 20µl sample was withdrawn from each solution and analyzed daily for the first 7 days and then on days 14 and 21 using the HPLC method described in chapter 2. The concentration of melatonin is expressed as a percentage of the initial concentrations of the melatonin in solution.

4.3 RESULTS

As shown in figure 2.1, the chromatogram obtained from the melatonin solutions show sharp and symmetrical peaks, which were well resolved from the solvent peak with a retention time for melatonin at 7.2 min.

It is evident in table 4.1, showing the % of melatonin remaining that no degradation was observed in the first 2 days. From days 3 - 21, there was a gradual decrease in melatonin present at all pH's, with the % degradation not exceeding 30% at pH 12. As shown in table 4.2, the melatonin remained stable for the first 2 days at 37°C. From day 3 - 21, melatonin levels decreased gradually, not exceeding 29% degradation at pH 12.

Table 4.1: % Melatonin remaining after storage at room temperature (25±2ºC)

pH						
	1.2	**2**	**4**	**7.4**	**10**	**12**
Time (Days)						
0	100	100	100	100	100	100
0.25	100	100	100	100	100	100
1	100	100	100	100	100	100
2	100	100	100	100	100	100
3	99	99	99	99	100	99
4	99	99	99	99	99	97
5	99	92	92	91	97	88
6	95	92	92	83	97	88
7	92	92	91	83	88	80
14	82	80	84	77	88	79
21	76	73	78	71	77	70

Table 4.2: % Melatonin remaining after storage at 37 ±2ºC

pH						
	1.2	**2**	**4**	**7.4**	**10**	**12**
Time (Days)						
0	100	100	100	100	100	100
0.25	100	100	100	100	100	100
1	100	100	100	100	100	100
2	100	100	100	100	100	100
3	99	100	100	100	100	100
4	96	92	96	98	95	92
5	95	88	95	90	92	89
6	94	88	94	84	92	86
7	94	88	87	82	92	81
14	85	79	83	75	88	74
21	78	75	78	72	77	71

4.4 DISCUSSION

Due to the increased popularity of melatonin, numerous dosage forms of have become available, ranging from intranasal to transdermal dosage forms. However the most popular dosage form for melatonin remains the oral dosage form. These oral dosage forms namely capsules and tablets include modified release dosage forms. Considering that melatonin in the oral dosage form would be exposed to large variations in pH in the gastro-intestinal tract, the question arises as to whether melatonin would be stable in these environments. It has previously been shown that melatonin is stable in aqueous solution for at least six months when stored at 4°C in vials under vacuum (Cavallo & Hassan, 1995). However these authors did not demonstrate the stability of melatonin at temperatures higher than 4°C, and at different pH's.

The results of the present study demonstrate that solutions of melatonin are relatively stable at room temperature (25±2°C), and at 37±2°C, for at least 2 days, and that these levels do not decline by more than 30% after 21 days. Similarly, the results show that as expected pH does not play a significant role in the stability of melatonin and that melatonin is not sensitive to temperature changes with similar degradation profiles observed for both temperature conditions.

4.5. CONCLUSION

At present there are numerous dosage forms of melatonin, with oral route of administration being most popular. Presently, there is little information on the stability of melatonin over a pH range. With changes in pH in the gastrointestinal tract, as well as in different experimental conditions, information on the stability of melatonin is important. Using the HPLC method developed in chapter 2, the stability of melatonin solutions over a pH range (1.2 – 12) at room temperature and at 37^{o}C over a period of 21 days was assessed. These findings imply that melatonin should be relatively stable at body temperature when ingested orally, particularly as this hormone is known to be very lipophilic and can cross membranes, such as the stomach wall, with ease. This also suggests that orally administered slow release preparations of melatonin should be relatively stable and therefore exhibit favourable bioavailability. This study thus provides

the first evidence of the stability of melatonin over a pH range. However it should be noted that melatonin in solution is not stable within acceptable limits (95-105%) after 3 days, providing important information and a challenge to the formulators of this drug substance in a liquid dosage form. Further studies are required to determine the bioavailability of melatonin from the gastro-intestinal tract to confirm these findings.

CHAPTER FIVE

MELATONIN PHOTOSTABILITY - ICH

5.1. INTRODUCTION

Much attention has been focused in recent years by the Pharmaceutical Industry on photostability and the issues of protecting drug substances and products from light. Several important reviews of this topic appeared in the literature before the introduction of the ICH photostability guidelines in 1997 (ICH, 1997; Moore, 1996). Surveys on the photostability practices in the pharmaceutical industry conducted before the introduction of the ICH guideline showed diverse applications of photostability testing globally (Anderson *et al*., 1991; Thorma, 1996). Due to the variation of photostability protocols and in experimental design, it became apparent that some harmonization of photostability practices was needed (Tonnesen & Karlsen, 1995).The ICH Q1B guideline is now the official guideline to which the pharmaceutical industry is expected to adhere to when conducting photostability tests (ICH, 1997). This photostability guideline primarily pertains to the photostability of drug substances and manufactured finished drug products but does not specifically address the photostability of a product under in-use conditions or the photostability of analytical samples.

The ICH decision flow chart is illustrated in figure 5.1. (www.ifpma.org/ich5q.html). The first law of photochemistry states that only radiation that is absorbed by a molecule can be effective in producing chemical changes in the molecule (Thatcher *et al*., 2001). Primary photochemical reactions occur only when a molecule absorbs radiant energy and becomes electronically excited and the energy absorbed by such a molecule can be dissipated in many ways, including heat (internal conversion), emission of photons (fluorescence or phosphorescence), energy transfer to another molecule (sensitization), and direct photoreaction (Turro, 1982).

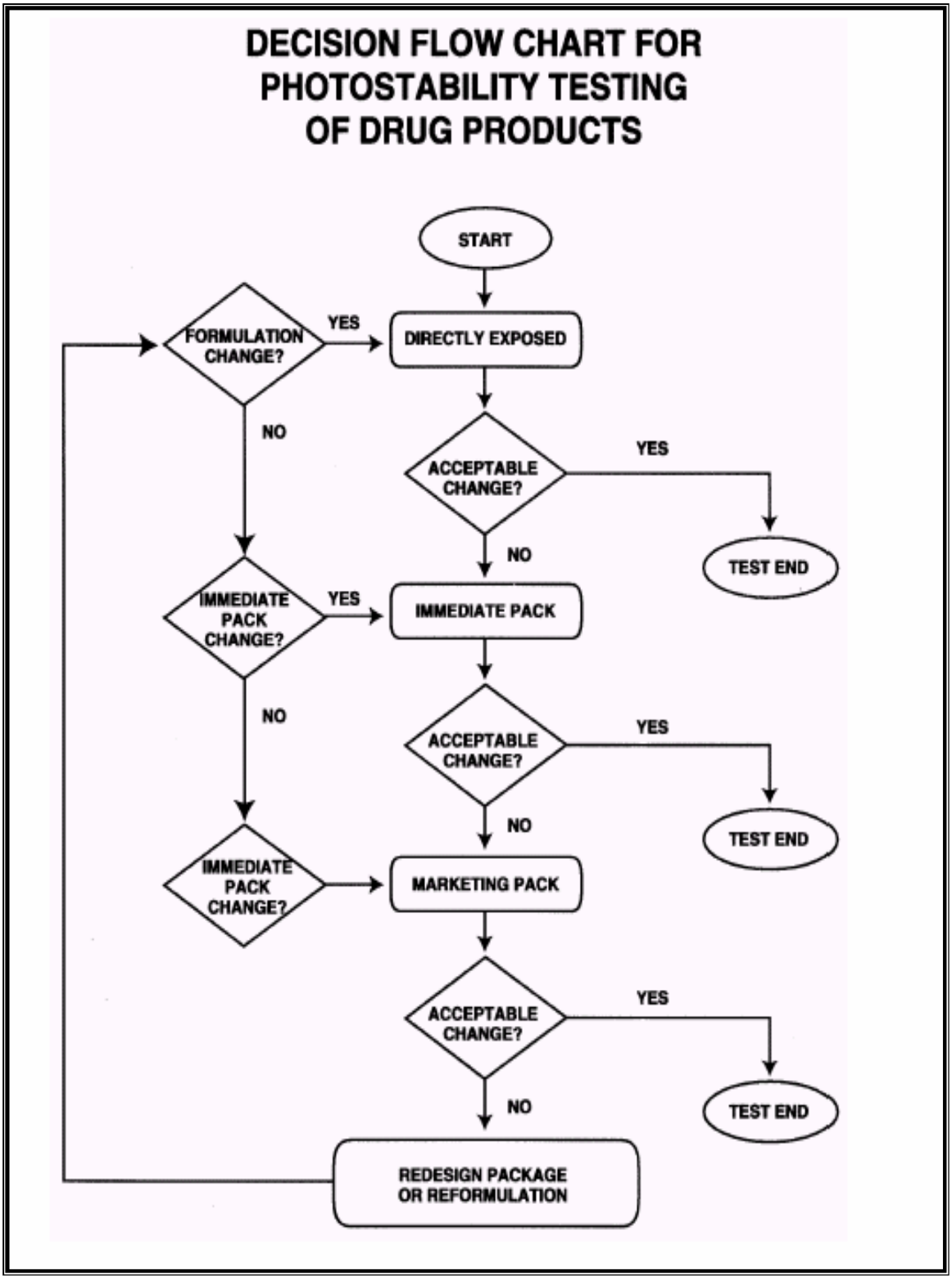

Figure 5.1: Decision flow chart for photostability testing of drug products. (ICH, 1997).

The photoliability of the final dosage form depends on three main factors: the active ingredient (s), the excipient (s) in the dosage form, and the physical state of the dosage form (e.g. solution, solid, or suspension). A molecule may be photoreactive in solution but not as a solid. Solid dosage forms typically are more photostable than solutions because the drug is protected (shielded) in the interior portions of the dosage form (i.e. photodegradation is a surface phenomenon). Of all dosage forms, solutions are the most susceptible to photodegradation (see table 5.1). Pharmaceutical products especially solutions may continue to degrade after exposure to radiation (Thoma, 1999).

Table 5.1: Susceptibility of dosage forms to photodegradation (Thoma, 1999).

Very High	High	Low
Parenterals	Soft gelatin capsules	Tablets
Infusions	Ointments	Capsules
Ophthalmic drops	Creams	Powders
Nasal solutions	Lotions	Coated Tablets

The manner in which samples are prepared, packaged, and aligned relative to the photolysis source for photostability testing can have a significant effect on the outcome of a photostability experiment. Therefore, all experiments in this chapter were designed such that the physical characteristics of the sample being tested (melatonin) were conserved.

5.2. PHOTOSTABILITY TESTING OF MELATONIN UNDER ICH CONDITIONS.

5.2.1 INTRODUCTION

Melatonin synthesis is under the control of the sympathetic nervous system. At night, during the dark phase, the pineal gland is activated by norepinephrine released from sympathetic fibers innervating the gland. This results in enhanced conversion of tryptophan to melatonin. Melatonin, once formed by the pineal gland is not stored in the gland but released immediately into the bloodstream. Light entering through the eyes inhibits the synthesis of melatonin. Thus, melatonin is secreted diurnally (Reiter, 1991).

Melatonin being highly lipophilic is able to traverse most barriers in the body and there is presently wide speculation that this antioxidant could be used as a neuroprotectant in neurodegenerative disorders such as Alzheimer's disease (Tan *et al*., 1993a). In addition, because of its protective properties, it has also been suggested that melatonin could be potentially useful if incorporated into sunscreens. It has been reported that topically administered melatonin, when applied to the skin immediately after UV irradiation, significantly suppresses the formation of UV-induced erythema (Bangha *et al*., 1997).

We have demonstrated previously (Maharaj *et al*., 2002), that irradiation of melatonin in solution (quartz photoreactor and medium pressure mercury lamp) results in rapid degradation of melatonin with only 18% of melatonin remaining after 20 min. For this reason, if melatonin is to be incorporated into pharmaceuticals, its stability in the presence of light needs to be thoroughly investigated. The evaluation of drug photostability is important not only due to the fact that photodecomposition leads to a loss of potency and therapeutic inactivity, but also due to the possible occurrence of adverse effects as a result of the formation of minor degradation products during storage and administration (De Vries *et al*., 1984). In addition, knowledge about the photostability of drug substances and drug products is thus also important to provide information in the handling, packaging and labeling of drug products (Tønnesen, 1996).

Photostabilty testing in formulations adds another dimension to the testing, as there are excipients, which are susceptible to free radical attack and are able to participate in a photochemical process. Although there have been many reports on photostability testing (Andersen *et al.*, 1991; Hibbert, 1991), the ICH Harmonized Tripartite Guideline has made recommendations to be adopted on 1 January 1998 covering the stability of new drug substances and products and notes that light testing should be an integral part of testing the agent (www.ifpma.org/ich5q.html) with the implementation of these ICH photostability study guidelines being reported on in the literature (Helboe, 1998).

The present study is thus the first report describing the photostability of melatonin raw material, tablets, capsules and solution under ICH conditions to include information on the effect of packaging on the photostability of melatonin.

5.2.2. MATERIALS AND METHODS

5.2.2.1. Chemicals and Reagents

The commercially available capsules were packaged in white securitainers and the tablets in amber plastic containers. All other chemicals and reagents were of the highest purity available.

5.2.2.2. Analytical Method

The HPLC system and method for quantitation of melatonin was the same as that described in chapter 2.

5.2.2.3. Sample Preparation

Aqueous solutions of 3 mg/ml of melatonin in clear (USP Type 1) (see figure 5.2) and amber glass ampoules, melatonin raw material (40 mg evenly spread in a 1-2 mm layer thickness on a flat, clear petri dish covered with cling wrap (Glad Wrap®), tablets/capsules (packaged and unpackaged) in flat, clear petri dishes covered with cling wrap and all dark controls were irradiated according to ICH guidelines.

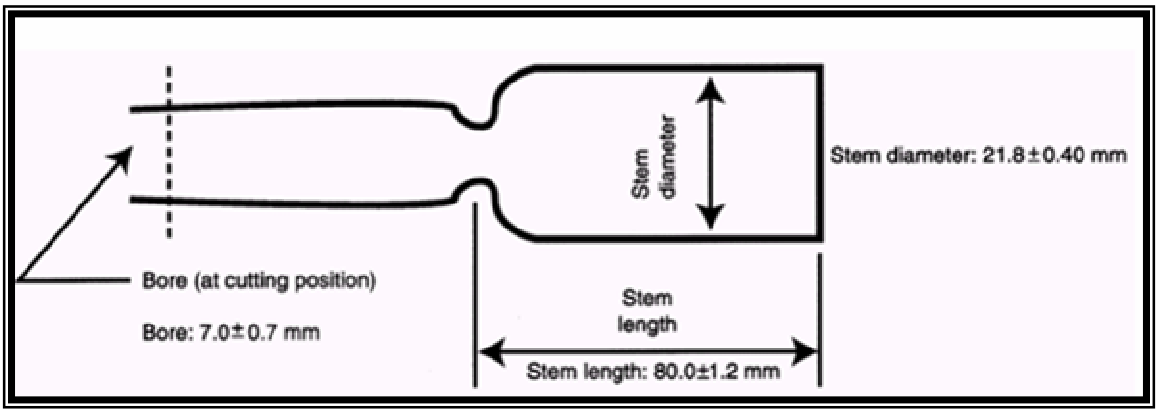

Figure 5.2: Diagrammatic representation of the USP type 1 clear glass ampoule. (ICH, 1997).

5.2.2.4. ICH conditions

Irradiation was according to ICH conditions for confirmatory studies samples in the visible wavelength range from 400-800 nm at 1.2 million lux hours and in the UV wavelength range from 300-400 nm at 200 watt hours/m^2 using the Hereaus Suntest CPS+ (ATLAS, Gelnhausen, Germany) (see figure 5.3) equipped with a light source designed to produce an output similar to the ID 65 emission standard, which is the equivalent indoor indirect daylight standard.

Figure 5.3: Photograph of the Hereaus Suntest CPS+ (ATLAS, Gelnhausen, Germany) used to irradiate the melatonin samples according to ICH guidelines.

After irradiation, samples were analyzed using the validated HPLC method described in chapter two.

5.2.3. RESULTS

The effect of irradiation under ICH conditions for melatonin in solution and the solid state (raw material, tablets and capsules) is reported in tables 5.1 and 5.2. In all cases negligible degradation (97-100% melatonin remaining) was noted for the dark controls, confirming that the degradation occurring on exposure to be due to light and not due to the heat (Hereaus Suntest CPS+ was maintained at 40^{o}C) that was generated during the exposure.

The results in table 5.2, clearly shows 82% of melatonin remaining in solution in the clear glass ampoules, while 98% of melatonin remained in the amber glass ampoules after exposure at 1.2 million lux hours, confirming the light-protective effect of the amber glass.

Furthermore, the results in table 5.3 also indicate that melatonin raw material is more stable than melatonin capsules and tablets (packaged and unpackaged). It is also evident when looking at the results for both tables that melatonin in the solid-state is less susceptible to photodegradation than in solution.

Table 5.2: Percentage melatonin remaining in solution after irradiation.

Percentage Melatonin, in Solution Remaining After Irradiation at 200 Watt hours/m^2 and 1.2 Million Lux Hours		
Container	Percentage Melatonin Remaining 200 Watt hours/m^2	1.2 million lux hours
Amber glass ampoule (Control)	100	100
Amber glass ampoule	100	98
Clear glass, USP Type 1 ampoule (Control)	100	99
Clear glass, USP Type 1 ampoule	97	82

Table 5.3: Percentage melatonin remaining in solid state after irradiation.

Percentage Melatonin, Solid-State (raw material, tablets, capsules) Remaining After Irradiation at 200 Watt hours/m^2 and 1.2 Million Lux Hours		
Container	Percentage Melatonin Remaining 200 Watt hours/m^2	1.2 million lux hours
Raw Material (Control)	99	99
Raw Material	91	91
Tablet, unpackaged (Control)	99	99
Tablet, unpackaged	88	83
Tablet, packaged (Control)	100	99
Tablet, packaged	94	91
Capsule, unpackaged (Control)	99	97
Capsule, unpackaged	86	85
Capsule, packaged (Control)	100	100
Capsule, packaged	99	99

5.2.4. DISCUSSION

The first law of photochemistry states that only radiation that is absorbed by a molecule can be effective in producing chemical changes in the molecule (Draper and Hadley, 1990). The evaluation of photostability of a drug is important as decomposition leads to loss of potency and therapeutic inactivity, and the possible occurrence of adverse effects due to the formation of degradation products during administration and storage.

The results show that melatonin in solution is susceptible to photodegradation with 82% melatonin remaining in clear glass ampoules after exposure at 1.2 million lux hours with an 8% loss of potency. This instability may be attributed to photodegradation, as the amount of melatonin remaining in the dark control is 99%, ruling out the effect of heat. However the exposure at 1.2 million lux hours exceeds the required radiant exposure in

the UV-range by a factor of 2.5, while the percentage degradation after the required exposure at 200watt hours/m^2 is only 3%.

Although melatonin in the solid-state is less susceptible to photodegradation than in solution, 9%, 17% and 15% degradation occurs for the raw material, the tablets and capsules (unpackaged) respectively. In all cases this degradation is attributed to the effect of light since the percentage degradation of melatonin in the dark controls is between 0-3 %.

This study highlights the photo-instability of melatonin both in the solid-state and solution on exposure to light according ICH conditions and the importance of suitable packaging. The packaging of melatonin in solution in amber ampoules and the capsules in securitainers has proved effective with only 2% and 1% degradation occurring, while the amber plastic containers were not suitable in protecting the tablets against light according to ICH conditions with only 91% melatonin remaining after exposure at 1.2 million lux hours.

5.3. CONCLUSION

Melatonin is marketed as tablets, capsules and an oral spray. In this study the photostability of melatonin raw material, tablets and capsules (packaged and unpackaged) and a 3 mg/ml aqueous solution are evaluated for photostability according to the guidelines of the ICH. Radiant exposure at approximately 1.2 million lux hours showed melatonin to be light sensitive with 9%, 17%, 15% and 18% degradation of the melatonin raw material, tablets, capsules and solution occurring, requiring consideration of the packaging of these drug products.

CHAPTER SIX

PHOTODEGRADATION OF MELATONIN AND THE IDENTIFICATION OF ITS PHOTOPRODUCTS

6.1. INTRODUCTION

Photodegradation studies can be performed either on an analytical or on a preparative scale. Analytical apparatus enables the reaction vessels to be moved varying distances from the light source, thereby controlling the rate of the reaction. This technique also enables the use of a shutter, placed between the lamp and vessel which facilitates the analysis of the solution without the lamp having to be switched off and restarted (Moore, 1987). This is useful since a warm-up time of about five minutes is required before a constant intensity is achieved. The use of preparative scale apparatus results in higher yields of photoproducts. Vigorous stirring is essential, as the majority of the absorption of light takes place in the layer of solution closest to the light source.

The immersion-well photoreactor (figure 6.1), a useful and popular instrument for photodegradation studies, consists of an outer Pyrex vessel and an inner removable double-jacketed immersion-well. The lamp is contained in the double-walled immersion-well, which is made of either quartz or borosilicate glass. This allows water cooling, and filtering of excitation radiation. A small diameter inlet tube extends to the bottom of the annular space to allow flow from the bottom of the well upwards. All reactions flasks (figure 6.1; 2) are made of borosilicate glass and are fitted with one central ground socket (to take an immersion well) and other small sockets for a reflux condenser or dropping funnel, sampling port, etc. The flask is generally supported by conventional laboratory stands and clamps. Due to the lamp being surrounded by the solution being irradiated, the immersion-well photoreactor is among the most efficient reactors used for photochemical reactions (Photochemical Reactors, Applied Photophysics).

Since the absorption of light is necessary to effect a photochemical change, the choice of light source is important and dictated by the absorption spectrum of the reactant to be

studied (Moore, 1987). The most widely used sources of ultraviolet and visible light for conventional photochemical experiments are the mercury and xenon lamps. All irradiations carried out in this study involved using a 400W high pressure mercury lamp, emitting over the ultraviolet-visible range. According to the first law of photochemistry, the generation of free radicals by melatonin is possible in this case, since the excitation wavelength is such that radiation absorbed by the molecule may result in a chemical reaction (Gilbert & Baggott, 1991).

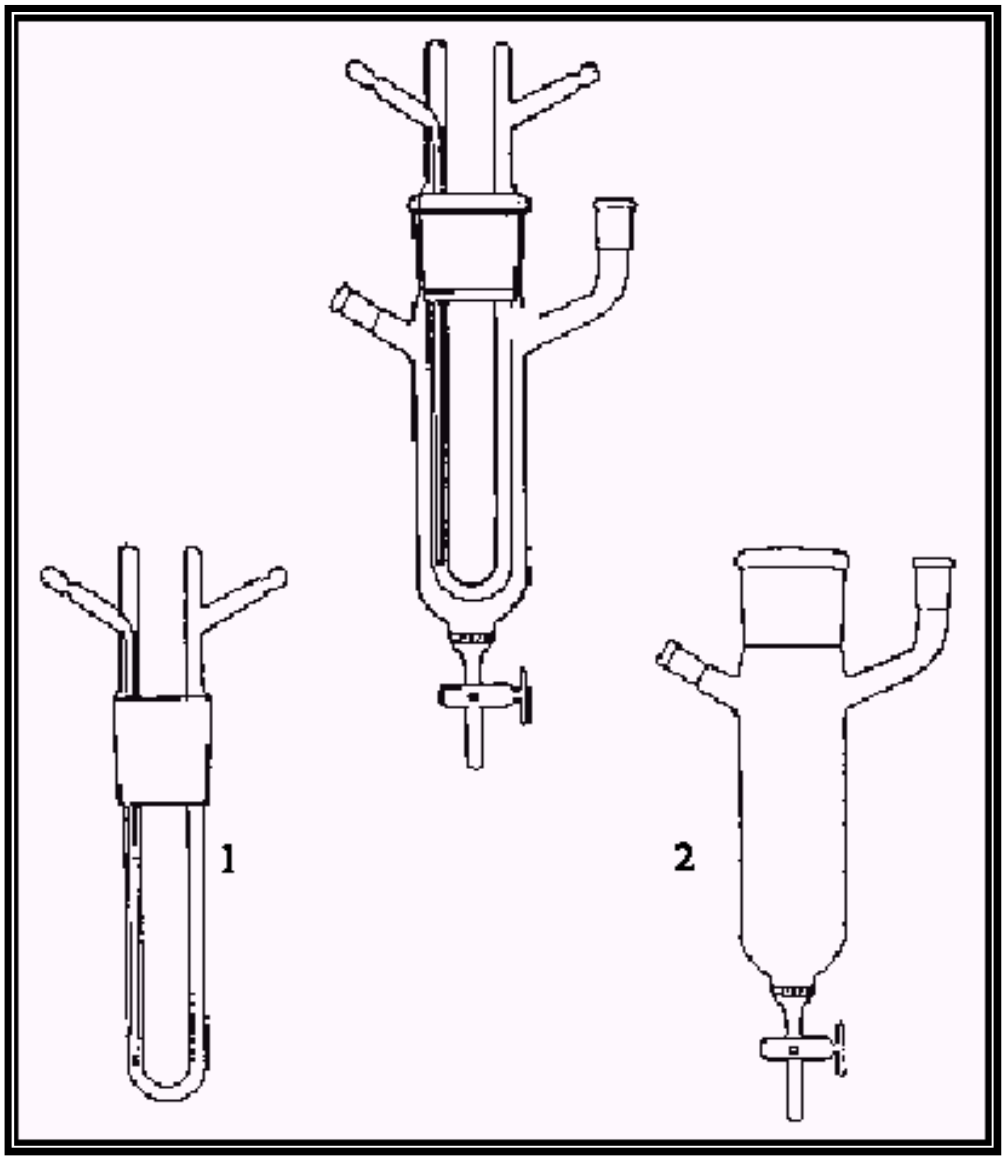

Figure 6.1: The immersion well photoreactor with detail of the double-walled immersion well (1), and the outer borosilicate flask (2) (Photochemical Reactors, Applied Photophysics).

6.2. PHOTOSTABILITY STUDY OF MELATONIN.

6.2.1. INTRODUCTION

Many pharmaceutical compounds are known to be unstable to light (Moore, 1987; Albini & Fasani, 1998) and are required to be stored in sunlight-protected containers; moreover, significant phototoxic effects have been ascertained for several drugs. Accordingly, there is now an increasing attention to photochemistry of bioactive compounds including identification of their photodegradation products and control of their photobiological effects, requiring that selective, stability-indicating analytical methods are available for the assessment of photostability. Limited information is available regarding the photochemical and photobiological properties of bioactive compounds such as melatonin.

Melatonin was recently reported to be photolabile (Andrisano *et al*., 2000, Anoopkumar-Dukie *et al*., 2000) but detailed investigations on its photochemistry have not been reported. Thus, the aim of the present chapter was to assess the stability of melatonin in solution in the presence of UV light and to identify the resulting photoproducts.

6.2.2. MATERIALS AND METHODS

6.2.2.1. Chemicals and Reagents

Absolute ethanol (HPLC grade) was purchased from Saarchem (Krugersdorp, South Africa). All other chemicals were of the highest quality available and were purchased from commercial distributors.

6.2.2.2. Instrumentation

The photodegradation apparatus consisted of a quartz immersion well photoreactor (Applied Photophysics, Leatherhead, UK), and a 400W medium pressure mercury lamp, emitting over the UV/Vis range of 300-575 nm with maximum irradiance in the UVA at 365 and 565 nm in the visible region (figure 6.1).

A modular, isocratic HPLC system as described in chapter two, section 2.2.3 was used in order to analyze the samples. In addition, the samples were monitored with a Cary 500 UV/VIS/NIR spectrophotometer (Varian Inc., Palo Alto, CA, USA).

6.2.2.3. Chromatographic Conditions

The chromatographic conditions for this assessment were the same as that described in chapter 2, section 2.2.4.

6.2.2.4. Sample Preparation

A stock solution of melatonin (0.1 mg/ml) was freshly prepared by accurately weighing 1mg of melatonin and dissolving it in 10% v/v of absolute ethanol. Fresh melatonin solutions were prepared each day and the beakers containing the melatonin solutions were protected from light with aluminium foil. Dilutions of this stock solution were made to prepare the required standard solutions for the concentration range to be studied. A calibration curve was obtained using 0.01 mg/ml – 0.1 mg/ml of melatonin (figure 6.2).

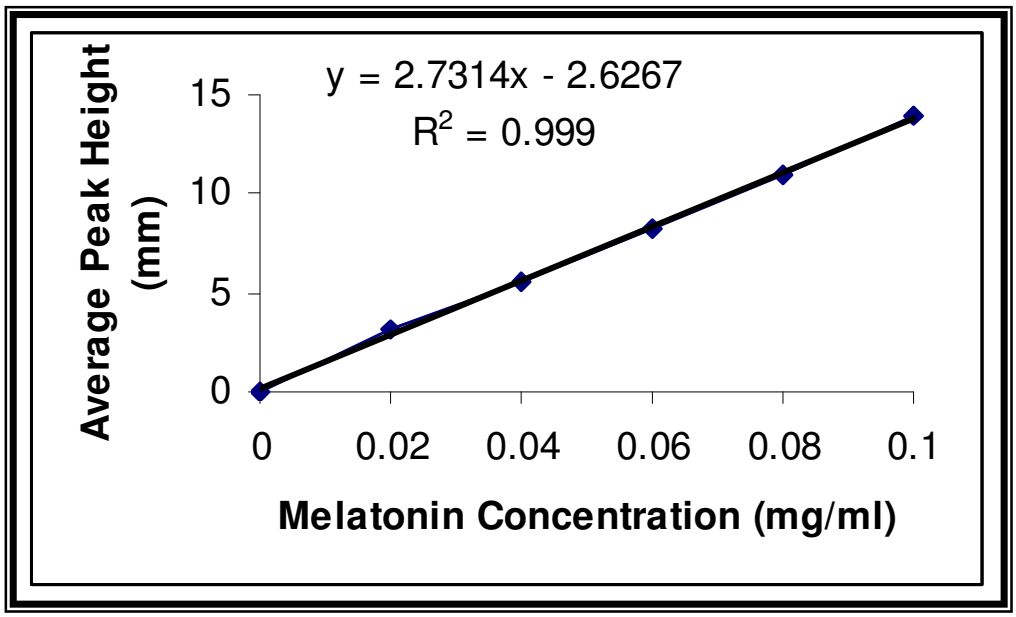

Figure 6.2: Typical calibration curve constructed by plotting mean peak height against the concentration (0.01 mg/ml to 0.1mg/ml) of melatonin solutions prepared in 10%v/v absolute ethanol/ water.

6.2.2.5. Irradiation Studies

Melatonin (0.1 mg/ml) was placed in the immersion-well photoreactor and irradiated continuously with a 400-W medium pressure mercury lamp, for three hours, whilst bubbling air or nitrogen through the solution, at ambient temperature. The selected times for UV irradiation were predetermined.

Aliquots of 5mL were removed periodically and were analyzed using a validated HPLC method as described in chapter 2. In addition, the samples were monitored with a Cary 500 UV/VIS/NIR spectrophotometer (Varian Inc. Palo Alto, CA, USA).

6.2.3. RESULTS

6.2.3.1. HPLC Study

The mobile phase was optimized for a rapid and interference free chromatogram. The chromatograms obtained show well resolved, sharp and symmetrical peaks as shown in chapter two, figure 2.5. Regression analysis showed that the concentration and peak height were linear over the concentration range studied (see figure 6.2). The height of the peak at time (0) was taken to represent 100% of the melatonin. The decrease of peak height during the study was taken to be an indication of the percentage of drug remaining.

As shown in figure 6.3, irradiation of melatonin (0.1 mg/mL) as described above resulted in a significant decrease of the melatonin present in solution. The rate of melatonin photodegradation is shown to be accelerated when the solution is aerated, compared to purging with nitrogen only. In air, only 18% of melatonin remained after 20 minutes of irradiation, whereas under nitrogen, ± 50% remained after the same period. After one and a half hours of irradiating the aerated solution there was 0% of melatonin remaining. While, with purging with nitrogen ± 5% of melatonin remained after three hours of irradiation.

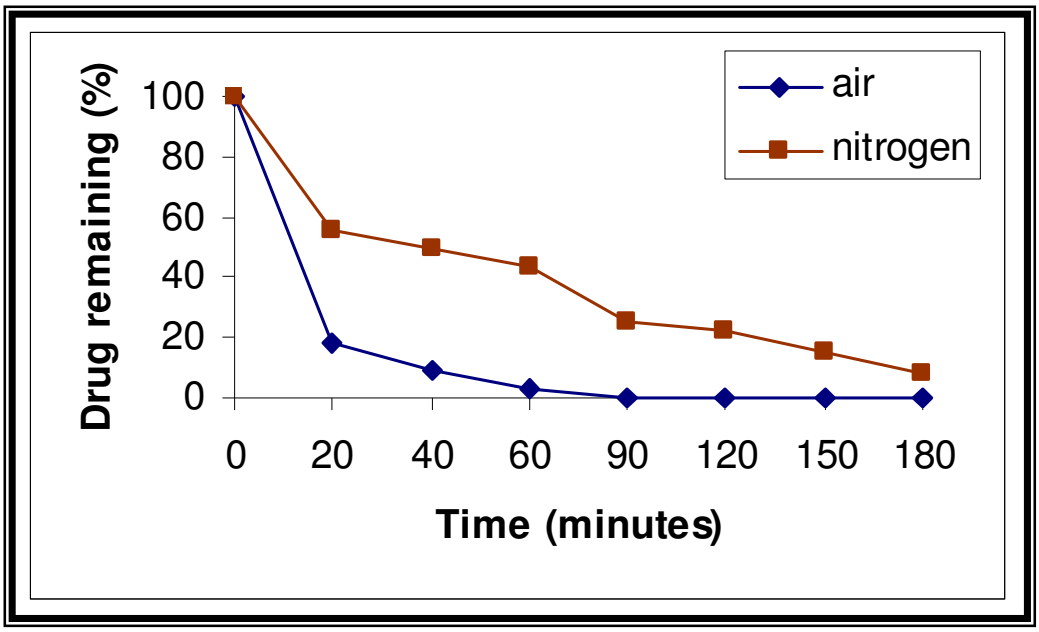

Figure 6.3: The effect of 400 W UV/Vis irradiation in the presence of air or nitrogen on the photodegradation of melatonin.

6.2.3.2. UV/Vis Spectrophotometry Study

Melatonin (0.1 mg/mL) was dissolved in a 50:50 ratio of ethanol and water and irradiated while the solution was aerated as described above in section 6.2.2.4. The spectra of melatonin at time 0 minutes (figure 6.4, **a**) shows a lambda max (λmax) band at ± 275nm with an absorbance of 1.213. At time 10 minutes of irradiation it is clearly evident that the λmax of the melatonin peak exhibited a hypsochromic shift by ± 3nm to 272nm and there is a reduction in its absorbance (figure 6.4, **b**) At time 20 minutes (figure 6.4, **c**) there is a further reduction in the melatonin peak absorbance and a further hypsochromic shift. These decreases in absorbance are an indication of a decrease in the concentration of melatonin, while the shifts are an indication of the possible appearance of photoproducts. At time 30 and 60 minutes (figure 6.4, **d and e**) of irradiation it is clearly evident that the melatonin peak at 275nm is no longer present indicating that all the melatonin has been degraded.

6.2.4. DISCUSSION

It is known that solutions of melatonin maintained in sterile, pyrogen-free conditions, may be stored at 4°C for six months without degradation (Cavallo & Hassan, 1995). The present study shows that irradiation of a melatonin solution causes rapid degradation of melatonin. These results further demonstrate that the presence of oxygen accelerates the photodegradation of melatonin, as opposed to purging with nitrogen. As shown in figure 6.3., irradiation of aerated melatonin (0.1 mg/mL) solution results in a significant decline of melatonin over the 60 minute irradiation period. These results are confirmed with the results obtained with the UV/VIS spectrometry scans as shown in figure 6.4.

One of the objectives of the present study was to determine the photostability of melatonin. The results from this study raise important concerns about the medical use of melatonin in sunscreens, since it is rapidly inactivated by UV light. Further studies need to be conducted to determine the exact nature of the photodegradants of melatonin.

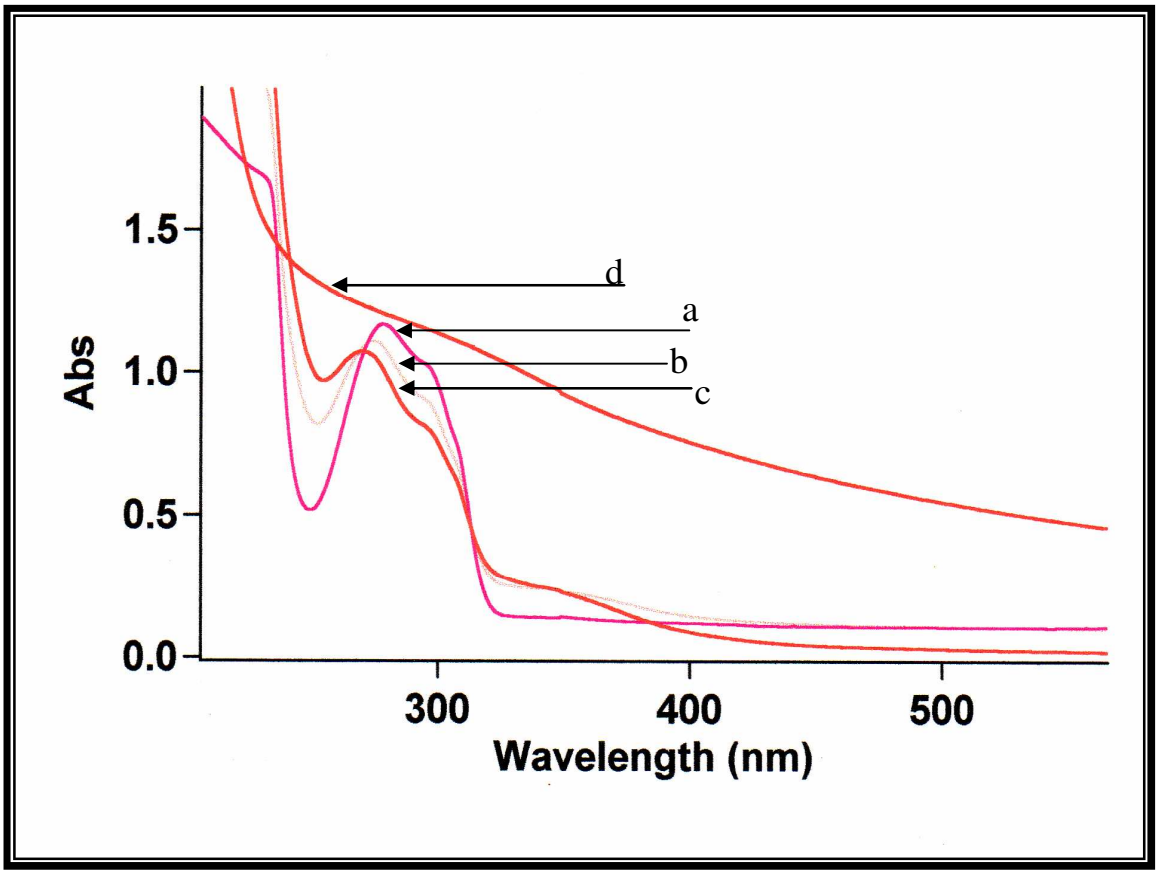

Figure 6.4: Absorption spectral changes observed for melatonin in a 50:50 ratio of ethanol: water. Spectra (a) melatonin, t = 0, (b) t = 20min irradiation, (c) t = 30 min irradiation while (d) is the spectra after 60 min irradiation.

6.3. IDENTIFICATION OF THE MELATONIN PHOTOPRODUCTS.

6.3.1. INTRODUCTION

Melatonin has been shown to be more potent than α-tocopherol, mannitol, and glutathione as a free radical scavenger (Reiter, 1997). Unlike classical antioxidants such as vitamin C, vitamin E and glutathione which undergo redox cycling, melatonin being an electron rich molecule may interact with free radicals via an additive reaction to form several stable end products, which are eliminated in the urine. Consequently melatonin does not undergo redox cycling and therefore does not function as a pro-oxidant (Tan *et al*., 2000b). Topically administered melatonin has been shown to significantly suppress the formation of UV-induced erythema when applied to the skin immediately after UV irradiation (Bangha *et al*., 1996). It has also been shown that pre-irradiation melatonin application significantly inhibits the development of erythema (Bangha *et al*., 1997).

The study conducted in section 6.2, raises concerns about the use of melatonin in topical applications especially the medicinal use of melatonin in sunscreens because it is rapidly inactivated by UV irradiation with 18% of melatonin remaining after 20 minutes of UV irradiation. The photoproducts of melatonin following exposure to UV light have not been properly identified, neither has it been demonstrated whether the degradants retain antioxidant activity.

Thus the aim of the present study was to determine the photodegradation profile of melatonin and to identify the main photoproducts that are formed upon UV irradiation of melatonin solution using combination of high-performance liquid chromatography and mass spectrometry (LC-MS).

The LC-MS has had a significant impact on drug development over the past decade. Continual improvements in LC-MS interface technologies combined with powerful features for structure analysis, qualitative and quantitative, have resulted in a widened scope of application. These improvements coincided with breakthroughs in combinatorial chemistry, molecular biology, and an overall industry trend of accelerated development.

New technologies have created a situation where the rate of sample generation far exceeds the rate of sample analysis. As a result, new paradigms for the analysis of drugs and related substances have been developed. The growth in LC-MS applications has been extensive, with retention time and molecular weight emerging as essential analytical features from drug target to product (Lee & Kerns, 1999).

6.3.2. MATERIALS AND METHODS

6.3.2.1. Chemicals and Reagents

All reagents were of the highest quality available and were purchased from commercial distributors.

6.3.2.2. Instrumentation

The photodegradation apparatus was the same as that described in section 6.2.2.2.

A modular, isocratic HPLC system as described in chapter 2, section 2.2.3 was used in order to analyze the melatonin samples and determine the photodegradation profile of melatonin.

6.3.2.3. Chromatographic Conditions

The chromatographic conditions for this assessment were the same as that described in chapter 2, section 2.2.4.

6.3.2.4. Irradiation Studies

Melatonin (0.1 mg/ml) was placed in the immersion-well photoreactor and irradiated continuously in the same manner as described above in section 6.2.2.3. Aliquots of 5mL were removed periodically and were analyzed using a validated HPLC method as described in chapter 2 to determine the photodegradation profile of melatonin. In addition, the samples were analysed using the LC-MS system.

6.3.2.5. Liquid Chromatography-Mass Spectrometry (LC-MS)

The melatonin photoproducts were identified using a Finnigan LCQ system equipped with an atmospheric pressure chemical ionization (APCI) source used for all the LC-MS studies was configured to scan the *m/z* range of 100 to 700 during the chromatographic run (figure 6.5). The capillary temperature at 138°C, vaporizer temperature 450°C, capillary voltage 38 V, discharge voltage 5 kV, tube lens offset 19 V, discharge current 5 μA and the sheath gas at 20 arbitrary units set, represented an optimum for production of both molecular ions as well as fragmentation products.

Figure 6.5: Photograph of the Finnigan LCQ system equipped with an atmospheric pressure chemical ionization (APCI) source.

6.3.3. RESULTS

6.3.3.1. Photodegradation Profile

The HPLC chromatograms (n=5) obtained for the UV irradiation of melatonin solution from time 0 to 90 minutes were examined for the presence of photoproducts. Four photoproduct peaks were evident on the chromatogram however only two of the peaks were sharp, resolved and symmetrical (as shown in chapter 2, figure 2.5).

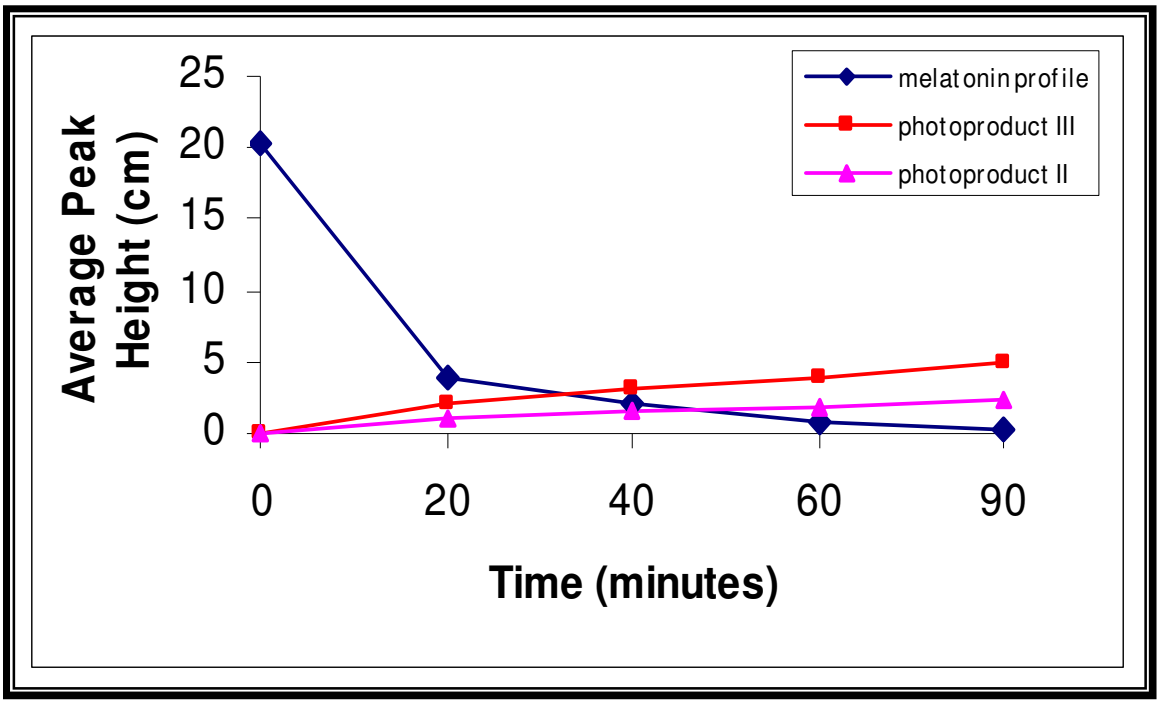

Figure 6.6: Photodegradation profile of melatonin in the presence of oxygen.

Melatonin eluted at 7.2 minutes. The 2 major photoproduct peaks were labelled photoproduct II which had a retention time of 4.88 minutes and photoproduct III which had a retention time of 6.42 minutes. As shown in figure 6.6, photoproduct III was formed to a larger extent than photoproduct II. The ratio of the two degradants when the melatonin concentration reached zero was found to be 2:1 for photoproduct III and photoproduct II respectively.

6.3.3.2. Identification of Melatonin Photoproducts Using LC-MS

As shown in figure 6.7 and the LC-MS scans in appendix six, the molecular ion $(M + H)^+$ at m/z = 233 confirmed the identity of the parent drug while the photodegradants are assigned molecular ions $(M + H)^+$ at m/z = 249 (II) and 265 (III) suggesting the addition of oxygen to the melatonin and as these photoproducts did not appear when the reaction was carried out under nitrogen. Melatonin eluted at a R_T of 7.23 min with photoproduct II eluting at 4.88 min and photoproduct III eluting at 6.42 min. The LC-MS scans of UV-irradiated melatonin solution at each time interval is present in appendix six. These photoproducts were identified as 6-hydroxymelatonin (II) (6-OHM) and N^1-acetyl-N^2-formyl-5-methoxykynurenamine (III) (AFMK). Figure 6.7 also illustrates that these two photoproducts also occur as metabolites in the brain and liver, which is not uncommon as there may be similarities between *in vitro* degradants and *in vivo* metabolites. Figure 6.8, illustrates the mechanism of photodegradation of melatonin and the formation of the two photoproducts.

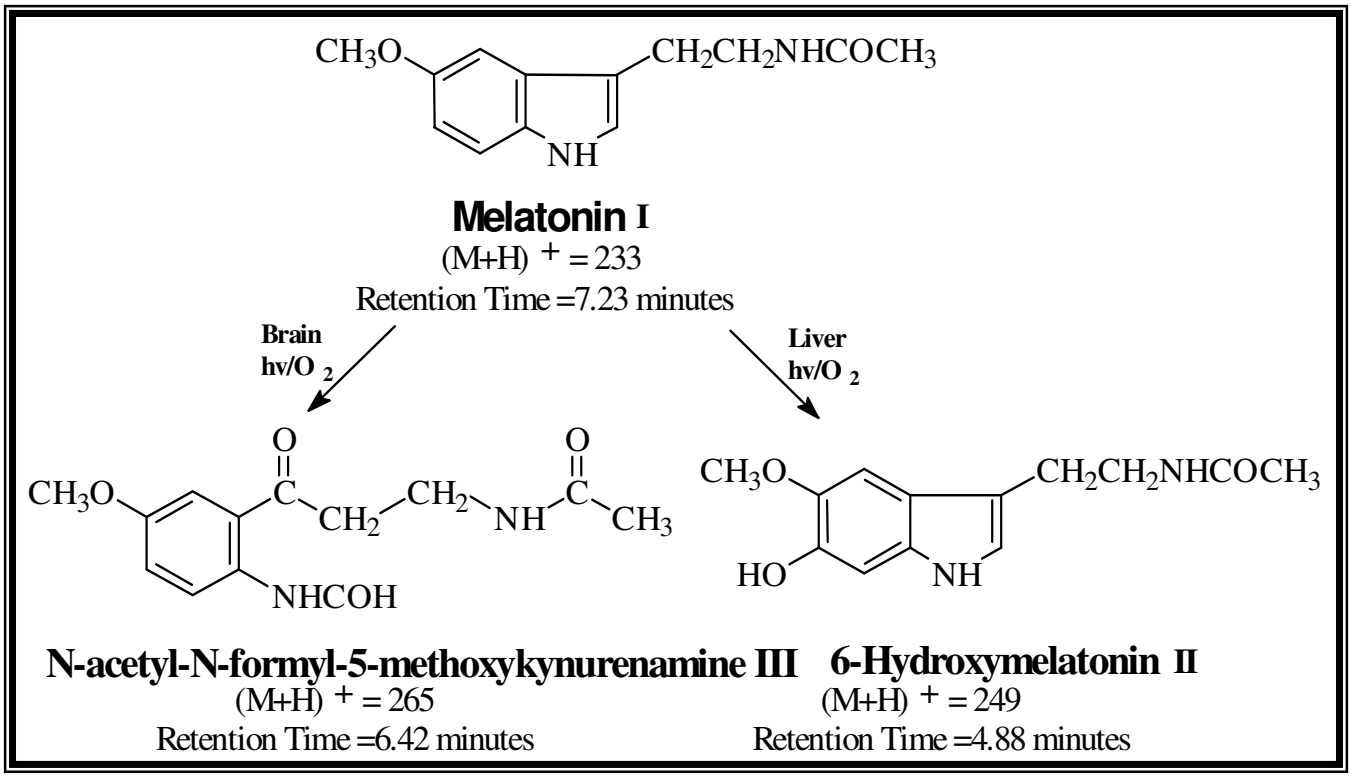

Figure 6.7: Degradation pathway of melatonin in the presence of oxygen

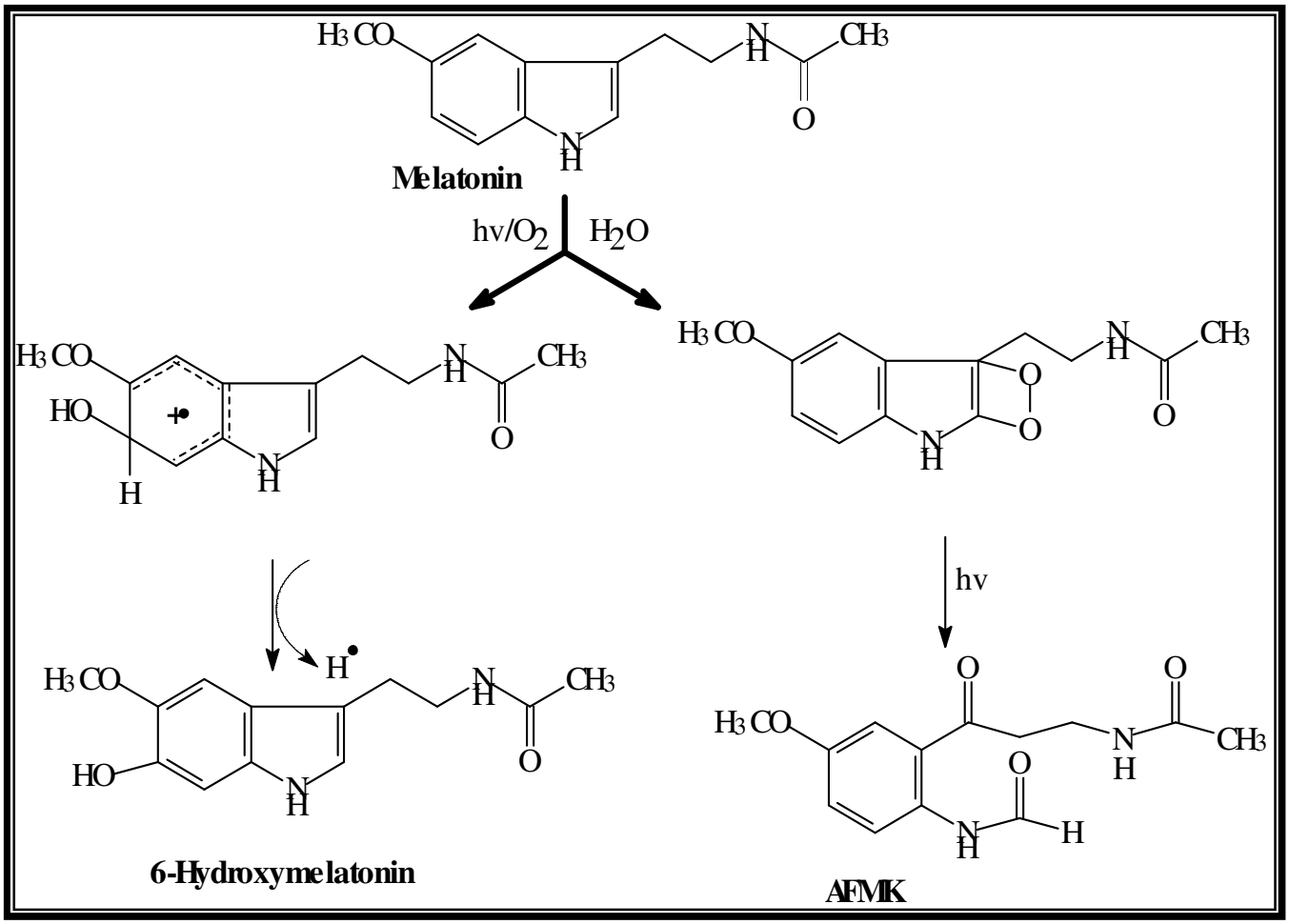

Figure 6.8: Mechanism of photodegradation of melatonin

6.3.4. DISCUSSION

Exposure of skin to UV radiation produces multiple deleterious responses, including photoageing (Ogura *et al*., 1988) and erythema. There is ample evidence that UV radiation produces toxic free radical intermediates, which are implicated in the pathogenesis of UV-induced skin damage. Under normal conditions the skin antioxidant defence mechanisms, which include superoxide dismutase, is able to protect the skin. However, the generation of free radicals depletes the skin of these antioxidant defence mechanisms, rendering it vulnerable to UV-induced oxidative stress (Gilchrest, 1996).

The possibility of melatonin as an additive to sunscreens to prevent the hazards of UV light has been raised. The HPLC chromatogram revealed the presence of two distinct photoproducts that eluted at a shorter retention time than melatonin, indicating that the photoproducts were more polar than the parent drug. The results of the LC-MS studies show that melatonin, after UV irradiation, is converted to two products, namely, AFMK and 6-OHM, existing in a ratio of 2:1, respectively, when melatonin concentration reached zero.

The photoproducts did not appear when the reaction was carried out under nitrogen, proving that the presence of oxygen is necessary for the melatonin photodegradation. The formation of photoproduct III is proposed to occur by photo-oxidation of the indole ring, giving an endoperoxide, which rearranges to the stable photoproduct III as suggested by Andrisano *et al*., (2000). The findings of this chapter are in accordance with the study performed by Andrisano *et al*., (2000). The authors reported that the photodegradation of melatonin is rapid at pH 9 and decreases as pH decreases; the same main photoproduct is obtained at the different pH values; the photodegradation of melatonin is prevented in deaerated solutions, with the photoproduct being obtained only in the presence oxygen and light-protected melatonin solutions were found to be stable.

Both of these compounds are also known metabolites of melatonin in the body and are also known to be generated when melatonin interacts with free radicals (Tan *et al*., 2001). It has recently been shown that AFMK functions as a potent antioxidant, reducing lipid peroxidation as well as DNA damage (Tan *et al*., 2000b; 2001). It has been reported by

Pierrefiche *et al*., (1993) and Hara *et al*., (1997; 2001) that that melatonin does not appear to be a major antioxidant in comparison to the more intense activity noted by its principal hepatic metabolite, 6-OHM, whose structure differs from that of melatonin by only one hydroxyl group in position six (Syh Tse *et al*., 1991), however this main melatonin metabolite in the liver, was shown by Matuszak *et al*., (1997) to have the ability to scavenging the hydroxyl radical as well as possibly promoting the generation of hydroxyl radicals. Thus, it was decided to investigate the ability of 6-OHM to generate or protect against the production of ROS and necrotic cell death in rats in the following chapters.

We have reported that (Maharaj *et al*., 2002) although melatonin disappeared after UV exposure, the degraded solution still provided equipotent protection against reducing the generation of superoxide anions and lipid peroxidation in rat brain homogenate; despite the absence of melatonin. The system that was used to investigate the ability of melatonin to reduce lipid peroxidation; albeit far removed from the UV irradiation of skin, enables investigation of the efficacy of UV irradiated melatonin as a free radical scavenger. By implication the reduction in UV-induced reactive oxygen species (ROS) by UV irradiated melatonin in the study carried out by Fischer *et al*., (2001) could be due to not only to melatonin but also due to the degradants which might have been produced during the UV-irradiation.

6.4. CONCLUSION

The present study on the photoreactivity of melatonin, allows the understanding of the mechanism of its photodegradation and the elucidation of the structure of its two main photoproducts. The present study implies that although melatonin is degraded by UV light, the two photodegradant(s) formed i.e. AFMK and 6-OHM have been shown to retain free radical scavenging properties of the parent compound, melatonin. This study further confirms the suitability of melatonin as an agent to protect tissues such as skin against UV-induced free radical damage. One of the concerns of using melatonin in sunscreens is its photoinstability. From this chapter it is evident that even though melatonin is rapidly degraded in the presence of UV light, the degradants retain antioxidant activity, thus making melatonin a likely candidate for inclusion in sunscreens.

CHAPTER SEVEN

SINGLET OXYGEN GENERATION

7.1. INTRODUCTION

Singlet oxygen ($^1O_2$) is formed in cells by the photosensitization reaction of substrates such as dyes used in photodynamic therapy and biological pigments (figure 7.1). It is well documented that $^1O_2$ itself is not only cytototxic due to the oxidative degradation of cell membranes, but it is genotoxic because it can oxidise DNA directly (Ravanat *et al.*, 2000).

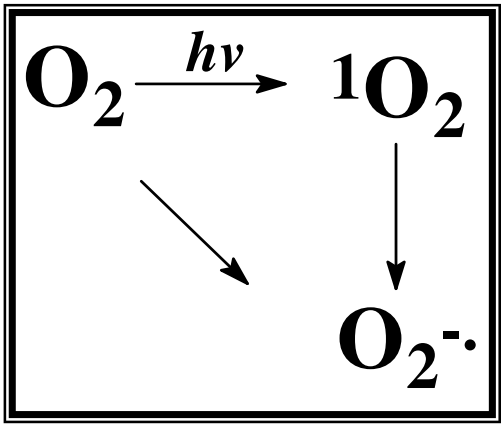

Figure 7.1: Photoexcitation of O_2 produces singlet oxygen (Reiter *et al.*, 2002).

One of the major precursors of free radicals is molecular oxygen (O_2, dioxygen). While O_2 is obviously an absolute requirement for the survival of aerobic organisms where it functions as an electron sink for energy-yielding processes and as an agent for a variety of metabolic transformations which involve oxidation and oxygenation, at the same time a small percentage (up to an estimated 4%) of the inhaled O_2 is converted to damaging metabolites (Grisham, 1992). The molecular destruction metered out by these reactants is generally identified as oxidative stress (Sies, 1986). The concurrent beneficial and destructive actions of O_2 are commonly referred to as the oxygen paradox (Hauptmann & Cadenas, 1997).

Oxygen toxicity occurs when O_2 is reduced to free radicals and other reactive species. In biological systems, oxidative stress can lead to cell death that is often characterized by

internucleosomal DNA fragmentation and is termed apoptosis (Sarafin & Bredensen, 1994). Apoptosis can be experimentally induced by an interaction of light with photosensitive compounds (Cagnoli *et al*., 1995). This photoexcitation reaction generates $^1O_2$ (Agarwal *et al*., 1991), which has both electrons in a single orbital, a characteristic that makes it a very reactive species which is capable of damaging molecules within the body (figure 7.1). $^1O_2$ is a non-radical reactant but, nevertheless, its high reactivity permits it to damage other non-radical species (Halliwell & Gutteridge, 1989) therefore $^1O_2$ falls under the reactive oxygen species (ROS) molecules. Since O_2 utilization by aerobes is by necessity continuous, molecular pummelling from oxygen–derived reactants is also incessant. $^1O_2$ can be generated by a range of enzymatic and non-enzymatic reactions including processes mediated by heme proteins, lipoxygenases and activated leukotrienes as well as radical termination reactions (Ravanat *et al*., 2000).

Photosensitization is the absorption of visible light by a coloured substance which initiates physical or chemical changes in a substrate (www.photobiology.com/ educational/len2/singox.html). The chemical reaction, in which a photoexcited molecule takes part is termed photochemistry, and it may lead directly to the final products (e.g. by isomerisation), or more frequently to an unstable or reactive chemical species (e.g. free radicals or radical ions). The reactive chemical species generated in this primary photochemical process may react further in secondary processes through a series of dark reactions that lead ultimately to the final products (Suppan, 1994).

Because many photochemical reactions involve the attack of excited singlet oxygen on a ground state reactant molecule, the photophysical properties of the oxygen molecule are important (www.photobiology.com/educational/len2/singox.html). Molecular oxygen has two unpaired electrons in its lowest energy state. The existence of unpaired valence electrons in a stable molecule is very rare in nature resulting in a high reactive chemical system (www.photobiology.com/educational/len2/singox. html). The electronic structure of singlet oxygen is ably described by the molecular orbital theory. The oxygen molecule is unique in that its lowest electronic state is the triplet ground state ($^3\Sigma_g$) and, with two unpaired electrons distributed in the highest orbitals (figure 7.2), two possible singlet excited states result upon the rearrangement of the electron spins within the degenerated orbitals. Oxygen is thus capable of having both triplet and singlet excited states. The first

excited state ($^1\Delta_g^+$), i.e. both electrons paired in the same orbital (figure 7.2), has the lowest energy and is expected to undergo two electron reactions. The excitation energy of this form is 0.98 eV or 22.5kcal/mol (figure 7.3). Alternatively, the higher energy singlet state ($^1\Sigma_g^+$) is expected to undergo one electron free radical reaction due to its spin-paired electrons occurring in different molecular orbitals (figure 7.3). The more reactive $^1\Sigma_g^+$, with an excitation energy of 1.63 eV (35.7 kcal/mol^{-1}), has a much shorter lifetime than the $^1\Delta_g^+$ state and decays to the lower energy state before any chemical reactions can occur. Neither ($^1\Delta_g$ or $^1\Sigma_g$) form exists as a radical, given that there are no unpaired electrons, nor are there any spin restrictions (Maree, 2002).

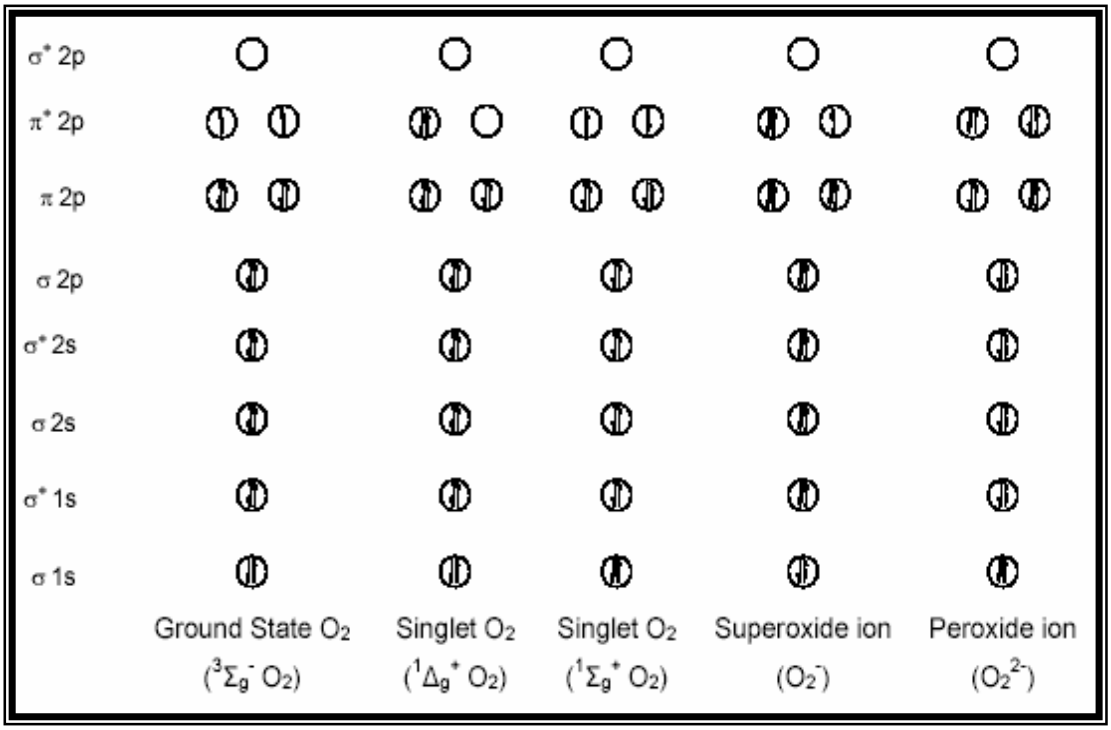

Figure 7.2: Bonding in the diatomic oxygen molecule (Halliwell & Gutteridge, 1989).

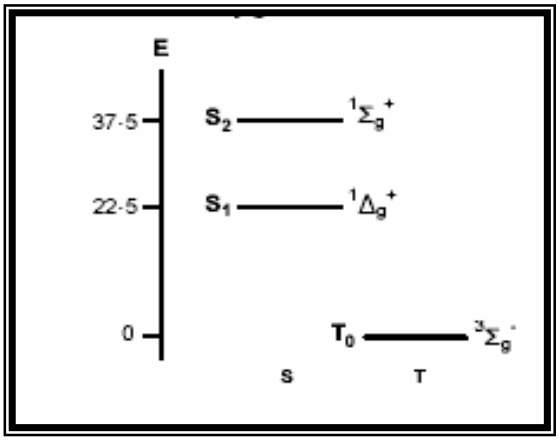

Figure 7.3: Jablonski diagram for an oxygen molecule (energy in kcal/mol) (Suppan, 1994).

The lifetime of the singlet oxygen has been found to be dependent on the solvent used in the reaction (www.photobiology.com/educational/len2/singox.html; Jenny & Turro, 1982). $^1O_2$ may be generated by either a) chemical methods, e.g. the biologically important reaction of hydrogen peroxide with sodium hypochlorite to produce singlet oxygen b) enzymatic reactions, e.g. by the myeloperoxidase enzyme during phagocytosis; c) gaseous exchange produced by passing an electric current through a gas or vapour, or d) by physical methods such as photosensitization which are used in photodynamic therapy (Antunes, 2003).

The pathway in which a photosensitiser triplet state reacts first with a substrate other than molecular oxygen is termed Type I, and reactions involving superoxide anion radicals ($O_2^{\bullet-}$) also occur. The alternative Type II pathway involves the photosensitiser triplet state reacting first with molecular O_2 (figure 7.4). Type II photosensitization of a biological system is known as photodynamic action. Type I reactions are characterized by the excitation of a sensitizer followed by electron transfer between the sensitizer and the substrate or solvent to give radicals or radical ions. These radicals then react with surrounding oxygen molecules ($^3O_2$) to form the $O_2^{\bullet-}$ that may be protonated at low pH to form the reactive peroxyl radical ($HO_2^{\bullet}$). The mechanism for a Type II reaction involves the transfer of energy from the excited sensitizer ($S^{\bullet}$) (as a result of the absorption of light) to $^3O_2$ molecules resulting in the formation of $^1O_2$. $^1O_2$ and $O_2^{\bullet-}$ thus formed can cause the oxidative destruction of tissue and leading to tissue necrosis, forming the basis for photodynamic therapy (Maree, 2002).

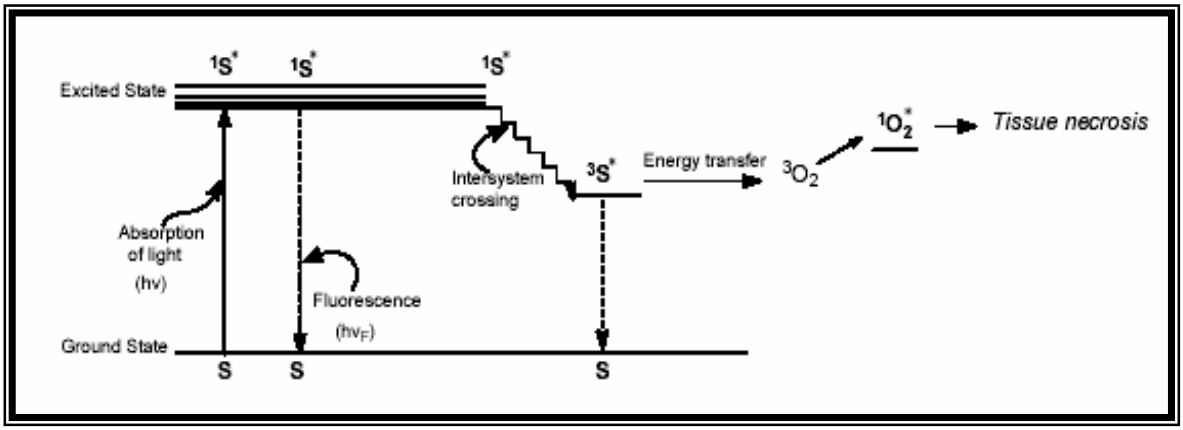

Figure 7.4: A modified Jablonski diagram showing the relevant reactions for a Type II mechanism, emphasizing the basis of PDT (S = sensitizer) (Maree, 2002).

The deactivation of $^1O_2$ back to its ground state is known as quenching and may be accomplished by either physical or chemical methods as described above. Physical deactivation is simply the reversion of the $^1O_2$ to its ground state without product formation or oxygen consumption. Chemical quenching consisting of energy transfer and electron transfer mechanisms incorporates the use of a quencher (Q) that reacts with the $^1O_2$ to produce ROS. Energy transfer involves the generation of a triplet state quencher together with the subsequent formation of ground state O_2, while electron transfer quenching entails the interaction between the electron deficient $^1O_2$ molecule and the electron donors to form a charge transfer complex (Antunes, 2003).

The potency of a drug in photodynamic therapy is determined by its ability to produce a photocytotoxic species, namely $^1O_2$ on interaction with light. The production of $^1O_2$ is measured as the $^1O_2$ quantum yield (Φ_Δ) (Maree, 2002). $^1O_2$ quantum yield is a key property of a photosensitizing agent since the ability of a compound to produce $^1O_2$ determines its potency in photodynamic therapy. The quantum yield gives an indication of the overall efficiency of a photochemical process and may be described as the number of molecules of $^1O_2$ generated for every photon absorbed by the photosensitiser. The production of $^1O_2$ by photosensitisation involves 4 steps (figure 7.4) 1) the absorption of light by the sensitizer, 2) the formation of the sensitizer triplet state, the quantum yield of this process is the intersystem crossing (ISC) efficiency or triplet yield (Φ_T), 3) the trapping of the triplet state by molecular O_2 within its lifetime (the fraction of trapped triplet state is given by f_T, 4) the energy transfer from the triplet state to molecular oxygen. Virtually all measurements of the quantum yield (Φ_Δ) are scaled to a reference substance, e.g. rose bengal (Φ_Δ 0.79) in aqueous medium (Antunes, 2003).

The protective effects of agents such as histidine, tryptophan, melatonin, ascorbates, classified as scavengers are well known and are thought to inhibit the rate of $^1O_2$ or photochemical reactions (www.photobiology.com/educational/len2/singox.html). The aim of this chapter was thus to determine if melatonin and its main photoproduct, 6-OHM serve as singlet oxygen quenchers.

The foundation for the analysis was based on the production of singlet oxygen upon irradiation of a sensitizer and a quencher, which then reacts with the resulting singlet

oxygen. 1, 3-Diphenylisobenzofuran (DPBF) with its absorption maximum at 417 nm, was used as the quencher and its disappearance was easily monitored. Only the first 20% decrease is applicable in order to obtain reliable or accurate first order kinetic data. The disappearance of the DPBF quencher is related to the production of $^1O_2$ and the following processes may take place:

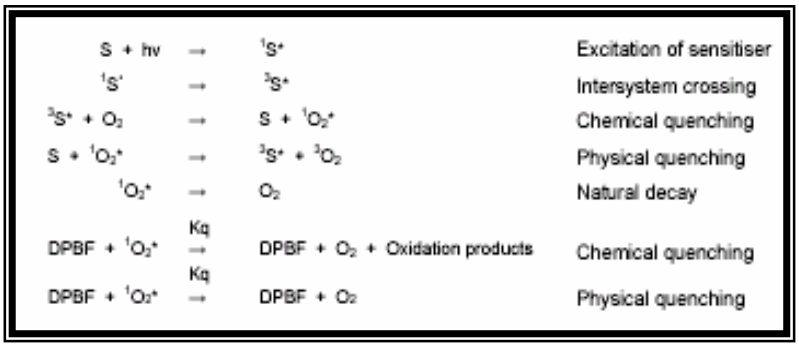

Figure 7.5: The processes involved in the disappearance of the DPBF quencher (Antunes, 2003).

The physical quenching processes (figure 7.5) noted above may be ignored because the quantum yield of $^1O_2$ is not dependant on the concentration of the sensitizer present and the DPBF is known to act as a chemical quencher only in organic solvents. Also compared to the potential sensitizer DPBF is highly reactive to $^1O_2$, making the first chemical quenching equation above in figure 7.5 invalid (Maree, 2002). Thus, the only equations of relevance are natural decay and second chemical quenching. The rate of disappearance of DPBF as a result of reaction with $^1O_2$ is given by equation 7.1 (Maree, 2002):

$$\frac{-[DPBF]}{dt} = k_q [DPBF] [^1O_2] \qquad \textbf{EQ. 7.1}$$

Following rearrangement and substitution the following equation 2 is derived (Maree, 2002):

$$\Phi_{\Delta}^{S} = \Phi_{\Delta}^{Std} \times \frac{(C_o - C_t)^{S}}{(C_o - C_t)^{Std}} \times \frac{(\alpha t)^{Std}}{(\alpha t)^{S}} \times \frac{[DPBF]^{Std}}{[DPBF]^{S}}$$

EQ. 7.2.

Where:

S = sample
Std = standard
$(C_o - C_t)$ = change in DPBF concentration (C_o = initial and C_t = final)
α = 1 (for the monochromatic laser light, previously determined by Maree (2002).
t = photolysis time-span in seconds.

It is important, though, to clarify the use of low concentrations of DPBF since first order kinetics are observed, while at high concentrations the reaction rate would become independent of the DPBF and a zero order reaction will be observed.

7.2. MELATONIN AND 6-OHM AS SINGLET OXYGEN QUENCHERS.

7.2.1. INTRODUCTION

$^1O_2$ is a ROS that can be produced by living cells and is capable of causing lipid peroxidation, DNA damage and cell death (Ravanat *et al*., 2000; Roberts *et al*., 2000). Thus, the use of antioxidant agents such as melatonin to protect tissues against $^1O_2$ generation is becoming popular. Besides melatonin's actions via receptors, a large amount of evidence has accumulated showing that melatonin is an effective direct free radical scavenger and indirect antioxidant (Cabrera *et al*., 2000). Melatonin has also been shown to scavenge the hydroxyl radical ($^{\bullet}OH$) which is generated from hydrogen peroxide (H_2O_2) via the Fenton reaction (Tan *et al*., 1993a; Tan *et al*., 1998; Stasica *et al*., 1998). Cagnoli *et al*., (1995) reported that melatonin protected rat cerebellar granule neurons from $^1O_2$ induced apoptosis. Furthermore, Zang *et al*., (1998) confirmed and provided direct evidence of the ability of this antioxidant to scavenge $^1O_2$ by demonstrating that melatonin reduced $^1O_2$-dependent 2, 2, 6, 6-tetramethyl-piperdine oxide radical generation during rose bengal photodynamic excitation.

In a purely chemical system, Poeggeler *et al*., (1994) found that riboflavin catalysed the oxidation of melatonin and the auto-oxidation of melatonin during bright light exposure. However, a photophysical study conducted by Roberts *et al*., (2000), using flash photolysis demonstrated that melatonin produces a small, yet detectable amount of singlet oxygen.

The aim of these studies was to determine whether melatonin possesses the ability to scavenge or generate $^1O_2$ using two different methods i.e. laser and lamp photolysis.

Horstman *et al*., (2002) demonstrated that when melatonin reacts with the hydroxyl radical generated via the Fenton reaction, it yields a number of primary products; one of the products identified was 6-OHM. Furthermore, 6-OHM is formed as one of the major products when melatonin reacts with peroxynitrite (Zhang *et al*., 1998). In chapter 5, it was demonstrated that melatonin degrades in the presence of UV light to yield two

photoproducts, one of which was identified as 6-OHM. Furthermore, the degraded solution of melatonin has been shown to reduce the generation of superoxide anions and lipid peroxidation in rat brain homogenate, despite the absence of melatonin (Maharaj *et al*., 2001, 2002). This indicates that the reduction of UV-induced reactive oxygen species (ROS) by UV-irradiated melatonin (Fischer *et al*., 2001) could be due not only to melatonin but also due to the photodegradants. This prompted an additional study to test whether 6-OHM was able to scavenge the $^1O_2$ that was generated using laser photolysis.

7.2.2. MATERIALS AND METHODS

7.2.2.1. Chemicals and Reagents

Melatonin and 6-OHM was purchased from Sigma Chemicals Co., St. Louis, USA. HPLC grade dimethylsulphoxide (DMSO), dried over alumina before use, naphthalene and 1, 3-diphenylisobenzofuran (DPBF) was purchased from Sigma-Aldrich. Zinc phthalocyanine (ZnPc), used as a standard was kindly donated by Dr. V. Derkacheva from the Organic Intermediates and Dyes Institute, Moscow. Methanol (HPLC grade) was purchased from BDH laboratory Supplies, Poole, UK. All other chemicals were of the highest quality available and were purchased from commercial distributors.

7.2.2.2. Instrumentation

For the laser studies, the excitation pulse source for the singlet oxygen studies was provided by an Nd-Yag laser (Laser Photonics, Orlando, Fl) (providing 47 mW, 9 ns pulses of laser light at 532 nm) and the basic setup is shown in figure 7.6. An energy meter was used to measure the pulse energy of the laser light (Antunes, 2003). Absorbance spectra were recorded on a Varian UV-Vis-NIR spectrophotometer. For the lamp photolysis studies, samples were irradiated with a lamp (at 70V) equipped with a filter which cut off any wavelengths of light above 500 nm. The basic setup is shown in figure 7.7

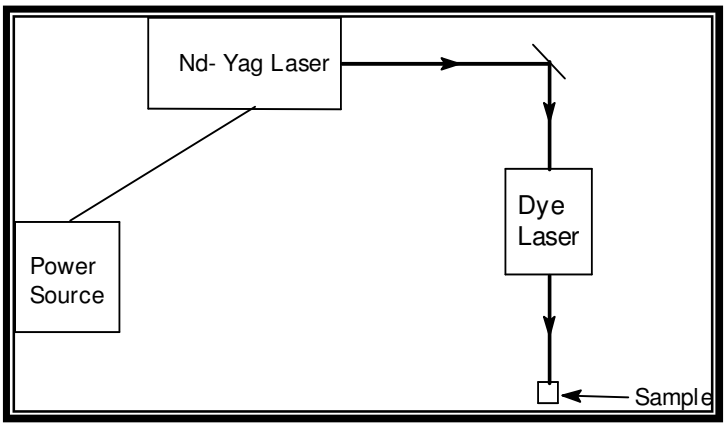

Figure 7.6: Set-up for singlet oxygen quantum yield determinations using the Nd-Yag laser (Antunes, 2003).

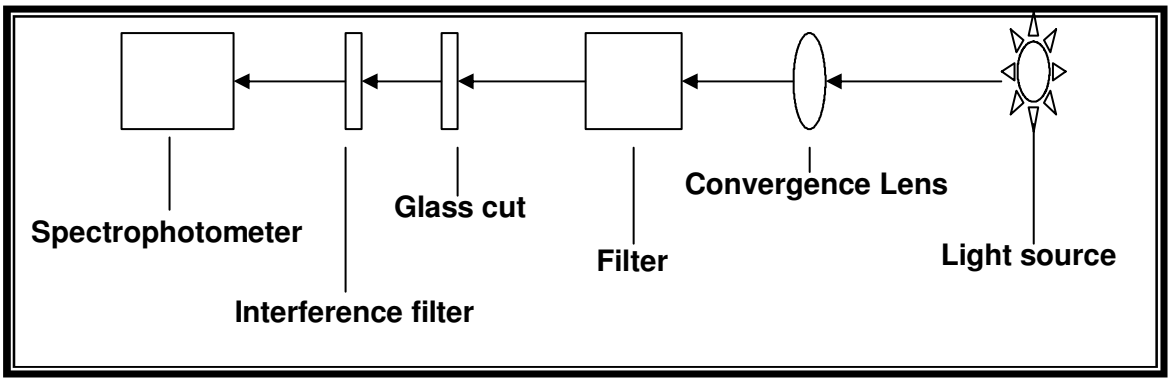

Figure 7.7: Set-up for singlet oxygen quantum yield determinations using lamp photolysis (Antunes, 2003).

7.2.2.3 Singlet Oxygen Determination

7.2.2.3.1. Nd-Yag Laser Studies

The experiment was based on the production of singlet oxygen upon irradiation of a sensitizer and a quencher. For this study, zinc pthalocyanine (ZnPc) was chosen as the sensitizer, while 1, 3-dipenylisobenzofuran (DPBF), which is highly reactive to singlet oxygen, was used as the singlet oxygen quencher for the standard solutions since it was easily monitored using the disappearance of its absorption maximum at 417 nm. Only the first 20% decrease is applicable in order to obtain reliable or accurate first order kinetic data. The sample solutions were thus composed of ZnPC, DPBF and melatonin or 6-OHM. Some competition is therefore expected between the known scavenger DPBF and the apparent scavenger's melatonin and 6-OHM. Since melatonin and 6-OHM also

have λmax values in the region of 278 nm and 272 nm, respectively and in this region there is likely to be an overlap with ZnPC and DPBF, the absorption maximum of DPBF at 417 nm was monitored and used to establish the effect of the presence of melatonin or 6-OHM upon the rate of disappearance of DPBF. The data for the sample solution would therefore be compared to the results obtained for the standard solution and any differences would therefore be attributed to the presence of melatonin or 6-OHM.

The photochemical experiments were carried out in a 4 mL UV cell with an optical pathlength of 1 cm. Air saturated solutions were used for the experiments (i.e. without deoxygenating or bubbling of oxygen) except where stated and the measurements carried out at room temperature. To determine singlet oxygen quantum yields the relative method using ZnPc as a reference and DPBF as a scavenger of singlet oxygen were used. The absorbances of the quencher (DPBF), the sample and sensitizer solutions were set to approximately 1 by dilution. The DPBF, melatonin or 6-OHM and ZnPc sample solutions were made up in DMSO prior to use and protected from light. The DPBF and ZnPc absorbances were both just below 1 and the Q-band irradiated by using the laser source described above.

Upon irradiation, the decrease in the DPBF band was monitored while ensuring that the bands belonging to the ZnPc remained unchanged (the light intensity was kept low enough to avoid this decrease, as any change would indicate photobleaching or photodegradation of the sample). ZnPc [Φ_{Δ} = 0.67 (Capraro *et al.*, 1994) in DMSO] was used as both the singlet oxygen generator and the reference solution. Samples were irradiated at a wavelength of 672 nm (corresponding to the λmax of the Q-band of ZnPc). Graphs were plotted to show the rate of disappearance of DPBF over time (Abs vs Time).

7.2.2.3.2. Lamp Photolysis Studies

For this study, naphthalene was used as singlet oxygen generator. Sample solutions of DPBF, melatonin and naphthalene were made up in DMSO and the absorbance once again set to approximately 1 by dilution. Upon irradiation, the decrease in the DPBF band was once again monitored while ensuring that the bands belonging to napthalene remained unchanged (as any change would indicate photobleaching or photodegradation

of the sample). Napthalene [Φ_Δ = 0.78 (Capraro *et al.*, 1994) in MeOH] was used as both the singlet oxygen generator and the reference solution. Since the Φ_Δ for napthalene, is given in methanol, it was thus necessary to determine the Φ_Δ for naphthalene in DMSO. Graphs were plotted to show the rate of disappearance of DPBF over time (Abs vs Time).

7.2.3. RESULTS

7.2.3.1. Nd-Yag Laser studies

In the determination of singlet oxygen quantum yields (Φ_Δ), the decay of the DPBF in the presence of the melatonin and 6-OHM was monitored upon irradiation with light. Figure 7.8, represents the UV-Vis spectrum of ZnPc-DPBF and it is clearly evident that there is a rapid decline in the absorbance of DPBF with an increase in the irradiation time. The intensity of the light is low enough so the phthalocyanine remains unaffected as can be seen in figure 7.8.

The quantum yields of singlet oxygen photogeneration (Φ_Δ) of melatonin, 6-OHM and DPBF, were determined using the equation described above (EQ. 2) and using ZnPc as the standard. No photobleaching or phototransformation of the melatonin was observed during the irradiation of melatonin as no decrease in the absorbance of ZnPc is noted, since these processes occur much slower than singlet oxygen generation.

The rate constants obtained for melatonin and ZnPc were calculated to be -9.98×10^{-3} (R^2 0.996) and -4.50×10^{-3} (R^2 0.997) respectively (figure 7.9). Unexpectedly, melatonin was found to increase the rate of disappearance of DPBF substantially when compared to the ZnPc reference solution (figure 7.9). The singlet oxygen quantum yield thus determined for this system was therefore calculated to be Φ_Δ = 1.41. In fact, it is likely that under these conditions, the melatonin is actually producing radicals i.e. $^1O_2$ and melatonin radicals ($MEL^\bullet$). In order to confirm this, a fresh sample mixture was deaerated by bubbling with nitrogen and irradiated at 672 nm. A decrease in the rate of disappearance of DPBF was then observed (rate constant -2.40×10^{-3}, R^2 0.993, figure 7.10) while the quantum yield was calculated to be Φ_Δ = 0.33.

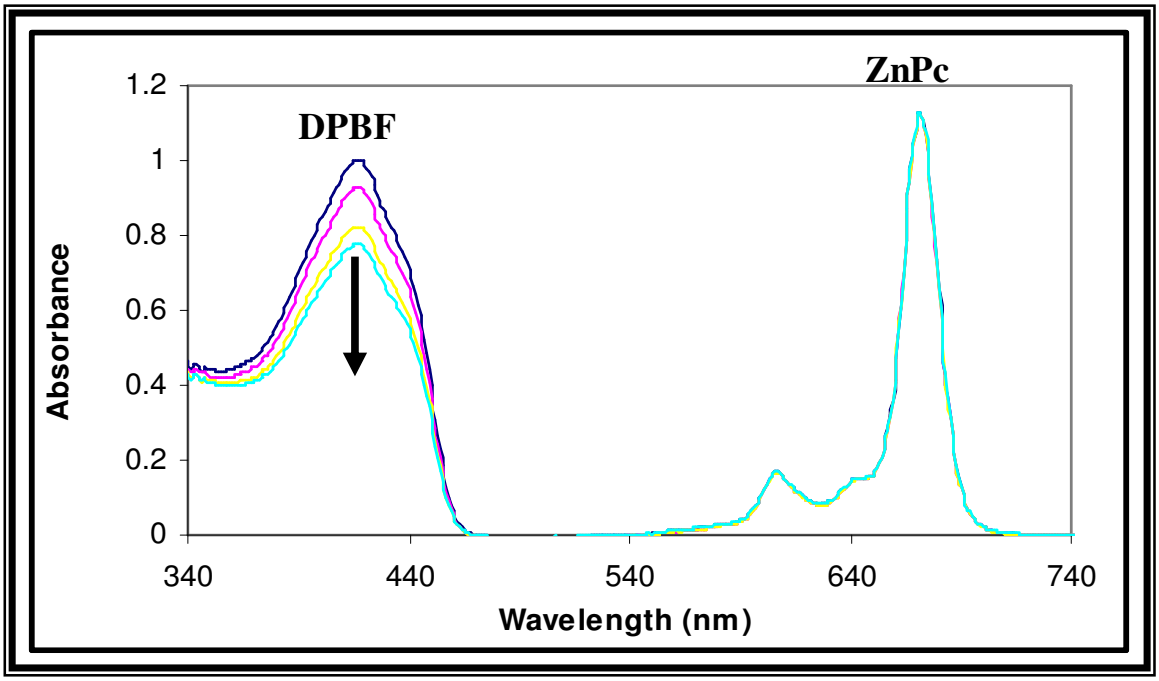

Figure 7.8: UV-Visible spectra of DPBF degradation by singlet oxygen in DMSO.

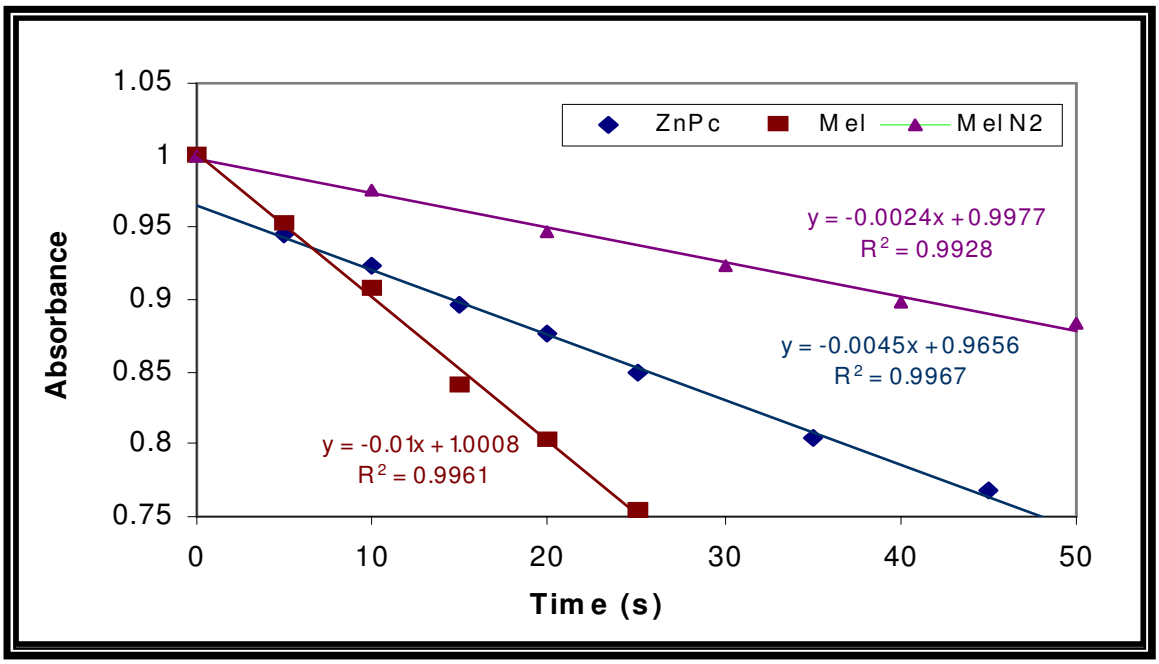

Figure 7.9: Representation of the decrease in absorbance of ZnPc-DPBF alone, ZnPc-DPBF in the presence of melatonin and ZnPc-DPBF in the presence of melatonin (nitrogen) over time (seconds) using laser irradiation.

A quantum yield value greater than 1 is often observed when photolysed compounds generate radicals. Bearing in mind that a quantum yield of a primary process is a value between 0 and 1 (since it represents the probability that an excited state will undergo a reaction), the quantum yield of an overall reaction (primary and secondary processes) can,

however, be greater than 1, depending on the secondary processes taking place. These yields can be quite large when chain reactions occur (Colye & Puttfarcken, 1993).

A decrease in the rate of disappearance of DPBF was observed (rate constant –2.40x 10^{-3}, R^2 0.993), which is still significantly high, while the quantum yield (Φ_Δ = 0.33) obtained confirmed the production of radicals by melatonin upon irradiation of the singlet oxygen generator ZnPc (figure 7.9), thus indicating the melatonin is producing $MEL^\bullet$ as well as $^1O_2$. Drawing from the observed data, the following mechanism is proposed:

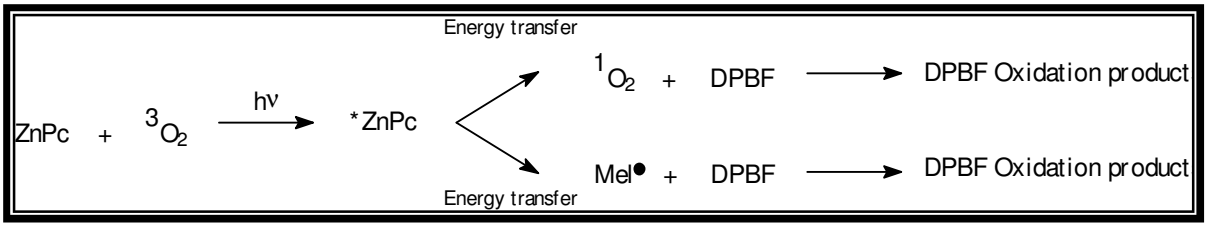

Figure 7.10, represents the decrease in absorbance of the ZnPc-DPBF solution alone and in the presence of 6-OHM. The rate constants obtained for 6-OHM and ZnPc were calculated to be –1.89 x 10^{-3} (R^2 0.988) and –4.76 x 10^{-3} (R^2 0.997) respectively. As expected, 6-OHM was found to decrease the rate of disappearance of DPBF quite substantially when compared to the ZnPc reference solution. These results confirm the ability of 6-OHM to scavenge singlet oxygen.

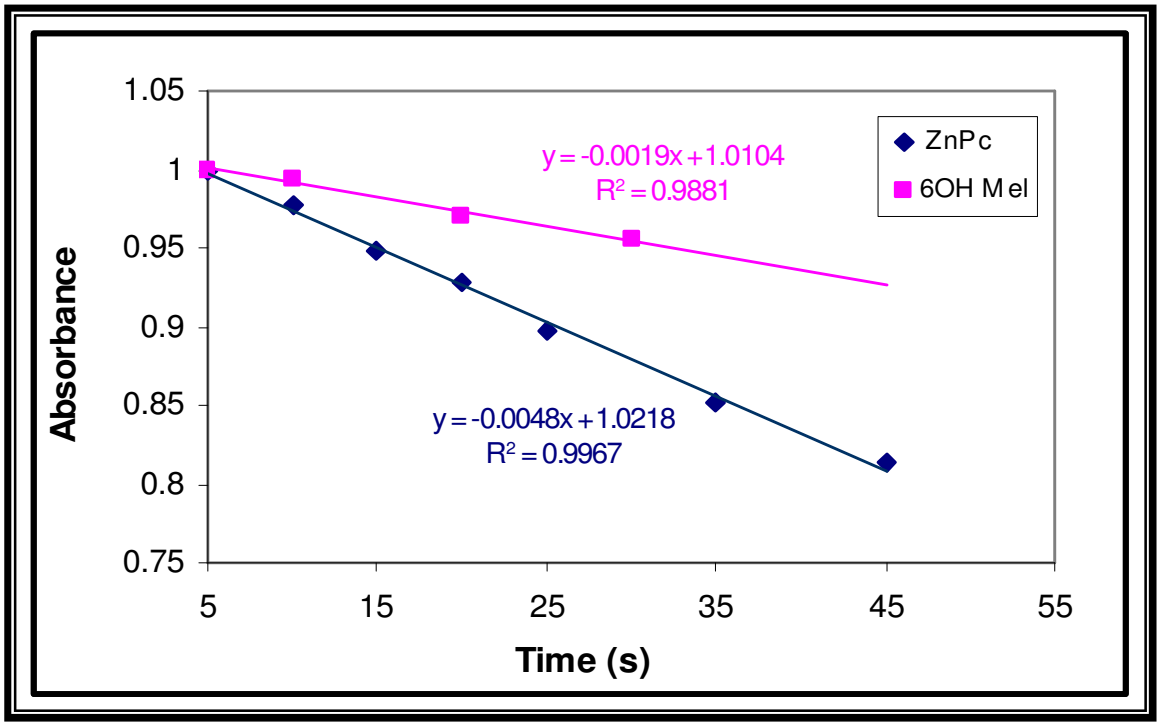

Figure 7.10: Representation of the decrease in absorbance of ZnPc-DPBF alone and ZnPc-DPBF in the presence of 6-OHM over time (seconds) using laser irradiation.

The singlet oxygen quantum yield thus determined for the 6-OHM system was calculated to be Φ_Δ = 0.26, which is a substantial decrease from the Φ_Δ = 0.67 for ZnPc, further evidence of the ability of 6-OHM to scavenge singlet oxygen. The following mechanism is therefore proposed:

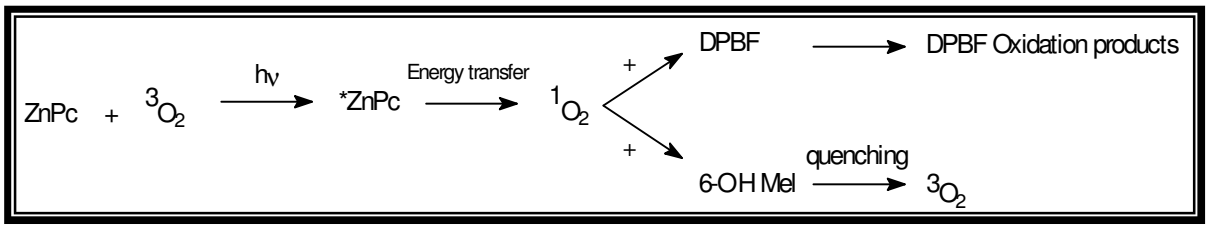

7.2.3.2. Lamp photolysis studies

The results of figure 7.10 show a rapid decrease in the absorbance of DPBF in the presence of naphthalene. The rate constants obtained for melatonin and naphthalene were calculated to be – 0.1 x 10^{-3} (R^2 0.9976) and –0.2 x 10^{-3} (R^2 0.9981), respectively (figure 7.10). In this study, melatonin was found to decrease the rate of disappearance of DPBF when compared to the napthalene (DMSO) reference solution. Thus indicating the melatonin was competing with the DPBF solution for the quenching of $^1O_2$.

The singlet oxygen quantum yield thus determined for this system (Napth+DPBF+Mel) was therefore calculated to be $\Phi_\Delta = 0.05$ which is a substantial decrease in comparison to the Φ_Δ of napthalene in DMSO which is 0.114. It is therefore likely that under these conditions, the melatonin is behaving as a singlet oxygen scavenger. The decrease in the rate of disappearance of the DPBF may be attributed to competition between the DPBF and melatonin to scavenge the singlet oxygen generated by naphthalene, which could therefore account for this decrease. The following mechanism is proposed:

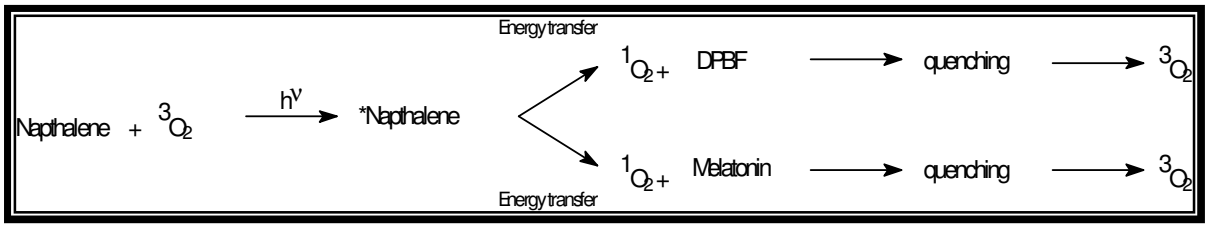

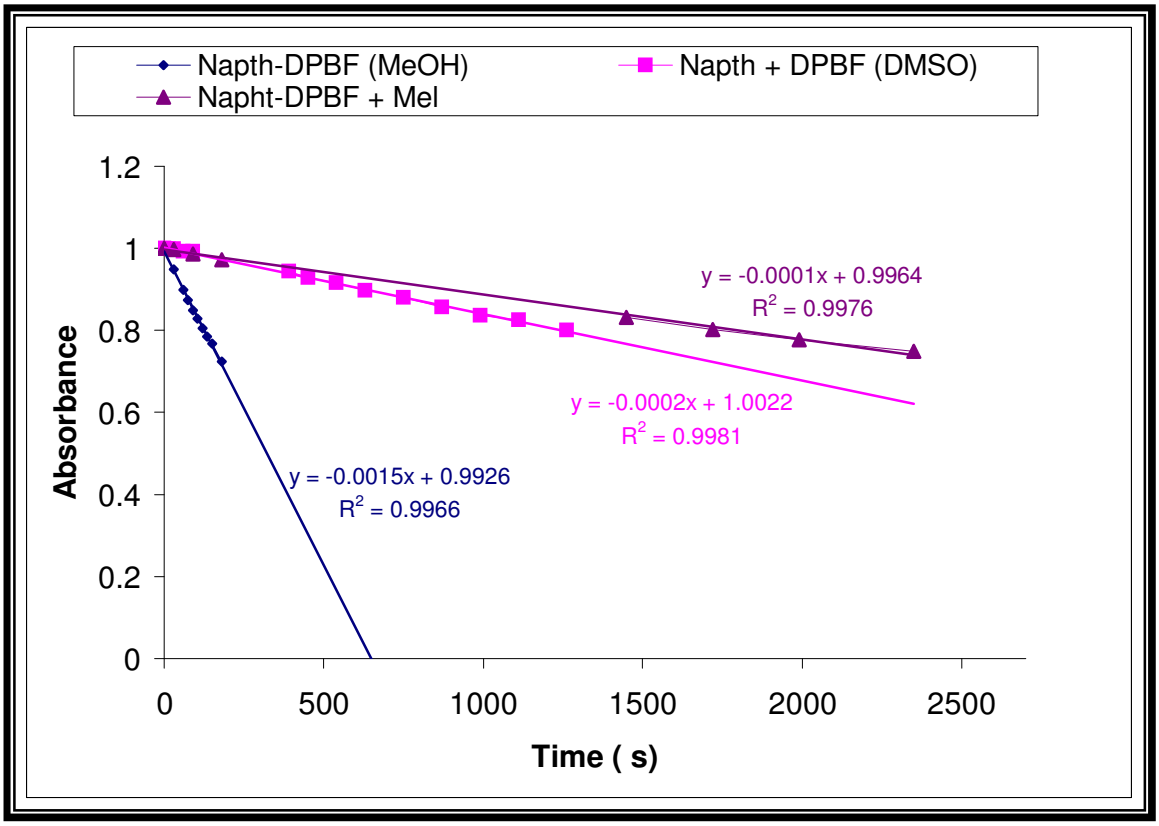

Figure 7.11: Representation of the decrease in absorbance of Napthalene alone, Napthlene-DPBF alone and Napthalene-DPBF in the presence of melatonin over time (seconds) using the lamp photolysis.

7.2.4. DISCUSSION

Given that melatonin neutralizes O_2-derived reactants, this indole would be expected to protect against hyperbaric hypoxia exposure. This has been shown to be the case. In the two organs that are most sensitive to increased O_2 levels, the lungs and the brain, melatonin given to rats exposed to 4 atmospheres of 100% O_2 for 90 minutes reduced the breakdown of polyunsaturated fatty acids and maintained high antioxidant enzyme activity (Pablos *et al*., 1997). The protection afforded by melatonin against O_2 toxicity is consistent with the *in vivo* free radical scavenging and antioxidant properties of melatonin (Cabrera *et al*., 2000).

$^1O_2$ is a reactive molecule that is produced in cells upon the electronic excitation of O_2. It is generally accepted that the $^1O_2$ is cytotoxic and has be postulated to play a role in neurodegenerative diseases such as Parkinson's disease (Perry *et al*., 1982). In the present study, using two different excitation sources i.e. the Nd-Yag laser and lamp photolysis, the ability of melatonin to scavenge and or generate singlet oxygen was shown. Using the laser source, melatonin was shown to increase the disappearance of DPBF indicating that melatonin under these conditions is actually producing radicals. Nitrogen was bubbled in the melatonin solution prior to irradiation (thus removing the presence of oxygen) and the rate of disappearance of DPBF decreased while the quantum yield that was obtained i.e. $\Phi_\Delta = 0.33$ confirmed the production of radicals by melatonin i.e. melatonin radical and $^1O_2$. Figure 7.12, illustrates the mechanism of formation of melatonin radicals. In detoxifying the hydroxyl radical, melatonin is believed to work *via* electron donation (Hardeland *et al*., 1993; Poeggeler *et al*., 1994; 1996). In so doing, melatonin itself became a radical first, the indolyl cation (or melatonyl) radical, of which there may be several isoforms (Stasica *et al*., 1998). Furthermore, Zhang *et al*., (1998) demonstrated the involvement of melatonyl radical cation formation in the peroxynitrite/melatonin reaction and with excess bicarbonate. Thus, in a similar manner melatonin in the presence of the laser source and $^1O_2$ species is producing melatonin radicals however; this product is not very reactive and is therefore non-toxic in the cell (Lewis *et al*., 1990).

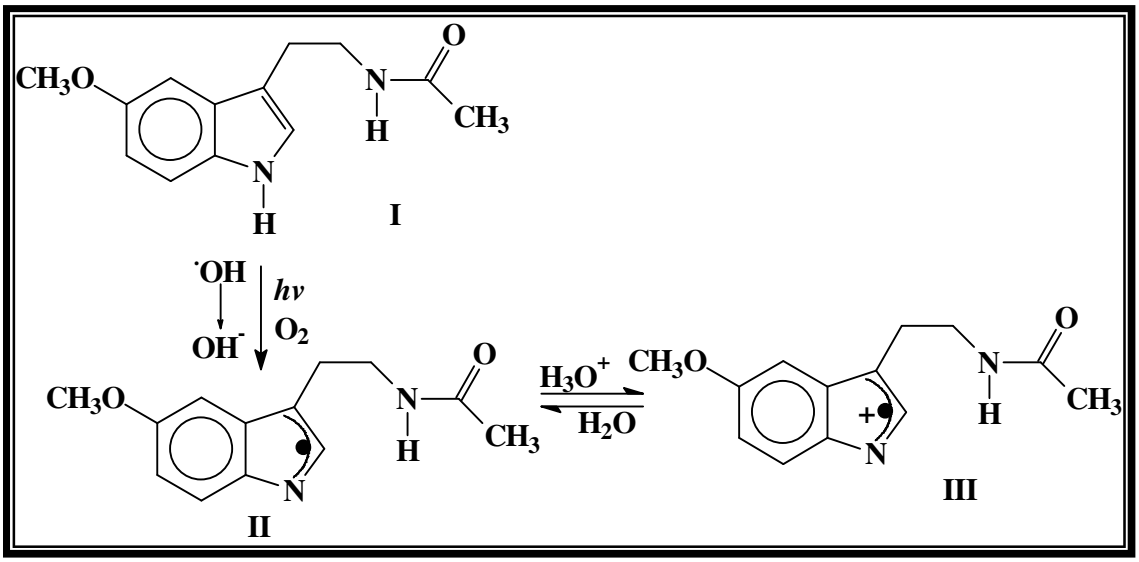

Figure 7.12: Melatonin (I) believed to detoxify highly toxic radicals by electron donation. In doing so, it becomes the indolyl cation radical, of which there may be more than one form (II and III) (Reiter, 1998).

However, with upon lamp photolysis , melatonin was shown as an effective scavenger of $^1O_2$ produced by naphthalene. This discrepancy may be explained in terms of a) the much higher energy systems employed by the laser to irradiate the ZnPc sensitizer at 672 nm (λ max of ZnPc); and b) the energy which could be transferred from the excited ZnPc molecules (which possess a large amount of energy) to both the ground state oxygen molecules as well as melatonin. These results however, correlate with the data obtained by Roberts *et al.*, (2000), where the authors demonstrated that melatonin produces a small, yet detectable amount of singlet oxygen when it is irradiated by a Nd-Yag laser. It has been shown that tumours are destroyed in photodynamic therapy (PDT), by singlet oxygen generated by porphyrins (Spikes, 1989). Thus, it can be speculated that melatonin under the following conditions can generate singlet oxygen which can be useful for the destruction of tumours. The optimum photosensitisers for PDT will have a high quantum yield for $^1O_2$ production (Roberts *et al.*, 2000). For example, hematoporphyrin has a Φ_Δ = 0.68 in CD_3OD (Scaiano, 1995) while for melatonin it is 1.14 indicating that it is a good photosensitiser for PDT.

Lamp photolysis operates at a lower energy and the wavelengths employed were those that were not filtered (i.e. those below 500 nm). Thus under the conditions of the lower energy system, melatonin serves as a $^1O_2$ scavenger. Cagnoli *et al.*, (1995) incubated cerebellar granule cells with a photosensitive dye, rose bengal and then exposed the

cultures to light, a process that generates $^1O_2$. Using this system, these authors found that melatonin inhibits DNA fragmentation, a marker of apoptosis, and cell death, induced by $^1O_2$. The findings, according to the authors (Cagnoli *et al*., 1995) are consistent with the ability of melatonin to directly neutralize $^1O_2$ toxicity.

The results of the laser study show that 6-OHM is able to effectively quench $^1O_2$ species. Thus, since 6-OHM is able to scavenge $^1O_2$ in this purely chemical system, it may be able to protect the body against the cytotoxic and deleterious effects produced by $^1O_2$ generation. This research serves as a basis of proving the ability of 6-OHM, the photoproduct and primary metabolite of melatonin, in scavenging the photocytotoxic species, $^1O_2$. However, in order to demonstrate the ability of melatonin and 6-OHM to scavenge $^1O_2$ *in vivo*, further research needs to be done using a lipid or protein source such as brain tissue.

In the skin and lung, even at low concentrations, $^1O_2$ has been shown to lead to direct oxidative damage to DNA (Ryter & Tyrrell, 1998). In the eye, $^1O_2$ may trigger an antioxidant defence even as it damages cells. However at the same time $^1O_2$ damage to DNA and lipids may accumulate in non-proliferative uveal melanocytes; this unpaired damage may play a role in the induction and /or proliferation of uveal melanoma (Roberts *et al*., 2000). The skin transmits both UVA and UVB radiation (Sterenborg & Wan der Leun, 1990), allowing light of both wavelength ranges to reach melatonin localized within the skin and be absorbed. The results in chapter 6 demonstrated the UV photo-instability of melatonin and the rapid formation of its photoproduct.

Amine substituted compounds are known to be singlet oxygen quenchers (Fiyer *et al*., 1988). The structure of 6-OHM is similar to that of melatonin and both indoleamines consist of two amine substituted groups in their structure. It is evident from figure 7.10, that 6-OHM is able to slow down the decrease in absorbance of DPBF which is a known quencher of $^1O_2$. Thus by slowing down the decay of DPBF, we can conclude that 6-OHM also serves as a $^1O_2$ quencher.

7.3. CONCLUSION

In vivo, roughly 4% of the molecular O_2 taken into the organism is normally converted to the O_2 byproducts, one such by product is $^1O_2$ (see figure 7.1). Thus the greater the concentration of O_2 in the inspired air, the more extensive is the molecular damage to the organism. This damage becomes increasingly clear when animals are exposed to 100% O_2 at increased atmospheric pressure (Jenkinson *et al*., 1989).

In order to generate $^1O_2$ *in vivo*, melatonin and 6-OHM must absorb light reaching the tissue where they are located. The skin transmits both UVA and UVB radiation (Sterenborg & Van der Leun, 1990), allowing light of both wavelength ranges to reach melatonin localized within the skin and be absorbed. In the eye, light of wavelengths shorter than 295nm is filtered by the cornea (Bachem, 1956) and prevented from reaching the aqueous humor.

Although, $^1O_2$ is produced in biological systems (Kukreja *et al*., 1993), as yet there is no information on the amount of singlet oxygen generated in pathological conditions associated with the neurodegenerative processes. It is possible that several pathways lead to its *in vivo* production, including the interaction of hydrogen peroxide with peroxynitrite (DiMascio *et al*., 1994). It is most likely that the $^1O_2$ generated by laser and lamp photolysis is very high, and that the damaging effects that we found in our *in vitro* system is much greater than the eventual biological damage induced by the amount of $^1O_2$ generated *in vivo*. Thus, it can be speculated that since melatonin and 6-OHM are able to scavenge the high concentration of $^1O_2$ produced, these compounds would be effective in quenching the biological concentrations of $^1O_2$ produced and thus be effective in counteracting the damaging action of photodynamic injury. This is supported by the results of Cagnoli *et al*., (1995) where melatonin was shown to counteract the cytotoxicity of singlet oxygen in rat cerebellar granule neurons.

Spikes (1989) showed that high concentrations of $^1O_2$ are able to destroy tumours. Furthermore, the ability of melatonin to generate $^1O_2$ in the presence of the laser source indicates that under these conditions melatonin may serve to destroy tumours by $^1O_2$

production. Melatonin can thus serve as an optimum photosensitiser as it possesses a high $^1O_2$ quantum yield under the Nd-Yag laser conditions.

Since, both melatonin and 6-OHM are able to scavenge $^1O_2$ in this purely chemical system; they may be able to protect the body against the cytotoxic and deleterious effects produced by $^1O_2$ generation. This research serves as a basis of demonstrating the ability of melatonin and 6-OHM, the photoproduct and primary metabolite of melatonin, in scavenging the photocytotoxic species, $^1O_2$. However, in order to demonstrate the ability of 6-OHM to scavenge $^1O_2$ *in vivo*, further research needs to be done using a lipid or protein source such as brain tissue.

Since O_2 and $^1O_2$ can be converted readily to $O_2^{\bullet-}$ these radicals are highly reactive and can readily cause neurodegeneration (Patel *et al*., 1996). Thus, the next question was whether these two indoleamines possess the ability to reduce or prevent the generation of $O_2^{\bullet-}$.

CHAPTER NINE

MITOCHONDRIAL FUNCTION

9.1. INTRODUCTION

The primary function of the mitochondrion, where aerobic eukaryotes generate most of their energy from, is to generate adenosine triphosphate (ATP), the energy currency of the cell. This is done by the rapid oxidation of NADH and FADH through the electron transport chain (ETC) to produce ATP (Acuña-Castroviejo *et al*., 2001). ATP is a ubiquitous store of energy needed for transport across membranes for all synthetic processes and for the mechanical work involved in motor activities of the cell (Hammans & Tipton, 1994). Remarkably, more than 90% of the body's O_2 consumption is utilized by a single enzyme, cytochrome *c* oxidase (Complex IV) (Nathan & Singer, 1999).

Aerobic organisms use ATP generated by an oxidative phosphorylation (OXPHOS) pathway involving a multienzymatic process, which includes Complex IV as an electron acceptor. Normally, there is no shortage of ATP production under aerobic conditions, since the amount of O_2 delivered to the tissues is in excess to the body's requirements. This situation is reversed when sufficient oxygen is available to the mitochondria, but they are unable to utilize it due to an inhibition at any of the several points in the electron transport chain (ETC) such as inhibition of Complex IV by cyanide. Such disturbances are common to aging and several pathologies, including neurodegenerative diseases, ischemia and sepsis where an increase in $O_2^{\bullet-}$, H_2O_2, $^{\cdot}OH$, nitric oxide, and peroxynitrite are known to inhibit the ETC Complexes (Murphy, 1989; Beal 1998; Lenaz, 1998; Bockowski *et al*., 1999).

As described in chapter eight, the mitochondria are involved as producers of ROS and the consequence of oxidative stress at the level of the mitochondria will be the failure of enzymatic, transport and receptor systems. A vicious circle (Ozawa, 1995; Ozawa, 1997) has been proposed to occur: any damage to the respiratory chain may enhance ROS production (Papa & Skulachev, 1997) and induce progressive and continuous perpetuation of damage through somatic mutations of mitochondrial DNA (mtDNA) and

defective mtDNA-encoded proteins. Although this idea is controversial and rejected by some authors (De Gray, 1998), an increase in both ROS production (Cavazzoni *et al*., 1999; Barogi *et al*., 2000) and mtDNA deletions (Lenaz, 1998) occurs during aging. Such alterations exclusively affect the four mitochondrial complexes (Complex I – IV) involved in energy conservation and can result in defective electron transfer and OXPHOS (Bai *et al*., 2000). Thus, mitochondria have been reported to undergo significant functional changes with aging (Benzi & Moretti, 1995; Cooper *et al*., 1992; Sastre *et al*., 2000) particularly changes to the activity of enzymes constituting the electron transport system. These changes may play a role in the progression of neurodegenerative diseases and the overall ageing process (Sharman & Bondy, 2001). Hence energetically compromised mitochondria may have detrimental effects on the survival of the cell. Furthermore, mitochondrial respiratory chain defects have been implicated in the pathogenesis of AD (Grunewald & Beal; 1999) and mitochondrial dysfunction has been associated with the neurodegeneration of PD (Berman & Hastings, 1999). Apoptosis is also believed to be triggered, *inter alia*, by the presence of energetically compromised mitochondria resulting in neuronal cell death (Heron *et al*., 2001).

9.2. THE EFFECT OF CYANIDE ON RAT BRAIN MITOCHONDRIAL RESPIRATORY FUNCTION.

9.2.1. INTRODUCTION

The ETC is constituted of four complexes and the electron transfer from one complex to another is driven by the reduced forms of the ubiquinone (UQ) and cytochrome c (cty c) (De Gray, 1999). Cyanide is implicated as a mitochondrial electron transport inhibitor of Complex IV, the cytochrome *c* oxidase enzyme, of the mitochondrial ETC as mentioned in chapter eight. Cyanide is known to cause severe depletion of cellular ATP (Ottino & Duncan, 1997) and prevents the cytochrome *c* oxidase mitochondrial defense mechanism against $O_2^{\bullet-}$ to occur effectively (Acuña-Castroviejo *et al.*, 2001). Cyanide has been shown to cause a rapid and severe depletion of cellular ATP and cell death that is dependent on cellular energy impairment (Maharaj *et al.*, 2003b). The final transport of electrons across the inner mitochondrial membrane is inhibited with cyanide, due to its inhibition of cytochrome a_1a_3, which reduces the number and rate of electron production by mitochondrial metabolism (Plummer, 1971). Therefore, cyanide is a well established respiratory poison, exerting its toxic effects on the mitochondria by virtue of its inhibition of Complex IV (Isom & Way, 1984).

In the present study, the extent of damage that cyanide causes on rat brain mitochondrial function due to impaired respiration was investigated using a modification of the biological oxidation assay described by Plummer (1971).

Briefly, the experiment used to study the electron transport chain function was done using a dye 2, 6-dichlorophenolindophenol (DPI) (blue) which acts as an artifical electron acceptor and changes colour on reduction or oxidation. In the present experiment, DPI accepts electrons from reduced flavoprotein (fp.2H) and is itself reduced to the colourless form as shown in figure 9.1. Thus, the rate of electron transfer can be measured by following the decolourization of this dye.

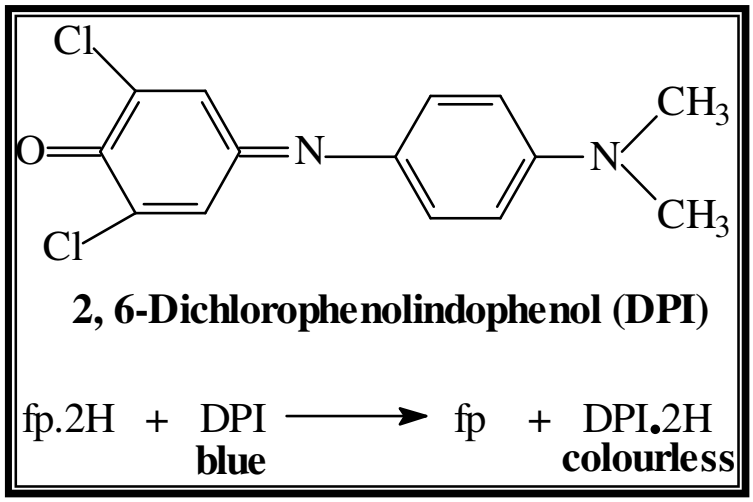

Figure 9.1: Schematic diagram of the reaction of DPI with a reduced flavoprotein (Plummer, 1971).

9.2.2. MATERIALS AND METHODS

9.2.2.1. Chemicals and Reagents

All chemicals and reagents were of the highest quality available and were purchased from commercial distributors. Potassium cyanide (KCN), nicotinamide adenine dinucleotide (NAD), sodium chloride (NaCl), 2, 6-diclorophenol-indophenol (DPI), and 3[*N*-morpholino]propanesulfonic acid (MOPS) were purchased from Sigma Chemical Corporation, St. Louis, MO, U.S.A. Sucrose was purchased from Saarchem (PTY) Ltd, Krugersdorp, South Africa. L-Malate was purchased from Eastman Organic Chemicals.

9.2.2.2. Animals

Adult, male, Wistar rats, weighing between 250 and 300g were used for the experiment and were housed and maintained under the conditions described in appendix one.

9.2.2.3. Sample Preparation

KCN was dissolved in Milli-Q water. The following concentrations were used for the biological oxidation assay: 0, 0.25, 0.5 and 1mM. All other reagents were prepared in 0.1M potassium phosphate buffer, pH 7.4.

9.2.2.4. Isolation of Mitochondria from Rat Brain Homogenate

The rats were sacrificed and their brains were rapidly excised as described in appendix two and chilled on crushed ice and thereafter these were rinsed in ice cold saline [0.9% (w/v) NaCl) solution to remove traces of blood. Rat brain mitochondrial suspensions were used for the biological oxidation assay of the electron transport chain. The whole brains were homogenized in 0.32M sucrose + 1M MOPS buffer at pH 7.4 in a manual glass Teflon homogenizer on ice to yield a 10%w/v homogenate. Mitochondrial suspensions were prepared by differential centrifugation to obtain relatively pure suspensions of intact mitochondria according to Plummer (1971). The brain homogenate was centrifuged at 600g for 10 minutes and then separated into supernatant and pellet. The pellet was resuspended in half the volume of sucrose and once again centrifuged at 600g for 10 minutes and the supernatant obtained was combined with the previous supernatant. The combined supernatant was centrifuged at 8000g for 10 minutes and the pellet obtained (crude mitochondria) was washed twice in sucrose and then stored on ice until required. All procedures were carried out at 0-4^{o}C. To ensure that the crude mitochondria was obtained, transmission electron micrographs (TEM; see figure 9.3) were prepared by the standard procedures (Rhodes University Electron Microscopy Unit Handbook).

9.2.2.5. Instrumentation

Samples for the biological oxidation assay were analyzed using a Shimadzu UV-160A UV-visible recording spectrophotometer.

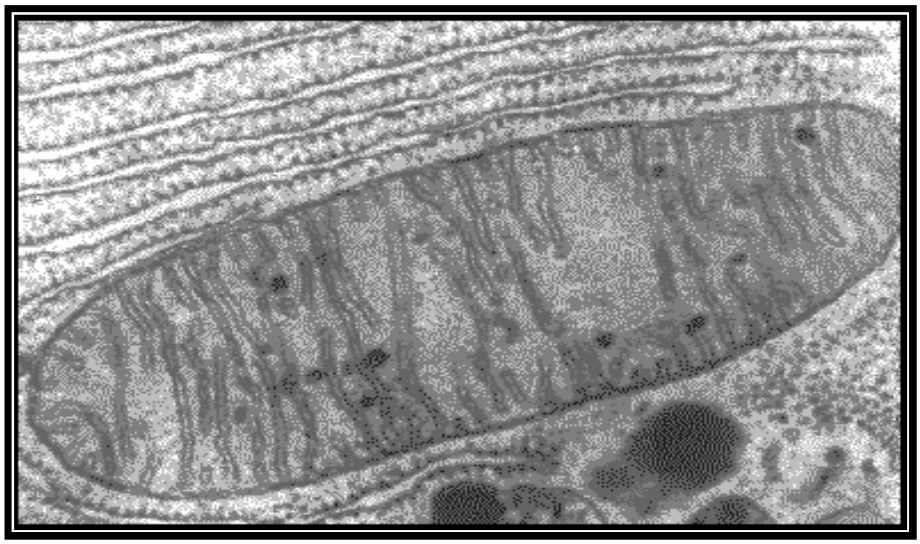

Figure 9.2: TEM micrograph showing the relatively pure mitochondria that was obtained by differential centrifugation (Magnification X 100 000).

9.2.2.6. Biological Oxidation Assay

This spectrophotometric technique was employed to determine the 'activity' of the inner mitochondrial membrane electron transport chain of the whole 'rat brain' mitochondrial suspension. The latter was determined by the rate of reduction of the synthetic electron acceptor dye 2, 6-dichlorophenol-indophenol (DPI: 50µM) in the presence of L-malate (substrate). L-malate is used as an indication of the extent of 'activity' of the inner mitochondrial ETC. The substrate and NAD^+ were present in saturating final concentrations of 0.0899mM and 0.5mM, respectively. Potassium phosphate buffer pH 7.4 (1.5mL) containing 300µL of mitochondrial suspension, 100µL of varying concentrations of KCN (0, 0.25, 0.5, and 1mM) were placed in a 37±2^{o}C water bath for varying preincubation times (5 and 60 min). Following incubation 1.5mL of incubated homogenate, 500µL of substrate/buffer (control), 500µL NAD and 100µL DPI was added in that order to a quartz cuvette. This was inverted once to mix solutions and the decrease in absorbance at 600nm was read over a 5 min period at 30 s intervals. Data was expressed as ΔAbs_{600nm}/min and corrected for appropriate controls.

9.2.2.7. Statistical Analysis

The differences in the means were analyzed using a one-way analysis of variance (ANOVA) for statistical significance. If the F values were significant, the Student Newman-Keuls test was used to compare the treated and control groups. The level of significance was accepted at $p<0.05$ (Zar, 1974).

9.2.3. RESULTS

The final results were corrected for all dilutions and expressed as rate of DPI reduction (change in absorbance at 600nm/min). The data represents the mean of five determinations and the mean ± SEM is represented.

The results obtained demonstrate a progressive decline of mitochondrial ETC activity in the presence of increasing concentrations of KCN as shown in figure 9.3. It is evident that mitochondrial ETC is time and dose dependently reduced by cyanide with malate as the substrate. The 0.25mM KCN concentration at 5min of incubation caused a ± 68% reduction of the ETC while the 1mM KCN at 60min of incubation reduced the activity to almost zero. Since the 1mM provided almost complete inhibition of he ETC activity, this dose was chosen for subsequent studies.

9.2.4. DISCUSSION

The brain has high energy requirements for normal functioning and the mitochondrion is known to be the intracellular fountain of the brain's energy supply and subtle functional alterations in these essential energy dynamos may lead to insidious pathological changes within neurons (Beal *et al.*, 1993; Beal, 1995). A decline in brain ETC activity has been linked to the etiology of neurodegenerative disorders, including Alzheimer's disease, Parkinson's disease and Huntington disease (Enns, 2003). Recent studies have shown that oxidatively modified proteins are found not only in the CNS of aged subjects but also in the brains of subjects affected with a range of neurological disorders including Alzheimer's disease and Parkinson's disease (Bondy, 1999). It is known that electron transport chain activity is reduced by excess levels of free radical reactions resulting in

ROS production (Sastre *et al*., 2000) as well as mitochondrial enzyme inhibitors which in turn leads to the obvious impairment in ATP production, and causes the diversion of electrons from their normal ETC recipients and further formation of damaging free radicals (Cassarino & Bennett, 1999). One such inhibitor is cyanide.

The present study shows that cyanide at all the concentrations tested for is capable of significantly reducing the activity of the ETC to levels below that of the control at 5 and 60 minutes of incubation time. A time and concentration dependent effect of cyanide on ETC activity of mitochondria is evident. The 1mM concentration at time 60min of incubation resulted in complete inhibition of mitochondrial ETC activity indicating that at this concentration cyanide has completely inhibited Complex IV activity (Maharaj *et al*., 2003b). These findings are in accordance with the fact that cyanide interacts with the haem-a-3 portion of cytochrome *c* oxidase (Slater, 1967), thus preventing oxygen utilization by the mitochondria, and resulting in respiratory dysfunction and oxidative stress. Impaired ETC functioning in the brain leads to cell death via a decrease in ATP production or an increase in ROS and RNS production (Curtin *et al*., 2002; Beal, 1995). The fact that the major neurodegenerative disease are age-related may well be accounted for by the fact that the efficiency of the mitochondrial electron transport decreases with age, and the production of hydrogen peroxide and superoxide radicals increases with age (Beal, 1995; Hagen *et al.*, 1997).

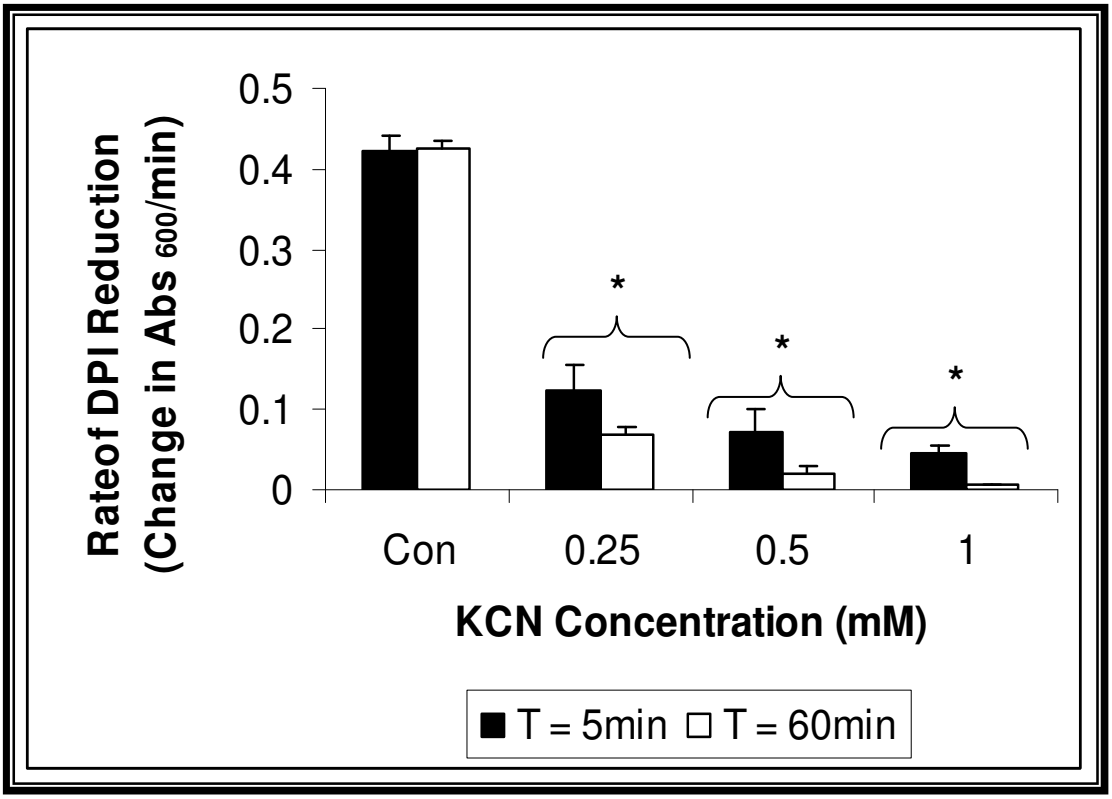

Figure 9.3: The effect of increasing concentrations of KCN on rat brain mitochondrial electron transport chain activity at time 5 and 60 min. Data represents the mean ± SEM (n=5) *($p<0.0001$) Control vs KCN (0.2, 0.5, and 1mM) at time 5 and 60min.

9.3. THE EFFECTS OF MELATONIN AND 6-OHM ON CYANIDE-INDUCED IMPAIRMENT OF THE RAT BRAIN MITOCHONDRIAL RESPIRATORY FUNCTION.

9.3.1. INTRODUCTION

The mitochondrion is the organelle in eukaryotes responsible for aerobic respiration and is the most common source of ROS as mentioned in chapter eight. Thus, a faulty electron transfer at any point in the ETC results in an electron being accepted by atomic oxygen thus resulting in the creation of free radicals. The respiratory chain loses two to three percent of the electrons during their transfer to molecular oxygen, most of them participating in the production of $O_2^{\bullet-}$ (Boveris, 1977). Thus agents that can scavenge ROS and promote mitochondrial ETC activity can serve to protect against neurodegenerative diseases and the deleterious effects of aging.

In chapter eight, melatonin and 6-OHM were shown to be effective scavengers of $O_2^{\bullet-}$ in rat brain homogenate with 6-OHM being the potent scavenger of the two indoleamines. Since much of the superoxide free radicals originate in the mitochondria, the following experiment was conducted to assess the effects of melatonin and 6-OHM on the ETC, and whether these agents were able to offer protection against cyanide induced impairment of the mitochondrial respiratory functioning.

9.3.2. MATERIALS AND METHODS

9.3.2.1. Chemicals and Reagents

All chemicals were of the highest quality available and were purchased from commercial distributors. Melatonin and 6-OHM were purchased from Sigma Chemical Corporation, St. Louis, MO, U.S.A.

9.3.2.2. Sample Preparation

Melatonin and 6-OHM were dissolved in a mixture of absolute ethanol and water for the purposes of this experiment. The final concentration of ethanol in the samples was less than 0.5% and all other reagents were prepared in 0.1M potassium phosphate buffer, pH 7.4.

9.3.2.3. Isolation of Mitochondria from Rat Brain Homogenate

Rats were sacrificed and the rat brains were rapidly excised as described in appendix two and chilled on crushed ice. Thereafter these were rinsed in ice cold saline [0.9% (w/v) NaCl). The whole rat brain was homogenized and brain mitochondrial suspensions were prepared as described in section 9.2.2.4

9.3.2.4. Biological Oxidation Assay

Potassium phosphate buffer pH 7.4 (1.5mL) containing 300µL of mitochondrial suspension, 100µL of varying concentrations of KCN alone or in combination with melatonin or 6-OHM (0, 0.25, 0.5, and 1mM) were placed in a 37±2^{o}C water bath for varying preincubation times (5 and 60 min). The procedure described in section 9.2.2.6 was followed. Final results were expressed as ΔAbs_{600nm}/min and corrected for appropriate controls.

9.3.3. RESULTS

The results obtained from this study show significant protection afforded by melatonin and 6-OHM against cyanide induced brain mitochondrial respiratory dysfunction, with respect to an increase in the activity of the ETC in the presence of these agents.

As evident in figure 9.4, the activity of the mitochondrial ETC of the mitochondria treated with melatonin only is significantly higher in comparison to the cyanide and control (no drug or toxin added) treated mitochondria. In addition, melatonin alone was able to time

dependently increase mitochondrial ETC function above that of the control value indicating that it is capable of increasing the basal levels of the ETC activity within the mitochondria. A similar effect is seen with the mitochondria treated with 1mM melatonin and 1mM cyanide and this is indicative of the complete protection offered by melatonin against cyanide inhibition of mitochondrial ETC function. Furthermore, the cyanide-induced inhibition of the mitochondrial ETC activity is dose and time dependently reversed by melatonin as shown in figure 9.4.

From figure 9.5, it is also evident that the reduction of mitochondrial ETC activity caused by the 1mM KCN was reversed by the addition of increasing concentrations of 6-OHM, with the greatest effect observed for the 1mM 6-OHM. There is no significant difference noted between the protection offered by different concentrations of 6-OHM at time 5 min and time 60 min of incubation. However, the 1mM 6-OHM at time 60 min of incubation was able to return ± 60% of the mitochondrial respiratory chain activity that was lost due to the addition of 1mM KCN. In addition, the activity of the ETC of mitochondria treated with 1mM 6-OHM alone was significantly higher in comparison to the control value as shown in figure 9.5.

However, in comparing figure 9.4 and 9.5, it is evident that melatonin offers significantly greater protection against cyanide induced inhibition of the mitochondrial ETC activity than 6-OHM. Furthermore, melatonin increases the ETC activity to much higher level than 6-OHM.

9.3.4. DISCUSSION

Cyanide is known to cause a rapid and severe depletion of cellular ATP and cell death due to its distal inhibition of the mitochondrial ETC (Maharaj *et al*., 2003b). In section 9.2, the extent of intoxication by cyanide on the ETC of brain mitochondria has been demonstrated and discussed.

The present study shows that melatonin affords significant protection to the mitochondria against cyanide-induced insult with respect to the activity of ETC, and this protection has been shown to increase with time and concentration of melatonin utilized. This however,

was unexpected, considering the fact that this experiment is an *in vitro* one, and that the vulnerability of the mitochondria is bound to increase with an increase in time. Thus, the results show that melatonin is able to prolong the lifespan and decrease the vulnerability of the mitochondria under the experimental conditions. The 6-OHM was able to dose-dependently reverse the cyanide-induced inhibition of the mitochondrial ETC activity; however no significant difference in mitochondrial ETC function was noted with an increase in incubation time. This implies that both melatonin and 6-OHM are capable of reducing cyanide-induced inhibition of the mitochondrial ETC activity, with melatonin causing complete abolishment while 6-OHM results in only partial reversal of this cyanide-induced inhibition. This implies that melatonin serves as a superior agent in promoting and protecting the mitochondrial ETC against cyanide. Both agents were also shown to increase the basal levels of respiration and ETC activity within the brain mitochondria. However, melatonin results in a more significant induction of the mitochondrial ETC activity in comparison to 6-OHM.

Melatonin has been shown to improve mitochondrial function and activity by increasing reduced glutathione (GSH) levels (Urata *et al*., 1999) which is required by the mitochondria for normal functioning (Acuña-Castroviejo *et al*., 2001) and by counteracting cyanide-induced inhibition of Complex IV (Yamamoto and Tang, 1996a, b) and restores levels of cytochrome a_1a_3 (Martin *et al*., 2000a). Melatonin has also been shown to increase Complex I and Complex IV activity of the mitochondrial ETC in rat liver and brain tissue in a time dependent and concentration dependent manner (Absi *et al*., 2000b; Martin *et al*., 2000b; Martin *et al*., 2000c). This data further supports the results of the present study where melatonin alone and in combination with cyanide was shown to increase ETC activity in a time and concentration dependent manner. Furthermore, melatonin augments the activities of several antioxidant enzymes including superoxide dismutase (SOD), glutathione peroxidase (GPx) and glutathione reductase (GRx), thereby reducing the oxidative state of cells (Pablos *et al*., 1997; Barlow-Walden *et al*., 1995; Antolin *et al*., 1996; Okatani *et al*., 2000). In light of this, there is a possibility that 6-OHM also increases Complex I and Complex IV activity as it also was shown to increase mitochondrial ETC levels above that of the basal levels. However, further studies have to be conducted to prove this theory and thus in section 9.4, the effect of 6-OHM on mitochondrial Complex I activity was determined. However, the results show that both melatonin and 6-OHM have a direct effect on the mitochondria. In other

studies, melatonin has been shown to increase ETC activity coupled with OXPHOS, which was reflected by an increase of ATP synthesis, both in normal mitochondria and in mitochondria depleted of ATP by cyanide (Martin *et al*., 2000a).

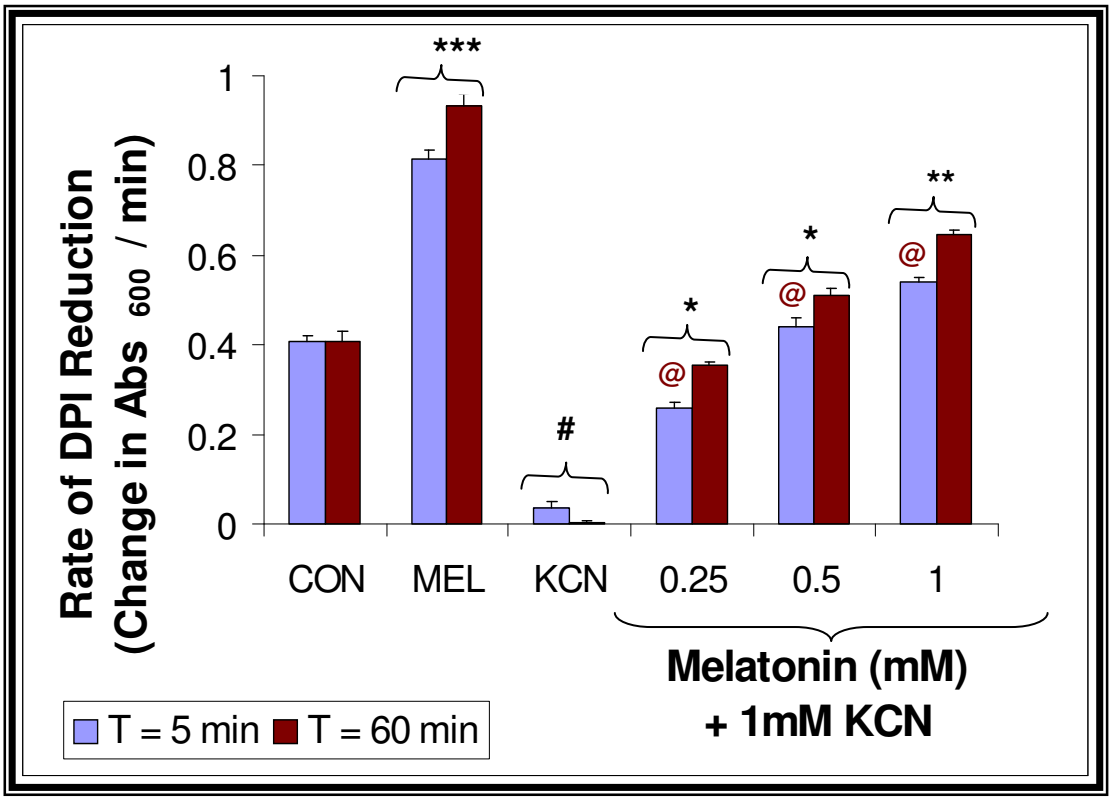

Figure 9.4: A comparison of the *in vitro* effect of melatonin alone or in combination with cyanide (1mM) on rat brain mitochondrial electron transport utilizing L-malate as a substrate, at time 5 and 60 minutes of incubation. Data represents the mean ± SEM (n = 5) $^{\#}p < 0.001$ vs control, at time 5 and 60 min; *p < 0.05 vs 1mM KCN alone, at times 5 and 60 min; **p<0.01 vs 1mM KCN and control; ***p<0.001 vs control, at times 5 and 60 min and @p<0.01 vs the respective melatonin value at time 60 minutes of incubation. (Student Newman-Keuls Multiple Range Test).

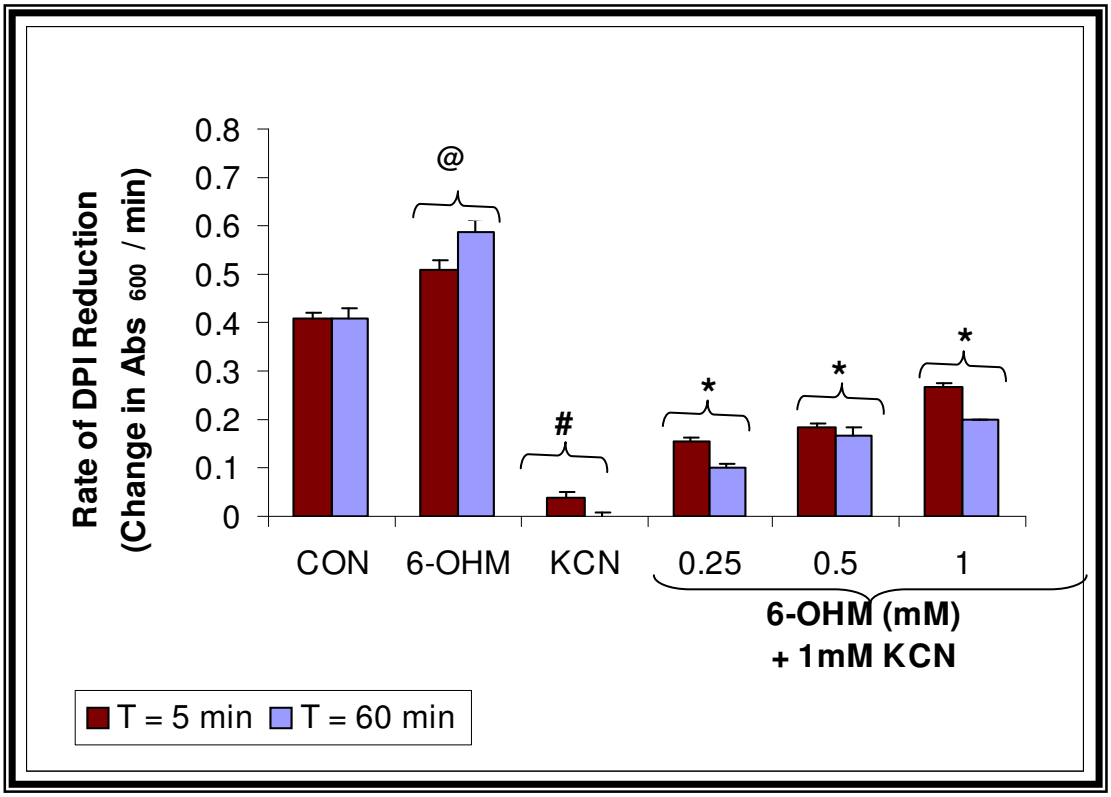

Figure 9.5: A comparison of the *in vitro* effect of 6-OHM alone or in combination with cyanide (1mM) on rat brain mitochondrial electron transport utilizing L-malate as a substrate, at time 5 and 60 minutes of incubation. Data represents the mean ± SEM (n = 5) $^{\#}p < 0.001$ vs control, at time 5 and 60 min; *$p < 0.05$ vs 1mM KCN alone, at times 5 and 60 min; and $^{@}p<0.05$ vs control, at times 5 and 60 min. (Student Newman-Keuls Multiple Range Test).

9.4. THE EFFECT 6-OHM ON COMPLEX I MITOCHONDRIAL RESPIRATORY CHAIN ACTIVITY.

9.4.1. INTRODUCTION

NADH-ubiquinone (coenzyme Q) oxidoreductase (EC 1.6.99.3), Complex I is a large and very complicated membrane bound multi-subunit enzyme complex that plays an important role in energy production by the mitochondrial OXPHOS system (Figure 9.6a). As evident in figure 9.6a, Complex I appears to have an 'L-shape' and this unique figure is conserved between eukaryote and prokaryote Complex I (Yano, 2002) Complex I is located at the entry point of the ETC and initiates electron transfer by oxidizing NADH and the electrons are transferred to the lipid-soluble electron carrier quinine (coenzyme Q) as an electron acceptor.

Complex I is known to produce ROS, as electrons leak from the intra-molecular electron transfer pathway of complex I (Yano, 2002). (Figure 9.7) and as discussed earlier the mitochondria are themselves targets of oxidative stress. Thus, if energetic impairment derives from the stochastic damage to the mitochondria, then it is important to select the mitochondrial activity that is most likely to be affected. Since seven out of 13 polypeptides encoded by mtDNA belong to Complex I, it is expected that this enzyme should be most affected by aging (Lenaz *et al*., 1997). A decreased activity of Complex I was indeed found in different tissues from aged animals and in bioptic specimens from old aged individuals (Cooper *et al*., 1992; Sugiyama *et al*., 1993; Castelluccio *et al*., 1994).

In addition a number of devastating neurodegenerative disorders has been found in connection with the defects of OXPHOS and complex I activity (Yano, 2002). Considering the fact that neurons demand a large amount of energy for their normal functions, decline of the energy production system considerably affects the ability of the nervous system to function properly. Melatonin was recently found by Martin *et al*., (2000a) and Absi *et al*., (2000) to prevent both oxidative mitochondrial damage induced

by toxin exposure and also increases the activities of the respiratory chain complexes I and IV in the rat liver and brain. In addition, melatonin was shown to increase complex I activity in the senescence-accelerated mouse (SAM) which commonly serves as a murine model of aging (Okatani *et al*., 2003). In the previous study, 6-OHM was shown to be effective in partially reversing the inhibition of the mitochondrial ETC activity induced by cyanide. Furthermore, this indoleamine was shown to increase the activity of the mitochondrial ETC above basal levels. It was further postulated in the above study that similar to melatonin, 6-OHM possibly could be increasing complex I activity. Thus, the present study investigates the effect of 6-OHM alone and in combination with rotenone (a complex I inhibitor, figure 9.3.) on rat whole brain mitochondrial complex I activity *in vivo*.

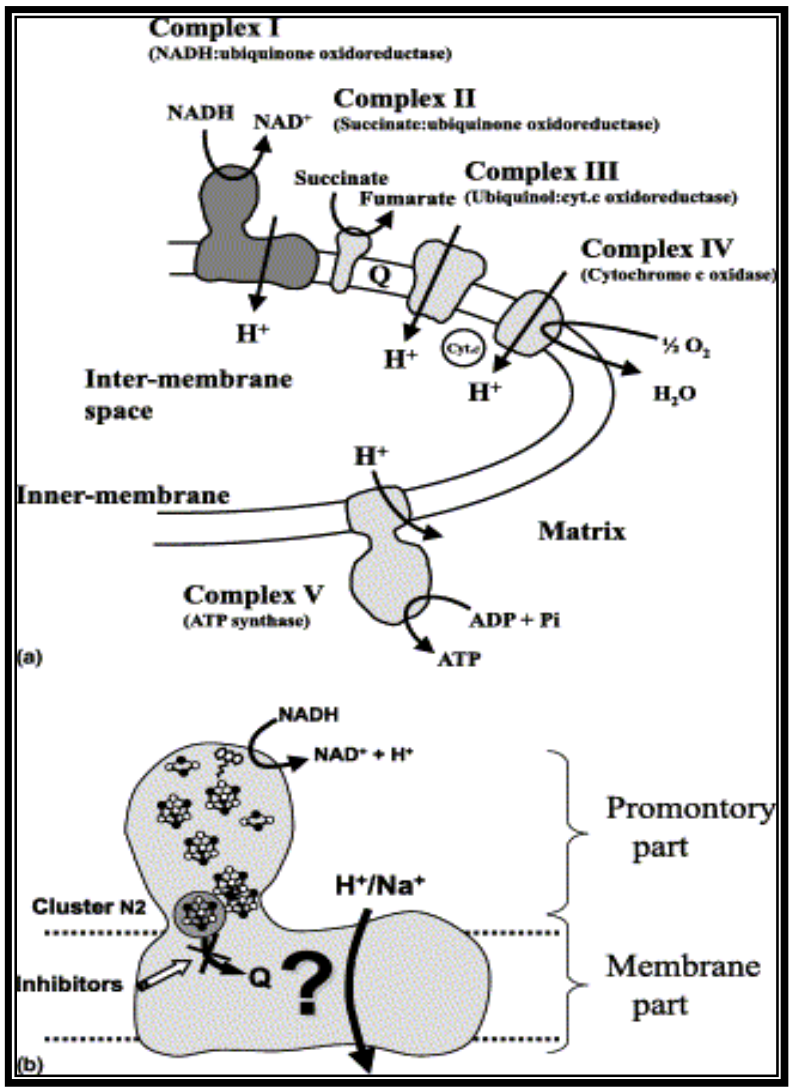

Figure 9.6: (a) Oxidative phosphorylation system of mitochondria. (b) L-shaped appearance of Complex I and its cofactor locations (Yano, 2002).

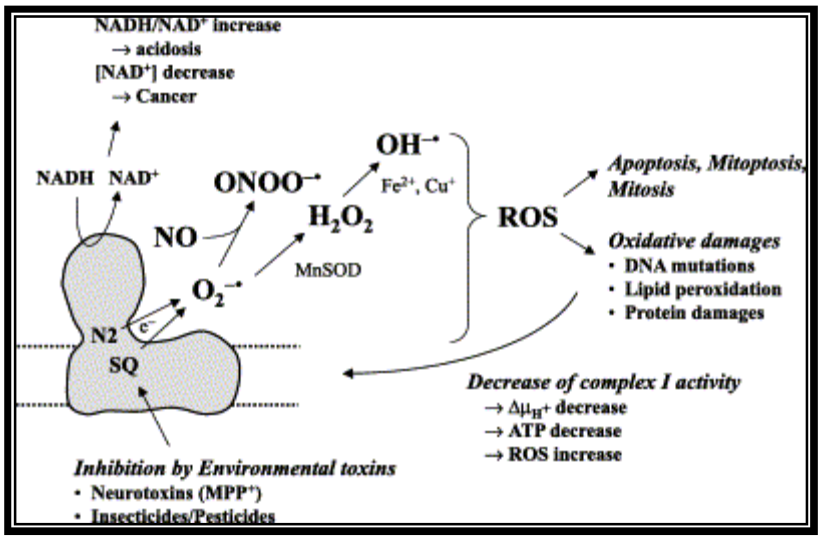

Figure 9.7: Generation of ROS by Complex I and its implicated consequences. $O_2^{\bullet-}$ is generated by a single electron reduction of O_2 by SQ or cluster N2. H_2O_2 and $^{\cdot}OH$ are formed by MnSOD and by Fenton's reaction in the presence of Fe or Cu, respectively. NO seems to react with $O_2^{\bullet-}$ or $SQ^{\bullet}$ species, generating a perinitrate species, $ONOO^{\bullet-}$ (Yano, 2002).

9.4.2. MATERIALS AND METHODS

9.4.2.1. Chemicals and Reagents

All chemicals were of the highest quality available and were purchased from commercial distributors. 6-OHM, potassium dihydrogen phosphate (KH_2PO_4), potassium hydroxide, Trisaminomethane (Tris), sucrose, Coenzyme Q_0, NADH, potassium cyanide (KCN), antimycin A and rotenone were purchased from Sigma Chemical Corporation, St. Louis, MO, U.S.A.

9.4.2.2. Dosing of animals

Male Wistar rats were used for this experiment and were housed according to the conditions described in appendix one. 6-OHM was dissolved in a minimum amount of absolute ethanol and diluted to 2.5 mg/mL with isotonic saline. The 6-OHM solution was prepared immediately prior to use and the unused portions were discarded at the end of each session. The concentration of ethanol in the final solution was 0.5%.

For the *in vivo* study, rats were divided into 4 groups of five animals each. Group I rats were injected with an equivalent amount of the vehicle only (2.5 mg/mL with isotonic saline and ethanol solution) for 24 hours while group II rats were treated the same way but for 5 days. Group III rats were treated with 6-OHM (10mg/kg/d, i.p.) alone for 24 hours while group IV rats were treated the same way for 5 days.

Rats were sacrificed 24 hours after the first injection of 6-OHM and on the fifth day, an hour after the last injection. Rats were sacrificed, their brains were rapidly excised as described in appendix two, chilled on crushed ice and thereafter these were rinsed in ice cold saline [0.9% (w/v) NaCl). The whole rat brains were homogenized and mitochondrial P_2 fraction was isolated as described below in section 9.4.2.3.

9.4.2.3. Isolation of Mitochondrial P_2 Fraction

Mitochondrial P_2 fraction was isolated according to a modification of the method described by Shults *et al*., 1995). Briefly, rat whole brain was homogenized in ice cold 0.32M sucrose dissolved in 10mM potassium phosphate buffer (pH 7.2), in a Teflon glass homogenizer with clearance of 0.1cm, to yield a 10% w/v homogenate. The homogenate is then centrifuged at 1 500 x g for 10min at 4^{o}C. Thereafter, the pellet that forms is discarded and the supernatant is spun at 10 000 x g for 30 min at 4^{o}C. At this stage, the supernatant that forms is discarded and the pellet is resuspended in the same volume of ice cold 50mM Tris in 10mM potassium phosphate buffer, pH 7.2 (1:1 v/v) and this is centrifuged at 10 000 x g for 30min at 4^{o}C. The supernatant is discarded and the pellet is resuspended in cold 10mM potassium phosphate buffer, pH 7.2. Finally the pellet is sonicated until it is uniformly dispersed. The mitochondrial P_2 fraction was used immediately or stored for 24 hours at -20^{o}C until use. Test samples revealed that storage of the mitochondrial P_2 fraction did not alter complex I activity levels compared to fresh samples. The submitochodrial particles were prepared by sonication. All procedures were carried out at 0-4^{o}C. Protein content was determined by the method of Lowry *et al*., (1951) as described in chapter nine, section 9.2.2.8.

9.4.2.4. Complex I (NADH:ubiquinone oxidoreductase) Assay

Complex I (reduced nicotinamide-adenine dinuleotide (NADH)-CoQ reductase) was determined using a modified protocol from Shults *et al*., (1995). The oxidation of NADH to NAD^+ by complex I was monitored by a fall in absorbance over a period of 2 min. DB, a synthetic water-soluble analogue of ubiquinone (coenzyme Q_o) (Estornell *et al*., 1993). For the *in vivo* study, the final 1ml assay mixture contained; an aliquot of the submitochondrial suspension sample (100µl), 850µl of assay buffer (10mM KH_2PO_4, pH 7.2, 5mM KCN, 2µg/ml Antimycin A, 5mM $MgCl_2$, 2.5 mg/ml of defatted BSA) and CoQ_O (54.9µM). The antimycin was added in order to inhibit complex II and III activity while KCN was used to inhibit complex IV activity (figure 9.3). After adding the buffer, mitochondrial fraction sample and CoQ_o the absorbance at 340nm was recorded for 0 and 2 min. The change in absorbance was noted and an incubation time with CoQ_o of 2 min was given. Thereafter, NADH (0.12mM) was added to the above assay mixture and the absorbance at 340nm was noted at time 0 and 2 min. This assay was repeated with rotenone at a final concentration of 2µM, allowing for the calculation of the rotenone-sensitive complex I rate. The change in absorbance without NADH was deducted from the change in absorbance with NADH (ε_{NADH} = 159nmole). The complex I activity was expressed as nmol of NADH oxidized/min/mg protein.

9.4.2.5. Statistical Analysis

The differences in the means were analyzed for statistical significance as described in section 9.2.2.7.

9.4.3. RESULTS

All data represents the mean ±SEM of three independent experiments assayed in duplicate of pooled rat brains from 5 rats each. The activity of complex I in the rat brain mitochondria from control treated rats were significantly lower than those treated 6-OHM, for the respective treatment period as evident in figure 9.8. There was no significant difference in mitochondrial complex I activity between the control rats treated

for 1 day and those treated for 5 days, indicating that the vehicle had no effect in increasing complex I activity over time. However, a significant increase in complex I activity is noted for rats treated with 6-OHM for 5 days in comparison to the rats treated with 6-OHM for 1 day. Thus, indicating that 6-OHM increases complex I activity with an increase in treatment period.

9.4.4. DISCUSSION

The results reported herein demonstrate that 6-OHM increases brain mitochondrial complex I activity above basal control values. An important observation in the present study is that a single, acutely administered pharmacological dose of 6-OHM stimulates mitochondrial complex I activity, similar to its parent compound melatonin (Martin *et al*., 2000a; Absi *et al*., 2000). The mechanisms underlying the beneficial actions of 6-OHM are unknown, but since complex I activity is elevated, 6-OHM ameliorative effects may relate to an increased efficiency of oxidative phosphorylation. Inhibition of complex I reportedly augments production of $O_2^{\bullet-}$. H_2O_2 and $^{\bullet}OH$ which trigger cell damage (Livera *et al*., 1997). Acuña-Castroviejo *et al*., (2001) noted that melatonin promotes OXPHOS and ATP synthesis after interacting with complexes I and IV both in normal mitochondria and in those depleted of ATP by cyanide. 6-OHM has been shown in the previous study to partially reverse cyanide inhibition of mitochondrial ETC activity which is probably due to the fact that 6-OHM promotes complex I activity. Thus, stimulation of the respiratory chain complex I activity by 6-OHM may be an indirect process by which 6-OHM limits molecular destruction of essential molecules by ROS.

One dire consequence of the ability of 6-OHM to increase complex I activity, is that complex I activity is known to result in the production of $O_2^{\bullet-}$ (Curtin *et al*., 2002) which is generated by the cycling of ubiquinol and $O_2^{\bullet-}$ which are highly toxic and can lead to cell damage as shown in figure 9.7. However, in chapter eight, 6-OHM was shown to a more potent $O_2^{\bullet-}$ scavenger than melatonin. In addition, Yoshida *et al*., (1993) showed that 6-OHM was able to significantly decrease the intensity of $O_2^{\bullet-}$. Thus, whilst this agent may increase complex I activity, it is also a direct scavenger of $O_2^{\bullet-}$.

A number of studies have measured the change in activity of ETC enzymes within cerebral tissue with age (Sharman and Bondy, 2001). Complex I activity is known to decline in aged animals and old individuals (Cooper *et al*., 1992; Sugiyama *et al*., 1993; Castelluccio *et al*., 1994; Lenaz *et al*., 1997). Genetic investigations of several patients with diseases associated with OXPHOS abnormality have revealed pathogenetic mutations of mtDNA and nDNA as potential causes of the symptoms with complex I deficiency (Yano, 2002). Furthermore, complex I deficiency has been documented to be intimately associated with the onset of several neurodegenerative disorders and the aging process (Yano, 2002; Ventura *et al*., 2002). Therefore, 6-OHM can serve to stimulate complex I activity and possibly prevent the age and neurodegerative disease-related decline. Further research is however warranted to determine the effects of 6-OHM against neurotoxin induced inhibition of complex I activity e.g. 1-methyl-4-phenyl-1, 2, 3, 6-tetrahydropyridine (MPTP) and rotenone which are known inhibitors of complex I activity and inducers of ROS production (Cleeter *et al*., 1992).

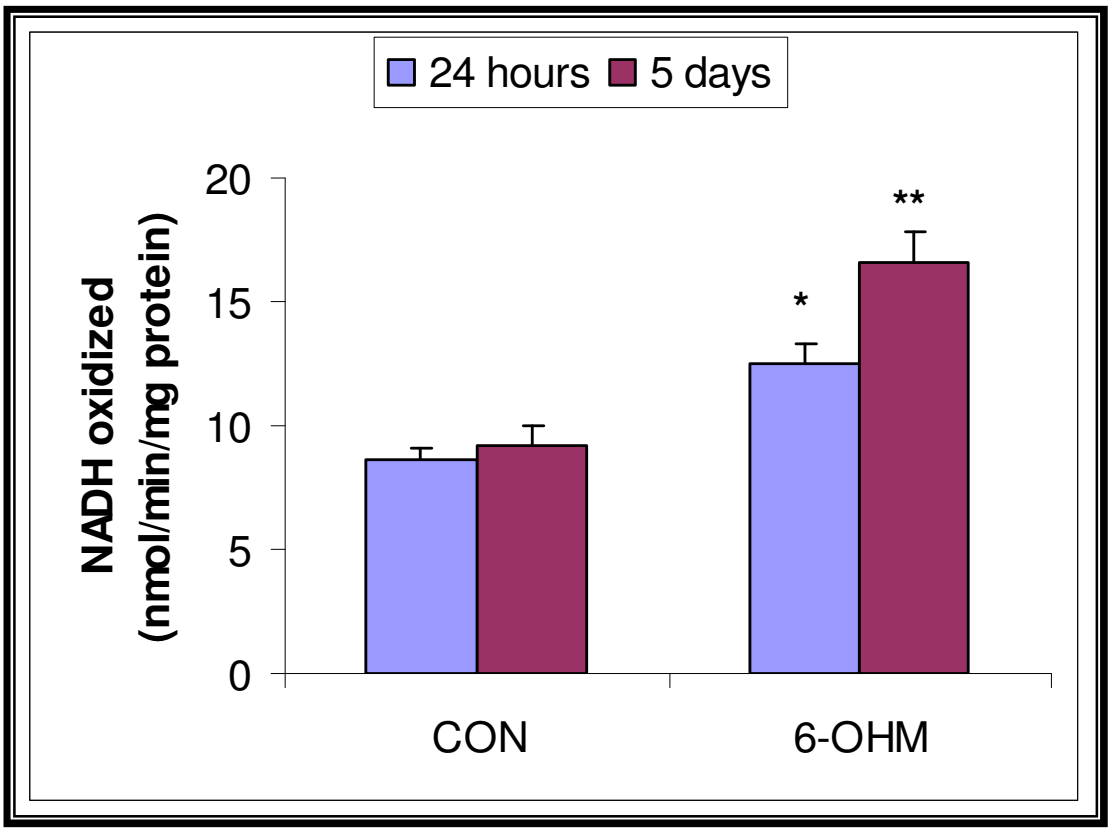

Figure 9.8: The effect of 6-OHM treatment on complex I activity in rat brain mitochondria *in vivo*. Data represents the mean ± SEM (n = 5) $^{*}p < 0.05$ vs control, 24 hours after treatment and $^{**}p < 0.01$ vs control, 5 days after treatment. (Student-Newman-Keuls Multiple Range Test).

9.5. CONCLUSION

The brain is acutely dependent on energy supplies for normal functioning. The mitochondrion is known to be the intracellular fount of the brain's energy supplies and subtle functional alterations in these essential energy dynamos may lead to insidious pathological changes within neurons (Beal *et al.*, 1993; Beal, 1995). Free radical reactions as well as mitochondrial inhibitors can decrease the activity of the ETC, which in turn leads to the obvious impairment in ATP production, and causes the diversion of electrons from their normal ETC recipients and further formation of damaging free radicals (Cassarino & Bennett, 1999).

The progressive decline of cell functions with age has been attributed to either a genetic program inborn in all organisms or to the accumulation of stochastic errors in somatic cells leading to loss of cell functions (Medvedev, 1990). Among the stochastic theories the mitochondrial theory of aging (Miquel *et al*., 1980; Linnane *et al*., 1989) proposes that mitochondria are involved both as producers and as targets of ROS whose aggressive behaviour can result in oxidative damage of all biological molecules. The consequence of this action at the level of the mitochondria will be the failure of enzymatic transport or receptor systems. A vicious cycle (Ozawa, 1995; Ozawa, 1997), has been proposed to occur; any damage to the respiratory chain may enhance ROS production (Papa & Skulachev, 1997) and induce a progressive and continuous perpetuation of damage through somatic mutations of mitochondrial DNA (mtDNA).

Melatonin is known to be an effective scavenger of ROS and RNS (Acuña-Castroviejo *et al*., 2001) as well as counteract cyanide-induced toxicity by blocking C-IV of the mitochondrial ETC. Both these properties of melatonin support its intra-mitochondrial role (Yamamoto and Tang, 1996a). Melatonin is also known to increase the activity of C-I and the C-IV enzymes of the mitochondrial ETC in a time dependent manner (Martin *et al*., 2000a). Figure 9.10, is a schematic diagram of the hypothesized involvement of melatonin in the mitochondrial ETC and in ATP synthesis (Acuña-Castroviejo *et al*., 2001). The results of the present study further support this action of melatonin. However, the indoleamine 6-OHM was also shown to increase the ETC activity of mitochondria and partially reverse cyanide induced inhibition of the ETC activity, implying that it

possibly acts in a similar way as to melatonin. However, melatonin was shown to have a more pronounced effect on mitochondrial ETC activity than 6-OHM. The above results demonstrate that melatonin and 6-OHM have the ability to stimulate the ETC and possibly ATP production in the mitochondria and this has relevance for these indoleamines as agents that could alter processes of aging as a progressive decline in ETC activity is known to occur (Cooper *et al.*, 1992).

Impaired ETC functioning in the brain leads to cell death via a decrease in ATP production or an increase in free radical or ROS production (Beal, 1995). The fact that the major neurodegenerative diseases are age-related may well be accounted for by the fact that the efficiency of the mitochondrial electron transport decreases with age, and the production of hydrogen peroxide and superoxide radicals increases with age (Beal, 1995; Hagen *et al.*, 1997). In chapter eight, both melatonin and 6-OHM have shown to potently scavenge superoxide anions. By increasing the basal level of respiration in the brain mitochondrial electron transport chain, and protecting against cyanide induced impairment of the same, both indoleamines could serve as a valuable defence system against mitochondria generated dysfunctions in the body.

Dietary supplementation with antioxidants capable of entering the brain mitochondria and reacting with the ROS generated there, may maintain the ETC enzyme activity level by preventing ROS-induced damage to these enzymes (Sharman & Bondy, 2001). To the extent that maintaining high ETC activity is critical for preventing age-related decline in brain function and the occurrence of neurodegenerative diseases, antioxidants may prevent or slow the development of these conditions. Melatonin and 6-OHM are both lipophilic compounds and can enter the circulatory system and cross the BBB and be transported into the mitochondrial inner membrane. These indoleamines have been shown in the present chapter to be antioxidants that are capable to scavenging $O_2^{\bullet-}$ formed in the mitochondria and increase mitochondrial ETC activity. However, in order to be effective, it may be necessary to begin supplementation at a fairly young age, before substantial loss of enzyme activity has occurred (Sharman & Bondy, 2001).

CHAPTER TEN

LIPID PEROXIDATION STUDIES

10.1. INTRODUCTION

The membranes of living cells are remarkable in molecular architecture, displaying a variety of different functions. The plasma membrane surrounds all animal cells, including neurons, and separates the cell interior from the extracellular environment, and also compartmentalizes the internal structures of the cell which is essential for cell functioning (Campbell, 1996). Membranes are not static boundaries that segregate regions but are dynamic systems responsible for among other things; function as permeable barriers for the selective transport of molecules into and out of the cell, are also responsible for the production of ATP and the binding of regulatory molecules such as hormones, growth factors and binding of neurotransmitters that mediate neurotransmission (Bohinski, 1987). Therefore, biological membranes function as important barriers, protecting cells from possible harmful compounds in the surrounding medium.

The structure of these membranes has been described by Singer and Nicholson as the 'Fluid Mosaic Model" (Matthews & Van Holde, 1991). According to the model, biological membranes are believed to be dynamic, irregular lipid mixtures of phospholipids and cholesterol, with globular proteins embedded within the membrane (Mathews & Van Holde, 1991). The membranes possess machinery for the transportation of molecules across them, and are also the site of metabolic activities such as electron transport. Membranes are also the site of cell-cell and cell-organelle interactions, such as hormone-cell interactions (Clark & Switzer, 1977).

Changes in membrane fluidity, by either physical or chemical disturbances, e.g. oxidative stress, cause changes to neuronal characteristics and the activities of the transport proteins and therefore alter membrane functions and this could ultimately lead to increased permeability to ions such as Ca^{2+} resulting in cell destruction.

This oxidative deterioration of polyunsaturated lipids i.e. lipids that contain more than two carbon-carbon double covalent bonds, is defined as lipid peroxidation (Halliwell & Gutteridge, 1989) and is extremely damaging as a result of the self-perpetuating chain reactions these cause (Fahn & Cohen, 1992). Lipid peroxidation, via the action of radical species, results in the attack of membrane lipids resulting in the destruction of the cell membrane and ultimately destroying the integrity of the cell (Southgate, 1999). If this occurs in neuronal membranes, neuronal characteristics are altered as well as the activities of transport proteins. Neuronal membranes are particularly vulnerable to oxidative attack by free radicals since the brain consumes a large portion of the total body oxygen, it is deficient in protective mechanisms such as glutathione, contains large amounts of polyunsaturated lipids, and some areas of the brain are rich in iron (Halliwell & Gutteridge, 1990). Free radical damage is further assisted by the presence of large amounts of iron (Braughler & Hall, 1989; Halliwell, 1992), required by the Fenton reaction (Fahn & Cohen, 1992). Since some free radical production is inevitable in cells, several enzymatic and non-enzymatic defence mechanisms have evolved to protect cells. Any alterations though, in either the defence mechanisms or the production of free radicals, could upset this balance and lead to neurotoxicity.

In chapter eight, cyanide and quinolinic acid (QA) were shown to increase $O_2^{\bullet-}$ production in rat brain tissue. The $O_2^{\bullet-}$ through the Haber-Weiss reaction is capable of producing the hydroxyl radical ($^{\bullet}OH$) in the presence of H_2O_2 (Halliwell & Gutteridge, 1985). Thus, this series of experiments were conducted to investigate the effect of cyanide, QA and iron (II) (Fe^{2+}) on lipid peroxidation levels. A comparative study was also conducted to determine the use of melatonin and 6-OHM as free radical scavengers.

The measurement of putative elevated end products of lipid peroxidation in animal material is probably the evidence most frequently quoted in support of free radical-induced tissue damage (Gutteridge & Halliwell, 1990). The thiobarbituric acid (TBA) test is most widely used as an indicator of hydroxyl radical generation (Gutteridge & Halliwell, 1990). The TBA test was introduced to biological systems for the first time by Kohn & Liversedge in 1944 (Kohn & Liversedge., 1944) as a measurement for lipid rancidity in the food industry (Gutteridge *et al*., 1983). This test is now the most widely employed technique used in the determination of peroxidation in biological materials

(Yamamoto *et al.*, 1990). Malondialdehyde (MDA) is a degraded lipid product from cell membranes, and is taken as a reliable indicator of oxidative stress (Reiter *et al.*, 1995). The foundation of this test is based on the reaction of one molecule of MDA with two molecules of TBA to yield a pink coloured chromagen (figure 10.1.). However, the simplistic methods described by Gutteridge and Halliwell (1990) and Southgate and Daya (1999) is subject to several errors (Anoopkumar-Dukie *et al.*, 2001).

For this above stated reason, a validated HPLC method which is a simple, accurate and cost effective method that has been designed for the determination of lipid peroxidation in biological tissue samples (Anoopkumar-Dukie *et al.*, 2001) was used to detect MDA-TBA complex. This method involves a modification of the method of Sagar *et al.*, (1992) and Draper and Hadley (1990). This assay method isolates the MDA-TBA complex using solid phase extraction columns which should be a standard part of the TBA method for MDA determination (Draper & Hadley, 1990). Materials of animal origin usually contain large amounts of protein, to which MDA may be bound (Draper & Hadley, 1990). In addition, the methanol evaporation procedure is carried out under nitrogen to prevent further oxidation of the complex. The MDA-TBA complex has an absorption maximum at 532nm. Materials of animal origin usually contain large amounts of protein, to which MDA may be bound (Draper & Hadley, 1990). It is therefore imperative to release the protein-bound MDA, which is achieved by hot acid hydrolysis (pH of 2-3) using TCA. This allows for the formation of the complex (MDA-TBA) and the release of protein bound MDA. Butylated hydroxytoluene (BHT) in methanol is added prior to TCA precipitation to ensure that no lipid oxidation occurs during the assay and interferes with the results obtained.

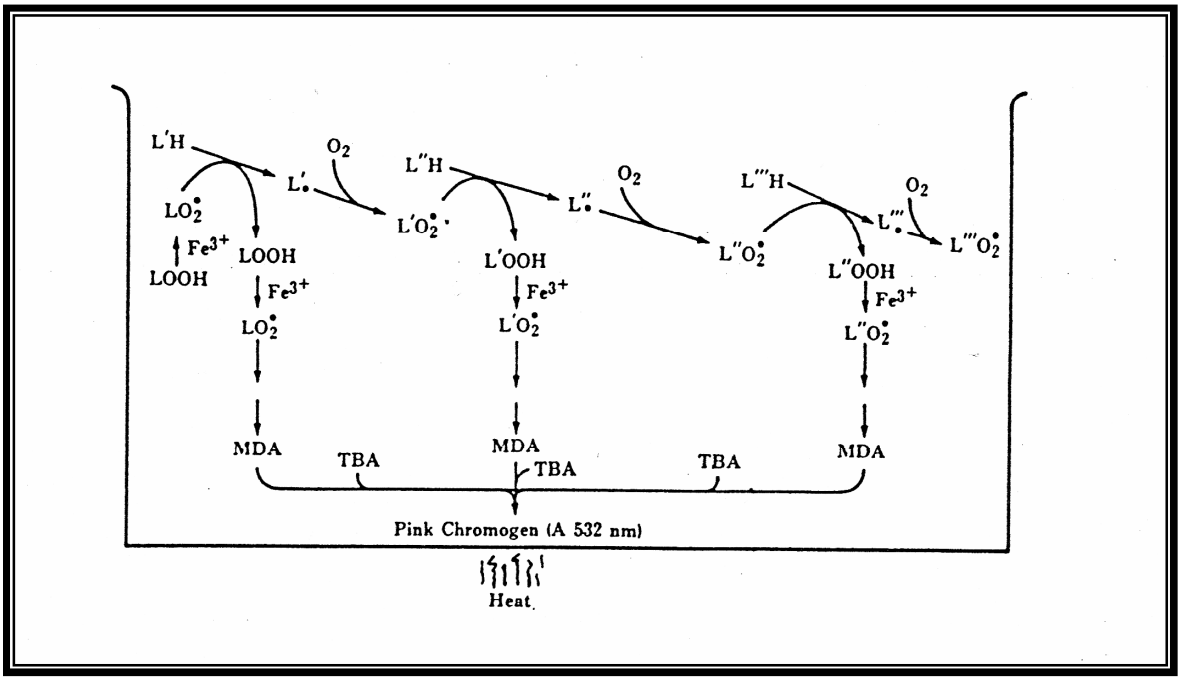

Figure 10.1: The formation of MDA by lipid peroxidation during incubation and to a much greater extent during the acid-heating stage (Gutteridge, 1987).

10.2. EFFECT OF CYANIDE, QA, AND IRON (II) ON LIPID PEROXIDATION IN RAT BRAIN HOMOGENATE *IN VITRO.*

10.2.1. INTRODUCTION

Since the brain is particularly susceptible to oxidative attack by free radicals, lipid peroxidation is able to cause extensive damage and is known to play a major role in the deterioration of the brain and spinal cord that occurs after traumatic, excitotoxic or ischemic injury. Such injuries to the brain result in more extensive tissue damage than do equivalent insults in other tissues and free radical reactions have been implicated in such damage (Halliwell & Gutteridge, 1990). The brain has been demonstrated to be the primary target organ of cyanide, QA and iron toxicity (Gunasekar *et al*., 1996; Stone, 1993; Fahn & Cohen, 1992; Minotti & Aust, 1987).

Cyanide-induced neurotoxicity is mainly attributed to its production of cellular anoxia in the brain (Yamamoto & Tang, 1996a). Due to the number of antioxidant enzymes inhibited by cyanide; it is also believed that oxidative stress plays an important role in cyanide-induced neurotoxicity (Ardelt *et al*., 1989). QA-induced neurotoxicity results from the activation of ionic channels through which sodium, potassium and calcium flood into the cell (Stone, 1993). The increased intracellular calcium sets off a cascade of events that culminate in the generation of free radicals.

Free iron or its chelates, are involved in a number of radical reactions at a number of different levels. Fe^{2+} is also oxidized in the presence of hydrogen peroxide (H_2O_2) to form $^{\bullet}OH$ or ferryl ion (Fe^{3+}-OH) according to the Fenton reaction (Bielski, 1991). The role of iron in free radical and lipid peroxidation reactions has been studied extensively and its role in this regard is widely accepted (Fahn & Cohen, 1992; Minotti & Aust, 1987). Both ferric (Fe^{3+}) and ferrous ions (Fe^{2+}) or their chelates can participate in the formation of oxygen radicals and may either initiate or take part in lipid peroxidation (Gutteridge *et al*., 1979). Formation of $^{\bullet}OH$ or decomposition of lipid hydroperoxides, both catalysed by iron has been implicated in lipid peroxidation (Braughler *et al*., 1987;

Sreejayen & Rao, 1993). The crucial role of iron in initiating and propagating lipid peroxidation was recently reviewed by Halliwell and Gutteridge (1990).

The aim of this study was to determine the effect of three neurotoxins, cyanide, QA and Fe^{2+}, on lipid peroxidation in rat brain homogenate *in vitro*. These neurotoxins have been previously reported to increase lipid peroxidation levels in brain homogenate (Southgate, 1999; Stipêk *et al*., 1997; Daya *et al*., 2000; Anoopkumar-Dukie *et al*., 2003).

10.2.2. MATERIALS AND METHODS

10.2.2.1. Chemicals and Reagents

All reagents used were of analytical grade. Cyanide, QA (2, 3-pyridinedicarboxylic acid), 2-thiobarbituric acid (98%) (TBA), 1, 1, 3, 3-tetramethoxypropane (98%) and butylated hydroxytoluene (BHT) were purchased from Sigma Chemical Corporation, St. Louis, MO, U.S.A. Methanol (HPLC grade), anhydrous ferrous sulphate were purchased from BDH Laboratory Supplies, Poole, England. Trichloroacetic acid (TCA), resorcinol, ascorbic acid, and ethylenediaminetetraacetic acid (EDTA) were obtained from Saarchem, Johannesburg, South Africa. IsoluteJ C_{18} solid phase extraction (SPE) columns were obtained from International Sorbent Technology, Mid Glamorgan, and UK. HPLC grade water was prepared by reverse osmosis and purification through a Milli-Q system, Millipore, Bedford, MA, USA.

10.2.2.2. Animals

Adult male rats of the Wistar strain, weighing between 200-250g were used in this experiment. The rats were randomly assembled into groups of five, and housed in separate cages, in a controlled environment as described in appendix one. All protocols for the experiments were approved by the Rhodes University Animal Ethics Committee.

10.2.2.3. Sample Preparation

BHT (0.5 mg/mL) was dissolved in methanol; TCA (15%) and TBA (0.33%) were prepared in Milli-Q water. All reagents were made up under de-aerated conditions.

Stock solutions were prepared so that on addition of 100µL of the toxin, the stock solution would be diluted to the correct incubation concentration. KCN, QA and Fe^{2+} were tested at the following concentrations; 0, 0.25, 0.5, 1, 1.5mM.

10.2.2.4. Brain Removal

Rats were sacrificed and their brains removed as described in appendix two.

10.2.2.5. Tissue Preparation

Rat brain homogenate is a useful model for determining the efficacy of agents to reduce or potentiate lipid peroxidation (Maharaj *et al*., 2002). Each brain was homogenized according to the method described in chapter eight, section 8.2.2.6. The homogenate was either used immediately or frozen in liquid nitrogen and stored at -70°C until use. All samples were used within 7 days of homogenate preparation. Test samples revealed that storage of the homogenate did not alter the lipid peroxidation levels compared to fresh brains.

10.2.2.6. Instrumentation

Samples were analyzed on a modular, isocratic HPLC system. The chromatographic system consisted of a Spectraphysics Iso Chrom LC Pump, a Linear UVIS 200 Detector, and a Perkin Elmer 561 Recorder. Samples were introduced into the system using a Rheodyne Model 7125 fixed loop injector that had been fitted with a 20µL loop. An N-EVAP analytical evaporator was used to evaporate the methanol using nitrogen.

10.2.2.7. Chromatographic Conditions

Analytical separation was achieved using a C_{18} (Waters Spherisorb, 5µm, 250 x 4.6 mm i.d.) column. Following injection, samples were filtered using an in-line 2µm pre-column filter (Upchurch Scientific). The mobile phase composition for the analysis was 14% methanol in Milli-Q water and was degassed using a 0.45µm membrane filter before use. The mobile phase flow rate was 1.2ml/min and the chart speed on the recorder was 5mm/min. The detector sensitivity was set at 0.05 AUFS and the TBA-MDA complex was detected at 532nm. The analytical procedure was validated by assessment of linearity of calibration (5-25 nmol/L), repeatability, sensitivity, precision, LOQ and LOD (Anoopkumar-Dukie *et al*., 2001). Resorcinol (0.05 mg/ml) was used as the external standard. This HPLC analytical procedure was validated and optimized to suit our laboratory requirements before use.

10.2.2.8. Preparation of the Standard Curve

1, 1, 3, 3-tetramethoxypropane was used as a standard. A series of reaction tubes each containing appropriate aliquots of water and standard solution were prepared with Milli-Q water to a final volume of 1ml. A calibration curve was generated by measuring the absorbance at 5nmoles/ml intervals. The procedure described in section 10.2.2.9 was followed. The detection λ was set at 532nm. The ratio of the peak height of MDA-TBA to the peak height of resorcinol (external standard) was plotted against the concentration of MDA in the complex injected (appendix five).

10.2.2.9. Lipid Peroxidation Assay

A modification of the thiobarbituric acid (TBA) assay described by Anoopkumar-Dukie *et al*., (2001) was used to measure the level of MDA in the rat brain homogenates. This compound is the final product of lipid peroxidation chain reactions and is used as an estimation of the degree of lipid breakdown.

Briefly, rat brain homogenate (1mL) containing varying concentrations of KCN or QA were incubated in an oscillating water bath for 1hr at 37^{o}C.

For the iron-induced lipid peroxidation experiments, 1mL of the homogenate containing varying concentrations of Fe^{2+} together with 100µM ascorbate, 100µM EDTA, and H_2O_2 was incubated at 37°C for 1hr. All solutions were prepared in deaerated water to prevent the rapid oxidation of Fe^{2+} to Fe^{3+}.

Termination of the incubation period was followed by the addition of 0.5mL of BHT (0.5 mg/mL in methanol) and 1mL of TCA (15% in water) to the mixture. The tubes were sealed and heated for 15 min in a boiling-water bath to release protein-bound malondialdehyde (MDA). To avoid adsorption of MDA onto insoluble protein, the samples were cooled and centrifugated at 2000 x g for 15 min. Following centrifugation, 2mL of the protein-free supernatant was removed from each tube and 0.5mL thiobarbituric acid (0.33% in water) was added to this fraction. The tubes were sealed and incubated in a boiling water bath at acidic pH for 30 min. This step was not necessary when generating the calibration curve. The effect of incubation time and temperature were determined in order to optimize the assay.

After cooling, TBA-MDA was separated from other possible thiobarbituric acid-reactive substance (TBA-RS) using an IsoluteJ C_{18} SPE columns that was pre-washed with 2mL methanol followed by 2mL distilled water. The sample (1mL) was loaded onto the column, which was subsequently washed with 2mL distilled water. The TBA-MDA complex was eluted with 1mL methanol. The methanol was then evaporated using an N-EVAP analytical evaporator at 60°C under a gentle stream of nitrogen. This is necessary to prevent further oxidation of the complex. The pink residue was dissolved in distilled water (0.5mL) containing 0.05 mg/mL of resorcinol. These samples were analyzed by the HPLC method described in section 10.2.2.7. The MDA levels were obtained from a calibration curve as described in section 10.2.2.8. The ratio of the peak height of TBA-MDA to the peak height of resorcinol was plotted against the concentration of MDA in the complex injected and the final results were expressed as nmol MDA/mg tissue.

10.2.2.10. Statistical Analysis

The results were analyzed using a one-way analysis of variance (ANOVA). If the F values were significant, the Student's Newmans-Keuls Multiple Range test was used to compare the treated and control groups. The level of significance was accepted at $p<0.05$ (Zar, 1974).

10.2.3. RESULTS

Range finding tests were conducted in order to optimize the assay and the effect of incubation time and temperature on lipid peroxidation was determined. As shown in figure 10.2 and 10.3, the optimum incubation time and temperature was 60 min and 37^{o}C, respectively.

The retention time for the TBA-MDA complex and the external standard (resorcinol) was approximately 2.4 and 6.45 min, respectively. As shown in figure 10.4, 10.5 and 10.6, exposure of rat brain homogenate to increasing concentrations of KCN, QA or Fe^{2+}, resulted in a concentration-dependent increase in lipid peroxidation levels which was found to be significantly higher in comparison to the control value (no toxin added).

As shown in figures 10.4 and 10.5, it is evident that co-incubation of rat brain homogenate with increasing concentrations of cyanide and quinolinate caused significant increases in MDA level in the brain homogenate in comparison to the control value, respectively. No significant differences were noted between the MDA levels generated by the 1mM KCN or 1mM QA and that of the 1.5mM KCN or 1.5mM QA. Thus the 1mM KCN and 1mM QA were chosen for subsequent studies since they yielded the highest amount of lipid peroxidation products. Furthermore, it is evident from figure 10.6, that 5mM Fe^{2+} generated the greatest amount of lipid peroxidation products resulting in this concentration being chosen for subsequent studies.

10.2.4. DISCUSSION

Free radicals have been postulated to be important mediators of tissue injury in several neurodegenerative models (Bautista & Spitzer, 1990; Shuter *et al*., 1990; Yoshikawa *et al*., 1994). The brain is particularly susceptible to free radical damage because of its high utilization of oxygen, its relatively low concentration of antioxidative enzymes and free radical scavengers (Reiter, 1995a). Free radical generation in the brain is further assisted by the presence of large amounts of iron (Daya, 1999; Halliwell, 1992; Braughler & Hall, 1989) required by the Fenton reaction (Halliwell, 1992; Braughler & Hall, 1989; Fahn & Cohen, 1992). Radical damage has long been suspected to play a role in the progression of various neurological conditions (Kedziora & Bartosz, 1988; Götz *et al*., 1994; Simonian & Coyle, 1996; Pappolla *et al*., 1997; Schapira, 1999).

Johnson *et al*., (1987) proposed that increased intracellular calcium after cyanide treatment generates reactive oxygen species leading to peroxidation of lipids and subsequent neuronal damage. The result of the present study is consistent with this finding. It has also been proposed that nitric oxide, a promoter of $^{\bullet}OH$ formation, is a mediator of convulsions associated with cyanide toxicity (Yamamoto & Tang, 1996a). Studies have also shown the activation of NMDA receptors during cyanide toxicity (Gunasekar *et al*., 1996). Cyanide induced seizures are inhibited by MK-801, an agonist of the NMDA receptor (Yamamoto & Tang, 1996b). MK-801 is also known to inhibit cyanide-induced cerebellar granule cell death (Gunasekar *et al*, 1996).

QA is an established agonist of the glutamate receptor and previous research has shown that among a number of glutamate receptor agonists including QA, kainic acid and NMDA, only QA potentially induces lipid peroxidation in rat brain homogenate (Rios & Santamaria, 1991). The results of the present study are consistent with this finding and show that QA causes a significant induction of lipid peroxidation products in rat brain homogenate *in vitro* in a concentration dependent manner. Since QA is not readily metabolized in the synaptic cleft, it stimulates and activates the NMDA/ion channel complex for prolonged periods, followed by cytosolic accumulation of free Ca^{2+} (Daniel, 1991), which is believed to promote lipid peroxidation (Gutteridge, 1977; Babizhayev, 1988) and to induce delayed nerve cell death (Keihoff *et al*., 1990). However, in rat brain

homogenate the mechanism by which QA induces oxidative stress is not well understood. Stipêk *et al*., (1997) showed that QA is only able to stimulate lipid peroxidation in the presence of iron while in the presence of an iron chelator, QA does not induce lipid peroxidation. The authors further demonstrated that QA is able to chelate Fe^{2+} ions (but not Fe^{3+} ions) to form a complex, and it is this complex that stimulates lipid peroxidation. The results suggest that *in vitro*, QA does not have a direct peroxidative effect, but that it modulates lipid peroxidation via its interaction with Fe^{2+}. Tissue disruption by homogenization tends to undergo lipid peroxidation more easily than healthy, intact tissue (Halliwell & Gutteridge, 1989). This explains the formation of MDA obtained in the absence of QA. Reasons for this increased peroxidisability of damaged tissue include inactivation or dilution of some antioxidants as well as the release of metal ions (especially iron) from intracellular storage sites (Halliwell & Gutteridge, 1989). QA has been reported to increase lipid peroxidation in brain homogenate and that this is dependent on the presence of iron and in particular, Fe(II) (Stipêk, *et al*., 1997). These authors showed that QA complexes with Fe(II) but not Fe(III).

The role of iron in free radical and lipid peroxidation reactions has been studied extensively and its role in this regard is widely accepted (Braughler & Hall, 1989; Fahn & Cohen, 1992). Under physiological conditions, iron is only slightly soluble, tending to form precipitates with anions such as the hydroxyl radical. However, a variety of agents greatly increase the solubility of iron. For example, the addition of ethylenediaminetetraacetate (EDTA) to a free radical generating system in the presence of iron, markedly potentiates cytotoxicity, hydroxyl radical formation and, consequently, lipid peroxidation (Fahn & Cohen, 1992). Kaptanoglu *et al*., (2003) demonstrated that incubation of brain tissue with ferrous iron, ascorbate and H_2O_2 resulted in increased lipid peroxidation *in vitro* which further supports the above findings. In the above system, $^{\bullet}OH$ radicals were generated and the iron is oxidized to its ferric form. In the presence of ascorbate, a reducing agent, ferrous iron is recovered from its oxidized form and $^{\bullet}OH$ radical generation persists.

Cyanide, QA and Iron (II) are thus known neurotoxins that have the potential to induce neurotoxicity by causing oxidative damage, which results in extensive peroxidation of the lipid layers of neuronal membranes (Daya *et al*., 2000; Cabrera *et al*., 2000; Lin & Ho,

2000). In chapter eight, cyanide was shown to cause a concentration dependant increase in $O_2^{\bullet-}$ generation in rat brain homogenate *in vitro* while QA generated $O_2^{\bullet-}$ *in vivo* in rat hippocampus. Since $O_2^{\bullet-}$ give rise to the highly toxic $^{\bullet}OH$ via the Haber-Weiss reaction which is known to cause peroxidation of lipid layers.

The results of the present study supports the findings of the above mentioned studies and imply that the neurotoxins cyanide, QA and iron (II) are capable of causing a concentration dependent increase in lipid peroxidation in rat brain homogenate *in vitro*. The concentrations of the neurotoxins in this study were suprapharmacological and above the concentration that is normally present *in vivo,* in aging and in neurodegenerative diseases. However in order to generate sufficient free radicals and peroxidation of the lipids *in vitro* these concentrations were chosen. Thus, the results of the study imply that cyanide, QA and Fe^{2+} ions act as neurotoxins and are capable of potentiating lipid peroxidation in rat brain homogenate *in vitro*.

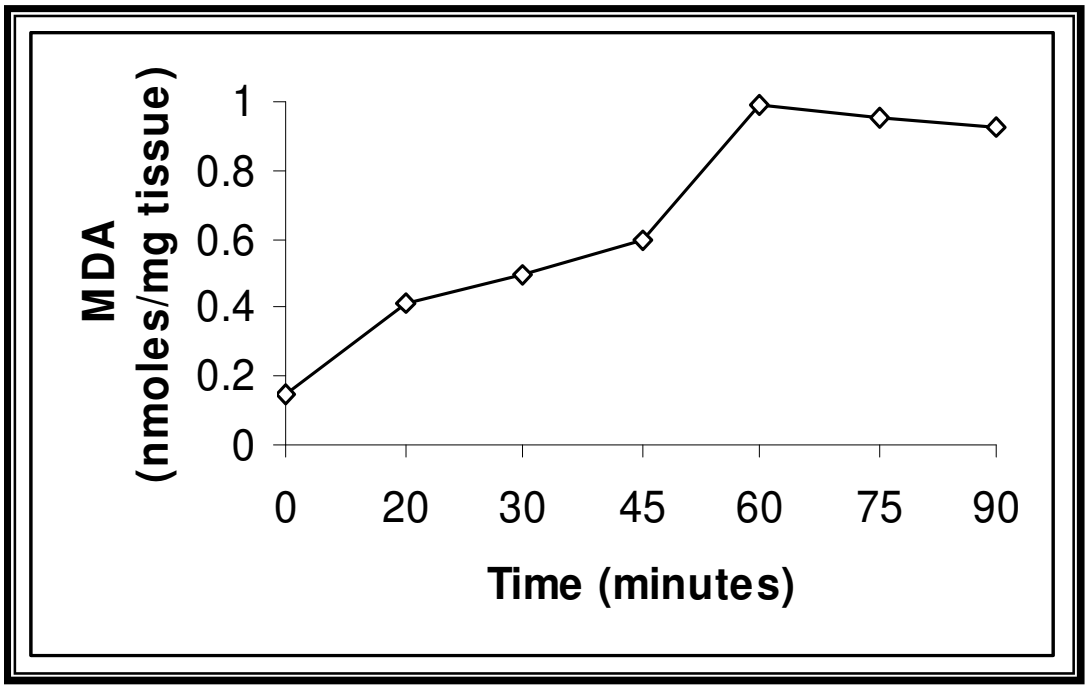

Figure 10.2: The effect of incubation time on lipid peroxidation. Each point represents the mean of triplicate determinations.

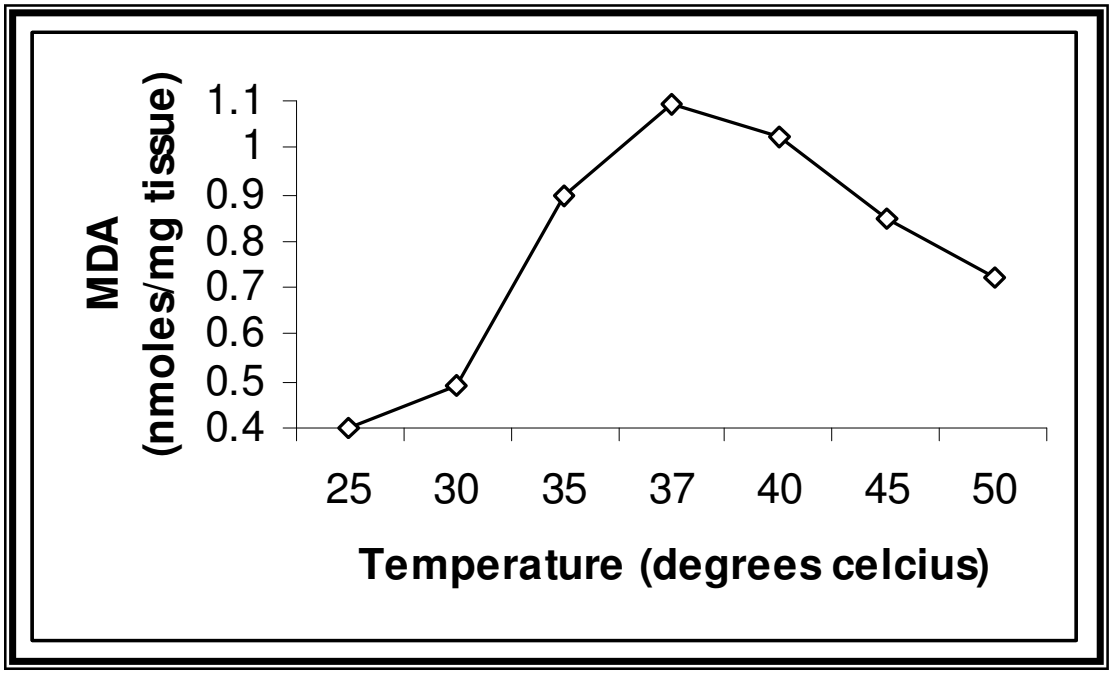

Figure 10.3: The effect of incubation temperature on lipid peroxidation. Each point represents the mean of triplicate determinations.

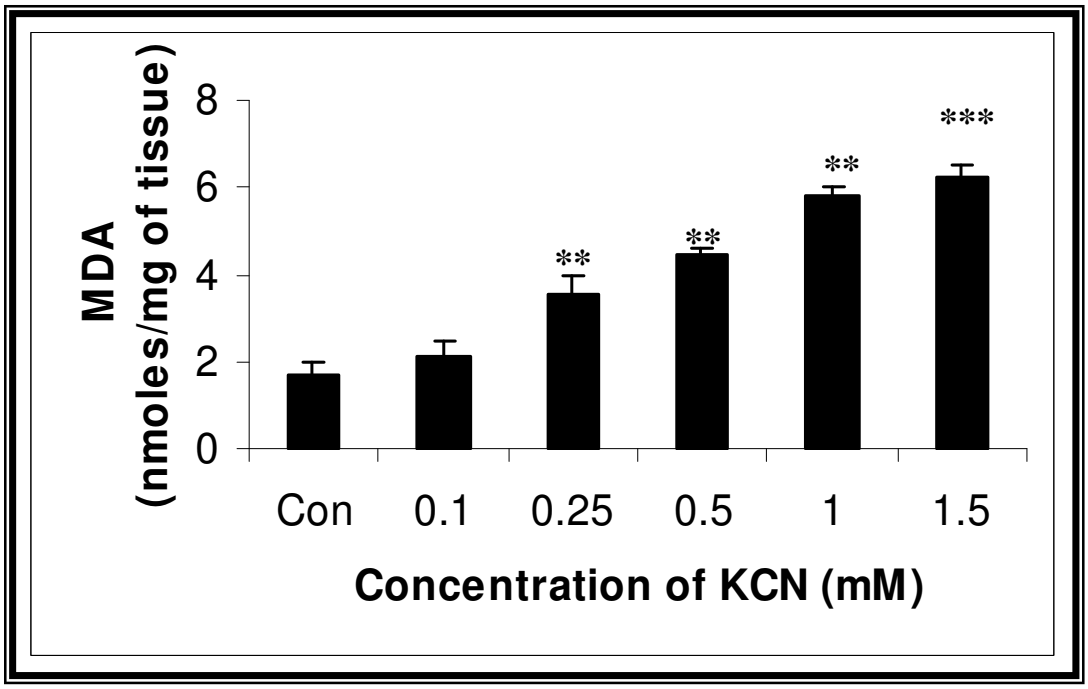

Figure 10.4: Concentration-dependent effect of KCN on lipid peroxidation generation in whole rat brain homogenates *in vitro*. Each bar represents the mean ± SEM; n=5.(**p<0.001 ; ***p<0.001 in comparison to control. Student-Newman-Keuls Multiple Range Test.

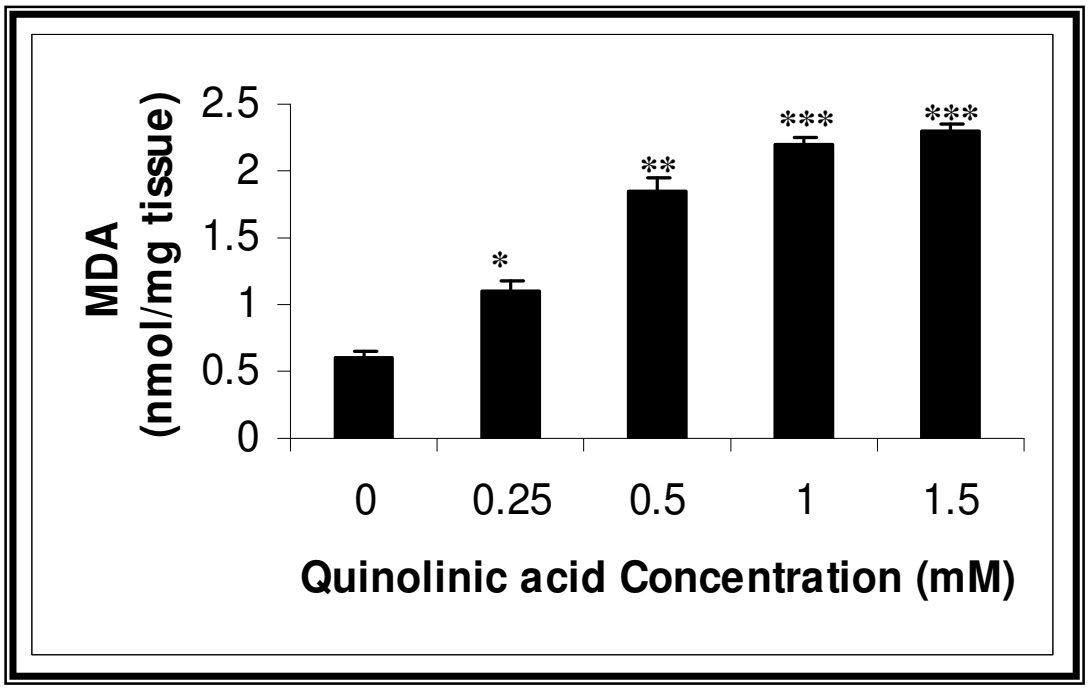

Figure 10.5: Concentration-dependent effect of QA on lipid peroxidation generation in whole rat brain homogenates *in vitro*. Each bar represents the mean ± SEM; n=5.(*p<0.05, **p<0.01 ; ***p<0.001 in comparison to control. Student-Newman-Keuls Multiple Range Test.

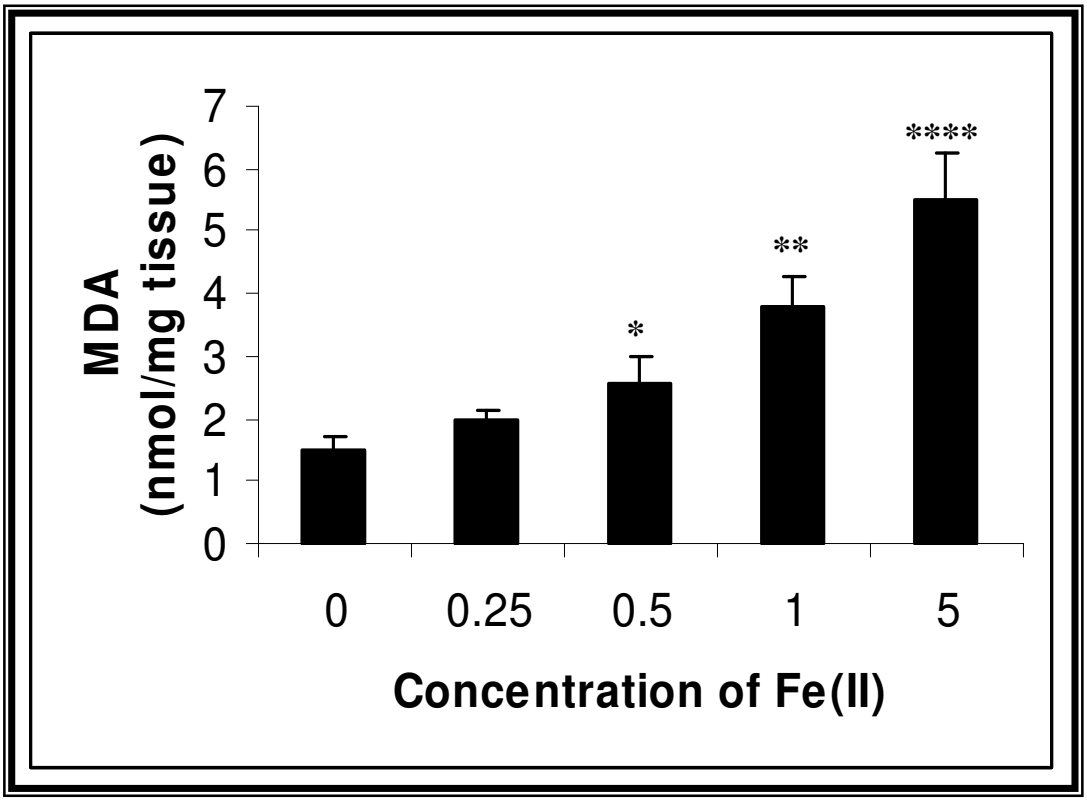

Figure 10.6: Concentration-dependent effect of Fe (II) on lipid peroxidation generation in whole rat brain homogenates *in vitro*. Each bar represents the mean $\pm$ SEM; n=5.(*p<0.05, **p<0.01 ; ****p<0.0001 in comparison to control. Student-Newman-Keuls Multiple Range Test.

10.3. THE EFFECT OF UV-IRRADIATED SOLUTION OF MELATONIN ON QA-INDUCED LIPID PEROXIDATION IN RAT BRAIN HOMOGENATE *IN VITRO*.

10.3.1. INTRODUCTION

Photochemical reactions with UV light result in the formation of ROS including $O_2^{\bullet-}$, and the highly toxic $^{\bullet}OH$ (Sasaki *et al*., 2000). Of the free radicals produced in the cell, the $^{\bullet}OH$ radical is the most destructive followed by the $O_2^{\bullet-}$ (Maharaj *et al*., 2002). These radicals can cause tissue damage by reacting with biomolecules such as lipids and proteins (Dreher *et al*., 1999) and result in the formation of lipid peroxides. These in turn elicit a chain reaction, causing formation of further lipid peroxides. The cell membrane is thus damaged as a consequence of this phenomenon. Melatonin, being an electron rich molecule, interacts with free radicals via an additive reaction to form several stable end products and has been shown to reduce UV-induced free radical production and lipid peroxidation (Bangha *et al*., 1996; Bangha *et al*., 1997).

In chapter six, concerns about the use of melatonin in topical formations were raised because of the rapid inactivation of melatonin by UV irradiation. However, in chapter eight, the results of section 8.3 demonstrate that the degraded solution of melatonin is able to produce equipotent protection against reducing $O_2^{\bullet-}$ as melatonin; despite the absence of melatonin. Thus the aim of this study was to determine whether the irradiated melatonin solution offers protection against lipid peroxidation induced by the neurotoxin, QA, which has been shown in the previous study to be a potent inducer of lipid peroxidation in rat brain homogenate. Rat brain tissue is widely used as a rich source of membrane lipids to assess general lipid peroxidation; therefore this tissue was used to assess the protection offered by the UV-inactivated melatonin solution. This would provide an indication of whether the photodegradants of melatonin are able to reduce QA-induced peroxidation of rat brain tissue.

10.3.2. MATERIALS AND METHODS

10.3.2.1. Chemicals and Reagents

All reagents used were of analytical grade and of the highest quality available. MEL was purchased from Sigma Chemical Corporation, St. Louis, MO, U.S.A.

10.3.2.2. Sample Preparation

Samples for the lipid peroxidation assay were prepared according to the method described in section 9.2.2.3.

A 0.1mg/ml solution of MEL was prepared by dissolving it in absolute ethanol, and subsequently diluting it with Milli-Q water so that the final ethanol concentration in the brain homogenate was less than 0.5%.

10.3.2.3. Animals and Tissue Preparation

Rats of the Wistar strain were used in this experiment and randomly assembled into groups of five, and housed in separate cages, in a controlled environment as described in appendix one. Rats were sacrificed and the brains removed as described in appendix two. Rat brain homogenate was prepared according to the method described in section 10.2.2.5.

10.3.2.4. UV Irradiation of Melatonin

Melatonin (0.1 mg/ml) was placed in the immersion-well photoreactor and irradiated continuously with a 400 W high pressure mercury lamp, emitting over the UV-VIS range (300-575nm) with maximum irradiance in the UVA at 365 and 565nm in the visible region, for two hours, whilst bubbling air through the solution at ambient temperature (figure 6.1). Aliquots of 5 ml were removed periodically and were assayed in order to determine if the irradiated solution offers protection against QA-induced lipid

peroxidation and possesses free radical scavenging properties. The selected times for UV irradiation were predetermined.

10.3.2.5. Lipid Peroxidation Assay

The instrumentation and chromatographic condition are described in sections 10.2.2.6 and 10.2.2.7, respectively. A calibration curve was constructed according to the method described in section 10.2.2.8.

Lipid peroxidation was determined using a modified method of Anoopkumar-Dukie *et al*., (2001) as described in section 10.2.2.9. Briefly, homogenate (1ml) containing 1mM QA alone or in combination with melatonin solution irradiated at different time intervals (0, 10, 20, 30, 40, 60 min) were incubated in an oscillating water bath for 1hr at 37^{o}C. These time intervals were chosen as after 60 min of irradiation the amount of melatonin in solution was zero as shown in chapter six. The procedure described in section 10.2.2.9 was then followed. Final results were expressed as nmoles MDA/mg tissue. All results were analyzed for statistical significance using the method described in section 10.2.2.10.

10.3.3. RESULTS

It is evident from figure 10.7, that the exposure of rat brain homogenate to 1mM QA causes a rapid and significant rise in lipid peroxidation product in comparison to the control, which contained no QA or irradiated melatonin solution. It is also evident that unirradiated melatonin (0.1mg/ml) at zero time significantly reduced the 1mM QA-induced increase lipid peroxidation by ± 50%.

Co-treatment of the rat brain homogenate with 1mM QA together with the irradiated melatonin solution at different time intervals (figure 10.7) resulted in a significant reduction in lipid peroxidation in comparison to 1mM QA level. Furthermore, this reduction in lipid peroxidation caused by the melatonin solution irradiated for 10-60 min was equivalent to the level of reduction of lipid peroxidation caused by the unirradiated melatonin solution. Furthermore, there is no significant difference between the protection

offered by the irradiated melatonin solution at each time interval, the unirradiated melatonin solution and the control value.

10.3.4. DISCUSSION

The increasing solar UV radiation and changes in lifestyle strengthen the necessity to seek preventative measures against the deleterious effects caused by intense or prolonged UV light exposure. It is the region between 280 and 320nmn (UVB) that has been found to be primarily responsible for vitamin D production, melanisation, sunburn (erythema and hyperplasia), premature aging of the skin and skin tumours (Epstein, 1970; Dermer, 1979). In particular, administration of antioxidants represents a successful strategy for preventing the occurrence and for reducing the severity of UV-mediated oxidative damage (Saija *et al*., 2002). Furthermore, UV exposure of human and animal tissue causes significant accumulation of non-heme iron in comparison to non-exposed areas (Trommer *et al*., 2001), thus accounting for the increase in lipid peroxidation observed in the presence of QA in the results (figure 10.7).

The skin transmits both UVA and UVB radiation (Sterenborg & Van der Leun, 1990), allowing light of both wavelength ranges to reach melatonin localized within the skin and be absorbed. Since melatonin has an absorption tail that extends to wavelengths longer than 295nm, it can absorb some UVB light (Roberts *et al*., 2000). Thus, endogenous melatonin can undergo photo-inactivation in the skin.

The results demonstrate that melatonin solution irradiated at 10-60 min time intervals reduces QA-induced lipid peroxidation *in vitro*. Furthermore, the irradiated melatonin solution was able to decrease the levels of MDA produced to levels similar to that in the absence of QA, demonstrating complete protection against this neurotoxin with regard to lipid peroxidation. From the results it is evident that irradiated melatonin solution at time 10-60 min has equivalent protection against lipid peroxidation to that of unirradiated melatonin solution. These results confirm that even though the amount of melatonin present in the irradiated melatonin solution at time 60 min is zero the solution is able to protect rat brain homogenate against QA-induced lipid peroxidation and reduce oxidative neurotoxicity due to QA.

From these results we can conclude that the photoproducts of melatonin which were found in chapter two i.e. 6-OHM and AFMK possess neuroprotective and antioxidant properties. Furthermore, there is no significant difference between the protection offered by melatonin at time zero and the irradiated melatonin solution (time 10-60 min) and the control value, indicating that melatonin and the irradiated melatonin solution which contains the photoproducts offer complete protection against QA-induced peroxidation of the brain lipid layers. This implies that the photoproducts of melatonin possess equipotent free radical scavenging ability as the parent compound. From the results obtained, it can be concluded that even though melatonin is degraded in the presence of UV-light, the degraded solution possesses equipotent antioxidant scavenging properties as melatonin and this sets to rest the concerns about the incorporation of melatonin in sunscreens (Maharaj *et al*., 2002) as the results show that the degraded solution possess antioxidant properties, making melatonin a likely candidate for inclusion in sunscreens.

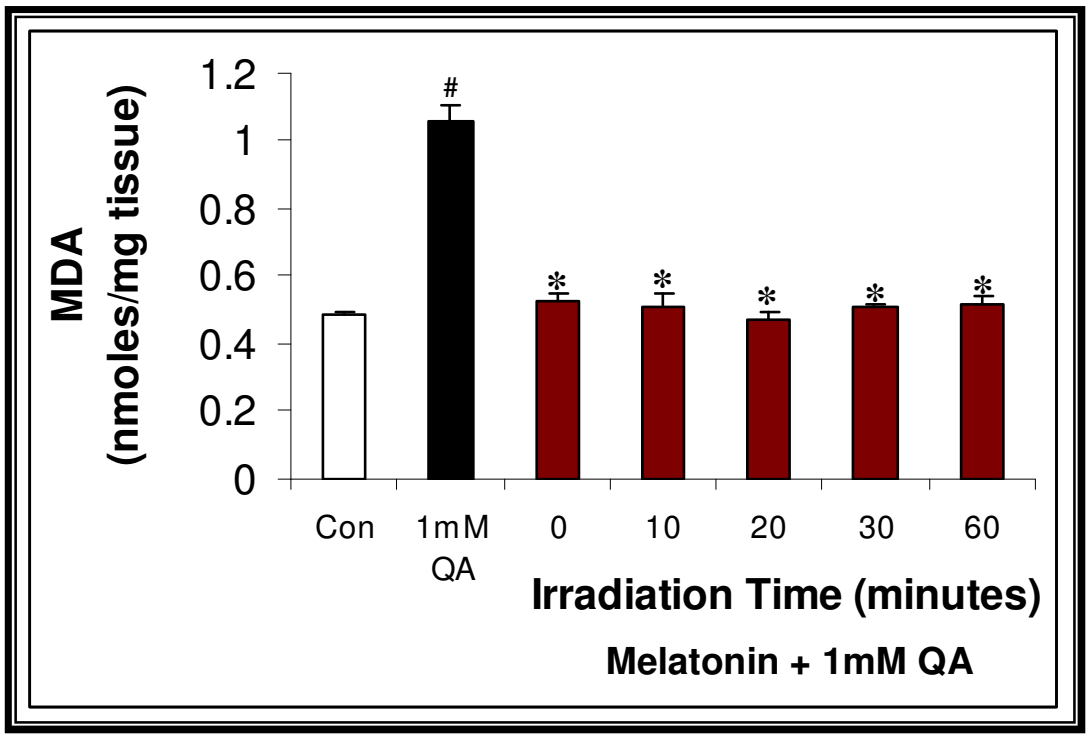

Figure 10.7: The effect of irradiated melatonin on quinolinic acid-induced lipid peroxidation in rat brain homogenate. Each bar represents the mean ± SEM of three determinations. # ($p<0.05$) QA vs control; *($p<0.05$) melatonin vs quinolinic acid, Student-Newman-Keuls Multiple Range Test.

10.4. COMPARISON OF THE EFFECTS OF 6-OHM AND MELATONIN ON CYANIDE, QA AND IRON (II)-INDUCED LIPID PEROXIDATION IN RAT BRAIN HOMOGENATE *IN VITRO*.

10.4.1. INTRODUCTION

Under normal conditions, the antioxidant defence system within the body can easily handle free radicals that are produced. During times of increased oxygen flux, free radical production may exceed that of removal and ultimately result in lipid peroxidation. The hydroxyl radical, specifically, is the most damaging of all free radicals and ultimately causes the most damage (Halliwell & Gutteridge, 1985).

The $O_2^{\bullet-}$ can react with membranes to set off membrane destroying reactions (Poeggeler *et al.,* 1993). As membranes are vital for proper cell function, any damage to membranes could be toxic to neurons. Among the products of the membrane destroying reactions is MDA (Reiter *et al.*, 1995). In addition, the brain is known to be rich in iron, which plays a crucial role in initiating and propagating lipid peroxidation (Halliwell & Gutteridge, 1989). In the previous study, the oxidative damage caused by the neurotoxins; cyanide, QA and Fe^{2+} in rat brain homogenate has been demonstrated and discussed.

Since the brain is particularly susceptible to oxidative attack by free radicals, lipid peroxidation is able to cause extensive damage and is known to play a major role in the deterioration of the brain and spinal cord that occurs after traumatic or ischemic injury. Such injuries to the brain result in more extensive tissue damage than do equivalent insults in other tissues. Free radical reactions have been implicated in such damage (Halliwell & Gutteridge, 1990) and therefore the use of antioxidant agents to protect the brain against this free radical damage is becoming increasingly popular.

In the chapter eight, cyanide and QA were shown to potentiate $O_2^{\bullet-}$ production which was effectively reduced by the co-administration of melatonin and 6-OHM. Furthermore, melatonin has been shown to protect against cyanide, QA and iron induced peroxidation

of brain tissue *in vitro* and *in vivo* (Yamamoto & Tang, 1996a; Cabrera *et al*., 2000; Lin & Ho, 2000; Kaptanoglu *et al*., 2003). 6-OHM in recent studies has been shown to reduce $O_2^{\bullet-}$ generation and lipid peroxidation in rat brain tissue (Maharaj *et al*., 2003a,b). Furthermore, Pierrefiche *et al*., (1993) showed 6-OHM to be a more potent antioxidant than melatonin.

The aim of these studies was to determine whether 6OHM, which was found in chapter eight to be a more potent scavenger of $O_2^{\bullet-}$ than melatonin is able to protect against lipid peroxidation induced by the neurotoxins, cyanide, QA and iron (II). In addition, a comparative study was performed to compare the protection offered by melatonin to that offered by 6-OHM.

10.4.2. MATERIALS AND METHODS

10.4.2.1. Chemicals and Reagents

Melatonin and 6-OHM were purchased from the Sigma Chemical Company, St. Louis, MO (USA). All other chemicals used were of the highest quality available from commercial sources.

10.4.2.2. Sample Preparation

Samples for the lipid peroxidation assay were prepared according to the method described in section 10.2.2.3. Melatonin and 6-OHM were prepared by dissolving in absolute ethanol, and subsequently diluting with Milli-Q water so that the final ethanol concentration in the brain homogenate was 0.5%. The following concentrations of MEL or 6-OHM were used 0, 0.25, 0.5, 1, 1.5 mM.

10.4.2.3. Lipid Peroxidation Assay

Adult male rats of the Wistar strain were used for this experiment and were maintained as described in appendix one. The rats were sacrificed and the brains were rapidly removed

and placed on ice as described in appendix two. Each brain was homogenized as described in section 10.2.2.5.

The instrumentation and chromatographic conditions were as described in sections 10.2.2.6 and 10.2.2.7, respectively and a calibration curve was constructed according to the method described in section 10.2.2.8.

Lipid peroxidation was determined using a modification of the method described in section 10.2.2.9. Briefly, homogenate (1ml) containing 1mM QA or 1mM KCN or 5mM Fe^{2+} alone or in combination with varying concentrations of melatonin or 6-OHM were incubated on an oscillating water bath at 37^{o}C for 60min. The procedure as described in section 10.2.2.9 was then followed. Final results were expressed as nmoles MDA/mg tissue and analyzed for statistical significance as demonstrated in section 9.2.2.10.

10.4.3. RESULTS

The exposure of rat brain homogenate with 1mM KCN at 37^{o}C for 1hr caused a significant increase in the concentration of MDA compared to the control as evidenced in figure 10.8. However, this increase in lipid peroxidation products was attenuated or completely abolished by the co-incubation of the homogenates with different concentrations of melatonin or 6-OHM (figure 10.8). Furthermore, treatment with 2mM melatonin or 6-OHM significantly lowered the basal level of lipid peroxidation when compared to the control value. As shown in figure 10.8, there is no significant difference between the protection offered by melatonin and that offered by 6-OHM.

As can be observed in figure 10.9, 1mM QA caused a significant rise in the levels of MDA in comparison to the control value. Furthermore, figure 10.9, illustrates MEL and 6-OHM's inhibitory effect on QA-induced lipid peroxidation in rat brain homogenate. The response proceeds in a dose-dependent manner and the suppression of oxidatively damaged lipid products is highly significant for each concentration chosen. Melatonin concentration of 0.05mM and higher significantly reduces levels of MDA below those treated with QA only. Likewise, concentrations of 6-OHM of 0.25mM and higher were able to significantly reduce lipid peroxidation levels below those treated with QA only.

Concentrations of melatonin of 0.5mM and higher show significantly more protection against the QA-induced lipid peroxidation than the respective concentrations of 6-OHM. However, there was no significant difference noticed between the protection offered by the 1.5mM concentration of melatonin and the 1.5mM concentration of 6-OHM (figure 10.9). The 1.5mM melatonin and 1.5mM 6-OHM concentrations significantly reduced MDA levels below those of the control basal samples (no indoleamine or QA added).

Incubation of brain homogenates with 5mM Fe^{2+} significantly increased the formation of peroxidised lipids in comparison to the control samples (no indoleamine or iron) (figure 10.10). Co-incubation of the rat brain homogenate with increasing concentrations of melatonin or 6-OHM together with 5mM Fe^{2+} is able to dose-dependently prevent the iron-induced increase in lipid peroxidation as seen in figure 10.10. All concentrations of MEL and 6-OHM tested for proved to be able to significantly reduce the rise in lipid peroxidation caused by Fe^{2+}. Furthermore, as is evident from figure 10.10, the 1mM MEL concentration is able to significantly reduce iron-induced lipid peroxidation in comparison to the same concentration of 6-OHM. However, there is no significant difference between the protection offered by the two indoleamines and the control samples.

10.4.4. DISCUSSION

Research on compounds with antioxidative properties has become the major focus of attention for preventing CNS neurodegenerative diseases. Several antioxidative strategies may be therapeutically useful, including supplementation with antioxidative and upregulation of endogenous antioxidative defence mechanisms (Cicone, 1998; Marsden & Olanow, 1998; Simom & Standaert, 1999; Ebadi *et al*., 1996). Recently melatonin has been suggested as an antioxidant that may protect biological organisms from oxidative stress (Reiter, 1998). Melatonin has been shown to be effective in suppressing lipid peroxidation induced by iron, cyanide and QA as stated above. However not much evidence exists demonstrating the ability of 6-OHM against lipid peroxidation induced by different neurotoxins. In addition, the dose response protective effect against Fe^{2+}-induced rise in MDA levels demonstrated by melatonin is supported by Kaptanoglu *et al*.,

(2003) where the authors demonstrate that melatonin dose-dependently reduces lipid peroxidation induced by this neurotoxin.

The results of the present study show that melatonin and 6-OHM are able to protect against QA, cyanide and Fe^{2+}-induced lipid peroxidation in rat brain homogenate *in vitro* and the protection offered by 6-OHM is shown to be equivalent to that offered by the antioxidant, melatonin. However, melatonin in this study was shown to be more potent in reducing lipid peroxidation generated by Fe^{2+}. Although the concentrations of the indoleamines used in this experiment is suprapharmacological, it is necessary to use such high concentrations, as the concentration of neurotoxins use to generate free radicals and induce lipid peroxidation is required to be high. Furthermore, it is likely that the interaction of the neurotoxins with brain tissue generates very high levels of MDA and that the damaging effects found in this study is much greater than the eventual biological damage induced by the neurotoxins *in vivo*. Nevertheless, even under these conditions, the indoleamines provide significant protection. Thus, it can be speculated that although a high concentration of melatonin and 6-OHM is required to counteract the peroxidation of the lipid layers by the three neurotoxins, a much lower concentration of the indoleamines might be effective *in vivo*.

High concentrations of 6-OHM and melatonin are also shown to completely abolish lipid peroxidation induced by all three neurotoxins to below that of the basal control values, indicating that at these concentrations the indoleamines provide complete protection against the neurotoxin induced lipid peroxidation.

QA-induced increase of lipid peroxidation in brain homogenate is dependent on the presence of iron (Stipêk, *et al*., 1997). These authors showed that QA complexes with Fe^{2+} but not Fe^{3+}. Once a QA-Fe^{2+}complex forms, this reacts with preformed lipid peroxides, generated by tissue disruption, to produce peroxyl radicals (Halliwell & Gutteridge, 1989). Furthermore, Fe^{2+} participates in the Fenton reaction to produce damaging $^{\bullet}OH$ in the brain (Halliwell, 1992). These radicals can attack other molecules within the homogenate and so the chain of lipid peroxidation can continue. One means by which 6-OHM, could protect against QA-induced and Fe^{2+}-induced lipid peroxidation *in vitro*, is by possible binding the free Fe^{2+}, thereby preventing the complex formation

between QA and Fe^{2+} to occur. Thus without Fe^{2+} the Fenton reaction cannot proceed (Braughler & Hall, 1989). In addition, the autooxidaiton of Fe^{2+} results in the formation of $O_2^{\bullet-}$ (Halliwell, 1992). Melatonin has been previously shown to bind a number of metal ions such as Fe^{3+} but not Fe^{2+} (Limson *et al.*, 1998). The possibility that 6-OHM may be competing with QA for Fe^{2+} complexation and inhibiting the Fenton reaction by binding to ferrous ions has been investigated in chapter eleven.

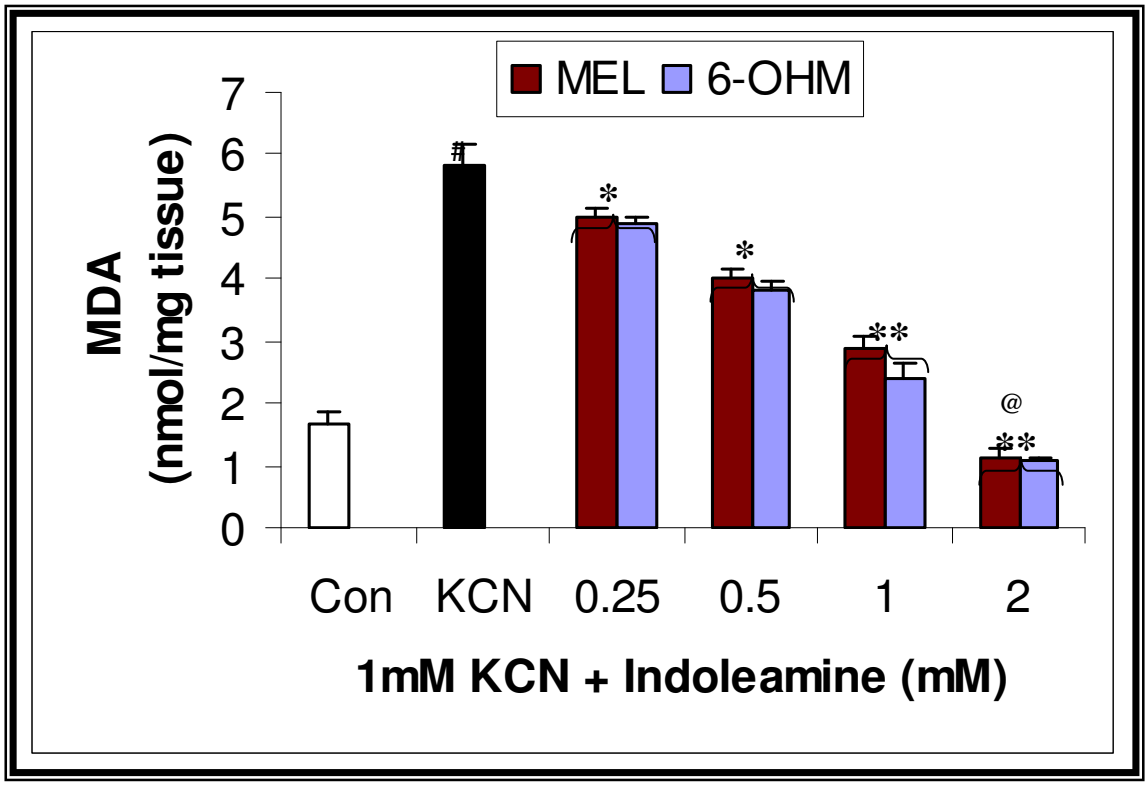

Figure 10.8: The effect of different concentrations of melatonin or 6-OHM on 1mM cyanide-induced lipid peroxidation in rat brain homogenate. Each bar represents the mean ± SEM of five determinations. # ($p<0.001$) KCN vs. control; *($p<0.05$) 0.25mM and 0.5mM MEL and 6-OHM vs. KCN; ** ($p<0.01$) 1mM and 2mM MEL and 6-OHM vs. KCN; and @ ($p<0.05$) 2mM MEL and 6-OHM vs. control. (Student-Newman-Keuls Multiple Range Test).

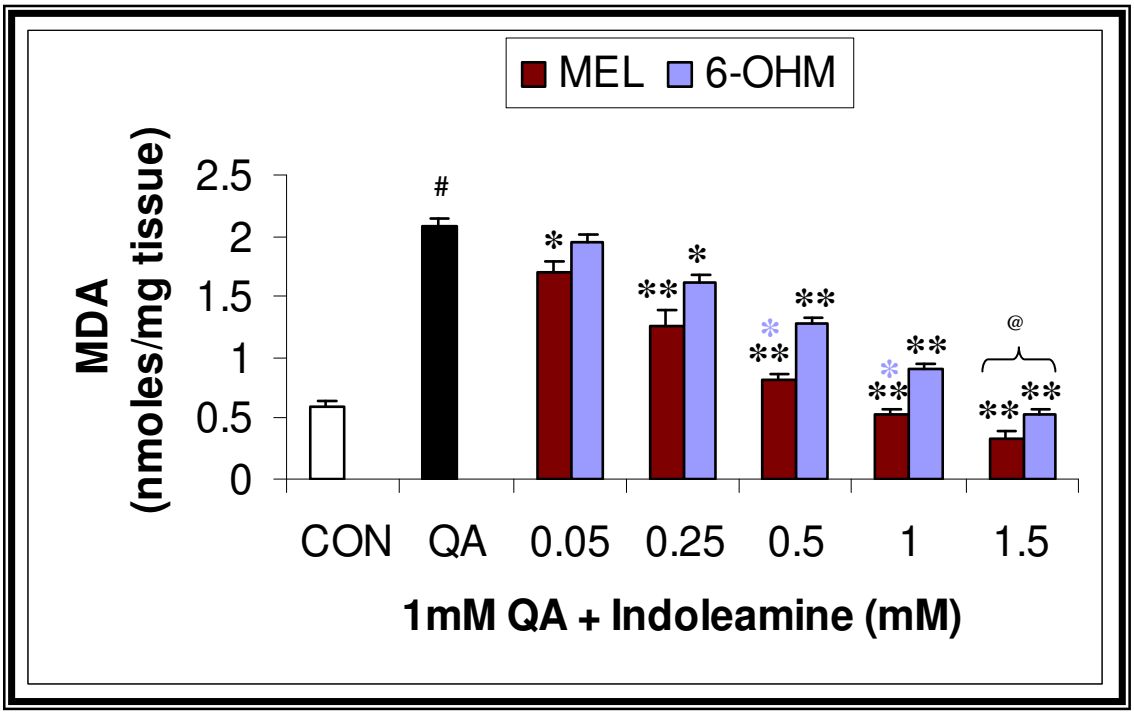

Figure 10.9: The effect of different concentrations of melatonin or 6-OHM on 1mM quinolinic acid-induced lipid peroxidation in rat brain homogenate. Each bar represents the mean ± SEM of five determinations. # ($p<0.001$) QA vs control; * ($p<0.05$) 0.05mM MEL vs QA and 0.25mM 6-OHM vs QA; **($p<0.01$) 0.25mM, 0.5mM, 1mM and 1.5mM MEL vs QA, and 0.5mM, 1mM, and 1.5mM 6-OHM vs QA; * ($p<0.05$) 0.5mM and 1mM MEL vs 0.5mM and 1mM 6-OHM, respectively; $^{@}$($p<0.05$) 1.5mM MEL and 1.5mM 6-OHM vs. control. (Student-Newman-Keuls Multiple Range Test).

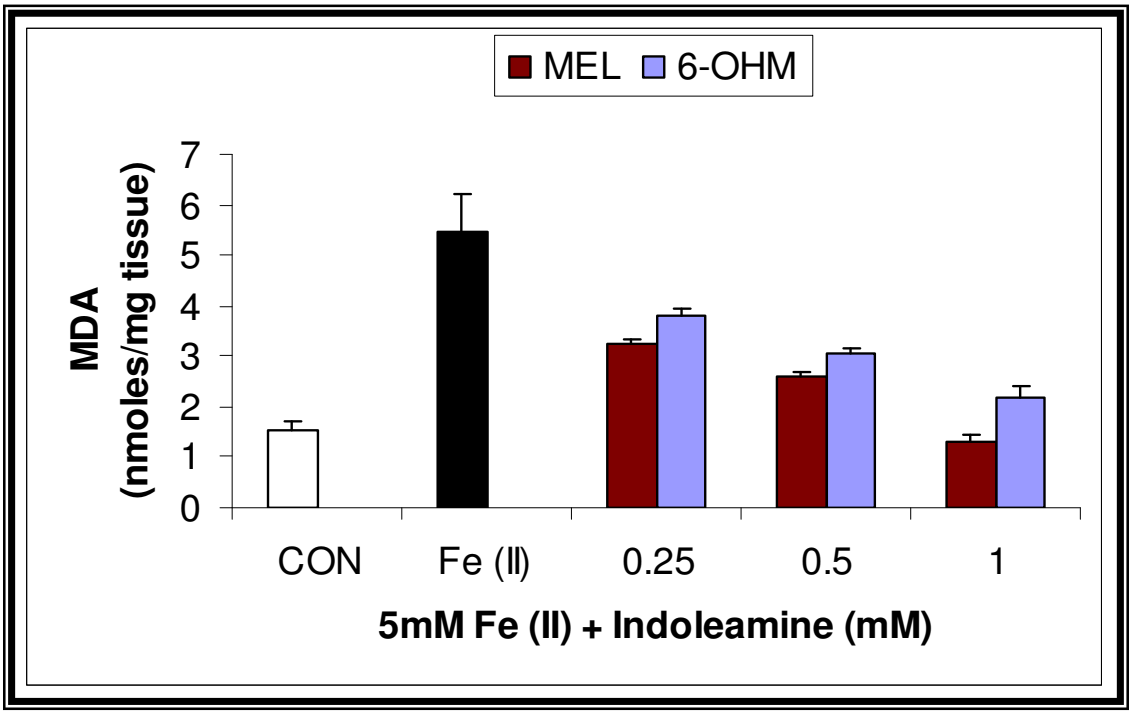

Figure 10.10: The effect of different concentrations of melatonin or 6-OHM on 5mM Fe (II)-induced lipid peroxidation in rat brain homogenate *in vitro*. Each bar represents the mean ± SEM of five determinations. # ($p<0.0001$) Fe (II) vs control; **($p<0.01$) 0.25mM and 0.5mM MEL vs Fe (II) and 0.25mM and 0.5mM 6-OHM vs Fe (II); ***($p<0.001$) 1mM MEL vs Fe (II), and 1mM 6-OHM vs Fe (II); * ($p<0.05$) 1mM MEL vs 1mM 6-OHM. There is no significant difference between the control and the 1mM MEL.

10.5. COMPARISON OF THE EFFECTS OF 6-OHM AND MELATONIN ON QA AND IRON (II)-INDUCED LIPID PEROXIDATION IN THE RAT HIPPOCAMPUS *IN VIVO*.

10.5.1. INTRODUCTION

The results of the previous experiment demonstrated that 6-OHM and melatonin protect against lipid peroxidation in rat brain homogenate following exposure to cyanide, iron (II) and QA. Since QA is known to be present in the brain at concentrations in the nM range and that this concentration increases with age (Moroni, *et al*., 1984a). Substantial increases of QA up to 400 fold in brain and systemic tissue occur in human patients with a broad spectrum of inflammatory conditions (Heyes *et al*., 1991; 1992a, b; Vogelgesang *et al*., 1996), levels substantially greater than those capable of causing neurotoxicity. For example in patients with pronounced neurological disease, CSF QA levels may exceed plasma concentrations (Heyes *et al*., 1991). The neurotoxic effects of the excitotoxin, QA are well established. Heyes (1996) reported that microglia and macrophages may be an important source of this neurotoxin and it has been implicated in the pathogenesis of a broad spectrum of degenerative, infectious, inflammatory and non-inflammatory human neurological diseases (Stone & Perkins, 1981; Moroni *et al*., 1986; Schwarz *et al*., 1988; Heyes, 1996). Cabrera *et al*., (2000) showed that both *in vivo* and *in vitro* pharmacological levels of melatonin confer protection against QA-induced lipid peroxidation and oxidative toxicity in the rat brain.

In normal brain iron is not reactive despite its high concentration, probably because its absorption, transport, storage are tightly regulated however, if there is an excess of ionic iron, iron induced oxidative damage can occur (Floyd & Carney, 1992). Abnormal iron metabolism is implicated in human neurological disorders such as Alzheimer's disease, Parkinson's disease and Huntington's disease (Gerlach *et al*., 1994). Furthermore, a hallmark of biological aging is the accumulation of iron in tissues such as brain (Cook & Yu, 1998) indicating that a causal relation between age-related iron accumulation and lipid peroxidation exists. Massie *et al*., (1985) proposed that the rate of age-related iron

accumulation correlates inversely with the life span in some species. In physiological systems, iron is sequestered by chelators, such as citrate and by macromolecules, such as transferring (Aisen, 1977). At biological pH and oxygen tension, Fe^{2+} is oxidized to Fe^{3+} via one electron transfer reactions that result in the formation of free radical intermediates (Czapski & Ilan, 1978; Koppenol *et al*., 1978). Although, the hippocampus is a brain area with low Fe^{2+} and catecholamine content (Sloot *et al*., 1994), prior studies have shown that direct injection of µL volumes of an aqueous solution of Fe^{2+} into the rodent hippocampus causes acute epileptiform discharges (Reid & Sypert, 1980; Willmore *et al*., 1978) and a significant increase in lipid peroxidation products, as measured by TBA-MDA assay (Boehme *et al*., 1977), within 5 min of injection.

Since both QA and Fe^{2+} do not cross the BBB under normal conditions (Kim *et al*., 2000; Haik *et al*., 2000), these need to be administered directly into the brain, usually via acute injections, for use in most animal models of neurodegeneration. Thus, it was decided to investigate whether 6-OHM could offer protection against lipid peroxidation following an intrahippocampal injection of QA or Fe^{2+} *in vivo*. A comparative study was done with melatonin to determine, which indoleamine is more potent in this respect.

10.5.2. MATERIALS AND METHODS

10.5.2.1. Chemicals and Reagents

As described in section 9.4.2.1. Ferrous chloride ($FeCl_2$. $4H_2O_2$; >99% pure) was obtained from Merck, Darmstadt. The Fe^{2+} was made up in de-aerated PBS buffer, pH 7.4, to prevent the oxidation of Fe^{2+} to Fe^{3+}.

10.5.2.2. Dosing of the Animals

The animals were separated into seven groups of six animals each (Table 10.1). The animals in group 4 and 6 received a dose of 10mg/kg/day of melatonin in 100µl sweet oil, injected subcutaneously, 20 mins prior to intrahippocampal QA and Fe^{2+} injections, respectively. Similarly the animals in group 5 and 7 received a dose of 10mg/kg/d of 6-OHM in 100µl of sweet oil, administered in the same manner as melatonin. The

animals in groups 1, 2 and 3 received the vehicle for these drugs, viz. sweet oil. On day one, 20 mins after dosing the animals with the respective drug or vehicle, the animals of groups 2, 4 and 5 were injected bilaterally into the hippocampal regions with QA while animals of groups 3, 6 and 7 were injected with Fe^{2+} in the same way. QA and Fe^{2+} were dissolved in PBS made up to pH 7.4. A dose of QA (120nmol) was used to induce neurotoxicity as this concentration of QA is known to cause severe behavioural disturbances and total loss of hippocampal neurons (Lekieffre *et al*., 1990; Schwarcz *et al*., 1984). A dose of Fe^{2+} (0.4µmol in 3µl of PBS) was used to induce hippocampal neurotoxicity as this dose has been shown previously to induce lipid peroxidation, seizures, extensive Ca^{2+} accumulation and neurodegeneration in the hippocampus of rats (Willmore *et al*., 1986; Triggs & Willmore, 1984; Sloot *et al*., 1994).

Following the intrahippocampal injections of QA or Fe^{2+}, the animals in groups 4 and 6 received subsequent daily doses of melatonin while animals of groups 5 and 7 received 6-OHM, each day for seven days. The animals in groups 1, 2 and 3 received daily doses of sweet oil for seven days.

10.5.2.3. Surgical Procedures

Rats were anaesthetized with diethelyether as described in chapter eight, section 8.5.2.3.1.

10.5.2.3.1. Bilateral Intrahippocampal QA and Fe^{2+} Injections

QA and Fe^{2+} were dissolved in phosphate buffered saline (PBS), pH= 7.4. QA (120nmol in 2µl PBS) and Fe^{2+} (0.4µmol in 3µl PBS) were infused bilaterally into the hippocampii employing a rat brain stereotaxic apparatus (Stoelting, IL, USA) (figure 8.8). The same procedure as described in chapter eight, section 8.5.2.3.2 was used.

10.5.2.3.2. Sham Lesioned Rats

The rats used as controls were subjected to the same surgical procedures described in section 8.5.2.3.3. However, bilateral stereotaxic injections into the hippocampal regions were free of QA and Fe^{2+} and comprised solely of PBS.

Table 10.1 Treatment regime for each group of animals

Treatment Group	**Received 20 mins prior to stereotaxic surgery (s.c.)**	**Intrahippocampal injection**	**Daily treatment for 7 days after stereotaxic surgery (s.c.)**
1. Control	100µl Sweet oil	PBS	100µl Sweet oil
2. QA	100µl Sweet oil	120nmol QA in PBS	100µl Sweet oil
3. Fe^{2+}	100µl Sweet oil	0.4µmol Fe^{2+} in PBS	100µl Sweet oil
4. MEL(+) QA	100µl melatonin in sweet oil	120 nmol QA in PBS	100µl melatonin in sweet oil
5. 6-OHM(+) QA	100µl 6-OHM in sweet oil	120 nmol QA in PBS	100µl 6-OHM in sweet oil
6. MEL(+) Fe^{2+}	100µl melatonin in sweet oil	0.4µmol Fe^{2+} in PBS	100µl melatonin in sweet oil
7. 6-OHM(+) Fe^{2+}	100µl 6-OHM in sweet oil	0.4µmol Fe^{2+} in PBS	100µl 6-OHM in sweet oil

10.5.2.4. Dissection of the Hippocampus

On the eighth day following the intrahippocampal injection of QA, the brains were removed as described in 8.5.2.4 and the hippocampii rapidly dissected according to a modified method of Glowinski and Iversen (1966).

10.5.2.5. Homogenate Preparation

Rats were sacrificed by cervical dislocation and then decapitated as described in appendix two. The brains were rapidly removed and placed on ice. Each brain was homogenized as described in section 10.2.2.5.

10.5.2.6. Lipid Peroxidation Assay

The instrumentation and chromatographic conditions are described in sections 10.2.2.6 and 10.2.2.7, respectively. A calibration curve was constructed according to the method described in section 10.2.2.8.

Lipid peroxidation was determined using a modified method of Anoopkumar-Dukie *et al*., (2001). Briefly, the incubation step at 37^{o}C for 1hr was excluded and the homogenate (1ml) for each treated group was heated for 15 min with 0.5mL BHT and 1 mL TCA in a boiling water bath to release protein bound MDA and the procedure described in section 10.2.2.9 was then followed. Final results were expressed as nmoles MDA/mg tissue and the results were statistically analyzed using the method described in section 9.2.2.10.

10.5.3. RESULTS

The QA or Fe^{2+} only treated rats often exhibited motor seizure activity. Roughly, 24 hours after intrahippocampal QA or Fe^{2+} injections, classical signs of neurobehavioral changes were observed such as arching of the tail, tremor, and seizures. The seizure behaviour varied from chewing and scratching movements, 'wet-dog shakes', body tremor; backward walking and rearing with falling. However, rats treated with MEL or 6-OHM together with QA failed to produce any detectable behavioural changes. While the seizure activity was not as pronounced in the rats treated with melatonin or 6-OHM and Fe^{2+} in comparison to the rats treated with Fe^{2+} alone.

Levels of lipid peroxidation products (figure 10.11) in the hippocampal homogenates of animals receiving the vehicle was 0.0089 ± 0.001 nmoles/mg tissue; following quinolate injection into the hippocampus, the MDA levels increased 0.021±0.0005 nmoles/mg tissue. The increase, when compared to the vehicle treated rats was greater than 50%. In QA + MEL treated rats the level of lipid peroxidation was reduced to 0.0042±0.0007 nmoles/mg tissue; this is a ~80% decrease relative to levels measured in the hippocampus of rats that received QA only. In the QA + 6-OHM treated rats the level of MDA was measured at 0.0065±0.0006 nmoles/mg tissue; which is a ~70% reduction relative to the levels of MDA measured in QA only treated rats. Thus, the injection of MEL or 6-OHM

in combination with QA significantly inhibited lipid damage in the hippocampus induced by the neurotoxin (figure 10.11). It is also evident that the co-administration of MEL or 6-OHM with the neurotoxin QA was able to significantly lower the levels of MDA below that of the control basal samples (rats treated with vehicle only).

Fe^{2+} injection into the hippocampus resulted in a significant increase in MDA levels. An increase of 0.0491±0.00055 nmoles/mg tissue in comparison to the control value is evident from figure 10.12. However, in Fe^{2+} + MEL treated rats the level of lipid peroxidation was reduced to 0.024±0.00087 nmoles/mg tissue. This is a ±50% decrease relative to levels measured in the hippocampus of rats that received Fe^{2+} only. In the Fe^{2+} + 6-OHM treated rats the level of MDA was measured at 0.037±0.0009 nmoles/mg tissue, which is a ±40% reduction relative to the levels of MDA measured in Fe^{2+} only treated rats. Thus, the injection of MEL or 6-OHM in combination with Fe^{2+} significantly inhibited lipid damage in the hippocampus induced by the neurotoxin (figure 10.12). It is also evident that there is a significant difference between the protection offered by the administration of MEL in comparison to the administration of 6-OHM.

10.5.4. DISCUSSION

Both QA and Fe^{2+} resulted in an increase in lipid peroxide product, MDA in the rat hippocampus. This action by QA and Fe^{2+} is further supported by a number of reports in which the authors describe that these neurotoxins cause an increase in lipid peroxidation levels (Rios & Santamaria, 1991; Willmore & Rubin, 1982; Triggs & Willmore, 1984; Chen *et al*., 2003). The results obtained show that melatonin and 6-OHM are both able to protect against QA-induced lipid peroxidation *in vivo*. Since QA is known to be an endogenous agonist of the NMDA receptor that causes neuronal damage due to an influx of calcium into the cell, it is possible that these indoleamines (melatonin and 6-OHM), in addition to their antioxidant ability, also act on the NMDA receptor. This assumption is based on the results of the present study, which shows that both indoles decrease the level of lipid peroxidation to below that of the control, suggesting total protection against QA. Furthermore, if melatonin and 6-OHM were to only act as an antioxidant, then cell damage due to QA would still occur and they would then only be preventing further damage. However, if these agents were to act on the NMDA receptor thereby competing

with QA to bind, then greater protection would be displayed by the indoles, which is shown in these results. There are several means by which melatonin is postulated to alter the NMDA receptor physiology and thereby decrease QA-induced lipid peroxidation. For example melatonin may change membrane fluidity (Garcia *et al*., 1998), which alters the affinity of the receptor, for the ligand and thereby could interfere with the binding of QA to the NMDA receptor (Cabrera *et al*., 2000). Recent research is directed at examining these potential actions of melatonin and thus 6-OHM could be acting in a similar manner. However, this needs to be investigated further.

In addition, the brain is known to be rich in iron, which plays a crucial role in initiating and propagating lipid peroxidation (Halliwell & Gutteridge, 1989) and the concentration of iron is known to increase with age. It serves as a catalyst for *in vivo* lipid peroxidaiton (Minotti & Aust, 1992; Floyd and Carney, 1993). Willmore *et al*., (1986) and Triggs and Willmore (1984) demonstrated that intracerebral injections of Fe^{2+} particularly into the hippocampus significantly increases lipid peroxidation levels and induces neuronal damage (Sloot *et al*., 1994). Both melatonin and 6-OHM have been previously shown to significantly reduce Fe^{2+}-induced lipid peroxidation in rat liver homogenate (Karbownik *et al*., 2000; Maharaj *et al*., 2003a). In addition, recently melatonin has been reported by Chen *et al*., (2003) to protect against Fe^{2+}-induced lipid peroxidation *in vivo*. The above findings are consistent with these results and further indicate that melatonin and 6-OHM are effective in partially reversing the damage caused by Fe^{2+} in the hippocampus. Melatonin has been shown previously to effectively scavenge $^{\bullet}OH$ (Stasica *et al*., 1998) and one of the primary products formed is 6-OHM (Horstman *et al*., 2002). This implies that even though melatonin interacts with the Fenton-type $^{\bullet}OH$ to form 6-OHM, 6-OHM retains significant ability to scavenge the $^{\bullet}OH$ and reduce lipid peroxidation induced by the Fenton reaction. However, melatonin remains superior in protecting the hippocampus against Fe^{2+}-induced lipid peroxidation.

The 6-OHM and melatonin are capable of rapidly crossing the blood brain barrier. It has also been reported that melatonin accumulates in high concentrations in brain cells after entering the brain. Cabrera *et al*., (2000) and Menéndez-Peláez *et al*., (1993) found that 30 min after a s.c. injection of 0.5 mg/kg melatonin, the concentrations of melatonin in the cell nuclei in rat cerebral cortex and cerebellum were five times higher than those of

control rats. From the results above, both melatonin and 6-OHM were able to inhibit the QA-induced and minimizing Fe^{2+}-induced seizure and neurobehavioral changes in rats. This provides evidence that 6-OHM, similar to melatonin, is able to protect the hippocampus against the seizure activity and neuronal damage caused by the neurotoxins and the protection offered by 6-OHM is equivalent to that of melatonin, indicating that 6-OHM is an effective antioxidant. These results are supported by Hara *et al.*, (1997; 2001) where the authors show that 6-OHM prevents lipid peroxidation in the liver, muscle and brain, with the same or greater potency as melatonin.

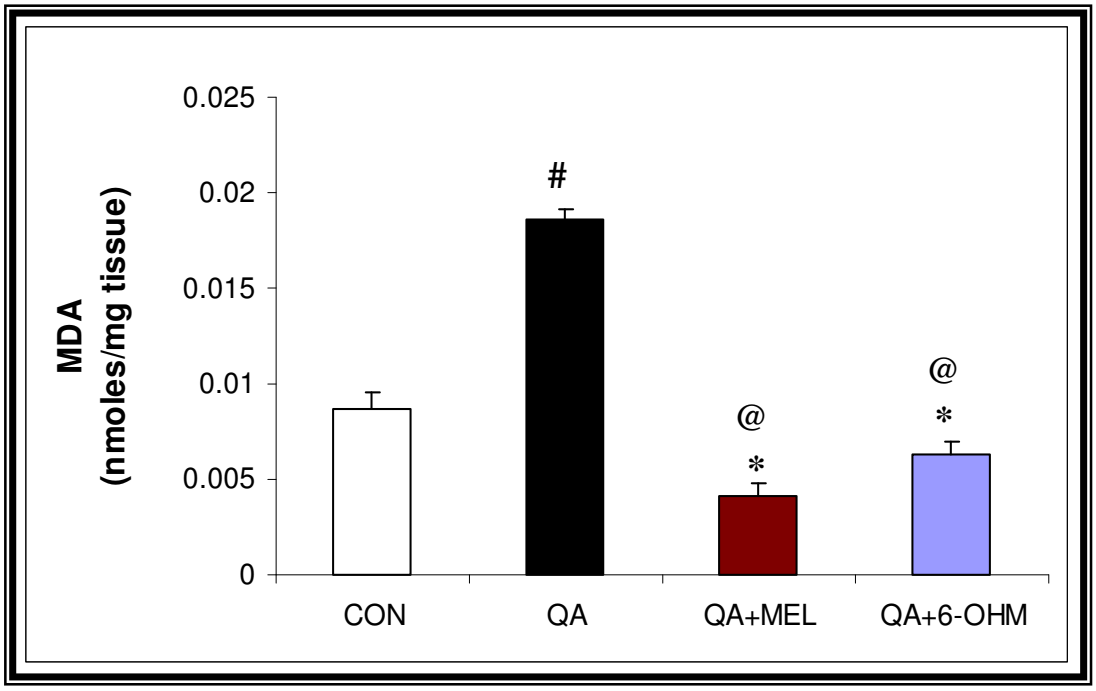

Figure 10.11: The effect of the MEL and 6-OHM on QA-induced lipid peroxidation in rat hippocampal homogenate *in vivo*. Each bar represents the mean ± SEM; n=6. # ($p<0.001$) QA vs CON; *($p<0.01$) MEL+QA vs QA, and 6-OHM + QA vs QA; @($p<0.05$) MEL and 6-OHM versus CON. (Student-Newman-Keuls Multiple Range Test).

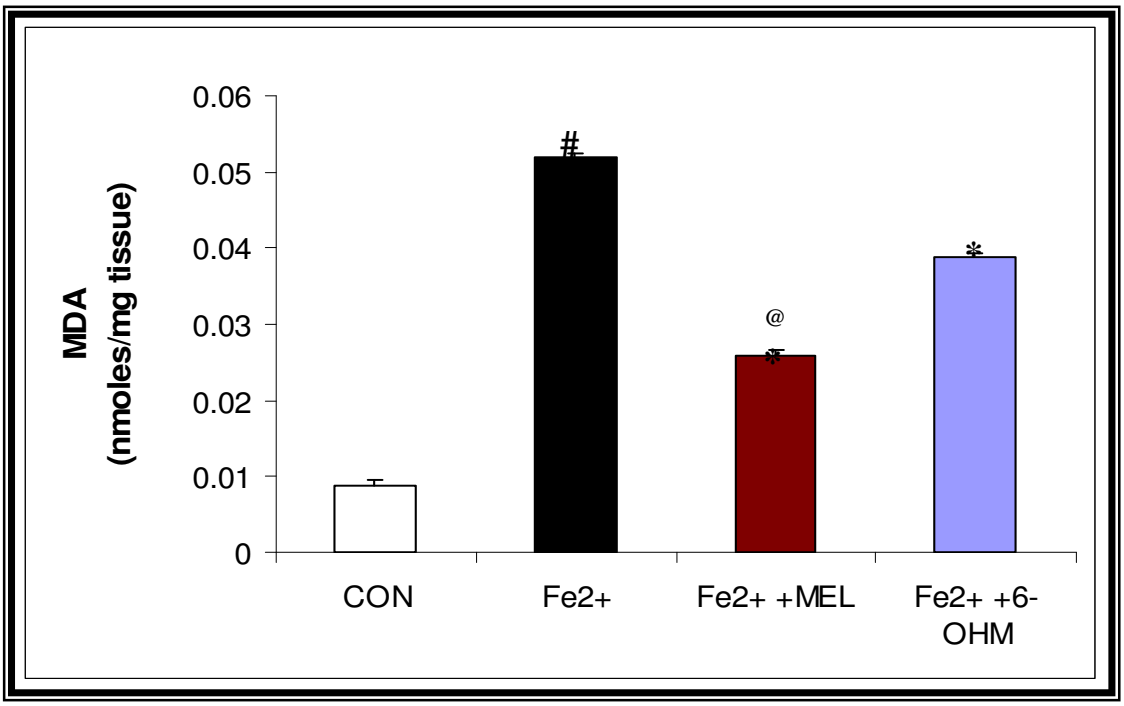

Figure 10.12: The effect of the MEL and 6-OHM on Fe (II)-induced lipid peroxidation in rat hippocampal homogenate *in vivo*. Each bar represents the mean ± SEM; n=6. $^{\#}(p<0.001)$ Fe (II) vs CON; *($p<0.01$) MEL+ Fe (II) vs Fe (II), and 6-OHM + Fe(II) vs Fe (II); $^{@}(p<0.05)$ MEL vs. 6-OHM. (Student-Newman-Keuls Multiple Range Test).

10.6. EFFECT OF UV-IRRADIATION ON LIPID PEROXIDATION ON RAT SKIN HOMOGENATE ALONE OR IN THE PRESENCE OF MELATONIN *IN VITRO.*

10.6.1. INTRODUCTION

It was earlier postulated that UV radiation was not energetic enough to generate free radicals and that without evidence these species could not be invoked as causing photodamage. There is now evidence that ROS are generated *in vivo*, by UV irradiation of skin (Black, 1987). Products of lipid peroxidation, lipid radicals, melanin radicals, and antioxidant depletion have all been noted in UV irradiated skin (Darr & Fridovich, 1994). Both UVA and UVB radiation interacts with several biomolecules to induce the generation of free radicals in biological tissues such as skin. Of these free radicals, the $^{\bullet}OH$ radical can induce cellular damage including lipid peroxidation, erythema, oedema, as well as premature skin aging (Maharaj *et al*., 2002; Ogura *et al*., 1988). Furthermore, significant levels of H_2O_2 are almost certainly generated by UV in human skin cells, and $^{\bullet}OH$ is generated by the Fe^{2+} ion-catalyzed Fenton reaction (Pantopoulous & Hentze, 1995). These radicals cause tissue damage by reacting with biomolecules such as lipids and proteins (Dreher *et al*., 1999) and result in the formation of lipid peroxides. These in turn elicit a chain reaction, causing formation of further lipid peroxides and the cell membrane is thus damaged as a consequence of this phenomenon. Under UV irradiation photoperoxidation of the chains of unsaturated fatty acids is induced in the skin and in the surface lipids (Diezel *et al*., 1975; Meffert & Reich, 1969). The opinion based on this fact, was put forward that UV-induced erythema is caused by photoperoxidation of lipids (Diezel *et al*., 1975). Lipid peroxidation in the membrane structures of cells (Goldstein & Harber, 1972; Lordkipanidze *et al*., 1978) and some other photoxidation reactions of biomolecules (Fahrenholtz *et al*., 1974; Goldstein & Harber, 1970) are inhibited by antioxidants. Therefore, one of the possible approaches to the elucidation of the photoxidation role in the UV-induced erythema may be the study of antioxidants' action.

In addition, the generation of free radicals following UV irradiation depletes the skin of endogenous enzymic and/or nonenzymic antioxidants (Shindo *et al*., 1993). It is widely accepted that human skin is particularly vulnerable to injury by free radicals (Gilcrest, 1996). Under normal conditions the skin has an antioxidant defence mechanism that can protect the skin. However, the generation of free radicals depletes the skin of this antioxidative defence mechanism, rendering it vulnerable to UV-induced oxidative stress (Gilchrest, 1996). Recently, Ito and Kawanishi (1997) reported that UV-mediated electron transfer does not require oxygen to induce damage to target molecules including DNA.

Antioxidants may intervene at different levels in the oxidative process e.g., by scavenging free radicals and lipid peroxyl radicals, removing oxidatively damaged biomolecules and other types of action (Briviba & Sies, 1994). Therefore apart from using chemical and/or physical sunscreens, supplementation of the skin with antioxidants and thereby strengthening its antioxidant capacity is a further approach in limiting UV-induced skin damage (Fryer, 1993; Darr & Pinnell, 1997). The photoprotective effect of topical antioxidants applied before UV exposure is being recognized (Bissett *et al*., 1990a, b; Gensler & Magdaleno, 1991).

Thus, the use of antioxidants to prevent such damage induced by UV irradiation has received much attention recently. One such antioxidant, which has the potential to be incorporated into sunscreens, is the pineal secretory product, melatonin. One of the concerns of using melatonin in sunscreens is its photo-instability (Maharaj *et al*., 2002) which was demonstrated in chapter six. In chapter eight, section 8.5, it was demonstrated that the protection of rat skin homogenate with melatonin prior to irradiation resulted in a decrease in $O_2^{\bullet-}$ generation. Thus, the basis of the present study is to provide evidence that the irradiation of rat skin homogenate with UV light results in an increase in peroxidation of the skin lipid layers, and to determine if the protection of rat skin homogenate with melatonin prior to exposure with UV light, results in a decline in lipid peroxidation.

10.6.2. MATERIALS AND METHODS

10.6.2.1. Sample Preparation

Stock solution of 0.1 mg/ml of melatonin was prepared by dissolving 40mg of melatonin in 400ml of a mixture of absolute ethanol and water. The final concentration of ethanol in the incubation samples was 0.5%.

10.6.2.2. Rat Skin Removal and Homogenate Preparation

Male Wistar rats were used for these experiments and housed according to the conditions described in appendix one. The rats were sacrificed swiftly by cervical dislocation and rapidly decapitated and the skin was removed as described in appendix two. A 2% rat skin homogenate was prepared according to the method described in section 8.5.2.2.

10.6.2.3. UV Irradiation Studies

Rat skin homogenate in the absence and presence of melatonin (0.1 mg/ml) was placed in the immersion-well photoreactor and irradiated continuously with a 400-W high pressure mercury lamp (figure 6.1), emitting over the UV/Vis range (300-575nm) with maximum irradiance in the UVA at 365nm and 565nm in the visible region, for 90 minutes, whilst bubbling air through the solution, at ambient temperature as described in chapter six, section 6.2. All irradiations were stopped at 90min, as previous results showed that 0% of melatonin was present in solution after 90min of irradiation (chapter six, section 6.2). Aliquots of 5mL were removed periodically at predetermined time intervals and analyzed for free radical scavenging properties.

The lipid peroxidation assay preformed as described in section 10.2.2.9. Briefly, the lipid source viz. rat skin homogenate (1mL) alone or in combination with melatonin at the different time intervals of UV irradiation was incubated with BHT and TCA in a boiling water bath for 15min. Thereafter the procedure described in section 10.2.2.9 was followed.

All results were analyzed to show statistical significance as described in section 10.2.2.10. Final results were expressed as nmoles MDA/mg tissue.

10.6.3. RESULTS

The irradiation of 2% w/v rat skin homogenate using an immersion-well photoreactor resulted in a time-dependent rise in the production of lipid peroxidation products (figure 10.13). As shown in figure10.13, the marked rise in lipid peroxidation in the rat skin homogenate for each irradiation time interval was significantly higher compared to the control value (rat skin homogenate that was not irradiated). After 90min of irradiation the level of lipid peroxidation product increased by ±80% in comparison to the control value.

However, the co-treatment of rat skin homogenate with melatonin (0.1 mg/ml) prior to irradiation significantly reduced the lipid peroxidation levels at each consecutive time interval in comparison to the rat skin homogenate without melatonin as is evident in figure 10.14. The melatonin at time 90 min of irradiation was able to inhibit the rise in lipid peroxidation by ±55%. Furthermore, as is evident in figure 10.14, in the melatonin treated rat skin homogenate, there is no significant increase in levels of lipid peroxidation above irradiation time of 20mins, implying that melatonin offered equipotent protection against UV-induced rise in MDA.

10.6.4. DISCUSSION

Currently sunscreens are widely used to prevent acute solar damage to skin and if used on a daily basis, should significantly reduce the incidence of the chronic photodamaging events.

Chronic exposure of skin to ultraviolet radiation produces multiple deleterious responses including photoaging (Gilchrest, 1996). There is ample evidence that UV radiation produces toxic free radical intermediates, which are implicated in the pathogenesis of UV-induced skin damage. Under normal conditions the skin antioxidant defence mechanisms, which include SOD, are able to protect the skin. However, the generation of free radicals depletes the skin of these antioxidant defence mechanisms, rendering it

vulnerable to UV-induced oxidative stress (Gilchrest, 1996). Melatonin has been shown to increase the activity of SOD and this contributes to its antioxidant activity (Antolin *et al*., 1996).

Free radical scavengers have become increasingly popular as a means of reducing or preventing the hazardous effects of free radicals and their inducers. Melatonin, the principal antioxidant of the pineal gland, now known to be a potent free-radical scavenger at physiological concentrations (Tan *et al*., 1993a; Daya, 1999), is an ideal candidate for scavenging such radicals. This agent is produced by the pineal gland in mammalian brains, predominantly at night (Sasaki *et al*., 2000). It is not stored in the pineal but released into circulation and due to its lipophilicity, is rapidly distributed to all tissues where it has been proposed to act as a free radical scavenger.

The results of the present report show that exposure of rat skin homogenate to UV irradiation induces a time-dependent increase in lipid peroxidation levels. However, this phenomenon is significantly reduced when the homogenate is exposed to UV light in the presence of melatonin. Melatonin was shown to rapidly disappear in the presence of UV light (Maharaj *et al*., 2002), with no melatonin left in solution after 90min of irradiation as shown in chapter six. However, the results of this assay demonstrate that melatonin offers equipotent protection against UV-induced lipid peroxidation at all time intervals of irradiation. The ability of irradiated solution of melatonin to scavenge free radicals and curtail the damaging properties of these agents can be attributed to its photodegradants which arise on exposure of melatonin to UV light. These photoproducts have been shown to be equally potent as melatonin as free radical scavengers (Maharaj *et al*., 2002). Bangha *et al*., (1997) demonstrated a dose-dependent suppression of UV-induced erythema by topical melatonin treatment in a human study. Since melatonin, which is not metabolized in human skin (Lee *et al*., 1994), does not absorb UVA or UVB, a direct sunscreen effect of this indoleamine can be excluded. Therefore, excluding a sunscreen effect, its protection can be attributed to its known antioxidant properties. Among the various types of free radicals, the $^{\bullet}OH$ is known to have the highest noxious potential and to be implicated in the sunburn reaction of the skin (Taira *et al*., 1992; Masaki *et al*., 1995). Several *in vitro* and *in vivo* studies have shown that melatonin acts as a highly potent free radical scavenger (Ianas *et al*., 1991; Hardeland *et al*., 1993; Pierrefiche *et al*.,

1993; Reiter *et al*., 1994), most probably by quenching these $^{\bullet}OH$ (Poeggeler *et al*., 1994). Thus, topical application of melatonin most likely reduces the number of acutely generated $^{\bullet}OH$.

It is known that during UV radiation of the skin, the skin's antioxidant defence is compromised. A decline in catalase and GPx activities is noted (Shindo *et al*., 1993). These enzymes, as discussed in chapter eight, section 8.6, and figure 8.14, are assigned the function of metabolizing H_2O_2 and thereby reducing the formation of the devastatingly toxic $^{\bullet}OH$. Melatonin has been shown to stimulate the activities of these enzymes (Okatani *et al*., 2001; Reiter *et al*., 2000b) and thereby promote the destruction of the $^{\bullet}OH$. This indirect antioxidative action of melatonin could certainly magnify its protective function in the skin.

Besides its antioxidant properties, melatonin is also known to modulate arachidonic acid metabolism (Franchi *et al*., 1987; Martinuzzo *et al*., 1991). Interactions with the eicosanoid system may result in an anti-inflammatory effect and thus complement antioxidative photoprotection in skin (Dreher *et al*., 1999).

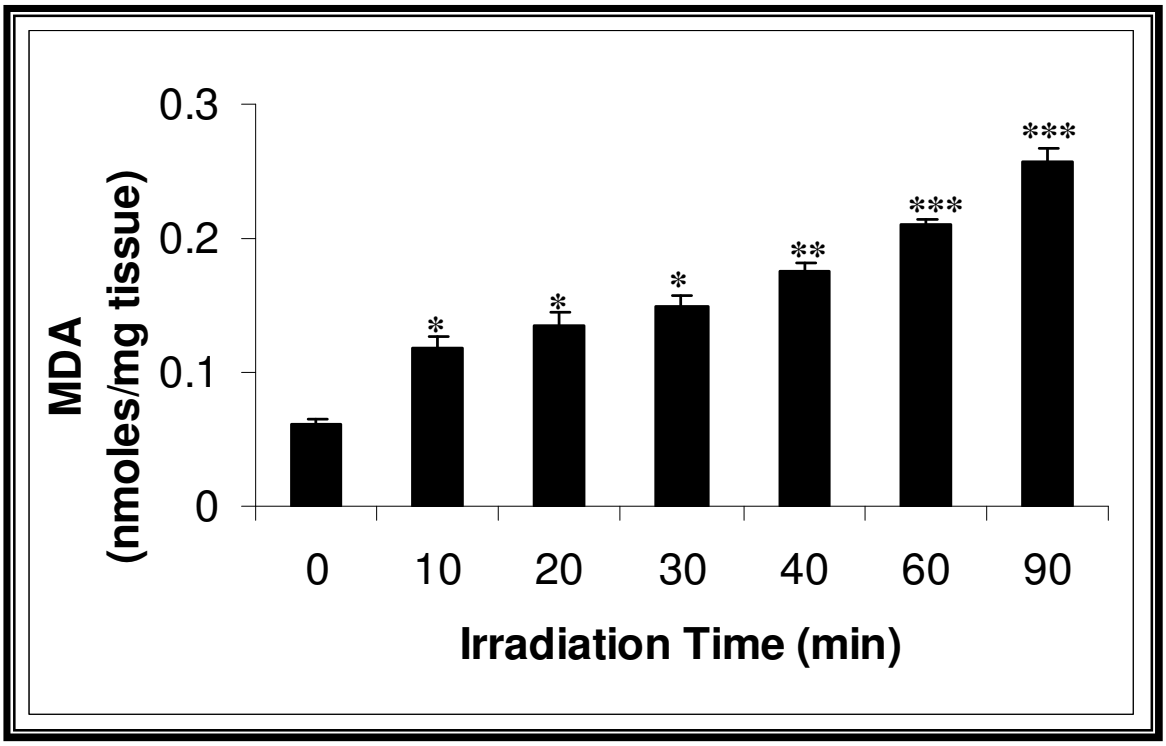

Figure 10.13: The effect of increase in UV-irradiation time on lipid peroxidation formation in rat skin homogenate. Each bar represents the mean ± SEM of five determinations. *($p<0.05$) 10-30 min irradiation time versus zero time; **($p<0.01$) irradiation time 40 mins versus zero time; and ***($p<0.001$) irradiation time 60 and 90 mins versus zero time. (Student Newman-Keuls Multiple Range Test).

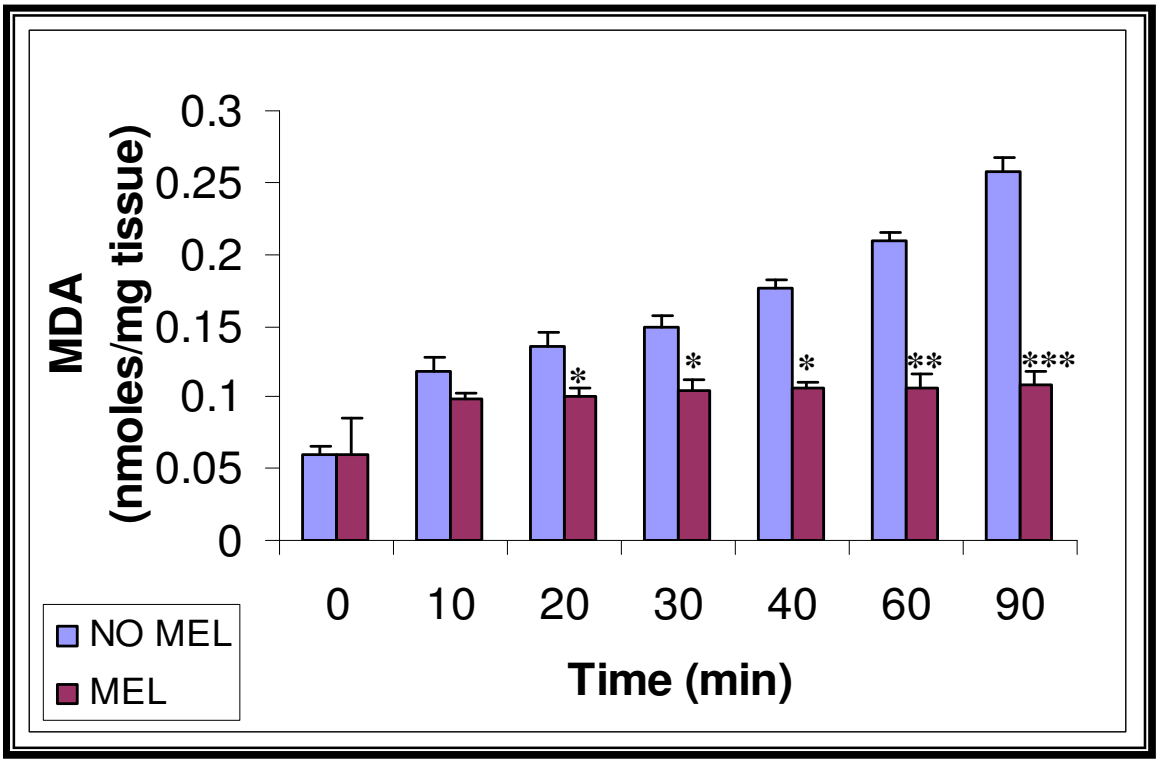

Figure 10.14: The effect of increase in UV-irradiation time on lipid peroxidation formation in rat skin homogenate in the presence of melatonin. Each bar represents the mean ± SEM of five determinations. *($p<0.05$); **$p<0.01$ and ***$p<0.001$ MEL versus NO MEL for each respective irradiation time interval. (Student-Newmans-Keuls Multiple Range Test).

10.7. CONCLUSION

Free radical damage has been implicated in a wide variety of diseases and in experimental models of a diverse range of these conditions, melatonin has been shown in all cases to be protective (Reiter, 1998; Reiter *et al*., 2002). Examples of situations in which melatonin has been found to lower the induced oxidative damage include; heavy metal toxicity such as Fe^{2+}, excitotoxin toxicity such as QA (Southgate *et al*., 1998; Southgate, 1999) exposure to UV radiation (Bangha *et al*., 1996), iron administration (Lin & Ho, 2000; Shamir *et al*., 2001). Each of these is believed to involve, as part of the destructive processes, free radical damage to essential macromolecules. Given the virtual absence of toxicity of melatonin (Reiter *et al*., 2002), reports of its use in humans to combat free radical damage will probably continue to appear. However, a major concern surrounds the fact that melatonin rapidly degrades in the presence of UV light and that it interacts with free radicals to produce a number of stable metabolites. 6-OHM has been shown to be a photoproduct and a metabolite of melatonin when it reacts with hydroxyl

radicals in the body (Horstman *et al.*, 2002). Furthermore, melatonin reduction of free radical induced lipid peroxidation in rat skin homogenate could be attributed not only to its free radical scavenging ability but also due to its interference with arachidonic acid metabolism, which leads to lower concentrations of prostaglandins and leukotrienes (Franchi *et al.*, 1987; Martinuzzo *et al.*, 1991). These agents have been recognised as having a role to play in UV-induced skin damage (Bissett *et al.*, 1990a, b; Anderson *et al.*, 1992). Thus, melatonin by diminishing the local concentration of these agents may result in suppressing erythema formation.

6-OHM is a main enzymatic metabolite of melatonin produced in the liver (Reiter, 1991). It has been claimed that this main photodegradation product of melatonin (Maharaj *et al.*, 2002) may be more potent than melatonin in inhibiting lipid peroxidation (Pierrefiche *et al.*, 1993; Hara *et al.*, 1997). Matuszak *et al.*, (1997), however, reported that this hydroxylated indole, in contrast to non-hydroxylated melatonin functions both as an $^{\bullet}OH$ scavenger and $^{\bullet}OH$ promoter. However, 6-OHM which is a metabolite formed when melatonin interacts with $^{\bullet}OH$ (Tan *et al.*, 2000b), in the system described by Qi *et al.*, (2000), was found to oxidative damage to purified DNA possibly by scavenging the $^{\bullet}OH$. However, its IC_{50} was found to be 1.00 μM, which was twice that of melatonin. The findings of this chapter support the above and confirm that 6-OHM is a potent $^{\bullet}OH$ radical scavenger with equipotent free radical scavenging properties as melatonin. Furthermore, in the present study, 6-OHM was shown to completely inhibit lipid peroxidation induced by QA and cyanide and partially reverse the peroxidation induced by Fe^{2+}. However, the present results show that melatonin remains a superior $^{\bullet}OH$ radical scavenger generated via the Fenton reaction than 6-OHM. The structure of these indoleamines plays a role of a buffer towards ROS forming stable indolyl radicals with them at the level of the pyrrole ring. It is of interest to note, as did Syh Tse *et al.*, (1991) that hydroxylation of the structures involved generally increases their antioxidant power significantly, whereas dehydrogenation produces the opposite effect. Pierrefiche *et al.*, (1993) demonstrated in their model, the high antioxidant power of 6-OHM in comparison to melatonin. Thus, it is speculated that the antioxidant properties of melatonin *in vivo*, can not be explained exclusively by its indole structure and suggests the possibility that melatonin combines an intrinsic antioxidant activity *in vivo* with that of 6-OHM. This hypothesis is supported by the short half-life of melatonin in organisms is 20-30 min and

that it is rapidly converted to 6-OHM (Raynaud *et al*., 1993; Liu *et al*., 2001). In addition Reiter and Tan (2003) suggest that even when melatonin itself is metabolically converted to 6-OHM before it can function in the direct detoxification of a radical(s), its major hepatic metabolic product may be capable of doing so.

It is thus postulated that 6-OHM possibly acts on the NMDA receptors and inhibits QA from binding. Another mechanism of action of 6-OHM is the possibility that it binds to Fe^{2+}, thus preventing the QA-Fe^{2+} complex from forming which is essential for QA induction of lipid peroxidaiton. Furthermore, by binding to Fe^{2+} it prevents it from taking part in the Fenton reaction and producing $^{\bullet}OH$ radicals. Since, 6-OHM is the chief hepatic metabolite of melatonin in the rat, the antioxidant effect of melatonin *in vivo* could be attributed in part to 6-OHM. 6-OHM is reportedly 30-fold more potent than melatonin in inhibiting lipid peroxidation (Pierrefiche *et al*., 1993). However in the above experiments, 6-OHM prevents lipid peroxidation in the brain with the same or slightly lesser potency than melatonin. Furthermore, melatonin has been shown to protect against UV-induced damage to the rat skin homogenates, thus providing further evidence supporting the use of melatonin in sunscreens.

Anti-inflammatory agents, antioxidants, and free radical scavenging agents and iron chelators, are all known to inhibit UV induced changes in mouse skin. Melatonin possesses all of the above characteristics, thus making it a useful agent to reduce and even inhibit UV-induced skin damage.

Considering previous investigations (Reiter, 1995a,b,c; Reiter *et al*., 1998a,b; Southgate *et al*., 1998; Maharaj *et al*., 2003a; b) as well as the results presented in the present study with regard to the neurological protection of MEL and 6-OHM, their ability to readily penetrate the BBB and melatonin's wide margin of safety, both these agents may find utility as pharmacological agents in preventing and treating neurological disorders in which free radical formation is a pathogenic factor (Reiter, 1998).

CHAPTER FOURTEEN

HEAT SHOCK PROTEIN STUDIES

14.1. INTRODUCTION

Organisms ranging from bacteria to plants and humans respond to hyperthermia or a variety of other stresses, e.g. heavy metals, free radical, amino acid analogues, ethanol, by the preferential synthesis of a group of highly conserved proteins referred to as the heat shock proteins (Hsp's) (Lindquist, 1986). Hsp's have basic and indispensable functions in the life cycle of proteins as molecular chaperones as well as protecting cells from deleterious stresses (Bechtold *et al*., 2000; Lindquist, 1986) and are known for increasing the ability of cells to recover from the toxic effects of heat and/or other physiological stresses. Molecular chaperones are able to inhibit the aggregation of partially denatured proteins and facilitate their refolding to the native state as shown in figure 14.1. It is suggested that Hsp's might bind to denatured or abnormal proteins produced by stress and aid in their elimination (Finley *et al*., 1984). Hsp's are also present in the absence of stress; they have further been hypothesized to play a role in the normal assembly and disassembly of proteins (Pelham, 1986) and serve as an indicator by which the extent of cellular stress is monitored (Craig & Gross, 1991). It has been shown that an enhanced expression of Hsp's can confer tolerance against stress in a variety of cell types, while their insufficient expression makes the cells vulnerable to stress, supporting the concept that Hsp's play a protective role against irreversible cell damage (Johnston & Kucey, 1988; Lavoie *et al*., 1993; Parsell & Lindquist, 1993; Riabowol *et al*., 1988; Sanchez *et al*., 1992). Some Hsp's are expressed constitutively in unstressed cells in which they act as molecular chaperones that play pivotal roles not only in folding/unfolding, assembly/disassembly, and translocation of cellular proteins but also in preventing inappropriate protein-protein interactions during maturation of the cellular protein structures (Gething & Sambrook, 1992; Hartl, 1996).

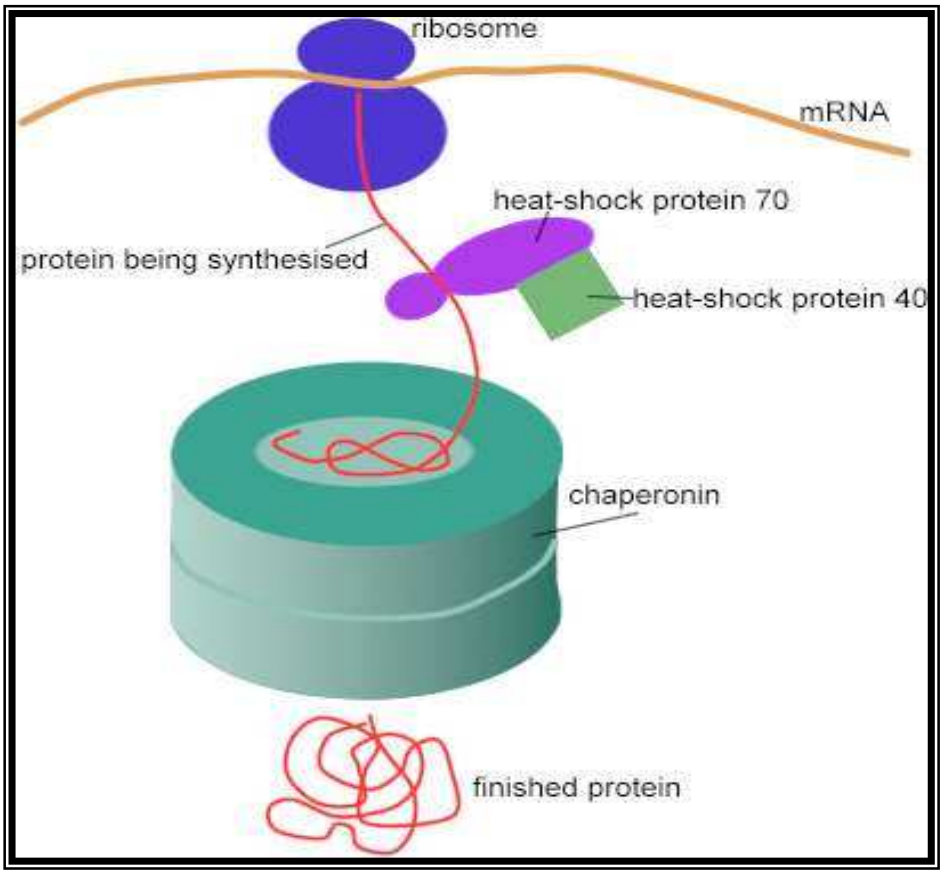

Figure 14.1: Diagram showing the role of heat-shock proteins and a chaperonin in protein folding. As the ribosome moves along the molecule of messenger RNA, a chain of amino acids is built up to form a new protein molecule. The chain is protected against unwanted interactions with other cytoplasmic molecules by heat-shock proteins and a chaperonin molecule until it has successfully completed its folding. www.nurseminerva.co.uk/ chaperon.htm.

Amongst these chaperones, the most frequently studied Hsp is the group of proteins of approximately 70kDa comprising the Hsp 70 gene family. Hsp 70 has received a lot of attention due to its role in the central nervous system. Hsp 70 is a prominent cytoprotective factor: its down regulation is sufficient to kill tumour cells or to facilitate the induction of apoptosis (Nylandsted *et al*., 2000; Burkart *et al*., 2000). Hsp70 has been reported to block apoptosis by binding apoptosis protease activating factor-1 (Apaf-1), thereby preventing the constitution of the apoptosome, the Apaf-1/cytochrome/caspase-9 activation complex (Saleh *et al*., 2000; Beere *et al*., 2000). Hsp70 has two major members, Hsp70, an inducible form and the heat shock cognate protein Hsc70, a constitutively expressed form. Hsp70 inducible is not expressed under unstressed conditions (Suzuki, *et al*., 1999), but is induced after brain hyperthermia. In contrast,

Hsc70 expression remains unchanged. Recently, Hsc70 was found to play a role in the CNS and has been found to be localized to the synapse, indicating a synaptic role for this molecular chaperone (Ohtsuka & Suzuki, 2000).

Furthermore, Hsp70 has been shown to protect the brain and heart from severe ischemia (Carroll & Yellon, 1999; Chopp, *et al*., 1989). This together with its role in protein refolding has resulted in several reports implicating Hsp70 for protection against and therapeutic treatment of inherited diseases caused by protein misfolding.

Recently, the cytoprotective functions of Hsp's in stress tolerance and neurodegenerative diseases are being investigated (Ohtsuka & Suzuki, 2000). Kainic acid (KA) a powerful seizure-producing analogue of glutamate (Olney *et al*., 1974) has been shown to produce neuronal expression of Hsp70 protein in various regions of the rat brain including the hippocampus (Armstrong *et al*., 1996; Sloviter & Lowenstein, 1992; Gonzalez *et al*., 1989; Longo *et al*., 1993). The Hsp70 positive neurons occur in regions that are known to be damaged by KA induced seizures in the rat brain (Armstrong *et al*., 1996; Ben-Ari, 1985). Ischemic injury caused by occlusion of the right middle cerebral artery in the rat brain caused neuronal and glial expression of Hsp 70 protein in an around areas of infarction (Gonzalez *et al*., 1989; Kinouchi *et al*., 1993). Thus neurons express detectable levels of Hsp70 protein after some forms of injury.

14.2. THE EFFECT OF MELATONIN, 6-OHM AND QA ON THE LEVEL OF HSP-70 IN THE RAT HIPPOCAMPUS

14.2.1. INTRODUCTION

While the name is derived from their response to heat stress, the heat shock proteins are induced by a variety of cellular stresses (Lindquist & Craig, 1988; Schlesinger *et al*., 1982). They appear to play a protective role in responding to these stresses and may also function to protect cells against subsequent challenges (Finley *et al*., 1984; Gershon & Rott, 1988; Barbe *et al*., 1988). Authors Gonzalez *et al*., (1989) found that there is an increase in Hsp72-positive cells due to injury by KA or ischemia and suggests that Hsp72 immunohistochemisty may be a useful cellular marker of trauma or injury in the brain. This conclusion is supported by the following fact a) Hsp's are stress indicators in a wide variety of cells (Lindquist, 1986), b)the induction of Hsp's in the brain by ischemia and trauma has been demonstrated biochemically (Currie & White, 1981). c) In some systems the Hsp synthesis is proportional to the degree of stress (Lindquist, 1986).

QA has been shown to induce lipid peroxidation in the rat brain *in vivo* and *in vitro*, and as a result destroys biological membranes. Subsequently, membrane proteins are also affected. Since heat shock proteins, and in particular, Hsp70 are induced in response to any stress that perturbs protein structure, it follows that the level of Hsp70 should increase in response to QA-induced neurodegeneration. Furthermore, Qin *et al*., (2001) showed that an intrastriatal injection of QA causes a rise in both Hsp72 and Hsp70 expression in rat brain.

The hippocampus is involved in memory formation and thus any damage to these neurons would have deleterious effects on learning and memory and could lead to various types of dementia. In view of the previous experiments, which have shown that 6-OHM protects against QA-induced neuronal damage, the present study was performed to investigate a further possible mechanism for this protection at the molecular level. Melatonin has been shown to protect against QA-induced oxidative neurotoxicity (Cabrera *et al*., 2000).

However to date no work has been done on the effect of melatonin on Hsp70 expression. Thus, it was decided to analyze the level of Hsp70 expression in hippocampal neurons, in response to treatment with QA alone, MEL alone, 6-OHM alone and the combination of each drug with QA using Western analysis.

Western analysis is more commonly referred to as immunoblotting. The principle of this technique is simple: protein, which is separated in a gel by means of electrophoresis, is extracted from the gel by means of diffusion, transport of solvent or electrophoresis and transferred to a solid surface. This is usually a membrane, which is permeable to molecules of the solvent and proteins. Despite the fact that the membrane is permeable, protein molecules will bind to the surface of the membrane until all binding sites are occupied. These can easily be reached by other molecules so that reactions, such as immune reactions, are possible.

14.2.2. MATERIALS AND METHODS

14.2.2.1. Chemicals and Reagents

Sodium dodecyl sulphate (SDS) was purchased from BDH Chemicals, Poole, England. Quinolinic acid (QA), melatonin (MEL), 6-hydroxymelatonin (6-OHM), N,N,N,N-tetramethylethylenediamine (TEMED), N,N-methylene-bis-acrylamide, acrylamide, Ponceau S, Monoclonal Anti-Heat Shock Protein 70 (Anti HSP70 antibody) and horseradish peroxidase conjugated secondary antibody were purchased from Sigma, St. Louis, U.S.A. Broad range SDS-PAGE Molecular Weight Standards (pre-mixed) was purchased from BIO-RAD, California, U.S.A. Hybond-C Extra Nitrocellulose (for protein transfer) was purchased from Amersham. BM Chemiluminescence Western Blotting Kit (Mouse/Rabbit) was purchased from Roche, Indianapolis, U.S.A.

14.2.2.2. Animals

The rats used in the experiment were cared for as described in appendix one

14.2.2.3. Surgical Procedures and Dosing

Male rats were used for the experiment and were separated into 5 groups as shown in Table 14.1. The treatment regime was the same as that described in section 8.5.2.4. Stereotaxic procedures were followed as described in section 2.5.2.5.

Table 14.1. Treatment regime for the determination of HSP 70 levels.

Group	Daily s.c. injection for 7 days	Intrahippocampal injection of:	Daily s.c. injection for 7 days
MEL	100µg Melatonin in 100µL PBS	2µl PBS	100µg Melatonin in 100µL PBS
6-OHM	100µg 6-OHM in 100µl PBS	2µl PBS	100µg 6-OHM in 100µl PBS
QA	100µl PBS	240nmol QA in 2µl PBS	100µl PBS
QA + MEL	100µg Melatonin in 100µL PBS	240nmol QA in 2µl PBS	100µg Melatonin in 100µL PBS
QA + 6-OHM	100µg 6-OHM in 100µl PBS	240nmol QA in 2µl PBS	100µg 6-OHM in 100µl PBS

14.2.2.4. Tissue Preparation

The rats were sacrificed, the brains removed and the hippocampii dissected as described in sections 8.2.2.5. and 8.5.2.7., respectively. The hippocampii were homogenized in lysis buffer containing: 50mM Tris-HCl pH 8, 150mM NaCl, 0.02% Sodium azide, 100µg/ml phenylmethylsulphonylfluoride (PMSF), 1µg/ml Aprotinin and 1% Triton X-100. The lysates were centrifuged at 13000 x g for 20min and the supernatant carefully removed. Total protein concentration of the homogenate was determined as described in appendix two. Equal volumes of the lysate and protein sample treatment buffer were mixed and heated for 3-5min at 95°C. Sample treatment buffer contained: 100mM Tris-HCl pH 6.8, 5% β-mercaptoethanol, 4% SDS, 0.2% bromophenol blue, 20% glycerol.

14.2.2.5. SDS-Polyacrylamide Gel Electrophoresis

The lysate together with a positive control (NIH 3T3 Mouse fibroblast cell extract) was resolved on a 12% sodium dodecyl sulphate polyacrylamide gel electrophoresis (SDS

PAGE) using a Biorad PAGE apparatus (figure 14.2). A positive control is used as a guide to determine where the Hsp70 band should be in the samples. The gels were prepared according to Table 14.2 and allowed to set for 20 minutes at room temperature. Samples were loaded as in Table 14.3 and run in 1 x SDS electrophoresis buffer containing 3.02 g Tris-base, 18.8 g glycine, 2 g SDS in 1 litre. The sample was run at 80 V for 2 hours after one gel was stained with Coomassie brilliant blue stain (0.25% Coomassie Blue, 50% methanol, 7.5% glacial acetic acid) and the other gel was transferred onto nitrocellulose membrane. The gel was stained for 2-3 hours and destained in a solution containing 20% methanol and 7.5% glacial acetic acid.

Table 14.2. Preparation of a 12% SDS PAGE Gel

Reagents	Running Gel (12%)	Stacking Gel (5%)
Distilled water	4.9 ml	4.1 ml
30% Acrylamide mix	6.0 ml	1.0 ml
1.5 M Tris-HCl, pH 8.8	3.8 ml	-
1.0 M Tris-HCl, pH 6.8	-	0.75 ml
10% SDS	0.15 ml	0.06 ml
10% Amm. Persulphate	0.15 ml	0.06 ml
TEMED	0.006 ml	0.006 ml

Table 14.3. Loading of the samples for SDS-PAGE

Sample & Well No.		μg Protein	*Volume (μl)
MW marker	(1)	-	25
Melatonin	(2)	300	25
QA alone	(3)	300	25
6-hydroxymelatonin	(4)	300	25
6-hydroxymelatonin+QA	(5)	300	25
Melatonin + QA	(6)	300	25
Pos. control	(7)	250	25

* The volume was calculated according to the protein concentration that was measured.

14.2.2.6. Western Blotting Analysis

Transfer buffer containing 25mM Tris base, 192mM glycine and 20% methanol was prepared and allowed to chill until use. Sheets of 3MM Whatmann filter paper and the nitrocellulose membrane were cut to the size of the SDS PAGE gel and soaked in ice cold transfer buffer for 30min to equilibrate. The SDS PAGE gel was carefully removed from the glass plates, the stacking cut off and the remaining gel placed in ice-cold transfer

buffer to equilibrate. The sandwich for the western transfer was constructed as follows: 2 sheets of 3MM Whatmann filter paper placed on a Scotchbrite fibre pad, the nitrocellulose membrane placed on top followed by the gel and finally the other 2 sheets of Whatmann paper and the fibre pad respectively. The sandwich was placed into the transfer panel with the nitrocellulose facing the anode and the gel facing the cathode. The cooling block was inserted and the tank filled with transfer buffer. The transfer was done at 100 V for 1 hour.

At the end of the run, the sandwich was dismantled and the nitrocellulose membrane was stained with Ponceau S (0.5g Ponceau S, 1ml glacial acetic acid in 100ml water), to visualize the protein. The membrane was stained for 5min, scanned and thereafter destained by rinsing in two washes of Tris-buffered saline (TBS) pH 7.5.

The membrane was blocked with 5% non-fat milk powder in TBS and left at 4°C overnight. The block was removed and the membrane incubated with primary antibody (Anti HSP70 antibody) (1:5000 in block) for 1 hour before washing twice in TBS each for 20 min. Thereafter, another two washes in block followed before incubating with the horseradish peroxidase conjugated secondary antibody (1:1250 in block) for 30 min. Finally, the membrane was washed four times with TBS-tween 20 for 15 min each before developing it.

All developing stages were performed in a dark room. After the last wash, the TBS-tween 20 was decanted and substrate added and left to incubate for 60 seconds. The membrane was transferred to a X-ray film cassette and cling wrap neatly placed on top. A piece of X-ray film was carefully placed on top of the cling wrap and the cassette closed tightly. The film was exposed to the blot for 15 min. Finally, the film was placed in developer for 3 min, then passed through the stop solution and transferred to the fix solution for 2min before rinsing under tap water and hung to dry.

14.2.3. RESULTS

The Coomassie-stained gel is shown in figure 14.2. It is evident from this that the SDS-PAGE was successful in separating out the various proteins present in the hippocampal homogenate within the molecular weight range shown. The arrow shown in figure 14.2 and 14.3 on the positive control lane indicates the Hsp70 band.

The Ponceau S stain of the nitrocellulose membrane confirmed the successful transfer of proteins from the SDS PAGE gel to the nitrocellulose membrane (figure 14.3).

Figure 14.4 shows the immunoblots of the western transfer. Hsp70 expression in the treated groups and the positive control is evident (figure 14.4.) indicating that there was successful transfer of the Hsp70 protein from the nitrocellulose membrane to the X-ray film. It is evident by the signals obtained, that all four treatments groups (i.e. MEL, QA, 6QA and MELQA) displayed expression of Hsp 70. However, an increase in the amount of Hsp70 is evident in respect to the control and untreated group were the basal hippocampal levels of Hsp70 were undetectable. The band for QA appears to be larger than that obtained for the MEL alone and MELQA treatment groups. The stronger the signal, the higher the level of Hsp70 in the hippocampal tissue used. However as is evident in figure 14.5, the signal for the Hsp70 expression is much stronger for 6 alone and the 6QA treatment groups in comparison to the QA alone treatment group.

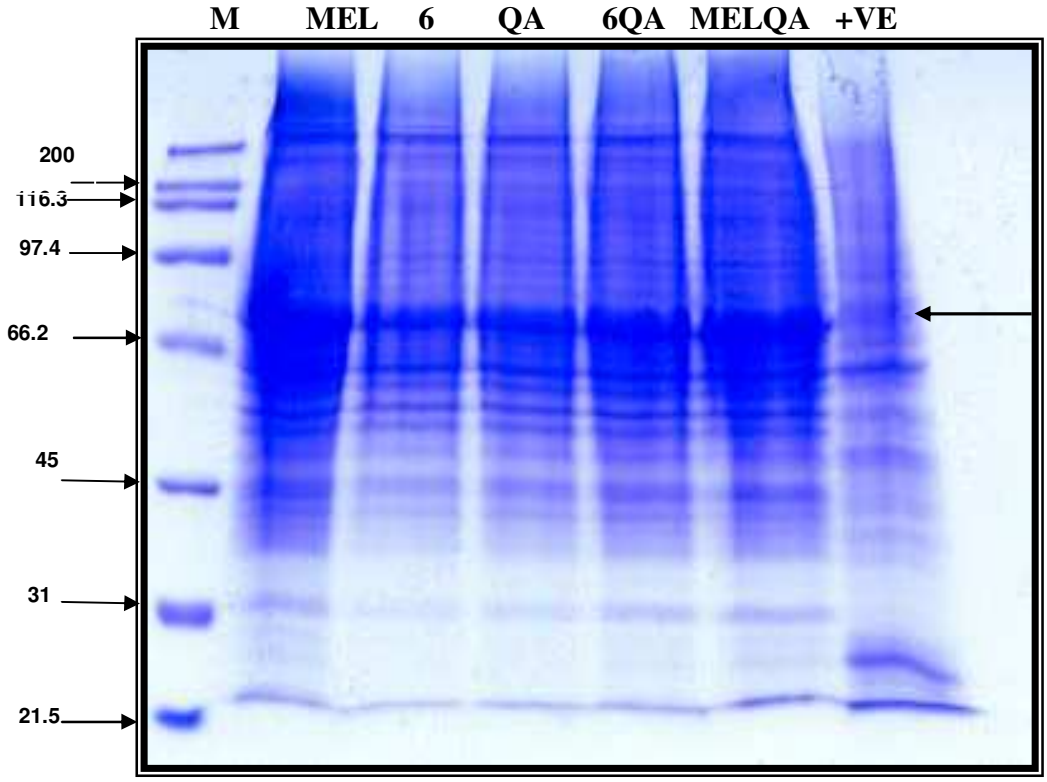

Figure 14.2: The gel stained with Coomassie stain, illustrating successful separation of proteins. (Molecular weights alongside are in kDa) M = Biorad broad range SDS PAGE enzyme molecular weight marker, MEL = Melatonin alone group, 6= 6-OHM alone group, QA = QA alone group, 6QA = 6-OHM and QA combined, MELQ = Melatonin and QA combined, and +VE = positive control (NIH 3T3 Mouse fibroblast cell extract).

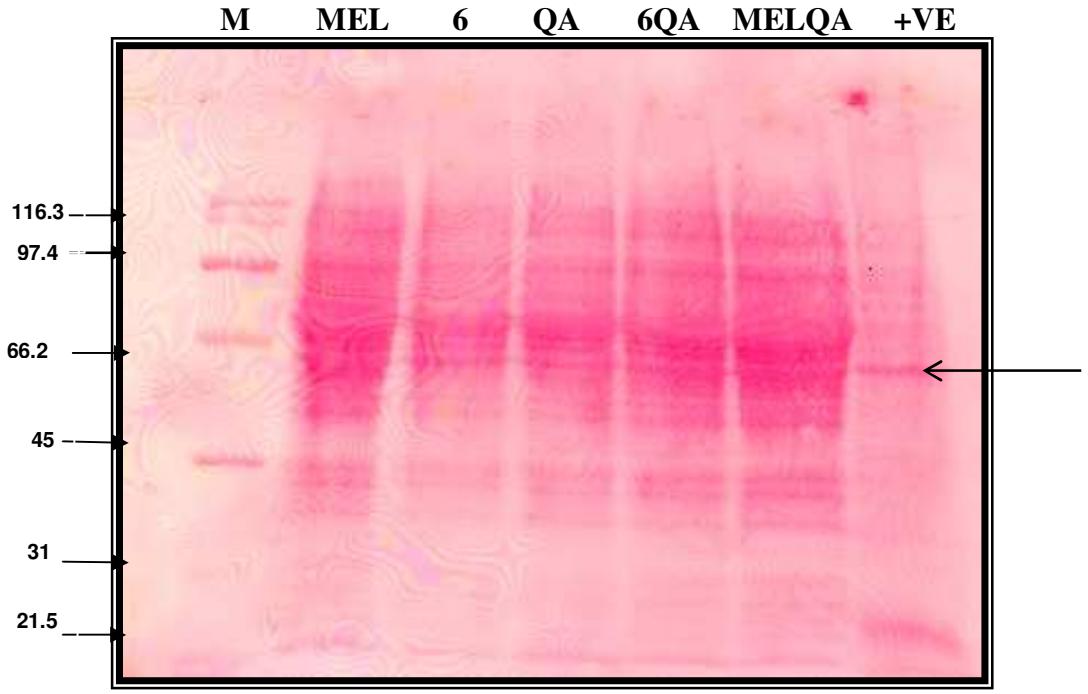

Figure 14.3: The membrane stained with ponceau stain (Molecular weights alongside are in kDa) M = Biorad broad range SDS PAGE enzyme molecular weight marker, ML = Melatonin alone group, 6= 6-OHM alone group, Q = QA alone group, 6Q = 6-OHM and QA combined, MLQ = Melatonin and QA combined, and +VE = positive control (NIH 3T3 Mouse fibroblast cell extract)

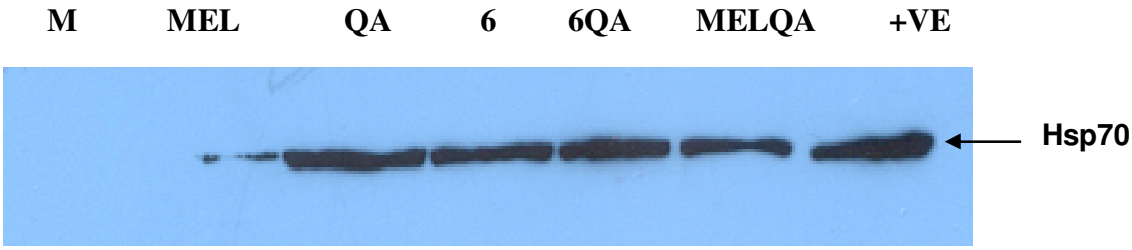

Figure 14.4: Western analysis to detect Hsp70/Hsc70 in the various treatment groups. M = Biorad broad range SDS PAGE enzyme molecular weight marker, MEL = Melatonin treated group, 6= 6-OHM alone group, Q = QA alone group, 6Q = 6-OHM and QA combined, MLQ = Melatonin and QA combined, and +VE = positive control (NIH 3T3 Mouse fibroblast cell extract).

14.2.4. DISCUSSION

Hsp's are produced by all prokaryotic and eukaryotic cells in response to heat stress and other noxious stimuli (Lindquist & Craig, 1988). Neurons express a detectable level of Hsp70 protein after some forms of injury such as damage caused by the excitotoxin, QA

(Qin *et al*., 2001). The results of the western blotting show that the level of Hsp70 in the hippocampus increases in response to treatment with QA. This was expected since Hsp70 is expressed when the cell is under stress such as that resulting from free radical attack, which is initiated by QA-induced damage. This evidence is supported by authors Qin *et al*., (2001) who demonstrated that QA levels increase after intrastriatal injection of QA. Authors Gonzalez *et al*., (1989) showed that Hsp72 levels increase in response to neuronal damage and thus hsp's can be used as markers of neuronal injury and this further supports the increase in Hsp70 in rat hippocampal tissue due to QA.

One limitation of this study was that the antibody used was unable to indicate whether the Hsp70 induced by the various groups, were that for Hsp70 inducible or the Hsc70 constitutive form, since the antibody detects both forms of this chaperone. However, this study gives an idea of whether Hsp70 is being expressed and thus we can conclude whether neuronal cells are under stress.

A slight increase in the level of Hsp70 in response to treatment with melatonin is noted and this could be due to the fact that Hsp's are also present in the absence of stress; they have been hypothesized to play a role in the normal assembly and disassembly of proteins (Pelham, 1986). Unfortunately it was not possible to quantify the exact level of expression of this chaperone protein, but from the thickness of the band it appears as though QA showed a significantly higher level of Hsp70 expression than that induced by melatonin. This is important as it indicates that melatonin treatment does not cause stress to the hippocampal neurons thus the lower expression of Hsp70. Melatonin was further able to protect the hippocampal neurons against QA-induced hippocampal damage as evident by the fact that a smaller Hsp70 band (i.e. a slightly thinner band is evident) is noted for the melatonin and QA treated group in comparison to the QA alone group. This would be expected as melatonin treatment was shown to protect the hippocampus against QA-induced neurotoxicity in *vitro and in vivo* and the level of protection was shown to be lower than that observed for basal control values (see chapter 10, section 10.5).

It was surprising that the control animals did not show any expression of Hsp70 since stress can be induced from the handling of the animals and the operating procedures (results not shown). However, an explanation for this could be that Hsp70 was indeed

expressed during these stressful times for the animals, but that the levels declined from the time of operating to the time of sacrifice, which was 7 days (Heron, 2002).

From the results presented in this chapter, it can be observed seen that melatonin administered alone causes a slight induction of Hsp 70; however this induction is minute in comparison to the expression caused by the administration of QA. Also melatonin treatment was able to decrease the QA-induced expression of Hsp70 and this indicates that melatonin is able to protect the hippocampal neurons in a manner that they do not need to express a large amount of Hsp70.

However, 6-OHM alone and in combination with QA resulted in overexpression of Hsp 70. The expression of Hsp 70 by 6-OHM is even more than that of the QA treated group, indicating that 6-OHM plays a role in causing some damage to the hippocampus. Another possibility for the increased expression of Hsp70 in response to 6-OHM treatment is that the result obtained actually represents Hsc70 expression. Hsc70 is the constitutively expressed form of Hsp70. Hsc70 chaperone protein has been reported to be involved in synaptic plasticity-related events; an electroconvulsive seizure induced Hsc70 mRNA but not Hsp70 (Kaneko *et al.*, 1993) and these authors also reported that Hsc70 could also be induced by synaptic activation. Chaperones localized at postsynaptic sites (including Hsc70) are involved in the mechanisms that activate AMPA receptors in the synapse during induction of long term potentiation (LTP) (Song *et al.*, 1998). Furthermore, Hsc70 is fundamental to synaptic transmission and plays a role in local protein synthesis at postsynaptic sites (Frydman *et al.*, 1994), which is essential for the maintenance of the already expressed synaptic plasticity, such as LTP and the consolidation process of memory (Tiedge & Brosius., 1996). However, further studies have to be conducted to prove the presence of Hsp70c.

The induction of Hsp's is a highly conserved, finely regulated, cellular defence mechanism against adverse environmental conditions (Sloviter & Lowenstein, 1992). More specifically, Hsp's induction has been associated with the protection of neurons against the injurious effects of heat shock and ischemia, probably mechanisms involving the inhibition of apoptosis (Rordorf *et al.*, 1991; Samaili & Cotter, 1996; Yenari *et al.*, 1998). Indeed, Hsp70 has neuroprotective effects against various insults including glutamate toxicity (Rordorf *et al.*, 1991). Overexpression of Hsp70 *in vivo* with viral

vectors protects striatal and hippocampal neurons from ischemia and KA induced damage (Yenari *et al*., 1998). Authors, Qin *et al*., (2001) showed that prostaglandin A_1 markedly increased the levels of Hsp70 and 72 in the rat striatum and this Hsp70 induction serves as an important mediator of the ability of prostaglandin A_1 to protect striatal neurons against excitotoxin-induced apoptosis (Mailhos *et al*., 1993). Taken together, these observations could suggest that 6-OHM could act to attenuate excitotoxic neuronal damage by increased induction of this highly conserved cellular defence mechanism of the body. Thus, Hsp70 induction may contribute to the protective effects of 6-OHM against QA-induced apoptotic cell death as evident in chapter thirteen.

14.3. CONCLUSION

Hsp's have attracted increasing attention in neuroscience because of their induction in the brain following a number of metabolic stressors including neuronal damage caused by excitotoxic agents such as KA or QA. Melatonin shows to be protective to hippocampal neurons by itself and in combination with QA as it decreases the rise in Hsp70 expression caused by QA.

It may be possible that 6-OHM induces the expression of both forms of Hsp70, but that the level of Hsc70 that is expressed in response to 6-OHM is much higher than the inducible form. The reason for this rationale stems from the fact, that although 6-OHM is implicated as a prooxidant (Matuszak *et al*., 1997), it is also a potent neuroprotectant, and thus if it was causing stress to such an extent then one wouldn't observe the protective effects against agents such as QA and the results seen in this chapter would then represent that for the inducible Hsp70. Another possibility is the fact that Hsp70 induction may contribute to the protective effects of 6-OHM as Hsp's protect neural cells from subsequent stress that would normally be damaging or lethal (Bechtold *et al*., 2000).

CHAPTER ELEVEN

IRON INTERACTION STUDIES

11.1. INTRODUCTION

Metallochemical reactions can be the underlying cause of free radical formation leading to disease. The highly reactive and biologically reactive hydroxyl radical can be formed in biological tissues when suitable transition metals are available. Lipid peroxidation is known to be initiated by any species that has sufficient reactivity to abstract a hydrogen atom from a methylene group of a polyunsaturated fatty acid in a membrane. Reactive species able to accomplish this include, the hydroxyl radical ($^{\bullet}OH$), the protonated form of the superoxide radical ($O_2^{\bullet-}$) and various iron-oxygen complexes (Halliwell & Gutteridge, 1989). Iron ions are themselves free radicals, which when added to a peroxide-free unsaturated lipid initiates peroxidation. However, it is extremely difficult to obtain a tissue fraction that is peroxide-free since lipid peroxides are formed enzymatically in tissues by cyclo-oxygenase and lipoxygenase enzymes. Thus, injured cells and membrane fractions isolated from disrupted tissue contain lipid peroxides. Consequently, brain homogenate, for example, is known to undergo lipid peroxidation much more rapidly than isolated intact brain (Halliwell & Gutteridge, 1989). Iron ions therefore are known to accelerate lipid peroxidation rather than initiate it. This occurs in the presence of certain iron complexes, which react with preformed lipid peroxides to produce alkoxyl and peroxyl radicals. These then initiate further damage in the propagation of lipid peroxidation.

Free radical generation in the brain is further assisted by the presence of large amounts of iron (Braughler & Hall, 1989; Halliwell, 1992), required by the Fenton reaction (Fahn & Cohen, 1992). Free iron and chelates of iron are involved in radical reactions at a number of different levels (Halliwell, 1992). The autooxidation of Fe^{2+} results in the formation of $O_2^{\bullet-}$. Conversely, the reduction of Fe^{3+} to Fe^{2+} by $O_2^{\bullet-}$ also occurs and competes with the dismutation of $O_2^{\bullet-}$ for available $O_2^{\bullet-}$. Thus, in theory, Fe^{2+} autoxidation could result in the redox cycling of iron due to the reaction of $O_2^{\bullet-}$ produced with Fe^{3+}. Furthermore,

Fe^{2+} is also oxidized in the presence of H_2O_2 (Fenton reagent) to from $^{\bullet}OH$ or ferryl ion (Fe^{3+}-OH). Both of these are very potent oxidants and will react with a wide range of biological substrates such as lipids, DNA and protein (Halliwell, 1992; Ottino & Duncan, 1997).

Iron accumulation in tissues is seen as one of the hallmarks of biological aging. In 1985, Massie *et al*., (1985) reported that the rate of iron accumulation inversely correlates with the life span in some species; this was recognized as strong evidence that iron accumulation has an adverse effect on aging. In addition, the involvement of iron toxicity in the aetiology/pathogenesis of AD has gained considerable attention (Lovell *et al*., 1998). Several studies have indicated imbalances of bulk iron (Samudralwar *et al*., 1995; Thompson *et al*., 1988) and iron at the microprobe level (Goodman, 1953; Switzer *et al*., 1986). The imbalances in iron, an element that participates in the generation of ROS (as shown in chapter ten and discussed above), is particularly significant in light of recent studies that indicate an increase in protein oxidation (Hensley *et al*., 1995), lipid peroxidation (Balazs & Leon, 1994; Lovell *et al*., 1995) and DNA oxidation (Meccoci *et al*., 1994) in the AD brain. Furthermore, iron also has been shown to induce aggregation of amyloid beta peptide (Aβ), but without fibril formation (Bush *et al*., 1995).

Stipêk *et al*., (1997) demonstrated that the ability of QA to induce lipid peroxidation is dependent on the presence of iron, in particular Fe^{2+}. These authors state that at concentrations between 0.015 mM and 1.5 mM, QA does not significantly increase lipid peroxidation in rat brain homogenates. However, paradoxically at higher concentrations of 3mM -15 mM, QA inhibits lipid peroxidation. This behaviour is attributed to the finding that QA forms a complex with Fe^{2+} and as a result chelates this iron, rendering it unavailable to play a role in lipid peroxidation (Stipêk *et al*., 1997). The complex between QA and Fe^{2+} has been reported to have a metal:ligand ratio of 1:2 and the overall formation constant to be 10^7, thus indicating a weak complex. Stipêk, *et al*., (1997), therefore suggest that the increase in lipid peroxidation observed in brain homogenate is due to the action of iron and not QA alone. However, other studies (Southgate & Daya, 1999; Rios & Santamaria, 1991) as well as those of the chapter ten have shown that QA at low concentrations does indeed cause a significant increase in lipid peroxidation but this is attributed to the presence of endogenous iron in the rat brain homogenate. Reasons for

this increased peroxidisability of damaged tissue include inactivation or dilution of some antioxidants as well as the release of metal ions (especially iron) from intracellular storage sites (Halliwell & Gutteridge, 1989). QA has been reported to increase lipid peroxidation in brain homogenate and this is dependent on the presence of iron, in particular, Fe^{2+} (Stipêk *et al*., 1997).

A Fe^{2+} complex reacts with lipid peroxide to generate Fe^{3+} and an alkoxyl radical. Halliwell (1992) showed the role of iron in the generation of free radicals and it is known that iron and its complexes stimulate membrane peroxidation (Halliwell & Gutteridge, 1989). Melatonin has been shown to play an important role in AD by its ability to bind Fe^{3+} but not Fe^{2+} (Limson *et al*., 1998). This is relevant to the Fenton reaction, in which Fe^{2+} generates the toxic hydroxyl radical and is oxidized to Fe^{3+}. It is for these reasons that it was decided to investigate the possible interaction between 6-OHM and Fe^{2+} or Fe^{3+} as a mechanism for 6-OHM's protection against lipid peroxidation induced by QA, which is known to complex Fe^{2+} and lipid peroxidation induced by Fe^{2+}. The formation of the complex between QA and iron Fe^{2+} may be the cause of QA's stimulatory action in increasing lipid peroxidation in rat brain homogenate. It has been shown by Sreejayan and Rao (1993), that Fe^{3+} ions stimulate the greatest amount of lipid peroxidation in comparison to Fe^{2+} ions. Thus, it was also decided to investigate the interaction between 6-OHM and Fe^{3+}. Three techniques were used to investigate the interaction between 6-OHM and Fe^{2+} or Fe^{3+}, namely, UV/VIS spectrophotometry, electrochemistry and HPLC.

11.2. INTERACTION BETWEEN 6-OHM AND Fe^{2+} AND Fe^{3+}: A UV/Vis AND HPLC STUDY.

11.2.1. INTRODUCTION

6-OHM has been shown as stable product when melatonin reacts with Fenton-type $^{\bullet}OH$ (Horstman *et al*., 2002). In chapter ten, it was established that 6-OHM is capable of protecting the rat brain in *vitro* and *in vivo* against QA and Fe^{2+}-induced lipid peroxidation. Furthermore in this chapter a mechanism of neuroprotection offered by 6-OHM was postulated to involve possible complexation of Fe^{2+} or Fe^{3+} ions by 6-OHM. Thus, absorption spectra in the near UV and Vis region were studied to observe the interaction of 6-OHM with Fe^{2+} and Fe^{3+} ions. UV spectroscopic studies were chosen as a starting point to observe any possible changes in the absorption spectra of Fe^{2+} and Fe^{3+} alone due to the addition of 6-OHM because of the relative simplicity of this method.

Spectroscopy involves the technique of measuring the absorption of a beam of light after it passes through a sample or after reflection from a sample surface. Ultraviolet and visible spectroscopy involves the energy absorbed by a transition from one electronic energy level to another. Any species with an extended system of alternating double and single bonds will absorb UV light, and anything with colour absorbs visible light, making UV-Vis spectroscopy applicable to a wide range of samples. Different chemicals may absorb light at different wavelengths so a qualitative analysis of an unknown chemical may be made by determining the absorption spectrum of that chemical. Any change in structure or composition of a compound will result in an electronic change, resulting in a change in the spectrum, either a shift in wavelength or a change in the extinction coefficient of the absorbance (Newman, 1969).

In addition, the spectra of metal-ligand interactions, such as metalloproteins and metalloenzymes, may also exhibit bands arising from 1) the d-d transitions of the metal ion, 2) ligand-to-metal charge transfer transitions (LMCT) involving the metal centre and surrounding ligands or 3) metal-to-ligand charge transfer bands (MLCT) also involving the metal centre and the surrounding ligands (Kendrick *et al*., 1992). However, transitions that are assigned as d-d transitions are usually weak and hence the band related to 6-OHM

in the visible region border was monitored. In optimum cases this technique may be used to determine differences in the metal-ligand geometry as well as metal oxidation states (Cowan, 1997). Although this may not be the case in this study, the technique is indeed useful in studying metals in biological systems.

HPLC allows for the separation and measurement of the desired components making it without a doubt, the most popular techniques in laboratories today. It also allows for the detection of degradants and metal complexes that may arise due to the addition of 6-OHM with the relative metal ions. Thus this method was also chosen to detect changes in the peak of 6-OHM in the presence of Fe^{2+} or Fe^{3+} and the presence of new peaks can be identified and integrated using this technique.

11.2.2. MATERIALS AND METHODS

11.2.2.1. Chemicals and Reagents

All reagents used were of analytical grade. 6-OHM was purchased from Sigma Chemical Corporation (St. Louis, MO, USA). Ferrous sulphate and anhydrous ferric chloride were purchased from were purchased from BDH Laboratory Supplies, Poole, England.

11.2.2.2. Instrumentation

A Varian Cary 500 Scan UV-VIS NIR Spectrophotometer (EL 99053199) was used to record the absorbance spectra of 6-OHM alone and in combination with Fe^{2+} or Fe^{3+}. The wavelength range was set to scan each sample from 800nm to 200nm.

The modular, isocratic HPLC system consisted of a Spectraphysics IsoChrom pump (Spectraphysics, San Jose, California, United States of America), a Linear UVIS 200 Detector and a Perkin Elmer Model 561 strip chart recorder (Hitachi, Japan). Samples were injected onto the system using a Rheodyne Model 7125 (Rheodyne, Cotati, California, United States of America) fixed loop injector that had been fitted with a 20µl loop.

11.2.2.3. Chromatographic Conditions

Separation on HPLC was achieved with a C18 Waters Spherisorb (250 x 4.6 mm, 5µm particle size) analytical column (Waters Corporation, Milford, MA, USA). The mobile phase for the analysis of 6-OHM was acetonitrile/water (40:60); 25mM ammonium acetate buffer (pH 7) and the flow rate was 1ml/min. The mobile phase was filtered through a 0.45µm filter and degassed prior to use. The UV detector was set at a wavelength of 295nm and the response time was set at 0.1s. The detector sensitivity was set at 0.2 AUFS. Data was recorded at a chart speed of 5mm/min.

11.2.2.4. Sample Preparation

For the UV-Vis and HPLC study 1mM 6-OHM was prepared in 10% absolute ethanol-water while equimolar concentrations of Fe^{2+} and Fe^{3+} were made up in de-aerated Milli-Q water to prevent oxidation of Fe^{2+} ions. Fresh solutions of 6-OHM and the ions were prepared daily.

11.2.2.5. UV/Vis Studies

An absorbance spectrum of Fe^{2+} and Fe^{3+} were run alone and these were used as the control scans. These solutions were made up to a concentration of 1mM in Milli Q water just prior to the experiment to prevent oxidation of Fe^{2+} taking place. Similarly the absorbance spectra of 6-OHM alone was run. Finally, the interaction between 6-OHM and the metal ions was studied by comparing the absorption spectra of the 6-OHM alone and then upon addition of an equimolar solution of Fe^{2+} or Fe^{3+} and the spectrum of these solutions were recorded. The solutions were added to 4mL quartz cuvettes and prior to reading the solution in the cuvettes was inverted twice to allow for even mixing of the solutions.

Changes in absorbance values, shifts in the peaks of the 6-OHM, the presence of new peaks and colour changes in the solutions were noted upon addition of the 6-OHM with the Fe^{2+} or Fe^{3+} in solution.

A new peak formed upon addition of 6-OHM with Fe^{3+}. Thus, this interaction between 6-OHM and Fe^{3+} was followed over a period of time to determine the effect of time on the complex that formed. The absorbance spectra of combination of 6-OHM and Fe^{3+} were recorded at predetermined time intervals.

11.2.2.6. HPLC Study

A 1mL aliquot of 1mM 6-OHM was mixed with 1mL of mobile phase solution and this was injected onto the HPLC system. The retention time and peak height were recorded. Thereafter, 1mL of 6-OHM solution was mixed with a 1mL of an equimolar concentration of Fe^{2+} solution and injected onto the HPLC system. Similarly, 1mL of 6-OHM was mixed with 1mL of Fe^{3+} was injected and any changes in the chromatogram were noted. Colour changes in solution, changes in retention time and peak height of 6-OHM were noted.

Changes in the 6-OHM and Fe^{3+} chromatogram was noted and thus a time-dependent study was conducted and solutions of 6-OHM and Fe^{3+} were injected onto the HPLC at the following time intervals; time 0 min, 5min, 20min, 30 min, 1hr.

11.2.3. RESULTS

11.2.3.1. UV/Vis Studies

Scans of both Fe^{2+} and Fe^{3+} alone were recorded in order to rule out the possibility that any interaction noted was because of a complex formation and not because of the metal ions. The λmax of the 1mM solution of 6-OHM was noted at 295nm with a maximum absorbance of ± 2.98, as shown in figure 11.1. The peak for the 1mM solution of Fe^{2+} on the other hand was present at 288nm with an absorbance value of 2.00. Upon addition of the 6-OHM and Fe^{2+} solutions, there was no colour change noted in solution. Figure 11.1 shows the absorbance spectrum of the combination of Fe^{2+} with 6-OHM (black spectrum) in solution. It is apparent from this plot that upon the addition of 6-OHM to the sample of Fe^{2+}, there is shift in the λmax to the left i.e. 287nm with an increase in the absorbance value of 3.6. However, this slight shift of the λmax of the peak and increase in

absorbance value can be attributed to the addition of these two agents together as both have similar λmax values.

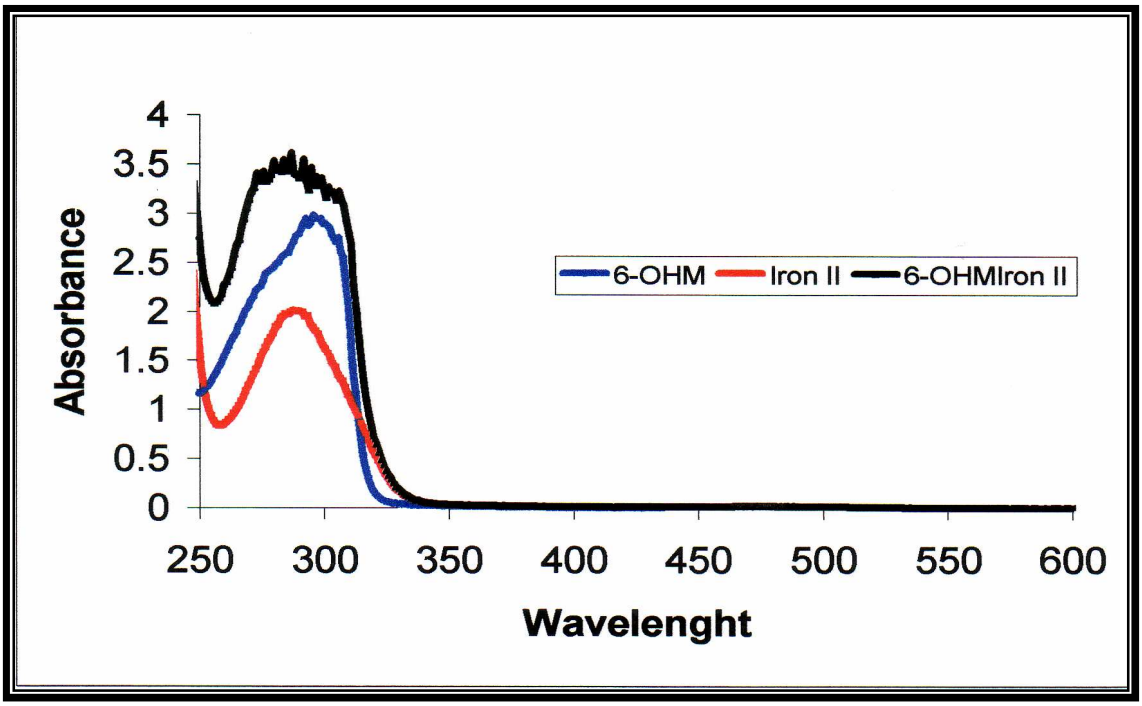

Figure 11.1: Absorbance spectra of 6-OHM alone, Fe^{2+} and 6-OHM mixed with Fe^{2+}.

As shown in figure 11.2, the peak for the 1mM solution of Fe^{3+} is present at 305 nm with an absorbance value of 1.43. Upon addition of the 6-OHM to the Fe^{3+} in solution, an immediate colour change was noted. The solution changed from a pale yellow to a dark purple colour, indicating a complex formation between the 6-OHM and the Fe^{3+}. Figure 11.1 shows the absorbance spectrum of the combination of Fe^{3+} with 6-OHM (black spectrum) in solution. It is apparent from this plot that upon the addition if 6-OHM to the sample of Fe^{3+}, there is a shift in the λmax of the 6-OHM peak to the left, it is now at 265nm with an absorbance value of 3.65. This shift in the λmax of 6-OHM is indicative of metal-ligand complexation. In addition, a new peak is present that absorbs in the region of 485nm with an absorbance value of 1.24. The presence of this new peak is further evidence of the formation of a 6-OHM/Fe^{3+} complex.

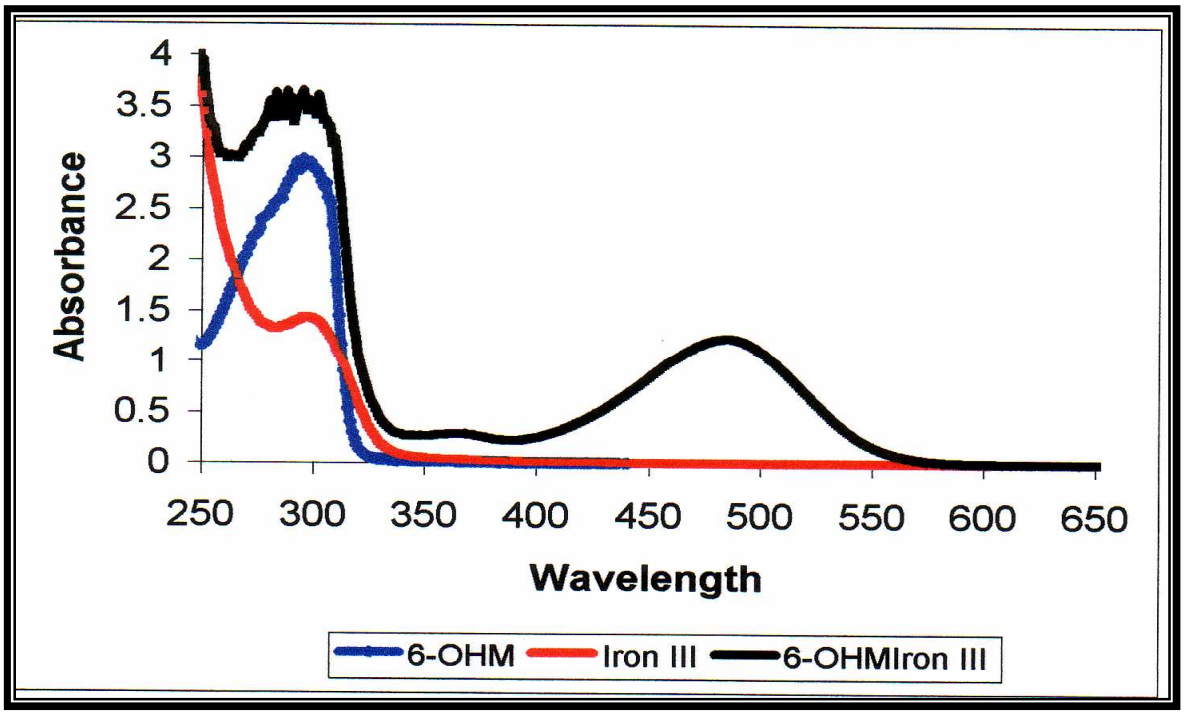

Figure 11.2: Absorbance spectra of 6-OHM alone, Fe^{3+} and 6-OHM mixed with Fe^{3+}.

The 6-OHM/Fe^{3+} combination solution was left to stand and it was noted that after ±5 mins, the dark purple colour began to turn a dark orange colour. The spectra of this solution were recorded at 5 min, 10 min, 20 min and 30mins. As can be seen from figure 11.3, at time 5 min the 6-OHM/Fe^{3+} complex peak increased in height by ± 1.14, while the peak at λmax of 265 nm decreased in height by 1.15. Thereafter, at the subsequent time intervals no significant increases can be noted in the 6-OHM/Fe^{3+} complex. The peak at λmax of 265 nm continued to decrease over the time intervals investigated with a decrease of 1.5 noted at 30 mins. This provides evidence that with time the 6-OHM/Fe^{3+} complexation becomes stronger with time and finally reaches maximum interaction at 30min. As is evident in figure 11.3, a new peak is present at time 5 min at λmax of 365nm which increases in absorbance as time increases. This indicates the formation of another 6-OHM/Fe^{3+} complex.

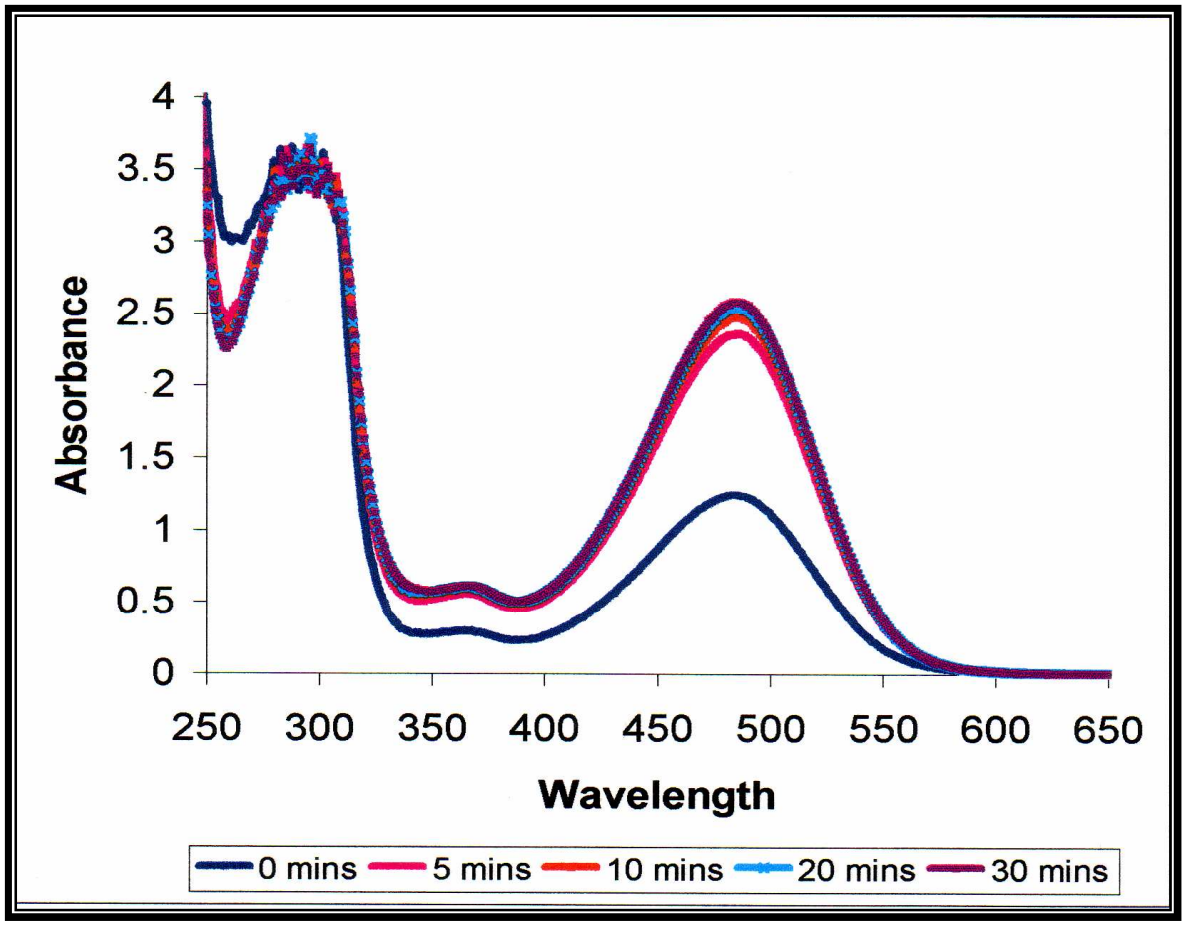

Figure 11.3: Absorbance spectra of the time course study of the 6-OHM/Fe^{3+} complex formation**.**

11.2.3.2. HPLC Study

The mobile phase was optimized for a rapid and interference free chromatogram. The chromatogram obtained from the 6-OHM samples demonstrated sharp, symmetrical and well resolved peaks. Each sample was run in triplicate. The HPLC chromatograms showing the interaction of 6-OHM with Fe^{3+} is shown in appendix seven. The wavelength of analysis of 6-OHM was 295 nm and the peak was released at a retention time of 4.4 min and it had a peak height of 56 mm. The retention time remained the same upon addition of the Fe^{2+} to the 6-OHM sample, while the peak height increased to 59mm. However, no colour change in the sample was noted and no new peaks were present on the chromatogram. The increase in peak height was thus attributed to the fact that Fe^{2+} absorbs at a λmax of 288 nm and the increase in peak height could be due to 6-OHM and Fe^{2+} absorbing in a similar UV region.

However, when the Fe^{3+} was mixed with the 6-OHM solution, the immediate purple colour change was noted as for the UV/Vis study. The chromatogram revealed the presence of three new peak, the first one was present at 3.5 min and was split with a peak height of 0.5 mm, a second one was present at 5 min with a peak height of 20 mm, and the third was present at 5.4 minutes with a peak height of 0.8. The 6-OHM peak on the other hand was present at its original retention time; however the peak height decreased drastically to 27 mm. The peaks for all the complexes were sharp and well resolved. Fe^{3+} was injected alone to determine whether one of the complexes is due to Fe^{3+} alone. However, no peak appeared on the chromatogram when Fe^{3+} was injected alone. Thus, indicating that all three peaks are due to the presence of 6-OHM-Fe^{3+} complexation and chelate formation.

The time response study revealed that at 5 min, the 6-OHM peak height decreased to 20 mm, while the new peak at 5 mins also decreased in height to 15 mm. The two other peaks remained present and no change in their heights was noted. At this time the solution changed from the purple colour to a dark orange. At time 10 mins the 6-OHM peak height increased to 32 mm while the peak at 5 min decreased further to 10 mm. After time 30 mins, the 6-OHM peak stabilized at 32 mm and no further increases or decreases were noted. The peak at 5 min disappeared after 30 minutes. The peaks at 3.4 min and 5.4 min, remained present and no changes in the peak heights were noticed. This is indicative that a 6-OHM/Fe^{3+} complex does form. However this complex decreases with time and disappears after about 45 mins and no changes in the 6-OHM peak is present after this time. At time 1hr, a new peak presents at 2.5 min with a peak height of 10 mm. This peak coincides with the peak of Fe^{2+} injected onto the same HPLC system, indicating that with time, 6-OHM converts Fe^{3+} to Fe^{2+}.

11.2.4. DISCUSSION

Iron is one of the most abundant metals in the body. Approximately two thirds of total body iron is present in the blood as haemoglobin and myoglobin with the remainder bound to the iron regulatory proteins, ferritin and transferrin (el Lozy *et al*., 1980). In the brain, iron is thought to play a crucial role in the maintenance of dopaminergic and GABAergic neurotransmission (Ben-Shachar *et al*., 1987; Willmore *et al*., 1978; Youdim

& Ben-Shachar, 1987). An excess of ferrous iron or ferric ions has been shown to lead to neuronal degeneration through the generation of reactive oxygen species and may be of importance in light of the report of Hensley *et al.*, (1994) in which Aβ was shown to induce free radical formation.

A colour change to dark purple was noticed in the 6-OHM solution upon addition of Fe^{3+} and this colour changed to a dark orange with time, indicating that a metal-ligand complex had formed. The change in the UV/Vis absorption spectrum of 6-OHM would suggest that 6-OHM is able to interact with the Fe^{3+} and result in the production of a new 6-OHM/Fe^{3+} complex. Sreejayan and Rao (1993) showed that Fe^{3+} ions stimulate a greater amount of lipid peroxidation than Fe^{2+} ions, implying that Fe^{3+} the more toxic of the two. Thus, 6-OHM is able to interact with Fe^{3+} ions. Such binding will prevent Fe^{3+} from producing toxic radicals. The results show that no interaction was noted between 6-OHM and Fe^{2+}. Fe^{2+} is known to play a role in the Fenton reaction to give rise to $^{\bullet}OH$ radicals resulting in peroxidation of lipids. The HPLC chromatograms further confirmed these results and show the absence of any interaction between Fe^{2+} and 6-OHM but show that 6-OHM is able to bind Fe^{3+} and result in a complex formation. However, the time study indicates that this complex is not very stable and after 1hr degrades resulting in a new symmetrical peak at 2.5 mins which coincides with a peak of Fe^{2+} injected onto the same system. However, it was shown in chapter ten and eleven, that 6-OHM significantly decreases Fe^{2+}-induced lipid peroxidation in rat brain homogenate *in vitro* and protects against Fe^{2+}-induced lipid peroxidation and neuronal damage in the rat hippocampus *in vivo*.

The colour changes noticed and presence of a new peak on the UV/VIS spectrum and HPLC chromatograms of 6-OHM upon addition of Fe^{3+} indicates that 6-OHM probably binds to Fe^{3+}. This could be another mechanism by which it brings about protection against neuronal damage. Also by binding Fe^{3+}, 6-OHM can convert Fe^{3+} to Fe^{2+} which is a more usable form of iron in the body. However, this study is not sufficient on its own to elucidate the exact mechanism of action by which 6-OHM might interfere with Fe^{3+} to form a complex.

11.3. INTERACTION BETWEEN 6-OHM AND Fe^{2+} AND Fe^{3+}: AN ELECTROCHEMICAL STUDY

11.3.1. INTRODUCTION

To further characterize the role played by 6-OHM in protecting against iron-induced lipid peroxidation in rat brain homogenate, an electrochemical study was performed to test whether 6-OHM is able to interact with Fe^{2+} or Fe^{3+} ions. Such an interaction would render the Fe^{2+} ions unavailable to play a role in the Fenton reaction and as a result lipid peroxidation would not be stimulated. The protection against QA-induced lipid peroxidation has been shown to occur by the addition of desferoxamine, an iron chelator, to rat brain homogenate (Stipêk, *et al*., 1997). Thus, if 6-OHM could bind to Fe^{2+} or Fe^{3+}, this would be a mechanism by which 6-OHM would be able to reduce both iron-induced and QA-induced lipid peroxidation. However, the results of the previous study showed that 6-OHM binds Fe^{3+} and not Fe^{2+} ions similar to its parent compound melatonin (Limson *et al*., 1998). Therefore, electrochemical analysis was another technique used to probe any interactions between 6-OHM and Fe^{2+} or Fe^{3+} and further confirm the results of the previous two studies.

A chemical reaction in which one or more electrons are transferred from one species to another is the basis for electrochemical analysis (Pecsok *et al.*, 1968). Electrochemistry has been used with much success in metal-ligand studies (Limson *et al.*, 1998, Limson & Nyokong, 1997, Lack *et al*., 2001). Limson *et al.*, (1998) used electrochemistry to show metal-ligand interactions between the pineal antioxidant melatonin and a range of metals. In the following experiments two dynamic electroanalytical techniques, cyclic voltammetry and adsorptive stripping voltammetry were employed to determine whether 6-OHM is capable of interacting and thereby inactivating Fe^{2+} and Fe^{3+} and to further confirm the capability of 6-OHM to bind Fe^{3+} *in situ* and form a 6-OHM/Fe^{3+} complex.

Most dynamic electrochemistry utilizes the classic three electrode system depicted in figure 11.4. Thus the electrochemical cell used in these studies comprises of three electrodes, the working, reference, and auxiliary electrode as depicted in figure 11.4. The first electrode is the working electrode, where the analyte is oxidized or reduced i.e.

electron transfer reactions occur at the surface of this electrode. These reactions are monitored in relation to a reference electrode, which maintains a constant potential. The current passes between the working electrode and the auxiliary electrode, the latter serving to complete the circuit (Bard & Faulkner, 1980).

The most utilized working electrodes are those of metallic origin. The basic requirements of the selected material considered ideal for constitution of a working electrode is that it provide a large potential range, it must be durable under various solution conditions, it has a low electrical resistance, and that it has an easily reproducible surface. In the studies conducted, the glassy carbon electrode (GCE) was used due to its ideal surface chemistry for adsorption of analytes. It also possesses excellent mechanical and electrical properties, a wide potential window and is chemically inert exhibiting reproducible performance (Limson, 1998). Electron transfer rates at carbon electrodes are, however, slower than at metal electrodes, therefore electrode pre-treatment procedures were used to increase the electron-transfer rates (Wang, 1994).

The reference electrode is the standard electrode, with which the potential of the working electrode is measured. It maintains a constant potential, and is also referred to as the primary electrode. Commonly used reference electrodes are the hydrogen electrode, smooth platinum electrode, saturated calomel electrode, silver/silver chloride (Ag/AgCl) electrode, and the glass electrode. The Ag/AgCl electrode was used due to its suitability in working with aqueous solutions. It consists of a silver wire anodised with silver chloride in a glass tube, the wire being in direct contact with saturated or concentrated solutions of AgCl and either KCl or NaCl (Limson, 1998). The electrode is protected from the solution by a semi-permeable salt bridge (Sole, 1995, Hawkridge, 1996).

The third electrode used is called the auxiliary electrode, which is usually constructed of an inert material such as platinum, either as a wire, a loop or foil, and it is used to prevent voltage drop across the working and reference electrodes. This electrode is not usually isolated from the working electrode while the reference electrode is (Sole, 1995, Hawkridge, 1996). Thus, current passes between the working and auxiliary electrode.

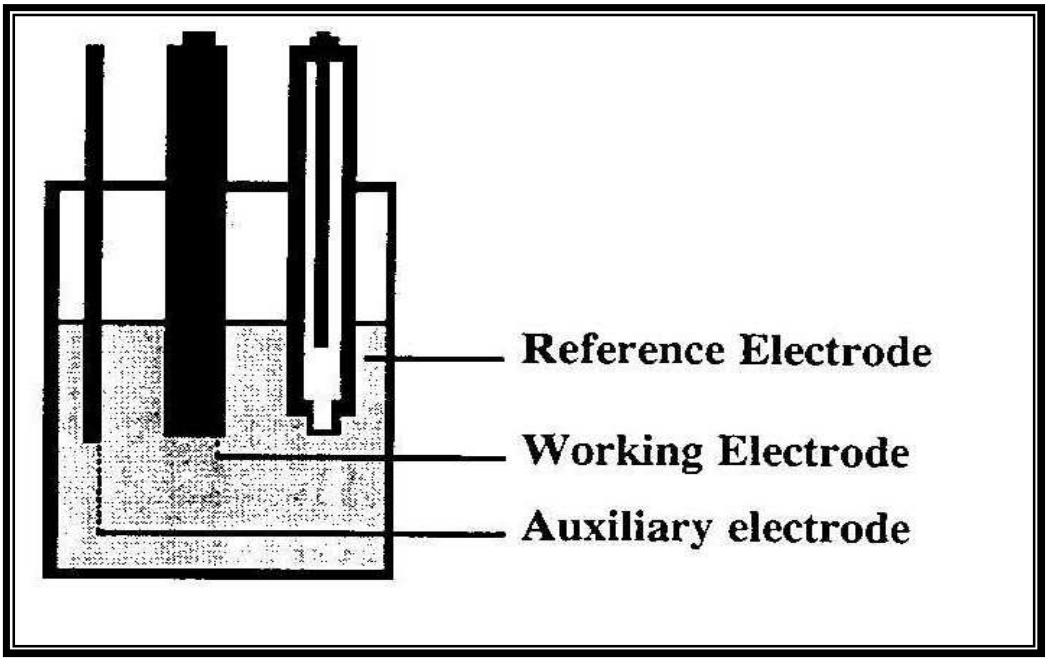

Figure 11.4: Most dynamic electrochemistry utilizes the classic three-electrode system as shown here (Limson, 1998).

Oxygen is electroactive at almost all electrodes, and seriously interferes with voltammetric and electrochemical measurements (Sawyer & Roberts, 1974). To remove the oxygen, nitrogen or other inert gas is bubbled through the solution.

Cyclic Voltammetry

Cyclic voltammetry is a relatively new methodology used extensively as the initial electrochemical technique for characterizing or providing a fingerprint of electro-active species in solution, mapping the current response produced at an electrode as a function of potential. It is an electroanalytical technique used to characterize and determine redox properties of molecules or species in solution (Chevion *et al*., 1997). Simply, an electrical potential gradient is applied (relative to a reference electrode) across an electrode-solution interface (working electrode) to oxidize or reduce species present in solution (in case of cyclic voltammetry, a linear potential gradient is applied). Electroactive species produce characteristic redox patterns. Changes in the redox behaviour and current intensity of the redox waves observed provide insight into the interaction of species in solution. All potentials were referenced against the standard Ag/AgCl electrode. During cyclic voltammetry, the electrode potential is rapidly scanned in search of redox couples. Once

located, a couple is characterised from the potentials of peaks on the cyclic voltammogram and from the changes caused by variation of the scan rate (Kissinger *et al.*, 1996). The forward scan generates the oxidised species and the reverse scan, the reduced species (Limson, 1998). Changes in current response and potential are good indicators of alterations in the chemistry of a target compound, such as that which occurs during an exchange of electrons in a metal-ligand bond.

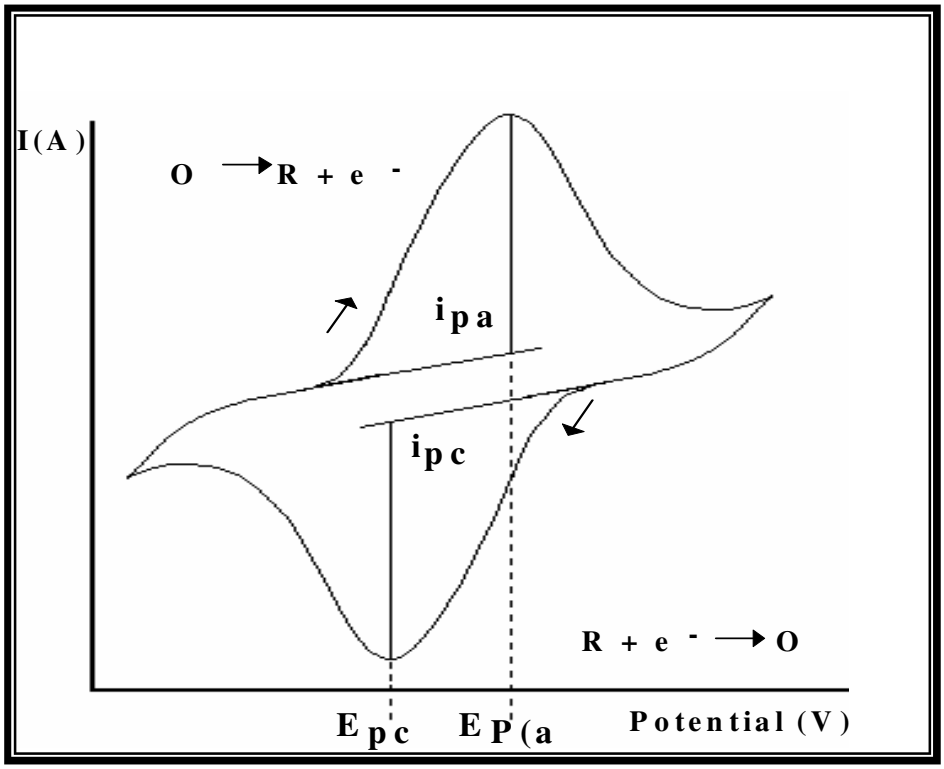

Figure 11.5: A typical cyclic voltammogram (Limson, 1998).

A typical cyclic voltammogram (CV) is shown in figure 11.5, depicting the resulting current versus the potential recorded. The voltammogram supplies information concerning the thermodynamic, kinetic and analytical features of the electrochemical couple under investigation. Although many factors determine the current shape and value (from the applied potential, electrode size, and geometry, size of energy barrier for electron transfer, interaction between the electrode surface and the electroactive molecules), voltammetric waves are usually obtained in a peak shaped or sigmoidal mode as seen in figure 11.5. Thus, the position of the current wave on the voltage axis (x-axis of the voltammogram) can be determined and is referred to as the potential where the peak current [peak potential Ep(a)] or inflection point (half –wave potential, $E_{1/2}$) occurs. The oxidation potential of a compound may be defined phenomenologically as the potential

where Ep(a) is observed for a given set of conditions. The size of the current (anodic current, AC) (Ia) (calculated from the y-axis of the voltammogram) depends on a number of parameters (area of the electrode, the rate in which the potential is applied) and is proportional, at any potential to monitor concentration. These two parameters (peak potential and AC) are characterized as the reducing power parameter and supply information concerning the type of reducing antioxidants (their ability to donate electrons) and their total concentration (Tan *et al*., 2001).

Adsorptive Stripping Voltammetry

Adsorptive stripping voltammetry (AdSV) exploits the natural tendency of analytes to pre-concentrate at an electrode and is a useful technique for gauging metal-ligand interactions. The electrode is polarised at a more negative potential than the reduction potential of the metal, and this serves to preconcentrate the analyte at the electrode. AdSV has been used with success to gauge the affinities of metals for target ligands. This technique relies on the natural tendencies of analytes in solution to absorb at the surface of the electrode in solution. Theoretically, when a suitable ligand is added to a metal solution, the reduction wave observed for the metal ligand complex should exhibit a significant change in current strength as well as a potential shift over the reduction potential of the metal alone in solution (Limson, 1998).

A metal species at an electrode will produce a characteristic response at a specific potential, with current being proportional to the amount of analyte at the electrode. When a suitable ligand is added to a metal solution, the ligand facilitates movement of the metal to the surface of the electrode. Theoretically then, a ligand which forms a bond with a metal will bring about a change in the current response observed, as well as a shift in potential resulting from the reduction of a new species, the metal-ligand complex at the electrode. The affinity of the ligand toward the metal is expressed by the extent of increase in current response of the metal on addition of the ligand. A lowering in current response indicates possible competition by the ligand for binding sites at the electrode at relatively high analyte concentrations. A negative potential shift indicates a strong metal-ligand interaction while a large positive shift is associated with a weaker metal-ligand interaction (Limson *et al.*, 1998; Lack *et al*., 2001).

The first step in AdSV is the formation of a metal-ligand complex, followed by controlled interfacial accumulation of the complex formed onto the electrode (in the presence of mercury) during the deposition step, and the reduction of the absorbed metal complex by application of a potential in the negative direction during the stripping step (equations 1 to 3).

$$M^{n+} + xLig_{aq} \rightarrow M(Lig)_{xaq} + xnH^{+} \quad (1)$$

$$M(Lig)_{xaq} \rightarrow M(Lig)_{xads} \quad (2)$$

$$M(Lig)_{xads} + xnH^{+} + ne^{-} \rightarrow M^{n+} + xLig_{aq} \quad (3)$$

Where Lig = Ligand.

An efficient ligand must satisfy several requirements; it must freely bind the analyte in solution, adsorb onto the electrode, and freely release the analyte during the stripping step. The extent of the increase in current response of the metal on addition of the ligand is an indication of the affinity of the ligand for the metal. The extent of the shift in the reduction potential of the metal after the formation of the metal-ligand complex is a measure of the stability of the complex (Limson, *et al*., 1998; Lack, *et al*., 1999).

In this study the ability of 6-OHM to bind Fe^{2+} and Fe^{3+} ions under de-aerated conditions using electrochemistry was investigated. The study was conducted in aqueous media and under biological pH conditions. The study was conducted using a CV and the AdSV technique (Wang *et al*, 1993; Zhang *et al*, 1993; Limson & Nyokong, 1997; Limson *et al*, 1998).

11.3.2. MATERIALS AND METHODS

11.3.2.1. Chemicals and Reagents

All reagents were of analytical grade. Tris-HCl was purchased from Sigma, St. Louis, U.S.A. Anhydrous ferric chloride (Fe^{3+}) and iron sulphate (Fe^{2+}) were purchased from BDH Laboratory Supplies, Poole, England. Tris-HCl (pH 7.3) was used as the electrolyte

in all voltammetric experiments and all reagents were prepared under deaerated conditions to prevent oxidation of Fe^{2+} from occurring.

11.3.2.2. Instrumentation

Cyclic and stripping voltammograms were obtained with a Bio Analytical Services (BAS, Lafayette, Indiana, USA) CV-50W voltammetric analyzer using a BAS C2 cell stand to maintain constant atmosphere. An undivided cell was used for the AdSV. The working electrode was the model MF-9058 controlled growth glassy carbon electrode (GCE) for voltammetric experiments. A silver/silver chloride (Ag/AgCl) [(KCl = 3 mol dm^{-3})] and a platinum wire were employed as the reference and auxiliary electrodes, respectively, in all electrochemical work. Prior to use, the GCE was cleaned by polishing with alumina on a Buehler pad, followed by washing in nitric acid and rinsing in water and the buffer solution. Between scans, the GCE was cleaned by immersion in a dilute acid solution and rinsed in water.

11.3.2.3. Sample Preparation

0.2M Tris-HCl buffer (pH 7.3) was used as the buffer solution and prepared in Milli-Q water. The Fe^{2+} and Fe^{3+} were prepared from the appropriate salts and dissolved in Milli-Q water under de-aerated conditions. While 6-OHM, was dissolved in absolute ethanol and subsequently diluted in Tris-HCl buffer. The final concentration of ethanol in solution was 0.2% w/v. Fresh solutions of 1mM 6-OHM, 1mM Fe^{2+} and 1mM Fe^{3+} was prepared daily. Tris-HCl buffer (pH 7.3) was the chosen electrolyte since this has a wide potential window.

11.3.2.4. Cyclic Voltammetry

For cyclic voltammetric experiments, appropriate concentrations of the metal and 6-OHM in pH 7.3, Tris-HCl buffer were introduced into a glass cell, degassed for 5 min with nitrogen before scanning a potential window. The metal-ligand complex is expected to have formed at this stage.

11.3.2.5. AdSV Technique

For AdSV experiments, pH 7.3, Tris-HCl buffer and appropriate concentrations of the metal (Fe^{2+} or Fe^{3+}) and the ligand (6-OHM) were introduced into an electrochemical cell. The solution was then de-aerated with nitrogen for 5 min and simultaneous solution stirring, after which a flow of nitrogen was maintained over the solution throughout the measurement. The metal complexes of 6-OHM were expected to have formed at this stage. The reason for purging the solution is to minimize any oxygen effects that may occur. All experiments were run under a blanket of nitrogen gas. The potentials quoted are cited with reference to the silver/ silver chloride reference electrode for all data accumulated. Optimum deposition potential 0.10V or 0.00V vs Ag/AgCl was applied for 60 s to effect the formation and adsorption of the metal and ligand species onto the GCE.

The voltammograms were then scanned in the negative direction from the deposition potential of -1.0V vs Ag/AgCl at the san rate of 0.1V/s to strip the adsorbed metal-ligand species from the electrode. During the stripping step, current responses due to the reduction of the metal-ligand species were measured as a function of potential. All potential values quoted are referenced against the Ag/AgCl reference electrode.

11.3.3. RESULTS

11.3.3.1. Cyclic Voltammetry

6-OHM is electrochemically active at the bare glassy carbon electrode, meaning that redox waves are observed for this compound. The cyclic voltammograms (CV) obtained for 6-OHM alone in solution is shown in figure 11.6 (a). An oxidation peak at 0.11V is shown with a quasi-reversible return peak at -0.08 V. Figure 11.6 (b), shows the CV of Fe^{3+}in solution, with an oxidation potential of -0.36 V and a return peak at -0.09V. In the presence of Fe^{3+}, fig. 11.6 (c) shows the potential shifts for 6-OHM. The 6-OHM peak shifts to a more positive potential of 0.12 V with a slight increase in current strength while the Fe^{3+} oxidation wave shifts to less positive potentials with a significant increase in current strength.

CV's of 6-OHM in the presence of increasing concentrations of Fe^{3+}, showing increasing shifts in the oxidation potential of the 6-OHM wave at 0.11V without any significant change in its current strength. No observable potential shifts are observed for Fe^{2+} and 6-OHM when CV was run of the two species in solution.

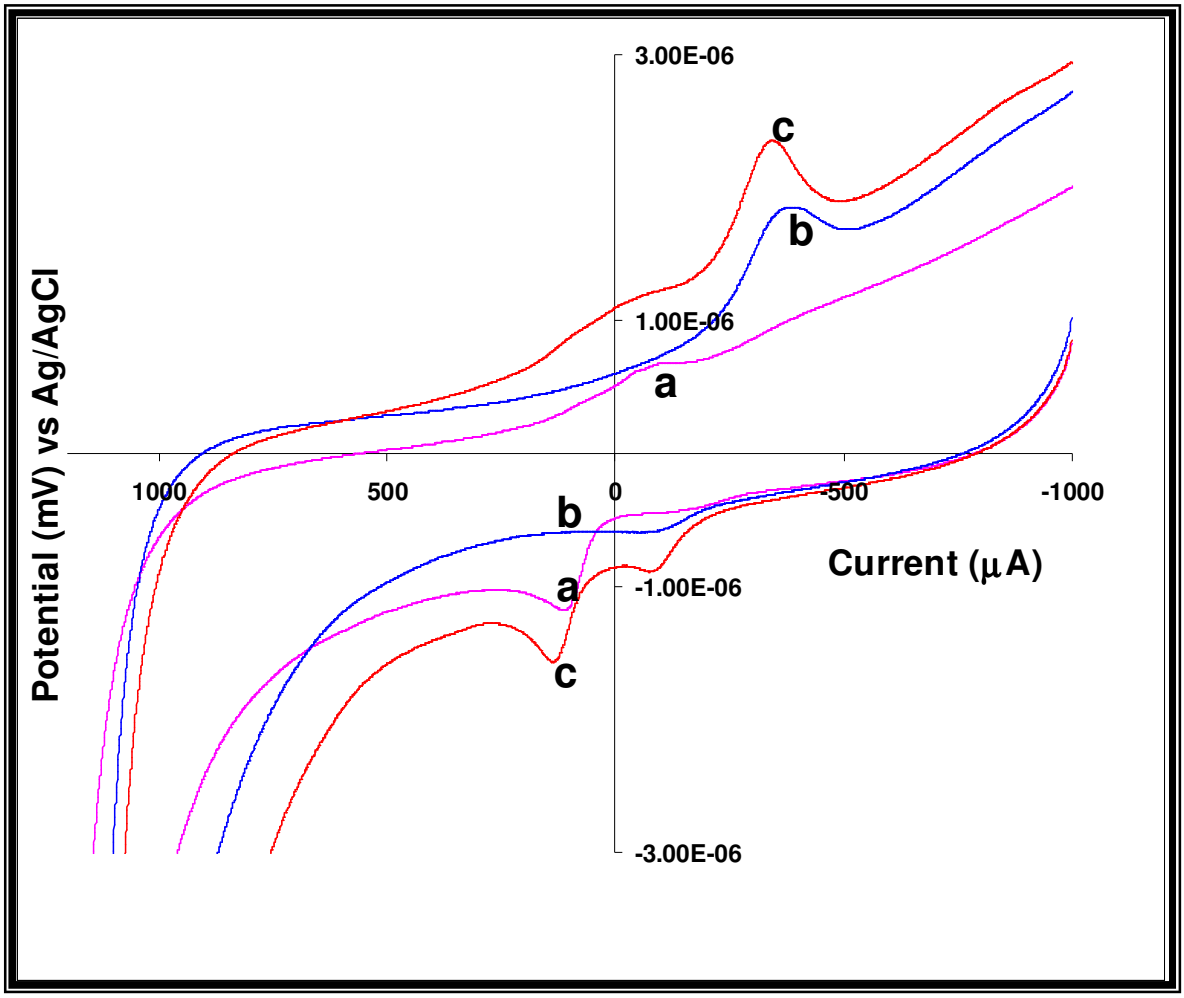

Figure 11.6: (a) CV of 6-OHM (1 x 10^{-5} M), and (b) CV of Fe^{3+} alone in solution (1 x 10^{-6} M). (c) CV of 6-OHM and Fe^{3+}. Electrolyte : 0.2M Tris-HCl.

11.3.3.2. AdSV Technique

Figure 11.7 (a), shows the AdSV for Fe^{3+} in solution, with a reduction potential of -0.39V. The reduction potential of 6-OHM alone is -0.14 V (Fig. 11.7 (b)). In the presence of 6-OHM, figure 11.7 (c) shows that the Fe^{3+} reduction potential shifted to -0.33 V accompanied by a sharp decrease in current intensity. The 6-OHM peak shifted to a less negative potential of -0.08V. The significant shift in potentials for both Fe^{3+} and 6-

OHM strongly suggests immediate metal-ligand interaction. A negative shift of 3mV for the Fe^{3+} reduction peak on the addition of 6-OHM, shows the resulting iron-6-OHM complex is less easily reduced than the Fe^{3+} alone. The shift of 0.03V is relatively small; indicating that the complex formed is not very stable. A potential shift is a strong indication that a new species is being reduced at the electrode, in this instance a 6-OHM/Fe^{3+} complex as opposed to just the Fe^{3+} or 6-OHM alone. These potential shifts were not observed for AdSV of 6-OHM and Fe^{2+}, therefore no interaction between Fe^{2+} and 6-OHM is concluded.

An immediate purple colour was evident upon addition of the 6-OHM to the Fe^{3+} in solution. This colour began to turn a dark orange after about 5 minutes. Thus, the changes occurring in solution upon addition of 6-OHM to Fe^{3+} were monitored electrochemically by running several successive AdSVs. Figure 11.8A, shows that with time, the peak due to 6-OHM increases with intensity as the peak due to Fe^{3+} decreases.

After 14 min, figure 11.8B, shows that the 6-OHM peak returns to its original potential of -0.14V (see figure 11.7 b) while the Fe^{3+} peak completely disappears by the final scan. A new broad peak appears at the high negative potentials of -0.57V which is attributed to the formation of Fe^{2+}. A scan of Fe^{2+} alone shows its reduction potential in the same region. A shift in potential is noticed for both 6-OHM and Fe^{3+} during the first and third scans (Figure 11.7 b).

11.3.4. DISCUSSION

These electrochemical results are in keeping with earlier electrochemical studies of melatonin (Limson *et al*., 1998), where weak interactions were found between melatonin and essential metals such as iron.

The changes in oxidation potentials for both Fe^{3+} and 6-OHM when both are present in solution strongly suggest an interaction between these two species (figure 11.6). This is most evident when examining a similar set of CV experiments obtained for Fe^{2+} and 6-OHM. Since there were no changes in the peaks, no observable potential shifts between Fe^{2+} and 6-OHM were observed and thus, it was concluded that 6-OHM was not binding

to Fe^{2+}. Similar results were obtained for the AdSV study. Furthermore, the significant shift in potentials for both Fe^{3+} and 6-OHM strongly suggests an immediate metal-ligand interaction (figure 11.7).

As shown in figure 11.8B, after 14 min the 6-OHM peak returns to its original potential while the Fe^{3+} peak completely disappears by the final scan. However, the presence of a new broad peak appears at a high negative potential which was attributed to the formation of Fe^{2+}. This was confirmed by a scan of Fe^{2+} alone. It is thus likely that 6-OHM may be reducing Fe^{3+} to Fe^{2+} while the 6-OHM becomes oxidized. It is postulated that the shift in potential for both 6-OHM and Fe^{3+} during the first to third scans may be attributed to the formation of a weak Fe^{3+}-6-OHM bond. After a certain time, at the fourth scan (figure 11.8A) it is postulated that the weak Fe^{3+}-6-OHM bond breaks and the 6-OHM returns to its original position. It is assumed that this bond breaks as all the Fe^{3+} is converted to Fe^{2+} observed electrochemically. No potential shifts were observed between Fe^{2+} and 6-OHM thus it was concluded that there is no interaction between Fe^{2+} and 6-OHM.

The AdSV were also run of 6-OHM in solution with varying concentrations of Fe^{3+}, keeping the 6-OHM concentration constant (1mM). Increasing concentrations of Fe^{3+} between 0.5mM and 4mM showed a decrease in the 6-OHM reduction peak, providing further evidence for a Fe^{3+}-6-OHM. Thus, the electrochemical data reported above clearly supports the postulation that 6-OHM binds Fe^{3+} and that chelation of ferric ions is the mechanism involved in the reduction of iron-induced lipid peroxidation (Reddy & Lokesh, 1994). The above results do not support the likelihood of an interaction between Fe^{2+} and 6-OHM and thus it does not support the postulation that 6-OHM-iron interaction being the mechanism involved in reducing QA-induced lipid peroxidation because QA binds with Fe^{2+} and not Fe^{3+} ions. Thus, 6-OHM in this case is probably acting as a free radical scavenger and thereby reducing oxidative stress induced by QA within the membranes and this is supported by the study conducted in chapter eight where 6-OHM was shown to scavenger $O_2^{\bullet-}$ produced by intrahippocampal injection of QA.

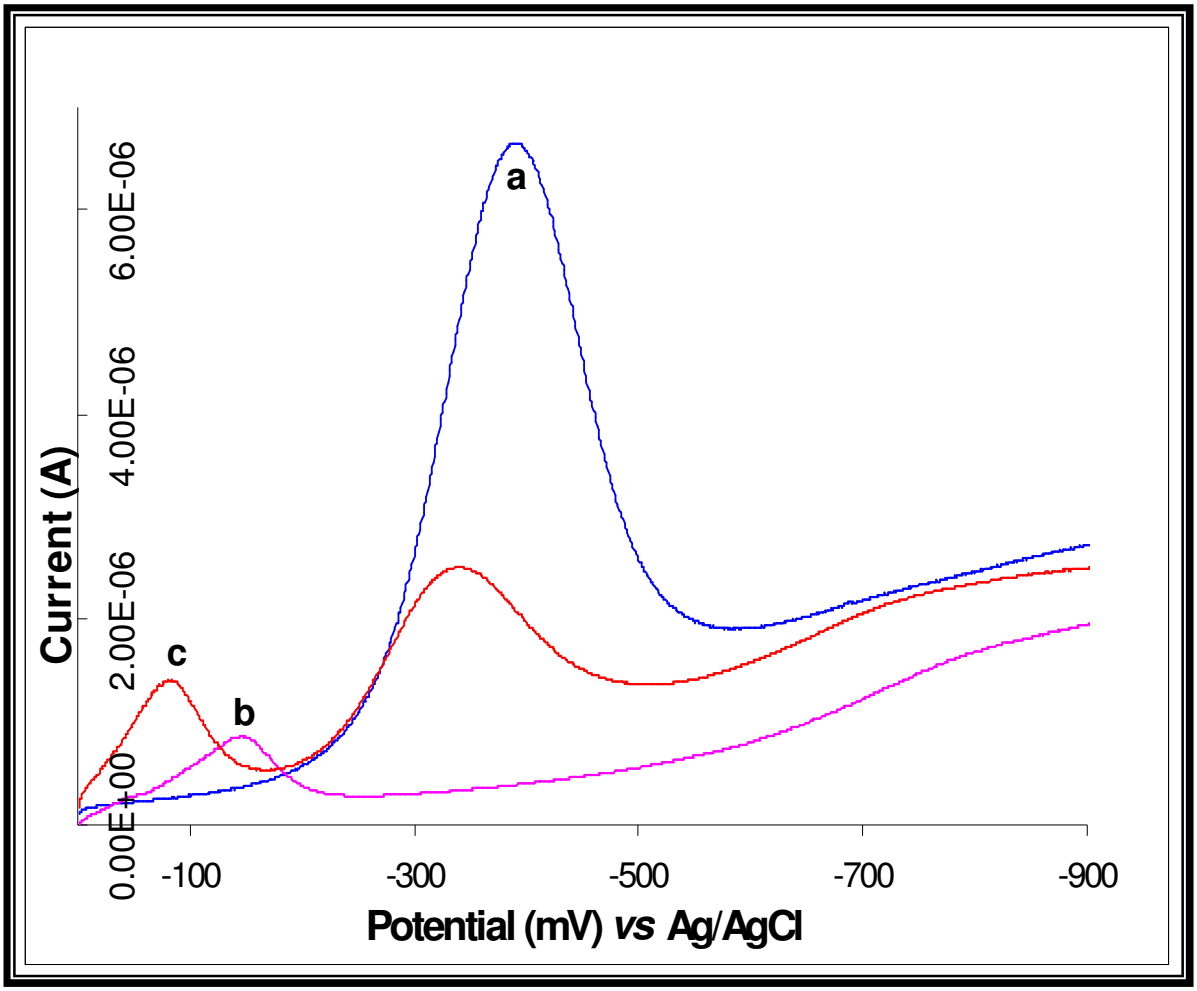

Figure 11.7: (a) Adsorptive stripping voltammogram (AdSV) for Fe^{3+} (5×10^{-5} M). (b) AdSV of 6-OHM (6×10^{-5} M). (c) AdSV of Fe^{3+} and 6-OHM with concentrations as in (a) and (b). Electrolyte: 0.2M Tris-HCl.

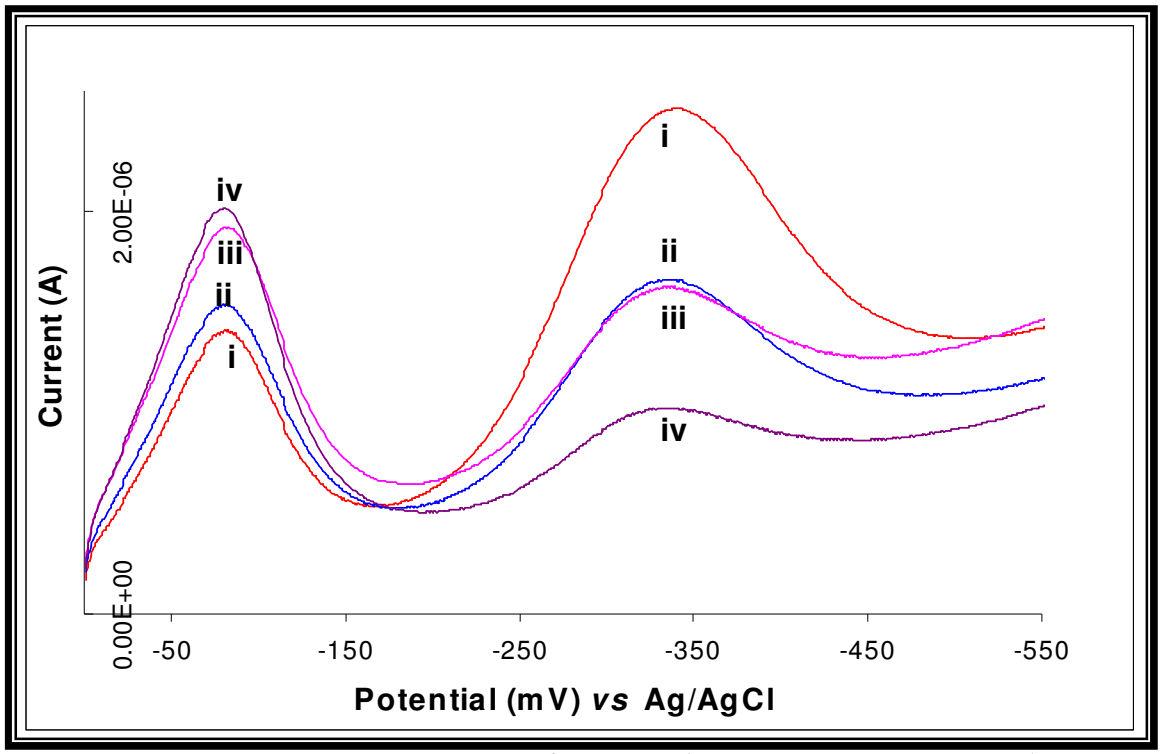

Figure 11.8: **A)** Successive AdSV of Fe^{3+} (5 x 10^{-5} M) and 6-OHM (6 x 10^{-5} M) taken from 0 to 12 min represented in (i) to (iv). The 6-OHM peak increased with time while the peak due to the Fe^{3+} decreased.

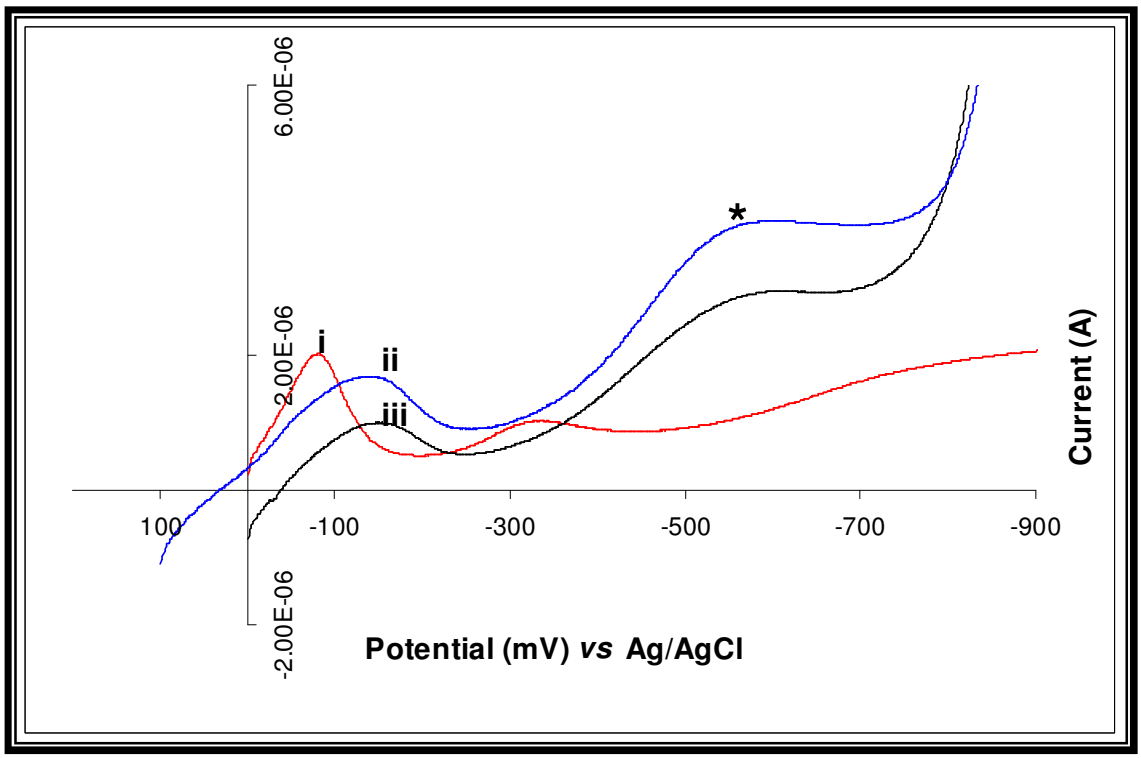

Figure 11.8: **B)** Successive AdSV of Fe^{3+} (5 x 10^{-5} M) and 6-OHM (6 x 10^{-5} M) taken from 14 to 30 min represented in (i) to (iii). After 14 min the peak shift is observed. (i) shows the AdSV at 12 min, (ii) the AdSV at 14 min shows the 6-OHM peak shifted back to its original potential while the Fe^{3+} peak disappeared. * a new peak at -0.57V is attributed to Fe^{2+}, (iii) shows the AdSV after 30 min. No observable changes were noted after this time.

11.4. CONCLUSION

The purpose of this chapter is to elucidate another possible mechanism of protection shown by 6-OHM against QA and Fe^{2+}-induced lipid peroxidation. The impetus of these studies arose as a result of reports which stated that QA-induced lipid peroxidation in rat brain homogenate is dependent on Fe^{2+} and that Fe^{2+} is required by the Fenton reaction to produce toxic $^{\bullet}OH$ (Stipêk *et al.*, 1997; Halliwell, 1992). Furthermore, melatonin has been reported to bind to iron. As a result, it was reasoned that an interaction between 6-OHM and iron would render the iron unavailable to cause extensive tissue damage.

6-OHM has been shown to be a powerful antioxidant in chapter eight and ten. In addition, 6-OHM was shown to increase complex I activity of the electron transport chain. However, the extent and mechanism by which this indoleamine is able to protect against QA and Fe^{2+}-induced lipid peroxidation is unknown. One mechanism by which 6-OHM offers protection could be an interaction with iron i.e. Fe^{2+} and Fe^{3+} ions since these oxidation states of iron are known to react with hydroperoxides (Hallwell & Gutteridge, 1989; Sreejayan & Rao, 1993).

The UV and HPLC studies showed that there exists a definite interaction between 6-OHM and Fe^{3+} but not Fe^{2+}. Sreejayan and Rao (1993) reported that Fe^{3+} ions stimulate a greater amount of lipid peroxidation than Fe^{2+} ions. This interaction itself would be somewhat effective in protecting against Fe^{3+}-induced oxidative damage.

The electrochemical data reported above clearly supports the postulation that 6-OHM binds to Fe^{3+}, thus supporting the UV/Vis study and HPLC study done earlier. However, the 6-OHM/Fe^{3+} resulting complex is not stable and after 14 min of interaction time between 6-OHM and Fe^{3+}, the complex disappears and a new Fe^{2+} peak is evident. Thus, 6-OHM acts similar to melatonin in binding to Fe^{3+} (Limson *et al.*, 1998). However, it is able to reduce the damaging Fe^{3+} to the more usable form of iron in the body, viz. Fe^{2+}. This observation is supported by the HPLC study. Thus it is likely that the chelation of ferric ions is the mechanism involved in reduction of iron – induced lipid peroxidation (Reddy & Lokesh, 1994).

Within the brain the trace metals such as iron play an important role as components of proteins essential for neural functioning. However, these metals have also been implicated in neurodegenerative diseases and they elicit damaging effects through oxidative stress (Ben-Shachar *et al*., 1992; Gutteridge, 1994; Halliwell, 1992) and energy failure (Brown *et al*., 2000). Disorders of iron accumulation are known to cause potential damage of vital organs including the liver. Thus, agents that are capable of reducing excess iron could be potentially useful in treating disorders such as hemochromatosis. It has been previously shown in our laboratory (Limson *et al*., 1998) that the pineal antioxidant, melatonin is able to bind to a number of metal ions including Fe^{3+}. The present study showed that 6-OHM binds Fe^{3+} and in so doing, converts it to Fe^{2+}. The implications of this are that 6-OHM converts Fe^{3+} to a more biologically usable form viz. to Fe^{2+}. This can be incorporated into important biomolecules including heme. These findings raise interesting questions concerning the manner in which 6-OHM acts to reduce free radical damage and lipid peroxidation and suggests that 6-OHM binds to Fe^{3+} in a non-toxic form, thereby preventing this metal from generating free radicals. It has been shown by Sreejayan and Rao (1993), that Fe^{3+} ions stimulate the greatest amount of lipid peroxidation in comparison to Fe^{2+} ions.

One dire consequence of this would be the ready provision of Fe^{2+} to drive the Fenton reaction. Matuszak *et al*., (1997) reported that 6-OHM promotes the production of $^{\bullet}OH$ radicals and the authors postulate that this prooxidant action is due possibly to 6-OHM reducing Fe^{3+}, thus producing sufficient Fe^{2+} to drive the Fenton reaction. However, the lipid peroxidation study conducted in the liver by Maharaj *et al*., (2003a) showed that 6-OHM significantly reduces Fe^{2+}-induced lipid peroxidation in rat liver homogenate. This is further supported by the results of chapter ten, where 6-OHM was able to reduce Fe^{2+}-induced lipid peroxidation in rat brain homogenate *in vitro* and hippocampal homogenate *in vivo* and this protection was shown to be equivalent to the protection offered by melatonin. Thus, while this agent has the potential of promoting the Fenton reaction, it also scavengers the hydroxyl radical (Matuszak *et al*., 1997) and at the same time reduces the consequent rise in Fe^{2+}-induced lipid peroxidation. Matuszak *et al*., (1997) postulated that 6-OHM possibly reduces Fe^{3+} to Fe^{2+} and this study is able to confirm this. In addition, 6-OHM retains the methoxy group in C5 which appears to keep melatonin from exhibiting prooxidative activity (Tan *et al*., 2002), thus we can postulate that this indoleamine should be devoid of prooxidative activity as well.

In conclusion, since some free radical production is inevitable in neuronal cells, and lipid peroxidation is the major consequence of free radical action, antioxidant defence mechanisms have evolved to protect such cells from extensive damage (Uchida & Kawakishi, 1990). Thus, a new mechanism of action is noted for 6-OHM and thus it can be concluded that 6-OHM can be used to enhance the antioxidant defence mechanism of the body by binding Fe^{3+}, thereby providing a role as a possible free radical scavenger.

CHAPTER TWELVE

HISTOLOGICAL STUDIES

12.1. INTRODUCTION

Histology is derived from the Greek word *histos* for web or tissue, and *logia*, meaning "the study of" or knowledge and involves the examination of preserved, sectioned and stained tissues. Literally, then, it refers to the knowledge, or science, of tissues, both plant and animal. Most of our knowledge of internal tissue structure has come from this branch of science (Hodgeson & Bernard, 1992). Neural tissues have a wide distribution throughout the body, innervating most visceral and peripheral tissues. Within the neural system, there are two basic types of cells, neurons and supportive cells. Neurons are highly specialised cells that easily conduct nerve impulses and are easily excited to produce them. Typical neurons show a large cell body with a large central nucleus and many cytoplasmic extensions of which there are two types: dendrites and axons. These features are also visible on a stained section of neural tissue observed under the microscope depicted in figure 12.1.

Excitotoxicity is associated with the excessive release of glutamate and related excitatory amino acids that may play central roles in the pathogenesis of neuronal injury (Choi & Rothman, 1990). One such excitatory toxin is QA. This agent has been shown to induce lesions after intrastriatal and intrahippocampal injections in rat brain (Schwarz & Köhler, 1983; Schwarz *et al*., 1983). These lesions closely resemble those observed in the brains of individuals who have Huntington's disease (Beal *et al*., 1986; Popoli *et al*., 1994). QA has been shown to cause dose dependent selective pyramidal cell death in the hippocampal CA1, CA3 and CA4 regions (Southgate *et al*., 1998; Behan *et al*., 1999) and results in the infiltration of the pyramidal cell layers and surrounding tissue by microglial cells (Stone *et al*., 2000). QA injected directly into the hippocampus, has been shown to cause neuronal cell damage, which was evident by the appearance of swelling and overall neuronal degeneration. This quinolinate damage was prevented by the co-

administration of melatonin (Southgate *et al*., 1998; Behan *et al*., 1999; Stone *et al*., 2000).

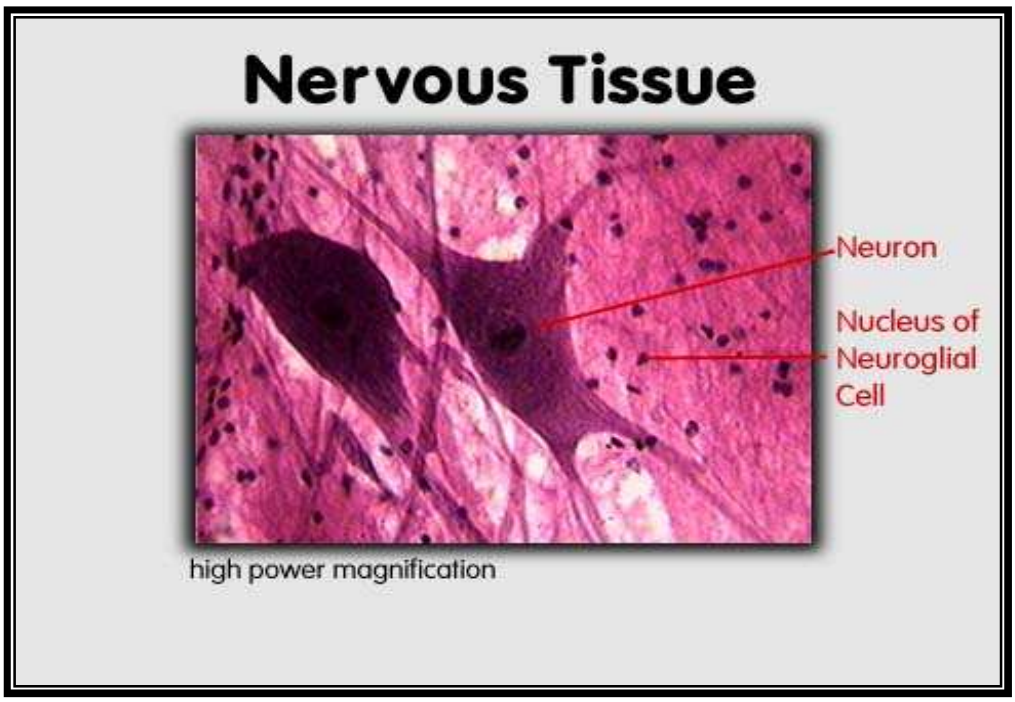

Figure 12.1: A high power magnified section of neural tissue showing large star shaped neuronal cell body and the nerve cell processes (bioweb.uwlax.edu/.../ neural_tissue__spinal_neuron_.htm).

Iron is one of the most abundant metals in the body with approximately two thirds of the total body iron being present in the blood (el Lozy *et al*., 1980). In the brain, iron is thought to play a crucial role in the maintenance of dopaminergic GABAergic neurotransmission (Ben-Shachar *et al*., 1987; Wilmore *et al*., 1978; Youdim & Ben-Shachar, 1987). An excess of Fe^{2+} can lead to neuronal degeneration through the generation of ROS and may be of importance in light of the report of Hensley *et al*., (1994) in which Aβ was shown to induce free radical formation. The increase of iron in this micro-environment could possibly catalyze further free radical generation, thus leading to an increase in Aβ fibril formation. Iron has been shown to be imbalanced in an AD brain by Goodman in 1953. However numerous studies thus far have confirmed the presence of iron and ferritin in AD brains (Connor *et al*., 1992; Connor & Menzies, 1995; Grundke-Iqbal *et al*., 1990). Connor *et al*., (1992) reported decreased transferrin in the brain of AD suggesting decreased mobility and utilization of iron in the disease. Prior studies have shown that direct injection of Fe^{2+} into the rodent brain shows focal oedema formation within 24hrs, followed by necrosis, neuronal loss and gliosis over 30 days (Willmore & Rubin, 1982; Willmore *et al*., 1978). Furthermore, Sloot *et al*., (1994)

demonstrated that after intrahippocampal injection of Fe^{2+}, an increase in Ca^{2+} accumulation in the hippocampus results and since Ca^{2+} accumulation is associated with neurodegeneration, this suggests that degeneration has occurred. The authors also demonstrated that Fe^{2+} causes severe neuronal loss in the hippocampal regions. A number of authors have reported melatonin to be effective in protecting against iron-induced lipid peroxidation and neuronal damage in rats (Cabrer *et al*., 2001; Chen *et al*., 2003; Kaptanoglu *et al*., 2003). Furthermore, Chen *et al*., (2003) demonstrated that melatonin was able to reduce iron-induced programmed cell death.

In chapter ten, it was shown that 6-OHM, protects against QA and Fe^{2+}-induced lipid peroxidation both *in vivo* and *in vitro*. Since, these studies were only a measure of the MDA, which is a degraded lipid product, and even though the decline in the formation of this is indicative of decreased cell damage, it is still important to examine the cells following QA and Fe^{2+} administration. The present study aims to examine the hippocampal neurons following an intrahippocampal injection of QA or Fe^{2+}, and pretreatment with subcutaneous injections of 6-OHM. Two different histological techniques were employed and the hippocampal neuronal cells were examined under a light microscope attached with an Olympus camera.

12.2. HISTOLOGICAL ANALYSIS OF THE EFFECT OF 6-OHM AGAINST QA AND Fe^{2+}-INDUCED DAMAGE TO HIPPOCAMPAL NEURONS USING CRESYL VIOLET STAIN.

12.3.4. INTRODUCTION

The Nissl stain, introduced by the German neurologist Franz Nissl in the late nineteenth century, is commonly used to study neurons under the light microscope. This stain is extremely useful since it distinguishes neurons and glia from one another and allows histologists to study the arrangement or cytoarchitecture of neurons in different parts of the brain (Bear *et al*., 2001).

In this experiment it was decided to investigate the hippocampal neuronal structural events that intrahippocampal injections of QA and Fe^{2+} induce in the CA1 and CA3 regions of the hippocampus. Since 6-OHM has been shown to afford protection against QA and Fe^{2+} mediated oxidative stress in chapter eight and ten, it was decided to determine whether 6-OHM offers neuroprotection against QA-induced and Fe^{2+}-induced intrahippocampal lesions in the rat brain. After treatment, the brains of the rats were sectioned and the hippocampus was stained with cresyl violet stain and examined microscopically to detect changes in neuronal structure and size, for evidence of any morphological changes.

12.2.2. MATERIALS AND METHODS

12.2.2.1. Chemicals and Reagents

Quinolinic acid, ferrous sulphate and 6-OHM were purchased from Sigma St. Louis, MO, U.S.A. Paraffin wax was obtained from Lasec (South Africa). Cresyl violet stain was purchased from BDH Chemicals Ltd (England), while DPX was purchased from Philip Harris Ltd (England). Haupt's adhesive consisted of the following: 1 g gelatine, 100 ml

water, 2 g phenol and 15 ml glycerol. All other chemicals were of the highest quality available and were purchased from commercial distributors.

12.2.2.2. Animals

Adult male rats of the Wistar strain housed in separate cages, in a controlled environment as described in appendix one.

12.2.2.3. Surgical Procedures

The bilateral injection of QA and Fe^{2+} into the hippocampus was carried out as in chapter ten, section 10.5.2.5.

12.2.2.4. Treatment Regime

The rats were dosed s.c. as described in chapter ten, section 10.5.2.4. However, the melatonin treated groups were excluded from this study. Care was taken to rotate the injection site as to allow for optimum absorption of the drug.

12.2.2.5. Histological Techniques

The histological techniques were performed according to the methods described by Southgate, 1999.

12.2.2.5.1. Fixing the brain

The animals were sacrificed and the brains removed as described in appendix two. Neural tissues are extremely fragile and easily subjected to rapid anoxic and postmortem changes. Immediately after death, animal tissues begin to break down as a result of autolysis and bacterial attack. To prevent this, immediate fixation of these tissues is required (Chang, 1995). This process usually entails submerging the tissues in stabilizing or cross– linking agents or perfusing them with these substances in order to preserve as much as possible of the morphological and molecular characteristics. The role of the

fixative is to maintain the morphology of the tissues as close to *in vivo* morphology as possible and to prevent post-sampling necrosis. A recommended fixative used for the study of brain tissue is Davidson's solution. The ratio of fixative to tissue volume should be at least 10:1 to ensure good fixation. Thus, fixation functions to chemically stabilize proteins, and thus preserve structures (Southgate, 1999).

There is no universal fixative and choice should be made taking into account later use of fixed material as well as practical aspects of fixative use (price, component availability, etc). Davidson's solution is an excellent choice for preserving the structure of the tissues (Lighter, 1996). In addition, tissue sections fixed with Davidson's solution can be stained later by different histochemical methods, as well as *in-situ* hybridization with DNA proteins. Davidson's alcohol formalin acetic acid fixative consists of 220mL of formalin (100%), 115mL of glacial acetic acid, 330mL of ethanol, and 335mL of water. This mixture is stored at room temperature prior to use (Lighter, 1996).

Brains were rapidly fixed in the Davidson's fixative mixture for 48 hours. After fixation, a slice of brain, 2mm thick was prepared to exclude the location of the injection track, which was normally apparent from the residual dimpling of the cortical surface produced by the needle penetration. Exclusion of the tissue directly below the site of the injection ensured that all damage was due to neurotoxin or drug and not due to the physical damage caused by the cannula needle. The 2mm block of brain tissues were then stored in 70% ethanol.

12.2.2.5.2. Specimen Preparation and Embedding

In order to be cut, the slices need to be supported. Embedding involves the infiltration and orientation of tissue in the paraffin wax support medium. Moisture was extracted from the tissue fragments by bathing them successively in a graded series of mixtures of ethanol. This step was followed by the clearing process which involves the removal of ethanol by immersing the tissue in xylene twice for one hour each. The tissue was then submerged in molten paraffin wax at 57^0C twice for one hour each, which facilitated the removal of xylene and while infiltrating the tissue without encountering water. This stage provides the hardness and support that the tissue requires for sectioning. The method used is shown in Table 12.1

Table 12.1: Procedure for embedding brains in paraffin wax.

Step	Processing Agent	Time (Hours)
1	70% Ethanol	1
2	90% Ethanol	1
3	Absolute Ethanol	1
4	Absolute Ethanol	1
5	Xylene	1
6	Xylene	1
7	Melted Paraffin Wax	1
8	Melted Paraffin Wax	1

12.2.2.5.3. Blocking Out

The brain material was fixed into a block and this procedure was performed in order to form a support that would facilitate sectioning using the rotary microtome. The mould used was a plastic ice tray and this was coated with ethanol-glycine to prevent the block sticking to the mould. The brain was removed from the final molten wax stage (previous section) and placed into the mould with warmed forceps. The brain was then completely covered in molten wax. Air was gently blown over the surface of the wax until the top solidified. The entire mould was then immersed in cold water overnight to facilitate quicker solidification and to prevent the formation of crystals that might disrupt the tissue.

12.2.2.5.4. Sectioning

Sectioning is a technique performed using a microtome. This is an instrument, which consists of a sharp metal knife held in a fixed position, and a chuck in which a block of wax with the tissue is held. Depending on the type of microtome, a particular mechanism oscillates the chuck up and down and with each oscillation; the chuck is brought closer to the knife by a fixed distance. In this way sections are cut from the wax block (Hodgeson & Bernard, 1992). The wax block was trimmed with a razor blade so that two of the sides were parallel, while the other two converged slightly (figure 12.3). The sides were cut so as to leave about 2 mm of wax around the tissue. The wax block was attached to a small wooden block with a small amount of molten wax.

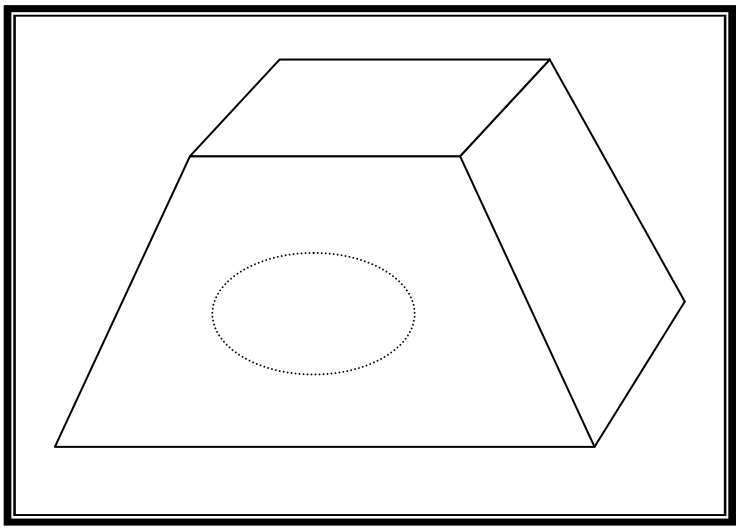

Figure 12.2: Diagram of wax block ready for sectioning with rat brain embedded in the centre (Southgate, 1999)

Sectioning was done using a RMC MT-7 rotary microtome. The microtome was set to cut sections of 10µm thickness. As sections were cut these would stick to one another, so as to form long ribbons. When the part of the brain containing the hippocampus was reached, every second section was removed and placed in a water bath (40° C) using forceps, which smoothens out the wrinkles.

12.2.2.5.5. Transferring Sections to Slides

Three sections at a time were removed from the water bath and placed onto glass microscope slides using a thin paint brush. The glass slide was initially brushed with a thin layer of Haupt's adhesive before the sections were mounted. The slides were left overnight in an oven at 40^0C to enable the section to adhere to the slide.

12.2.2.5.6. Staining

This stain stains the Nissl substances intense purple and the nuclei purple. The background is left clear (Bauer *et al*., 1974). Figure 12.1 shows a Nissl-stained coronal section through the caudal telencephalon of a rat brain depicting the hippocampus.

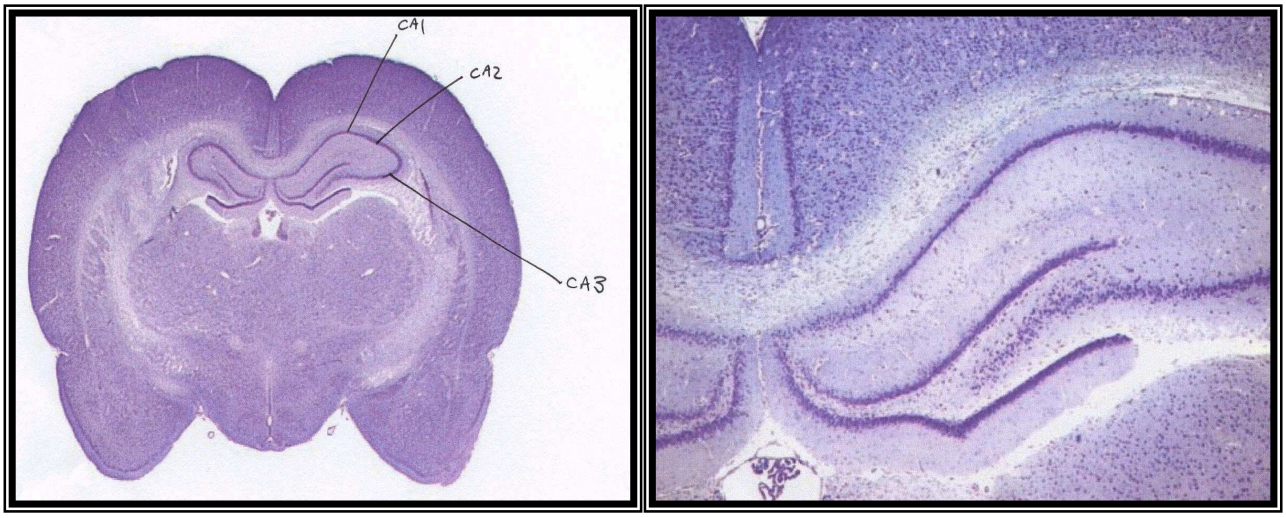

Figure 12.3: (Left) A coronal section through the caudal telencephalon of a rat brain displaying the hippocampal structure and three subdivisions. (Right) A magnified view of the rat hippocampus.

Since this dye is water soluble, the entire embedding process had to be reversed in order to remove the paraffin wax from the tissue and allow penetration of the dye. The paraffin was removed by running the slides through xylene twice for five minutes each, followed by immersion in a mixture of xylene and absolute ethanol (1:1) for three minutes. This step was followed by immersion in absolute ethanol for five minutes, and then re - immersion in absolute ethanol overnight. This was done as per Table 12.2.

Table 12.2: Procedure for dewaxing and rehydrating brain sections

Step	**Processing Agent**	**Time (minutes)**
1	Xylene (dewaxing)	5
2	Xylene	5
3	Xylene / Absolute Ethanol (1:1)	3
4	Absolute Ethanol	5
5	Absolute Ethanol	Overnight at 30°C

Sections were stained by placing in a 0.1% cresyl violet solution for 2 hours. The cresyl violet solution contained 0.25g cresyl violet, 250 ml Milli-Q water, 0.75 ml glacial acetic acid and 0.0512g sodium acetate. The pH was adjusted to 3.5 before use. The slides were differentiated rapidly in 95% ethanol by rinsing in a flat dish until the background was clear. Sections were then dehydrated again as shown in Table 12.3.

Table 12.3: Procedure for dehydrating brain sections after staining

Step	Processing Agent	Time (minutes)
1	Absolute Ethanol	5
2	Absolute Ethanol	5
3	Xylene	5
4	Xylene	5

12.2.2.5.7. Mounting of the Slides

The stained section on the slide must be covered with a thin piece of plastic or glass to protect the tissue from external damage like scratching, and to provide better optical quality for viewing under the microscope. While the slides were kept moist with xylene, enough DPX was added to just cover the tissue. A cover slip was placed over the tissue. The slides were allowed to dry on a flat surface for 48 hours.

12.2.2.5.8. Photo-microscopy

The slides were photographed using a combination Olympus camera and light microscope.

12.2.3. RESULTS

Neurons in the CA1 and CA3 regions of the hippocampus were examined microscopically. Sections of the CA1 and CA3 regions of the control treated rats (figure 12.4(a) and (f) respectively) showed optimally sized, pyramidal shaped neuronal cells with a clearly observable cell nucleus and continuous cell membrane. The cells are grouped closely together to form a band – like appearance, which is characteristic of both the CA1 and CA3 regions. Thus the neurons in both the CA1 and CA3 region appear to be undamaged. The neurons and nuclei were stained an intense purple colour while the background appeared light purple to a pink colour.

The hippocampal neuronal cells of both regions of the QA treated animals (figure 12.4 (b) and (g), respectively) show extensive degeneration by virtue of their roundness and swelling. The cells appear scattered with little integrity of cell membrane and appearance of dense nuclei. Necrosis of the neuronal cells in many areas is also evident. Similarly,

the neurons of the CA1 and CA3 regions (figure 12.4 (c) and (h), respectively) of the Fe^{2+} treated animals show extensive damage. The neurons appear even more scattered than the neurons in the QA treated rats. Most of the neurons in both the CA1 and CA3 regions of the hippocampus of the Fe^{2+} treated appear to have burst and lost their shapes (see figure 12.4 (c) and (h) arrows). Considerable cerebral oedema characterized by loss of cellular staining and vacuolisation is surrounded by a margin of pyknotic neurons adjacent is evident in the CA1 and CA3 region of rats treated with Fe^{2+}. Necrosis is evident in the CA1 and CA3 region of rats treated with QA and Fe^{2+}.

It is evident from figure 12.4 (d) and (i), the CA1 and CA3 regions of the rats treated with QA and 6-OHM, these neurons show significant protection in comparison to the neurons of the QA only treated rats. Similarly, the CA1 and CA3 regions of the 6-OHM and Fe^{2+} treated rats, (figure 12.4 (e) and (j) respectively), appear to be undamaged.

The majority of the neuronal cells in the 6-OHM and QA treated rats and the Fe^{2+} and 6-OHM treated rats (figure 12.4 (d), (i), (e) and (j)) appear to have retained their pyramidal appearance and are not as inflamed as those present in the hippocampus of the QA alone and Fe^{2+} alone treated rats. The cells show better orientation, integrity of cell membrane and appear closer to each other as though in an attempt to reconstruct their typical “band-like” appearance. It is also apparent that the neurons of the 6-OHM treated rats look healthier than the neurons of the control treated group.

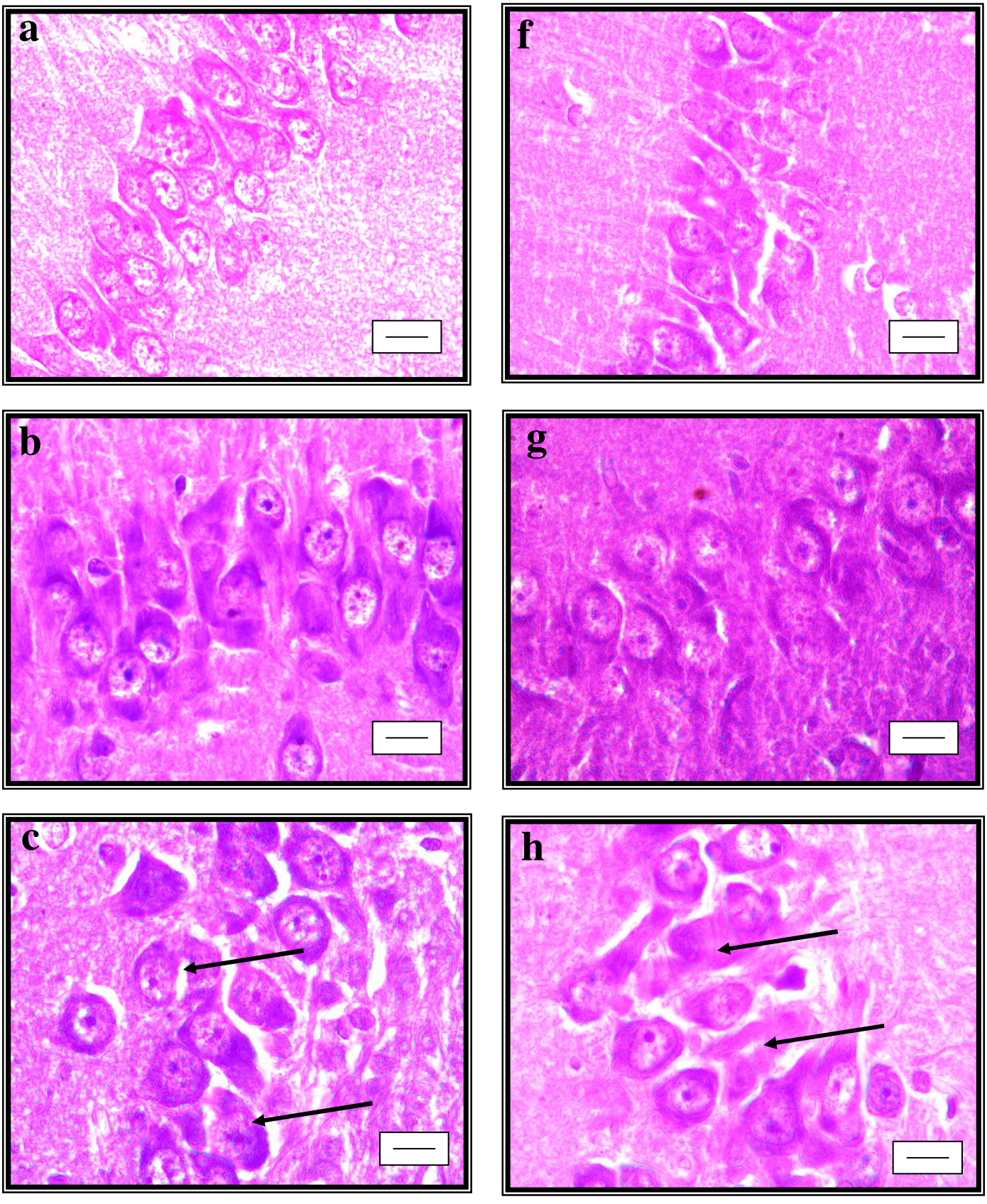
a
f
b
g
c
h

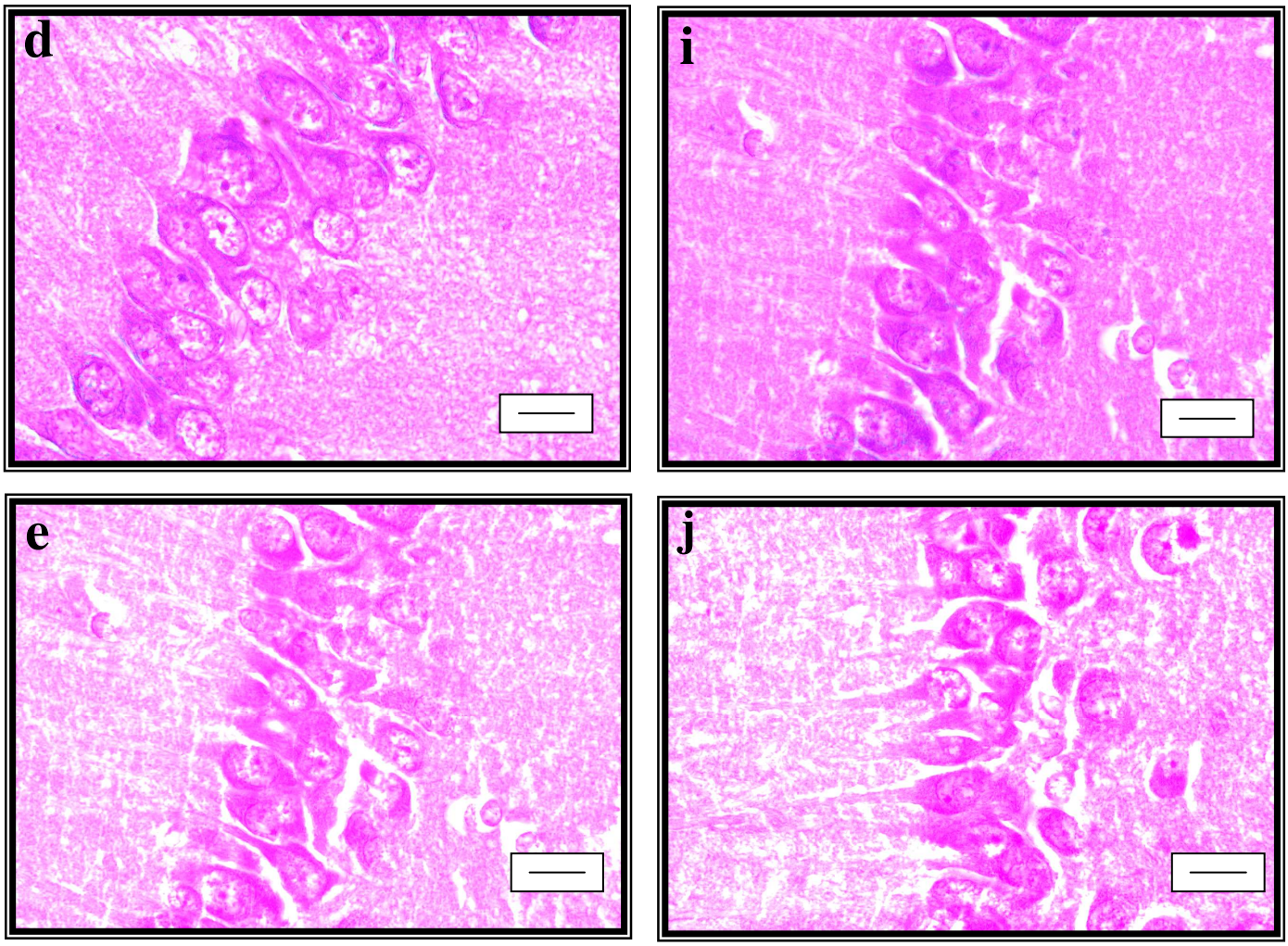

Figure 12.4: QA and Fe^{2+} toxicity and the protective effects of 6-OHM on rat hippocampal neurons. Micrographs (a-e) indicate cells in the CA1 region of the hippocampus from a control animal (a), an animal treated with QA (b), animal treated with Fe^{2+} (c), animal treated with QA and 6-OHM (d) and animal treated with Fe^{2+} and 6-OHM (e). Micrographs (f-j) indicate cells in the CA3 region of the hippocampus from a control animal (f), a QA treated animal (g), an animal treated with Fe^{2+} (h), an animal treated with QA and 6-OHM (i) and an animal treated with Fe^{2+} and 6-OHM (j). (Bar = 10µm).

12.2.4. DISCUSSION

Traumatic injury of the brain is characterised by disruption of cell bodies and axons, followed by little or no axonal regeneration and virtually no recovery of function by the lesioned tissue. These results clearly demonstrate the structural damage that a neurotoxin QA and the trace element Fe^{2+} causes in the CA1 and CA3 regions of the hippocampus, the part of the brain responsible for learning and memory processing.

The cell damage induced by QA is dependent on the NMDA receptor, since pretreatment with an antagonist prevents this damage. However, in order for NMDA receptors to be activated, another non-NMDA glutamate receptor such as AMPA must be activated. This activation results in an influx of Na^+ ions into the cell causing a depolarization of the membrane. The depolarization results in the removal of the magnesium block, allowing the opening of the channel once QA has bound. Once opened, Ca^{2+} ions move through and into the neuron. In cases where there are high concentrations of glutamate within the synapse, excessive activation of glutamate receptors occurs; resulting in a Ca^{2+} dependent rise in free radicals and acute toxicity follows. Acute toxicity occurs because of the rapid influx of Na^+ ions into the neurons, which causes passive water and Cl^- entry via osmotic pressure. This toxic process may be associated with abnormalities in membrane permeability and may be lethal, via osmotic lysis (Southgate, 1999). The process that takes place may be direct, by over-stimulation of the neuron leading to prolonged depolarization and depletion of energy reserves, or exchange. In addition, the activation of the NMDA receptor by QA results in a further influx of Ca^{2+} ions. This together with the water uptake results in the swelling of the cells evident in the photomicrographs. Similarly, Fe^{2+} lesions in the hippocampus have been shown to cause an increase in glutamate levels (Engström *et al*., 2001) and Ca^{2+} concentration (Sloot *et al*., 1994) in the hippocampus and result in focal oedema formation within 24 hours (Willmore *et al*., 1986).

A further possibility is that the damage produced by QA is partly dependent on the gliosis and inflammatory reaction which occurs in response to excitotoxic challenge (Behan *et al*., 1999). Activated microglia as well as activated macrophages which infiltrate the CNS in the aftermath of insults or lesions are known to produce ROS which could account for some of the neuronal damage *in vivo*. QA could act synergistically with the ROS produced from this source to produce a degree of damage which is dependent on both the activation of NMDA receptors and the oxidative stress imposed by free radical generation. However, QA must also be able to generate ROS independently of such cells, in view of the $O_2^{\bullet -}$ generation and lipid peroxidation which was noted *in vitro* and *in vivo* in chapter eight (figure 8.12) and chapter ten (figures 10.5 and 10.11). The above observations reported in this experiment demonstrate the hippocampus as an excellent model for examining the neurotoxic effects of QA and Fe^{2+} and further strengthens the

suggestions that the hippocampus may have a crucial role to play in mediating many of the behavioural and memory problems associated with QA and Fe^{2+} toxicity. In addition, neurons damaged due to the cannula needle were excluded ensuring that all damage was of an excitotin-induced nature and not due to physical damage caused by the needle tract.

From the histology studies (figure12.4.), it appears that 6-OHM not only protects neurons from structural damage induced by QA and Fe^{2+} but cells treated with 6-OHM appear healthier than cells from controls. External observations in the rats treated with QA and 6-OHM and those with Fe^{2+} and 6-OHM showed a relatively greater activity and faster response when compared to those that were treated with QA alone and Fe^{2+} only.

12.3. HISTOLOGICAL ANALYSIS OF THE EFFECT OF 6-OHM AGAINST QA AND Fe^{2+}-INDUCED DAMAGE TO HIPPOCAMPAL NEURONS USING ACID FUCHSIN STAIN.

12.3.1. INTRODUCTION

Acidophilia is considered one of the hallmarks of acute neuronal damage and death in brain ischemia, excitotoxic and traumatic lesions and epileptic seizure (Victorov *et al*., 2000). Acidophilic ("red") neurons intensively stain with acidic (anionic) dyes, such as eosin and acid fuchsin. Histochemical analysis of the staining by these anionic dyes shows that nuclear and cytoplasmatic acidophilia of degenerating neurons is due to proteins rich in arginine and lysine (Kiernan *et al*., 1998). The principal features of damaged neurons expressing acidophilia were initially described by Spielmeyer (1922) in autopsy material. According to Spielmeyer, the main pathomorphological signs of neuronal damage in the human ischemic brain ("ischamische Zellveranderungen", ischemic cell change) include shrinkage of neuronal somata, deformation and displacement of strongly stained nuclei, chromatolysis, and acidophilia of the cytoplasm.

Shrunken neurons displaying ischemic cell changes are necrotic, but they differ from swollen "truly" necrotic cells (Garcia *et al*., 1995; Rosenblum, 1997). In subsequent studies, acidophilic (red) neurons were observed in experimental brain (Auer & Siesjo, 1988; Brown, 1977; Garcia & Conger, 1986; Garcia *et al*., 1995; Kawai *et al*., 1992; Kirino *et al*., 1985). This type of acute neuronal damage is not unique to ischemia (*Kirino et al*., 1985), but was also found in hypoglycaemia (Auer *et al*., 1985; Auer & Siesjö , 1984; Auer *et al*., 1984), epilepsy (Chang & Braham, 1994), excitotoxic neuronal lesions (Kiernan *et al*., 1998), and brain trauma (Sutton *et al*., 1993). Initially, necrotic neurons were considered to be only those neurons subsequently removed from brain tissue in separate experiments studying the time course of the tissue damage. However, it soon became apparent that all neurons which demonstrated a pronounced affinity for acid dyes were moribund.

Acidophilia is generally considered as a sign of irreversible (necrotic) neuronal damage (Kirino *et al*., 1985). However, reversible acidophilia was observed in the hippocampus of rats after epileptic seizures induced by kainic acid (Chang & Braham, 1994). In this experiment it was decided to investigate whether 6-OHM offers neuroprotection against QA and Fe^{2+}-induced intrahippocampal neuronal death in the rat hippocampus. After treatment, the brains of the rats were sectioned and the hippocampus was examined microscopically for evidence of acidophilic and hyperchromatic shrunken neurons.

12.3.2. MATERIALS AND METHODS

12.3.2.1. Chemicals and Reagents

Quinolinic acid, ammonium metavanadate, borax (sodium tetraborate), sodium acetate, 6-OHM, acid fuchsin, and toluidine blue were purchased from Sigma St. Louis, MO, U.S.A. Acetic acid glacial was purchased from Saarchem (PTY) Ltd., Krugersdorp, South Africa. All other chemicals were of the highest quality available and were purchased from commercial distributors.

12.3.2.2. Solution Preparation

a) Ammonium metavanadate solution. 500mg of ammonium metavanadate was dissolved in 100mL of hot (80-90^{o}C) distilled water with constant stirring.
b) Vanadium acid fuchsin (VAF). 100mg of acid fuchsin was dissolved in 75mL of distilled water and to this solution, 25mL of 0.5% ammonium metavanadate solution and 1mL of glacial acetic acid was added.
c) Acetic acid –sodium acetate buffer (pH 3.3). 130mg of sodium acetate was dissolved in 100mL of distilled water; to this solution 1.2mL of glacial acetic acid was added.
d) Toluidine blue. 25mg of toluidine blue was dissolved in 100mL of acetic acid-sodium acetate buffer.
e) 0.01% solution of borax. This solution needs to be changed regularly.
f) Acid alcohol (1% hydrochloric acid in 70% absolute alcohol).
g) 1% solution of sodium bicarbonate. This solution needs to be changed regularly.

12.3.2.3. Treatment Regime

Adult male rats of the Wistar strain housed in separate cages, in a controlled environment as described in appendix one. Surgical procedures were conducted according to the method described in 10.5.2.5 and the rats were dosed s.c. as described in section 10.5.2.4.

12.3.2.4. Histological Techniques

The histological techniques were followed according to the methods described by Victorov *et al*., (2000).

12.3.2.4.1. Fixing the brain

The animals were sacrificed and the brains removed as in section 2.2.2.4., and immediately fixed as described in section 12.2.2.5.1.

12.3.2.4.2. Specimen Preparation and Embedding

Dehydration of tissue fragments and embedding of tissue in paraffin wax was conducted as described in section 12.2.2.5.2.

12.3.2.4.3. Blocking Out

The brain material was fixed into a block as described in section 12.2.2.5.3.

12.3.2.4.4. Sectioning

Sectioning was done using a rotary microtome and 8-10 μm thickness sections were cut as described in section 12.2.2.5.4.

12.3.2.4.5. Transferring Sections to Slides

Sections placed onto glass microscope slides using a thin paint brush as described in section 12.2.2.5.5.

12.3.2.4.6. Staining

Paraffin wax was removed from the tissue to allow penetration of the dye. The paraffin was removed by running the slides through xylene for five minutes, followed by hydrating the slides in a graded ethanol solutions (100%, 96%, 70%) for 5 min each. Thereafter the slides were washed in distilled water. The slides were then stained with VAF for 1 min (maximum of 2 min) and thereafter rinsed in distilled water. The slides were then rinsed with 0.01% borax solution for 20-30sec until a light red colour of the section was obtained and then rinsed again in distilled water. The slides were immersed in acetate buffer for 30s and then counterstained with toluidine blue for 20-30s (maximum of 1 min).

The slides were then rinsed with acetate buffer for 30 s until the sections were a pale sky blue colour with at pale reddish brown background. The slides were examined using a light microscope to determine if staining was satisfactory. Abnormal neurons are stained a deep red colour while healthy neurons stain a dark blue colour. Once staining has been achieved satisfactorily the slides were rinsed with distilled water, blotted gently dry with filter paper and dehydrated as described above in Table 12.3.

The stained sections were mounted with cover slips as described in section 12.3.2.5.6 and photographed using a combination Olympus camera and light microscope.

12.3.2.4.7. Quantification of Brain Damage

Cell counts of CA1 and CA3 regions were made from every fifth section throughout the rostrocaudal extent for each animal and it control using an image analyzer. To differentiate surviving neurons from injured neurons, injured neuronal cells were determined according to the criteria of Eke and Conger (1989; 1990). Neurons were examined at a magnification of x 1000. The hippocampus was examined at the CA1 and

CA3 regions and a damage score with 0% representing an absence of detectable cell loss and 100% representing the absence of any normal pyramidal neurons in the field of view. A difference was considered statistically significant at $p<0.05$ using the Student-Newman-Keuls test for multiple comparisons (Zar, 1974).

12.3.3. RESULTS

From the photomicrographs it was evident that the nuclei and cell membrane of healthy, undamaged neurons were stained blue while abnormal hippocampal neurons stood out as bright red objects against a brownish pink background (figure 12.5). It is evident from figure12.5, by the extensive red staining of damaged neurons, that both QA and Fe^{2+} caused excessive damage to the CA1 and CA3 regions of the hippocampus. The abnormal neurons were variable in appearance and distribution. It was also observed that the number of AF positive neurons was greater in the CA1 region of the hippocampus for the rats treated with QA only.

The rats that received Fe^{2+} only, the pyramidal cell layer of the hippocampus consisted largely of strongly red stained neurons. It is evident in figure 12.5 (c) and (h), there is dense cellular staining pattern of the CA1 and CA3 neurons with macrophage and glial cells present in the surrounding area. However, a dose of 6-OHM (5mg/kg/d) was effective in protecting the neurons of the CA1 and CA3 regions of the hippocampus from QA and Fe^{2+} induced neuronal damage (figure 12.5). It is clearly evident in figure 12.5 (c) and (h) that there is intense staining of the white matter of the rat brain which is due to the Fe^{2+} causing damage to the surrounding area in addition to the hippocampus. As evident in figure 12.4, the number of AF positive neurons are markedly decreased by the administration of 6-OHM.

As shown in figure 12.6 and 12.7, treatment of rats with QA only and Fe^{2+} only resulted in a significant increase in AF positive neurons in both the CA1 and CA3 regions of the hippocampus. However, the administration of 6-OHM is able to significantly reduce the number of AF positive neurons as compared to the QA only and Fe^{2+} only treated groups.

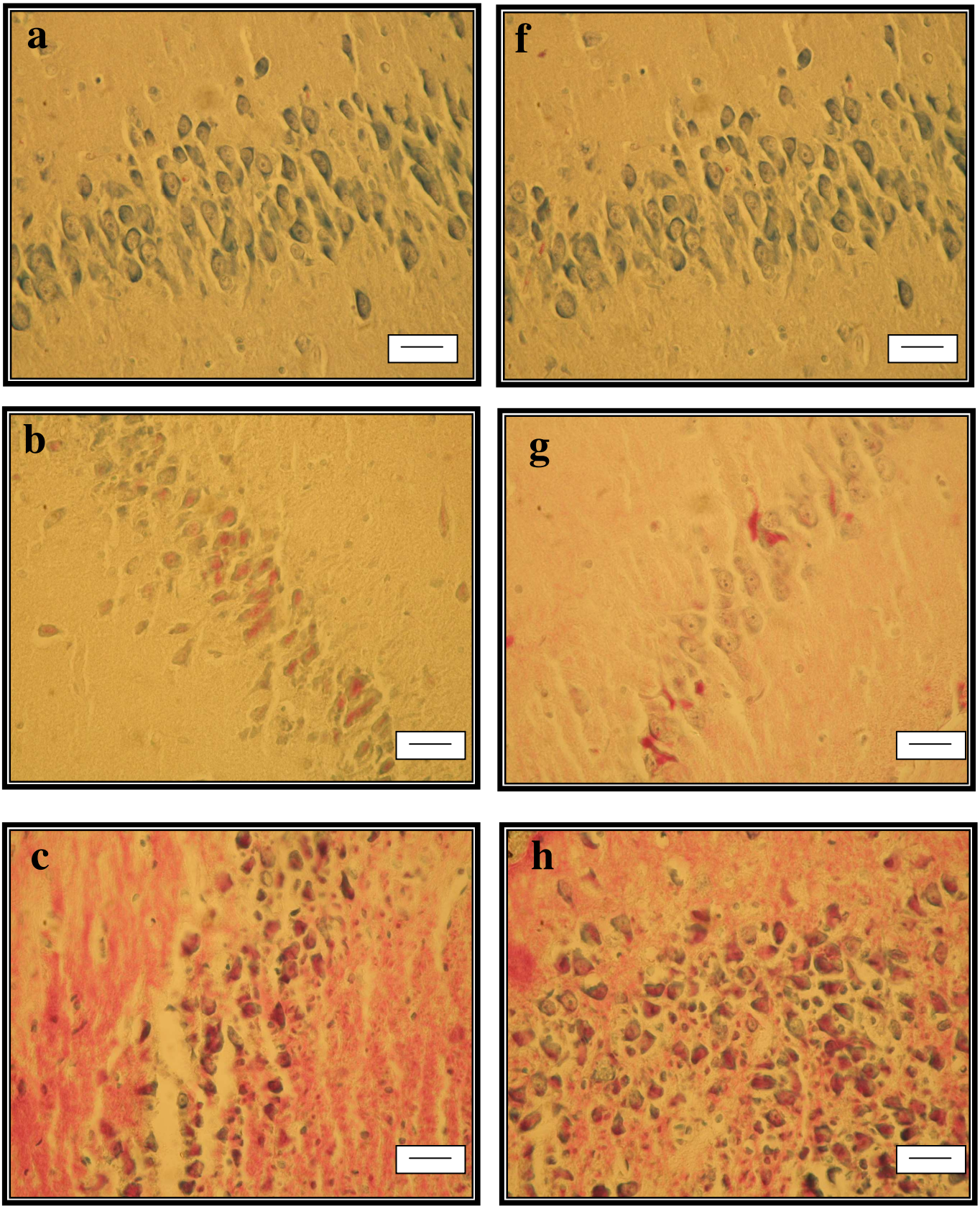
a
f
b
g
c
h

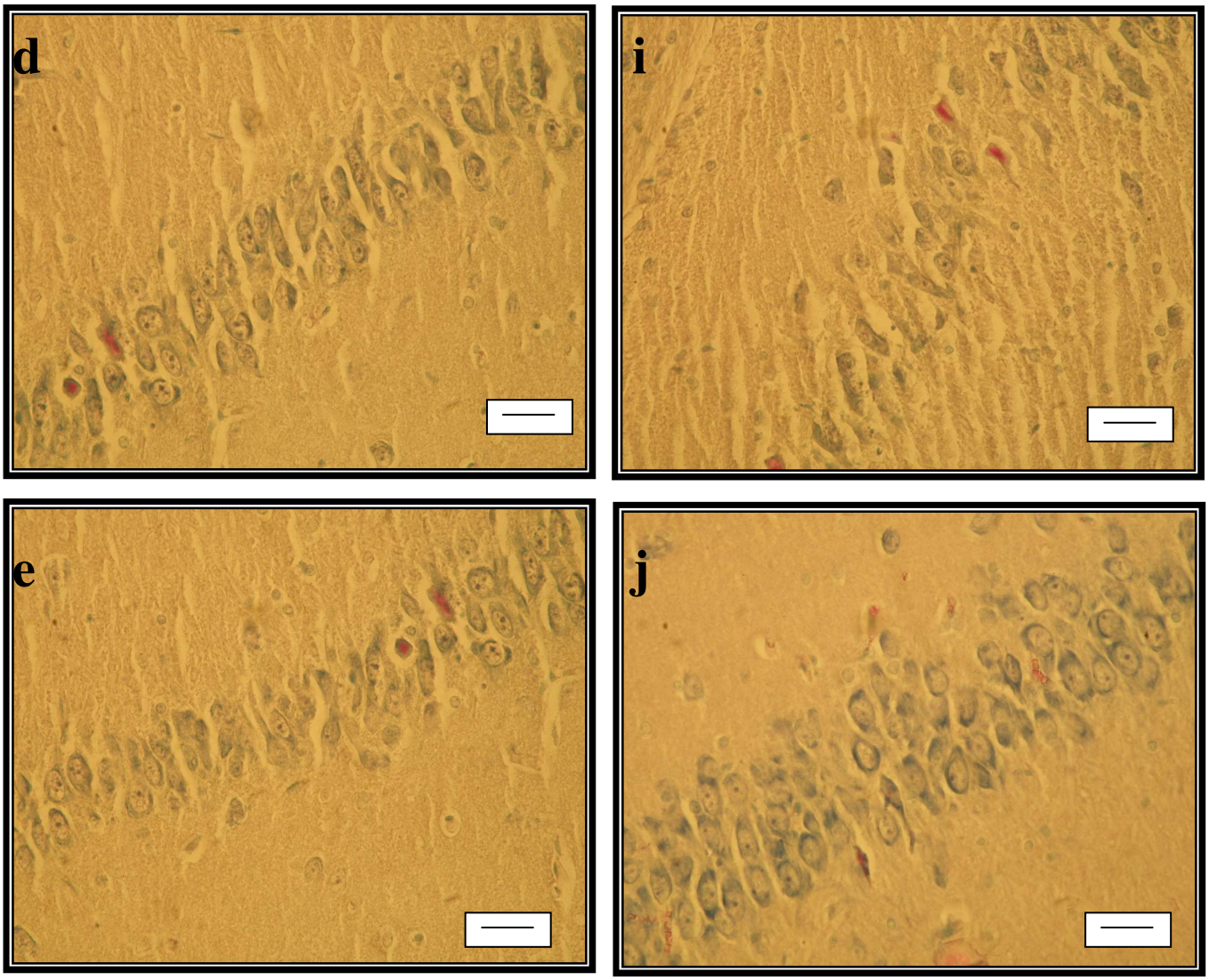

Figure 12.5: QA and Fe^{2+} toxicity and the protective effects of 6-OHM on rat hippocampal neurons. Micrographs (a-e) indicate cells in the CA1 region of the hippocampus from a control animal (a), an animal treated with QA (b), animal treated with Fe^{2+} (c), animal treated with QA and 6-OHM (d) and an animal treated with Fe^{2+} and 6-OHM (e). Micrographs (f-j) indicate cells in the CA3 region of the hippocampus from a control animal (f), a QA treated animal (g), an animal treated with Fe^{2+} (h), an animal treated with QA and 6-OHM (i) and an animal treated with Fe^{2+} and 6-OHM (j). (Bar = 10µm).

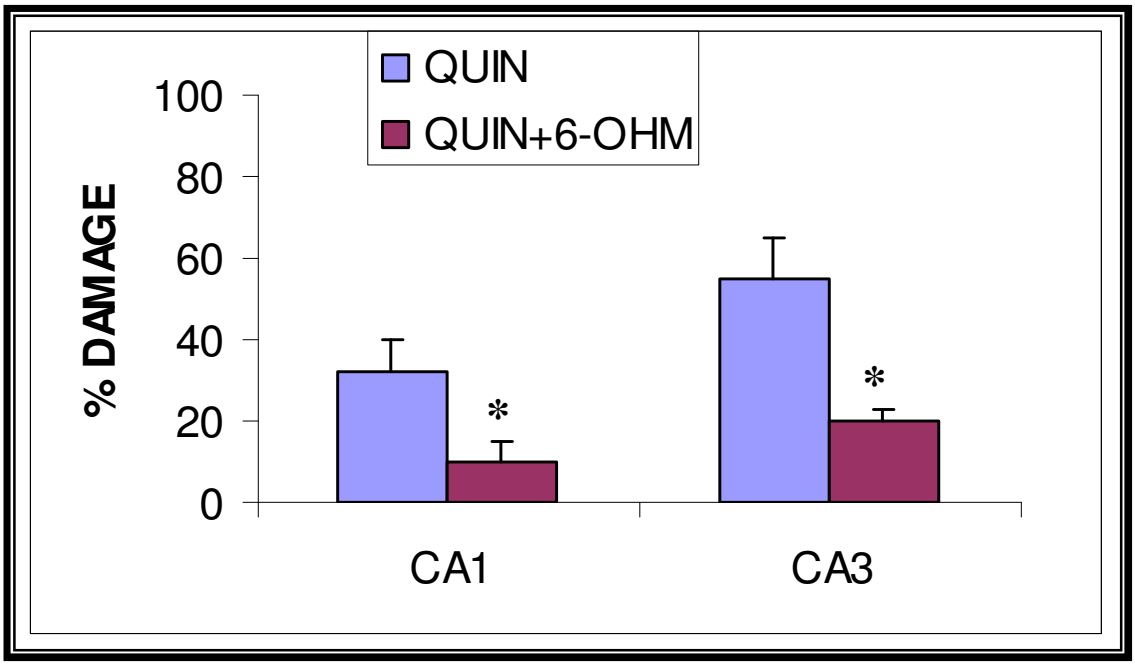

Figure 12.6: Effect of 6-OHM on neuronal damage after QA injection. Each bar shows the mean ± SEM (n=5 rats) of the neuronal damage assessed in CA1 and CA3 regions. * ($p<0.05$) as compared with QA only treated rats.

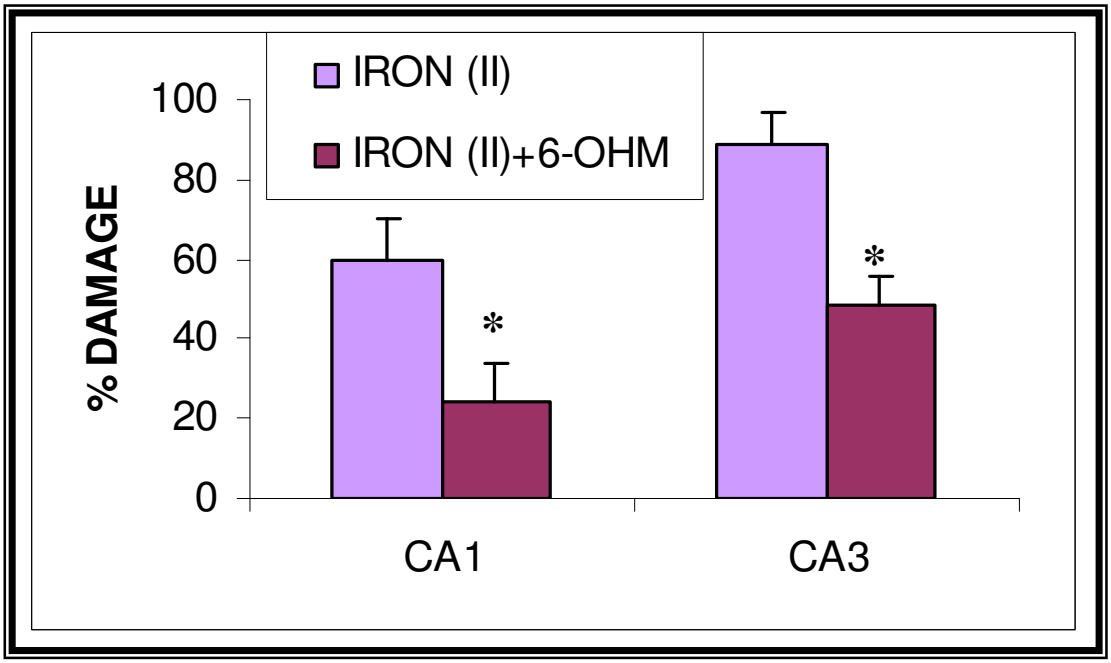

Figure 12.7: Effect of 6-OHM on neuronal damage after Fe^{2+} injection. Each bar shows the mean ± SEM (n=5 rats) of the neuronal damage assessed in CA1 and CA3 regions. * ($p<0.05$) as compared with Fe^{2+} only treated rats.

12.3.4. DISCUSSION

Acid fuchsin, a biological stain, has been utilized in cell death of hypoglycaemia, traumatic injury and excitotoxicity (Auer *et al*., 1984). In any necrotic tissue the cells that remain recognizable commonly exhibit increased affinity for anionic dyes. In the CNS, acidophilic neurons are a useful indicator of the extent of damage in incomplete lesions such as the dispersed damage caused by the administration of an excitotoxin (Tanaka & Simon, 1994).

Two such excitotoxins are QA and Fe^{2+}, both these agents are known to cause oxidative damage to the hippocampus of rats as shown in chapter 8 and chapter 9. In the present study it is evident that both these toxins bring about hippocampal neuronal death in both the CA1 and CA3 region. These result further support the Nissl stained sections seen in figure 11.4. However, the administration of 6-OHM is able to significantly protect the neurons in these regions of the hippocampus from QA and Fe^{2+} induced neurotoxicity. The mechanism of action 6-OHM acting as an antioxidant and protects the neurons against QA and Fe^{2+} induced ROS and lipid peroxidation as was shown in chapter 8 and chapter 9. In the experiment the intrahippocampal injection of Fe^{2+} caused brain oedema, and this is supported by Chan & Fishman (1980) that phospholipids peroxidation may initiate a cascade leading to the formation of oedema.

12.4. CONCLUSION

From the results obtained in this chapter, it is evident that 6-OHM attenuates QA and Fe^{2+} insult in the rat hippocampus. Heyes (1996), Willmore & Rubin (1982) and Armstrong *et al*., (2001) reported that microglia and macrophages may be an important source of QA and Fe^{2+} neurotoxicity and since macrophages were often present in the affected areas, cell death in the hippocampus was likely due to necrosis. This protection elicited by 6-OHM as well as that shown against the increase in lipid peroxidation in chapter ten, could be due to its antioxidant property, in this way preventing further damage induced by the free radicals formed during the initial QA and Fe^{2+} damage. However, considering the extent of the protection that 6-OHM has against this potent neurotoxin, it is more likely that the protection involves the NMDA receptor and the scavenging of $^{\bullet}OH$

radicals. It is possible that 6-OHM, similar to melatonin, is able to bind to the receptor to the same site at which QA binds (Southgate, 1999), and the indoleamine would compete with QA and thus prevent QA induced neuronal damage. Another mechanism of action of 6-OHM against QA induced oxidative stress was postulated to be that 6-OHM could be binding Fe^{2+} or Fe^{3+} and thus preventing these ions from playing a role in neuronal damage, was investigated in chapter eleven. 6-OHM was found not to bind to Fe^{2+}, but was effective in binding to Fe^{3+} and converting it to Fe^{2+}. Thus, indicating that complexation of 6-OHM with Fe^{2+} is not its mechanism of neuroprotection but its protection is elicited more by its antioxidant ability. In chapter eleven, it was postulated that 6-OHM by bind to Fe^{3+} and reducing it to Fe^{2+}, is possibly promoting the Fenton reaction and serving as a pro-oxidant. However, this chapter provides histological evidence demonstrating that 6-OHM does not promote oxidative neurotoxicity but protects hippocampal neurons against QA and Fe^{2+}-induced necrosis.

The cell damage induced by QA is dependent on the NMDA receptor, since pre-treatment with an antagonist prevents this damage. However, in order for NMDA receptors to be activated, another non-NMDA glutamate receptor, such as AMPA must be activated. This activation results in an influx of Na^{+} ions into the cell causing a depolarization of the membrane. The depolarization results in the removal of the magnesium block, allowing the opening of the channel once QA has bound. Once opened, Ca^{2+} ions move through and into the neuron.

In cases where there are high concentrations of glutamate within the synapse, excessive activation of glutamate receptors occurs, resulting in acute toxicity. Acute toxicity occurs because of the rapid influx of Na^{+} ions into the neuron, which causes passive Cl^{-} and water entry via osmotic pressure. This toxic process may be associated with abnormalities in membrane permeability and may be lethal, via osmotic lysis (Southgate, 1999). The process that takes place may be direct, by over-stimulation of the neuron leading to prolonged depolarization and depletion of energy reserves, or indirect, by excessive Na^{+} ion influx resulting in Ca^{2+} build up via Na^{+}-Ca^{2+} exchange. In addition, the activation of the NMDA receptor by QA results in a further influx of Ca^{2+} ions. In addition, iron neurotoxicity has been shown to be associated with elevation of intracellular Ca^{2+} concentration (Sloot *et al.*, 1994) and this can be attenuated with NMDA receptor

antagonists (Zhang *et al*., 1993). It has been suggested that the NMDA receptor complex may contain a novel site sensitive to blockade by Fe^{2+} iron in rat brain (Nakamichi *et al*., 2002). This together with the water uptake results in the swelling of the cells evident in the photomicrographs.

It is evident from this chapter that both QA and Fe^{2+} result in extensive loss and damage to the morphology of hippocampal neurons. From the characteristics of the cell damage, the mechanism of neuronal death for both QA and Fe^{2+} was interpreted as necrosis. This is supported by a number of authors, who have shown QA and iron to cause cell death in the hippocampus by necrosis (Southgate *et al*., 1998; Armstrong *et al*., 2001; Sloot *et al*., 1994; Willmore & Rubin, 1982; Willmore *et al*., 1978). However, some authors have shown that intracerebral QA injection results in increases in glutamate levels and p53 levels (a transcription factor whose main function is to control cell cycle progression and apoptotic process) and display signs of apoptosis (Uberti *et al*., 2003). Thus, the ability of QA to induced programmed cell death in the hippocampus was investigated in chapter thirteen.

The pineal antioxidant, MEL has been shown to protect against QA-induced hippocampal neuronal degeneration (Southgate *et al*., 1998), while Lin *et al*., (2000) and Chen *et al*., (2003) demonstrated the effectiveness of melatonin in preventing iron-induced oxidative damage and neuronal death to the rat brain *in vivo*. The result confirms that 6-OHM, the primary photoproduct and stable metabolite of melatonin, is able to protect against QA and Fe^{2+} induced hippocampal damage. Thus 6-OHM, like melatonin, has a role to play in reducing neuronal degeneration which the above two toxins are known to produce.

CHAPTER THIRTEEN

APOPTOSIS

13.1. INTRODUCTION

Apoptosis is gene-directed cell death with distinct morphological and biochemical features which are characterized by membrane blebbing, nuclear fragmentation, nucleosomal DNA fragmentation (DNA ladder), and formation of apoptotic bodies in comparison to necrosis (Steller, 1995). Some of these changes are illustrated in figure 13.1, which shows time-lapse microscopy images of a trophoblast cell undergoing apoptosis.

Apoptosis is generally characterized by chromatin condensation, intracellular fragmentation associated with membrane-enclosed cellular fragments (apoptotic bodies), and internucleosomal DNA fragmentation (Kerr *et al*., 1972; Wyllie *et al*., 1984). One of the hallmarks of apoptosis is fragmentation of DNA, which is visible as 'laddering' on an electrophoresis gel. However, not all forms of apoptosis appear to involve the same amount of laddering (Wyllie *et al*., 1984), or this phenomenon may occur at a relatively late stage in apoptosis. Additionally, this method does not allow for the identification of individual apoptotic cells. The TUNEL method was designed as a histochemical technique to detect internucleosomal DNA fragmentation at the level of individual cells (Gavrieli *et al*., 1992; Ben-Sasson *et al*., 1995). The TUNEL reaction preferentially labels DNA strand breaks generated during apoptosis and this allows discrimination of apoptosis from necrosis and from primary DNA strand breaks induced by cytostatic drugs or irradiation (Gorczyca *et al*., 1993).

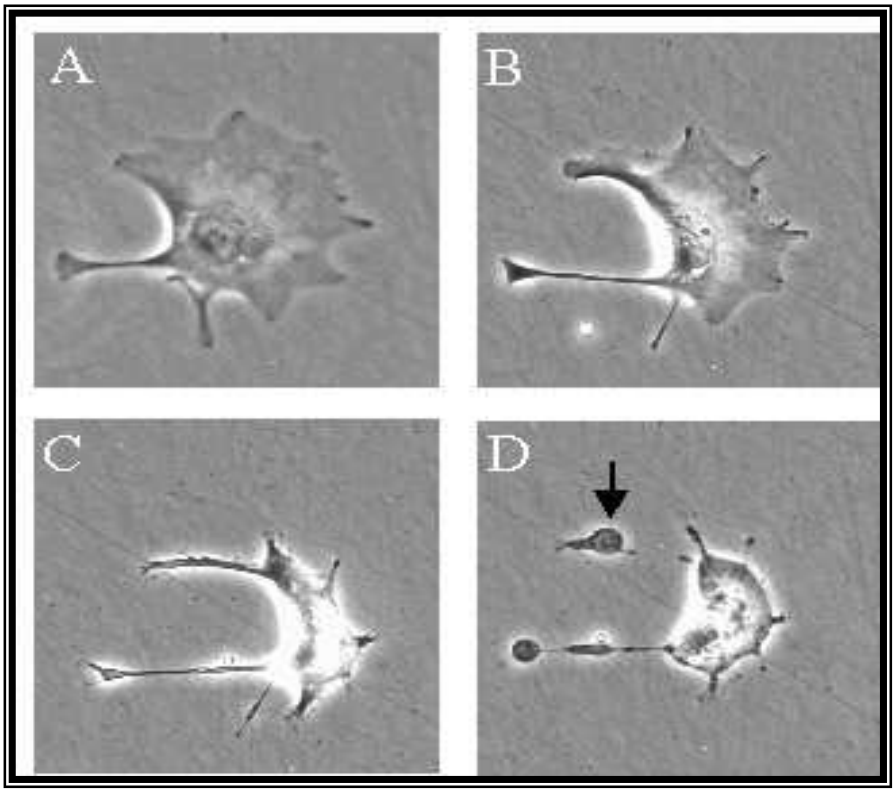

Figure 13.1: Shows time-lapse microscopy images of a trophoblast cell undergoing apoptosis (www.sghms.ac.uk/depts/immunology/%7Edash/apoptosis/intro.html). Typically, the cytoplasm begins to shrink following the cleavage of lamins and actin filaments (**A**). Nuclear condensation can also be observed following the breakdown of chromatin and nuclear structural proteins, and in many cases the nuclei of apoptotic cells take on a "horse-shoe" like appearance (**B**). Cells continue to shrink (**C**), packaging themselves into a form that allows for easy clearance by macrophages. These phagocytic cells are responsible for removing apoptotic cells from tissues in a clean and tidy fashion that avoids many of the problems associated with necrotic cell death. In order to promote their phagocytosis by macrophages, apoptotic cells often undergo plasma membrane changes that trigger the macrophage response. One such change is the translocation of phosphatidylserine from the inner leaflet of the cell to the outer surface. Membrane changes can often be observed morphologically through the appearance of membrane blebs (**D**) or blisters which often appear towards the end of the apoptotic process. Small vesicles called apoptotic bodies are also sometimes observed (**D**, arrow).

Several methods have been described to identify apoptotic cells (Afanasyev *et al*., 1993; Bryson *et al*., 1994; Darzynkiewicz *et al*., 1992). Endonucleolysis is considered as the key biochemical event of apoptosis, resulting in cleavage of nuclear DNA into oligonucleosome-sized fragments. Therefore, this process is commonly used for detection of apoptosis by the typical 'DNA ladder" on agarose gels during electrophoresis. This method, however, cannot provide information regarding apoptosis in individual cells nor relate cellular apoptosis to histological localization or cell differentiation. This can be done by enzymatic *in situ* labelling of apoptosis induced DNA strand breaks.

DNA polymerase as well as terminal deoxynucleotidyl transferase (TdT) (www.roche-applied-science.com) has been used for the incorporation of labelled nucleotides to DNA strand breaks *in situ*. The tailing reaction using TdT, which was also described as ISEL (*in situ* end labelling) (Gorczyca *et al*., 1993) or TUNEL (TdT-mediated dUTP nick end labelling) (Gavrieli *et al*., 1992; Sgonc *et al*., 1994) technique, has several advantages in comparison to the *in situ* nick translation (ISNT) using DNA polymerase:

- Label intensity of apoptotic cells is higher with TUNEL compared to ISNT, resulting in an increased sensitivity (Gorczyca *et al*., 1993).
- Kinetics of nucleotide incorporation is very rapid with TUNEL compared to the ISNT (Gorczyca *et al*., 1993).
- TUNEL preferentially labels apoptosis in comparison to necrosis thereby discriminating apoptosis from necrosis and from primary DNA strand breaks induced by antitumour drugs, irradiation or excitotoxins (Gorczyca *et al*., 1993).

Cleavage of genomic DNA during apoptosis may yield double stranded, low molecular weight DNA fragments (mono-and oligonucleosomes) as well as single strand breaks ('nicks') in high molecular weight DNA. Those DNA strand breaks can be identified by labeling free 3'-$^{\cdot}$OH termini modified nucleotides in an enzymatic reaction. The working procedure described below was published by Sgonc *et al*., (1994) and the TUNEL method used for the experiments of this chapter involves the use of fluorescein-dUTP to label DNA strand breaks. Stage one involves the labeling of DNA strand breaks with TdT. This catalyses polymerization of labeled nucleotides to free 3'-OHM DNA ends in a template-independent manner (TUNEL-reaction). In stage two, the fluorescein labels incorporated in nucleotide polymers are detected and quantified by fluorescence microscopy (www.roche-applied-science.com).

Apoptosis has been found to be implicated in clinical outcomes, such as Alzheimer's disease, Parkinson's disease; Huntington's disease, and heart failure (Wylie, 1998). Thus, in this chapter it was decided to investigate the ability of QA to promote apoptosis in the hippocampus and protection offered by the treatment with melatonin and 6-OHM using the *In Situ* Cell Death Detection Kit, Fluorescein. This kit is designed as a precise, fast, and simple, non-radioactive technique for the detection and quantification of apoptosis at single cell level in cells and tissues, based on labeling of DNA strand breaks (TUNEL technology) using fluorescence microscopy.

13.2. THE EFFECT OF MELATONIN AND 6-OHM AGAINST QA-INDUCED APOPTOSIS.

13.2.1. INTRODUCTION

Excitotoxicity has been proposed to contribute the pathologenesis of a number of neurodegenerative disorders, including stroke, Huntington's diseases, Parkinson's disease, AD, and amyotrophic lateral sclerosis (Qin *et al*., 2001). Apoptotic mechanisms appear to contribute to excitotoxic neuronal injury in the rat striatum (Portera-Cailiau *et al*., 1995; Qin *et al*., 1996). Excessive generation of $O_2^{\bullet-}$ has been linked to programmed cell death and to the diminution of the life span of organisms (Greenland *et al*., 1995; Orr & Sohal, 1994).

In chapter eight, QA was shown to cause extensive production of $O_2^{\bullet-}$ in the rat hippocampus *in vivo* and thus apoptosis is postulated as a possible mode of neuronal cell death. The role of QA in DNA fragmentation has been reported by (Ogata *et al*., 2000). Ogata *et al*., (2000) showed that QA induced apoptosis via the caspase pathway in HL-60 cells. QA is a natural metabolite in the NAD cycle for NAD biosynthesis and metabolism in animals and NAD is known as the substrate for PARP involved in apoptosis (Ogata *et al*., 2000). The results of a number of studies have suggested that NAD metabolism, especially PARP participates in the processes of apoptosis induced by various stimuli (Shiokawa *et al*., 1997). Moreover, QA has a pharmacological function as an analeptic in the brain (Perkins & Stone, 1982) and has a suppressive effect on bone marrow erythroid growth and lymphocyte blastoid transformation (Kawashima *et al*, 1987). Furthermore, the excitotoxin, QA is known to induce apoptosis in the striatum of rats (Qin *et al*., 2001; Nakai *et al*., 1999). Henchcliffe & Burke (1997) showed extensive apoptosis 24 hrs after striatal QA lesion. This was further supported by recent observations that suggest that QA induced destruction of striatal cells occurs, at least in part, by an apoptotic mechanism (Portera-Cailliau *et al*., 1995; Qin *et al*., 1996; Dihné *et al*., 2001). In addition recently, QA lesioned neuronal cells have been shown to undergo programmed cell death (Uberti *et al*., 2003).

Since the ability of QA to induce necrotic cell death in the CA1 and CA3 hippocampal neurons was shown in chapter twelve, it was decided to investigate if QA resulted in apoptotic cell death as well. In the previous chapters, the indoleamines, melatonin and 6-OHM have been shown to protect against QA-induced oxidative stress, excitotoxicity and necrotic cell death in the hippocampus. Thus, the aim of this chapter was to investigate whether lesioning of the hippocampus with QA results in apoptotic neuronal death and if co-treatment of rats with QA and melatonin or 6-OHM results in a reduction in positive apoptotic neurons, using the *in situ* cell death detection kit, fluorescein described above.

13.2.2. MATERIALS AND METHODS

13.2.2.1 Chemicals and Reagents

Quinolinic acid, melatonin, and 6-hydroxymelatonin were purchased from Sigma St. Louis, MO, U.S.A. Aminopropyltriethoxysilane (APES) was purchased from NT lab Fluka. Paraffin wax was obtained from Lasec (South Africa). *In situ* cell death detection kit, fluorescein, proteinase K (nuclease free) and DNase 1, grade 1 (positive control) were purchased from Roche Diagnostics, (Nonnenwald, Penzberg). Formaldehyde, glacial acetic acid, absolute ethanol, xylene, and chloroform were purchased from Saarchem, Gauteng, SA while the aqueous mountant, SHUR/MOUNT™ was purchased from Triangle Biomedical Sciences Inc, Durham, USA. All other chemicals were of the highest quality available and were purchased from commercial distributors.

13.2.2.2. Animals

Adult male rats were cared for as described in appendix one.

13.2.2.3. Surgical Procedures

Animals were dosed as described in section 10.5.2.2., while the bilateral injection of QA into the hippocampus was carried out as in section 10.5.3.2.1. However, the Fe^{2+} treatment was excluded from this study.

13.2.2.4. Histological Techniques for Apoptosis Detection

The histological techniques were followed according to the method described by the *in situ* cell death detection kit, fluorescein instruction manual (www.roche-applied-science/pack-insert/1684795a.pdf).

13.2.2.4.1. Fixation and Processing of Brain Tissues

Fixation of the brain tissue can have dramatic effects on the cellular morphology of histological sections. Fixation of brain tissue should be performed rapidly without unnecessary handling beforehand, because neuronal staining artifacts generated by manipulation can be misinterpreted as pyknotic nuclei in neurons. The brain tissue was fixed according to the method described in chapter twelve, section 12.2.2.5.1.

The fixation process was terminated by dehydrating the brain tissue. For apoptosis detection, traditional processing and embedding techniques can not be used as described in chapter twelve, section 12.2.2.5.2. Thus, in order to reduce residual damage and improve the fluorescence of the tissue, reagents that could affect the fluorescence were eliminated from the procedure. Moisture was extracted from the tissue fragments by bathing them successively in a graded series of mixtures of ethanol, and this step was followed by the clearing and defatting process that involves the removal of ethanol by immersing the tissue in chloroform. The tissue was then submerged in molten paraffin wax (MP 57-58^{o}C) at 60^{o}C for one hour, which facilitated the removal of chloroform and while infiltrating the tissue without encountering water. At the end of this 1 hr period the brain tissue was placed under vacuum to remove any air that was trapped in the wax for 15min. Thereafter, the brain tissues were placed in new wax twice for a period of 1hr each. Finally the brain tissue was embedded in molten wax and this stage provides the hardness and support that the tissue requires for sectioning. The method used here is a modification of the method described by Geiger *et al*., (1997) and is described in Table 13.1. The tissues can be stored in paraffin indefinitely without visible influence on the quality of TUNEL reactions (Geiger *et al*., 1997).

Table 13.1: Fixation and Processing of Tissues for Paraffin Embedding.

Step	Processing Agent	Time (Hours)
Fixation	Davidson's Fixative solution	48 hrs
Dehydration	50% Absolute Ethanol	1 x 2 hrs
	70% Absolute Ethanol	1 x 2 hrs
	80% Absolute Ethanol	1 x 2 hrs
	90% Absolute Ethanol	1 x 2 hrs
	96% Absolute Ethanol	2 x 2 hrs
	100% Absolute Ethanol	3 x 2 hrs
Clearing	Absolute Ethanol: Chloroform (1:1)	1x 2 hrs
	Chloroform	1 x 2 hrs
	Xylene: Chloroform (1:1) at 60^{o}C	1 x 1 hr
Wax Immersion	Melted Paraffin Wax (MP 57-58^{o}C) at 60^{o}C	1x 1 hr
	Vacuum at 60^{o}C	15min
	Melted wax	2 x 1hrs
Embedding	In molten Wax	Overnight

13.2.2.4.2. Sectioning

Paraffin sections were cut by standard methods as described in chapter twelve, section 12.2.2.5.4. The sections of paraffin-embedded tissue was cut 5µm thick and placed on the APES coated slides. The treatment procedure for the slides is described below.

13.2.2.4.3. Treatment of Slides

When mounting paraffin sections on slides, it is important to use an appropriate adhesive to avoid loss of sections during the subsequent washing procedures. Sections can be mounted on Superfrost slides or on glass slides that have been coated (subbed) with either aminopropyl triethoxysilane (APES) or poly-L-lysine. APES has been shown to be superior to poly-L-lysine in preventing tissue detachment from the glass (Ben-Sasson *et al.*, 1995) and thus, APES was use to treat the glass slides prior to use. The slides were subbed at least 2 days prior to the application of the paraffin sections.

The method described by Herrington and McGee (1992) was used for treating the slides. Briefly, the slides were placed in a rack and cleaned by immersion for 30 min in 2% Decon 90 made in warm (60^{o}C) distilled water. This was followed by rinsing in distilled water, and then in acetone and finally air dying. The slides were then immersed into 2% APES made in acetone for 30 min. Finally the slides were rinsed with acetone, washed in distilled water and air dried at 37^{o}C. The slides were then stored in a dry place for 2 days prior to use.

13.2.2.4.4. Transferring Sections to Slides

One or two sections at a time were removed from the water bath and placed onto glass microscope slides using a thin paint brush. The paraffin slides were stored at room temperature until use to enable the section to adhere to the slide.

13.2.2.4.5. Deparaffinising Sections

Deparaffination should be as complete as possible, since remaining paraffin adversely affects the TUNEL reaction. The sections were heated 60^{o}C for 20 min (Gavrieli *et al*., 1992) and then hydrated through several baths of xylene and a graded series of ethanol at concentrations ranging from 100 to 70% with an immersion time of 3 min per bath as shown in table 13.2. Thereafter, the sections were rinsed in PBS (pH 7.4) for 30sec. Care was taken to ensure that the slides did not dry out during the deparaffinising.

Table 13.2: Procedure for dewaxing and rehydrating brain sections

Step	Processing Agent	Time
1	Heat at 60^{o}C	20 min
2	Xylene	2 x 5 min each
3	100% Ethanol	2 x 3 min each
4	90% Ethanol	1 x 3 min
6	80% Ethanol	1 x 3 min
7	PBS	30 sec

13.2.2.4.6. *In situ* Cell Death Detection Kit, Fluorescein

For the TUNEL reaction, tissue sections were processed according to the procedure described below.

13.2.2.4.6.1. Deproteinisation with Proteinase K

After the PBS wash, the tissue sections were partially deproteinised by incubation with Proteinase K. Proteinase K treatment digests cross-linked proteins and thereby increases cell permeability and access to the nucleic acid targets i.e. DNA. Proteinase K is preferred because it does not require predigestion to reduce residual nucleases (Willson & Higgins, 1990). The concentration, incubation time, and temperature of proteinase K are extremely important and have to be optimized for each type of tissue as high concentrations can cause tissue damage and increase nonspecific staining (Tornusciolo *et al*., 1995). The slides were incubated in 20µg/ml proteinase K which was made up in 10mM Tris-HCl buffer, pH 8, for 15min at 37^{o}C in a humidified chamber. Care was taken to ensure that the sections did not dry out and drying out would prevent fluorescence.

Since the final immunohistochemical stain is peroxidase-independent (Geiger *et al*., 1997), no inhibition of endogenous peroxidases that can produce high levels of background staining and interfere with the interpretation of the results, was performed because H_2O_2 weakens TdT activity (Migheli *et al*., 1995) and induces DNA breaks (Wijsman *et al*., 1993). Thus, incubation step was terminated by washing the slides four times in PBS for 3min each. The experimental slides were kept in PBS while the positive control slide was removed for DNase treatment as described below.

13.2.2.4.6.2. Positive DNase Controls

There is a substantial amount of variation in positive staining when using the TUNEL method; therefore, at least two DNase control slides should be included with each experimental run. The type, size and fixation of the tissue are contribution factors to the variation in staining. Since DNA fragmentation is characteristic of apoptosis, application of DNase I to control slides is ideal. DNase I is an endonuclease that introduces breaks by hydrolyzing double-stranded, or single-stranded DNA, preferentially at sites adjacent to

pyrimidine nucleotides (Sambrook *et al.*, 1989); therefore, pretreatment with DNase I results in intensive labelling of all nuclei. If the DNase I controls do not stain, staining on the experimental slides may be artifact and not positive staining.

The concentration of DNase I used was 3000U/ml prepared in 50mM Tris-HCl, pH 7.4 containing 1mg/ml BSA. After finger flicking for 10sec, sufficient DNase mixture was applied to the desired DNase control slides in order to cover the entire section and incubated for 10min at 25^{o}C. This mixture should not be made until needed, since thawing of the DNase I causes its inactivation. After DNase I pretreatment, the positive control slides were washed thoroughly with PBS, since residual DNase activity can introduce high background.

13.2.2.4.6.3. Labelling Protocol

In the TUNEL method, TdT is used to incorporate biotinylated deoxyuridine at the sites of DNA breaks. Both single-stranded DNA and 3' overhangs of double-stranded DNA are good substrates for TdT. The TdT is generally inefficient at catalyzing the transfer of biotinylated dUTP to blunt or recessive ends (Deng & Wu, 1983). The *in situ* cell death detection kit, fluorescein (Roche) contains two vials; vial 1 is the enzyme solution which contains the TdT from calf thymus (EC 2.7.7.31) in storage buffer while vial 2 which is the label solution contains the nucleotide mixture in reaction buffer. To prepare the reaction mixture 100µl label solution is removed from vial 2 and kept away for the 2 negative controls. The total volume of the enzyme solution (vial 1) is added to the remaining 450µl of label solution (vial 2) to obtain 500µl of TUNEL reaction mixture. The mixture is mixed well to equilibrate the components. To maximize efficiency the TUNEL reaction mixture is prepared during the 10min DNase treatment step and kept on ice until use. In addition, the TUNEL reaction mixture is sensitive to light therefore it was prepared in the dark.

50µl/section of TUNEL reaction mixture containing the enzyme and digoxignenin-labeled dUTP was added to both the experimental and DNase control slides while, 50µl of the labelling solution was added to each of the negative controls. All the slides were covered with a zip-lock bag, in order to prevent the slides from drying out and this also

imposes an even layering of the reaction mixture over the whole tissue section. All the slides were then incubated in a humidified chamber for 60min at 37^{o}C in the dark. TdT is temperature-sensitive; temperatures above 40^{o}C inactivate the enzyme (Geiger *et al.*, 1997) therefore the temperature was constantly monitored in the humidified chamber to ensure that a temperature of 37±2^{o}C was maintained throughout the incubation period.

The reaction was then terminated by immersing the slides in PBS. The slides were washed three times in PBS.

13.2.2.4.6.4. Mounting of Slides

In order to preserve the fluorescence and prevent the drying out of the sections, the sections need to be mounted. However, normal xylene mounts such as DPX destroys the fluorescence of the tissue therefore, while the slides were still wet enough SHUR/MOUNT™ was added to them. SHUR/MOUNT™ is an aqueous mountant that also assists in preserving the fluorescence of the tissue. Tissue sections were then covered with coverslips and allowed to dry in the dark.

13.2.2.4.6.5. Photo-microscopy

To detect apoptotic neuronal death, once the mountant had dried, the tissue sections were viewed and photographed using an Olympus DX-61 motorized epifluorescence microscope (Wirsam Scientific, Gauteng) that is controlled by the Soft Imaging Systems analysis 3.2 software (SiS Systems GmbH, Munster, Germany). Photographs were taken using a Peltier cooled Colorview camera. Apoptotic cells can be detected using an excitation (ex) wavelength in the range of 450-500nm or by detection the range of 515-565nm (green) therefore, two filter cubes, i.e. U-YFP filter (ex= 513nm and emission (em)= 527nm) and Texas Red U-MWIYZ filter (ex= 596nm and em= 620nm), that are capable of detecting fluorescence in this wavelength region were utilized to detect the apoptotic cell death. Filter cubes were obtained from Chroma Corp. (Battlebro, USA). Sections were protected from light at all times.

13.2.3. RESULTS

The primary difference between normal cells and apoptotic cells is in the nucleus (Mahalik *et al*., 1997). The DNase I controls are used as a guideline to ensure that the staining on the experimental slides is not artifact and is actually positive staining. The positive control slides, pretreated with DNase I resulted in intensive labelling of all nuclei throughout the rat brain. The apoptotic positive cells are shown in figure 13.2 with arrows. The subpopulation of apoptotic cells, scattered throughout the tissue section are intensely stained green by the TUNEL treatment and are easily visible.

The experimental control sections appeared quiescent with no TUNEL positive apoptotic cells in the CA1 and CA3 regions of the hippocampus as evident in figure 13.3. The neurons are clearly visible with the absence of the green staining of the nucleus and thus indicate that apoptotic cell death has not occurred (figure 13.3, arrows).

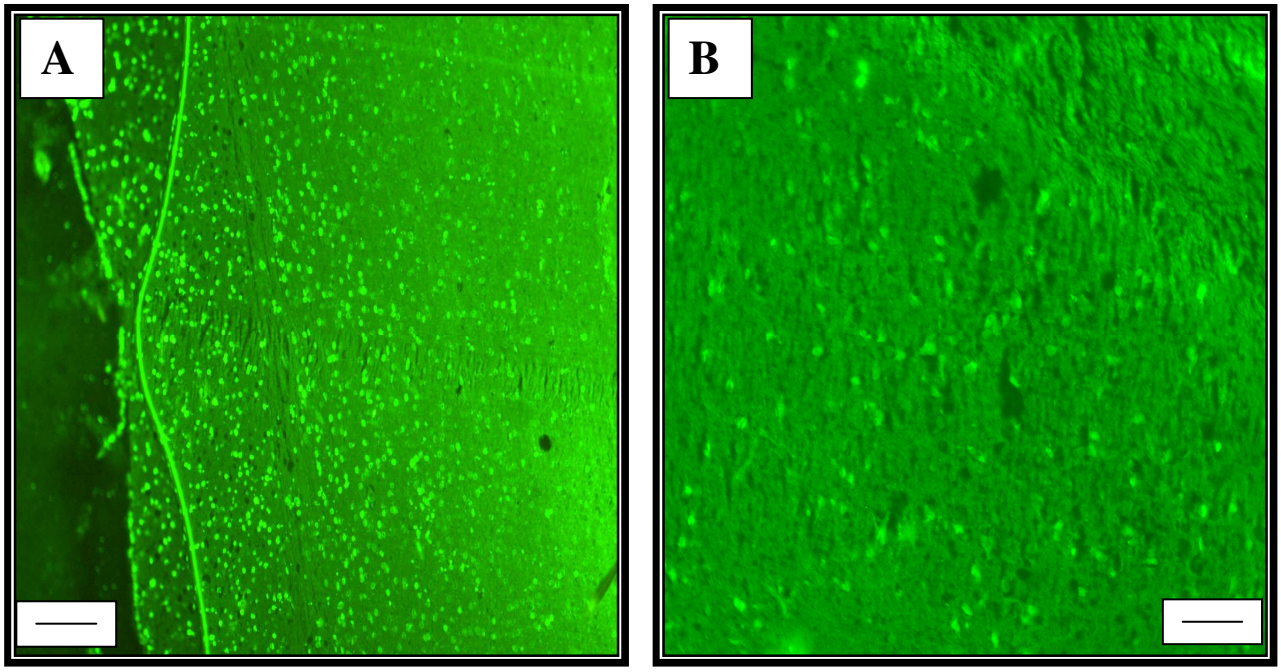

Figure 13.2: Detection of apoptotic cells (green spots) by fluorescence microscopy in the positive control tissue section from a rat brain. The section was assayed with the *in situ* cell death detection kit, fluorescein. **A**. Bar, 200µm and **B**. Bar, 100µm.

Figure 13.4, shows the hippocampus cells of the QA treated rat. As evident from this figure, the TUNEL positive cells appear surrounded by unstained neurons (arrows). However, it is also evident from figure 13.4, that QA does cause some apoptotic cell death which is more prominent in the CA1 region than the CA3 region of the

hippocampus. In order to confirm that apoptotic cell death that was occurring, a composite picture was taking using two different filter cubes i.e. a YFP and Texas Red filter cube as shown in figure 13.5. It is evident from this figure that the apoptotic cell death is true as there is co-localization of the staining. The co-localized apoptotic cells appeared a yellowish orange colour. However, the treatment of rats with QA together with melatonin or 6-OHM was able to prevent the QA-induced apoptotic cell death as seen in figure 13.6 and 13.7. As evident from figures 13.6 and 13.7, the CA1 and CA3 regions of the indoleamine treated rats were quiescent and lacked apoptotic positive stained cells. In addition, there was no indication of aggregation of apoptotic cells into multicellular clusters. Furthermore, there is no visible difference between the hippocampal neurons of the control treated rats and the melatonin and 6-OHM treated rats, indicating that the indoleamines were able to protect the CA1 and CA3 region of the hippocampus against QA-induced apoptotic cell death.

13.2.4. DISCUSSION

Apoptotic mechanisms appear to contribute to excitotoxic neuronal injury in rat brain (Portera-Cailliau *et al*., 1995; Qin *et al*., 1996). The TUNEL kit proved extremely sensitive and easy to use providing a good signal-to-background ratio. The TUNEL method specifically labelled individual apoptotic nuclei in the CA1 and CA3 regions of the rat hippocampus. The intense staining of the apoptotic cells in the DNase treated positive control section provide evidence that the experimental method was carried out correctly and that any staining on the experimental sections could be attributed to apoptotic cell death. In addition, necrosis generally appears in clusters of neighbouring cells and is associated with an inflammatory process in which immune cells infiltrate the area and disrupt the tissue structures as shown in chapter twelve. However, as shown in this chapter apoptotic cells appear scattered or follow a distinct pattern of distribution.

Ogata *et al*., (2000) demonstrated that QA causes DNA fragmentation when analysed by flow cytometry at 10mM for 24hr in HL-60 cells. However, these authors further showed that QA, which has two carboxyl groups in the molecule, generally acts as a weak inducer of apoptosis. This weak ability of QA to induce programmed cell death is further confirmed by the results obtained TUNEL reaction as shown in figure 13.4 and 13.5. The

result of this experiment confirms that QA causes modest apoptotic neuronal death. This is more predominant in the CA1 region than in the CA3 region of the hippocampus. The mechanism by which QA induces apoptosis is suggested to be via the caspase pathway (Ogata *et al*., 2000). This is supported the findings of a number of authors that QA weakly induced apoptotic neuronal death in the hippocampus and striatum cells (Portera-Cailliau *et al*., 1995; Qin *et al*., 1996; Dihné *et al*., 2001). The QA-induced apoptotic cascade has been shown to be initiated by the stimulation of NMDA receptors (Qin *et al*., 1996).

From the results of this chapter it is also evident that both the indoleamines were able to prevent the modest induction of apoptotic cell death in the CA1 and CA3 region of the hippocampus caused by QA. The CA1 and CA3 hippocampal neurons resemble those of the control treated rats thus indicating that both melatonin and 6-OHM provided complete protection against QA-induced apoptosis. Kunduzova *et al*., (2003) demonstrated that melatonin plays a critical role in preserving the functional integrity of membrane lipids and has the ability to reduce ischemia-induced cell apoptosis, suggesting that melatonin may act through apoptotic transduction pathways. The authors further conclude that melatonin may protect against oxidative stress induced cell death. In addition, Chen *et al*., (2003) demonstrated that melatonin protects the locus coeruleus against oxidative stress induced apoptosis.

13.3. CONCLUSION

Programmed cell death occurs during normal development of the nervous system. Moreover, features of apoptosis may be evident after cell death induced through physical or chemical insults. Ferrer *et al*., (1995) using morphological and biochemical studies demonstrated that prevailing necrosis together with apoptosis occur following intrastriatal injection of QA. This is further supported by the results of chapter twelve, where QA was shown to induce extensive necrotic cell death in the hippocampus. Thus, it can be concluded that QA induces marked necrosis with a modest amount of apoptotic cell death. This is further supported by the findings of Qin *et al*., (2001). This further confirms the results of chapter twelve. It is suggested that different antioxidant substances can suppress the apoptotic cell death. Besides being highly potent direct scavengers of oxygen

radicals, melatonin and 6-OHM were shown in this study to prevent the weak induction of apoptosis by QA in hippocampal neurons. Apoptosis is also characterized by caspase-independent processes, which may be inhibited by Hsp70 (Creagh *et al*., 2000). Thus, the effect of QA and the indoleamines on Hsp70 expression was investigated in chapter fourteen.

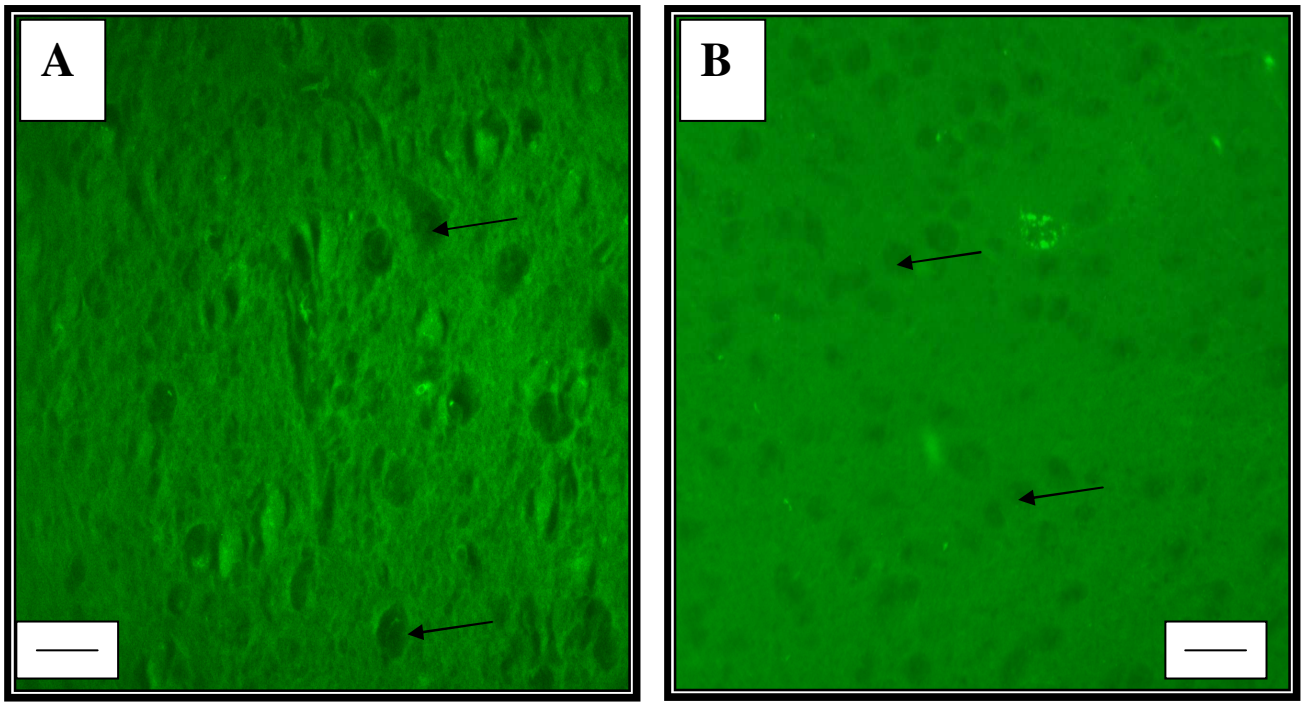

Figure 13.3: Hippocampus cells from a control treated rat. Bar 50µm. **A**. CA1 region and **B**. CA3 region of the hippocampus. Arrows show pyramidal neurons lacking the green stained nuclei.

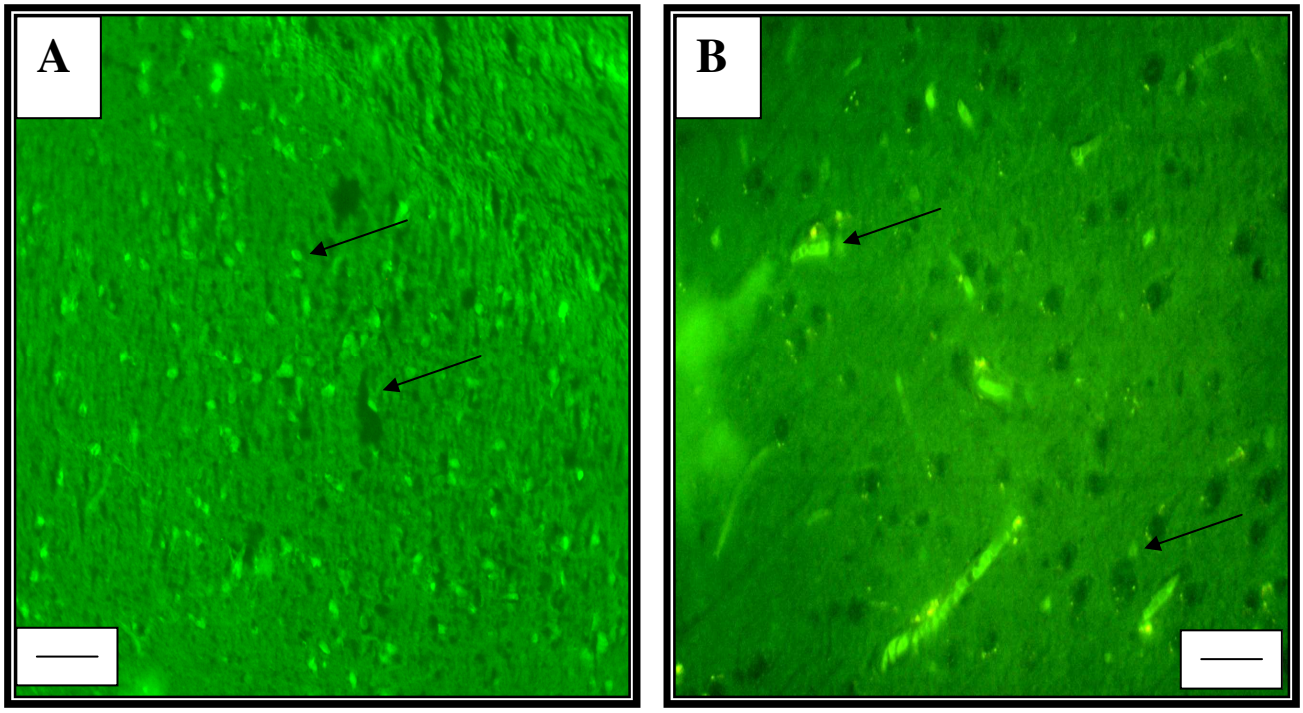

Figure 13.4: Hippocampus cells from a QA treated rat. Bar 50µm. **A**. CA1 region and **B**. CA3 region of the hippocampus. Arrows show green stained nuclei of the apoptotic positive cells.

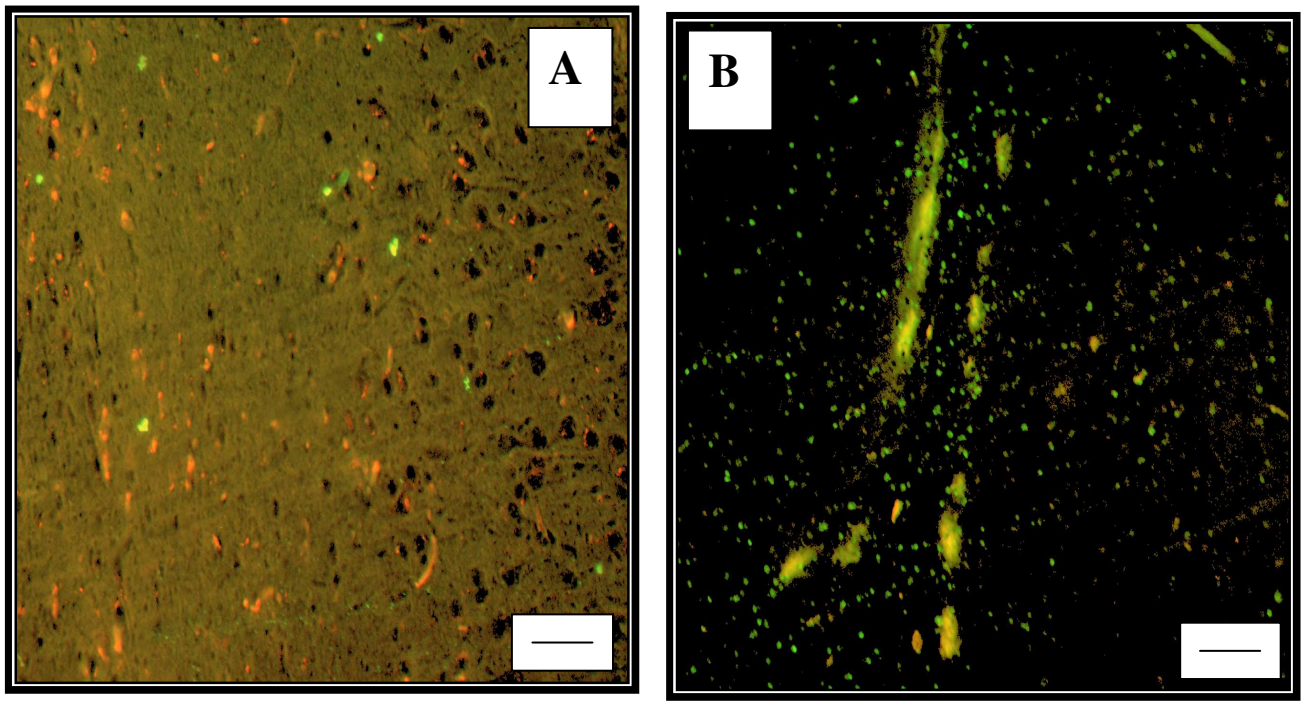

Figure 13.5: Hippocampus cells from a QA treated rat. A composite image using Texas Red and U-YFP filters. Bar 50µm. **A**. CA1 region and **B**. CA3 region of the hippocampus. The yellowish orange stained nuclei of the apoptotic positive cells indicate co-localization.

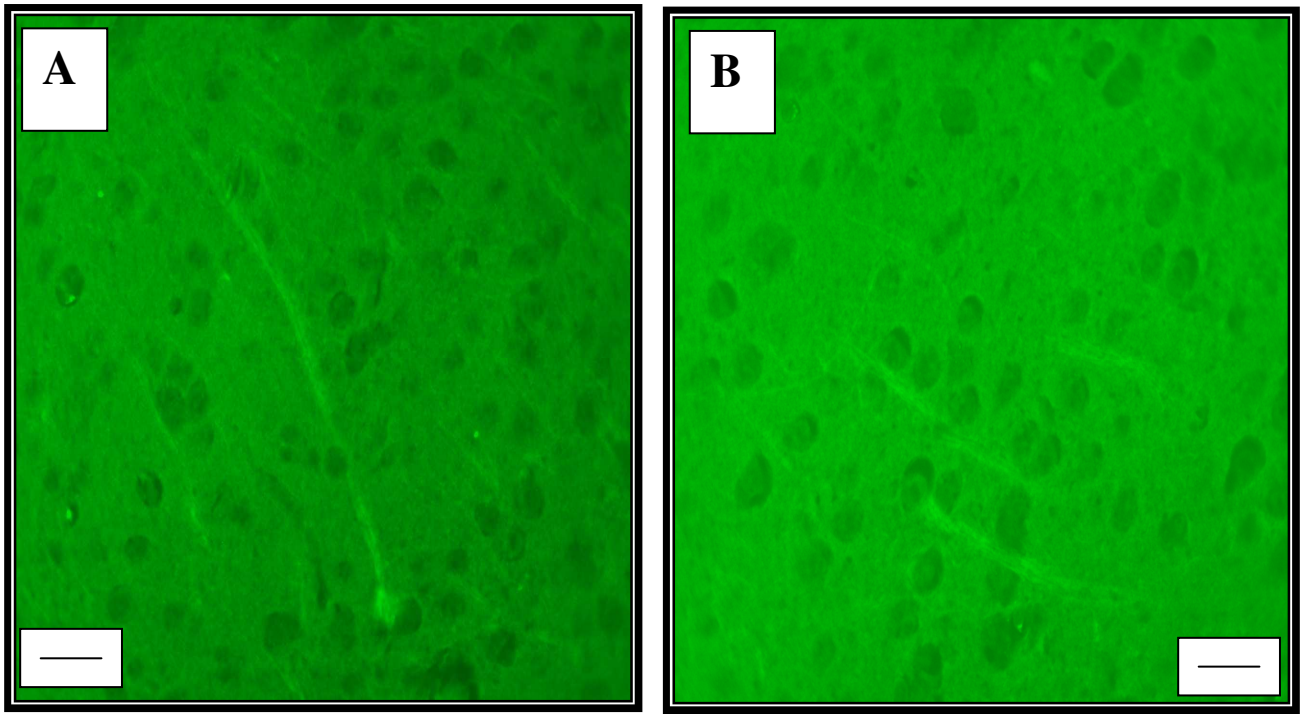

Figure 13.6: Hippocampus cells from a QA and melatonin treated rat. Bar 50µm. **A**. CA1 region and **B**. CA3 region of the hippocampus. The CA1 and CA3 neurons are clearly visible with a lack of apoptotic cell death.

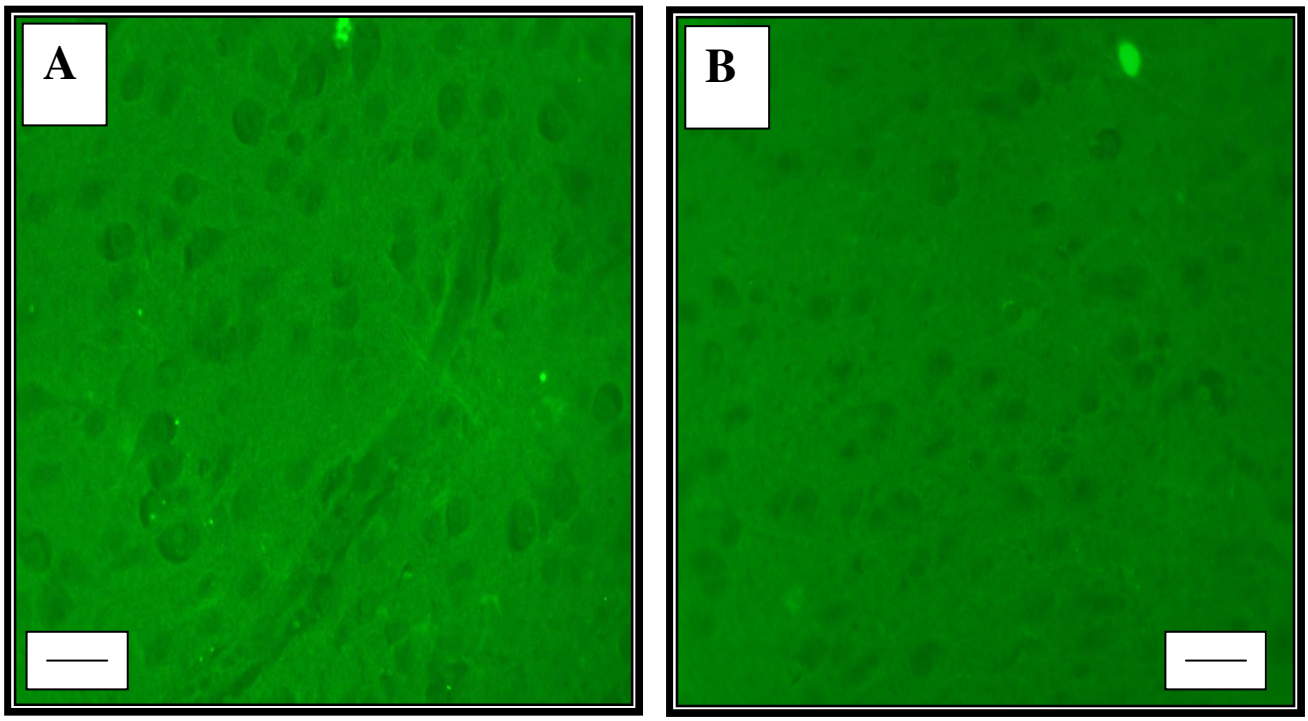

Figure 13.7: Hippocampus cells from a QA and 6-OHM treated rat. Bar 50µm. **A**. CA1 region and **B**. CA3 region of the hippocampus. The CA1 and CA3 neurons are clearly visible with a lack of apoptotic cell death.

CHAPTER FIFTEEN

CONCLUSION

The results of the first part of this study involves an in depth investigation into the physico-chemical, pH, temperature and photostability properties of the pineal hormone, melatonin. The results of these studies were conducted in order to assist future researchers in the identification of melatonin as well as provide important information for both consumers and manufacturers concerning the proper storage conditions required for melatonin formulations, considering the lack of this information in literature sources.

The possible use of melatonin as a therapeutic agent prompted the initial study which was the development of a simple, reliable, cost-effective HPLC method to analyze melatonin raw material and this was conducted in chapter two. In addition, this method may be applied to the determination of melatonin in dosage forms and to quantitate the amount of melatonin in combination with selected drugs remaining during and after photostability studies. In addition this HPLC method served as the basis for the assessment of the partition coefficient, hygroscopic, pH, temperature and photostability characteristics of melatonin.

Chapter three provides a detailed investigation into the physico-chemical properties of melatonin. Initially, the physical properties of melatonin were determined utilizing various chemical techniques. This provides important information to both characterize and confirm the identity of melatonin raw material used in this study. In addition, this study was essential as the physical properties of melatonin have not been reported in detail in literature to date. In addition, in chapter three, the partition coefficient and hygroscopic properties of melatonin was determined. The results indicate that melatonin partitions to a greater extent in octan-1-ol than in water confirming its lipophilic nature and providing essential experimental evidence regarding the preparation of melatonin in solution The results of the hygroscopic study indicated that melatonin raw material is extremely hygroscopic at temperatures above 40^{o}C, while melatonin tablets are hygroscopic when left out of the original container. Thus, this study highlights the need

for consumers to be aware of the proper storage of melatonin tablets to improve the stability and ensure long term integrity of the compound.

The most common route of administration melatonin is the oral route, thus exposing the indole group to large variations in pH, within the gastrointestinal tract and despite the common use of aqueous solutions of melatonin; its stability in solution has not been reported. Chapter four was focused on investigating the stability of melatonin over a range of pH's and temperatures. The findings imply that melatonin should be relatively stable at body temperature when ingested orally, particularly as this antioxidant is known to be very lipophilic and can cross membranes, such as the stomach wall, with ease. In addition the results suggest that orally administered slow release preparations of melatonin should be relatively stable and therefore exhibit favourable bioavailability. However it was noted that melatonin in solution is not stable within acceptable limits (95-105%) after 3 days, providing important information and a challenge to the formulators of this drug substance in a liquid dosage form.

Chapter five highlights the photo-instability of melatonin both in the solid-state and in solution on exposure to light according ICH conditions and the importance of suitable packaging. The results of this study imply that radiant exposure at approximately 1.2 million lux hours showed melatonin to be light sensitive with 9%, 17%, 15% and 18% degradation of the melatonin raw material, tablets, capsules and solution occurring, requiring consideration of the packaging of these drug products.

Chapter six is based on recent reports as well as the results of chapter five indicating that melatonin is photolabile (Andrisano *et al*., 2000, Anoopkumar-Dukie *et al*., 2000). However, detailed investigations on its photochemistry have not been reported. Thus, in chapter six the stability of melatonin in solution in the presence of UV light was assessed and the resulting photoproducts identified. The present study showed that irradiation of a melatonin solution with UV light causes rapid degradation of melatonin and the presence of oxygen accelerates the photodegradation of melatonin, as opposed to purging with nitrogen. The results of the LC-MS studies show that melatonin, after UV irradiation, is converted to two products, namely, AFMK and 6-OHM, existing in a ratio of 2:1,

respectively, when melatonin concentration reached zero. In addition, the degradation pathway for the formation of these two photoproducts was proposed in this chapter. Both these photoproducts have been shown to retain free radical scavenging properties of the parent compound, melatonin. This study further confirms the suitability of melatonin as an agent to protect tissues such as skin against UV-induced free radical damage. One of the concerns of using melatonin in sunscreens is its photoinstability. From this chapter it is evident that even though melatonin is rapidly degraded in the presence of UV light, the photodegradants retain antioxidant activity, thus making melatonin a likely candidate for inclusion in sunscreens.

Melatonin is available commercially from several unregulated health food suppliers and since the Wurtman report, melatonin sales have not declined. In 1994, one manufacturer of melatonin in USA increased the amount of melatonin sold the previous year by three fold. However, the melatonin formulations appear with no labelling for the correct storage conditions, dosage and side effects, as well as no control for purity and self-medicating with an unregulated product. Thus, the results of the present study provides important information for consumers and manufacturers regarding the proper storage conditions of melatonin formulations to improve its stability and ensure long term integrity of the compound. In addition, it provides information to future researchers regarding the preparation of melatonin solutions and identification of melatonin in different dosage forms and experimental specimens. Furthermore, this study confirms the incorporation of melatonin in sunscreen preparations and puts to rest some of the concerns surrounding the photoinstability of melatonin.

The experiments conducted for the second part of this study point conclusively to a new and emerging role of 6-OHM as a neuroprotective agent.

Initial studies were conducted to investigate whether melatonin and 6-OHM could scavenge, the cytototxic and genotoxic species, $^1O_2$. The result of this study provides interesting information because, using the laser source, melatonin was shown to increase the disappearance of DPBF indicating that melatonin under these conditions is actually producing radicals. Bubbling of nitrogen in the melatonin solution prior to irradiation confirmed the production of melatonin radicals by melatonin. However; these melatonyl radicals have been reported not to be very reactive and therefore non-toxic in the cell

(Lewis *et al*., 1990). However, upon lamp photolysis, melatonin was shown as an effective scavenger of $^1O_2$ produced by naphthalene. This dual action of melatonin under different $^1O_2$ generating systems, allows for the speculation that under the conditions using the laser source melatonin can be used in PDT as a useful agent in the destruction of tumours, and using the lower energy source, lamp photolysis, it can serve as an effective $^1O_2$ scavenger. However, surprisingly, 6-OHM was shown to be an effective scavenger of $^1O_2$ species produced using the laser source and DPBF. This is the first report showing the $^1O_2$ scavenging ability of 6-OHM and the results indicate that 6-OHM serves as a more potent $^1O_2$ scavenger than melatonin. This research serves as a basis of demonstrating the ability of 6-OHM, the photoproduct and primary metabolite of melatonin, in scavenging the photocytotoxic species, $^1O_2$. It is most likely that the $^1O_2$ generated by laser and lamp photolysis is very high, and that the damaging effects that we found in our *in vitro* system is much greater than the eventual biological damage induced by the amount of $^1O_2$ generated *in vivo*. Thus, it can be speculated that since melatonin and 6-OHM were able to scavenge the high concentration of $^1O_2$ produced, they would be effective in quenching the biological concentrations of $^1O_2$ produced *in vivo* and thus be effective in counteracting the damaging action of photodynamic injury. Since, $^1O_2$ has been postulated to play a role in neurodegenerative diseases such as Parkinson's disease (Perry *et al*., 1982), it is speculated the use of melatonin or 6-OHM could help reduce this effect of $^1O_2$.

The extent of protection that 6-OHM as an antioxidant could afford to the brain, against oxidative stress in the form of $O_2^{\bullet-}$ was investigated in chapter eight. Initially, the ability of the degraded melatonin solution to provide equipotent protection against reducing the generation of $O_2^{\bullet-}$, despite the absence of melatonin was investigated. The results of this study imply that the photoproducts i.e. 6-OHM and AFMK retain $O_2^{\bullet-}$ scavenging properties of melatonin. In addition, a further study was conducted to show that melatonin can reduce UV-induced $O_2^{\bullet-}$ generation in skin tissue. In addition, this provides supportive evidence for the use of melatonin in sunscreen preparations. Furthermore, the experimental results indicated that 6-OHM affords significant and complete protection against cyanide and QA-induced $O_2^{\bullet-}$ generation by reducing the levels of $O_2^{\bullet-}$ below that of the control value. In addition, 6-OHM proved to be superior to melatonin as an $O_2^{\bullet-}$ scavenger. The $O_2^{\bullet-}$ scavenging ability of melatonin was postulated to be due to its anti-

inflammatory actions as well as it ability to increase SOD activity, an important antioxidative enzyme involved in the dismutation of $O_2^{\bullet-}$. In addition, it is speculated that 6-OHM together with its ability to directly scavenge $O_2^{\bullet-}$ is also acting by increasing the activity of SOD enzyme, similar to melatonin.

Since 6-OHM showed protection against cyanide induced $O_2^{\bullet-}$ generation, and considering the fact that cyanide is a respiratory poison which acts by blocking complex IV activity of the ETC, the study in chapter nine was conducted to determine the effect of 6-OHM on cyanide induced depression of the ETC within the mitochondrial fraction isolated from the rat brain. The results indicate that melatonin and 6-OHM are able to dose-dependently reverse the cyanide-induced inhibition of the mitochondrial ETC function, with melatonin causing complete abolishment of the cyanide-induced inhibition and 6-OHM only partially reversing this inhibition. This implies that melatonin serves as a superior agent in protecting the mitochondrial ETC against cyanide. In addition, both indoleamines were shown to increase basal levels of respiration and ETC activity within the brain mitochondria with melatonin resulting in a more significant induction. This action of melatonin is postulated to be due to the fact that it augments the activities of a number of antioxidant enzymes and it increases complex I and IV activity in the mitochondrial ETC. In light of this, it was postulated that 6-OHM also increases complex I activity. This was therefore investigated and the results showed 6-OHM to increase complex I activity above basal control values *in vivo*. Since the mechanisms underlying the beneficial actions of 6-OHM are unknown, and since it is shown to elevate complex I activity, 6-OHM ameliorative effects may relate to an increased efficiency of oxidative phosphorylation. Furthermore, complex I deficiency has been documented to be intimately associated with the onset of several neurodegenerative disorders and the aging process (Yano, 2002; Ventura *et al*., 2002). In addition by stimulating complex I activity, 6-OHM can serve to possibly prevent the age and neurodegenerative disease-related decline of complex I activity. Considering the fact that respiratory inhibition of mitochondria by cyanide is the basis for its $O_2^{\bullet-}$ generation, it can be concluded that the protection offered by 6-OHM against $O_2^{\bullet-}$ generation by cyanide is not due only to its antioxidant properties, but also due to the direct inhibition of cyanide insult and complex I activation within in the ETC.

In chapter ten, the neuroprotective effects of 6-OHM against QA, cyanide and Fe^{2}-induced neurodegeneration and oxidative stress in the form of lipid peroxidation was investigated. Initially, the ability of the degraded melatonin solution to provide equipotent protection against reducing the QA-induced lipid peroxidation in brain homogenate, despite the absence of melatonin was investigated. The results of this study imply that the photoproducts i.e. 6-OHM and AFMK retain the ability to reduce QA-induced lipid peroxidation. In addition, a further study was conducted to show that melatonin can reduce UV-induced lipid peroxidation in skin tissue. This study further provides supportive evidence for the use of melatonin in sunscreen preparations. Thereafter, experimental studies were conducted to investigate the effect of 6-OHM on lipid peroxidation induced by the above three mentioned neurotoxins, demonstrated that 6-OHM significantly decreases lipid peroxidation both *in vitro* and *in vivo*. However, melatonin is shown to be a more potent inhibitor of lipid peroxidation than 6-OHM. The findings of this chapter support and confirm that 6-OHM is a potent $^{\bullet}OH$ radical scavenger (Matuszak *et al*., 1997) with equipotent free radical scavenging properties as melatonin. In addition, 6-OHM was shown to completely inhibit lipid peroxidation induced by QA and cyanide and partially reverse the peroxidation induced by iron (II). The significance of this is obvious when considering that damage to any plasma membrane, albeit the cell or mitochondrial membrane, results in a disruption of membrane fluidity and damage to proteins. The production of ATP may also be affected. Thus the effects of lipid peroxidation may be detrimental to the cell. Furthermore, neuronal damage due to oxidative stress has been implicated in several neurodegenerative disorders, in which case 6-OHM may be a therapeutic advantage. It was thus postulated that the protection 6-OHM offered to lipid peroxidation induced by QA and iron (II) was not only attributable to the antioxidant properties of this indoleamine, but also due to a possible chelation of iron (II) and iron (III).

Iron (II) plays an important role in accelerating lipid peroxidation and is itself a free radical. QA-induced lipid peroxidation has been reported to be dependent on iron (II). Therefore, chapter eleven was devoted to investigating whether the mechanism of protection elicited by 6-OHM against this damage may be due to an interaction with iron (II) and iron (III), thus rendering these metal ions unavailable to cause further damage. Results demonstrate the existence of a definite interaction between 6-OHM and iron (III)

but not iron (II). However, the results in this chapter demonstrate that by binding to iron (III), 6-OHM readily converts iron (III) to iron (II). It is therefore suggested that the chelation of iron (III) is one of the mechanisms involved in the reduction of iron-induced lipid peroxidation. However, one dire consequence of this conversion is the ready availability of iron (II) to drive the Fenton reaction. However, 6-OHM was shown in chapter ten to reduce iron (II)-induced lipid peroxidation *in vitro* and *in vivo*. Thus, it was demonstrated that while this agent has the potential to promote the Fenton reaction, it has been shown to scavenger the $^{\bullet}OH$ and at the same time reduce the consequent rise in iron (II) lipid peroxidation.

QA is an endogenous agonist at the NMDA receptor, which when activated, results in excessive calcium influx into the cell resulting in neuronal swelling. Iron (II) has also been shown to increase calcium accumulation in the hippocampus (Sloot *et al*., 1994). Histological investigation (chapter twelve) of hippocampal neurons illustrates that 6-OHM protects these neurons against QA and iron (II)-induced damage. Moreover, external observations in the rats treated with the toxin and 6-OHM showed relatively greater activity and faster response as compared to the toxin alone group. In addition, 6-OHM treatment was able to prevent the QA and Fe^{2+}-induced seizure activity and behavioural changes noted in the rats. It is further suggested that the cell death in the hippocampus due to the administration of these neurotoxins, was likely due to necrosis due to the macrophage infiltration and the inherent inflammation that was evident in the photomicrographs. Thus, the protection elicited by 6-OHM as well as that shown against the increase in lipid peroxidation demonstrated in chapter ten, is due to its antioxidant properties. However, considering the extent of the protection offered by 6-OHM, it is likely that the protection involves the NMDA receptor. In addition, this chapter provides evidence demonstrating that 6-OHM does not promote oxidative neurotoxicity and that 6-OHM does not act as a prooxidant by promoting the Fenton reaction.

QA has been reported by some authors to cause necrosis together with apoptotic cell death in the hippocampus (Uberti *et al*., 2003; Ferrer *et al*., 1995), thus, the ability of QA to induce programme cell death (apoptosis) in the hippocampus and the protection offered by both melatonin and 6-OHM was investigated in chapter thirteen. The results of this chapter further support these findings, showing QA to induce a moderate amount of

apoptotic cell death which was inhibited by the treatment of rats with either of the indoleamines. These results confirm the finding that QA induces necrotic cell death as shown in chapter twelve. This is one of the first studies done to show that melatonin and 6-OHM are effective inhibitors of QA induced apoptotic cell death.

Since apoptosis is also characterized by caspase-independent processes, which may be inhibited by Hsp70 (Creagh *et al.*, 2000). Thus, in chapter fourteen it was decided to investigate the effect of QA and the indoleamines on Hsp70 expression. The results demonstrated that QA as well as 6-OHM act as inducers of Hsp70 expression, with 6-OHM serving as a more potent inducer. These results imply that the moderate apoptotic induction observed by QA in chapter thirteen is due to the Hsp70 induction. An explanation of the observed enhancement of expression of HSP70 by 6-OHM treatment could be twofold. Either 6-OHM increases the level of expression of Hsp70 (inducible). However, in light of the experiments showing 6-OHM's protective effects against QA-induced damage, it is not likely to be significantly large. It may be possible that the signal observed for the western blotting in response to 6-OHM treatment largely represents Hsc70. This cognate protein enhances synaptic transmission and stimulates long term potentiation, thus it may be possible that 6-OHM elicits these effects on the brain via a mechanism dependent on Hsc70 expression. Another possibility is the fact that Hsp70 induction may contribute to the protective effects of 6-OHM as Hsp's protect neural cells from subsequent stress and apoptotic cell death that would normally be damaging or lethal. Melatonin treatment was shown to be protective to hippocampal neurons by itself and in combination with QA as it decreased the rise in Hsp70 expression caused by QA, indicating that melatonin relieved the oxidative stress induced by this neurotoxin in a manner that the neurons did not need to express a large amount of Hsp70.

Although, the results of this study serve as a basis to point to a possible role of 6-OHM as a neuroprotectant, further investigations are warranted to conclusively confirm these findings. The metal chelating property of 6-OHM shown in this study is an exciting finding which requires to be analyzed in depth as to characterize the complexes formed with other metals, their biological and toxicological properties as well as pharmacokinetic properties. Iron deficiency not only leads to anaemia but can also lead to adverse effects on cells in the CNS and on neurotransmitters. Iron-deficiency anaemia can also lead to reduced oxygen delivery to the brain. The results of chapter eleven provide new,

important information and imply that 6-OHM converts iron (III) to a more biologically usable form viz. iron (II) which can prove helpful in cases of iron deficiency. However, further biological investigations are warranted to confirm this finding conclusively.

Another area of future research would be to investigate the molecular mechanisms by which 6-OHM exerts its various neuroprotective abilities. The ability of 6-OHM to stimulate complex I activity in the mitochondria was shown in this study and postulated as one of its protective mechanisms against oxidative stress. However, further investigations into the effect of 6-OHM on complex IV activity as well as SOD, GPx and GRd activities are warranted. In addition, the effect of 6-OHM on the receptors in the brain, such as those involved in excitotoxicity, e.g. NMDA receptors also needs to be explored.

While pharmaceutical companies continue to invest huge resources into identifying agents which could be used to alleviate debilitating neurodegenerative diseases, a source of potentially beneficial agents, namely the indoleamines, appear to offer significant benefits that are yet to be fully exploited. In conclusion, from the above research conducted it is evident that even when melatonin itself is metabolically converted to 6-OHM before it can function in the direct detoxification of radical(s), its major hepatic metabolite and primary photoproduct may be capable of doing so. Thus, it is desirable and of benefit, that more studies on the potential benefits of 6-OHM as a neuroprotectant be conducted.